Smith, Benjamin Anthony Visocchi (2016) Assessment of carbon and nutrient export from a peatland windfarm construction site. PhD thesis.

http://theses.gla.ac.uk/7080/

Copyright and moral rights for this thesis are retained by the author

A copy can be downloaded for personal non-commercial research or study, without prior permission or charge

This thesis cannot be reproduced or quoted extensively from without first obtaining permission in writing from the Author

The content must not be changed in any way or sold commercially in any format or medium without the formal permission of the Author

When referring to this work, full bibliographic details including the author, title, awarding institution and date of the thesis must be given

Glasgow Theses Service
http://theses.gla.ac.uk/
theses@gla.ac.uk

# Assessment of carbon and nutrient export from a peatland windfarm construction site

Benjamin Anthony Visocchi Smith

BSc (Joint Hons) Environmental Chemistry and Geography

Submitted in fulfilment of the requirements for the Degree of Doctor of Philosophy


School of Geographical and Earth Sciences

College of Science and Engineering

University of Glasgow

February 2016

# Abstract

The full extent of a landscape's resilience to the environmental impact of siting wind-based renewables on peats is currently unknown. This research explores if windfarm construction activities have caused disturbance by investigating; time series of fluvial carbon (C) and nutrient concentrations; constructing aquatic organic C fluxes, before, during and after the windfarm construction period. Additionally, C sequestration rates of peat and nearby lake sediments (Loch Brora) were calculated to provide a historical context to, i) calculated aquatic C fluxes and ii) sediment export from surrounding catchments, considering both a catchment hosting the windfarm construction and one that does not. Furthermore, the effectiveness of a peatland restoration technique, drain-blocking, was assessed as a means of undertaking a whole system approach to assessing the potential impact of the windfarm development, considering how these management strategies can help mitigate potential C losses associated with construction.

The research field site was located on the Gordonbush Estate, near Brora, where construction started in July 2010 (the same time this research began) on Scottish and Sothern Energy Renewables (SSER) 35 turbine windfarm. Construction work finished in May 2012 and data collection continued until September 2014. Throughout this period, fieldwork was focussed on storm event sampling (collecting samples for dissolved organic carbon (DOC), particulate organic carbon (POC), total phosphorous (TP), soluble reactive phosphorous (SRP) and total oxidised nitrogen (TON)), collecting peat and lake sediment cores, samples of modern day sediment export and monitoring water table depth in an area where old drainage channels were blocked as part of a peatland restoration initiative.

Three river catchments were studied, two affected by windfarm construction activities (GB10 and GB11) and one control site (GB12), DOC concentrations ranged from 1.1 mg $l^{-1}$ to 48.3 mg $l^{-1}$, POC from <0.1 mg $l^{-1}$ to 21.3 mg $l^{-1}$, TP from <0.5 µg $l^{-1}$ to 264 µg $l^{-1}$, SRP from <0.5 µg $l^{-1}$ to 39 µg $l^{-1}$ and TON from <1 µg $l^{-1}$ to 141 µg $l^{-1}$. These were all within ranges of macronutrient concentrations measured at other northern temperate peatland sites. Comparing macronutrient concentrations between catchments, generally GB10 > GB11 > GB12 for all determinants. Seasonal patterns in fluvial macronutrient concentrations were observed at Gordonbush: summer maxima and winter minima in DOC and TP concentrations and the opposite trend in TON concentrations. SRP data collected indicates a legacy of forest felling in the Bull Burn Plantation has contributed to increased concentration in the Allt Mhuilin river (GB10) compared to the two other catchments, Allt Smeorail (GB11) and Old Town Burn (GB12) where no forest felling occurred during the data collection period. Differences in DOC and TP concentration in Allt Mhuilin compared to other catchments could also be related to forest felling activities

but catchment characteristics such as peat coverage may have also influenced results. For all relevant measures of water quality, macronutrient concentrations from Gordonbush shows studied streams consistently achieved “Good” or “High” status throughout the data collection period. Apart from the legacy of forest felling, a discernible impact of windfarm construction was not observed from macronutrient concentration time series.

Calculating annual aquatic C fluxes from studied catchments offered a means of assessing potential impact. Various techniques of estimating fluxes were explored but splitting storm event DOC and POC data based on time of year and whether samples were collected on the rising or falling limbs were concluded to give the best estimates. Calculated fluxes ranged from 3 – 38 g C $m^{-2}$ $yr^{-1}$ and DOC consistently accounted for ~90% of total aquatic C export. These values were within limits of other C flux based studies from peatlands but the time series constructed at Gordonbush suggested windfarm construction, between July 2010 and May 2012, may have contributed to an increase in aquatic C export from affected catchments during this time, relative to the control site.

Long term C sequestration rates from within the Gordonbush estate were 20-25 g C $m^{-2}$ $yr^{-1}$, the same magnitude as aquatic organic C fluxes. However, peat C sequestration was shown to be variable over the last ~9000 years since Scottish peatlands became established, with rates ranging from 10-60 g C $m^{-2}$ $yr^{-1}$. Controls on this variation are likely climatic with delivery of moisture influenced by the North Atlantic Oscillation (NAO) a key factor. Calculated lake C sequestration also varied over time, 22-82 g C $m^{-2}$ $yr^{-1}$ but an inconclusive radiocarbon dating chronology meant historical comparison of C export dynamics between the, C ‘source’, peatland to the, C ‘sink’, lake was unfortunately not possible. Modern day sedimentary export data showed higher sediment yields from windfarm affected catchment than the control site. Physical characteristics varied considerably between the two catchments so although this observation could not definitively be attributed to a direct windfarm impact, it remains a possibility.

Whilst studying and quantifying the impact of drain blocking, manual measurements of water table depth (WTD) ranged between -53 cm to +14 cm in dip-wells and -36 cm to +20 cm in automated logging pressure transducers. The response of WTD throughout both data sets indicates meteorological conditions were more influential as a factor controlling peat hydrology across the site compared to topography. Manual measurements from dip-wells shows the drainage channels investigated (~0.5-0.7 m deep and ~0.5 m wide) had the greatest influence on effect WTD 0-2 m from the main channel but no statistically significant difference was detected in mean WTDs measurements before or after blocking, in relation to distance from the drainage channels themselves or

comparisons between drained and un-drained (control) areas. However, data from PTs indicate the net effect of multiple parallel drains can cause water table drawdown at a significant distance, ~ 25 m, from the drainage channel.

This is an important finding as methodology used to calculate the C 'payback time' of windfarms utilises the lateral drainage extent of peat when turbines bases are excavated. Drain blocking had no obvious effect (either positive or negative) on WTDs however it is acknowledged positive effects can take up to five years, after blocking has taken place, to be observed. Maximum DOC concentrations increased the year after blocking however this result has been recorded at other sites and the exceptionally dry summer of 2013 could have contributed to the noticed increased by promoting more peat oxidation and subsequently DOC production. There was no statistically significant difference between [DOC] collected up and downstream of the drainage channel inputs for samples collected before and after blocking. This suggests drain-blocking has had little impact on the larger site [DOC] signature one year after drain-blocking. However, as discharge from drainage channels was not measured, a potential reduction in overall DOC export could not be fully assessed and this is a highlighted future research need.

Combining averages of aquatic organic C fluxes and peat C sequestration rates calculated it is estimated net ecosystem exchange would have to be between -30 to -50 g C $m^{-2}$ $yr^{-1}$ for Gordonbush to be classed as a C 'sink'. If the observed increases in sedimentary export could be attributed to windfarm construction, Loch Brora is unlikely to act as a strong C sink for any potential increased losses as it is estimated ~90% of POC exported is not sequestered on a long-term basis in the lake sediments.

It has recently been recommended windfarms should not be developed on peatlands due to the marginal C savings achieved as our future energy mix changes (Smith et al., 2014). However, if similar projects are granted planning permission then findings from this research support the following recommendations: installation of buffer zones around areas of felled forestry to reduce nutrient export into surrounding streams; implementation of a water quality monitoring programme to assess impact of windfarm construction during construction and a period afterwards as it is still unclear from this research if there will be any lasting effects; installation of silt traps to reduce aquatic sediment export and disturbance; limit any high density excavation of drainage channels as the effects of water draw-down could be quite extensive; in addition, blocking all historical drainage channels and retaining as much moisture as possible within, and surrounding, areas of degraded peatland can increase long-term peat C sequestration rates and offset C losses experienced during construction.

This research has been funded by SSER, Engineering and Physical Sciences Research Council (EPSRC) and Energy Technology Partnership (ETP). This research has been undertaken and supported at the University of Glasgow within the College of Science and Engineering, specifically aligned to the work of the Carbon Landscapes and Drainage (CLAD) research group headed by Prof. Susan Waldron in the School of Geographical and Earth Sciences. Finally, this research has also been supported in partnership with Stirling University.





# Table of Contents

# List of Tables

# List of Figures

# Acknowledgements

It is commonly said, but without the help and support of the people listed below this research and thesis would not have been possible. I would like to take this opportunity to thank certain individuals for their contributions in helping me undertake this research.

Firstly, thank you to my sponsors Scottish and Southern Energy Renewables (SSER), Engineering and Physical Sciences Research Council (EPSRC) and The Energy Technology Partnership (ETP) for the funding to this research. Special thanks must go to Jane MacDonald of SSER for her initial effort and support in setting up this research.

For site access at Gordonbush I would like to thank John McKenzie and Iain Jappy of SSER and estate factor Tony Smith. Special thanks must go to Richard Sloman and Richard Knotts of SSER for their support throughout my field work. My requests for information regarding on-site works were always granted and considering they were not obliged to me help, the time taken by them both to give me updated information was always greatly appreciated. I recall fondly many nights spent in their company and I thank them both for being so accommodating when I stayed with them. A special mention is also reserved for Gordonbush gamekeeper Robbie Rowantree. I thank him for sharing with me his wealth of knowledge regarding the Gordonbush estate and his local nous proved useful when installing certain field equipment. Robbie, I was grateful for your consistent interest in my research activities and constant offer of help if, and when, I needed it.

For accommodation during my field work, I would like to thank Douglas Rushforth for the use of Oakleigh Cottage as continued access to it made life a lot easier. To all the people that accompanied me during those stays, a massive thank you is in order, your time and enthusiasm was greatly appreciated: Roger Grau-Andres, Hemanth Pasumarthi, Martin Coleman, George Manitas, Ian Boyd, Anthony Smith, Elliot Barnes, Richard Beck and Helen Murray. Special mention to Dr. Alona Armstrong for all her help and advice setting up regarding specific parts of my research, it was greatly valued. In regards to field work I owe the largest gratitude to Mr. Kenny Roberts. You were the best field work technician I could have asked for but more importantly your company was superb. You were a constant source of good advice and your time and commitment continually supporting me with field work was above and beyond the expected levels, so Kenny, thank you!

For extra data supplied which helped me analyse my results I must thank Ms. Anita Spurway and Mr. Andrew Revill from SEPA and Keith Johnson from MNV Ltd. Special thanks also to Mr. Ray Cranfield for weather data sourced from his station at West Clyne,

Brora and additionally to Dr. Tom Dargie for all data collated from Gordonbush Water Quality Monitoring Programme.

For laboratory work undertaken in relation to this research and for my benefit, I thank; Michael Beglan and Isabel Freer for all equipment requests no matter how strange, Mohammad Ali Salik and Fulton Murdoch for nutrient analysis, Gordon Cook of SUERC for all radiocarbon dating, Andy Tyler and Stuart Bradley of University of Stirling for $^{210}$Pb dating. Similarly, to all students who worked on aspects of my research during summer internships and dissertations I am grateful for all your hard work and enthusiasm: Rosie Atkinson, Leticia Beschus, Steven Silvestro, Colleen Mooney and Sofia Daouadji.

To all members of the Carbon Landscape Research Group past and present, your constructive comments and advice regarding oral and written pieces I have presented over the years has been warmly received and appreciated. You have all been great colleagues to work alongside and bounce ideas off throughout my Ph.D., so thank you.

To Kim Ross and Hazel Long, you have both been fantastic office mates. Thank you for putting up with all my banter, I most definitely enjoyed yours and the company of you both made life sitting at my desk considerably more bearable.

My team of four supervisors have been an enormous help over the duration of my research. Prof. David Gilvear, I thank you for your support, advice and commitment attending supervisor meetings despite our differing locations. Dr. Andrew Henderson, again despite our physical distance your support has always been keenly felt. Your advice has been has also been welcomed and appreciated. I always felt very comfortable in your company and working with you has been really enjoyable. To Dr. Hugh Flowers, for being my academic supervisor for almost a decade, I could have not selected anyone better. Your time, patience and guidance has been constant throughout my duration as a student at the University of Glasgow and made my life so much easier and more memorable, for this I will always be exceptionally grateful. To the last of my supervisors, Prof. Susan Waldron, your unwavering support, enthusiasm, patience and constructive advice has been far more than should be expected of a Ph.D. supervisor. I am extremely grateful for all the time you have invested in me and your commitment to make me a better scientist has been admirable and wholly appreciated. Simply, I could not have chosen a better principal supervisor, so I thank you for choosing me to undertake this research.

Finally, to my parents, Angela and Tony, I thank you for all your support without which the education I have received would not have been possible. Now you can ask me as many times as you like “when will it be finished?”…I hope it makes a good read!

# Author's Declaration

I declare that the work outlined and described in this thesis has been carried out by myself unless otherwise acknowledged. This thesis is completely my own composition and has not, in whole or part, been submitted for any other degree at this or any other university.

Benjamin A.V. Smith

February 2016

Thesis Citation: Smith, B.A.V (2016) *Assessment of carbon and nutrient export from a peatland windfarm construction site*. Ph.D. thesis, University of Glasgow, School of Geographical and Earth Sciences, Glasgow, UK

# Abbreviations

| | |
|---|---|
| A.D. | Anno Domini |
| AMS | accelerator mass spectrometry |
| Approx. | approximately |
| ASL | above sea level |
| Avg. | average |
| AWS | automatic water sampler |
| bdl | below detection limit |
| blq | below limit of quantification |
| cal. yr. BP | calibrated years before present (i.e. years before 1950 A.D.) |
| C | carbon |
| $CO_2$ | carbon dioxide |
| CA | catchment area |
| $CH_4$ | methane |
| DECC | Department of Energy and Climate Change |
| DEFRA | Department for Environmental and Rural Affairs |
| DIC | dissolved inorganic carbon |
| DOC | dissolved organic carbon |
| Eqn | Equation |
| EQR | ecological quality ratio |
| EU | European Union |
| Fo8 | figure of eight |
| g C $m^{-2}$ $yr^{-1}$ | grams carbon per metre squared per year |
| GHG | greenhouse gases (predominately $CO_2$ and $CH_4$) |
| HMP | habitat management plan |
| IPCC | Intergovernmental Panel on Climate Change |
| IUCN | International Union for Conservation of Nature |
| ln | natural logarithm / logarithm to base *e* |

| | |
|---|---|
| LOI | loss on ignition |
| mg $l^{-1}$ | milligrams per litre |
| µg $l^{-1}$ | micrograms per litre |
| MLR | multiple linear regression |
| N | nitrogen |
| NAO | North Atlantic Oscillation |
| NEE | net ecosystem exchange |
| $NO_3^-$ | nitrate |
| $NO_2^-$ | nitrite |
| NOAA | National Oceanic and Atmospheric Administration |
| NPP | net primary production |
| OM | organic matter |
| P | phosphorous |
| p | p-value indicating the marginal level of significance within a statistical test |
| PCC | Pearson's correlation coefficient |
| POC | particulate organic carbon |
| PT | pressure transducer |
| Q | discharge measured in cubic metres per second ($m^3$ $s^{-1}$) |
| RCPC | reference condition reactive phosphorous |
| RP | reactive phosphorous |
| S | S value representing the average distance of any observed values are from the proposed regression line |
| SAC | Special Area of Conservation |
| SE Mean | standard error of the mean |
| SEPA | Scottish Environmental Protection Agency |
| SD | standard deviation |
| SNH | Scottish Natural Heritage |
| SRP | soluble reactive phosphorous |
| SSER | Scottish and Southern Energy Renewables |
| SSSIs | Sites of Special Scientific Interest |

| | |
|---|---|
| SUERC | Scottish Universities Environmental Research Centre |
| SUVA | specific absorbance of ultraviolet wavelengths |
| TOC | total organic carbon |
| TON | total oxidised nitrogen |
| TP | total phosphorous |
| TRP | total reactive phosphorous |
| UK TAG | United Kingdom Technical Advisory Group |
| US EPA | United States Environmental Protection Agency |
| WFD | Water Framework Directive |
| WQMP | Water quality monitoring programme |
| WTD | water table depth |

Square brackets are used to indicate concentration, e.g. [DOC] = dissolved organic carbon concentration

# 1 Introduction

## 1.1 Abstract

This opening chapter provides an introduction to the recent increase of windfarm construction on peatlands and why these developments are seen as environmentally sensitive issues. The Scottish Government's target of generating 100% of Scotland's electricity demand from renewable energy sources has supported the rise in development of such projects. However, this policy has created a debate whether siting windfarms on peatlands is environmentally sustainable given this could disturb peatland carbon-storing potential, and the full impact of windfarm construction is currently unknown. This research examines the impact of windfarm construction on the aquatic and sedimentary carbon cycle in the windfarm development. This chapter will introduce the site where this research has been undertaken, The Gordonbush estate (near Brora), and outline the research aims, objectives and summarise the thesis structure.

## 1.2 Why studying the impact of windfarm construction on peatlands is of interest

In global society, the impact of anthropogenic-induced climate change, through the release of excess carbon (C) into the atmosphere from primarily burning of fossil fuels (IPCC, 2014a), is becoming an ever more prevalent issue. Consequently, there is a desire to lower future C emissions and construct economies based on low C renewable energy technologies, e.g., Scottish Government 2020 Renewable Energy Route map. The Scottish Government has a target of producing 100% of Scotland's electricity usage from renewables by 2020 (Scottish Government, 2011). Consequently, it has been government policy to encourage, through subsidies, energy companies to invest in renewable energy projects (OFGEM, 2014). In 2012, renewable projects displaced approximately (approx.) 10.3 million tonnes of $CO_2$ (British Parliament, 2013) equivalent to 20 % of Scotland's overall C emission in 2011 (Scottish Renewables, 2013). Total installed capacity of renewable electricity in Scotland has risen from 2.7 GW in 2007 to 6.7 GW in 2013, with 68% of the capacity coming from onshore windfarms (Scottish Government & DECC, 2014a).

Scotland has 25 % of Europe's wind energy resource with an estimated power generation potential of 36.5 GW (Scottish Government, 2014). Currently installed capacity of onshore windfarms is 4.67 GW with a further 4 GW consented to (Scottish Government & DECC, 2014b). Continued onshore windfarm expansion is seen as an integral part of helping Scotland achieve its 2020 target. Renewable energy generation in 2013 comprised 46.6

% of Scotland's electricity consumption (Scottish Government & DECC, 2014b), currently ahead of scheduled interim 2020 target of 50 % by 2015 (Scottish Government, 2012). Currently there are 160 onshore windfarms in Scotland (Scottish Renewables, 2014) most of which are located on or near areas of peatland. Thus, peatland landscapes are increasingly facing the relatively-new pressure of hosting renewable energy developments in the form of large scale commercial windfarms (Figure 1.3).

Often peatlands are preferred locations for situating windfarms because of their remoteness, limited agricultural land use and high wind yields (Nayak et al., 2009; Cowell, 2010). Much of the expansion of onshore windfarms is taking place in North-East Scotland (Caithness and Sutherland) (Figure 1.2A). This region is often referred to as the 'Flow Country' as over half of it is covered in blanket bog dominated by *Sphagnum* mosses (Wilkie & Mayhew, 2003). Peatlands (blanket bogs) generally have higher C storage densities per unit area than any other ecosystem (Freeman et al., 2012) and contain 56% of the total C held in all Scottish soils (Chapman et al., 2009). Consequently, the 'Flow Country' is the biggest and deepest single expanse of blanket bog peatland and largest terrestrial C store in Europe (see Figure 1.2B), covering an area approx. of 4000 $km^2$ (SNH, 2005; Chapman et al., 2009; Muller & Tankere-Muller, 2012) with many parts protected as Sites of Special Scientific Interest (SSSIs) and Special Areas of Conservation (SAC) (Wilkie & Mayhew, 2003). The 'Flow Country' region also represents 13% of blanket bogs distributed globally (Lindsay et al., 1988) and contains 48% of all soil C in the UK (Bradley et al., 2005).

Globally, peatlands are subject to various pressures including a historic legacy of drainage (Ramchunder et al., 2009; Turner et al., 2013; Parry et al., 2014) and changes in functioning arising from climate change (Freeman et al., 2001a; Tranvik & Jansson, 2002; Freeman et al., 2004; Fenner & Freeman, 2011). Both pressures can cause degradation such that these C 'sink' landscapes become major C 'sources'. Therefore, considering the increase of the construction of windfarms on peatlands (not only in Scotland (Artz et al., 2014) but in other European countries, e.g. Ireland and Spain (Fraga et al., 2009; Renou-Wilson & Farrell, 2009)) there is a need to better understand these ecosystems, and the pressures affecting them in order to support their management as a C sinks, including where necessary restoration of degraded sites.

Peatlands are subject to a level of disturbance during windfarm construction that can cause losses in terrestrial C storage meaning the effectiveness of reducing the energy production C footprint from windfarms built on peatlands has been questioned (Nayak et al., 2009; Renou-Wilson & Farrell, 2009; Smith et al., 2012). During windfarm construction, a large amount of on-site excavation of peat is undertaken for road building,

installation of turbine bases and the laying of all necessary power cables. Additionally, on-site borrow pits are commonly quarried to provide rock and raw materials for excavated road surfaces (see examples in Figure 1.1). Further disturbances may involve forest felling to reduce turbulence in air flow. The impacts of all these disturbances are not completely understood but the consequences of increased aquatic C and nutrient export from peatlands (due to windfarm construction) can include: negatively affecting ecology within surrounding rivers loss of natural habitat for local wildlife species and causing general degradation such peatlands become a source of C to the environment compared to their natural C sink status (these issues are discussed in more detail in section 2.3.3). Therefore, it is imperative, to better assess and quantify C losses (Renou-Wilson & Farrell, 2009), to fully investigate and evaluate the 'green credentials' of windfarm development on peatlands. This information can feed into and potentially improve, the 'carbon payback calculator' used in windfarm planning, which estimates times taken for the windfarm to generate enough electricity to offset C losses associated with its construction (Nayak et al., 2009; Smith et al., 2012).

Before, during and after construction, water quality in river and lakes surrounding the site must comply with European Union (EU) Water Framework Directive (WFD) guidelines; the potential impact of construction activities can make this challenging. Although construction companies aim to follow "Good practice during windfarm construction" guidelines, management strategies to limit environmental impact are continually being reviewed and updated (Scottish Renewables et al., 2013); thus this research can contribute to developing best land management practices regarding windfarm construction on peatlands. The aim of this research is to broaden the scientific evidence base of known effects of windfarms construction on aquatic C and macronutrient export and assess whether it is prudent to build windfarms on peatlands when there is disturbance of the terrestrial C store.

Increased dissolved organic carbon (DOC) losses, of approx. 5 g C $m^{-2}$ have been directly attributed to windfarm construction activities (Grieve & Gilvear, 2008) and increased [DOC] (from this point square brackets around a determinant, e.g. [DOC] = DOC concentration) have been observed in drainage systems from areas deforested to host windfarms in southern Scotland (Murray, 2012; van Niekerk, 2012). However, there are few studies, and research to understand peatland resilience and adaption to windfarms is still limited (Drew et al., 2013). This research aims to expand understanding here.

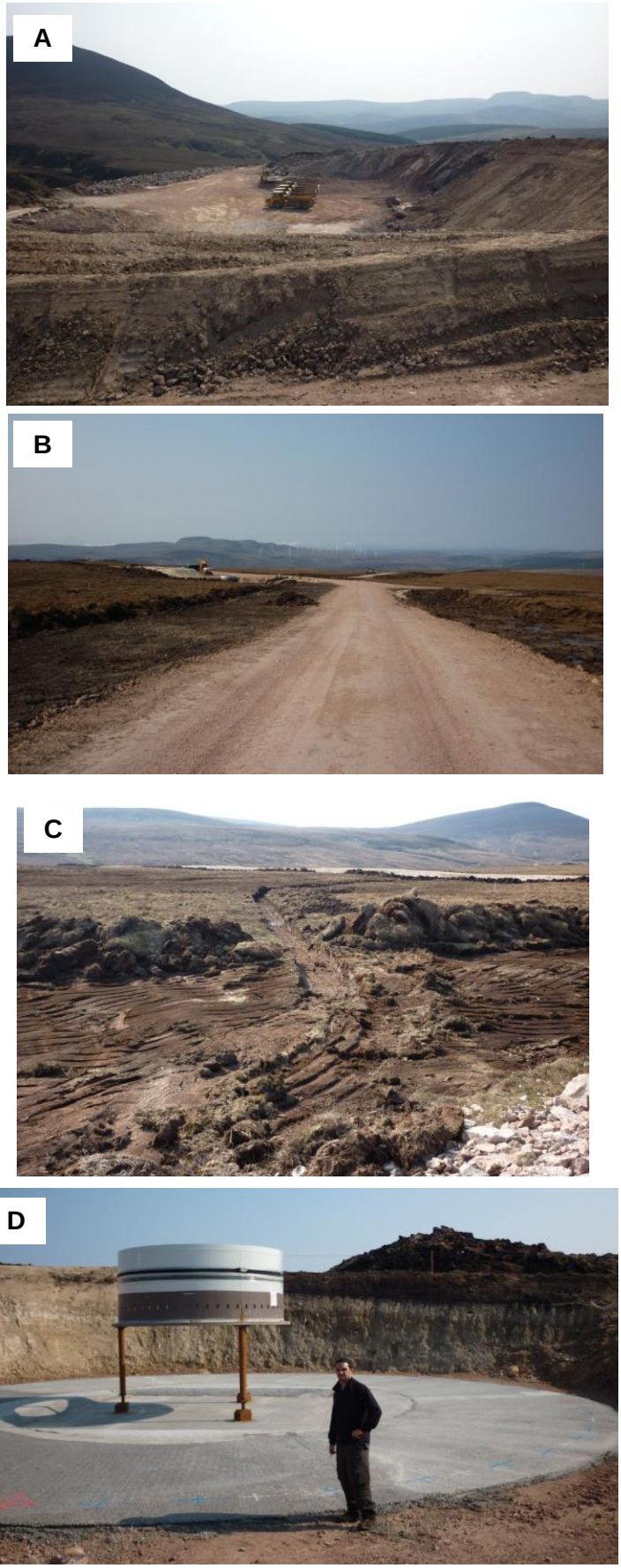


**Figure 1.1 - Examples of disturbance during wind farm construction at Gordonbush April 2011**
A = A borrow pit used to quarry rock for on-site road network. B = Disturbed peatland due to peat removal next to road network. C = Examples of peat removed for roads and cut trenches for electrical cabling. D = Deep excavation into bedrock need for the foundations of wind turbines. All presented photos are owned by Ben Smith ©.

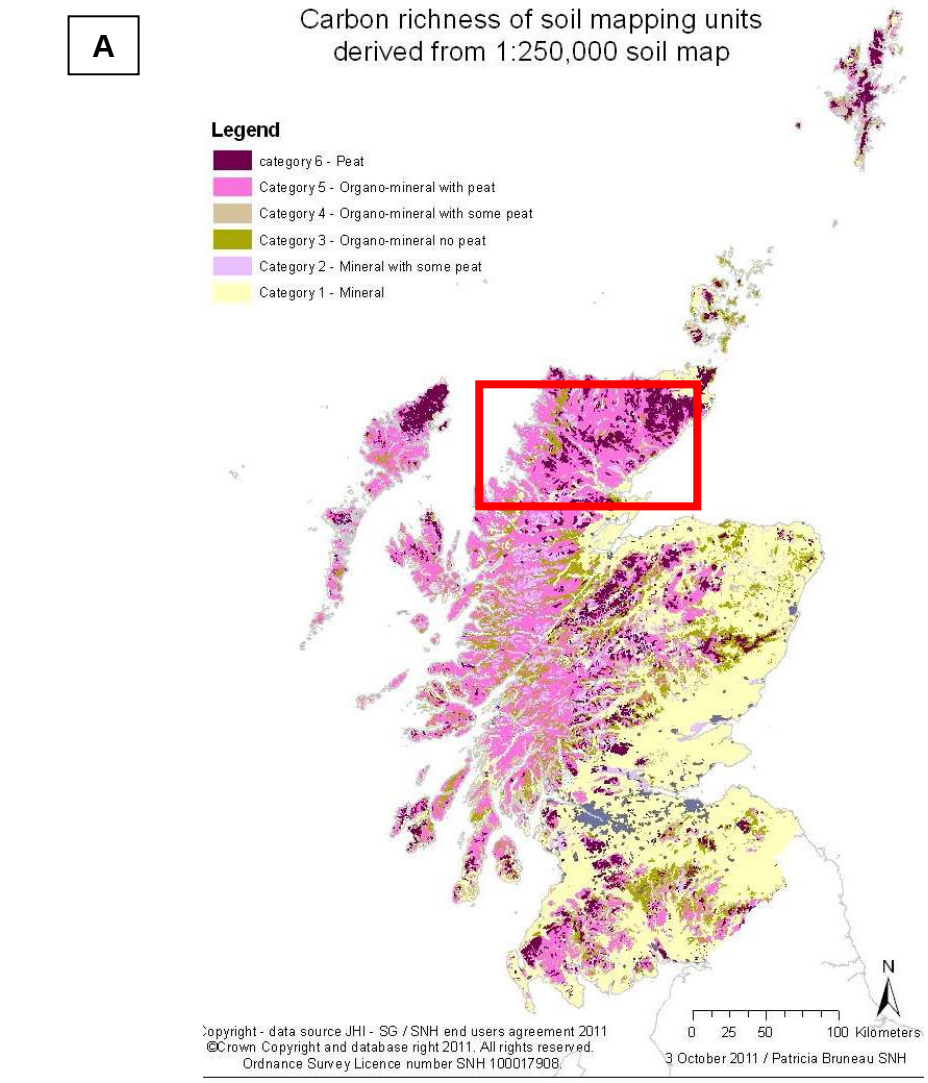


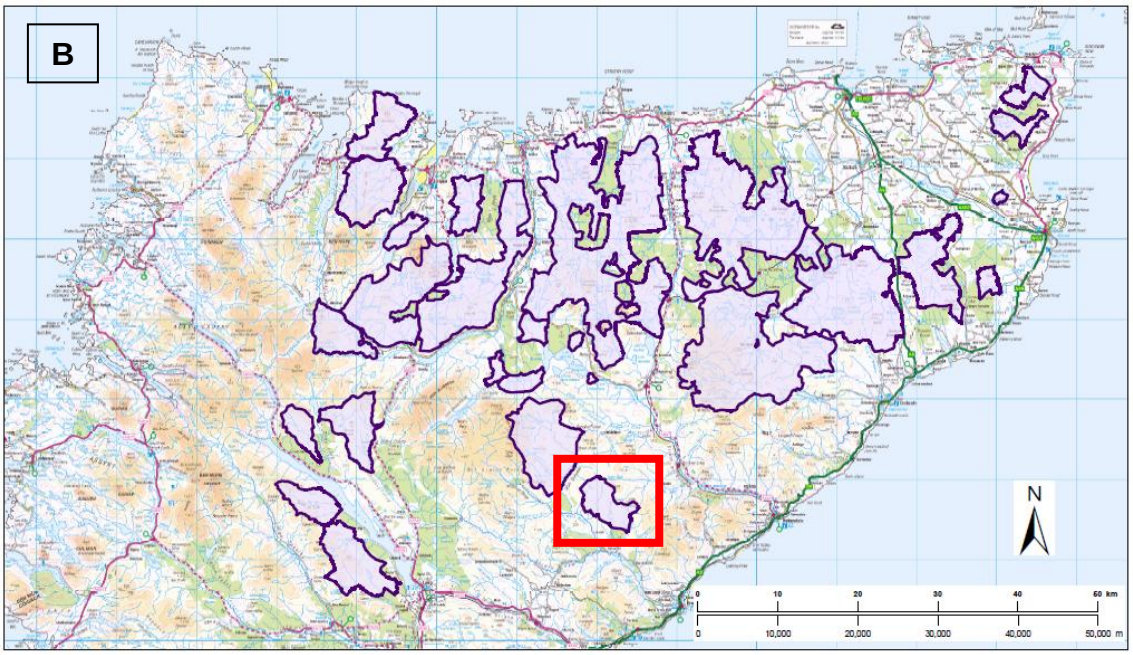


**Figure 1.2 - SNH carbon soil map and NE Scotland of special areas of conservation**
Both maps above were produced by Scottish Natural Heritage (SNH). A = Illustrates carbon content of soils in Scotland, with peat being the most carbon rich (purple) and mineral soils (yellow) having the lowest carbon content (SNH, 2012). A relevant key is provided. B = More detailed map of area highlighted in red in map A (SNH, 2013b). This map shows areas of special conservation in NE Scotland which have been given this designation based on the nationally important blanket bog habitat and populations of birds that breed in these areas, e.g. golden plover. Highlighted in red is the site of Coir An' Eoin which is the closest point of special conservation to the research field site, the Gordonbush Estate.

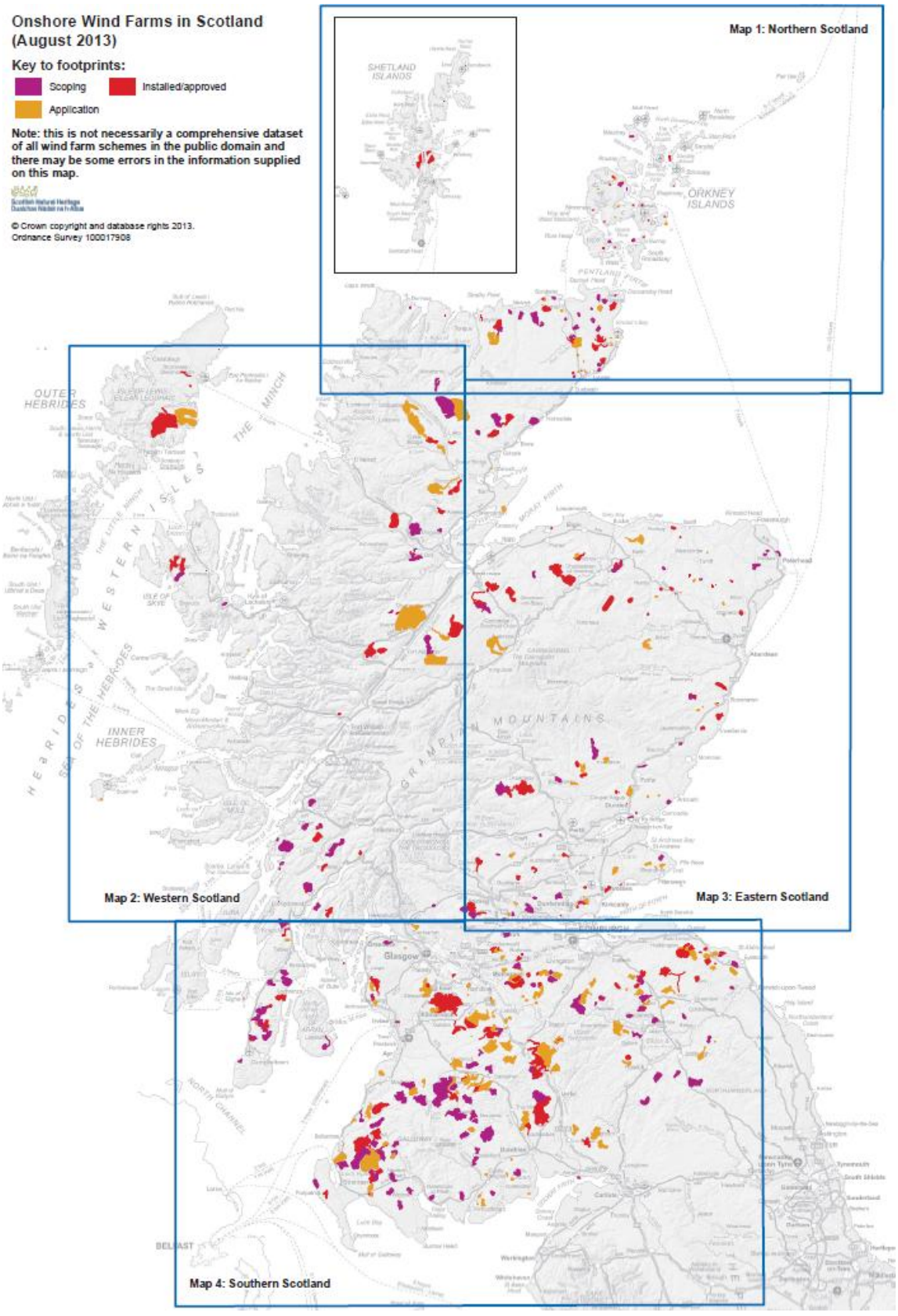


**Figure 1.3 - SNH map of Scottish on-shore wind farms**
SNH produced the map above in August 2013. The map displays the locations of wind farm developments which have been installed or approved (red), are currently the subject of an application (orange) and are being scoped as a potential wind farms (purple), (SNH, 2013a).

## 1.3 Introduction to field site

This research was carried out on the Gordonbush Estate (58° 06'33 N, 03° 56'11 W), situated approx. 7 miles west of the coastal town of Brora, Sutherland, North East Scotland (Figure 1.4A). The Estate covers an area of approx. 57 km$^2$ (Rowantree, 2013) of predominately moorland but with small plots of natural (Scots pine *Pinus sylvestris*) and commercial (Sitka spruce, *Picea sitchensis*) forestry. The estate is located at the southern end of the 'Flow Country' and includes a designated SSSI, Coir' An Eoin (SNH, 2013b) (Figure 1.2). The most recent and extensive land use change implemented at Gordonbush has been the construction of infrastructure to host a 35 turbine on-shore windfarm commissioned and managed by Scottish and Southern Energy Renewables (SSER). The areas suitability for commercial windfarm development is reinforced by the presence of the 27 turbine Kilbruar windfarm (initially completed in 2008 and extended in 2011) located on the opposite side of the River Brora valley, south of the Gordonbush estate (Falck Renewables, 2013).

The windfarm is situated in the NW of the estate, on a moorland plateau ranging from 280-390 m in elevation. Construction began in August 2010. The windfarm construction activities occurred only within the Allt Mhuilin and Allt Smeorail catchments (Figure 1.5). The windfarm was fully operational by June 2012, with a capability of generating sufficient electricity to power 60,000 households (based on average household consumption of 3,200 kWh a year) and plans exist (2015) for an extension to be constructed which would allow up to 20 new turbines to be installed (SSER, 2014). A more detailed field site description is presented in Field methodology chapter, section 3.1.

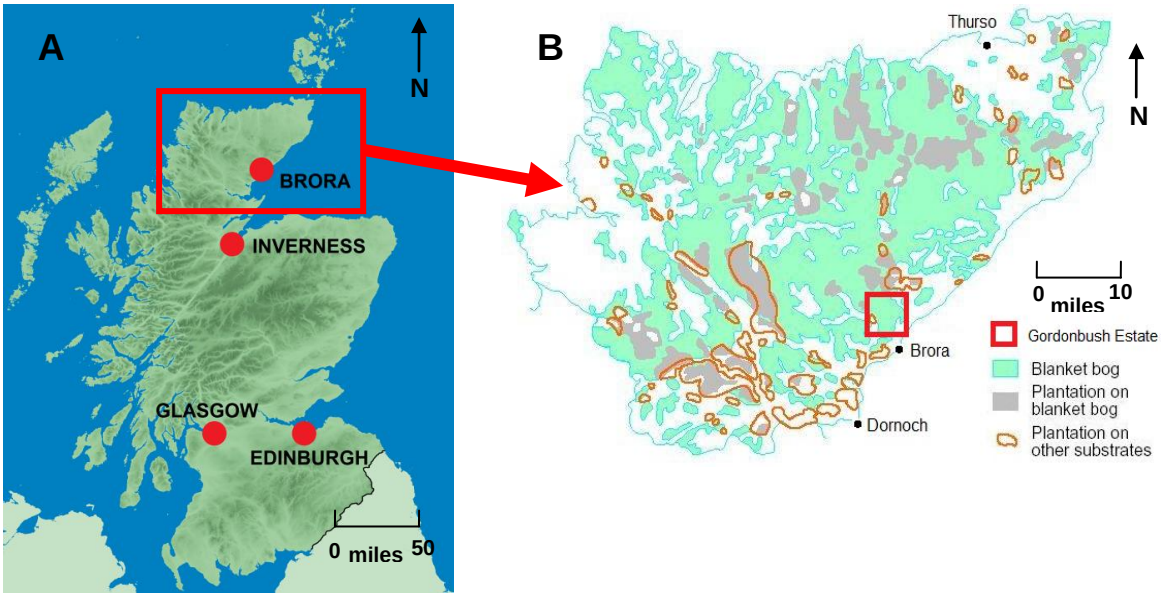


**Figure 1.4 - Maps of Scotland and 'Flow Country'**
A = Map of Scotland showing major cities, Edinburgh, Glasgow, Inverness and coastal town of Brora (map adapted from www.geolocation.ws), B = Map of NE Scotland "Flow Country" with Gordonbush estate highlighted (map adapted from (Oosthoek, 2005)). Figure 1.5 is an expansion of the red boxed highlighted and labelled "Gordonbush Estate" in Figure 1.4B.

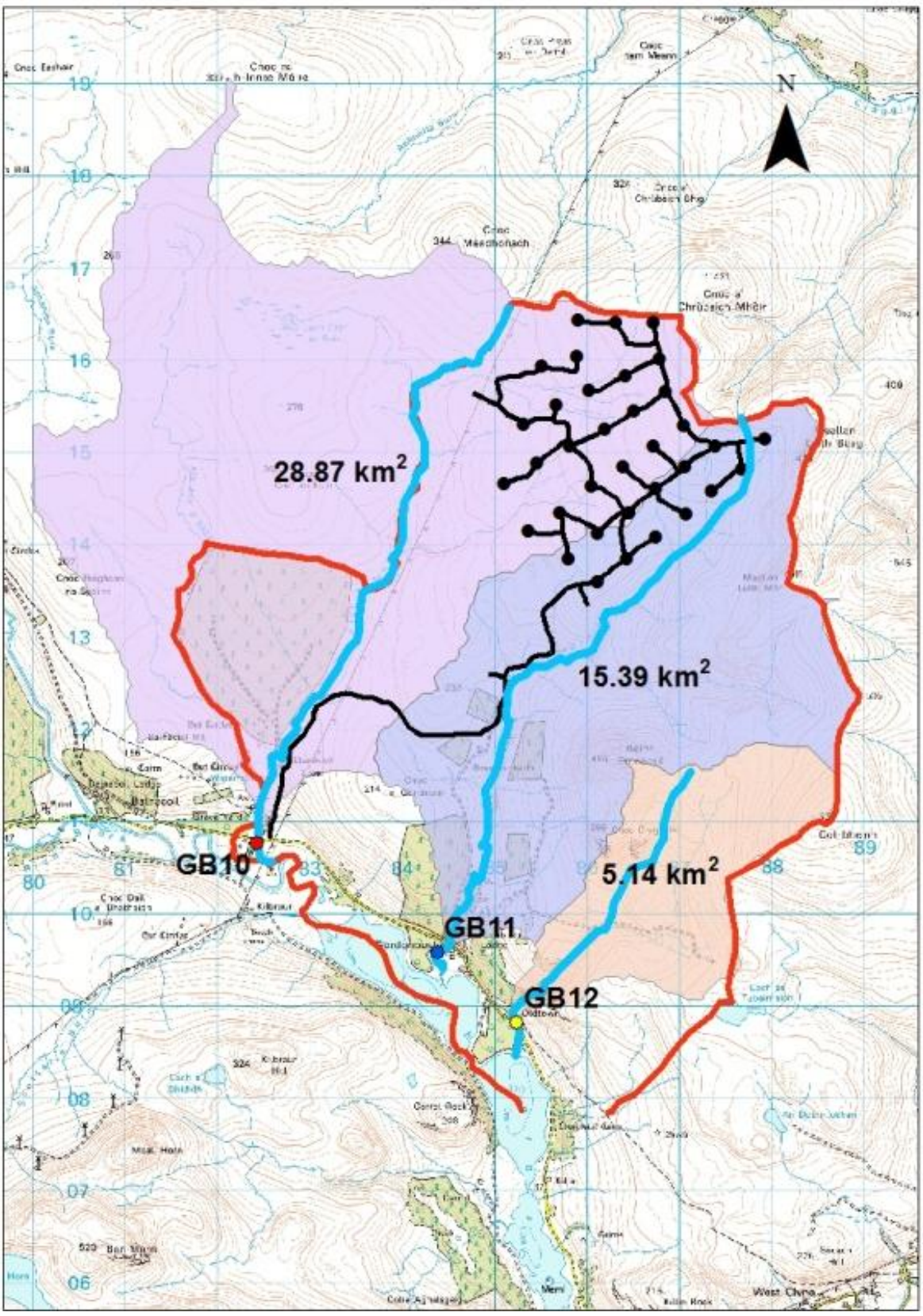


**Figure 1.5 - Gordonbush research field site**
The red line marks the boundaries of Gordonbush estate controlled by wind farm developer, SSER. The black lines represent the wind farm road network and black dots, the locations of individual turbines. The catchments of Allt Mhuilin (28.87 km$^2$), Allt Smeorail (15.39 km$^2$), and the OId Town Burn (5.14 km$^2$), are outlined by different colours. The rivers in each catchment have been highlighted in a light blue colour to make them stand out. Storm event sampling points (GB10, GB11 and GB12) are located at mouth of each catchment The original map (contained wind farm road network, turbines and estate boundary) was supplied by (Dargie, 2012a) and has been adapted and amended by K. Roberts.

## 1.4 Research objectives and aims

During this research I sought to better understand how windfarm construction impacts the peat land C cycle with specific focus on aquatic and sedimentary organic C losses. This research programme therefore has two principal aims:

1. To assess if windfarm construction causes changes in river [C] and [macronutrient] and if so, how long for.

2. To examine particulate C and sediment export from the landscape over timescales longer than windfarm construction, to provide a historical context for assessing the significance of potential losses during the construction period.

Specific objectives were to:

1. Characterise concentrations of DOC and particulate organic carbon (POC), TP, soluble reactive phosphorous (SRP) and nitrate ($NO_3^-$), during storm events to construct time series and investigate whether concentrations change during or after construction phase.

2. Combine storm event concentration data with river discharge data to calculate aquatic organic C fluxes from catchments hosting the windfarm and an adjacent control catchment to assess any windfarm impacts on export budgets.

3. Analyse peat cores within the wind turbine locations to produce C sequestration rates to better understand the DOC export significance.

4. Analyse sediment cores from the depositional delta in Loch Brora to investigate historical C export from the windfarm site in order to contextualise modern losses.

5. Install and monitor sediment traps in Loch Brora to characterise sediment export during and after windfarm construction.

6. Investigate the impact and effectiveness of drain blocking by installing a series of dip wells to monitor aquatic C export.

## 1.5 Thesis structure

This thesis consists of a further eight chapters.

Chapter 2 is a literature review of key background information to C cycling and functioning characteristics of peatlands, their formation and global distribution. Anthropogenic and climate-induced impacts of C cycling within peatlands, past, present and future will also be discussed.

Chapter 3 and 4 documents all field and laboratory techniques used to generate data for this thesis.

Chapter 5 will examine the fluvial time series of C and nutrient concentrations measured to consider whether windfarm construction has caused an impact (Aim 1)

Chapter 6 investigates different methods of calculating C fluxes estimates to assess if there has been a catchment wide loss of C with time (Aim 2).

Chapter 7 examines C sequestration rates in the Gordonbush peatland and in Loch Brora, the receiving water of the catchment drainage. This is undertaken to consider the range of natural variation that a system exhibits independently of a windfarm development (Aims 3, 4 and 5).

Chapter 8 explores the short-term response of drain-blocking as an effective management restoration approach in reducing C loss by raising water table depth (Aim 6).

Chapter 9 summarises the key findings and comments on windfarm construction in the context of C management and future policy of peatland construction as part of the Scottish Government's renewable energy targets. Future research needs are also identified.

# 2 Literature review

## 2.1 Abstract

This chapter reviews literature concerning peatland formation, distributions and the role they have as important global and UK terrestrial C stores. Knowledge regarding the current state, recently observed changes in functioning and the vulnerability of peatlands to potential global climate change will be also outlined. Impacts of historic and current peatland management on trends we are currently observing will be examined which in turn will help contextualise the potential impact of windfarm construction. Literature associated with the current known impacts of windfarm construction on peatlands will also be reviewed.

## 2.2 Peatland formation, distribution and classification

### 2.2.1 Peatland formation

Peatlands are areas where soils consist of decayed or partially decayed remains of plants species (Clymo et al., 1998). Peatlands are formed in areas where soils are poorly drained or are often waterlogged, i.e. swamps, mires and wetland bogs (Clymo, 1984) and therefore do not tend to form in steeply-sloping regions where water can easily drain away (Charman et al., 2013). Permanent saturation of water in the top soil leads to anaerobic conditions (Belyea, 1996; Waddington & McNeill, 2002; Quinty & Rochefort, 2003). Breakdown of organic matter (OM) is 1000 times slower in the anaerobic part of the soil profile (catotelm) compared to the aerobic (acrotelm) (Ingram, 1978; Belyea & Clymo, 1999; Belyea & Clymo, 2001), due to the slow diffusion and lack of availability of oxygen inhibiting microbial decomposition (Clymo, 1992; Clymo et al., 1998). Peatland growth is largely regulated by the position of the water table (the boundary between acrotelm and catotelm) (Ingram, 1978; Clymo, 1984; Kalbitz et al., 2000). Peat accumulation occurs when net primary production (NPP) exceeds annual decomposition and gaseous losses (Frolking et al., 2001; Turunen, 2008), consequently layers of OM build up. Rates of peat accumulation increase when the difference between NPP and decomposition losses increases. This produces ecosystems where C can be stored on a long-term basis (Waddington et al., 2009; Yu et al., 2010) making peatlands the most space-efficient C store in the terrestrial biosphere (Joosten et al., 2013). In Scotland peat soils, and therefore peatlands, are defined as where OM content is greater than 60% and depth exceeds 50 cm (Bruneau & Johnson, 2014; Scotland's Soils, 2014b).

## 2.2.2 Global distribution

It is thought the majority of peatlands in the northern hemisphere developed and expanded following the end of the last glacial period (Yu, 2012) due to increased warming and atmospheric moisture conditions (Smith et al., 2004). In North America, the retreat of the Laurentide ice sheet during the Younger Dryas period (approx. 14500 – 11500 cal. yr. BP) is thought to have triggered enhanced C extraction from the atmosphere, which was deposited in layers of peat and thus increased C sequestration at this time (Gorham et al., 2012). This assumption regarding the timing of peatland formation and development since the Last Glacial Maximum (LGM) is supported by the fact basal ages of peat cores do not generally exceed 16500 cal. yr. BP (MacDonald et al., 2006). Blanket bogs in the northern hemisphere most likely formed through the process of paludification (outward expansion of water-logged soils converting dry uplands to wetland habitats) (Charman, 2002) rather than terrestrialisation (or hydroseral succession), where peats form in aquatic habitats (basins/hollows) through infilling of sediment (Ireland et al., 2013). Peatlands in the mid-latitude northern hemisphere have been argued to have expanded faster than their high-latitude counterparts because of the relatively high mean annual temperatures (Beilman et al., 2009). Sometime between approx. 14000-17000 cal. yr. BP increased temperatures and warm conditions induced and coincided with extensive areas of peat being established in the southern hemisphere (Barker et al., 2009). Such, peatlands are found in at least 175 countries across all climate regions (except desert, i.e. tropical, temperate, boreal and arctic zones), see global map of C distribution (Figure 2.1).

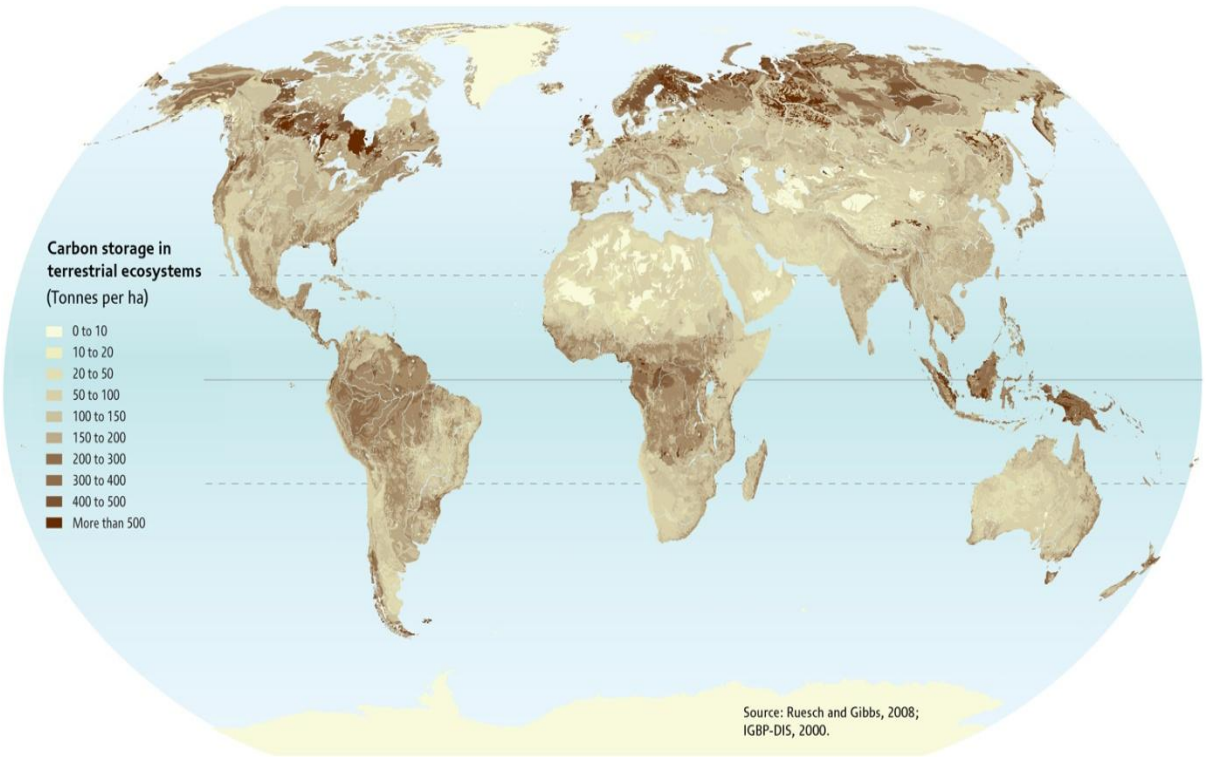


**Figure 2.1 - Map of global carbon/peatland distribution**
Map presented above was sourced from (Ruesch & Gibbs, 2008).

Despite covering only 4 million $km^2$, equivalent to 3 % of the world's land area ((Turunen et al., 2002; Limpens et al., 2008)), peatlands are estimated to contain approx. 30 % of the world's land-based C (Gorham, 1991; Koehler et al., 2011), almost all of which has accumulated since the most recent global ice age (Billett et al., 2010; Yu et al., 2010). The importance of peatlands (wetlands and permafrost) to the global C cycle is demonstrated by the amount of C they currently store, which exceeds the amount of C stored in the atmosphere (Davidson & Janssens, 2006) and is approx. equivalent to the amount of C contained in all living organisms (Geist, 2006). Of that total, 25 % of the world's soil C is stored in peatlands distributed in the northern hemisphere (Roulet et al., 2007). By area, the UK contains 15 % of global peatlands, (Tallis, 1998) and despite covering only 8% of our land mass; these areas contain approx. half of Britain's total soil C stocks (Milne & Brown, 1997; Bradley et al., 2005) with conservative figures estimating this equates to 3100 Mt of C (Lindsay, 2010). British peatlands began to form and sequester C in their soils since the end of the LGM, approx. 10,000 years ago (Charman, 1992).

## 2.2.3 Peatland classification

Peatlands are classified depending on their nutrient status and the sources of water they receive. Ombrotrophic (bog) peatlands exist where water is supplied exclusively by precipitation (Bragg, 2002; Geist, 2006). As such, they are characterised by low-nutrient levels, their waters are acidic and their vegetation is dominated by *Sphagnum* species (Charman, 2002; Yu et al., 2003). Of the main two classifications, ombrotrophic sites are more sensitive to climatic shifts than minerotrophic due to their extra reliance on rainfall sources to maintain optimum moisture and nutrient conditions (Frolking et al., 2001). Raised bogs (ombrotrophic peats) mostly form in natural depressions, e.g. lake basins (Langdon & Barber, 2005; Ireland et al., 2013) and peatlands of this type in Scotland have average depths of ~5 m (Hughes & Dowse, 2012) however the deepest recorded depth is 12 metres (Scotland's Soils, 2014a). Blanket bogs (also ombrotrophic) develop in areas where there is consistently high rainfall and low evapotranspiration rates which allow peat to develop, not only in depressions, but over large areas of uneven (and mostly upland) ground (Gorham, 1957; Keddy, 2010). Typically they are shallower than raised bogs with peat depths of 2-5 metres (Bruneau & Johnson, 2014). Blanket bog is the most extensive peatland type in UK comprising 90% of its total area (Worrall et al., 2011).

Minerotrophic peats (or fens) are supplied with water from precipitation, ground water and surface run-off sources (Bruneau & Johnson, 2014). Minerotrophic peats commonly have a higher mineral nutrient content (Ca, Mg, Na, K) and pH conditions are more variable compared to predominately acidic in ombrotrophic bogs (Charman, 2002). Plant types (e.g. grasses and sedges) are also more varied in minerotrophic peats (Mornsjo, 1971).

## 2.3 Contextualising the impact of windfarm development

To contextualise the significance of modern C losses from peatlands as a result of windfarm construction, understanding the sensitivity of historical peatland C sequestration rates to different environmental conditions is valuable.

### 2.3.1 Peatlands are important global C sinks but climatically sensitive

Since the beginning of the Holocene (approx. 11,500 years ago), peatlands have been net sinks of C (Yu et al., 2011). It has been estimated that peatlands situated above 40 degrees latitude in the northern hemisphere have sequestered >300 Pg of C over the last 8000 years (Kleinen et al., 2012), with the global total since the end of the last ice age closer to double that at ~600 Pg (Gorham et al., 2012; Charman et al., 2013). The process of C uptake and peat formation has exerted a negative feedback on climate change over last 10,000 years (Frolking et al., 2006). So much so, it has been estimated that the Holocene peatland expansion has been responsible for net cooling equivalent to one-third of radiative forcing caused by the increase of carbon dioxide ($CO_2$) emissions in last 150 years, (Frolking & Roulet, 2007); emphasising their importance in regulating and influencing the global C cycle (Yu, 2011). The processes governing peat accumulation are a result of complex interactions between plant productivity, decomposition and hydrology (Belyea & Clymo, 2001; Yu et al., 2001; Quillet et al., 2013) making it difficult to assess the extent and influence of physical, chemical and biological controls on their growth (Belyea & Baird, 2006).

Warm dry periods can lead to decomposition surpassing plant production rates as water table levels are lowered due to lack of precipitation; as peatlands dry out there is also an increased risk of peatland fires occurring (Kettridge et al., 2015). Both situations subsequently increases $CO_2$ release reducing C sequestration rates, making peatlands C sources rather than sinks (Quinty & Rochefort, 2003; Barber & Langdon, 2007; Charman, 2007; Charman et al., 2009). Conversely, warm wet conditions promote peat growth (Yu, 2011) as water tables stay high and decomposition rates are greatly reduced under waterlogged conditions (Ingram, 1978). It should be highlighted, under anoxic conditions, peatland will release methane ($CH_4$) (Smith et al., 2004; Gorham et al., 2012), which in terms of climate warming and C release from peatlands is considered a positive feedback (Frolking & Roulet, 2007). Despite this, overall C storage and C sequestering potential of peatlands are best maintained if waterlogged and anaerobic conditions are consistently preserved (Davidson & Janssens, 2006).

Peatlands and peat accumulation is sensitive to even minor climatic fluctuations (Bragg & Tallis, 2001; Yu et al., 2003). Consequently, peatlands are a function of hydro-climatic and geomorphic conditions (Quillet et al., 2013) and their archives therefore offer an excellent means for palaeo-environmental reconstruction, recording both natural and anthropogenic environmental changes (Cook et al., 1998; Charman, 2007; Blundell et al., 2008). Accurately interpreting changes within peatland sediment cores, understanding how positive warming and cooling feedbacks may influence peatland functioning and C storage (Pendea & Chmura, 2012), can help informing global climatic-C cycle models (Frolking & Roulet, 2007; Yu, 2011). These C landscapes have been more closely studied over the last 20 years and their role in the global C cycle has been increasingly recognised, given their potential to sequester but also release large amounts of greenhouse gases (GHG) (Whittington & Price, 2006; Frolking & Roulet, 2007).

## 2.3.2 Peatland functioning and present conditions

Peatlands are a balance between C inputs and outputs above and belowground. The main inputs are plant and root detritus, outputs are dominated by $CO_2$ and $CH_4$ efflux from soil surface and hydrologic leaching of dissolved and particulate C (Davidson & Janssens, 2006) (Figure 2.2). This research has focussed on aquatic C losses and long-term C sequestration rates as gaseous losses are more expensive and difficult to measure due to their diffuse nature (Billett et al., 2010).

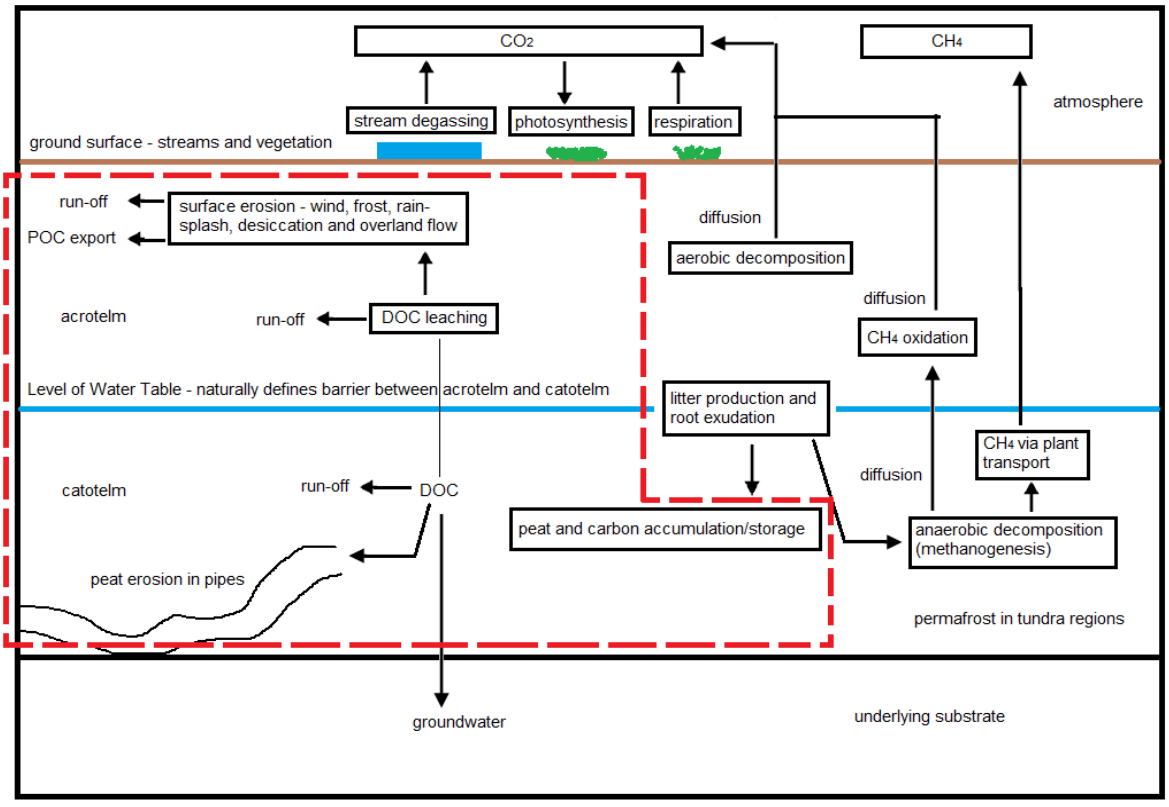


**Figure 2.2 - Cross section of peat and functioning processes**
Figure above adapted from (Holden, 2005b) showing cross section a typical peat and the processes that occur within with emphasis on carbon species, DOC, POC, carbon dioxide ($CO_2$) and methane ($CH_4$). The red highlighted square indicates the processes this thesis focuses on.

### 2.3.2.1 Aquatic carbon (C) export from peatlands

Total organic C (DOC + POC) generally accounts for over 90% of downstream aquatic C export (Billett et al., 2004). Aquatic [C] in rivers draining temperate peatlands varies seasonally (Dawson et al., 2004). Of the two organic forms of C exported in aquatic systems, DOC is most commonly a larger pool than POC regardless of seasonality (e.g. (Dawson et al., 2004)). The maximal [DOC] occur during the late summer and early autumn due to build up of OM during these warmer and drier periods supporting greater production of DOC than in winter and spring (Grieve, 1990; Worrall et al., 2003; Cooper et al., 2007; Dawson & Smith, 2007; Dawson et al., 2011). Biological DOC production and OM breakdown increases during this time due to increased water table draw down and subsequent aeration of the peat during dry periods (Clymo et al., 1998; Clark et al., 2007).

Peatland rivers are said to export 50% of their C loads during only 10% of the largest recorded discharges (Hinton et al., 1998) (Figure 2.3). After maximum DOC production has occurred (within the peat profile) during the summer, rainfall events at end of summer and early autumn are normally characterised by high [DOC] (Mattsson et al., 2015), commonly termed the 'autumn flush' (Worrall et al., 2002). Annually, this is the time period when C export from peatland is at a maximum (Worrall et al., 2004b; Lumsdon et al., 2005; Tipping et al., 2007; Mattsson et al., 2015). DOC export is also significantly affected by water table draw down, and by time between hydrological events (Worrall & Burt, 2008), with C export increasing when peat is re-wetted after periods of drought (Clark et al., 2012).

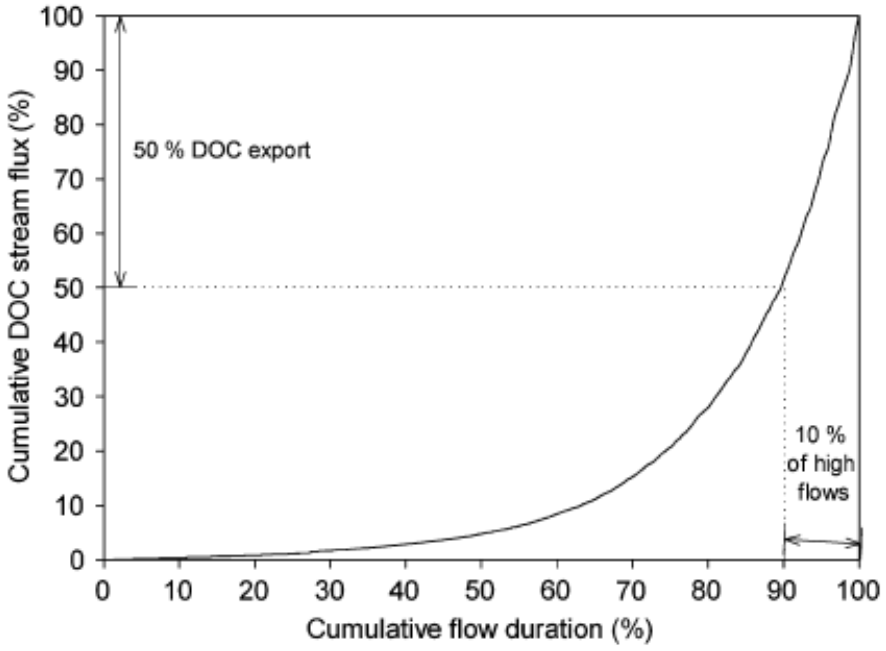


**Figure 2.3 - The relationship between DOC export and discharge**
The diagram above was taken from (Hinton et al., 1997).

### 2.3.2.2 Recent change in C export from peatlands

Over the last 30 years there is evidence DOC in rivers draining peatland catchments have been increasing in the UK (Hope et al., 1997b; Worrall & Burt, 2004; Worrall et al., 2004b; Evans et al., 2006a; Worrall & Burt, 2007b; Ryder et al., 2014) and Northern Europe (especially Scandinavia) (Freeman et al., 2001a; Clark et al., 2005). This increase has been correlated with a reduction of atmospheric sulphur deposition since the late 1980s and the clean-up of industrial gas emissions in the UK (Evans et al., 2005; Monteith et al., 2007). This legislative measure also reduced the deposition of multivalent ions (e.g. calcium and magnesium), which can increase the ionic strength and acidity of any given soil solution (Adamson et al., 2001; Hruska et al., 2009). High ionic strength and high acidity reduces solubility of OM and restricts the release of soil DOC (Tipping & Hurley, 1988; Tipping & Woof, 1991). Thus, a decrease in the deposition of such ions may also indirectly influence surface water [DOC] (Monteith et al., 2007; Clark et al., 2010; Evans et al., 2012) (Figure 2.4).

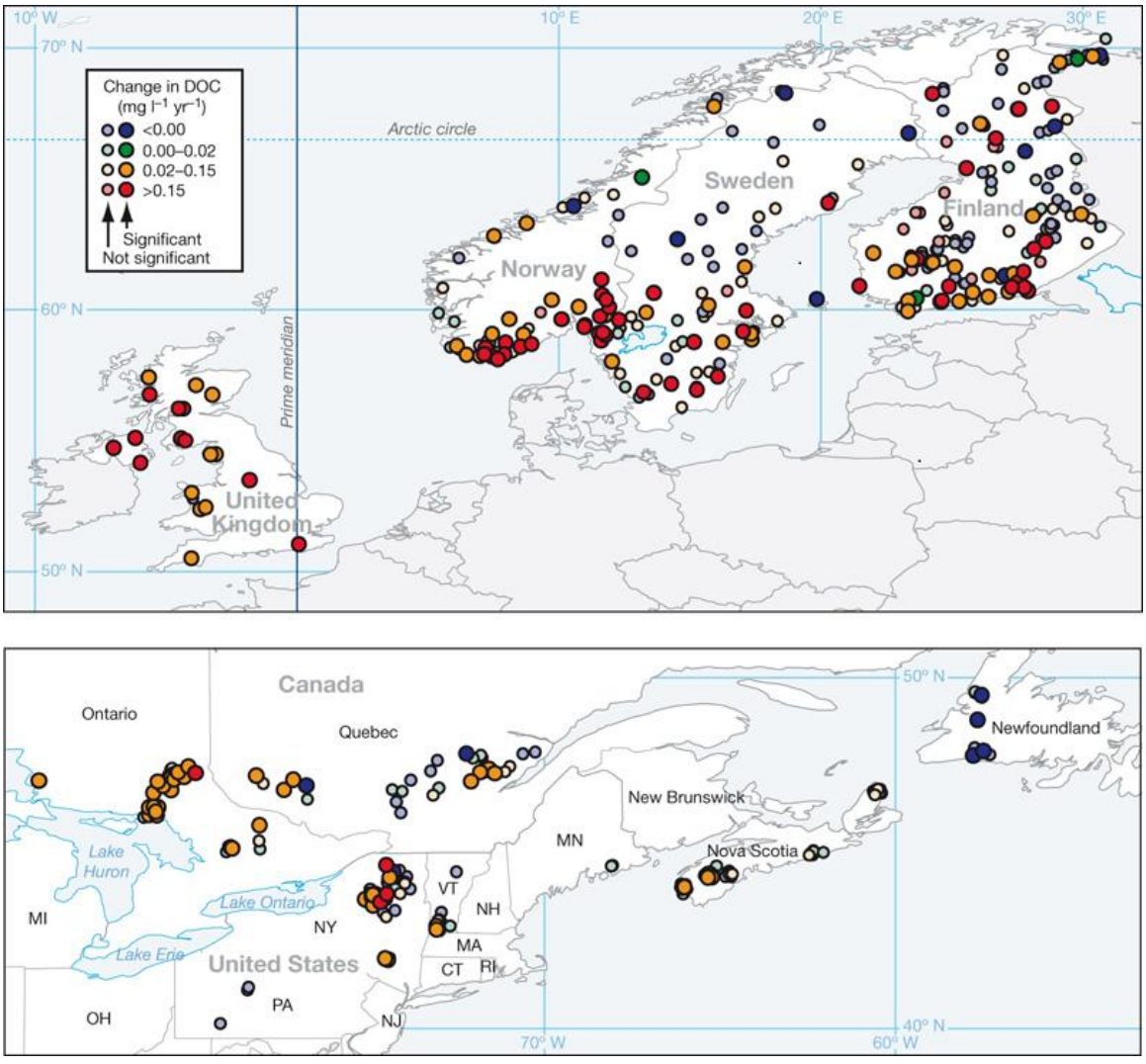


**Figure 2.4 - Changes in [DOC] across Northern Europe and North America**
The figure above was published in a Nature paper by (Monteith et al., 2007) and depicts changes in trends of [DOC] in water bodies at various monitoring sites in the UK, Scandinavian, Canada and Northern USA between 1990-2004.

Another possible explanation for increasing [DOC] in drainage systems is the rise in temperature affecting the activity of phenol-oxidase enzyme, present within peatland soils, which regulates C storage (Freeman et al., 2001b). As temperature increases, it prompts a decrease in water table levels and peatlands start to dry out. As the peat soil dries it becomes more oxic and as the activity of phenol-oxidase enzymes are limited in anaerobic environments, drying increases the prevalence of the phenolic compounds. Phenol-oxidase increases the breakdown of phenolic compounds breaking down OM and producing DOC (Freeman et al., 2001b). Enzyme activity can still be present when water table rises and anaerobic conditions return (Gibson et al., 2009). This mechanism has been attributed to increases in DOC after drought conditions (Clark et al., 2005) and the effects can allow decomposition to continue years after drought has happened (Worrall & Burt, 2004; Gibson et al., 2009). Additionally, successive periods of severe drought followed by re-wetting can increase DOC production and subsequently [DOC] (Kalbitz et al., 2000; Worrall & Burt, 2004) although it is acknowledged the consequences of wetting and drying peat are complex, and at times conflicting (Clark et al., 2009). Finally, increases in atmospheric [$CO_2$] are thought to have stimulated increased primary production, in turn producing more DOC which is available to be exported in river systems (Freeman et al., 2004). Despite all of these different mechanisms, it has been acknowledged that it may be unreasonable to expect to find one universal indicator responsible for the increases in [DOC] observed (Preston et al., 2011).

#### 2.3.2.3 Anthropogenic impacts and influence on C losses from peatlands

Direct anthropogenic activity has also impacted the C cycling characteristics of peatlands and their ability to effectively store C (Janssens et al., 2005; Worrall et al., 2011). Peatlands have been damaged on both local and global scales due to drainage, burning and peat extraction for agricultural and horticultural purposes (Peacock et al., 2013a; Blundell & Holden, 2015) and fuel consumption (Schilstra, 2001; Waddington et al., 2008; Strack & Zuback, 2013). These types of activities have increased over last century (Waddington et al., 2002; Evans et al., 2014) and make peatlands vulnerable to atmospheric and aquatic C losses (Glatzel et al., 2003; Waddington et al., 2010; Connolly & Holden, 2013).

In tropical regions, peatlands are mainly exploited for commercial agriculture, e.g., palm oil, forestry or rice paddy plantations (Koh et al., 2009; Page et al., 2009; Page et al., 2011). In northern temperate regions improving pasture for cattle, sheep and game animals (red deer and grouse) (Holden & Burt, 2003a; Holden et al., 2007b), peat extraction for fuel and horticulture (common practice in Ireland, Canada, Scandinavia and Baltic countries including Russia) (Schilstra, 2001), post WWII forestry plantations and

burning to support game bird production have been the main economic drivers of disturbance (Holden et al., 2004; Turunen, 2008; Evans et al., 2014). As a result of these anthropogenic activities and development, 10-20 % of world peatlands have been lost (Geist, 2006) with estimates as high as 80-90% in parts of Canada (Landry & Rochefort, 2012) and western Europe (Verhoeven, 2014). In the UK, over 80% of peatlands are said to be in a degraded state (Worrall et al., 2011) although it is acknowledged it is hard to identify all the impacted areas (Artz et al., 2014). Drainage and extraction land use management practices actively lower the water table (Worrall et al., 2003; Worrall et al., 2007b; Wilson et al., 2010) and modify peatlands hydrologically, biochemically and ecologically (Macrae et al., 2013), increasing the likelihood of them switching from net C sinks to C sources (Evans et al., 2014).

Peatlands are sensitive to small changes in environmental conditions (Holden et al., 2007a), however, mechanisms controlling C storage, C production and export are principally controlled by hydrology, but are highly complex (Freeman et al., 2001a). Water tables closer to ground surfaces restrict plant decay due to anaerobic conditions and limit fluvial C release (Holden, 2005b). Consequently, implementing drainage networks on peatlands actively inhibits C storage and peat accumulation (Evans & Lindsay, 2010; Evans et al., 2014). Further negative responses include increased susceptibility of peat erosion (Holden et al., 2007b; Evans & Warburton, 2008) due to increased aerobic decomposition (Clymo, 1984, 1987; Waddington et al., 2002). Typically POC fluxes for intact peatlands are <10 g C $m^{-2}$ $yr^{-1}$ (Hope et al., 1997b) whilst for severely eroding systems they can exceed 100 g C $m^{-2}$ $yr^{-1}$ (Worrall et al., 2011).

Increased decomposition also leads to increased production of DOC and leaching of C (Freeman et al., 2001b; Wallage et al., 2006; Strack et al., 2008; Waddington et al., 2008; Clark et al., 2009; Gibson et al., 2009; Armstrong et al., 2010; Wilson et al., 2010). Enhanced leaching of other macro-nutrients, phosphorous (P) and nitrogen (N), can also occur due to peat aeration and decomposition (Devito & Dillon, 1993; Geurts et al., 2010; Zak et al., 2010) and this can subsequently affect C sequestration (Holden et al., 2004; Ramchunder et al., 2009). Large gaseous C losses, e.g. $CO_2$ emissions, have been associated with, and measured at, drained and degraded peatland sites (Clark et al., 2008; Worrall et al., 2009; Evans & Lindsay, 2010). Degraded peatlands are responsible for 25% of $CO_2$ emissions from the land use sector (Bonn et al., 2014b). In addition, burnt areas of peat (encouraging bird game production) have been said to export double the amount of DOC than un-brunt areas (Yallop et al., 2010).

Evidence relating to $CH_4$ emissions from drained peatlands is more contradictory with some studies showing effects of drainage and lowering water tables increases emissions

(Waddington et al., 2009; Parry et al., 2014) but recent meta-data analysis shows an opposite decreasing trend (Haddaway et al., 2014). Although $CH_4$ emissions may increase after re-wetting (Landry & Rochefort, 2012) in the short-term, this does not outstrip the long term C saving benefits of enhanced $CO_2$ sequestration and reduction in DOC and POC losses from water logged peats (Bonn et al., 2014a). Regardless of the varied $CH_4$ results, the overall affect caused by the drainage of peatlands is a shift from ecosystems which were C sinks to C sources (Strack & Waddington, 2007; Cooper et al., 2014; Green et al., 2014; Haddaway et al., 2014; Vanselow-Algan et al., 2015)

Drainage of peatlands is widespread across all countries (Joensuu et al., 2002; Holden et al., 2004) but post-war government policies to maximise agricultural output across the UK led to large areas of blanket bog being drained to improve areas of peatlands for forestry (Turner et al., 2013) or animal grazing (Wilkie & Mayhew, 2003; Armstrong et al., 2009; Wilson et al., 2011a). In the UK, drainage channels are typically ~0.5 m deep and up to 1 m wide (Armstrong et al., 2009; Gibson et al., 2009) and although forestry plantations were established in areas of drained peat, initiatives to develop similar areas for grazing were less successful (Holden et al., 2007a). The UK government now discourages afforestation on land with peat over one metre deep (Anderson et al., 2000; Holden et al., 2004) and forestry guidelines promote the removal of plantations to enhance and improve the condition of peatlands surrounding SSSIs and SAC (Forestry Commission Scotland, 2015).

As forestry plantations on peatlands are common in the UK (Cannell et al., 1993), the environmental effects are quite well known. Increases in [DOC] (Neal & Hill, 1994; Nieminen, 2004; Neal et al., 2005; Tetzlaff et al., 2007; Murray, 2012; van Niekerk, 2012) and P (Ahtiainen & Huttunen, 1999; Cummins & Farrell, 2003; Neal et al., 2003; Nieminen, 2003; Neal et al., 2004; Nieminen, 2004; Kreutzweiser et al., 2008; Rodgers et al., 2010; Kaila et al., 2012) have been reported in rivers after harvesting at numerous locations draining forested peatland sites. Consequently, as a result of increases in [P], water quality downstream has deteriorated (Nieminen, 2004; Kaila et al., 2012) and the risk of eutrophication has increased (Forestry Commission Scotland, 2011). Since the introduction of the WFD by the EU, countries are legally obliged to improve and maintain ‘good’ water quality status in all waterways (European Union, 2012) and this has become a major consideration before, and during, any modern development happening within peatland areas.

### 2.3.3 Windfarm construction as an emerging disturbance on peatlands

The emergence of windfarm construction as a disturbance to peatland ecosystems is not only an issue that is relevant in Scotland / UK but in other parts of Europe. In Spain, peatland in parts of the Basque country under increasing pressure from windfarm developers and despite the presence of regionally rare or threatened species, develop on these sites is not automatically ruled out (Heras & Infante, 2009). In Galicia (NW Spain), windfarm construction on peatland has led to lower plant diversity and the spread of invasive species increasing the risk these habitats are to be replaced by grassland and heaths (Fraga et al., 2009). Windfarm construction in NW Spain has also made some previously remote peatland sites more accessible and caused pressures from intensive grazing and forestry to increase as new land resources look to be exploited (Fraga et al., 2009). In Ireland, it has been acknowledged the development of peatland sites for wind energy has a negative impact on local and regionally biodiversity including avian species (birds and bat) displacement and river ecology due to a decrease in water quality (Tosh et al., 2014). It has been recommended develop should focus areas where peat is already industrially extracted and 'pristine' peats should be protected (Renou-Wilson & Farrell, 2009). Issues related to preserving plant and animal biodiversity in the face of windfarm development pressures have also been investigated in Scotland and conclusions made SSSIs and SACs should continue to be protected (Artz et al., 2014) however less is known on the extent of direct C losses due to construction.

Specific research studies investigating the impact of windfarm construction on C losses from peatlands remain limited (Drew et al., 2013), however some examples do exist. Suspended sediment concentrations (i.e. proxy for [POC]) and [DOC] were markedly elevated in catchments affected by windfarm construction compared to control sites at Braes of Doune windfarm near Stirling (Grieve & Gilvear, 2008). The increased sediment loading in the rivers was attributed to a lack of effective sediment traps draining the road networks and the increase in aquatic C fluxes were estimated at 5 g C $m^{-2}$ $yr^{-1}$, directly as a result of construction activities (Grieve & Gilvear, 2008). Conversely, the efficient use of settlement ponds and drainage channels was noted as a measure which reduced the impact of windfarm construction at Whitelee near Glasgow (Murray, 2012). Of the 9 catchments monitored draining the windfarm site, only one was found to show an increase in total organic carbon (TOC) related to windfarm construction (Murray, 2012). Increases in aquatic [C] and [P] species were linked more to the large areas of deforestation associated with the windfarm installation rather than the implementation of infrastructure itself (Murray, 2012). Forest felling and windfarm construction were suspected to have caused an estimated 12 g C $m^{-2}$ $yr^{-1}$ increase in aquatic C exported from windfarm

affected catchments at the Arecleoch windfarm in Ayrshire from 2008 to 2010 (van Niekerk, 2012). DOC samples from disturbed sites had greater degree of humification, suggesting windfarm construction is potentially facilitating increased breakdown of OM in soils and rivers (van Niekerk, 2012).

Some research has been undertaken to estimate the time windfarms take to payback the C lost associated with their construction, identifying site selection, minimising peat excavation to ensure appropriate drainage is implemented and establishing site restoration projects (Nayak et al., 2008). Using the developed methodology, the best case scenarios predict C losses could account for <6% of potential C savings installing the windfarm (Nayak et al., 2009). However, the same research also highlights if the best management practices are not followed, over three quarters of potential C savings would be lost through C emissions, providing little overall benefit (Nayak et al., 2009).

In the past, developing windfarms on peatland sites has been seen as environmentally positive as the renewable energy produced was replacing power generated from fossil fuels (Smith et al., 2012). However, the energy mix of the UK's power generation is changing towards low C technologies and increased renewable production (DECC, 2011). This means the C losses associated with constructing windfarms on peatlands will not equate or be lower than the C emissions of the energy produced by another means over the established lifetime of a windfarm (25 years) essentially increasing the C payback time for windfarms in the future (Smith et al., 2014). As such, it has been recommended that windfarms should not be built on non-degraded peatland sites (Smith et al., 2012). It has been estimated only marginal C savings will be made in the future locating windfarms on peatlands and in doing so may affect countries abilities to meet C emission targets (Smith et al., 2014). Alternatively locating windfarms on sites with mineral soils, where practical, will reduce any associated C payback time compared to sites with peats and have a better chance of improving the 'green credentials' of future windfarm developments (Smith et al., 2014).

### 2.3.4 Practical problems of increased C export from peatlands

Aquatic C losses from peatlands have wider implications than may be reflected in reduced C sequestration. Approx. 50 % of the UK's drinking water supplies are sourced from organic soils such as peatlands (Tang et al., 2013). Increases in aquatic [DOC] leads to water becoming more highly-coloured (Wallage et al., 2006): colour changes from light yellow to darker shades of brown for increasing [DOC] (Weyhenmeyer et al., 2004; Ledesma et al., 2012). Water with a high DOC content is aesthetically undesirable (Worrall et al., 2003; Freeman et al., 2004) and drinking it is not advisable because of the

possible health risks (Lambert & Graham, 1995). Biological contamination (Gibson et al., 2009; Holden et al., 2012b) and production of carcinogenic disinfection by-products (e.g. trihalomethanes) as a result of chlorination (Chow et al., 2003; Worrall et al., 2003) are legitimate practical problems caused by high [DOC] in drinking supplies (Peacock et al., 2013a; Tang et al., 2013). Depending on where it is sourced, DOC quality within water courses can vary markedly (Thurman, 1985) thus treatment procedures are commonly site-specific (Tang et al., 2013). These types of practical problems will subsequently incur extra costs for water companies (Ledesma et al., 2012; Worrall et al., 2012; Turner et al., 2013) and increase pressure on already strained water treatment works (Holden et al., 2007b; Worrall et al., 2009).

Furthermore, certain peatland rivers can flow into lakes (as with the Gordonbush estate), systems recently acknowledged as important stores of C in the global cycle (Cole et al., 2007; Tranvik et al., 2009; Buffam et al., 2011; Ferland et al., 2012). Whether a lake is largely heterotrophic or autotrophic in nature will determine if it is a C sink or C source (Jansson et al., 2000; Hanson et al., 2004; Sobek et al., 2011; Fritz & Anderson, 2013). In heterotrophic lakes, typically where [DOC] is >10 mg $l^{-1}$ (Algesten et al., 2004), ecosystem respiration is generally greater than production and the lake surface is a source of C to atmosphere (Anderson et al., 2014) as a result of mineralisation of OM being greater than sediment burial (Hanson et al., 2004). Autotrophic systems fix $CO_2$ from atmosphere in quantities that equal or exceed whole-lake respiration making it a C sink (Jansson et al., 2000). Most lakes are net heterotrophic (Wetzel, 2002; Cole et al., 2007) and if C losses continue to increase from peatland catchments to lacustrine systems, $CO_2$ effluxes from many lakes could also increase.

Conversely, rising aquatic DOC export could affect lake ecology due to decreases in light penetration (this issue has not been examined during this research) prompting a lowering of heterotrophic potential. This issue is equally applicable in rivers and has a keen relevance in the Highlands of Scotland as fishing activities (including tourism) are a major part of the local economy. Reduction in light penetration due to increased [DOC] (and increased acidity) could negatively affect the food webs of salmonids and fresh water pearl mussel species and potentially reduce their populations. Maintaining desirable ecological conditions for these species are therefore a key concern when peatlands are subject to windfarm development in North East Scotland.

Additionally, with an historical context relating to the ecological status of inland water bodies, presently, there has been limited consideration of the changes between heterotrophic and autotrophic status of lakes through time (Fritz & Anderson, 2013) or to rates of change in organic C burial rates within these ecosystems surrounded by peatland

(Heathcote & Downing, 2012; Anderson et al., 2014). Assessment of whether these systems are C sinks or sources is important regarding their potential as C stores and understanding how their functioning will change in the future due to climate change, which ultimately could affect how they are managed (Buffam et al., 2011). For instance, depletion of oxygen in deeper water and stratification periods are estimated to be longer due to climate change effects, consequently meaning more C sequestration as breakdown of OM in more anoxic conditions is reduced (Gudasz et al., 2010). On the contrary, anoxic conditions lead to more $CH_4$ production which is 20 times more potent as a GHG compared $CO_2$ (Sobek et al., 2009; Pacheco et al., 2014). These short-term drivers may or may not be detectable in long-term lake-sedimentary records affecting lake functioning. However, within the context of this research evidence for natural variability has concentrated on changes in C sequestration rates, which can change in response to allochthonous delivery and reprocessing of that material.

Human disturbance and agricultural activity has also increased eutrophication in many lakes worldwide (Smith, 2003). However, increased [nutrient] in lakes have been correlated with greater rates of C sequestration (Anderson et al., 2014; Pacheco et al., 2014). This could be perceived as a potential positive effect of anthropogenic activities; even if C losses from peatlands increase, lakes could act as major C sinks, sequestering extra C and therefore overall C from terrestrial stores are not degraded, but rather transferred from one ecosystem to another.

## 2.4 Peatland change in the face of future climate change

Regardless of whether the increase in C losses from peatland is mainly climatic or due to anthropogenic activities, the current trends could be exacerbated by climate change (Strack et al., 2008; Smith et al., 2009; Ryder et al., 2014). There remains uncertainty on how on C cycling within peatland ecosystems will change under future climate scenarios and mismanagement of peatlands could lead to the UK failing to meet C emission targets (Ramchunder et al., 2009) or EU imposed standards on water quality, i.e. WFD and Habitats Directive (Bonn et al., 2014a). Future climate change scenarios predict an increase in the frequency and intensity of summer storms (Tranvik & Jansson, 2002; IPCC, 2007) and given discharge is seen a key regulating control on C export (Schiff et al., 1997; Clark et al., 2007, 2008), [DOC] in upland rivers may be expected to rise (Fenner & Freeman, 2011; Strohmeier et al., 2013; Ryder et al., 2014). Additionally, inorganic forms of C (e.g. $CO_2$ and carbonates) lost through evasion of river water (Billett et al., 2006) can represent significant terrestrial C losses (Moody et al., 2013) and these are also predicted to rise under increased storm events which create large amounts of

turbulence (Billett & Moore, 2008; Dinsmore & Billett, 2008; Alin et al., 2011; Aufdenkampe et al., 2011).

As the processes of human industry lead to increased global atmospheric [$pCO_2$] (Rafelski et al., 2009), this may have a knock-on effect fuelling root exudation in vascular plants (commonly found in peatland), enhanced production of labile C in turn promoting decomposition of OM and further increases in [DOC] with peatland soils (Freeman et al., 2004). Rising temperature and more frequent droughts (IPCC, 2014a) could dry out undisturbed peatlands or exacerbate problems (Erwin, 2009) in areas where impact historical impact of drainage channels has already lead to subsequent gully erosion (Evans & Lindsay, 2010) and increased DOC export (Pastor et al., 2003; Holden, 2005b).

## 2.5 Peatland restoration efforts increasing

Consequently, issues regarding measures to proactively reduce C export from peatlands and protect their C storage potential (e.g. International Union for Conservation of Nature (IUCN) Peatland Programme) are increasingly receiving more attention both politically and publicly (Bain et al., 2011; Evans et al., 2014). The IUCN has suggested a target of 1 million hectares of peatlands in good condition or under restoration management in the UK by 2020 (Bain et al., 2011). Blocking old drainage channels promotes rewetting of peatlands through raising water tables depths, which is known to reduce water export and lower C export (Holden et al., 2006; Armstrong et al., 2010; Evans et al., 2014). Drain-blocking is now used widely as a management tool to restore peatland deemed to be damaged by historical drains and [DOC] in associated channels have been shown to decrease 6-9 months after drain blocking (Wallage et al., 2006; Wilson et al., 2011b). Despite this, a meta data analysis shows that even although [DOC] is higher from drained peatland sites compared to un-drained, re-wetting has yet to be clearly linked to a decrease in [DOC] (Haddaway et al., 2014). However, one of the reasons for such a conclusion could be the short duration of impact studies, further strengthening the need for longer-term monitoring (Evans et al., 2014; Haddaway et al., 2014; Martin-Ortega et al., 2014). Although increases of $CH_4$ emissions have been recorded at some restored peatlands sites in the short-term (Landry & Rochefort, 2012; Haddaway et al., 2014), this is not considered to offset the long term C saving benefits of enhanced $CO_2$ sequestration and reduction in DOC and POC losses and restoration is still viewed as positive regarding climate change (Bonn et al., 2014b; Parry et al., 2014).

## 2.6 Balancing our carbon foot-print

Peatlands in good condition provide a number of important ecosystems services: climate regulation via C sequestration and storage, water regulation (helps prevent flooding), palaeo-environmental archives and habitats for internationally important wildlife (Bonn et al., 2014b; Evans et al., 2014). There is a newfound realisation that a number of peatland landscapes need to be restored so these important, and increasingly valued characteristics, are maintained (part of principle 1 of windfarm and peatlands good practice principles, (Scottish Renewables et al., 2012)). It is becoming more recognised that restoring peatlands could help offset some effects of climate change (Bonn et al., 2014b) which is important as global fossil fuel consumption is increasing in developing economies and GHG emissions continue to rise (IPCC, 2014b). Efforts to restore peatlands to minimise losses and mitigate GHG emissions is therefore juxtaposed with the current drive to maximise renewable energy generation, which often involves the development of peatland sites for windfarms. The C payback calculator (Nayak et al., 2008) was developed to try and better understand the conflict between these two issues.

The research generated from C payback time studies have highlighted that effective management is key to ensuring optimum C savings (Nayak et al., 2009). Best practices include; designing road networks which where possible avoid peat deeper than 1 m; appropriate drainage should be implemented to minimise affect on natural catchment hydrology characteristics and sediment settlement ponds installed and regularly maintained; peat should be restored as soon as possible after disturbance where possible; and setting up areas of restoration, i.e. drain blocking to re-wet areas are encouraged to improve peatland habitat and help offset any associated C losses through construction activities (Nayak et al., 2008). The main uncertainty related to C payback times is the extent of peat removal needed to ensure adequate drainage so the structural integrity of windfarm infrastructure (roads, turbines bases and cable trenches) on peatland sites is maintained (Nayak et al., 2009; Scottish Renewables et al., 2013). The larger the drainage areas needed, the more peat needs to be excavated and therefore the longer C payback time will be (Nayak et al., 2009). Perhaps most fundamentally, initial site selection should be carefully considered. For the greatest potential C saving, windfarm should be constructed on mineral soils or peatlands that have already been degraded (Nayak et al., 2009; Smith et al., 2012; Smith et al., 2014).

This research is aligned with principles 3 and 4 of ‘good practice for windfarms on peatland’ which is to cooperate with developers and stakeholders to implement scientific monitoring studies to broaden the knowledge base of impacts of windfarm construction on peatland functioning characteristics (Scottish Renewables et al., 2012). This research

aims to contribute to better understanding of the effects of drainage channels on water table levels and how effective draining blocking activities are as a re-wetting restoration management practice to promote improved peatland C sequestration and retention. In addition, from water quality monitoring and fieldwork carried out this research will attempt to assess and detect particular impacts of current windfarm construction techniques on aquatic and sedimentary aspects of the C cycle within a peatland. This will then provide a basis to comment on the effectiveness of windfarm construction management practices and highlight areas, where and if necessary, these could be improved.

| **Potential impact of windfarm construction on peatlands** | **Consequences of potential impact** | **References** |
|---|---|---|
| Loss of C storing potential – construction inducing loss of $CO_2$, $CH_4$, DOC & POC | Turns peatlands in C sources rather than C sinks and reduces green credentials of peatland windfarms | (Renou-Wilson & Farrell, 2009; Artz et al., 2014; Evans et al., 2014) |
| Increases in aquatic macronutrient concentrations and export through soil disturbance but also forestry removal (C, P and N) | Increases in [DOC] can negatively affect water supplies<br>Increased [DOC] in rivers can lower light penetration and affect ecology. Increased sediment (POC) and nutrient (P and N) export can affect river ecology with water becoming more eutrophic. This could have negative impact on environmentally sensitive and economically important species, e.g. salmonids and fresh water mussels | (Grieve & Gilvear, 2008; Rodgers et al., 2010; Worrall et al., 2011; Murray, 2012; Tang et al., 2013) |
| Loss of natural habitat for indigenous species | Birds and bat species can be displaced due to construction and this reduces biodiversity of affected peatland | (Fraga et al., 2009; Douglas et al., 2012; Tosh et al., 2014) |
| Construction on SSSI and SAC sites | Loss of biodiversity in environmentally sensitive areas and loss of unique habitats | (Heras & Infante, 2009; Artz et al., 2014) |
| Minimum C savings | Peatland based windfarms will produce ever smaller C savings as energy mixes change as larger proposition of renewables are integrated in energy supply.<br>Not following best management practices will lead to minimal C savings / losses | (Nayak et al., 2009; Smith et al., 2012; Smith et al., 2014) |

**Table 2.1 - Summary of potential impacts and consequences of windfarm construction**
Authors have been references who have and published existing evidence for some of the potential impacts of windfarm construction highlighted.

# 3 Field methodology

A detailed description and brief history of the research field site will be given along with an outline of field methods and techniques used to collect the data within this thesis. In addition, there will be a detailed explanation how stage-height discharge ratings curves were constructed (section 3.12).

## 3.1 Description and brief history of field site

This research was conducted on the Gordonbush Estate, situated approx. 7 miles west of the coastal town of Brora, Sutherland, North East Scotland. The majority of peat deposits at Gordonbush would be classified as ombrotrophic blanket bog, including special areas of conservation (SNH, 2013b) (see, Figure 1.2). Peat depths across the estate range from 0.5-5 metres (SSER, 2012). Attributes of the field site are similar to other UK peatlands making the results of this research applicable to other locations. The sparsely populated estate meant anthropogenic sources of C and macronutrients were minimal making it a prime site to investigate the impacts of constructing a windfarm on a peatland.

Research activities were exclusively concentrated in the western side of the estate within three river catchments, two of which drain the windfarm development (Figure 3.1). Situated furthest west is the Allt Mhuilin river, (catchment area (CA) 28.87 $km^2$) which drains into the River Brora, just upstream from the mouth of Loch Brora (length 5.7 km, area 2.3 $km^2$, maximum depth 20 m, mean depth 6.9 m, mean breadth 400 m). Above the Bull Burn forestry plantation, the Allt Mhuilin river forms the western edge of the estate boundary so approx. 60% of its catchment area is not part of the Gordonbush estate. Further east, the Allt Smeorail river, (CA 15.39 $km^2$), drains parts of the windfarm development and discharges directly into Loch Brora. The easternmost studied catchment was drained by the Old Town Burn river (CA 5.14 $km^2$), which was not subject to any windfarm construction activities, and also discharged directly into Loch Brora. Thus, this catchment was used as a 'control' site offering an insight into natural variation in C, macronutrient and sedimentary export occurring in the area (Figure 3.1). Water samples from the three rivers were assigned the following code names Allt Mhuilin = GB10, Allt Smeorail = GB11 and Old Town Burn = GB12.

Vegetation at Gordonbush is comparable to that identified at other peatland sites (Dinsmore et al., 2013; Parry et al., 2014) and comprises similar species adapted to water logged, nutrient poor conditions including: mosses (e.g. *Sphagnum spp.*), shrubs (e.g. *Calluna vulgaris*), sedges (e.g. *Eriophorum spp.*), grasses and species of carnivorous plants (e.g. *Drosera sp.*). Mean annual climatic conditions based on 1981-2010 data,

(sourced from the closest currently operating Met office weather station at Kinbrace, Euclidean distance ~20 km north east of Gordonbush) are as follows: mean maximum daily temperature 10-11 °C, mean minimum daily temperature 1-2 °C, rainfall is 970 mm and 1209 hours of sunshine (Met Office, 2014).

Catchment characteristics such as bedrock geology and surface sediments present influence river [C] and [macronutrients] and differences can be seen across the three studied catchments. The Allt Mhuilin and most western sections of Allt Smeorail catchments have Kildonan Psammite (KILD) bedrock formations. Moving east, NE-SW trending ribbons of Langwell Conglomerate (LACO) and Ulbster Sandstone (ULBS) are present before a change to Badbea Breccio-Conglomerate (BAB) and Berridale Sandstone (BDSA), which dominate the Old Town Burn catchment area. All of the above information was sourced from University of Edinburgh Digimap® service, Figure 3.2A. Information on superficial sediments at Gordonbush is presented in a table (Table 3.1) and on a map (Figure 3.2)

| | Soil types present on Gordonbush Estate<br>Coverage by percentage (%) and area ($km^2$) of each soil type | | | |
|---|---|---|---|---|
| Catchment & Research ID | **Peat** | **Peaty Podzols** | **Brown Forest Soils** | **Humus Iron Podzols** |
| **Allt Mhuilin (GB10)** | 84% (24.28) | 12% (3.50) | 4% (1.10) | n/a |
| **Allt Smeorail (GB11)** | 33% (5.06) | 64% (9.89) | 2% (0.32) | <1% (0.12) |
| **Old Town Burn (GB12)** | 17% (0.88) | 81% (4.16) | n/a | 2% (0.11) |

**Table 3.1 - Superficial sediments present on Gordonbush Estate**
Data was sourced from Scotland's soils website (www.soils-scotland.gov.uk) which is maintained on behalf of Scottish Government and in partnership with James Hutton Institute. Coverage percentage of total catchment area was calculated using ArcGIS® software.

The estate has a history of agriculture since the 1800s, before the Highland Clearances, mainly of sheep and cattle grazing, but also small areas of arable farming. Peat cutting for fuel and in support of the local whiskey distillery (Clyne Heritage Society, 2013) dates back 100s of years. Multiple drainage channels are still noticeable on areas of peat, a legacy of a grant scheme introduced by the UK government to try and improve the agricultural output from uplands areas (Milne, 2010), however such activities ceased at least 40 years ago. All forestry on the estate is privately owned and was planted due to increased timber demand in 1920s or grant money being available to re-introduce natural species e.g. Scots pine, back into area (Rowantree, 2013). In addition, a hydro electric dam was built on Allt Mhuilin river in 1920s and provided electricity to estate buildings until 1960s when it was decommissioned. It was dismantled in April 2013, during the course of this research, as it was in a poor state of repair. However, the two current main estate controlled activities remain management of wild deer populations and sport fishing.

Gordonbush has a deer population of approx. 900 animals and a cull is carried out each year to keep the population in balance with the natural habitat. Recent land use changes include the construction and installation, by SSER, of a 35 turbine windfarm on the peatland plateau, spanning across the Allt Mhuilin and Allt Smeorail catchments. Felling of Sitka spruce species in the Bull Burn Plantation in the Allt Mhuilin catchment was completed in May 2010 as part of the SSER Habitat Management Plan (HMP) for the Gordonbush estate (SSER, 2009). The trees were felled partly because they had reached maturity but also to prevent reductions in air flow, a common practice on windfarm sites. Similar types of forestry, in the Allt Smeorail catchment, were felled in 2013 because they had reached maturity.

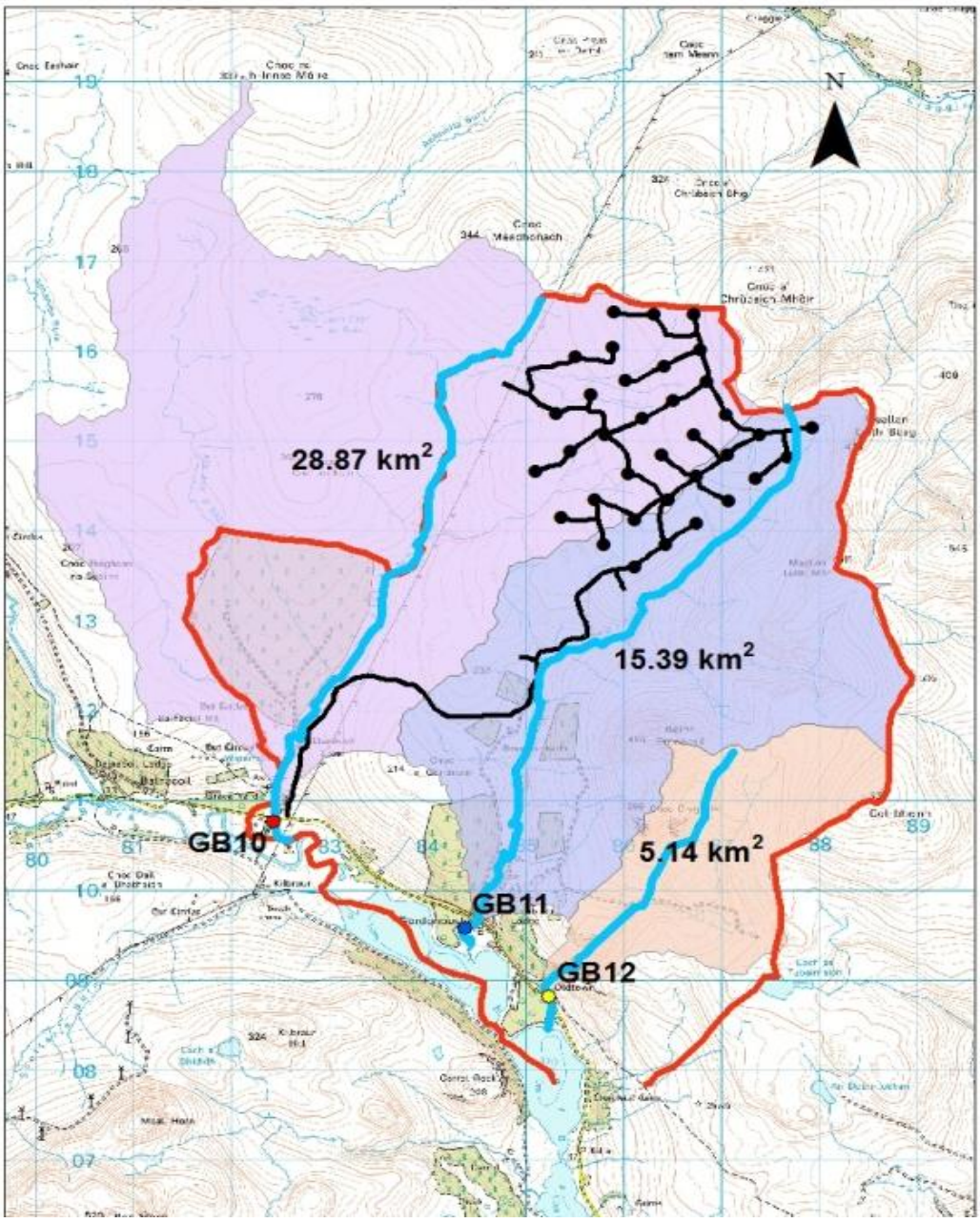


**Figure 3.1 - Gordonbush research field site**
Red lines mark the boundaries of Gordonbush estate controlled by wind farm developer, SSER. Black lines represent the wind farm road network and black dots, the locations of turbines. The catchments of Allt Mhuilin, Allt Smeorail and OId Town Burn are outlined and their rivers are bold in a light blue colour. Storm event sampling points are located at mouth of each catchment (GB10, GB11 and GB12). Map courtesy of Dr. T. Dargie (Dargie, 2012a) and adapted by K. Roberts.

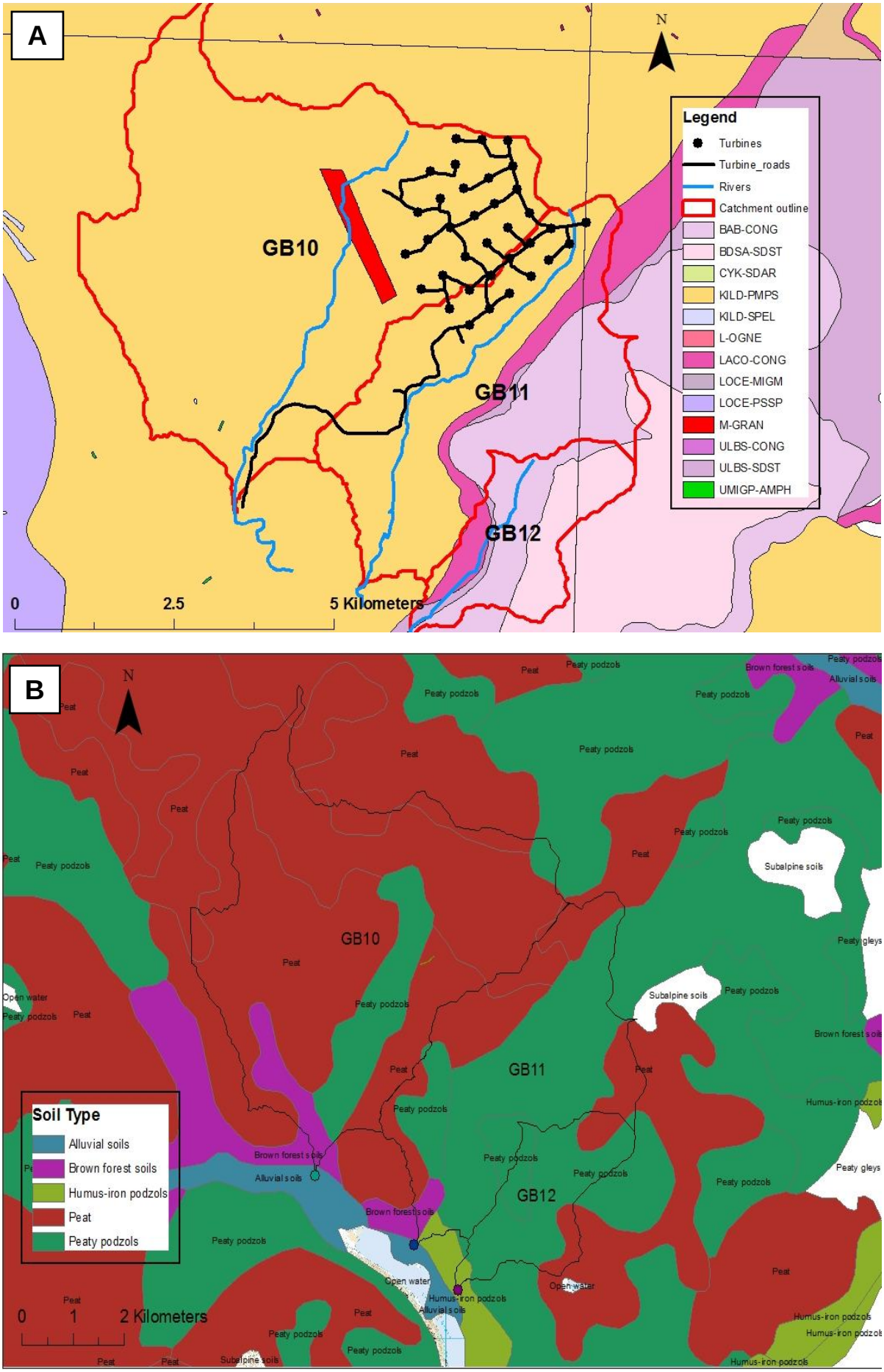


**Figure 3.2 - Gordonbush geology and surface sediment maps**
A = Gordonbush geology with accompanying legend. B = Surface sediment distributions in area around Gordonbush as well outlining Allt Mhuilin (GB10), Allt Smeorail (GB11) and Old Town Burn (GB12) catchments. The displayed above were courtesy of (British Geological Survey, 2014).

## 3.2 Gordonbush water quality monitoring programme

Additional to the data collected as part of this research, SSER oversaw an extensive water quality monitoring programme (WQMP) at Gordonbush site as part of their HMP (SSER, 2009; Dargie, 2012b). The WQMP consisted mainly of daily and weekly checks of basic stream water parameters; temperatures, turbidity, total suspended solids, pH and electrical conductivity. Monthly water samples were collected and measured for; colour, DOC, BOD, COD, Al, Mn, Ca, Na, Mg, Fe, Cl, nitrate ($NO_3^-$) and phosphate ($PO_4^-$). A final report based on the samples collected between December 2009 and May 2012 (Dargie, 2012b) was collated by Northern Ecological Services on behalf of SSER and this will be referred to in the relevant results section.

## 3.3 Storm event sampling procedure

To calculate annual aquatic organic C fluxes, measurement of [C] should include routine sampling and event flow. During the research period, monthly samples for [DOC] measurement were collected by the Ecological Clark of Works (ECoW) at Gordonbush as part of WQMP, therefore this research concentrated on characterising aquatic C export ([DOC] and [POC]) during event flow, which is generally under-sampled (Hinton et al., 1998). Omitting storm events can lead to large potential errors in flux calculations (Strohmeier et al., 2013) as more interpolation of data is needed (Hinton et al., 1997).

Event samples were collected for DOC, POC, TP, SRP and TON analysis. [SRP] and [TON] can change within a water sample after initial collection due to bacterial degradation. Analysis of [SRP] and [TON] should be performed as soon after initial collection as possible (for more detail, see 4.1.7 and work of (Bazeley, 2013). Therefore, these types of samples were only collected where time between sampling and analysis would not significantly compromise the concentration characterisation.

Storm event samples were collected from GB10, GB11 and GB12 where they crossed the main access road to the windfarm site at their respective catchment outlets (Figure 3.1). Generally storm event samples were collected every four hours after an initial sample and sampling would cease when river stages heights returned to levels similar to start of the event, in most cases after a period of 48-72 hours.

Samples for C and nutrient determination were collected, facing upstream, in one litre plastic containers and TP samples in 100 ml plastic tubs. All containers were rinsed three times with river water before the final sample was collected. When possible samples would be collected from the middle of the stream but during periods of high flow when this became too dangerous samples were collected closer to the river bank side but always in an area where the water was flowing. A life jacket was always worn.

**Figure 3.3 - Storm event water sampling**
Ben Smith collecting storm event water sample in Allt Mhuilin river (GB10).

## 3.4 Automatic water samplers

The purpose of installing automatic water sampler (AWS) equipment was to help collect samples at the start of storm events when visits on site were unplanned as it was logistically difficult to always be reactive to changeable weather forecasts given the 4.5 hour journey from Glasgow to Brora. Additionally, the AWS equipment allowed samples to be collected at high flow without having to physically get into the river which was far safer. Thus, a Teledyne ISCO 3700 AWS (ISCO 3700 product information, (ISCO Teledyne ISCO, 2013)) was installed at each of the main sampling locations, GB10, GB11 and GB12 on 12$^{th}$-14$^{th}$ December 2011.

Float switches were fitted, that triggered the AWS to collect a one litre river water sample when the stage height rose above the height of where the float switch was positioned (Figure 3.4). The decision on exactly where to position the float switches was based on an estimate of an increase in stage height of 10-15 cm, which was regarded to be the beginning of a reasonably sized storm event. Each AWS had the capacity to take 24 one litre samples and was programmed to take a sample every four hours when the float switch was enabled. This corresponds to the time intervals when manual water sampling was carried out during storm flow.

**Figure 3.4 - Automatic water sampler and float switch**
Left: Each ISCO automatic water sampler was powered by 12V lead acid battery (placed in plastic box to left of water sampler. The dexion seen was used to prevent the water sampler moving in high river flows however all samplers were placed beyond maximum river levels Right: Float switches were securely fastened to river bank, either against rock faces or trees.

## 3.5 Continuous measurement of stage height

Stage height data allow discharge to be measured (if the stage-discharge equation is known) and subsequently C fluxes to be constructed for when aquatic organic [C] data has been collected. Initially only manual measurements of stage height were taken at easily visible and retraceable markers on the river bank. Once equipment became available (November 2010 (GB10 & GB11) and December 2011 (GB12)), data loggers recorded stage height every 15 minutes using pressure transducers (PTs) installed close to all three storm event sampling points, GB10, GB11 and GB12.

### 3.5.1 Allt Mhuilin and Allt Smeorail

MNV Consulting Ltd were commissioned by SSER to install and maintain all automated in-stream data logging equipment associated with the Gordonbush WQMP. Stage boards and vented PTs were installed in the Allt Mhuilin and Allt Smeorail rivers on 17th and 18th November 2010 respectively. Responsibilities for PTs were taken over as part of this research once MNV's maintenance contract with SSER expired in May 2012. From July 2012 to September 2014, data was downloaded from the loggers approx. every six weeks using the same protocols employed by MNV to ensure the integrity of the data collected.

PTs installed were supplied by SEBA Hydrometrie (model No. DS-22, SEBA Hydrometrie loggers) and WinBedein Software (SEBA software) was used to download all data logged. Instruments were calibrated using manual readings taken from stage boards installed next to each logger. Stage height data exists from WQMP sampling point 6 on Allt Smeorail river (3 km upstream from sampling point GB11) from 18th November 2010 to 24th September 2014, and WQMP sampling point 10 on Allt Mhuilin river (the same position as GB10 sampling point) from 17th November 2010 to 24th June 2013. The PT located in Allt Mhuilin developed a fault after data were downloaded on 24th June 2013. Subsequently no more data was retrieved from this location, as MNV Consulting Ltd's maintenance contract had expired at the time and SSER, who own the equipment, chose not to repair it.

### 3.5.2 Old Town Burn

Waterra In-Situ Rugged Troll 100 instruments were installed at the storm event sampling location in the Old Town Burn, GB12, and stage height was recorded from 13th December 2011 to 16th September 2013. The In-Situ Rugged Troll 100 system uses two data loggers to measure stage height. The first was a non-vented PT which converts a pressure reading into a measure of water above it. However, the pressure recorded is not corrected for atmosphere pressure. Therefore, to obtain an accurate stage height reading a second logger must be deployed which measures atmospheric pressure and temperature. Win-Situ® Baro Merge™ (In-Situ Inc.) software combines data from both loggers and produces a corrected stage height from non-vented PT compensated for atmospheric pressure and temperature.

The non-vented PT was deployed within a plastic tube casing and secured to a tree on the river bank. The logger measuring atmospheric pressure was securely hung from a branch on the same tree. Both loggers recorded at the same time every 15 minutes and data from each was downloaded approx. every six weeks. Data from the loggers were used to create a stage-discharge ratings curve for Old Town Burn, GB12.

**Figure 3.5 - Stage height measuring equipment at Gordonbush**
Left: the stage board at GB10 sampling point was installed by MNV Ltd. The white box on top of wooden stake contains stage height measuring equipment. Right: plastic casing used to protect Rugged Troll used at GB12 to measure stage height.

## 3.5.3 Reconstructing stage height hydrographs

As accurately measured stage height data only existed from 17-18$^{th}$ November 2010 in Allt Mhuilin and Allt Smeorail rivers, and only from 13$^{th}$ December 2011 in Old Town Burn, a technique was needed to infer stage height back to August 2010 in all three rivers, to the time of the first event sampling (and start of windfarm construction). To reconstruct stage height at Gordonbush, stage height data recorded every 15 minutes from the nearest Scottish Environmental Protection Agency (SEPA) gauging station to the Gordonbush estate, Bruachrobie on the River Brora (Figure 3.6), were obtained for the period 1$^{st}$ August 2010 to 31$^{st}$ September 2013.

Although the gauging station at Bruachrobie is located further downstream on the River Brora than where Gordonbush rivers enter it (technically only Allt Smeorail and Old Town Burn rivers enter Loch Brora), it is still exposed to the same climatic conditions so it is reasonable to expect stage height trends at this location to be the same as at Gordonbush, thus offering a way to back calculate stage heights at GB10, GB11 and GB12 sites. Stage heights measured at Bruachrobie will be influenced by the particular residence time of water passing through Loch Brora therefore there was an associated time lag effect of various magnitudes between stage height data recorded at Bruachrobie and each studied river on Gordonbush estate.

The statistical technique of cross-correlation allows (time) lags to be identified between any two sets matching datasets. The technique has been used in previous studies when this type of problem occurred; estimating stage heights of river when no data has been collected directly (Brodie et al., 2008; Fiorillo & Doglioni, 2010; Bailly-Comte et al., 2011). Cross-correlation analysis was undertaken in Minitab V.16 when stage height data from Gordonbush rivers and River Brora data at Bruachrobie were available to derive best estimates of the time lags between the GB10, GB11, GB12 and Bruachrobie, respectively. These acquired relationships were used to estimate the stage heights in all three rivers (Allt Mhuilin, Allt Smeorail and Old Town Burn) back to 1st August 2010 using data recorded at Bruachrobie. Results from this method are presented in Appendix A.

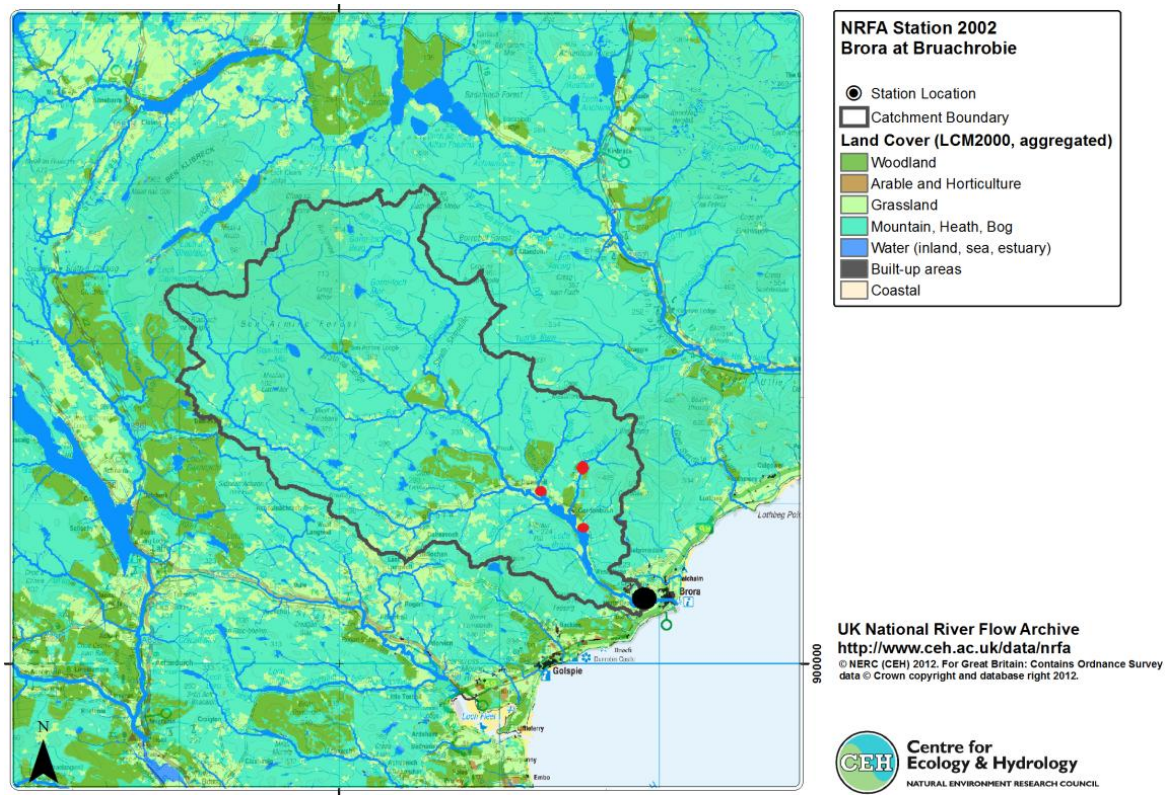


**Figure 3.6 - River Brora catchment area**
Map of River Brora catchment area provided by National River Flow Archive (NFRA). The map contains land cover information in the key. The points highlighted in red are points where stage height measurements were made on Gordonbush estate. The large black dot represents the location of the SEPA gauging station at Bruachrobie.

## 3.6 Measuring river discharge

To produce accurate annual aquatic C fluxes (g C $m^{-2}$ $yr^{-1}$), estimates of river discharge ($m^3$ $s^{-1}$) were needed over the full range of hydrological flows at each event sampling location. Measuring discharge manually is time-consuming and dangerous in high flows, therefore automated equipment was used. A stage-discharge profile was produced for each site by deploying an ISCO 2150 Area Velocity sensor and module (Figure 3.7) to provide a measure of discharge that could be compared to the adjacent measurement of stage height. The ISCO logger was pre-programmed with a manually-derived measure of the cross-sectional area, as discharge ($m^3$ $s^{-1}$) = velocity (m $s^{-1}$) * cross-sectional area ($m^2$) (Soupir et al., 2009), which was assumed to increase linearly with increasing bank fill. Over and under estimates of area using this river bed survey method generally cancel each other out (Figure 3.8). In the absence of using ground penetrating radar (Costa et al., 2000), this is the normal traditional alternative (Kuusisto, 1996). The logger was deployed until sufficient data over a range of flow conditions had been collected to construct a representative stage-discharge profile before being moved to the next site.

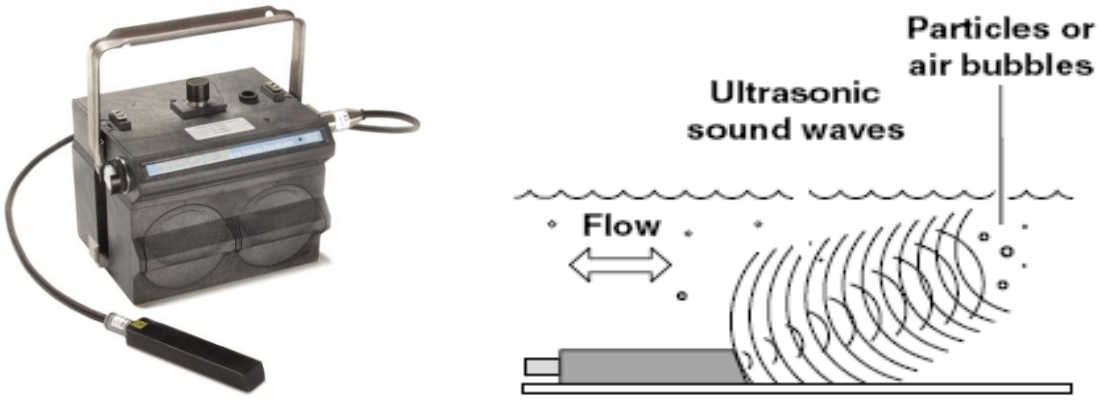


**Figure 3.7 - ISCO 2150 Area Velocity Module**
A = ISCO 2150 area velocity module and sensor (black rectangular object connected to black cable) (ISCO. Teledyne ISCO, 2013). B = An illustration of how ISCO 2150 sensor works to calculate water velocity. The sensor is placed on stream-bed, ultrasonic waves sent from the sensor bounce off particles or air bubbles in the water column and are returned to sensor. The time delay between waves being transmitted then received is converted into flow rate (metres per second) of water surrounding the sensor.

The ISCO logger is considered to function best in rivers no wider than 3 m, so at times, the logger was repositioned in Allt Mhuilin (approx. 9 m wide) and Allt Smeorail (approx. 7 m wide) effectively characterising how river velocity varied over the breadth of the river at any given stage height. The data generated from sensors positioned in different locations were pooled to produce a stage-discharge ratings curve representative of all velocities across the river (see section 3.12 – Formation of hydrographs and stage-discharge

relationships). The location chosen for deployment on the Old Town Burn was only approx. 3 m wide therefore data from only one velocity sensor were used to create stage-discharge ratings curve.

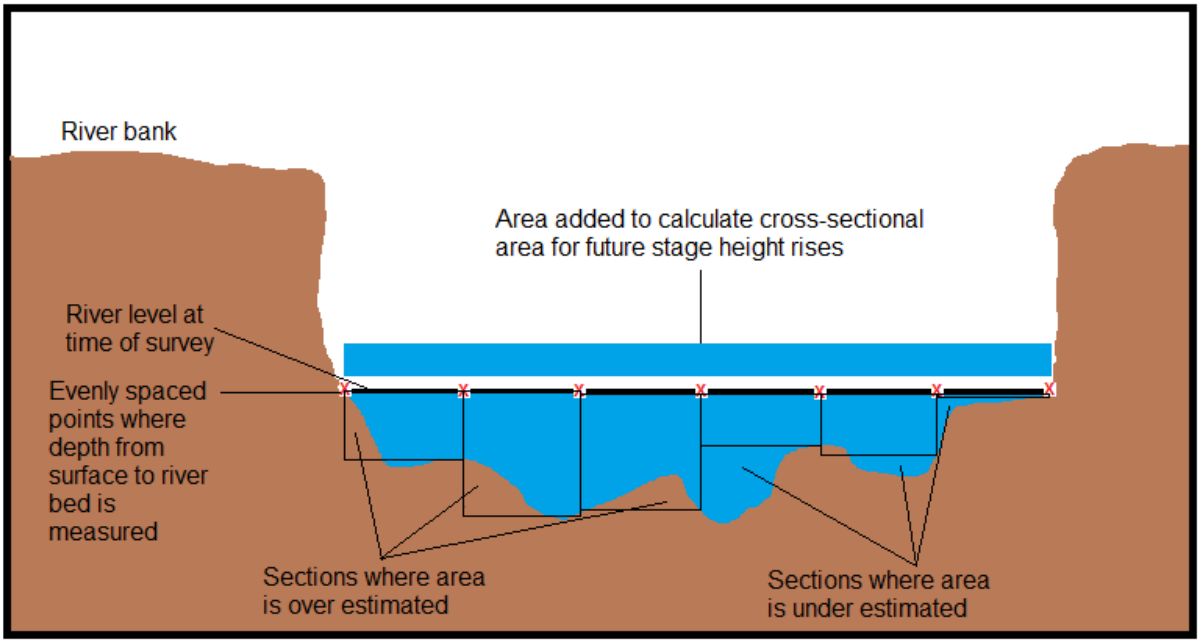


**Figure 3.8 - How cross sectional area of rivers were calculated**
An illustration of how initial cross-sectional area of river profile was calculated and how cross-sectional area is estimated when stage height rises. A similar example available of p4 (Kuusisto, 1996)

## 3.7 Tracking primary productivity rates in rivers

Artificial river substrates were used to quantify changing primary productivity rates within each of the three river sampling points. One artificial substrate, a polyvinyl tile measuring 14 cm x 14 cm attached to a lead weight sealed in duck-tape (used to stop movement of the tile after initial installation) by four cable ties, was placed in the Allt Mhuilin, Allt Smeorail and Old Town Burn close to water storm event sampling locations. To ensure the most conducive conditions for periphyton growth, these substrates were positioned where the surface was not shaded by surrounding vegetation, and where water would always flow over them. Substrates did occasionally move during periods of high discharge but after collection they were returned to the original locations. Substrate surfaces were replaced approx. every 6 weeks or when enough material had accumulated for analysis to be undertaken and samples collected were stored in the dark and refrigerated until analysis for % biomass and chlorophyll *a* content (see section 4.2.5).


**Figure 3.9 - Pictures of artificial river substrates**
A = A side profile of an artificial river substrate attached to lead weights by cable ties. B = An example of where substrates were deployed in any river, a position where the substrate was going to be constantly submerged and sunlight was never blocked. C = A freshly replaced substrate (left) adjacent on 25th June 2013. The substrate on the right had accumulated the material photographed since the 14th May 2013, 42 days (6 weeks) previously.

## 3.8 Sediment traps

To monitor sediment flux from Gordonbush catchments during and after windfarm construction, traps were deployed at mouths of the Allt Smeorail (affected) and Old Town Burn (control) rivers where both rivers enter Loch Brora (Figure 3.10A). The Allt Smeorail catchment (15.39 $km^2$) is three times as large as the Old Town Burn catchment (5.14 $km^2$) and drains the windfarm construction site, including two main on site borrow pits used for gathering hard standing material for the windfarm road network, whereas the Old Town Burn does not. No trap was deployed at the mouth of the Allt Mhuilin as it flows into River Brora 200-300 m upstream of the Loch Brora and therefore any sample collected would be influenced by exports characteristics of a large proportion of the River Brora (~432 $km^2$) catchment area which was not of interest in this research. Traps were placed approx. 20-30 metres, in a downstream direction from the mouth of each river to fully capture sediment transported fanning out on arrival to Loch Brora.

The light-weight mobile sediment traps used at Gordonbush were similar to a design used by Kattel (2009) and were custom-made by Kenny Roberts (field technician). The design is pictured in Figure 3.10B,C & D and consists of three plastic cylindrical sample tubes (5 cm diameter and 30 cm in length) with a buoyant foam material fixed in between an upper and lower triangular frame made of plastic. The sample tubes were fixed to the frame with bungee cord and a hole was drilled through the centre of the frame for a rope so a buoy and anchor could be attached above and below the trap.

Care was taken to ensure that traps were relocated in the same location after each collection. Each sample tube was emptied into 1 litre plastic containers which were pre-rinsed 3 times with lake water. Once all material was collected, the sample tubes were rinsed clean with lake water and securely attached back onto the sediment trap assembly.

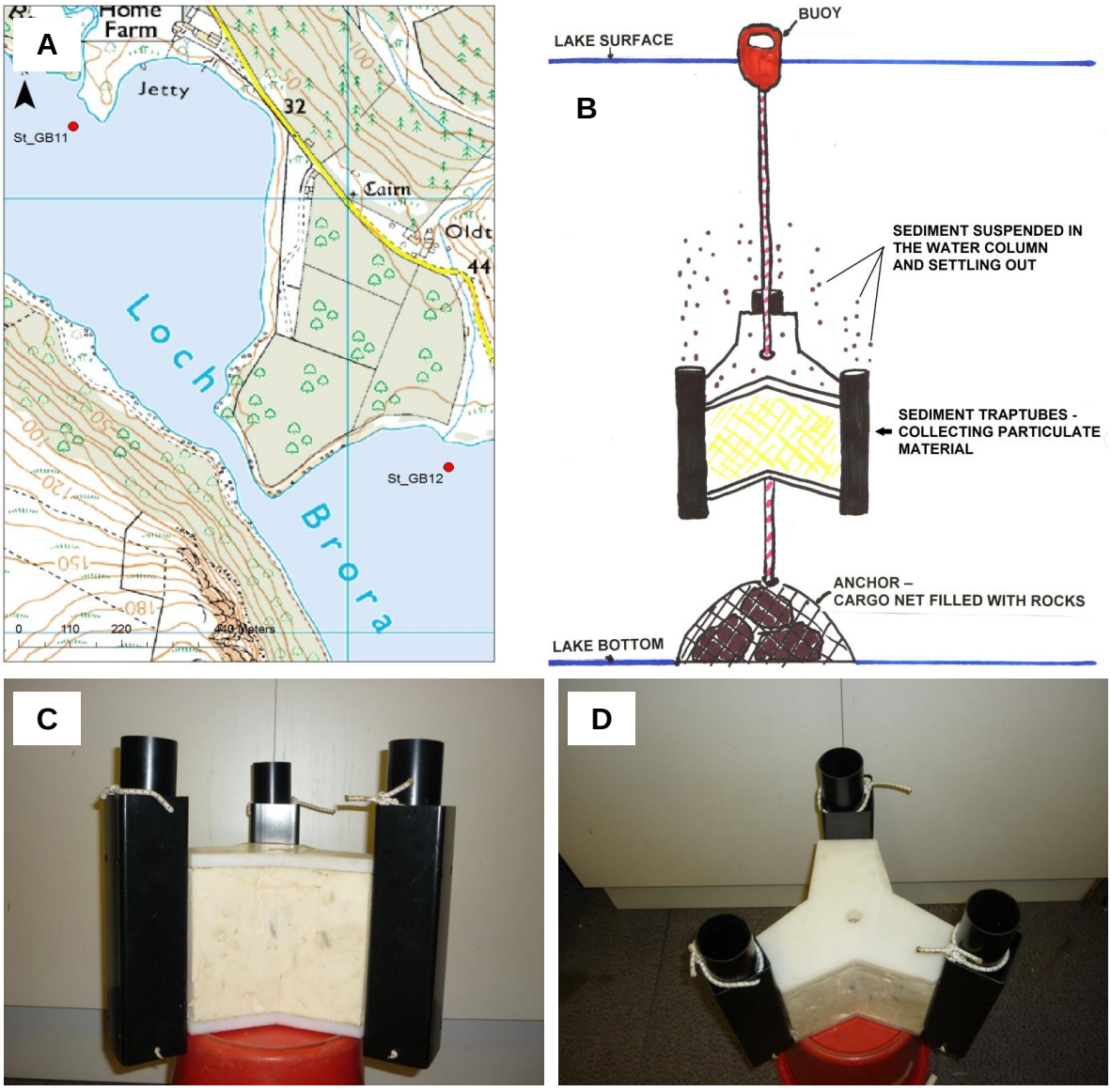


**Figure 3.10 - Sediment trap locations and design**
Figure 3,11 illustrates how they are deployed and operated - the buoy keep the traps suspended in the water column (approximately 1 metre off the bottom of the Loch) and anchor keeps the trap located in a stationary position in the lake. Pictures of sediment traps deployed in Loch Brora at mouths of Allt Smeorail and Old Town Burn rivers.

Of the three samples collected, from each trap one was to be used to monitor primary productivity rates measuring [chlorophyll *a*], C content of sediment using loss on ignition (LOI) analysis and particle size distribution by grain size analysis; the second was frozen and the third was spiked with Lugol's iodine solution (as soon as possible after field collection) to preserve the diatom communities within the samples should another researcher wish to make use of the samples. All samples were refrigerated as soon as possible after field collection until further analysis, including preparation for chlorophyll a (section 4.2.5), %LOI (section 4.2.1) and grain size analysis (section 4.2.2).

The sediment traps were emptied on an approximate 6-8 weekly basis which allowed time for sufficient sediment to accumulate for the analyses. Between installation on 27th March 2011 and the last collection date on 24th September 2014, sediment traps samples were collected 20 times from Allt Smeorail traps and 17 times from Old Town Burn. At times weather conditions and high water level (making it hard to find the surface buoy) meant it was not possible to collect and empty both sediment traps.

## 3.9 Lake coring – Loch Brora lake sediments

Sediment cores were collected on 25th May 2010 from the middle basin of the Loch Brora's three basins where the Allt Smeorail river enters the lake. Cores were collected to investigate long term lake C sequestration rates to provide a historical context of modern day sedimentation. The coring site was selected as it was thought to be best location that would be representative of C accumulated from inputs of both Allt Smeorail and River Brora rivers as well as an average of in-lake C production (Figure 3.11A).

A Livingstone piston corer (Livingstone, 1955; Wright, 1967) was used to collect the sediment, an approach routinely used for soft-sediment lake coring (Glew et al., 2001). The diameter and length of each core collected was approx. 5 cm and 1 metre, respectively. After retrieval, each core was wrapped in cling film then aluminium foil before being sealed in cylindrical plastic case (Figure 3.11B-D).

The total core length of recovered Loch Brora sediments was 2.1 m and overlap cores were taken every 0.5 m. The top 1 metre of the core was extruded at 1 cm resolution (Glew, 1988) on-site after collection and sediment transferred to labelled plastic bags, ensuring excess air was pushed out (Figure 3.11E-F). All cores (including extruded samples) were refrigerated as soon as possible after collection until further %LOI (section 4.2.1) and grain size (section 4.2.2) analysis was undertaken.

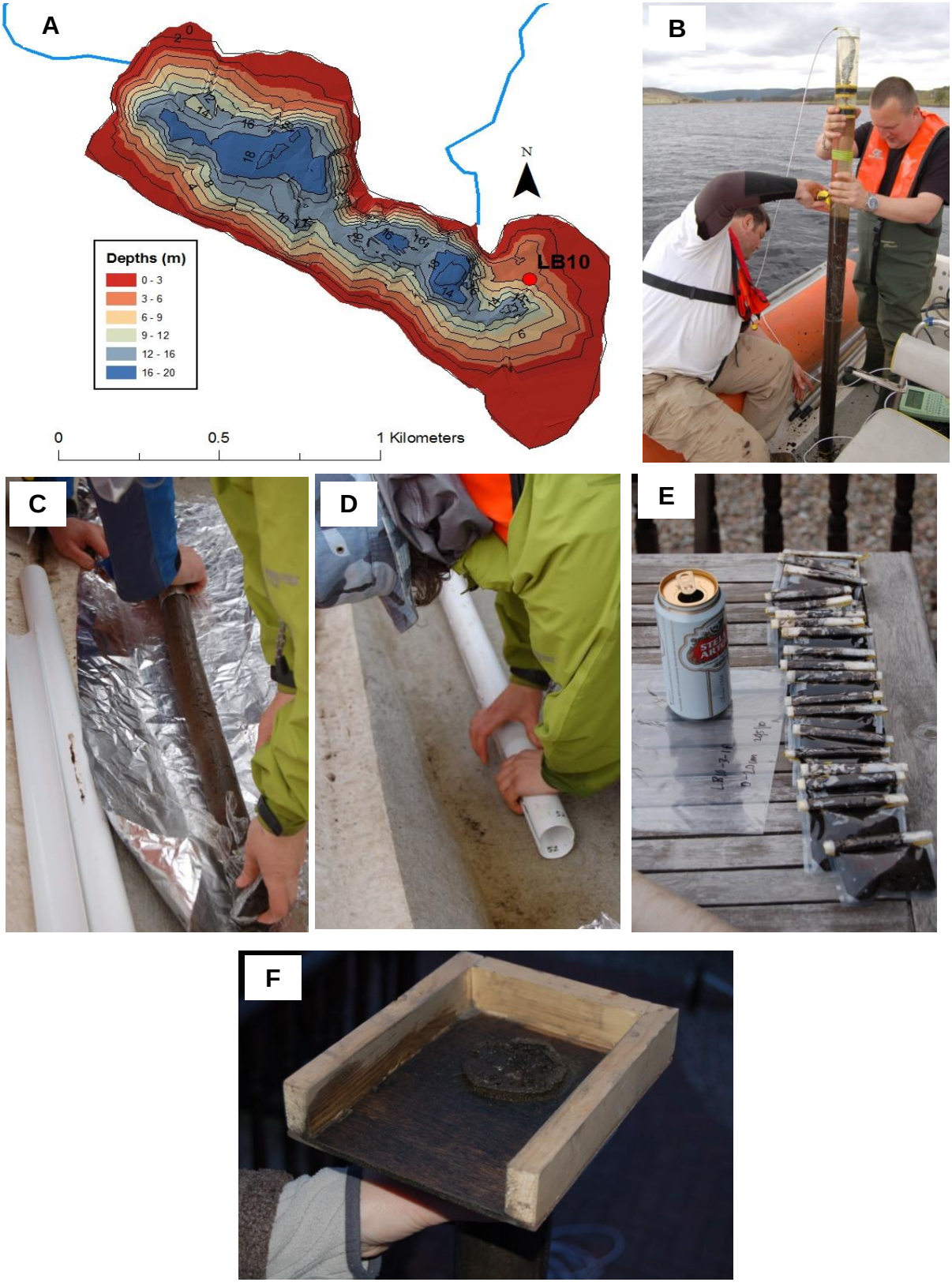


**Figure 3.11 - Loch Brora bathymetry map, coring and slicing procedure**
A = Loch Brora bathymetry map, data was collected by K. Roberts when Loch Brora core (LB10) was collected in May 2010. Incoming rivers of River Brora (top left) and Allt Smeorail (right) are shown by blue lines. B = Livingstone piston corer equipment used to collect Loch Brora sediment core. C = Wrapping of retrieved cores in cling film and aluminium foil to prevent them drying out until they could be refrigerated. D = Cores sealed in plastic casing for easy transport from field to laboratory. E = Loch Brora sediment samples in 1 cm sections sealed in sediment bags. After field collection, sediment was stored in refrigerator. F = Extruder apparatus used to slice Loch Brora sediment at 1 cm resolution. Extrusion of the top 1 metre of sediment collected was done on the day of sampling.

## 3.10 Peat coring at undisturbed and disturbed sites

Two sets of peat cores were retrieved using a Russian peat corer (Givelet et al., 2004; Vleeschouwer et al., 2010; Aquatic Research Instruments, 2013) on 19th June 2012 (see Figure 3.13). A section of undisturbed peat on the turbine plateau between turbine No. 20 and turbine No. 21 was selected as the pristine (uncut) site (GB1), (58° 06'40 N, 03° 55'07 W). A cut site (GB2) was selected and located just off main access road of the windfarm away from turbine plateau, (58° 04'57 N, 03° 58'11 W) (Figure 3.12). The rationale for selecting a pristine and cut site was to examine not only the natural variability in C sequestration rates across the Gordonbush plateau but if any differences in C sequestration could between observed disturbed and undisturbed sites which may have a relevance to disturbance caused by windfarm construction activities.

Each core was 50 cm long and had a diameter of approx. 5 cm. After collection each core was wrapped in cling film, labelled and stored in cylindrical plastic cases. Cores were refrigerated as soon as possible after collection and stored there until %LOI analysis was conducted. In total, approx. three metres, of peat cores were collected at each site, to determine C content and C sequestration rates over the Holocene timescale. A separate, 0.5 metre core was also collected from both sites, to be used for $^{210}$Pb radiometric dating helping determine C sequestration rates over the 100-150 year time scale.

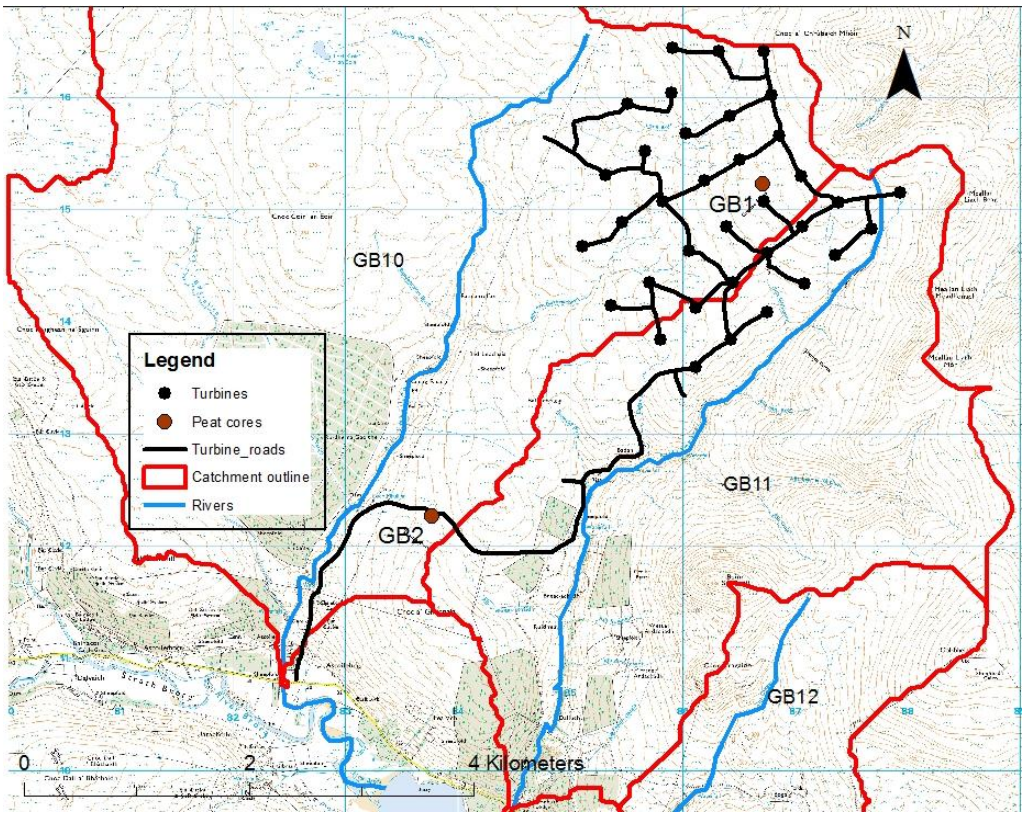


**Figure 3.12 - Peat coring locations**
Map showing peat coring locations of undisturbed (GB1) and disturbed sites (GB2). The outline of the catchments (red lines), their main rivers (blue lines) and codes names, GB10 (Allt Mhuilin), GB11 (Allt Smeorail) and GB12 (Old Town Burn) are shown. The wind farm road network and turbine locations are displayed. A legend, scale and North arrow are also included.


**Figure 3.13 - Peat coring fieldwork photographs**
A = Illustration of the depth of peat cored, approx. 3 metres from undisturbed site. B = transfer of peat cores from corer to plastic casing (wrapped in cling film). C = 50 cm peat core sections collected using Russian peat corer. D = collecting cores from site that had been subject to peat cutting. All pictures were taken in June 2012 during peat coring fieldwork on Gordonbush estate.

## 3.11 Monitoring of drain blocking site

The methodology here is most relevant to Chapter 8 and describes the field instrumentation and sampling protocol used to understand how drainage and subsequent restoration may influence water table depth (WTD) as well as [DOC] export from soils surrounded by drainage channels compared to areas with no drains. Drain blocking was implemented at Gordonbush as it is the simplest and most cost effective means of increasing water retention in a peatland with historic and artificial drainage channels.

### 3.11.1 Site description

The drains chosen to be blocked were identified in HMP from the following features: i) their parallel nature, similar width, and the proportion of drains already in-filled (with *Sphagnum* species), ii) the logistical ease of eventually performing drain-blocking activities, iii) the similarity in vegetation and slope across the area and iv) the location of a nearby area for a control site with similar vegetation, slope and aspect.

Drains numbered 0 to 6 were the best locations to focus the monitoring study Figure 3.14.

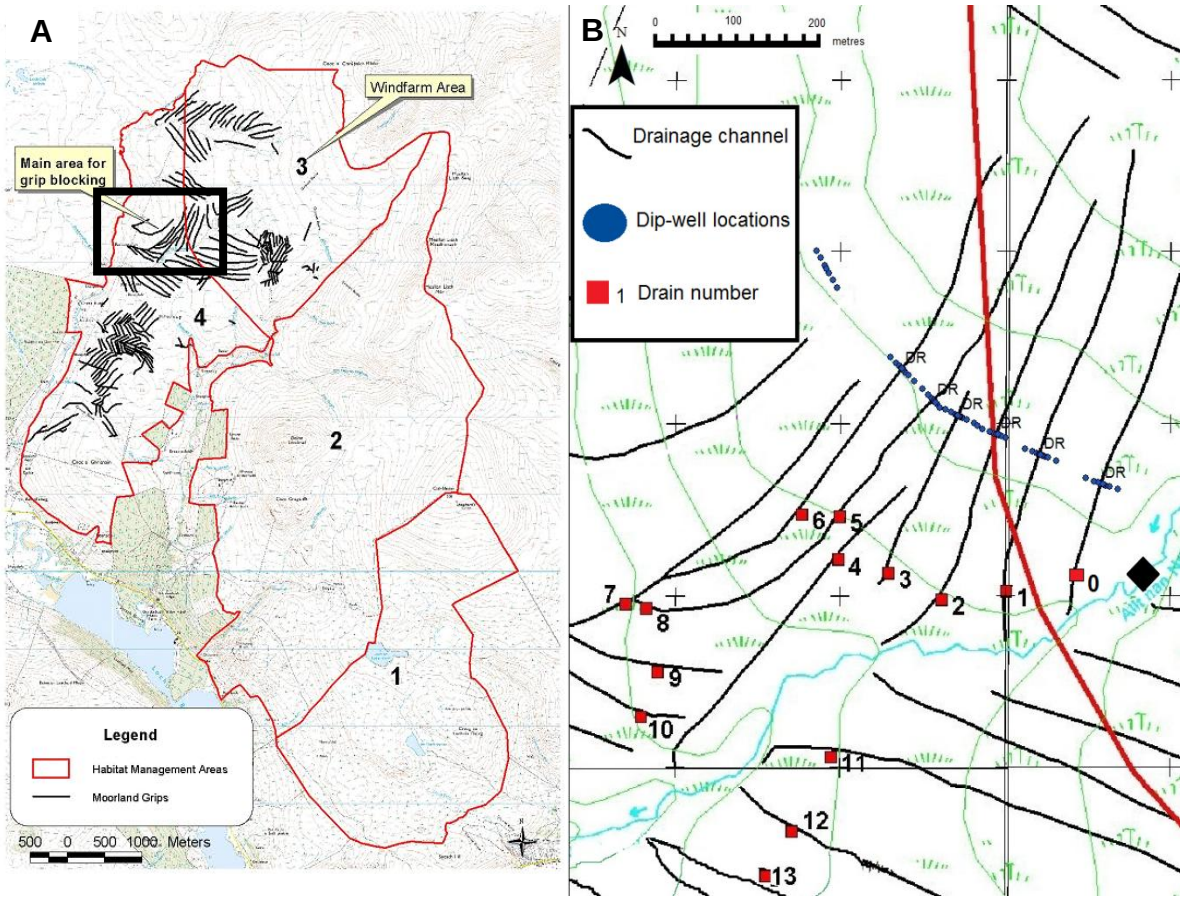


**Figure 3.14 - Maps of impact of drain blocking study site**
A = shows Gordonbush estate and marks locations of drains in black. B = a more detailed map of area highlighted in black is presented. Blue dots (right Map) represent dip-well positions (adapted from Milne, 2010). The dots to the NW of the diagram represent the control site. Drains 0, 1, 2, 3, 5, and 6 all drain into Allt nan Nathraichen river (blue thin on map B), a tributary of Allt Mhuilin which was sampled upstream of where any of the drains drain into the river (marked by black diamond).

On the 6th August 2011, dip-wells were installed either side of the drains, at a distance of 20, 10, 5, 2, 1 and 0.5 metres perpendicular to the drains. Additionally, an array of 'control' dip-wells was installed ~125 metres NW of drain 6 to represent WTD in peat not affected by drainage channels (Figure 3.14B). This area was chosen due to similarity in slope, vegetation and altitude to the drain transect. The control array contained six dip-wells spaced 10 metres apart. The first control dip-well was positioned ~70 metres (north) away from the nearest drain previously identified (Milne, 2010). However, this drain was partially in-filled but we were confident that it was located far enough away from the control transect and that it would not affect the WTD data subsequently collected (Figure 3.14B).

### 3.11.2 Automatic water table depth measurements

To measure WTD continuously, two Waterra In-Situ Level Troll® 700 data loggers (Level TROLL 700 – product description) were installed: one in the middle of the drain transect of dip-wells, between drains 3 and 2, the other in the middle of the control array, between the third and fourth dip-wells. These pressure transducers (PTs) had vented cables therefore accurate measurements could be recorded without the need to be corrected for atmospheric pressure and temperature.

The instruments were set-up to record the water depth above the sensor (Figure 3.15) every 15 minutes, therefore it was important it the PT stayed in a fixed positioned cased within the plastic dip-well and cable ties were used to ensure this. Data were downloaded approx. every 6-8 weeks using Win-Situ® software (In-Situ Inc.). The Level Troll 700 had the ability to record water depths to ± 0.001 of a centimetre, temperature ± 0.1°C and pressure sensor ± 0.1%, of full scale. A desiccator filled with silica gel beads, was used to protect cable download connections on each logger from water damage. Silica gel within desiccators was changed as required. The PTs were housed in plastic (PVC) pipes, 1.5 metres in length and 7 cm in diameter. These were larger versions of manufactured dip-wells used to record manual WTDs described below.

### 3.11.3 Manual water table depth measurements

Dip-wells were constructed using similar methodology to Patterson & Cooper (2007). In summary: dip-wells were constructed from lengths of cylindrical 1.4 cm diameter white PVC pipe, cut into 1 metre long sections with holes drilled approx. at 1-2 cm intervals along the length except the top 10 cm (to avoid precipitation ingress when installed and capped). Dip-wells were sealed at the bottom with duck tape so soil would not fill the pipe when installed in the ground. The drilled holes allowed peat water to enter the pipe and enable water table depth to be measured *in-situ* (Patterson & Cooper, 2007).

To measure water table depth at dip-wells locations, a hollow pipe (approx. 1 m in length and graduated every centimetre) was lowered inside the dip-well and air blown into it. When bubbling sounds were heard, caused by the air hitting the water, the depth the hollow pipe had been lowered to was noted (B). The height of the dip-well above the peat surface was also noted (A) and water table depth below the peat surface was calculated by subtracting B from A (Figure 3.15). PTs located at within drain and control transects constantly logged the water level in its own dip-well plastic casing. The protocol used to convert this measurement into an equivalent WTD is explained in Appendix H.

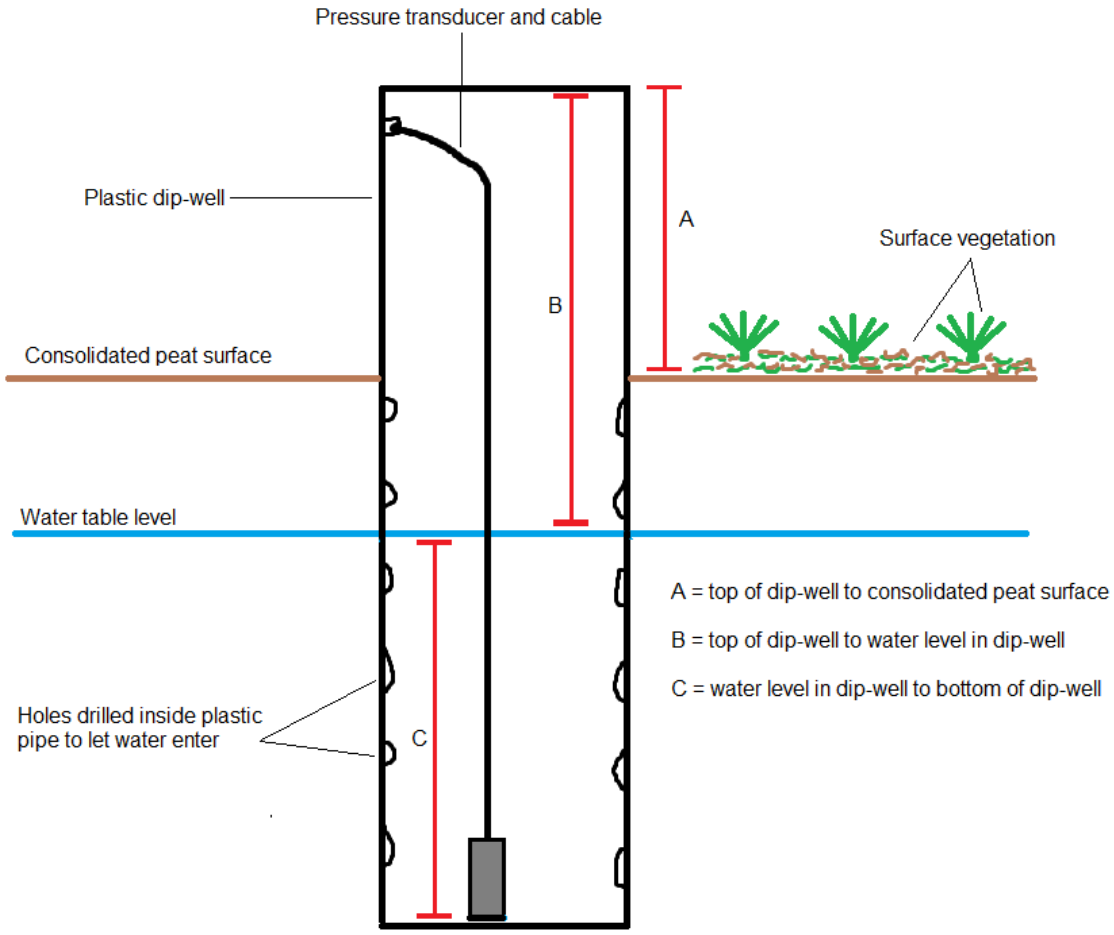


**Figure 3.15 - Water table depth measurements**
The diagram above illustrates what measurements were taken manually and automatically by pressure transducers in order to calculate water table depth in dip-wells.

## 3.11.4 Drain water collection

Water samples for [DOC] were collected from drains in 125ml plastic containers (rinsed 3 times with drain water) at same location on every monitoring date. Refer to subsequent sections is the Laboratory methodology chapter for protocols regarding filtration of water samples (4.1.2) and measurement of [DOC] (4.1.3).

## 3.12 Formation of hydrographs and stage-discharge relationships

Although this section is technically presenting results calculated from data collected, it has been inserted here, in the methods section, as its content is fundamental to subsequent parts of the thesis.

Construction of a stage-discharge relationship (ratings curve) allows discharge to be estimated continuously by only recording water level (stage). A stage-discharge relationship is described using the most statistically significant linear function (e.g. linear regression, power, exponential, polynomial etc). To quantify aquatic C fluxes, I constructed a specific stage-discharge relationship for all three rivers studied. This required a stage height time series (or hydrograph) spanning the period of study. Therefore, here I detail the stage-discharge relationships in one of the three studied Gordonbush rivers, Allt Smeorail (GB11) and working stage height profiles for all three studied rivers. Methodology used to construct stage-discharge ratings curve for the other two rivers (Allt Mhuilin – GB10 and Old Town Burn – GB12) was exactly the same and related data are presented in Appendix D. In addition, specific annual discharge estimates (inferred using stage height data and constructed stage-discharge ratings curves) will be presented for all three rivers.

### 3.12.1 Creating stage-discharge relationships

An ISCO logger was placed in Allt Smeorail very close to the sampling point GB11 for reasons relating to ease of access and the presence of a conducive channel shape for estimating discharge (rectangular shape with a flat river bed and well defined steep/vertical river banks). However, long-term hydrograph was located at GB6, 3 km upstream from GB11. To ensure that it was appropriate to use stage height data from GB6 to construct stage-discharge relationships, data from GB6 and stage height data collected by ISCO logger were plotted to assess linearity between the two data sets (Figure 3.17). A strong linearity was exhibited and reflected in $R^2$ values > 0.9. Consequently the use of stage height measured at GB6 to calculate long-term discharges profiles was deemed suitable. The continuous stage height record from GB6 used to create stage-discharge relationship for Allt Smeorail at GB11 is displayed with time periods highlighted when discharge was estimated at GB11 (Figure 3.16).

The maximum and minimum stage heights recorded at GB6 when the ISCO logger was placed at GB11 sampling point were 1.78 m (12/10/12) and 0.29 m (10/5/2013). The absolute maximum and minimum stage heights recorded at GB6 between November

2010 and September 2013 were 2.16 m (23/12/2012) and 0.24 m (21/7/2013), therefore a very wide range of all hydrological conditions were recorded by the ISCO logger. This is reinforced by construction of a flow duration curve for all stage height (stage height has been used as a proxy for discharge in this instance) collected at GB6 (Figure 3.18).

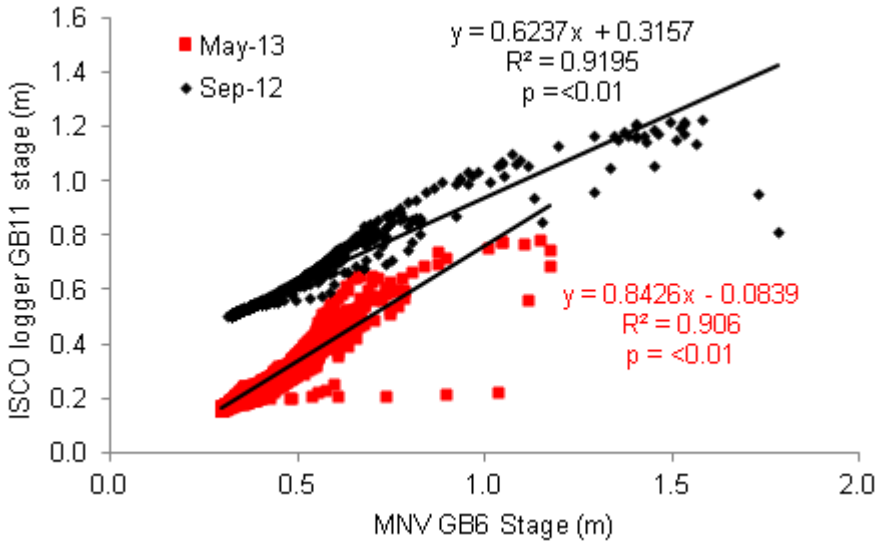


**Figure 3.17 - Comparison of stage height between GB6 and GB11**
Data points in black represent the time period when ISCO logger was placed at GB11 in Sept. 2012, and red points in May 2013, respectively. Linear regression equations, associated $R^2$ and p values are displayed for both sets of data presented in respective colours.

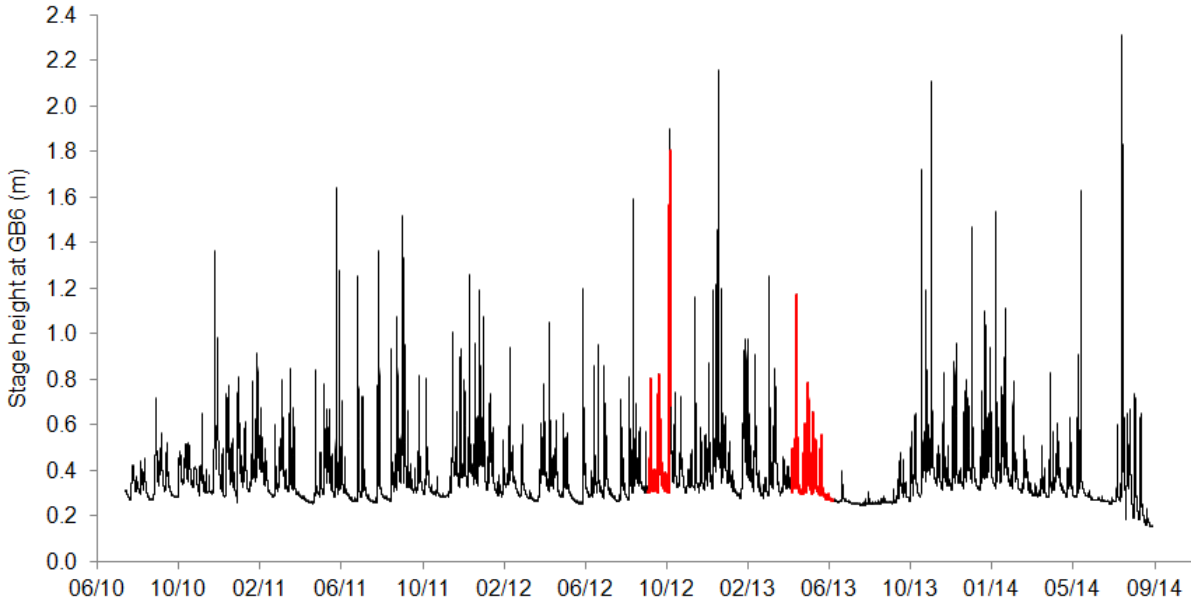


**Figure 3.16 - GB6 stage height time series with ISCO logger deployment dates highlighted**
GB6 stage height is shown in black and the time periods when ISCO logger was deployment in Allt Smeorail near GB11 are highlighted in red. The ISCO logger was placed in Allt Smeorail on two occasions between 10/9/12 to 12/11/12 and 10/4/13 to 10/6/13 capturing the flow range 0.2 to 2.2 m.

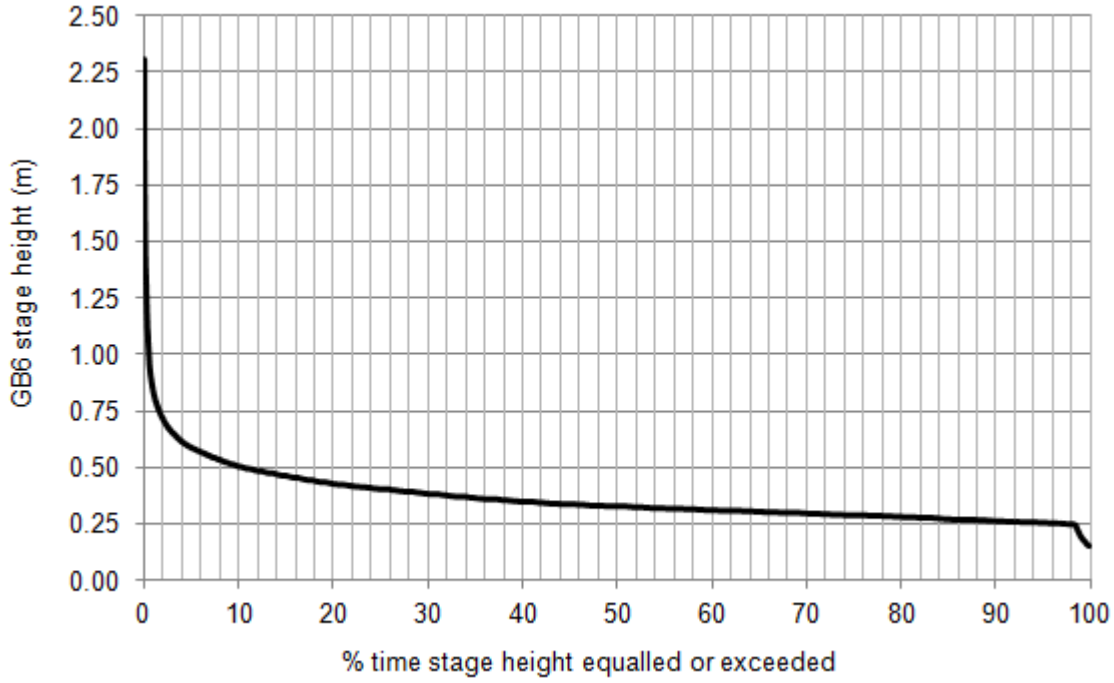


**Figure 3.18 - GB6 flow duration curve**
Stage height values recorded between November 2010 and September 2014 from GB6 station plotted against percentage of time that value was equalled or exceeded. Only 30 stage height readings were recorded above 1.78 m during the study period and the flow duration curve indicates exceedance above this value was less than 0.05 %. The minimum flow value during ISCO deployment had an exceedance value of 72.0 % which mean that the majority of low flow conditions were characterised.

Allt Smeorail is wider than the recommended 3 m limit extent of the ISCO logger, thus to ensure the stage-discharge curve effectively describes the system, two ISCO sensors were deployed on between 10/4/13 and 10/6/13 to assess flow velocity variability. ISCO loggers were placed in five different channel locations (Figure 3.19).

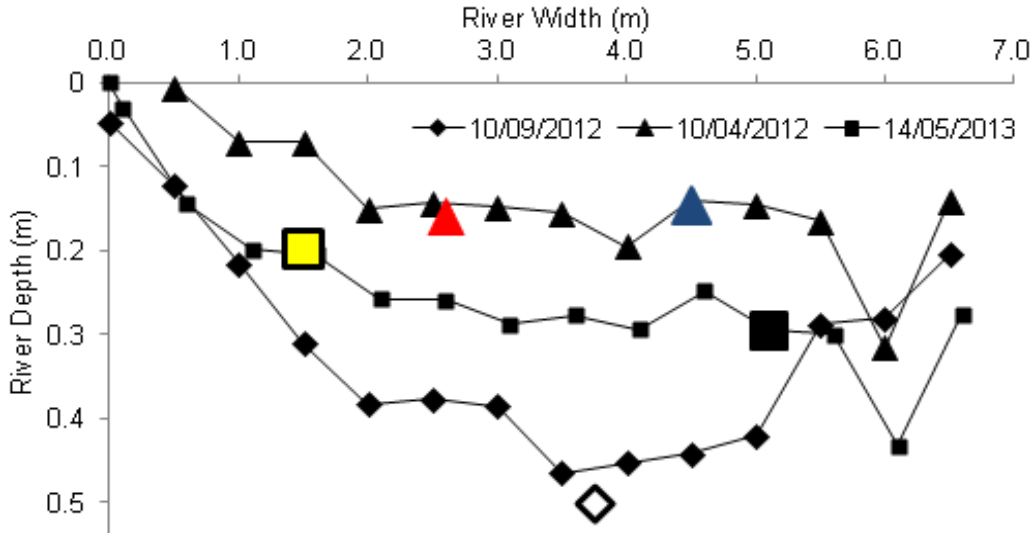


**Figure 3.19 - ISCO logger positions GB11**
Cross-sectional river profiles are shown for survey dates of GB11. The profiles are represented looking in an upstream direction to river flow. The coloured shapes are markers for the location of where the ISCO logger was placed after a specific survey had taken place. The shapes (circle, diamond and triangle) of the markers match up with the shapes used to represent cross-sectional profiles on different dates. The colours of the markers also correspond to data collected from each sensor which is displayed in Figure 3.20.

The data from the four sensor positions (red and blue triangles, black squares and black hollow diamonds) was deemed to offer best representation of natural variability in velocities across the river. Data from sensor in yellow did not show similar patterns to other sensors and was deemed to be too close to the bank and potentially could have been affected by swirling water and eddies in the shallowest part of the river. Combining data from red, blue and black coloured deployments produces a highly linear stage-discharge relationship (Figure 3.20).

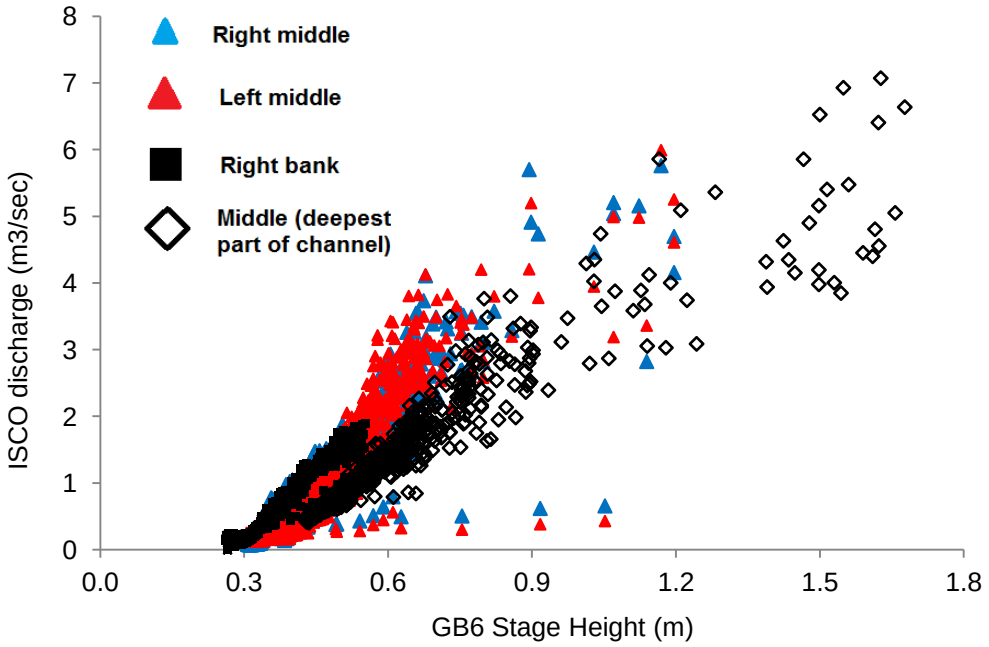


**Figure 3.20 - GB11 collated ISCO logger discharge data**
Discharge data collected from ISCO logger when positioned in Allt Smeorail at GB11. The colour coded markers correspond to same colour of makers and highlight the position of ISCO logger along cross-sectional area of river near GB11 that is displayed in Figure 3.19.

This relationship is less-well defined for discharge above ~0.75 m stage height partly due to the fact there are a relatively small number of measurements that exist during high flows which is a consequence of stage heights in the Allt Smeorail during the study period only exceeding 0.5 m 10% of the time. We might have expected the stage-discharge relationship to be curvi-linear as this is the typical shape associated with hydrological systems. From the data collected, a fitted curvi-linear relationship inferred discharge would decrease as stage increased at some points which is unrealistic. I did not want to 'cherry pick' data so I feel the linear relationship presented is the best representation of the data collected despite it might not have been what was expected. A graph of the final collated stage-discharge relationship data are shown below for GB11 (Figure 3.21) as well as a table presenting the stage-discharge rating curve equations for all three studied Gordonbush rivers (Table 3.2).

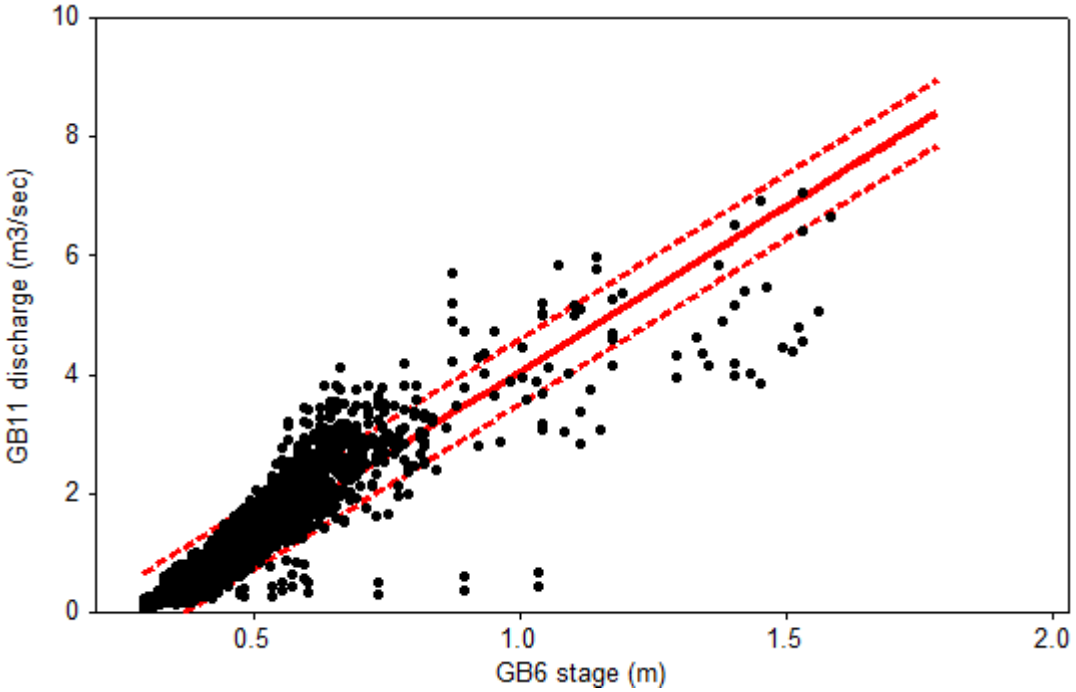


**Figure 3.21 - Stage-discharge ratings curve for GB11 (Allt Smeorail)**
All collated discharge data is plotted against corresponding stage height data from GB11. The red line shows the best fit linear relationship through the data. The dashed red lines are the prediction intervals for the fitted line.

The corresponding equation of linear regression line for GB11 is presented below along with equations from the other two rivers.

| River name and code | Stage-Discharge Relationship | $R^2$ value | p value |
|---|---|---|---|
| Allt Mhuilin (GB10) | Q = (10.16 * GB10 stage) – 2.614 | 0.90 | <0.01 |
| Allt Smeorail (GB11) | Q = (5.563 * GB6 stage) – 1.517 | 0.87 | <0.01 |
| Old Town Burn (GB12) | Q = (2.493 * (GB12 stage)$^3$) + (2.505 * (GB12 stage)$^2$) + (0.1453 * GB12 stage) + 0.03382 | 0.90 | <0.01 |

**Table 3.2 - Stage-discharge relationships for Gordonbush rivers**
Displayed are river names and code. Stage-discharge relationships for GB10 and GB11 are linear equations and GB12 is a cubic.

The stage-discharge relationship presented in this section for GB11 has been used in all subsequent analysis where a discharge value was required. The same is true for data presented regarding GB10 and GB12 in Appendix D.

### 3.12.2 Working stage height profiles

Working stage height profiles of all three rivers are presented below (Figure 3.22). This data was utilised to calculate all discharge estimates. A graph showing data from each individual river is available in Appendix B.

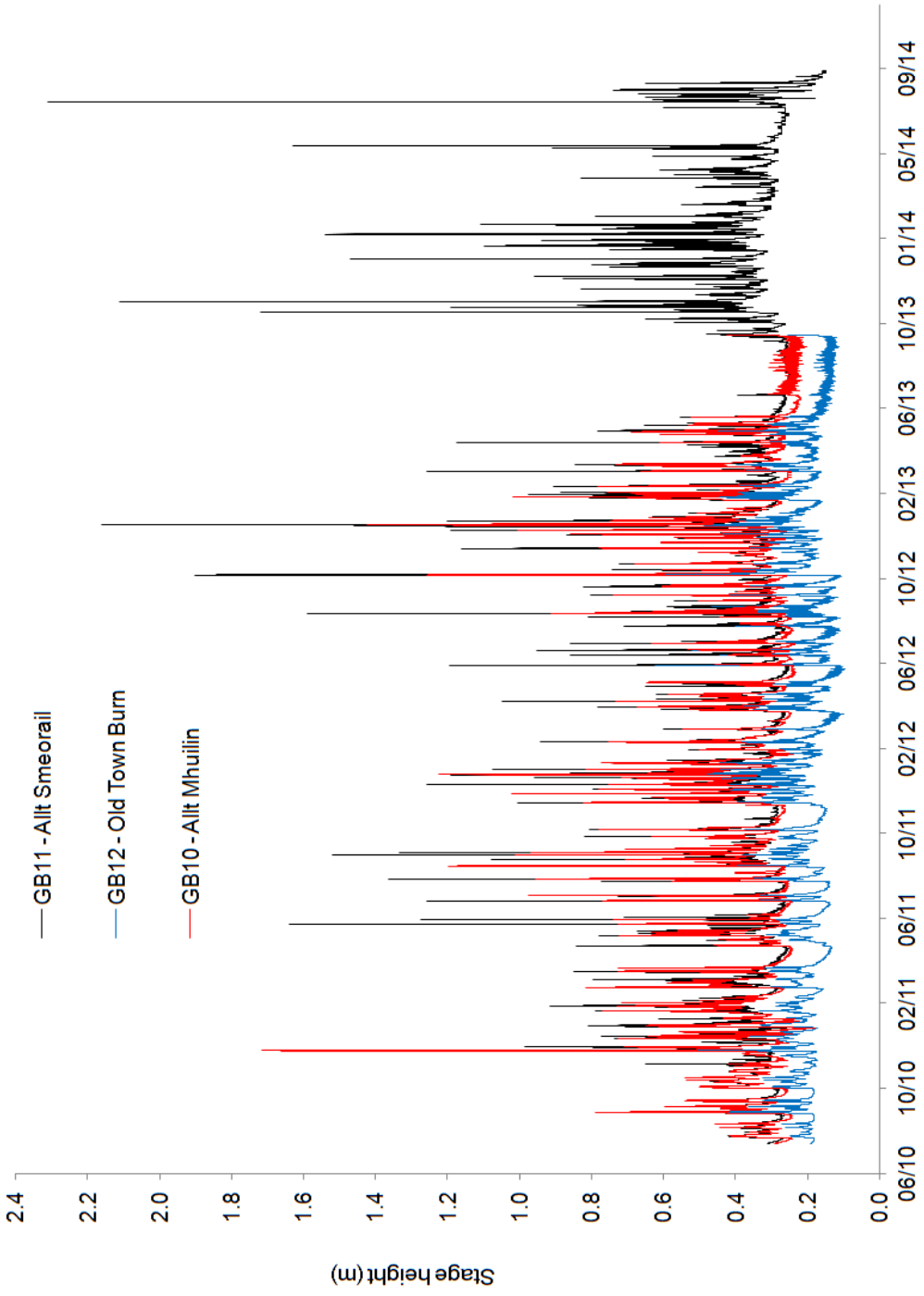


**Figure 3.22 - Stage height time series of all Gordonbush rivers from Aug. 2010 to Sept. 2014**
GB10 – Allt Mhuilin stage height is shown in Red, GB11 – Allt Smeorail in Black and GB12 – Old Town Burn in Blue.

### 3.12.3 Specific annual discharge estimates

Comparisons of annual river discharges between adjacent catchments of different sizes should be in proportion with their catchment area (Hendriks, 2010). An exception to this rule would be catchments that contain significant amounts of bedrock limestone however this does not apply at Gordonbush (see section 3.1 detailing underlying geology of Gordonbush catchments). The graph below shows annual specific discharge for each catchment per hydrological year.

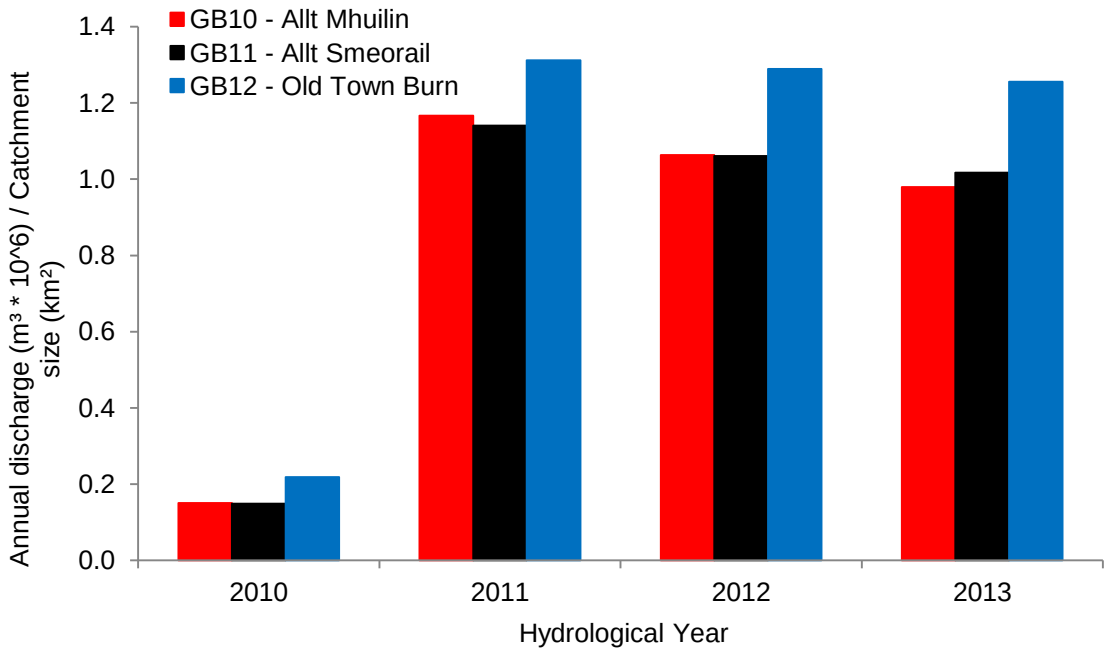


**Figure 3.23 - Annual discharges from Gordonbush rivers**
2010 results are markedly smaller than other years due to the fact only discharges in August and September of that year have been calculated.

All catchments should give similar annual specific discharge (Figure 3.23) as they are closely located, and exposed to a similar climate, and this is what is generally observed. GB12 is consistently higher is all years. The differences noticed in specific annual discharges between the three rivers are most likely related to the statistical variability associated with the stage-discharge ratings curves of each individual river. The highest statistical variability associated with stage-discharge ratings curve for all rivers is apparent for the highest stage heights recorded and the most probably source and reason for the inter-catchment differences. In the future, extra data collection of discharges at the highest recorded stage heights in all rivers would help better constrain the stage-discharge relationships of all rivers and would likely improve annual discharge estimates. However, as the flow duration curve (presented earlier) illustrates, hydrological events with high stage height (and discharge) are rare and challenging to capture with data loggers. Despite this, I am confident discharge data collected for this research is representative.

# 4 Laboratory methodology and data analysis

This section outlines techniques used to process and analyse samples after initial collection in the field. This chapter has three sub-sections: 1) water-based samples; 2) sediment-based samples; and 3) computer-based methods and statistical analysis.

## 4.1 Water Analysis

### 4.1.1 Cleaning of filter kits and filtration protocol

For DOC, POC, SRP and TON analysis, water samples needed to be filtered. Separate kits were used for samples filtered for DOC and POC analysis, and those for SRP and TON analysis. Filter kits used for DOC and POC were soaked in 5 M nitric acid overnight before being rinsed thoroughly with deionised water and dried in a drying cupboard, prior to use whilst on field work. For SRP and TON filter kits were instead soaked in phosphate-free 2% Decon®. Whilst on field work, the kits were rinsed with deionised water between filtering different samples.

Filtering was undertaken typically 1-2 hours after collection to minimise biological degradation of the samples. If filtration was not possible within this time-frame, samples were refrigerated until it could take place; a measure undertaken to minimise biological degradation (Kaplan, 1994). Sample bottles were always shaken prior to filtration to suspend any particulate material.

### 4.1.2 Filtration procedure for DOC and POC

For DOC and POC, ~900 ml from the 1 litre sample was vacuum-filtered through a pre-combusted (550 °C for 3 hours) 0.7 µm glass micro-fibre (Whatman GF/F) 47 mm filter paper to collect sufficient material for measurement of [POC] by loss on ignition (LOI) (section 4.2.1). The choice of glass fibre filter papers is deemed the most suitable for aqueous OM studies to prevent contamination (Dawson et al., 2012) and it will not combust during LOI analysis.

The exact volume of water filtered through each filter paper was accurately measured and recorded, as this is used in the final calculation of [POC]. Sometimes, more than one filter paper was used per sample if enough particulate material was present to cause filtering rates to approach zero before all ~900 ml was filtered. All filter papers were stored in labelled plastic Petri dish containers. After filtration, all samples were discarded expect for

a ~50 ml aliquot transferred to a 50 ml polypropylene (graduated) centrifuge tubes, which was retained for measurement of [DOC].

### 4.1.3 Dissolved organic C analysis

For measurement of DOC, dissolved inorganic carbon (DIC) must be removed. This was done by titrating a known volume of the filtrate with 0.01M $H_2SO_4$ to pH 3.9 using either a Mettler Toledo G20 or DL20 compact auto-titrator (Mettler Toledo). The volume of the filtrate titrated and the volume of acid added must be known to allow the final measured [DOC] to be volume-corrected for the samples dilution that occurred as acid was added.

After acidification and prior to analysis, samples were placed in an ultrasonic bath for 15 minutes to remove any trace sources of inorganic C. [DOC] of all water samples were measured using a Thermalox™ TOC Analyser (Analytical Sciences). Water samples (30 µl) were injected into a high temperature (680 °C), oxygen gas saturated furnace, where all organic C within samples was converted into $CO_2$ aided by a platinum coated catalyst. Subsequently, the quantity of $CO_2$-C produced was measured in a non-dispersive infra red detector. The measured $CO_2$ value was then converted to an equivalent [DOC] using a standard calibration line.

Standards were automatically prepared by the instrument prior to every analysis run from a 1000 mg $l^{-1}$ total organic C stock solution of potassium hydrogen phthalate, by dilution with (He) degassed, deionised water. Generally five standards were prepared for any one run dependant on the estimated [DOC] of the samples however these were commonly in the range between 5-100 mg $l^{-1}$. The linearity of the instrument prepared standards, along with zero standards was checked thoroughly before a sample run was started. A manually prepared check standard (~20 mg $l^{-1}$ C) and zero standards were analysed every 10 samples throughout every run to allow assessment of the stability of instrument readings and correction of any potential drift that may have occurred. Three replicated measurements were made for each sample and an average of all three formed the base of the final results. Samples were reanalysed if the coefficient of variation (defined as the ratio between the standard deviation and the mean of replicate sample results) percentage between the three replicates was <2%.

### 4.1.4 Loss on ignition analysis: POC

[POC] of water samples were measured using LOI techniques, i.e., the weight loss of GF/F filter papers used in the filtration process (previous section 4.1.2). This procedure included drying filter papers to remove all traces of water before combustion of OM at

higher temperatures, otherwise [POC] would be overestimated (Pribyl, 2010). Exposure at temperatures of 550°C for ~4 hours is recommended time for complete OM combustion in sediment samples (Dean, 1974; Heiri et al., 2001). However exposure at a lower, temperature of 375°C for a longer period of time is favoured for determination of POC as this reduces loss of water from clays and breakdown of inorganic C compounds, all of which would overestimate [POC] (Ball, 1964).

Firstly, papers were dried at 105°C for 4 hours and their weights recorded. POC filter papers were then combusted at 375°C for 16 hours (Hope et al., 1997a) and then weighed a final time. Between all transfers from furnace to weighing balance, filter papers were placed in sealed desiccators to avoid them absorbing any moisture. Filter papers were also only handled with tweezers at every stage of the above process to avoid moisture uptake from hands. All weights were recorded to 5 decimal places (i.e. 0.00001 g). [POC] was calculated using the following equation (Eqn):

$$POC\ (mg\ l^{-1}) = [(W_{105} - W_{375}) / Vf\ ] * 0.58 \qquad \text{Eqn (4.1)}$$

where W is the weight of filter paper (mg) after ignition at each temperature and V*f* is volume of water filtered (litres). The total weight loss is multiplied by a factor of 0.58 (the van Bemmelen factor) as it has been estimated 58% of OM is comprised of C in soils (Ball, 1964; Allison, 1965), and this figure has been commonly adopted for POC analysis in other studies (Hope et al., 1997a; Dawson et al., 2002; Dinsmore et al., 2013).

### 4.1.5 Filtration procedure for SRP and TON

The remaining 100 ml from the 1 litre water samples were vacuum-filtered through a 0.2 µm pore size (Whatman 47mm) nylon membrane filter for the purposes of SRP and TON analysis. It is not strictly defined what pore size of filter should be used prior to SRP analysis however the pore size being used should be stated (MEWAM, 1992; Eaton et al., 2005). The choice of 0.2 µm was influenced by previous work done by Murray (2012).

Due to the typically low [SRP] and [TON] measured during analysis some extra precautions were taken to minimise contamination during the filtration process. Filter papers were washed by filtering ~5 ml of deionised water before the sample was filtered. Then, ~40 ml of sample was filtered and discarded so the paper was conditioned with sample. Finally, ~30-50 ml of sample was filtered into a 50 ml centrifuge tube refrigerated and retained for analysis. Three blanks of deionised water were also prepared using the

same protocol as above before any river samples were filtered, so any background levels of SRP and TON could be accurately corrected for in the final analysis.

### 4.1.6 TP digestion prior to analysis

Samples designated for TP analysis (collected separately, see section 3.3) were not filtered and thus represented P in both the particulate and dissolved fractions. Before TP analysis could be undertaken, a digestion was needed (Eaton et al., 2005) to convert all insoluble P fractions into soluble ones and produce a suitable sample matrix for automated colorimetric analysis (Rowland & Haygarth, 1997). Before all TP digestions, all glassware used was cleaned with phosphate-free 2% Decon® solution and then soaked in 10% hydrochloric acid for at least 1 hour before rinsing thoroughly with deionised water.

For the digestion 30% sulphuric acid ($H_2SO_4$) and analytical grade potassium persulphate ($K_2S_2O_8$) reagents are needed. The 30% sulphuric acid solution can be made by carefully adding 150ml concentrated sulphuric acid to 300ml deionised water. This mixture was allowed to cool then made up to 500 ml with deionised water.

For the TP digestion, 20 ml of well-mixed, unfiltered sample, was pipetted into a 30 ml screw cap bottle and 0.4 ml 30% $H_2SO_4$ and 0.2g $K_2S_2O_8$ was added. The weight of each container (without lid) was recorded. Samples were placed in autoclave, above the water line and covered with aluminium foil to avoid contamination as water droplets were found to be entering bottles otherwise. For full digestion to take place samples were heated for 30 minutes at 126 °C. After the autoclave had finished, containers were removed and allowed to cool. Each bottle was then re-weighed (making sure the outside was dry and aluminium foil removed) and made back to the original weight with deionised water to replace water lost during the autoclaving procedure. The same procedure was undertaken creating blanks using 20 ml of deionised water rather than sample (Eaton et al., 2005).

### 4.1.7 Phosphorous and nitrogen colorimetric analysis

All [P] and [N] were measured using automated colorimetric techniques, where reagents react with the analyte to produce a colour of a certain wavelength whose absorbance is then measured. A Technicon® Autoanalyser II, utilising the air segmented continuous flow technique was used. The system consisted of eight major components; automated sampler, peristaltic pump, water bath (20 °C for reagents and 37 °C for chemical reactions and mixing manifold), manifold, colorimeter, analogue chart recorder, BBC computer and printer.

Each nutrient analysis was carried out using the same apparatus except for the chemistry manifold which has the appropriate tubing and mixing coils on it for the specific colorimetric reaction. After the sample reactions occur in the manifold, the sample passes through the flow cell in the colorimeter where the absorbance of light at a specific wavelength is measured. This is recorded as a peak height on the chart recorder. The concentration is calculated by reference to the peak heights produced by the standard solutions. A peak with a more distinct and better defined shape, the more precise the concentration value measured will be.

Even though SRP and TON samples were filtered as soon as possible after field collection, they were still susceptible to bacterial degradation and immediate analysis was always sought. In 2013, an undergraduate student project attempted to quantify the effect of time on concentration between filtration and analysis. Results, from Gordonbush samples indicated that samples filtered for SRP and TON analytical purposes were both stable for five days before concentrations of both began to decrease. The biggest decrease in concentration was caused by not refrigerating samples, emphasising the need to keep samples stored at approx. 4 °C after filtration (Bazeley, 2013). The same study also quantified the limit of detection (LOD) and limit of quantification (LOQ) for SRP, TP and TON analytical methods which are displayed in Table 4.1.

| Analytical Method | LOD (µg $l^{-1}$) | LOQ (µg $l^{-1}$) |
|---|---|---|
| SRP and TP | 0.2 | 0.5 |
| TON | 0.3 | 1.1 |

**Table 4.1 - Analytical measurements limits of Technicon system**
Limit of detection (LOD) and limit of quantification (LOQ) of Technicon analytical systems. Results in Table 4.1 were provided from work undertaken by Bazeley (2013).

The following methods used for SRP, TP and TON analysis are taken from the Technicon Methods Handbook and were developed for low level analysis (Flowers, 2014). Reagents were made using AnalaR® grade chemicals and helium de-gassed de-ionised water. All analytical reagents, standard stock solutions and working standards were stored below 4 °C between analyses. All glassware used for preparing reagents for purposes of SRP and TON analysis were soaked overnight in 2%, phosphate-free Decon® solution. Glassware was then rinsed thoroughly, firstly with tap water then with deionised water. Glassware was dried in a drying cupboard.

### 4.1.7.1 Technicon® Autoanalyser II standard set-up and maintenance

Wash Chamber

To help minimise cross-contamination between samples during colorimetric analysis, wash solution was injected by the auto-sampler between samples. For TON analysis the wash solution was 0.2 ml 15 % Brij-35 solution dissolved in 1 litre (L) of de-ionised water, whilst de-ionised water only was used for SRP analysis system as the wetting agent Brij-35 interferes with the SRP system. The TP system used an acid wash made by diluting 6 ml concentrated sulphuric acid in 1 L of deionised water.

Establishing a baseline prior to analysis

A steady baseline signal and a regular bubble pattern were required on the Technicon Autoanalyser before any analysis was conducted. During a sample run, drift occurred due to electronic drift and changes in room temperature. To quantify drift, the two standards with the largest concentrations followed by a wash and two zero standards were analysed after every twelve samples. The drift during the twelve samples was then calculated by the computer program from the two adjacent sets of standards and used to adjust the sample concentrations. Three blanks and the series of samples were run in duplicate and a mean concentration calculated.

Cleaning and Maintenance

Before each use, the rollers of the peristaltic pump were cleaned with ethanol to ensure smooth flow of reagents through the appropriate sample lines. Appropriate parts of the pump were also well oiled and greased. The manifold and tubing of the Technicon was cleaned when switching between determinants by rinsing for 15 minutes with either 5 % $H_2SO_4$ solution or, a 1 M NaOH solution, depending whether the reagent mix had been alkaline or acidic respectively. De-ionised water was then flushed through the system for a further 20 minutes.

## 4.1.8 SRP and TP analysis

An adapted version of ammonium molybdate-ascorbic acid method (Murphy & Riley, 1962) was used for low level analysis of SRP and TP. The method is based upon the orthophosphate ion reacting with ammonium molybdate in an acid solution to form phosphomolybdic acid, a faintly yellow coloured product. The product is then reduced using ascorbic acid to give an intense blue colour. Antimony potassium tartrate is added

to increase the rate of the reaction. This reaction is preferred over other methods as it is less temperature sensitive and the chromophore is more stable (Robards et al., 1994).

#### 4.1.8.1 Reagents for SRP and TP analysis

The same reagents were required for SRP and TP analysis however the recipes for the acid molybdate solutions differ slightly between the methods.

Acid molybdate solution

The following recipe is suitable for acid molybdate solution used for SRP analysis. 120 mL concentrated sulphuric acid was added to 700 ml de-ionised water in a 1 L glass amber bottle and the solution was allowed to cool. Ammonium molybdate (10.4 g) was added whilst stirring. Antimony potassium tartrate (0.2 g), was dissolved in 50 ml de-ionised water and added to the acid solution with gentle mixing to avoid the formation of a precipitate and made up to 1 L with de-ionised water. This solution was stored in the dark and was stable for at least 1 month after it was initially made.

To compensate for the background acid within digested TP samples, the acid content (concentrate sulphuric acid) for acid molybdate solution for TP analysis had to be reduced to 70 ml per litre rather than 120 ml. Apart from this adjustment, the recipe above should be followed. The increased acidity of TP digests is also the reason an acid solution is required for wash chamber during TP analysis.

Ascorbic acid solution

Ascorbic acid (1.5 g) was dissolved in 90 ml de-ionised water in a 100 ml volumetric flask, 2.5 ml of 10 % sodium dodecyl sulphate (SDS) wetting agent was added, and the volume made up to the mark with de-ionised water. This reagent was unstable and unsuitable for long term storage so was freshly prepared on the day of analysis. The SDS stock solution must be fully dissolved, so if necessary, it was placed in an ultrasonic bath for 15-20 minutes prior to analysis.

Background colour correction

Concentrated sulphuric acid (120 ml) was added to ~700 ml deionised water in a one litre glass bottle. After allowing the solution to cool 3.34 g ammonium sulphate was added and dissolved by stirring. The reagent was degassed and made up to 1 L with degassed water and mixed gently. This reagent was stable for several months and could be degassed ultrasonically during long intervals between uses if required to retain its function.

This reagent replaces the acid molybdate reagent when running an SRP colour correction analysis. No colour correction is needed for TP analysis as the TP digestion process eliminates all colour from the samples resulting in a clear liquid being formed.

### 4.1.8.2 Standard solutions for SRP and TP analysis

A 1000 mg $l^{-1}$ phosphate-P standard stock solution was made using potassium dihydrogen phosphate, dried at 105 °C for 1 hour and allowed to cool in a desiccator. Dry potassium dihydrogen phosphate (4.394 g) was dissolved in approx. 900 ml de-ionised water in a 1 L volumetric flask and made up to the volume with de-ionised water. A working standard of 0.1 mg $l^{-1}$ was typically prepared for SRP from this using the appropriate dilution.

A working standard of 0.1 mg $l^{-1}$ was prepared for TP analysis from the same stock solution. To keep the matrix the same as the samples, 1 ml 30 % $H_2SO_4$ plus 0.3 g $K_2SO_4$ was added to 100 ml of standard. In addition, 1 ml of 30 % $H_2SO_4$ plus 0.3 g $K_2SO_4$ was added to 100 ml de-ionised water and used as a zero standard.

### 4.1.8.3 SRP and TP manifold

SRP and TP analysis used the same manifold set up. The minor difference between the two set-ups was the wash chamber solution for TP analysis was acidic compared to deionised water for SRP analysis. TP wash chamber solution contained 6 ml concentrated sulphuric acid per litre of deionised water.

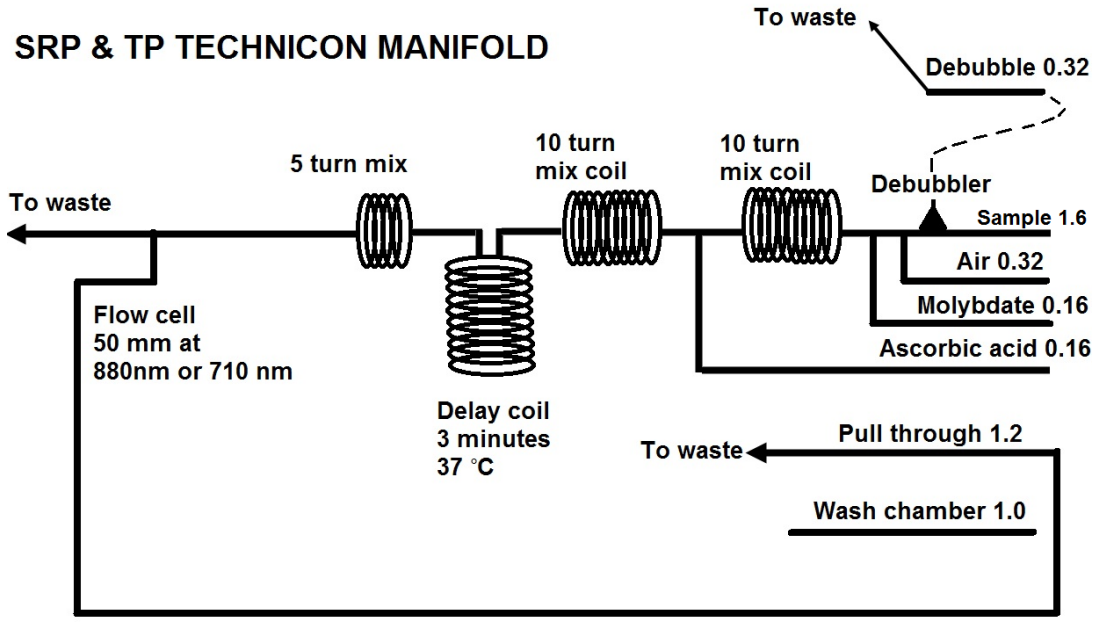


**Figure 4.1 - RP and TP Technicon manifold**
For example, “Air 0.32” means Air has a flow rate of 0.32 ml per minute through the manifold, etc. The manifold for RP and TP analysis had a sampling rate of 40 per hour. This system was capable of measuring phosphorous concentrations up to 0.5 mg $l^{-1}$.

## 4.1.9 TON analysis

TON in water samples comprises both nitrate ($NO_3^-$) and nitrite ($NO_2^-$) molecules. Nitrites usually only occur in trace amounts in natural waters (Lichvarova, 2001) therefore [TON] is routinely measured and interpreted to represent the maximum [$NO_3^-$] (Eurostat, 2012).

The [TON] was determined using a method based on the reaction in Mullin & Riley (1955) and the automated methods of Henriksen (1965) and Best (1976). $NO_3^-$ is quantitatively reduced to $NO_2^-$ by hydrazine under alkaline conditions using the copper (II) ion as the catalyst. The total $NO_2^-$ is subsequently treated with sulphanilamide and N-1-napthylenediamine dihydrochloride under acidic conditions to form a pink dye. This method therefore measures both $NO_3^-$ and $NO_2^-$ in the sample i.e. TON.

### 4.1.9.1 Reagents for TON analysis

Buffer solution

Sodium tetraborate (22.5 g) and 2.5 g sodium hydroxide were dissolved in 900 ml of degassed and de-ionised water and the solution was made up to 1 L in a volumetric flask.

Griess Reagent

Concentrated hydrochloric acid (100 ml) was added to 800 ml of degassed and de-ionised water in a 1 L volumetric flask. Sulphanilamide (10.0 g) and n-1-napthylenediamine dihydrochloride (0.5 g) were weighed into a 1 litre beaker and a quantity of the acid solution was added and stirred until compounds were dissolved. This solution was then added to the remaining hydrochloric acid and made up to 1 L in the volumetric flask using degassed and de-ionised water. This reagent was prepared in a fume cupboard.

Reducing agent

Hydrazine sulphate (0.3 g) was added to 900 ml of degassed and de-ionised water in 1 L volumetric flask. The mixture was stirred gently with a magnetic stirrer to dissolved hydrazine sulphate powder, avoiding the formation of a vortex to prevent the entry of oxygen into the flask, which can react with hydrazine and decrease the reducing power of the reagent. Brij-35 solution, 2 ml of 15 %, was added and mixed gently before 1 L volumetric flask was made up to the mark using degassed and deionised water. This reagent was prepared in a fume cupboard because of carcinogenic properties of hydrazine sulphate. The reagent was not stable and had to be made up fresh upon each day of TON analysis.

Catalyst solution

Copper sulphate solution, 1 ml of 2.47 %, and 2 ml of Brij-35 15 % solution were added to 900 ml of degassed and de-ionised water and the resulting solution was gently stirred. The solution was made up to 1 litre mark with degassed and deionised water.

Background colour correction

A 250 ml solution was made by adding 25 ml concentrated HCl acid to approx. 200 ml of helium de-gassed de-ionised water in a 250 ml volumetric flask and mixed gently before making up to volume with helium de-gassed de-ionised water. This colour correction reagent replaces the Griess reagent and does not contain sulphanilamide and n-1-napthylenediamine dihydrochloride.

### 4.1.9.2 Standard solutions for TON analysis

A 1000 mg $l^{-1}$ nitrate-N standard stock solution was made using sodium nitrate, dried at 105 °C for an hour and allowed to cool in a desiccator. 6.068 g of the dry sodium nitrate was dissolved in approx. 900 ml de-ionised water in a 1 litre volumetric flask and made up to the volume with de-ionised water. A working standard (e.g. 1 mg $l^{-1}$) was prepared by appropriate dilution.

### 4.1.9.3 TON manifold

The TON method (Flowers, 2014), was adapted slightly from the original method due to high OM content of the samples that was thought to increase complexation of the copper catalyst. The Brij-35 15% solution (wetting agent) content of both the copper catalyst and hydrazine sulphate reducing reagent were doubled to aid flow of reagents through the manifold and stop excess copper build up in reagent lines. The flow rate of reagents was increased to 1.9 ml per minute through a 50 mm flow cell so as to increase sensitivity of the instrument, which was an important amendment as generally measured [TON] from Gordonbush samples were very low.

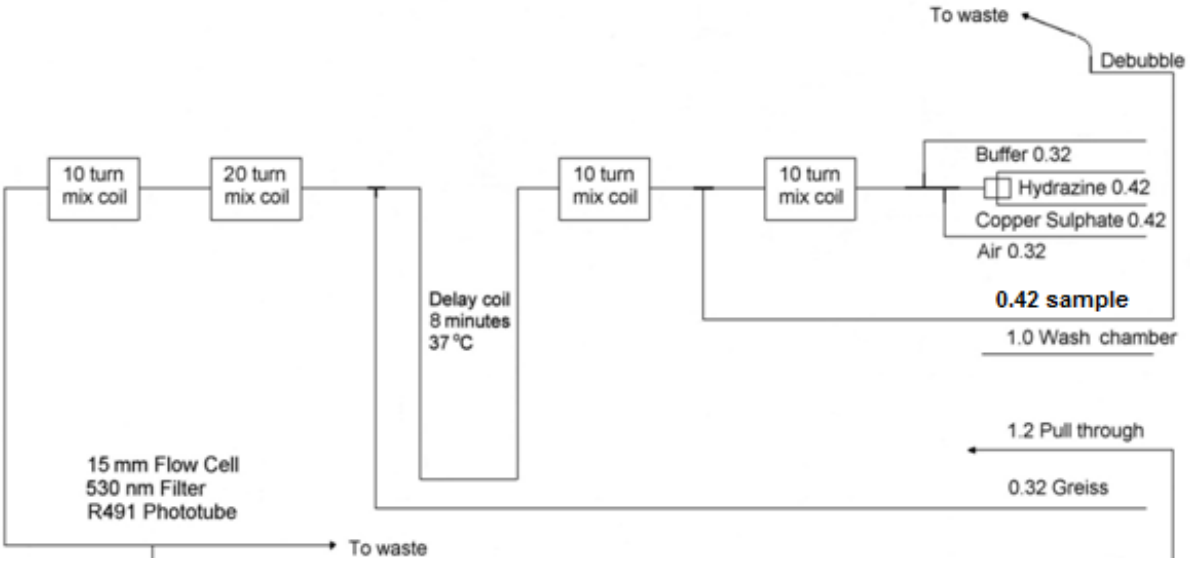


**Figure 4.2 - TON Technicon manifold**
For example, "Buffer 0.32" means the Buffer solution has a flow rate through the manifold of 0.32 ml per minute, etc. The manifold for TON analysis had a sampling rate of 50 per hour. This system was capable of measuring [TON] up to 5 mg $l^{-1}$.

### 4.1.10 SRP and TON analysis colour correction

During colorimetric analysis problems can occur when analysing naturally highly-coloured samples and where the ratio of colour to analyte required for very low level analysis is high, such as in this research. Here, the background colour of the sample may interfere at the same wavelength and lead to an increased measure of absorbance and thus an over-estimation of [nutrient] in the sample. Correction for the background colour of the sample is therefore required, as described in detail in Murray (2012).

To correct for background colour in the SRP and $NO_2^-$ analyses, the samples were first run using the standard procedure and reagents to obtain non-colour corrected concentrations. The relevant reagents were then replaced by the modified colour correction reagents (sections 4.1.8.1 and 4.1.9.1) and the baseline was re-established. All other settings were kept the same so that the peak heights could be directly related to the peak heights of the previous run. The same series of standards, blanks and samples were then run and, since no colour reaction was taking place, both standards and blanks gave the same low reading, and the peaks produced by them could be attributed to the background colour of the samples.

The method for correcting for background colour is based on the assumption that the peaks produced by the reaction colour and the background colour are additive so the true sample concentration can be quantified by subtracting the height of the peak produced by background colour in the absence of the colorimetric reagent from the sample peak height. Since no colour reaction takes place, the standards in the colour correction run give a reading at the base line (Figure 4.3). To calculate a correction expressed in concentration units on the Technicon computer, the peak heights of the colour correction standards were calculated using the peak heights from the non-colour corrected run (Eqn. 4.2) and inserted manually into the data file and the calculation programme was executed. The colour corrected concentration for a sample was obtained by subtracting the concentration determined in the colour correction run from the concentration determined in the non-colour corrected run as outlined in Eqn 4.2:

$$\text{colour correction}_{\text{standard peak}} = \left\langle \text{non-colour corrected}_{\text{standard peak}} - \text{non-colour corrected}_{\text{mean zero}} \right\rangle + \text{colour correction}_{\text{mean zero}} \quad \text{Eqn (4.2)}$$

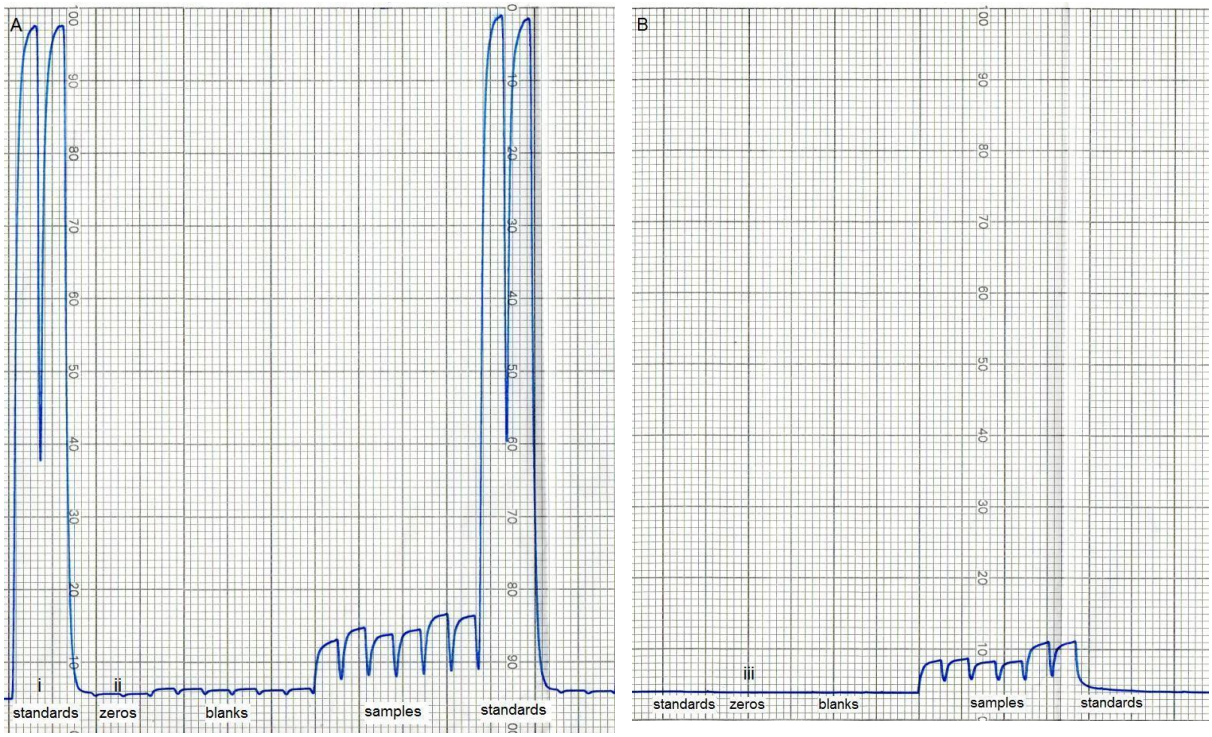


**Figure 4.3 - Standard and sample output from colorimetric analysis**
A (left) = non colour corrected data. B (right) = colour correction data, i = non-colour corrected standard peak, ii = non colour corrected zero and iii = colour correction zero.

# 4.2 Sediment analysis

## 4.2.1 Loss on ignition: Sediment core samples (lake and peat)

The same basic LOI technique that used for analysis of [POC] (section 4.1.4) was also used to analyse C content of lake and peat sediment core samples. For LOI analysis of lake and peat sediment core samples, one $cm^3$ sediments samples, sub-sampled of at one cm resolution for all cores, were placed into silica crucibles rather than on filter papers; the sediment was dried for 16 hours (overnight) at 105 °C and combusted at 550 °C for 4 hours, all of which is standard practice (Dean, 1974; Heiri et al., 2001; Beaudoin, 2003; Chambers et al., 2010). Similar to POC analysis, we used desiccators and tweezers to handle crucibles to avoid uptake of moisture. Both $\%LOI_{550}$ and % organic C content were calculated from Eqn's 4.3a and 4.3b, respectively.

$$LOI_{550} = [(S_{105} - S_{550}) / S_{105}] \quad \text{Eqn (4.3a)}$$

$$organic\ C = LOI_{550} * 0.58 \quad \text{Eqn (4.3b)}$$

where $S_{105}$ and $S_{550}$ are weights of sediment sample after drying at 105 °C and 550 °C respectively. In equation 4.3b the 0.58 represents the van Bemmenlen factor.

## 4.2.2 Grain size analysis

Grain size analyses were undertaken on materials from the sediment trap and Loch Brora core samples.

Following LOI analysis, samples were retained for particle size analysis. The remaining sediments were firstly gently ground to separate grains that had agglomerated during LOI analysis. Sediments were transferred to 50 ml plastic containers, 25 ml of tap water and 6 ml of an anti coagulating reagent (sodium hexametaphosphate dissolved in water) were added and the mixture placed in an ultrasonic bath (3 minutes) to help aid the separation of all individual particles and stop coagulation. The samples were then mixed using a magnetic stirrer.

Particle sizes (up to 2000 µm) were measured using laser diffraction on Coulter LS230 instrument. Particles sizes measuring less than 0.4 µm utilised additional Polarization Intensity Differential Scattering (PIDS) for characterisation. Further information about the method can be found on the Beckman Coulter Website.

## 4.2.3 Sediment (peat and lake) age dating

Two techniques were used: $^{210}$Pb dating for purposes of age model between 0-150 years; $^{14}$C radiocarbon dating to generate ages on a 0-60,000 year scale.

### 4.2.3.1 $^{210}$Pb and $^{137}$Cs radiometric dating

$^{210}$Pb is created by radioactive decay of $^{214}$Pb as part of the $^{238}$U natural decay series (Figure 4.4) and has a half life of 22.3 years making it a suitable isotope to date sediment accumulated over the last 150 years, (Appleby, 2008; MacKenzie et al., 2011). Sedimentation rates are always calculated using the dry mass of a material so all samples were freeze dried (see section 4.2.5.1) before analysis (Appleby, 2001). A typical $^{210}$Pb well preserved sediment profile that is not subject to disturbance would normally have unsupported activities starting at 100 to 250 mBq g$^{-1}$ (Appleby, 2008) trending to zero towards bottom of the core, forming a downward exponential pattern.

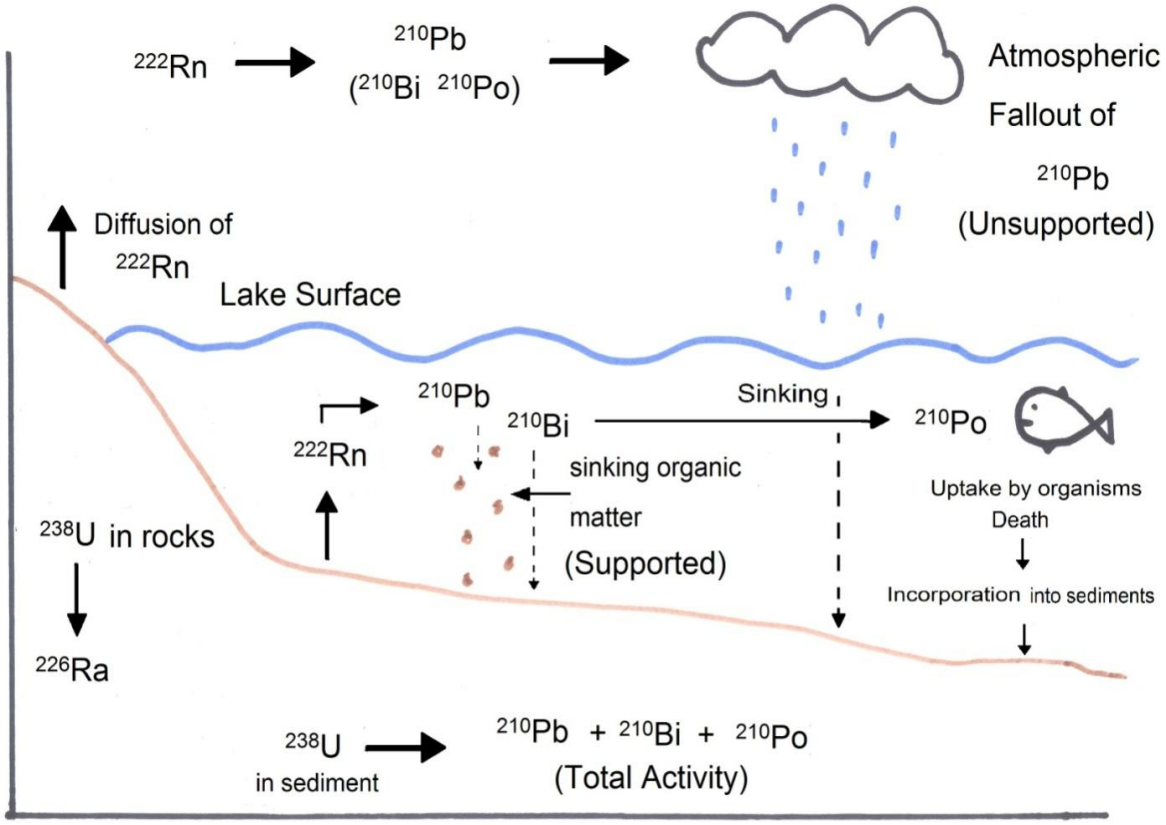


**Figure 4.4 - Transfer of lead in aquatic environments**
$^{210}$Pb transport and incorporation into lake sediments within natural environment, highlighting Supported and Unsupported elements of $^{210}$Pb deposition, adapted from (Oldfield & Appleby, 1984). Although an aquatic environment is illustrated above, exactly the same processes occur in land-based sediments i.e. peatland sediments.

Measurements of $^{137}$Cs concentrations can be used to refine and constrain core $^{210}$Pb chronologies (Appleby, 2001, 2008). Typical $^{137}$Cs profiles for undisturbed sediments in

the Northern Hemisphere, particularly NW Europe, show two distinct peaks which are associated with two specific historical events and subsequently known increases in atmospheric $^{137}$Cs and subsequent deposition. These relate to widespread nuclear bomb testing before a treaty prohibiting all open-air test detonations of nuclear weapons was signed in 1963 and the Chernobyl nuclear disaster in 1986 (Appleby, 2001).

High Purity Germanium (HPGe) gamma photon detectors were used to measure all radionuclides ($^{210}$Pb, $^{214}$Pb ($^{226}$Ra), $^{214}$Bi and $^{137}$Cs) during dating procedures following 3 weeks of storage in sealed containers to allow radioactive equilibration. Absolute efficiencies of the detectors were determined using calibrated sources and standards of known activity. Corrections were also applied for the effect of self-absorption of low energy γ-rays within samples (Appleby et al., 1986; Appleby, 2001). For full methodology please refer to the following papers (Oldfield et al., 1979; Appleby & Oldfieldz, 1983; Oldfield & Appleby, 1984; Appleby et al., 1986; Oldfield et al., 1995; Appleby, 2001).

$^{210}$Pb radiometric dating analysis on peat core samples from GB1 and GB2 (cut) was carried out at Durham University Environmental Radioactivity laboratory due to their ability to handle small samples sizes with low activity. Peat typically accumulates very slowly (0.2-0.7 millimetres per year (Borren et al., 2004; Gorham et al., 2012)) leading to measureable $^{210}$Pb activity only likely to be detected in the top 20 cm of peat sediment. Also, the peat cores retrieved only had a diameter of 5 cm leading to a small amount of measureable sample (<2 g of sediment (dry weight) at 1 cm resolution). Lake sediment from Loch Brora was $^{210}$Pb dated at University of Stirling Environmental Radioactivity Laboratory.

#### 4.2.3.2 Radiocarbon ($^{14}$C) dating

All radiocarbon ($^{14}$C) dating was performed using accelerator mass spectrometry (AMS) at Scottish Universities Environmental Research Centre (SUERC), East Kilbride. The half life of $^{14}$C is 5720 ± 30 (Godwin, 1962) making it an ideal radionuclide to date lake and peat sediment on 0-60,000 year scale. In the absence of suitable macrofossils (e.g. branch, stem, seed or leaf fragments), which is the preferred material for $^{14}$C dating (Nilsson et al., 2001), humic acids were alternatively extracted from bulk peat samples and dated (Piotrowska et al., 2011). A brief summary of techniques used are given however a more comprehensive review of $^{14}$C dating is available in (Björck & Wohlfarth, 2001).

Humic acid dating for peat samples (pre-treatment)

The aim of radiocarbon pre-treatment for peat is to separate and isolate the humic acid fractions of sample from the other two main components, the fulvic acid and humin fractions. The acid/alkali/acid (AAA) method outlined in (Cook et al., 1998) is commonly used in pre-treatment of peat samples to remove humic acids. Once separated, the humic acids are freeze dried, combusted to generate $CO_2$ then reduced to graphite to make a suitable target for AMS analysis (Björck & Wohlfarth, 2001; Piotrowska et al., 2011).

AMS radiocarbon dating

AMS is the most modern and commonly used technique in $^{14}C$ dating. The [$^{14}C$] is determined by counting $^{14}C$ atoms in an ion beam produced by the sample (Björck & Wohlfarth, 2001; Piotrowska et al., 2011). Calibration of results was undertaken using standard procedures (Stuiver & Reimer, 1993; Reimer et al., 2008; Heaton et al., 2009) and the most recent internationally recognised calibration curves (Reimer et al., 2007; Reimer et al., 2009; Reimer et al., 2011; Reimer et al., 2013).

## 4.2.4 Calculation of C sequestration rates

When LOI and age of peat and lake sediments have been calculated it is then possible to determine C sequestration rates within any particular core. C sequestration rates are conventionally expressed as a weight of C per area size, per period of time, i.e. g C $m^{-2}$ $yr^{-1}$. Below is an explanation of how grams C per $cm^3$ (g C $cm^3$) and accumulation rates (cm $yr^{-1}$) are multiplied together and converted into g C $m^{-2}$ $yr^{-1}$ (Eqn 4.4).

1. $\left[\left(\frac{g\ C}{cm^3} \times \frac{cm}{yr}\right)\right. = g\ C\ m^{-2}\ yr^{-1}$
2. $\left[\left(\frac{g\ C\ cm}{cm^3 yr}\right)\right] = g\ C\ m^{-2}\ yr^{-1}$
3. $\frac{g\ C}{cm^2 yr} = g\ C\ m^{-2}\ yr^{-1}$
4. $\frac{\frac{g\ C}{yr}}{m^2} = g\ C\ m^{-2}\ yr^{-1}$

Eqn (4.4)

Steps 1-3 for equation 4.4 follow simple rules of multiplying fractions and dividing through by common terms. To get from steps 3-4, both lines of the equation need to be divided by a period of time term, e.g. (yr) and $cm^2$ need to be converted to $m^2$ by multiplying by a factor of 1,000,000 (10^6).

C sequestration rates can be calculated between any two points where the age of the sediment is known (i.e. accumulation rate can be worked out) and the C content (i.e. %LOI). Ages and C content are typically determined at 1 cm resolution and this was the

case for all sediment cores collected at Gordonbush. Since accumulation rates and C content can vary considerably from 1 cm to the next, C sequestration rates can be quite variable throughout any particular core. Long term averages of C sequestration rates are also commonly quoted which are calculated by simply multiplying the long-term accumulation rate (basal depth divided by basal age) and average C content.

## 4.2.5 Quantifying chlorophyll *a*

Chlorophyll *a* converts light energy into chemical energy allowing photosynthesis (light-induced C fixation) to take place (Aminot & Rey, 2000). Therefore, it is a commonly used biochemical parameter used to measure primary production rates in aquatic environments (White et al., 1991; Peterson et al., 1993; Kritzberg et al., 2006). Chlorophyll *a* determination is complex, non-specific and since the substances being tested are light sensitive protection from light sources during analysis is a constant concern (Aminot & Rey, 2000). In addition, all traces of water must be removed prior to chlorophyll *a* analysis undertaken on solid substances, i.e. collected samples from sediment traps and artificial substrates. To do this, a **Christ Alpha 1-4 LD-2** freeze drier was used. Freeze drying (also known as lyophilisation), a process where ice is converted directly to water vapour (sublimation), occurs under vacuum when a substance is <10°C. Freeze drying is also the gentlest process for preserving the biological properties of sensitive tissue components (Operating Manual Freeze Dryer ALPHA 1-4 LD-2, (Christ, 2014)).

### 4.2.5.1 Chlorophyll *a* measure using spectrophotometry

Material collected on the artificial substrates was scraped from the tile using a glass slide and toothbrush, whilst rinsing with a small amount of deionised water. Excess water was removed by centrifugation (at 1400 rpm for > minutes), the supernatant decanted and the residue transferred to a pre-weighed plastic breaker. The sample was then frozen to solidify and aid the freeze-drying process. The sample material was freeze-dried (section 4.2.5) in the dark to minimise chlorophyll *a* degradation. The yield of dry material was calculated by weighing the full beaker and subtracting the weight of the empty beaker.

A minimum of 50 mg was required for chlorophyll *a* analysis. Recorded amounts of sample was then transferred into centrifuge tubes and 5 ml of acetone added before being refrigerated for 24 hours to allow the chlorophyll pigment to fully develop. Any remaining freeze dried material was placed in small glass vials, covered in aluminium foil and stored in a freezer preserved for any future analysis.

After 24 hours, acetone extract from each sample was pipetted into glass cuvettes (path length = 1 cm), ensuring that no particulate material was transferred. Absorbance of extracts was then measured using a spectrophotometer against a 90% acetone blank at range of wavelengths: 750, 665, 664, 647 and 630 nm respectively. Hydrochloric acid (0.2 ml of 1%) was then added to each sample and left for two minutes before absorbance was recorded again (against 90% acetone blank) at wavelengths 665 and 750 nm.

Two methods were then used to calculate [chlorophyll *a*] from a series of options (Aminot & Rey, 2000). The first method and formula (Eqn 4.5) is related to the monochromatic process of calculation (Wetzel & Likens, 2002), utilising the acidified sample absorbance's (Lorenzen, 1967):

$$\textit{Chlorophyll a } (\mu g\ ml^{-1}) = \boldsymbol{k} * \boldsymbol{F} * ((E_{665o} - E_{750o}) - (EA_{665a} - EA_{750a})) / \boldsymbol{z} \qquad \text{Eqn (4.5)}$$

In Eqn 4.5 (monochromatic method for calculating chlorophyll [*a*]), *k* is the absorption coefficient of chlorophyll *a* (11), *F* is a factor associated with the maximum absorbance ratio of $E_{665o}/E_{665a}$ in the absence of pheopigments (2.43) and *z* is path length of the sample cuvettes used (1cm). Therefore '*k* * *F/z*' can be simplified to 26.73.

The same steps outlined earlier were used to get from (µg $ml^{-1}$) to (mg $m^{-2}$ $day^{-1}$). This method is supposed to correct for presence of pheopigment *a* in chlorophyll *a* calculations (Aminot & Rey, 2000); however, it would often give spurious results (e.g. negative productivity rates). This raised suspicion that the acidification was the cause of these problems so an alternative method (Eqn 4.6) was found that did not involve acidification of samples, the trichromatic method (Jeffrey & Humphrey, 1975):

$$\textit{Chlorophyll a } (\mu g\ ml^{-1}) = (11.85*(E_{664} - E_{750}) - 1.54*(E_{647} - E_{750}) - 0.08*(E_{630} - E_{750})) \quad (4.6)$$

In Eqn 4.6 (trichromatic method for calculating chlorophyll [*a*]), for example, $E_{664}$ represents the absorbance value measured at 664 nm. This method gave no spurious results and became the preferred method. When both methods were compared, Eqn 4.6 (Jeffrey & Humphrey, 1975) normally returned a higher result than Eqn 4.5 (Lorenzen, 1967). This means productivity rates could have been underestimated from the start of the chlorophyll *a* time series (February 2011) until Eqn 4.6 (Jeffrey & Humphrey, 1975) was used from August 2012 to end of data collection in September 2013.

From the equations above results obtained were µg $ml^{-1}$. These were multiplied by amount of acetone used (5 ml) and divided by weight of material used to give (µg $g^{-1}$). Results were finally multiplied by 1000 and divided by the area of substrate (mg $m^{-2}$) and

then the number of days since last collection to give an overall rate of production per day (mg $m^{-2}$ $day^{-1}$).

## 4.3 Data analysis

### 4.3.1 Statistical analysis

Minitab v.16 statistical software was used to generate: linear regression equations and associated prediction intervals (e.g., DOC- discharge relationships and stage-discharge ratings curves for studied rivers), correlations (e.g. [TP] vs. [POC]), multiple linear regressions (e.g., to predict [DOC] from physical parameter), cross-correlation analysis to calculate time lags between two different stage height data sets and paired t-tests to compare various means (e.g. drain-blocking [DOC] data). In addition, linear modelling packages in R and R studio were utilised to assess drain-blocking had a significant statistical affect on WTD from the data collected. Frequency distributions and box-plots were also used to illustrate certain aspects of descriptive statistics and these were created in either R or Excel.

### 4.3.2 Sediment age-depth modelling using *Bacon*

R, R studio and open-source software package *Bacon* v2.2 was used to construct age-depth peat core and lake chronologies using Bayesian statistics (Blaauw & Christen, 2011). Radiocarbon dating results can be calibrated within the *Bacon* software program using the IntCal13 calibration curve (Reimer et al., 2013). This facility was utilised and all calibrated radiocarbon ages of peat and lake sediments were calculated using *Bacon* software. This in turn also allowed sedimentation and C sequestration rates to be calculated for all peat and lake sediment cores collected during this research. Additional information regarding *Bacon* software is given in the methods section of Chapter 7, section 7.3.

### 4.3.3 GIS analysis

ArcGIS® 10.1 software by Esri® and all associated subsidiary packages (ArcGIS® and ArcMap™, see www.ersi.com) were used to create maps and identify catchment features. Access to data files containing certain catchment attributers e.g. underlying geology, was granted by Digimap® (see Digimap website), a service run by University of Edinburgh.

# 5 Fluvial carbon and nutrient time series from Gordonbush windfarm

## 5.1 Abstract

Here I use time series of [DOC], [POC], [TP], [SRP] and [TON] covering the period prior to, throughout and after windfarm completion, to assess if there is a change in water quality associated with the construction activities. Time series data and hysteresis analysis will also be utilised to investigate macronutrient interactions to better understand source, export characteristics and fate of C and nutrients species in from Gordonbush peatlands. The bulk of sample collection was undertaken during storm events, ensuring that a maximum concentration of each determinant was captured. Seasonal patterns were observed for [DOC], [TP] and [TON] as well as for primary productivity rates calculated from measuring [chlorophyll *a*]. From the fluvial C and nutrient concentration time series data, it seems that deforestation in the Bull Burn Plantation, as part of the HMP, may have caused an increase in [DOC], [TP] and [SRP] relative to other catchments where forest felling did not occur. However, concentration ranges for all determinants are still comparable to other studies in temperate peatland sites and are indicative of the “Good” and “High” water quality as defined by standards set by European Union Water Framework Directive (EU WFD) (UK TAG, 2013). Therefore, apart from the legacy of forest felling, there is limited evidence to suggest the windfarm construction has impacted macronutrient fluvial concentrations in studied rivers.

Carbon concentration data presented in this chapter will be used when calculating aquatic organic C flux estimates later on in the thesis (Chapter 6). Additionally, hysteresis results will be utilised to best inform decisions on the methodology of constructing C export budgets and assess the strength of all estimates calculated.

Hysteresis analysis indicated A2 loops dominated in summer and spring-autumn [DOC] whereas winter [DOC] produced C2 loops for all three catchments. Data from GB12 showed the occurrence of more cross-over loops compared to GB10 and GB11 but this was attributed to its smaller catchment size. All hysteresis analysis of [POC] produced C2 loops in all studied catchments. A strong inverse relationship between [DOC]-[TON] was observed. It was attributed to differences in seasonal maximum but it is also possible that high [DOC] suppresses TON production and subsequently its export. A curvi-linear association between [DOC]-[SRP] suggests that SRP is mobilised in upper layers of peat soil and washed out of soil on rising limbs of storm events.

## 5.2 Introduction

Land use change and anthropogenic disturbance can increase concentrations of macronutrients and turbidity in rivers draining from peatlands which can have a negative effect on river biology and ecology (Muller & Tankere-Muller, 2012). Although there are guidelines to minimise this (Scottish Renewables et al., 2013) and measures aimed at controlling it (Scottish Renewables & SEPA, 2012), considerable amounts of soil disturbance can occur during the construction of windfarm developments on peatlands. Current environmental impact assessments (EIA) do not (and are currently not required to) investigate how resilient peatlands are to adaptations needed to host a windfarm. This information is vital however if the "carbon payback calculator" (Nayak et al., 2009) is to accurately be informed of recovery times, associated with construction activities and will help inform future management of these landscapes.

This research focussed on storm event sampling, so with the resultant time series, temporal and hydrological variability in fluvial C and nutrient concentrations could be examined. Ensuring measurement of [DOC], [POC], [TP], [SRP] and [TON] over the full range of natural variability before, during and after anthropogenic induced disturbance is important when trying to detect any discernible impact. Impact of windfarm construction may also be elucidated through comparison with other fluvial sites draining peatlands. Sampling over three years also allowed seasonal variability on aquatic C and nutrients concentrations to be considered and calculation of mean values to compare data to current water quality guidelines. From these time series, whether there is an impact of windfarm construction and whether these rivers approach the quality expected from the WFD can be assessed.

The high intensity sampling of all macronutrients also allowed hysteretic responses and macronutrient interactions to be studied. Stream water chemistry varies to the greatest extent when discharge increases (Evans & Davies, 1998) and although concentrations evidently change in response; the relationships are seldom linear (Walling & Webb, 1986). Through concentration-discharge hysteresis analysis, the hydrological sources most influential in controlling [C], [P] and [N] during storms events (on both rising and falling limbs) can be identified (Klein, 1984; Seeger et al., 2004). Additionally, an objective of this chapter was to investigate relationships between e.g. [DOC]-[SRP] and [DOC]-[TON] to help better understand source and fate of each species. Studying changes in rates of primary production (i.e. algal) allowed an integrated measure of macronutrient export and so an assessment of nutrient availability in rivers and whether this may be increasing in correspondence to construction activities.

## 5.3 Methods

### 5.3.1 Water sampling and analysis

The majority of DOC, POC, TP, SRP and TON sample collection was undertaken during targeted storm events between August 2010 and May 2013. Storm event samples were supplemented by spot samples between events; the last spot sample was collected in September 2013. Due to logistics, field work trips to Gordonbush always lasted a few days so spot samples were collected each day (sometimes multiple on the same day) during times of non-event flow. Thus, the mean of spot sample results is also presented.

Artificial substrates, made of polyvinyl tiles secured to lead weights, were used to quantify primary production rates at sampling points GB10, GB11 and GB12, and were replaced approx. every 6-8 weeks from November 2010 until September 2013 (section 3.7).

All methods used to collect and analyse data presented in this chapter can be found in the methods chapter (Chapters 3 & 4).

### 5.3.2 Procedure for calculating site-specific water quality standards

Water quality standards, to which Gordonbush results were compared, were calculated. The current guidelines, which are site-specific, were introduced for reactive phosphorous (RP) in 2013 (UK TAG, 2013). RP is defined as phosphorous measured using the molybdenum blue colorimetric method commonly using an unfiltered water sample (equivalent to total reactive phosphorous: TRP), but "samples can be filtered if necessary" (equivalent to SRP) (UK TAG, 2013). The previous generic guidelines, which were in force when this research started and throughout the data collection period, defined water quality in terms of [SRP] (UK TAG, 2008). SRP analysis uses the same colorimetric method but with a filtered sample. The differences between [SRP] and [TRP] results are acknowledged as being “small” (UK TAG, 2008) and the differences between [RP] and [SRP] as “usually minor” (UK TAG, 2013).

Where samples are filtered the current guidelines recommend a filter size ≥0.45 µm (UK TAG, 2013). The pore size of filter used in the process of SRP analysis may affect the exact matrix of phosphorous forms in any particular sample. During this research, samples analysed for [SRP] were filtered using a 0.2 µm pore size filter (section 4.1.5). However, filter pore size is not considered a crucial factor in determining [SRP], albeit it is important to clearly state what size has been used (MEWAM, 1992; Eaton et al., 2005). To confirm that my filtration with a 0.2 µm filter was a valid choice, an investigation was

undertaken, quantifying [SRP] when the same samples were filtered using different pore sizes: 1.2, 0.7, 0.45 and 0.2 µm. The choice of filter paper affected [SRP] by only 0.9 to 1.4 µg $l^{-1}$ (4 samples of differing concentrations were tested, mean = 1.3 µg $l^{-1}$). Of the four filter papers tested samples filtered using 1.2 µm always gave the largest results (followed sequentially by 0.7, 0.45 and 0.2 µm) and the largest difference in [SRP] recorded for the same sample was always between 1.2 µm and 0.2 µm. However, the range of differences observed equated to only 2-3 times the LOQ (0.5 µg $l^{-1}$) of the analytical method used. This difference was considered small enough to use the results generated using a 0.2 µm filter for comparison with current water quality limits for [RP].

The acceptable [RP] for a given water quality is influenced by altitude and mean alkalinity (mg $l^{-1}$ $CaCO_3$). Rivers with higher mean alkalinity values can better buffer and resist changes in pH (EPA, 2015b) and so can better withstand the effects of increased P levels (decreases pH) and consequently will have higher [RP] standards. Oxygen is more easily dissolved in water at low altitudes (Smith, 1990) consequently rivers at higher altitudes are more susceptible to increases in [RP] and associated increase in primary productivity and biological oxygen demand. Therefore, higher altitude sites will usually lower river specific [RP] standards. A reference condition reactive phosphorous (RCRP), said to represent [RP] at near natural conditions is calculated by the following equation using alkalinity and altitude (Eqn 5.1).

$$RCRP = 10 \text{ ^ } (0.454(\log_{10}alk) - 0.0018\ (altitude) + 0.476) \qquad \text{Eqn (5.1)}$$

is taken from Water Framework Directive UK Technical Advisory Group Updated Recommendations on Phosphorus Standards for Rivers Final Report (August 2013), p. 3 & 4. (UK TAG, 2013).

The table below (Table 5.1) presents mean alkalinity and altitude values of water quality sampling points at Gordonbush. This information is needed to calculate site-specific water quality guideline thresholds.

| **Sampling site** | **Alkalinity (mg $l^{-1}$ $CaCO_3$)** Mean | SD (±) | **Altitude (m ASL)** |
|---|---|---|---|
| GB10 (Allt Mhuilin) | 10.9 (389) | 11.2 | 31 |
| GB11 (Allt Smeorail) | 10.2 (387) | 9.1 | 39 |
| GB12 (Old Town Burn) | 18.6 (383) | 15.4 | 39 |

**Table 5.1 - Mean alkalinity and altitude of Gordonbush water sampling points**
Mean alkalinity for each sampling site represents mean value for all water samples collected between August 2010 and September 2013. In brackets next to mean values is the total number of samples collected. The standard deviation (SD) of all samples measured for alkalinity is also given. Altitude values were sourced using a mobile GPS device.

Gordonbush water sampling points heights are close to sea level and have relatively low mean alkalinity (< 50 mg $l^{-1}$ $CaCO_3$), due to relatively high acidity related to the nature of rivers draining peatland catchments (Mattsson et al., 2007). The recommended site-specific [RP] standard is calculated using the following equation involving the RCPC and ecological quality ratio (EQR) values (Eqn 5.2):

$$Standard = 10 \wedge (1.0497 \times log_{10}(EQR) + 1.066) * (log_{10}(RCRP) - log_{10}(3500)) + log_{10}(3500)) \quad \text{Eqn (5.2)}$$

is taken from Water Framework Directive UK Technical Advisory Group Updated Recommendations on Phosphorus Standards for Rivers Final Report (August 2013), p.3 & 4 (UK TAG, 2013) where full details of how the standards are devised are located. “EQR” refers to ecological quality ratio, of which ratios are set at a defined value (presented in brackets) for High (0.702), Good (0.532), Moderate (0.356) and Poor (0.166) water quality classes on a scale of [RP]. “RCRP” refers to reference condition [RP] which is said to represent [RP] at near natural conditions and is calculated based on annual mean alkalinity and altitude of sampling location (Eqn 5.1).

Using Eqn’s 5.1 and 5.2 and the information in Table 5.1, the following site specific water quality guidelines were produced for Gordonbush sampling points (Table 5.2).

| | Annual mean Reactive Phosphorous (µg $l^{-1}$) | | |
|---|---|---|---|
| **Water Quality status** | **GB10** | **GB11** | **GB12** |
| High | 14 | 13 | 17 |
| Good | 30 | 29 | 35 |
| Moderate | 92 | 89 | 105 |
| Poor | 772 | 760 | 813 |
| Bad | +772 | +760 | +813 |

**Table 5.2 - Standards for phosphorous in rivers based on [RP]**
The table above, river specific annual mean [RP] standards have been calculated from criteria outlined in WFD UK Technical Advisory Group Updated Recommendations on Phosphorus Standards for Rivers Final Report (August 2013), (UK TAG, 2013). For example in GB10, any annual mean less than 14 µg $l^{-1}$ is regarded “High” water quality status, between 14-30 µg $l^{-1}$ is “Good”, 30-92 µg $l^{-1}$ is “Moderate”, 92-772 µg $l^{-1}$ is “Poor” and greater than 772 µg $l^{-1}$ is “Bad”.

No water quality guidelines exist for [TP] in rivers. [RP] largely is a measure of orthophosphate (and easily hydrolysed P) within samples whereas [TP] is measure of all forms (insoluble and soluble) of P in samples (orthophosphate, condensed phosphate and organic phosphate) following an acid digestion (EPA, 2015a). Thus water quality has also been compared against [TP] as this will be larger than [RP] and so is a conservative approach to assessing water quality.

There are no standardised water quality guidelines for [DOC] and [POC]. The main water guideline associated with N, relates to the level of nitrate, ($NO_3^-$), in drinking water which is 50 mg $l^{-1}$ (or 11.3 mg N $l^{-1}$). This guideline has been set and enforced by European Drinking Water Directive to reduce risk of methemoglobinemia (caused by ingesting excessive amounts $NO_3^-$) in infants (DEFRA, 2010).

### 5.3.3 Presentation of time series graphs

Time series graphs are presented for all storm events for each river (Figure 5.1 - Figure 5.9). Additionally [DOC] from SSER's WQMP have been included in the GB10 and GB11 time series to indicate concentrations before this research started and for comparison when both monitoring programmes were running simultaneously (Figure 5.1). GB12 was not sampled and so there is no data for this. To see easily inter-catchments differences throughout research period, mean [DOC], [POC], [TP], [SRP] and [TON] from all three rivers have been plotted on one graph per determinant (Figure 5.2, Figure 5.5, Figure 5.7 and Figure 5.9). When all three rivers are represented on the same graph, GB10 data points are always black diamonds, GB11 red squares and GB12 blue triangles. Pink markers have been inserted to highlight the start and end of windfarm construction process on each time series. Additionally, when applicable, river water quality guideline thresholds have been highlighted on time series graphs.

### 5.3.4 Discharge-concentration hysteresis

Hysteresis plots are constructed by plotting the primary control variable, i.e. discharge or stage height, against a response concentration variable, i.e. [DOC] or [POC]. Consecutive corresponding points of discharge and concentration are joined up (for a relative small time series, e.g. one particular storm event) and the resulting patterns can help inform us about what source of water is likely to be controlling the concentration variable (Evans & Davies, 1998). Hysteresis analysis was used to identify hydrological source pathways of [DOC], [POC], [TP] and [TON] during storm events. Hysteresis analysis can also help evaluate the relevance and robustness of certain linear regression relationships and methods used to produce aquatic C flux results in the next chapter.

## 5.4 Results

### 5.4.1 [DOC], [POC], [TP], [SRP] and [TON] (Tables & Time Series)

Table 5.3 summarises some descriptive statistics (minimum, maximum, mean and median) of [DOC], [POC], [TP], [SRP] and [TON] recorded during storm event and spot sampling in each of the three studied rivers at Gordonbush. The data has been split according to which hydrological year the samples were collected and a collated summary for the whole study period is also presented.

The first set of time series graphs presented show [DOC] and [POC].

| River | DOC (mg $l^{-1}$) | | | | POC (mg $l^{-1}$) | | | | TP (µg $l^{-1}$) | | | | SRP (µg $l^{-1}$) | | | | TON (µg $l^{-1}$) | | |
|---|---|---|---|---|---|---|---|---|---|---|---|---|---|---|---|---|---|---|---|
| sample code | Min. | Max. | Mean | Med. | Min. | Max. | Mean | Med. | Min. | Max. | Mean | Med. | Min. | Max. | Mean | Med. | Min. | Max. | Mean | Med. |
| **GB10** | | | | | | | | | | | | | | | | | | | | |
| 2010 (33) (2 events) | 15.7 | 37.6 | 26.3 | 27.3 | 0.6 | 7.3 | 1.8 | 1.4 | 12.1 | 80.3 | 42.5 | 47.8 | 7.9 | 38.4 | 22.5 | 25.4 | bdl | 14.5 | 5.3 | 4.8 |
| 2011 (84) (5 events) | 5.7 | 41.5 | 22.4 | 19.4 | 0.1 | 7.5 | 1.4 | 1.0 | 7.2 | 102.8 | 28.1 | 25.6 | 1.34 | 27.1 | 11.7 | 11.9 | 1.6 | 70.5 | 16.4 | 14.4 |
| 2012 (155) (12 events) | 5.1 | 48.3 | 23.1 | 23.4 | 0.1 | 11.6 | 2.3 | 1.6 | 6.2 | 264.8 | 30.3 | 23.6 | bdl | 22.8 | 10.7 | 10.2 | bdl | 108.1 | 53.0 | 56.4 |
| 2013 (73) (4 events) | 5.1 | 42.6 | 16.8 | 16.0 | 0.3 | 13.0 | 1.9 | 1.3 | 6.1 | 106.8 | 21.9 | 16.8 | 3.1 | 21.6 | 10.1 | 10.1 | bdl | 121.9 | 27.9 | 32.0 |
| All years | 5.1 | 48.3 | 21.9 | 20.0 | 0.1 | 13.0 | 1.9 | 1.4 | 6.1 | 264.8 | 29.2 | 23.4 | bdl | 38.4 | 11.9 | 10.4 | bdl | 121.9 | 32.4 | 29.3 |
| **GB11** | | | | | | | | | | | | | | | | | | | | |
| 2010 (33) (2 events) | 2.6 | 30.8 | 17.1 | 18.5 | 0.3 | 7.6 | 1.5 | 1.1 | 3.9 | 45.8 | 17.5 | 12.4 | bdl | 2.9 | 0.7 | 0.5 | bdl | 5.5 | 1.0 | bdl |
| 2011 (84) (5 events) | 1.7 | 33.3 | 15.1 | 14.1 | <0.1 | 6.5 | 1.0 | 0.6 | 1.2 | 51.0 | 14.6 | 11.6 | bdl | 14.7 | 3.0 | 2.3 | 1.2 | 49.6 | 12.3 | 9.2 |
| 2012 (135) (10 events) | 1.5 | 27.1 | 14.7 | 13.8 | 0.2 | 10.5 | 1.7 | 1.1 | 1.0 | 151.3 | 17.2 | 11.1 | bdl | 4.1 | 1.5 | 1.3 | bdl | 140.8 | 55.7 | 46.5 |
| 2013 (93) (4 events) | 2.5 | 29.8 | 9.7 | 9.1 | 0.2 | 21.3 | 2.9 | 1.2 | 1.1 | 256.0 | 17.4 | 7.9 | bdl | 7.6 | 1.1 | 1.0 | bdl | 85.4 | 24.3 | 24.5 |
| All years | 1.5 | 33.3 | 13.7 | 11.6 | <0.1 | 21.3 | 1.8 | 1.1 | 1.0 | 256.0 | 16.7 | 10.2 | bdl | 14.7 | 1.9 | 1.3 | bdl | 140.8 | 33.4 | 29.0 |
| **GB12** | | | | | | | | | | | | | | | | | | | | |
| 2010 (33) (2 events) | 2.8 | 31.4 | 15.3 | 16.2 | 0.4 | 13.6 | 1.6 | 1.1 | 2.3 | 59.7 | 16.0 | 9.6 | bdl | 0.7 | 0.3 | 0.2 | bdl | 10.7 | 3.5 | 4.1 |
| 2011 (84) (5 events) | 1.1 | 32.8 | 12.9 | 11.4 | 0.1 | 5.5 | 0.8 | 0.6 | 0.2 | 54.6 | 12.5 | 9.6 | bdl | 10.4 | 2.3 | 1.7 | 3.3 | 35.6 | 16.8 | 15.7 |
| 2012 (144) (11 events) | 1.9 | 26.8 | 13.9 | 14.0 | 0.1 | 10.7 | 1.6 | 1.0 | bdl | 79.5 | 12.4 | 8.8 | bdl | 4.0 | 1.1 | 0.8 | bdl | 81.8 | 31.3 | 32.0 |
| 2013 (80) (4 events) | 1.3 | 23.4 | 8.8 | 8.8 | 0.3 | 16.5 | 1.5 | 1.0 | 0.8 | 94.2 | 8.6 | 5.0 | bdl | 3.2 | 1.0 | 0.9 | bdl | 100.2 | 13.4 | 9.6 |
| All years | 1.1 | 32.8 | 12.6 | 11.3 | 0.1 | 16.5 | 1.4 | 0.9 | bdl | 94.2 | 11.9 | 8.3 | bdl | 10.4 | 1.4 | 1.1 | bdl | 100.2 | 19.4 | 14.0 |

**Table 5.3 - Collated table of carbon and nutrient measured concentrations**

Min. = Minimum, Max. = Maximum., Med. = Median. Descriptive statistics are given for each hydrological year samples were collected. An extra row, "All years" has been added summarising all the data. In brackets next to each hydrological year is the number of samples collected during that period. The number of storm events sampled each year is given in brackets under each hydrological year. [DOC] and [POC] were measured with precision of 0.1 µg $l^{-1}$; bdl = below detection limit, which for [TP] and [SRP] analysis was 0.15 µg $l^{-1}$ and for [TON] was 0.33 µg $l^{-1}$.

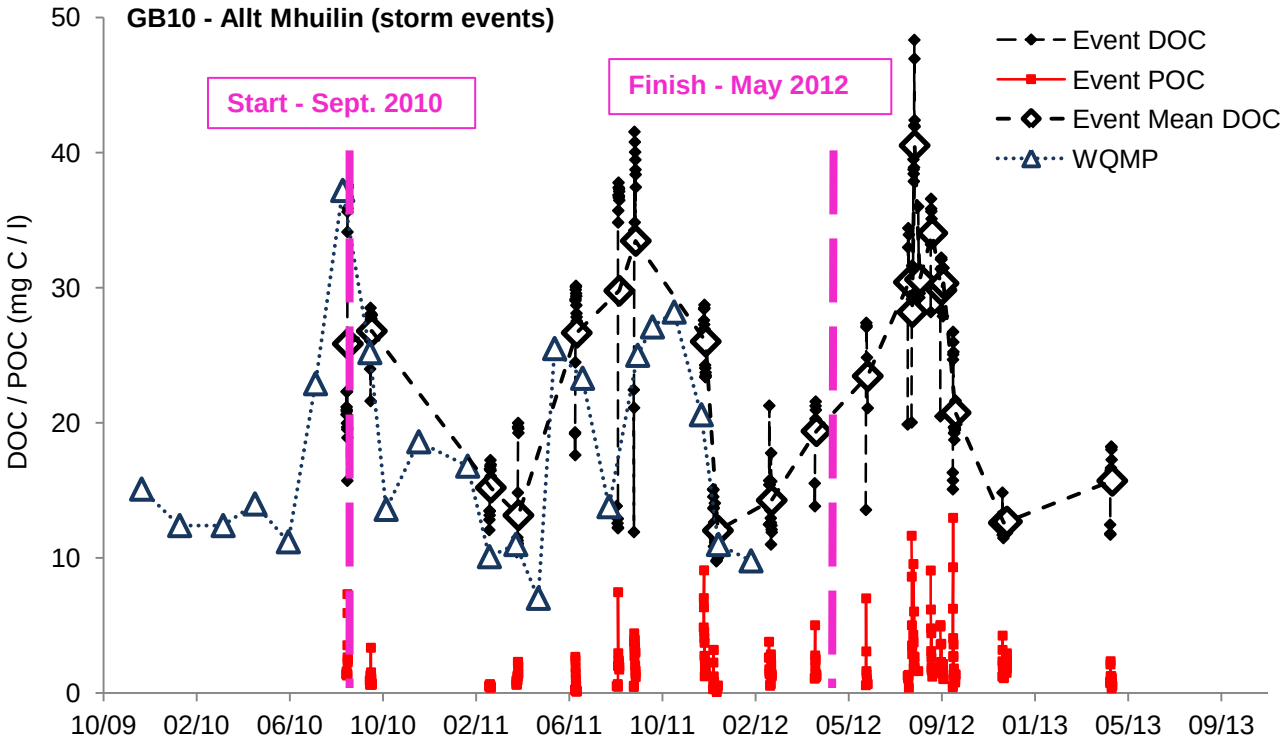


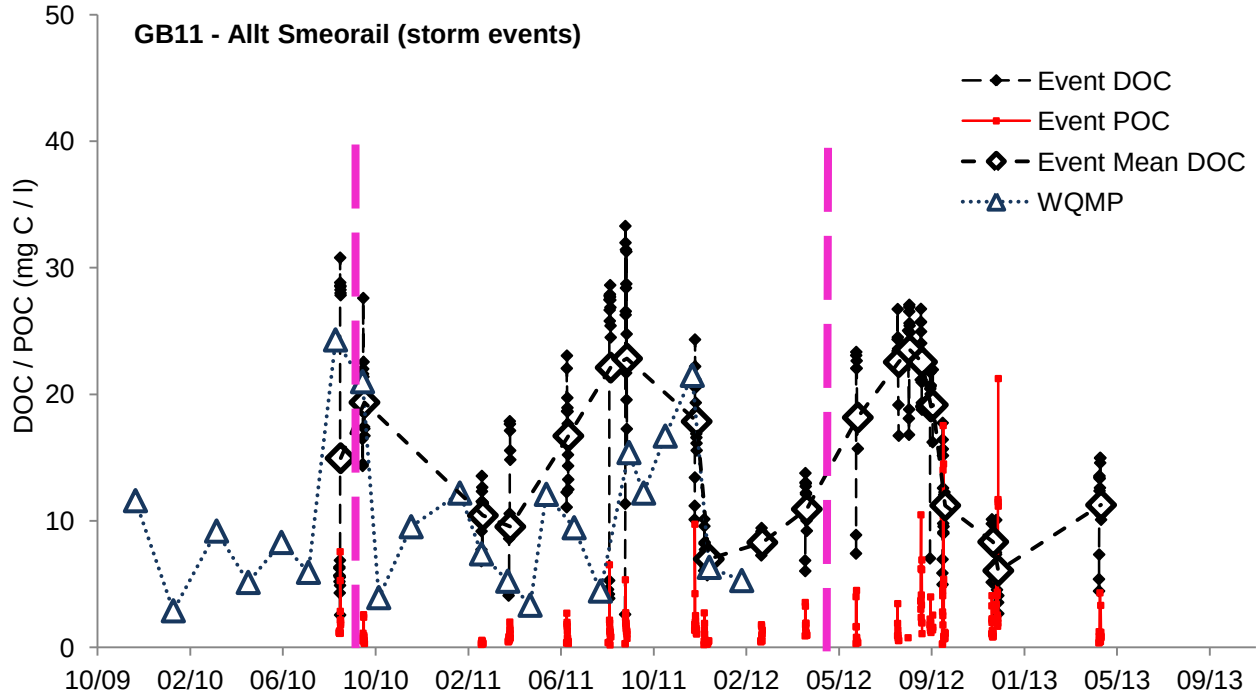


**Figure 5.1 - GB10 and GB11 [DOC] & [POC] storm event time series**
The small black diamonds and red squares linked by dashed vertical lines show individual sampling points during an event. The large hollow black diamond's represent mean [DOC] during any storm event and are linked by a black dashed line. Additionally the blue triangles in the graphs are the SSER WQMP [DOC] results, taken at GB1 on Allt Mhuilin (further upstream from GB10) and GB6 on Allt Smeorail (further upstream from GB11). The start and end dates of wind farm construction activities are marked by pink lines and text.

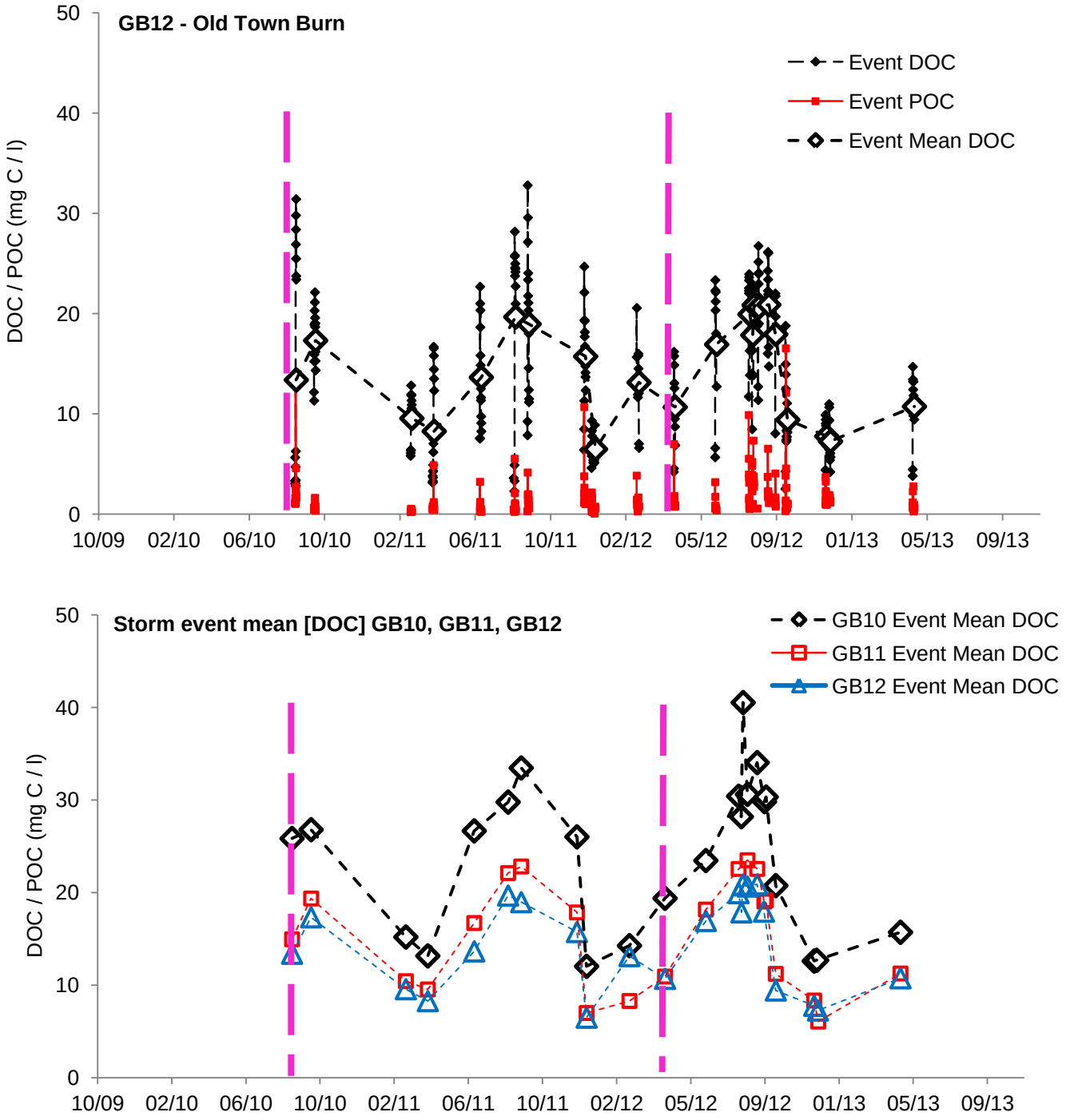


**Figure 5.2 - Storm event time series of [DOC] and [POC] for GB12 and Storm event mean [DOC] for GB10, GB11, GB12**
The SSER WQMP did not have a sampling on GB12 so no blue triangles are shown on graph above. Markers that indicate start and end of wind farm construction are shown. The colour marking on storm event mean [DOC] graph, where GB10 = black, GB11 = red and GB12 = blue, will be used throughout rest of this chapter.

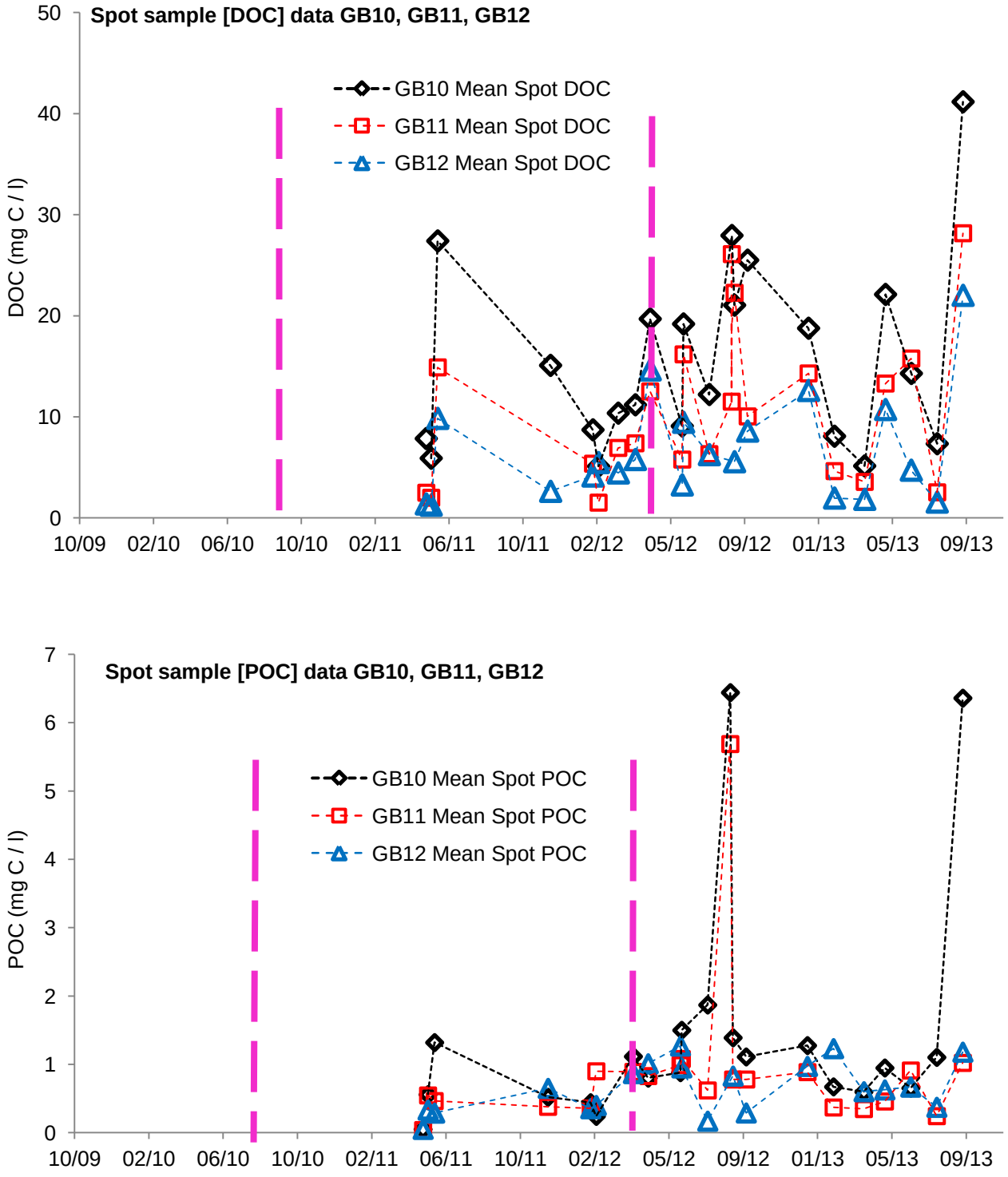


**Figure 5.3 - [DOC] and [POC] from spot samples in all three rivers at Gordonbush**
Graphs above cover samples collected from GB10, GB11 and GB12 out with storm event sampling between August 2010 and September 2013. The top graph shows [DOC] and the bottom [POC].

#### 5.4.1.1 Dissolved organic carbon (DOC)

Overall, [DOC] ranged from 1.1 mg $l^{-1}$ (GB12, May 2011) to 48.3 mg $l^{-1}$ (GB10, August 2012). GB10 had the largest [DOC] range from 5.1 mg $l^{-1}$ to 48.3 mg $l^{-1}$; in GB11 [DOC] ranged from 1.5 mg $l^{-1}$ to 33.3 mg $l^{-1}$ and in GB12 [DOC] ranged from 1.1 mg $l^{-1}$ to 32.8 mg $l^{-1}$. [DOC] were always higher in GB10 for comparable samples compared to GB11 and GB12. Generally, GB10 > GB11 > GB12 for [DOC] apparent from mean [DOC] during storm events (Figure 5.2) and in time series of spot samples (Figure 5.3)

The range in [DOC] during summer storm events was larger than in spring, autumn or winter events. The largest change during an event occurred in August 2011 in GB11 where [DOC] ranged from 2.6 mg $l^{-1}$ to 33.3 mg $l^{-1}$. For a spring/autumn event, the largest range occurred in November 2011 in GB12, when [DOC] moved from 6.4 mg $l^{-1}$ to 24.7 mg $l^{-1}$. The largest range observed during a winter event also occurred in GB12, in February 2012, with [DOC] varying from 6.6 mg $l^{-1}$ to 20.6 mg $l^{-1}$.

A strong seasonal trend is apparent in [DOC] storm event and spot sampling time series from all three rivers (Figure 5.1, 5.2 & 5.3) where maximum concentrations were recorded towards the end of summer months (August and September) each year and lowest concentrations were generally measured in winter months (February and December). This seasonal pattern is also visible from [DOC] data from SSER WQMP collected from sampling points GB1 on Allt Mhuilin and GB6 on Allt Smeorail (Figure 5.1).

#### 5.4.1.2 Particulate organic carbon (POC)

[POC] measured in all three rivers ranged from 0.04 to 21.3 mg $l^{-1}$. [POC] were generally lower than [DOC] (Figure 5.1, 5.2 & 5.3). [POC] ranged in GB11 from 0.04 mg $l^{-1}$ (April 2011) to 21.3 mg $l^{-1}$ (December 2012), followed by GB12, 0.05 mg $l^{-1}$ to 16.5 mg $l^{-1}$ and then GB10, 0.05 mg $l^{-1}$ to 13.0 mg $l^{-1}$. Mean [POC] during the sampling period were largest in GB10 (1.9 mg $l^{-1}$), followed by GB11 (1.8 mg $l^{-1}$) and GB12 (1.4 mg $l^{-1}$) (Table 5.3). Unlike [DOC], [POC] shows no clear seasonal trend (Figure 5.1, 5.2 & 5.3).

The next set of time series graphs to be presented will be of [TP].

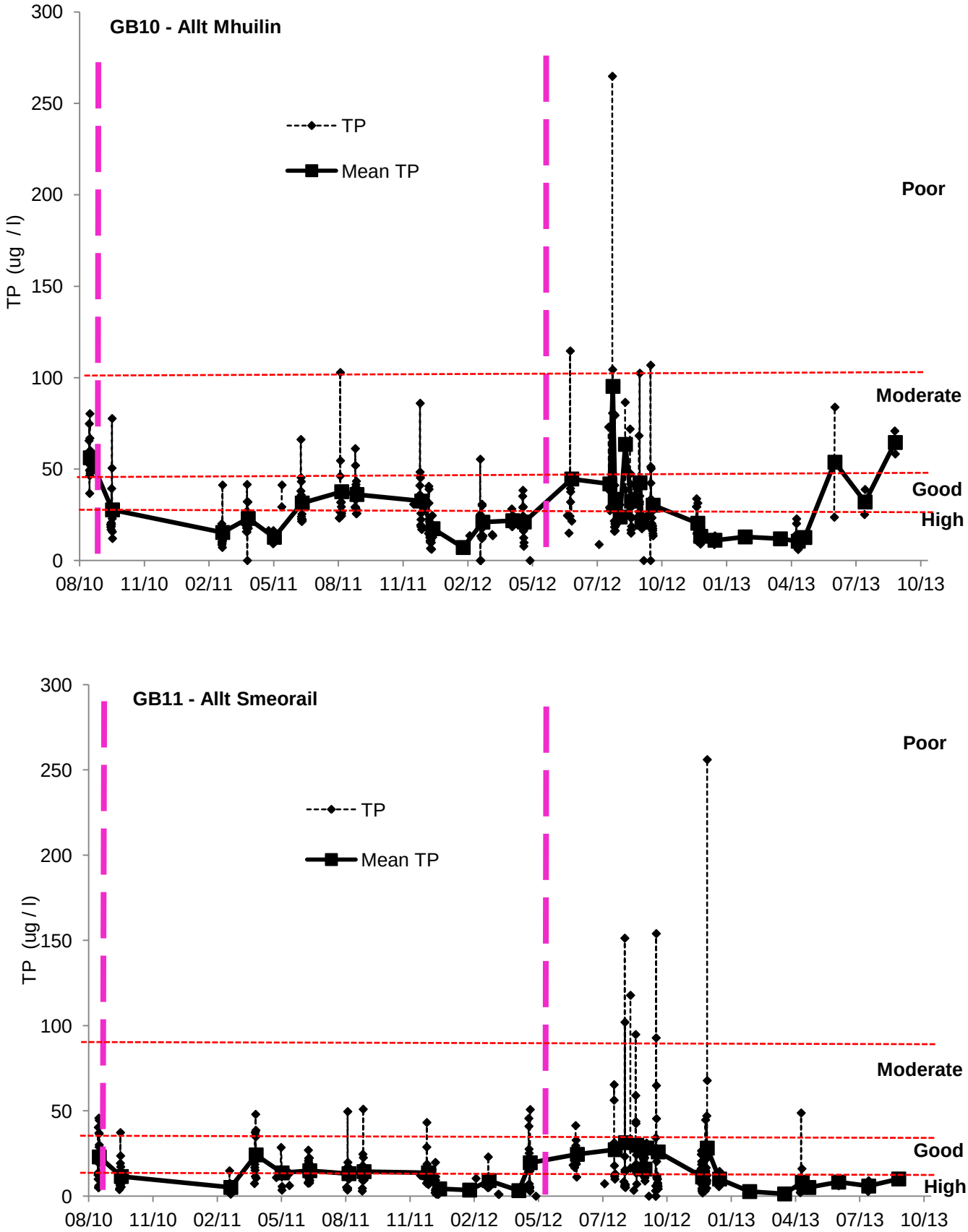


**Figure 5.4 - [TP] time series for GB10 and GB11**
The top graph shows GB10 time series and the bottom one GB11. TP samples were collected between August 2010 and September 2013. Dashed red lines show annual mean [RP] standards (refer to Table 5.2).

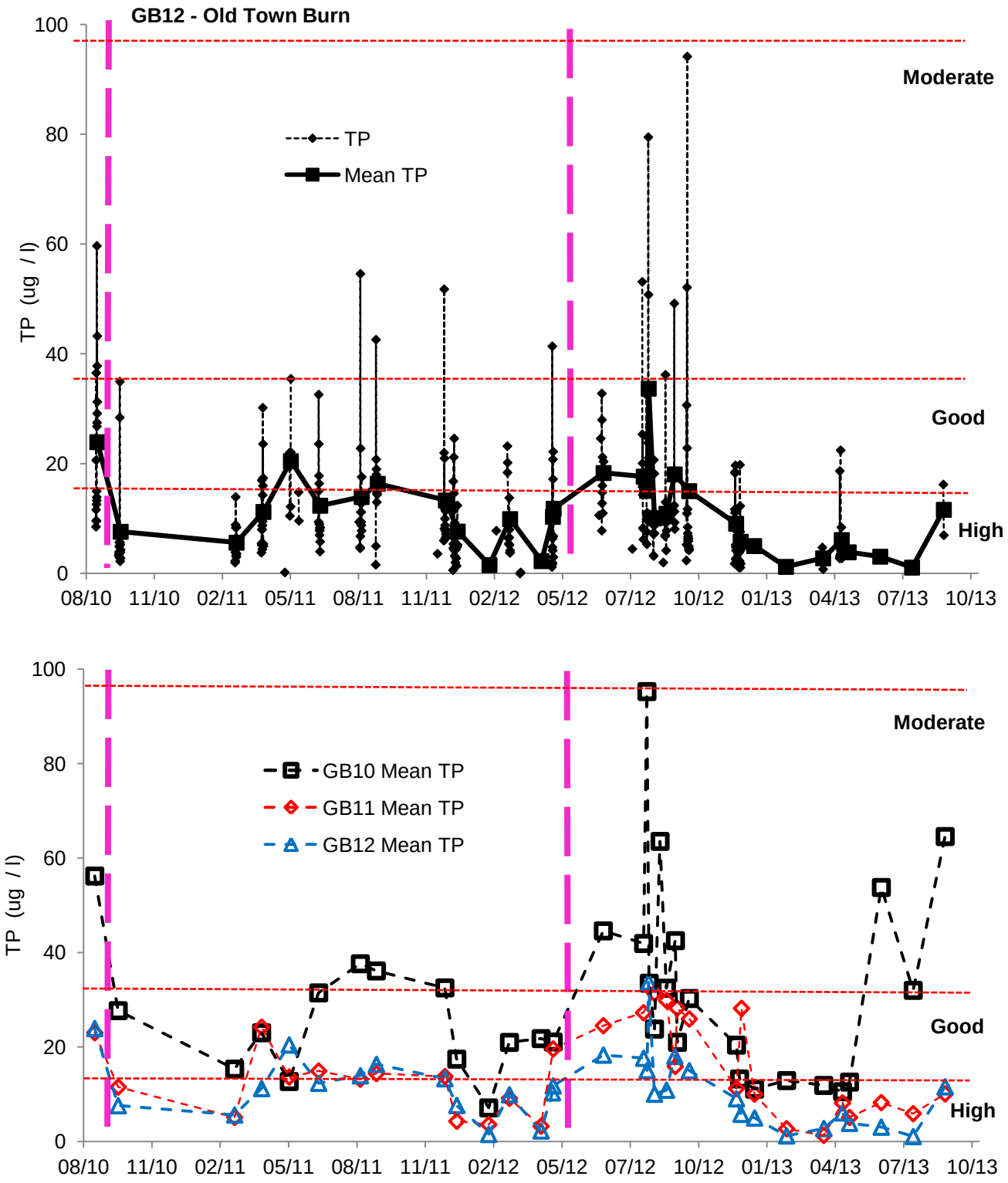


**Figure 5.5 - [TP] time series of GB12 and mean [TP] for GB10, GB11 and GB12**
GB10 = black squares, GB11 = red diamonds, GB12 = blue triangles. Dashed red lines show annual mean [RP] standards (refer to Table 5.2). GB12 [TP] time series of is represented over a smaller range (0-100 µg $l^{-1}$), than GB10 and GB11 in Fig. 4, 0-300 µg $l^{-1}$. The bottom graph of mean [TP] are shown is also on scale of 0-100 µg $l^{-1}$. The dashed lines between data points merely link points of the same river and are not representative of [TP] between different sampling dates.

### 5.4.1.3 Total Phosphorous (TP)

In the three studied rivers [TP] ranged from below detection limit (bdl, 0.15 µg $l^{-1}$) to 264.8 µg $l^{-1}$. The largest range occurred in GB10 (6.1 µg $l^{-1}$ to 264.8 µg $l^{-1}$). In GB11 and GB12, [TP] ranged from 1.0 µg $l^{-1}$ to 256.0 µg $l^{-1}$, and bdl to 94.2 µg $l^{-1}$, respectively. Generally, GB10 > GB11 > GB12 for [TP], with mean [TP] in GB10 of 29.2 µg $l^{-1}$, compared to 16.7 µg $l^{-1}$ in GB11 and 11.9 µg $l^{-1}$ in GB12 (Table 5.3). The range of [TP] measured in any particular event was greater during summer storm events compared to winter events.

Although it is not as pronounced as the seasonal trend observed with [DOC], generally largest [TP] occurred in the summer months (August and September) and the lowest [TP] in winter months (February and December). With the exception of six samples in each river [TP] did not exceed 100 µg $l^{-1}$ in GB10 or GB11 throughout the study period, while [TP] never exceeded 100 µg $l^{-1}$ in GB12. Thus the majority of water samples collected Gordonbush were classed either as “Good” or “High” in terms of water quality regarding [SRP] which is a minimum threshold which can be used to judge [TP] values against as a measured [TP] will include, and always represent more than, a [SRP] (Figure 5.5). The mean [TP] during all storm events and all spot samples in GB11 and GB12 were always classed in the “Good” or “High” water quality status.

The next set of time series graphs to be presented will be of [SRP].

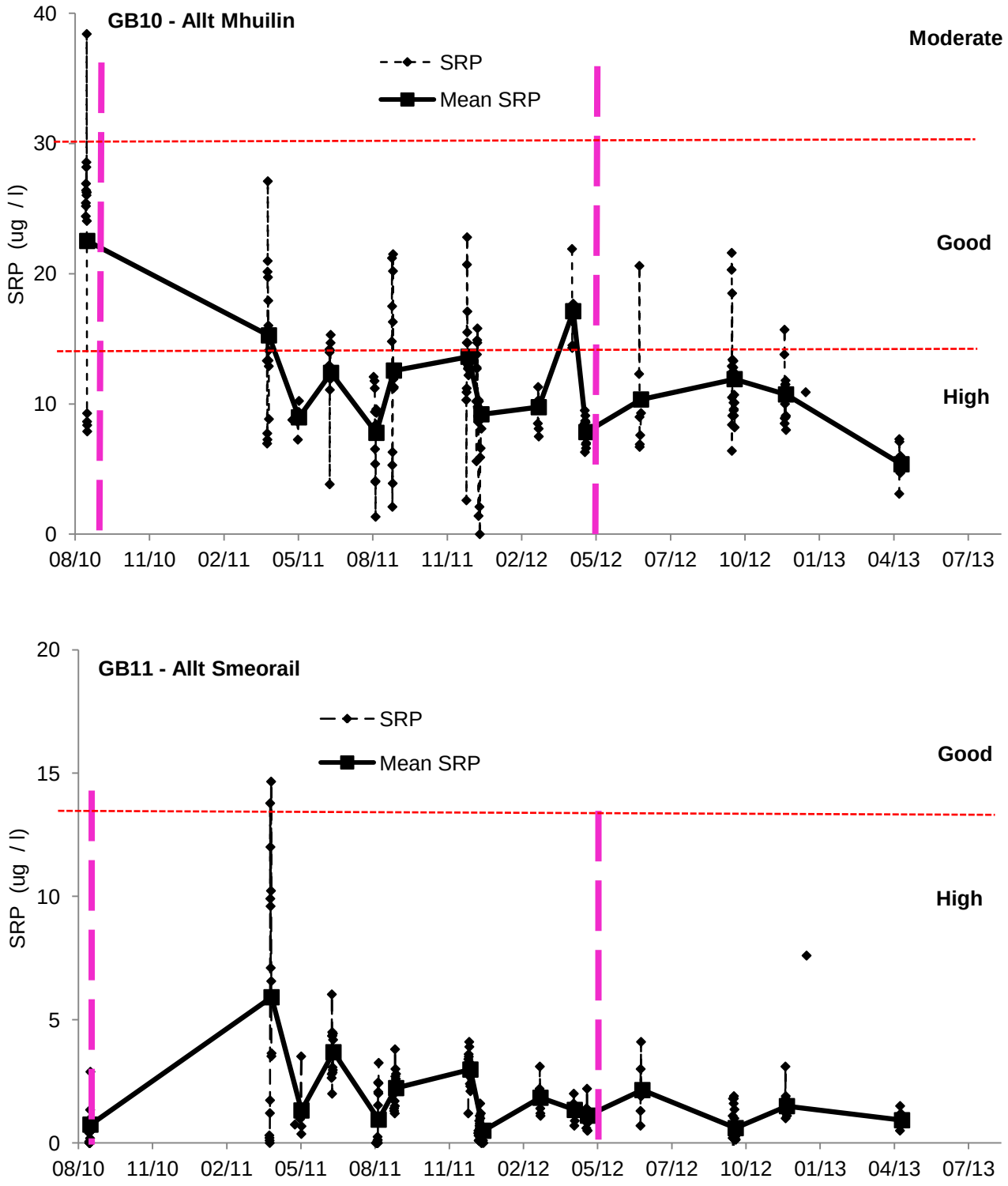


**Figure 5.6 - [SRP] time series from GB10 and GB11**
The top graph represents [SRP] time series from GB10 and the bottom from GB11. GB10 time series is displayed on SRP scale of 0-40 µg $l^{-1}$, whereas as GB11 is displayed on 0-20 µg $l^{-1}$. Samples were collected from August 2010 to May 2013. Dashed red lines show annual mean [RP] standards (refer to Table 5.3).

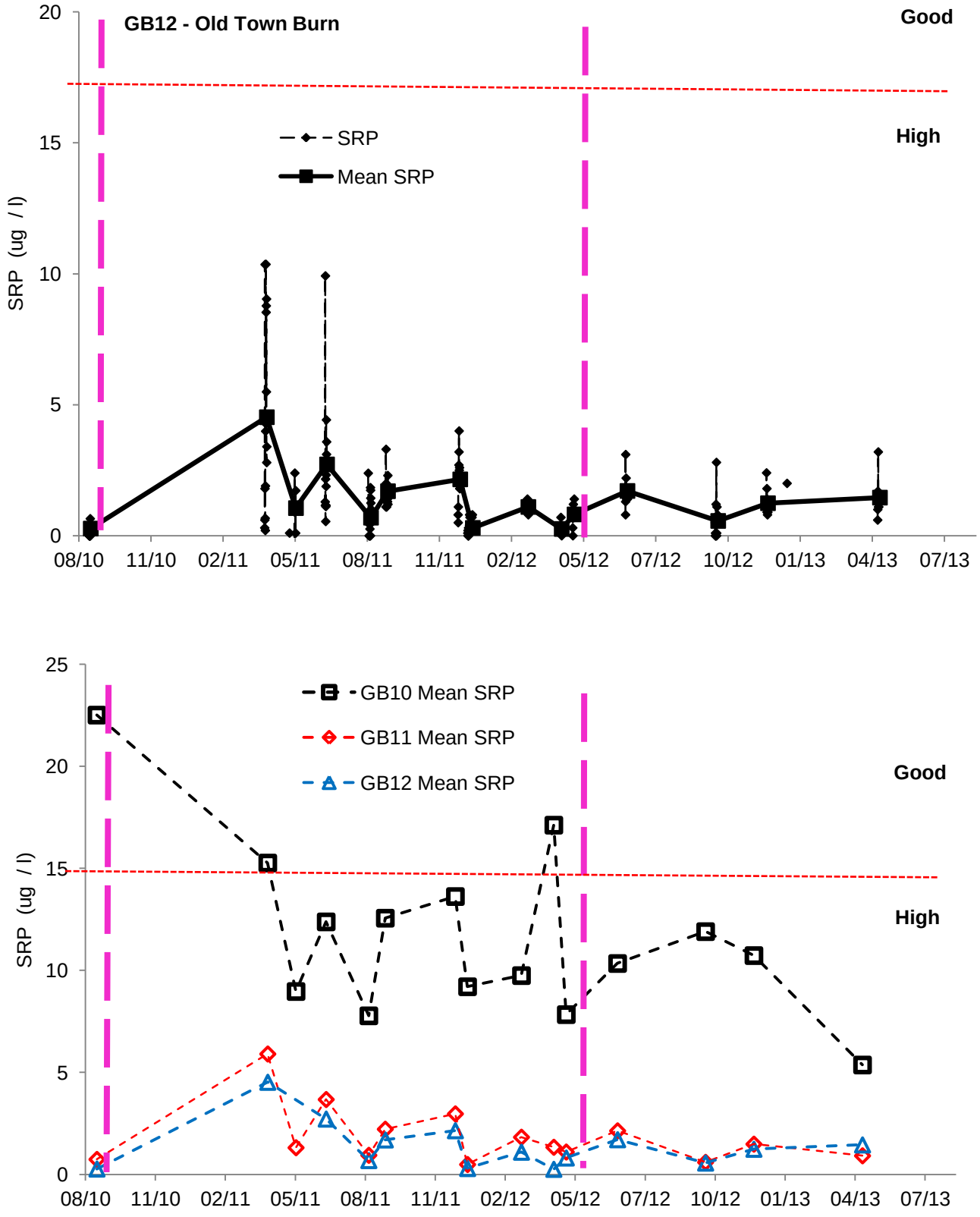


**Figure 5.7 - [SRP] time series from GB12 and mean [SRP] from GB10, GB11. GB12**
The top graph, GB12 [SRP] time series is has a [SRP] scale of 0-20 µg $l^{-1}$ similar to GB11 in Figure 5.6. The bottom graph showing mean [SRP] from all three rivers has a [SRP] of 0-25 µg $l^{-1}$. Again, the dashed lines between sampling points do not represent [SRP] between points be are used to clearly link data from the same river. Dashed red lines show Annual Mean [RP] standards (refer to Table 5.3).

#### 5.4.1.4 Soluble reactive phosphorous (SRP)

[SRP] measured at Gordonbush ranged from bdl (<0.15 µg $l^{-1}$) to 38.4 µg $l^{-1}$. The largest range occurred in GB10 and was bdl to 38.4 µg $l^{-1}$, [SRP] in GB11 and GB12 ranged from bdl to 14.7 µg $l^{-1}$ and bdl to 10.4 µg $l^{-1}$, respectively. Generally, GB10 > GB11 ≈ GB12 for [SRP].

There is no obvious seasonal trend, although the largest [SRP] were either measured in spring or summer months (Figure 5.6 & 5.7). Except for one sample from GB10 in August 2010, all water samples collected Gordonbush were either of “Good” or “High” water quality regarding [SRP] (Figure 5.6 & 5.7). During any storm events or spot samples in GB11 and GB12, [SRP] did not exceed 15 µg $l^{-1}$ and with the exception of two samples from GB11 in March 2011 event, were always classed in the “High” water quality status.

The next set of time series graphs to be presented will be of [TON].

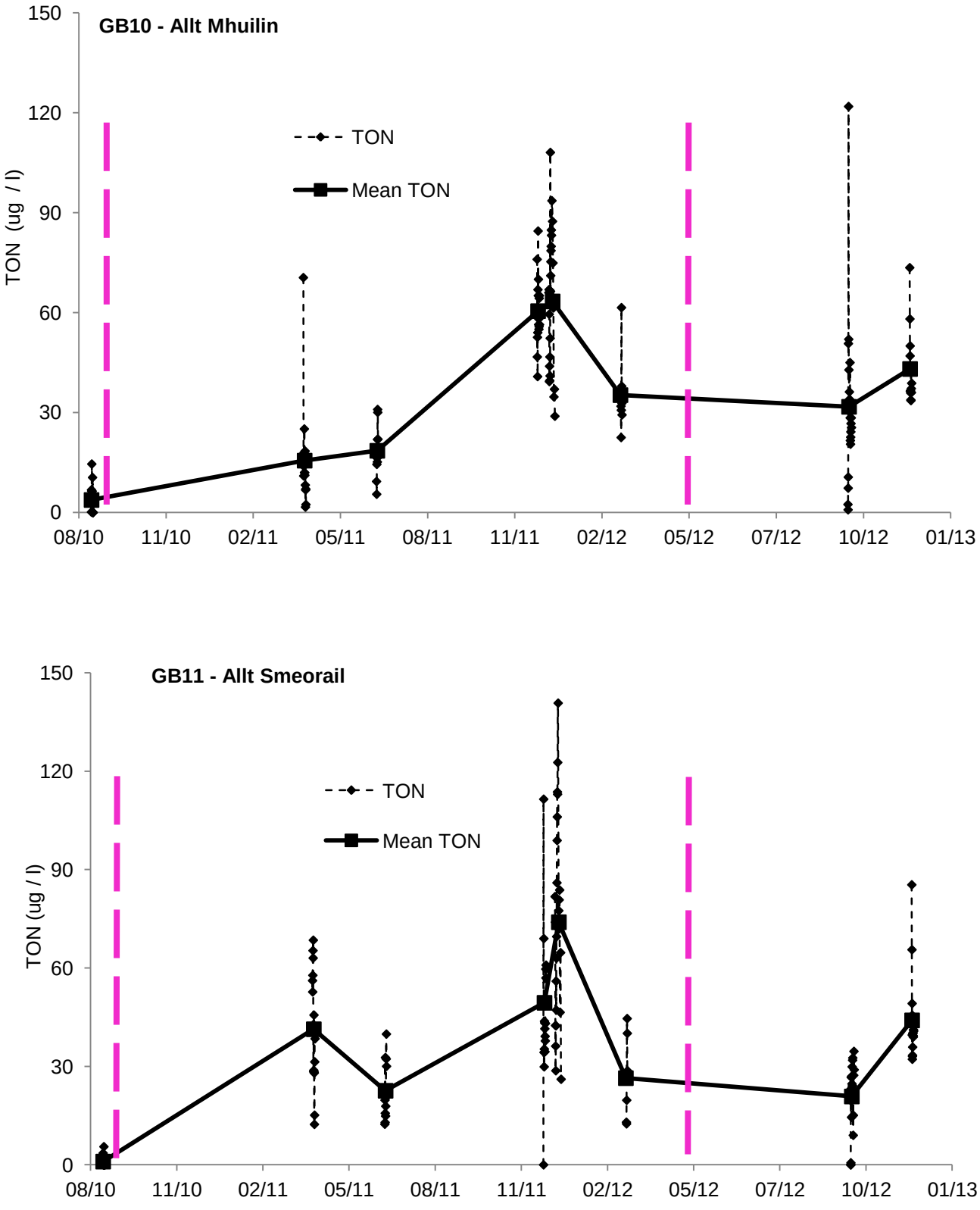


**Figure 5.8 - [TON] time series from GB10 and GB11**
Both graphs are displayed with [TON] scale of 0-150 µg/l. Samples measured for [TON] were collected between August 2010 and December 2012. Graphs presenting [TON] contain less data as successful analysis was not always possible as samples collected from some storm events did not register above the detection limit of 0.33 µg $l^{-1}$.

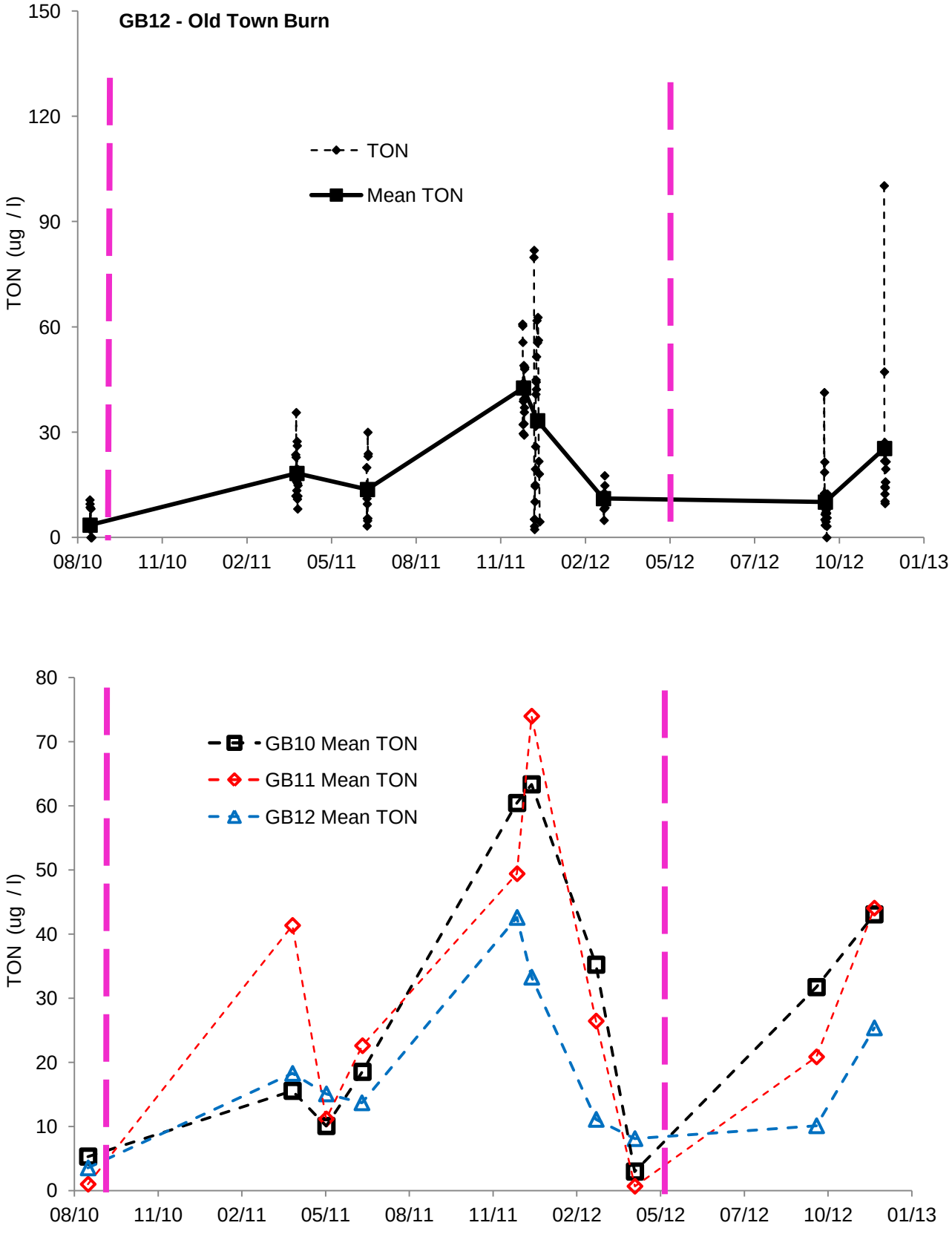


**Figure 5.9 - [TON] time series from GB12 and mean [TON] from GB10, GB11 and GB12**
The top graph is displayed with [TON] scale of 0-150 µg $l^{-1}$ whereas bottom graph has 0-80 µg $l^{-1}$.

#### 5.4.1.5 Total oxidised nitrogen (TON)

In all three rivers [TON] ranged from bdl of 0.33 µg $l^{-1}$ to 140.8 µg $l^{-1}$. The largest range occurred in GB11, from BDL to 140.8 µg $l^{-1}$, whilst in GB10 and GB12, [TON] ranged from bdl to 121.9 µg $l^{-1}$, and 100.2 µg $l^{-1}$ in GB12. There was no clear river ranking of concentration in mean [TON] data (Figure 5.8 & 5.9). An opposite seasonal trend was observed in [TON] compared with [DOC] and [TP]; with largest concentrations recorded in winter. As [TON] measured at Gordonbush were <1 mg $l^{-1}$ it was not necessary to contextualise results in relation to existing $NO_3^-$ water quality guidelines (50 mg $l^{-1}$).

### 5.4.2 Summary of water quality at Gordonbush

Water quality guidelines for [RP] are based on annual means (UK TAG, 2013). Below, a table is presented (Table 5.4) summarising mean [TP] and [SRP] data presented in Table 5.3 for each hydrological year. [TP] and [SRP] [P] have been compared to site-specific water quality guidelines calculated in section 5.3.2 (see Table 5.2).

| | Annual means of TP and SRP (all µg $l^{-1}$) & water quality status in brackets () | | | | | |
|---|---|---|---|---|---|---|
| | **GB10 – Allt Mhuilin** | | **GB11 – Allt Smeorail** | | **GB12 – Old Town Burn** | |
| Hydro. Year | [TP] | [SRP] | [TP] | [SRP] | [TP] | [SRP] |
| **2010** | 42.5 (M) | 22.5 (G) | 17.5 (G) | 0.7 (H) | 16.0 (H) | 0.3 (H) |
| **n** | 33 | 17 | 33 | 17 | 33 | 17 |
| **SD** | 19.9 | 8.7 | 13.0 | 0.8 | 14.7 | 0.2 |
| **2011** | 28.1 (G) | 11.7 (H) | 14.6 (G) | 3.0 (H) | 12.5 (H) | 2.3 (H) |
| **n** | 83 | 66 | 84 | 66 | 84 | 66 |
| **SD** | 14.6 | 5.1 | 10.8 | 3.3 | 9.1 | 2.6 |
| **2012** | 30.3 (G) | 10.7 (H) | 17.2 (G) | 1.5 (H) | 12.4 (H) | 1.1 (H) |
| **n** | 152 | 73 | 134 | 74 | 143 | n = 74 |
| **SD** | 27.6 | 4.4 | 22.0 | 2.5 | 11.8 | 0.9 |
| **2013** | 21.9 (G) | 10.1 (H) | 17.4 (G) | 1.1 (H) | 8.6 (H) | 1.0 (H) |
| **n** | 71 | 46 | 90 | 49 | 79 | 35 |
| **SD** | 17.9 | 3.9 | 33.3 | 1.2 | 12.5 | 0.7 |
| All years | 29.2 (G) | 11.9 (H) | 16.7 (G) | 1.9 (H) | 11.9 (H) | 1.4 (H) |
| **n** | 339 | 202 | 341 | 206 | 339 | 192 |
| **SD** | 22.9 | 6.0 | 22.9 | 2.3 | 11.8 | 1.8 |

**Table 5.4 -Summary of mean [TP] and [SRP] and related water quality statues**
The table displays annual means of [TP] and [SRP] from all three studied rivers at Gordonbush as well as the water quality category they fall in relation the site-specific guidelines (M = Moderate, G = Good, H = High). For all years for both [TP] and [SRP], number of samples (n) and the standard deviation (SD) of data collected is also presented.

From data collected during this research, annual means of [SRP] suggest 'High' water quality status was present in all rivers in all years, except for GB10 in 2010. For annual [TP], 'Good' status was present for all years in GB10 and GB11, except again for GB10 in 2010. Annual [TP] in GB12 for all studied hydrological years were low enough to achieve 'High' water quality status.

## 5.4.3 Hysteresis and macronutrient interactions

Here I consider flow-controlled hysteresis patterns and the interaction between macronutrients concentrations in storm event discharge. Changes in hysteresis between seasons and catchments for [DOC] and [POC] are presented (Figure 5.10, Figure 5.11 and Figure 5.12). Discharge-[DOC] hysteresis from all rivers are shown together as they are broadly similar. Figure 5.10 shows examples of anticlockwise (A2) and clockwise (C2) loops whereas Figure 5.11 presents examples of figure-of-8 (Fo8) loops. Some extra data is presented from GB12 (Figure 5.11C&D) to highlight the greater number of Fo8 loops observed in this river compared to the other two.

[POC]-[TP] hysteresis plots will also be presented with examples of hysteresis plots of POC and TP from selected storm events (Figure 5.13). This will be followed by hysteresis plots of [TON] (Figure 5.14).

[DOC]-[SRP] will be presented next to [DOC]-[TON] for each river, GB10, GB11 and GB12 (Figure 5.15).

### 5.4.3.1 DOC hysteresis in GB10, GB11 and GB12

All three Gordonbush rivers exhibit seasonality in [DOC] (see Figure 5.2). Storm events in the summer months have higher mean [DOC] (typically >20 mg $l^{-1}$) than those in the winter months (typically <15 mg $l^{-1}$). There are storm events with mean [DOC] that fall between these boundaries therefore it was decided events could be split into three categories that broadly map season: ‘Summer’ (storm events sampled between June-September), ‘Spring-Autumn’ (March, April, October and November) and ‘Winter’ (December-February). Analysis was undertaken to see if hysteresis patterns changed between the three ‘seasons’ and differed between the three studied rivers (Figure 5.10 and Figure 5.11).

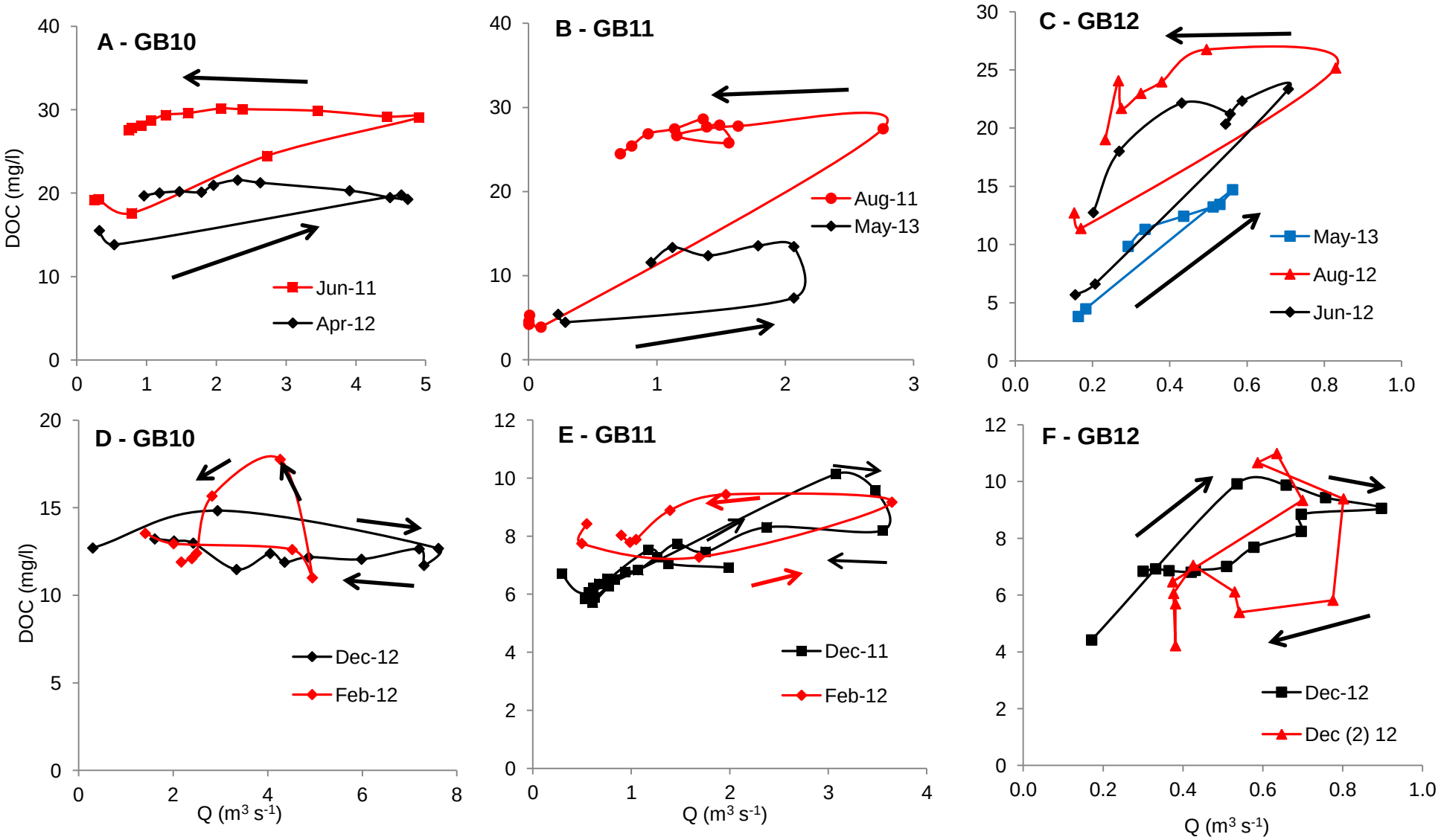


**Figure 5.10 - Hysteresis analysis of GB10, GB11 and GB12 [DOC] data showing A2 and C2 loops**
These plots show repeated hysteresis loops. Discharge (Q, $m^3$ $s^{-1}$) is represented on all x-axes. [DOC] (mg/l) is represented on all y-axes. A = Data from GB10 showing anticlockwise hysteresis (A2) loops in summer and spring-autumn, B = Data from GB11 showing A2 loops, summer and spring-autumn. C = Data from GB12 showing A2 loops, summer and spring-autumn. D = Data from GB10, a mixture of clockwise (C2) and anticlockwise (A2) loops in winter and spring-autumn, E = Data from GB11, a mixture of C2 and A2 loops, winter and spring-autumn F = Data from GB12 showing C2 loops only in winter. The black arrows show direction of hysteresis. The colour coded key shows dates of storm events.

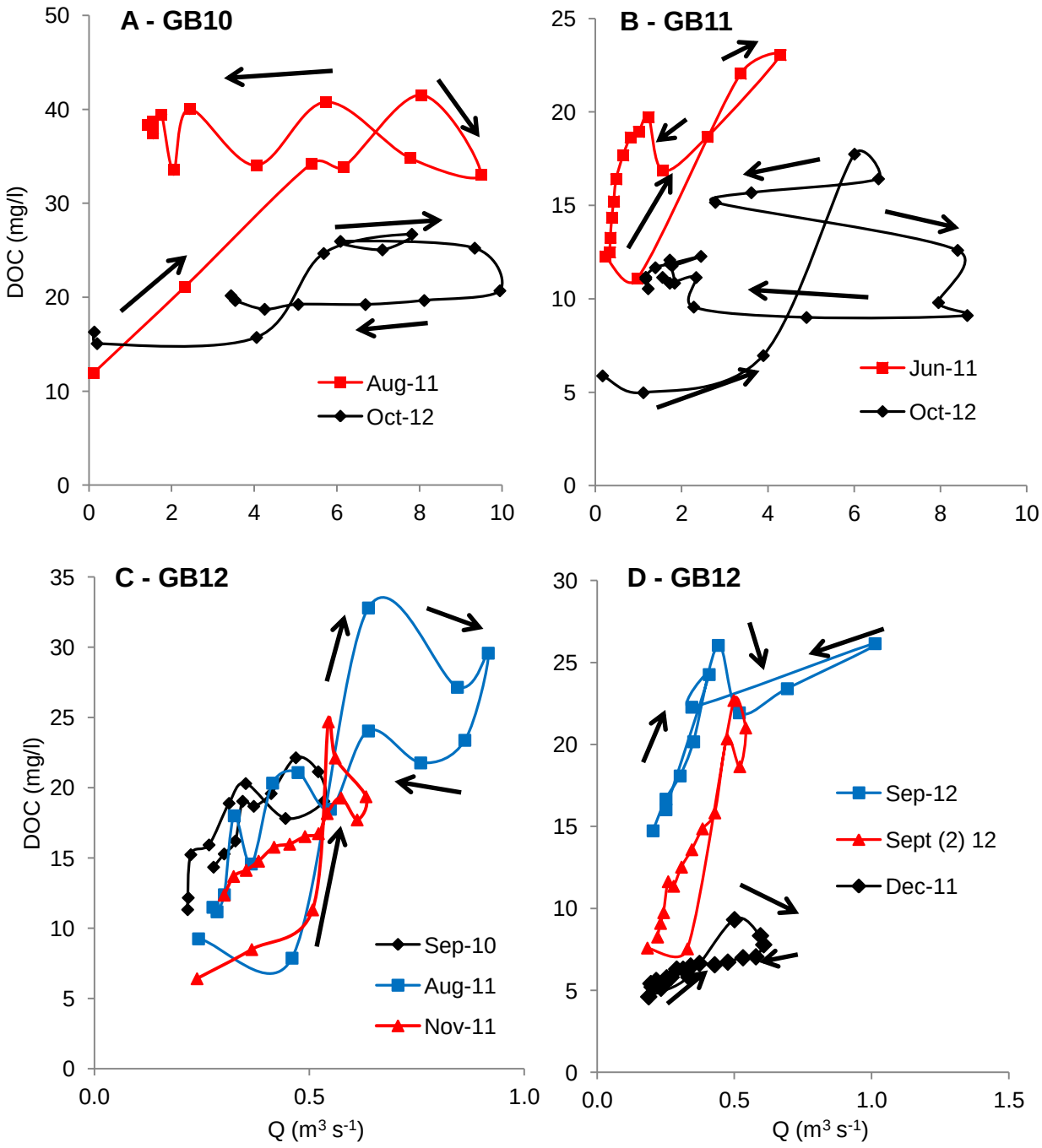


**Figure 5.11 - Hysteresis analysis showing cross-over (Fo8) loops in GB10, GB11 & GB12**
The above diagrams show repeated hysteresis loops. Discharge (Q, $m^3$ $s^{-1}$) is represented on all x-axes. [DOC] is represented on all y-axes. A = Data from GB10, figure 8 loops (Fo8) in summer and spring-autumn, B = Data from GB11, Fo8 loops, summer and spring-autumn. C = GB12, Fo8 loops in summer and spring-autumn, D = GB12, Fo8 loops, summer and winter. The black arrows show direction of hysteresis. The colour coded key shows dates of storm events.

**DOC in GB10 and GB11**

The [DOC] hysteresis loops for GB10 and GB11 in summer and spring-autumn events are predominately anticlockwise (Figure 5.10A&B). The loops presented exhibit patterns mostly associated with A2 loops (Evans & Davies, 1998) (Figure 5.17). A2 loops show [DOC] has a positive gradient on rising limb of an event whereas after peak discharge the [DOC] gradient on the falling limbs is shallower, with [DOC] either staying constant or decreasing at a slower rate than on the rising limb despite discharge decreasing. This implies soil flow (water washed through soil profile including duff layers) is exerting a greater influence on controlling [DOC] than surface flow, with groundwater exerting the least, over the complete duration of the storm event (Evans & Davies, 1998).

Some summer and spring-autumn GB10 and GB11 (Figure 5.11A&B), exhibit a Fo8 hysteresis pattern. A Fo8 clockwise loop is considered to be caused by surface flow being dominant in the early stage of a storm event supplying C to the river system (C2 hysteresis). However, as the event progresses, surface water becomes less important and soil flow becomes dominant, such that the hysteresis pattern is anti-clockwise (A2) and [DOC] remains constant, but discharge decreases. A Fo8 loop implies the DOC pool is not fully-depleted even after peak discharge and so the [DOC] becomes stable (Sander et al., 2011).

All GB10 and GB11 December storm events (winter) exhibited clockwise C2 loops (Figure 5.10D&E), produced when surface flow > soil flow > groundwater. Concentrations on rising limbs are commonly higher than those on falling limbs in C2 loops. [DOC] in GB10 and GB11 remains fairly constant throughout the duration of the events but concentrations decrease leading up to peak discharge. Events in winter from GB10 and GB11 exhibited the same anticlockwise (A2) hysteresis that was observed in summer and spring-autumn events (Figure 5.10A&B).

**DOC in GB12**

Although GB12 [DOC] hysteresis show some of same patterns as GB10 and GB11 - anticlockwise loops (A2) in the summer and spring-autumn events (Figure 5.10C) and clockwise loops (C2) in December (Figure 5.10F) – there are noticeable differences. Hysteresis analysis in GB12 shows more instances of Fo8 loops (between C2 and A2 types) forming (Figure 5.11C&D): hysteresis loops start in clockwise direction (C2), but [DOC] remains constant after peak discharge and the hysteresis has a more anticlockwise A2 shape.

### 5.4.3.2 POC in all catchments

[POC] varies between sites and events but GB10, GB11 and GB12 POC-discharge hysteresis plots all exhibit the same general clockwise rotation, most similar to a clockwise C2 loop (Figure 5.12).

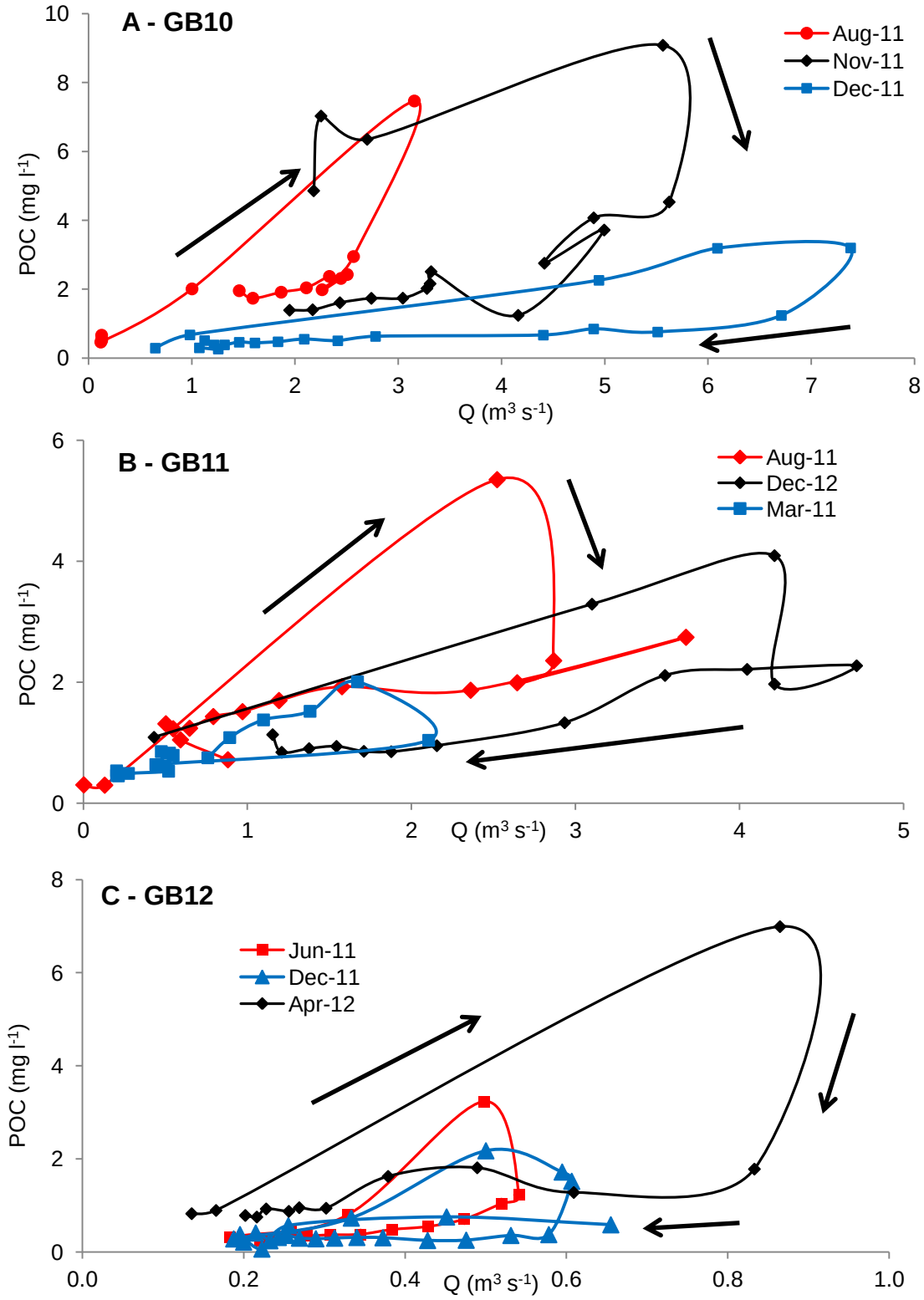


**Figure 5.12 - Hysteresis analysis of GB10, GB11 and GB12 [POC] data**
Graphs above show the clockwise nature of all POC hysteresis loops. Discharge (Q, $m^3$ $s^{-1}$) is represented on all x-axes. [POC] is represented on all y-axes. A = GB10, C2 loops, B = GB11, C2 loops, C = GB12, C2 loops. The black arrows show direction of hysteresis. The colour coded key shows dates of storm events.

The following graphs show [POC]-[TP] interactions and hysteresis (Figure 5.13) for the three river catchments.

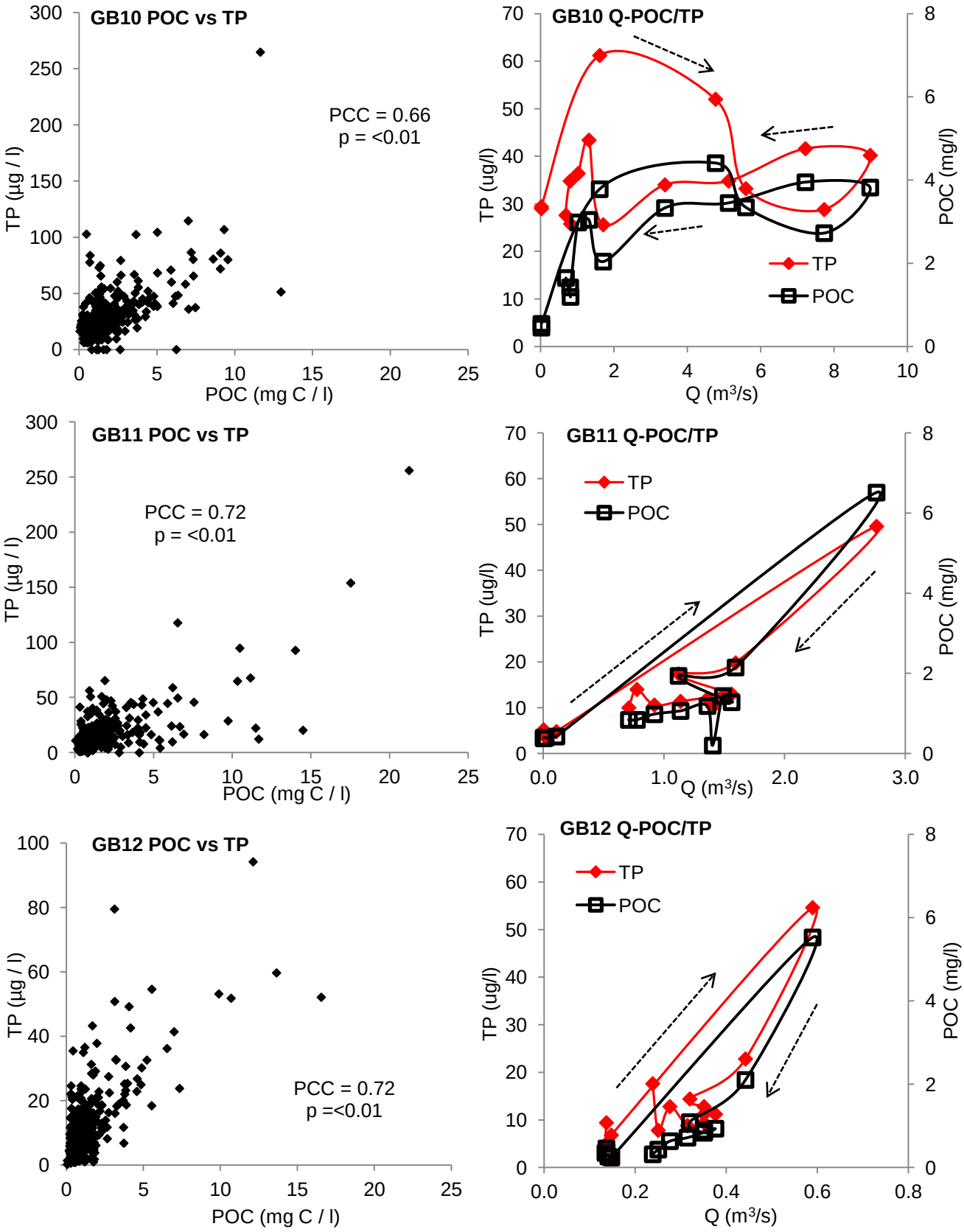


**Figure 5.13 - [POC]-[TP] relationships; correlations and hysteresis graphs**
[TP] scales from GB10 and GB11 is 0-300 µg $l^{-1}$, but for GB12 0-100 µg $l^{-1}$. Discharge-POC/TP hysteresis plots are presented adjacent to each [POC] vs. [TP] plots for each river from storm events in August 2011. Scales vary between the hysteresis plots. Data points that appear to be zero are samples that were below the detection limit or the limit of quantification. PCC = Pearson Correlation Coefficient.

The next graphs presented will be [TON] hysteresis plots (Figure 5.14).

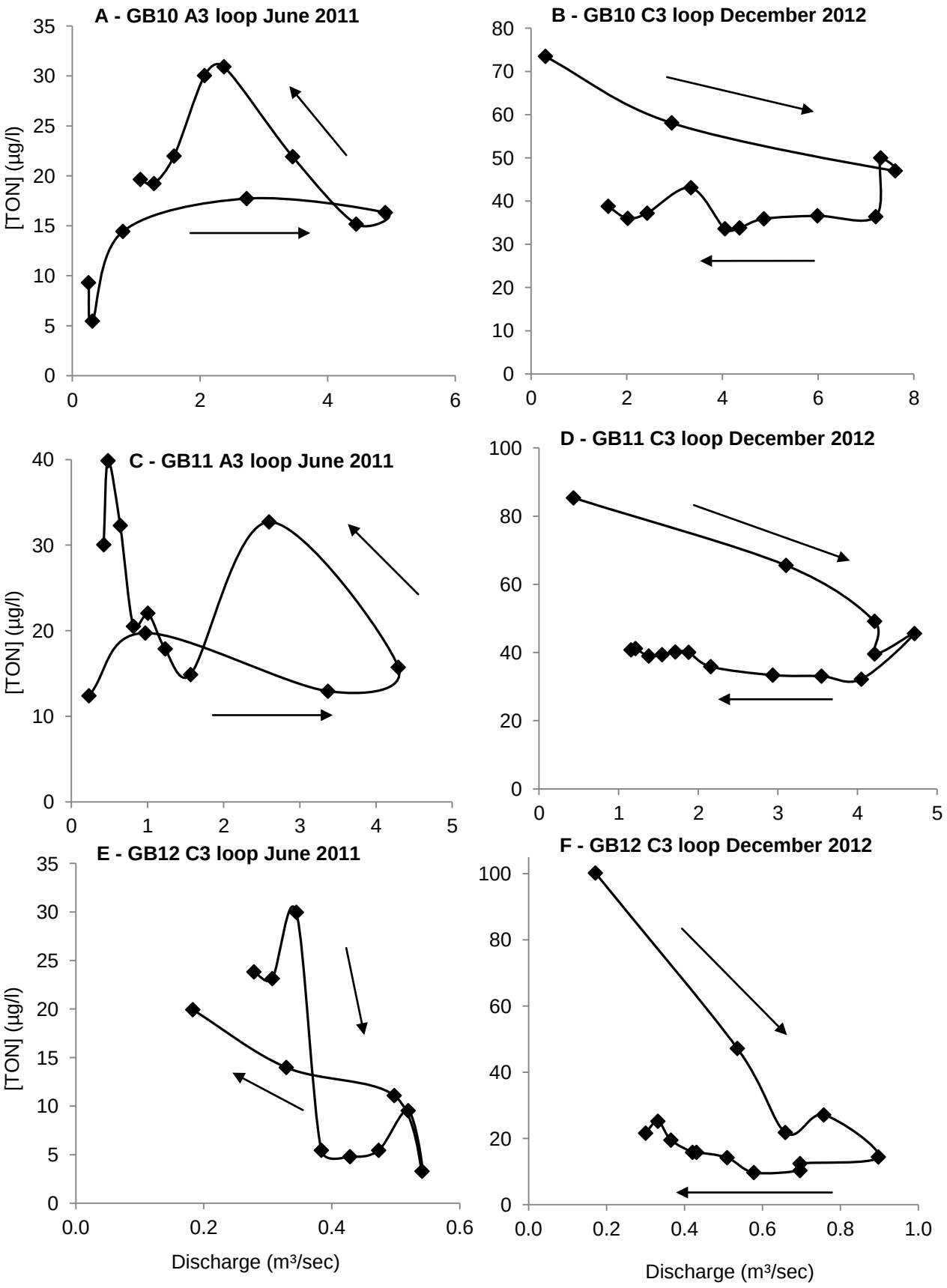


**Figure 5.14 - [TON] hysteresis for Gordonbush rivers GB10, GB11 and GB12**
All x-axis: discharge ($m^3$ $sec^{-1}$); y-axis [TON] (µg $l^{-1}$). The direction of the hysteresis is highlighted by black arrows. Graphs A, C and E – show hysteresis loops of GB10, GB11 and GB12, respectively, during a summer event in June 2011. Graphs B, D and F – show hysteresis loops of GB10, GB11 and GB12, respectively, during a winter event in December 2012.

#### 5.4.3.3 POC and TP

Pearson Correlation Coefficients (PCC) indicate [POC] and [TP] are positively correlated in all three rivers (Figure 5.13). Concentrations of POC and [TP] are more strongly correlated for GB11 and GB12 than GB10, but all relationships are statistically significant with p values <0.01.

The Discharge-POC/TP hysteresis plots for GB10, GB11 and GB12 August 2011 event (Figure 5.13) shows a similar clockwise hysteresis response for [POC] and [TP]. The patterns follow a C2 loop (see Figure 5.17), where surface run-off sources have the greatest influence on [determinant] compared to water inputs from the soil profile and least of all from groundwater sources (Evans & Davies, 1998). Although only one example is presented, a similar hysteresis response is exhibited in all other events.

#### 5.4.3.4 TON hysteresis

Hysteresis for [TON] varies in GB10 and GB11. For summer events (Figure 5.14A&C), A3 anticlockwise loops are observed. These loops imply groundwater sources are the dominant control on [TON], followed by inputs from soil profile with surface run-off supposedly having the least influence (Evans & Davies, 1998). For winter events (Figure 5.14B&D), C3 clockwise loops are observed, where groundwater is still the dominant control on [TON] but the surface water becomes more influential than water sourced from the soil profile (Evans & Davies, 1998). Hysteresis results differ slightly for GB12 compared to other two catchments, as regardless of season, loops are C3 clockwise in nature (Figure 5.14E&F). Although only examples one of each summer event (June 2011) and winter event (December 2012) are shown (Figure 5.14), these pattern observed were consistent for each river across all events when [TON] was analysed.

The following graphs show [DOC]-[SRP] and [DOC]-[TON] (Figure 5.15) interactions from the three Gordonbush catchments.

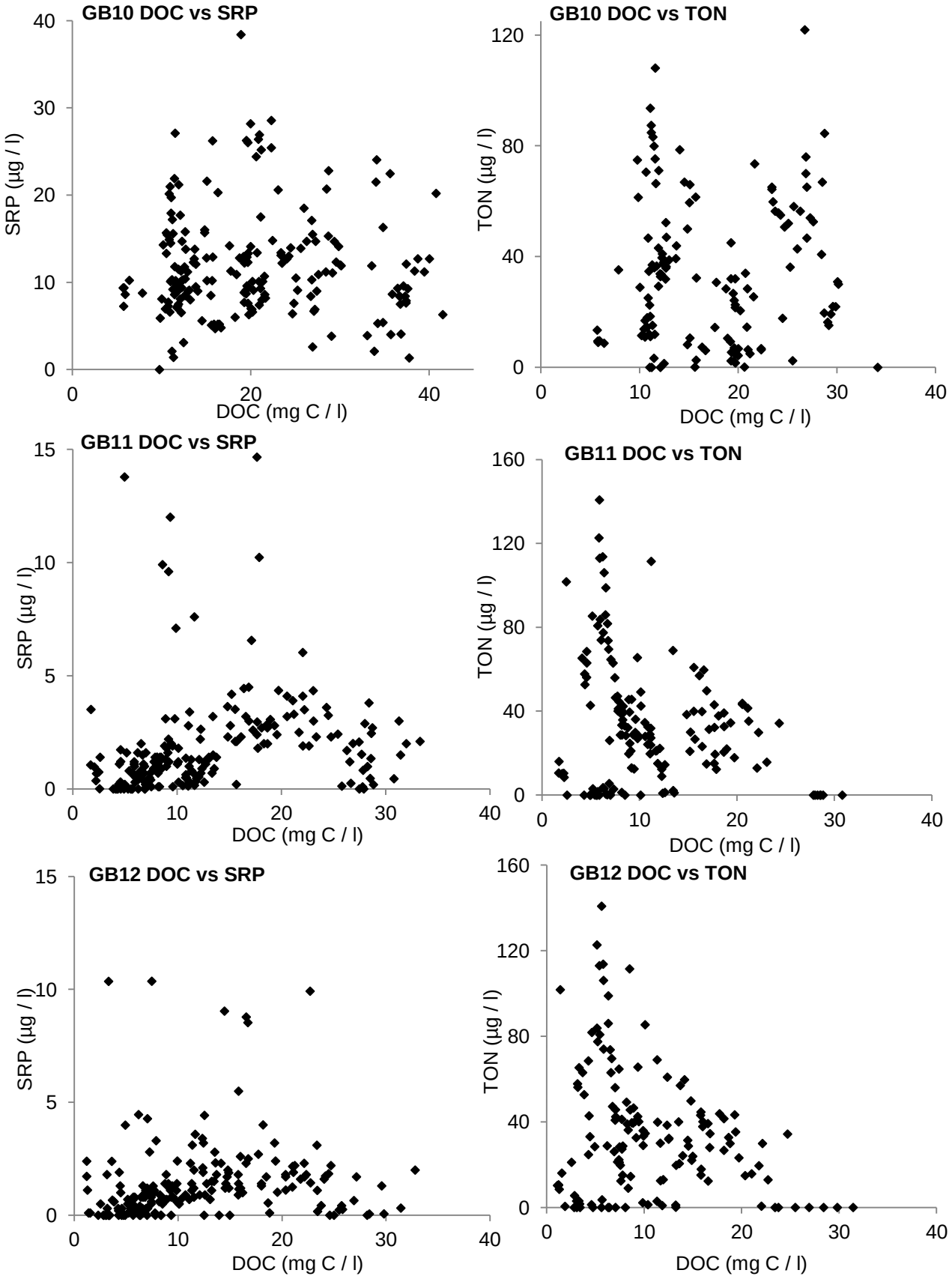


**Figure 5.15 - [DOC]-[SRP] and [DOC]-[TON] relationships from GB10, GB11 and GB12** [SRP] for GB10 are displayed on 0-40 µg $l^{-1}$, where GB11 and GB12 uses a 0-15 µg $l^{-1}$ [SRP] scale. All [TON] scales are 0-160 µg $l^{-1}$. All [DOC] scales are 0-50 mg $l^{-1}$. Data points that appear to have a value of zero are samples measured below the detection limit or below the limit of quantification.

#### 5.4.3.5 DOC and SRP

The relationship between [DOC] and [SRP] in GB10 (Figure 5.15) shows considerable scatter and a clear, definitive relationship between the two determinants is not apparent. However, in GB11 and GB12, a “curvi-linear relationship” with a maximum is apparent, although there are a small number of data points where [SRP] is higher than the bulk of the data. These outlying points of the curvi-linear [DOC]-[SRP] profiles of GB11 and GB12 are all associated with one event in March 2011 where [SRP] was also the greatest of the research period, but the reason for this is not fully understood. Here as [DOC] increases, [SRP] also increases, to a maximum [SRP] during mid-[DOC] and then [SRP] decreases whilst [DOC] continues to increase. When DOC-SRP data is compared between all three rivers, it is clear the curvi-linear relationships are stronger in GB11 and GB12 than GB10 but a similar relationship, albeit a weaker association, can be observed in GB10 data, especially when only [SRP] <10 µg $l^{-1}$ are considered.

#### 5.4.3.6 DOC and TON

The relationship between [DOC] and [TON] in GB10 shows considerable scatter and a clear relationship is not apparent. However, in GB11 and GB12, there is a weak inverse concentration relationship, with high [DOC] generally accompanied by low [TON]. The relationship is stronger in GB11 and GB12 than GB10 (Figure 5.15).

## 5.4.4 Primary productivity rates

From artificial substrates placed in each river, minimal primary production since deployment / last sampling was estimated and results are presented (Figure 5.16).

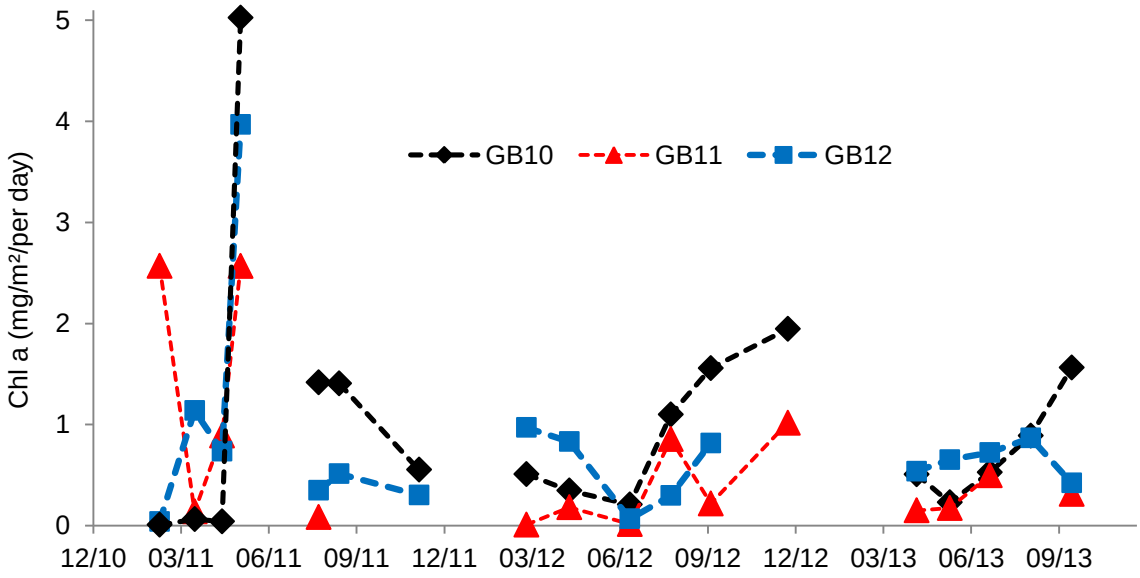


**Figure 5.16 - Rates of production of chlorophyll *a* over time**
Chlorophyll *a* results presented from all three rivers (GB10, GB11 and GB12). The first artificial substrates were installed in all three rivers on 17th November 2010. Primary productivity rates were calculated from 24th February 2011 up until 16th September 2013. All results >0.01 (mg/m$^2$/per day) are shown. Gaps in the each river time series indicate times when chlorophyll *a* analysis was not possible. Reasons for this included: no or insufficient material collected on the substrate between sampling dates, occasionally tiles were not found or overturned, presumably moved during flood events and at other times samples were analysed but results calculated were <0.01 mg/m$^2$/per day

Generally, rates of primary productivity measured ranged from 0.01 to 5.02 mg m$^{-2}$ day$^{-1}$ but rarely exceeded 2 mg m$^{-2}$ day$^{-1}$ (Figure 5.16). The largest concentrations were recorded in GB10 but this river did not consistently display the highest rates, with GB11 and GB12 sometimes having the highest [chlorophyll *a*] of any substrate material recovered. Chlorophyll *a* concentrations showed seasonal maxima in spring (May 2011, March-April 2012 and April-May 2013) and summer (August 2011, September-November 2012, June-September 2013) however the timings of these were not consistent in all three rivers. When samples were collected in the winter months (December, January, February) the measurement of primary production yielded values regularly close to or equal to 0.01 mg/m$^2$/per day.

# 5.5 Discussion

## 5.5.1 Seasonal trends observed in [macronutrient], hysteresis and macronutrient interactions.

Concentrations of all measured determinants changed during storm events, indicating that discharge is an important factor in terms of transporting aquatic C, P and N. Seasonal trends can be observed for [DOC], [TP] and [TON] data but also hysteresis patterns have been shown to differ throughout the seasons during the study period. By examining both macronutrient concentrations and hysteresis analysis, a better-informed understanding can be reached about the source of these determinants and the factors that control their export.

### 5.5.1.1 Seasonal changes in [macronutrient]

The seasonally changing time series observed in DOC is typical of that found elsewhere in other temperate catchments draining peat (Billett et al., 2004; Worrall et al., 2006a) (Clark et al., 2007; Cooper et al., 2007; Dawson et al., 2008; Dawson et al., 2011). Maximum [DOC] at Gordonbush are observed in the late summer and early autumn, commonly termed the “autumn flush”, (Worrall et al., 2008). Increased biological activity (and temperature effects on the enzyme phenol oxidase (Freeman et al., 2001a; Freeman et al., 2001b) in catchment soils during the summer months (higher temperatures, longer day length) (Grieve, 1990; Billett et al., 2006; Dawson et al., 2008; Koehler et al., 2009; Dawson et al., 2011; Muller & Tankere-Muller, 2012) produces DOC, which is then flushed from the soil with autumn rainfall (Tipping et al., 2007; Dawson et al., 2008). In winter [DOC] are lower, as biological activity is reduced due to lower temperatures and less labile C (reduced enzyme activity (Freeman et al., 2001a; Freeman et al., 2001b) is available within soil layers (Brooks et al., 1999; Worrall & Burt, 2004; Lumsdon et al., 2005; Tipping et al., 2007; Dawson et al., 2008). All events captured in December were influenced by surface run-off sources from snow melt which has a very low DOC content (Dyson et al., 2011) and this contributes to lower [DOC] by dilution (Schiff et al., 1998; Laudon et al., 2004; Agren et al., 2012).

Changes and ranges in [DOC] recorded during storm events implies DOC export is at least partly controlled by hydrological conditions and this control on [DOC] has been acknowledged in many other studies (Tipping & Hurley, 1988; Grieve, 1994; Hope et al., 1994; Hinton et al., 1997, 1998; Clark et al., 2007; Dawson & Smith, 2007; Clark et al., 2008; Dawson et al., 2011; Dinsmore et al., 2011). Specific hydrological controls on [DOC] will be explored further when the hysteresis analysis results are discussed in the next section 5.5.1.2.

Similarly, the observation that [DOC] are greater than [POC] is quite typical of aquatic organic C export from peatlands (Dawson et al., 2004; Dinsmore et al., 2013), where unless there is extensive gullying (Pawson et al., 2008; Evans & Lindsay, 2010; Rowson et al., 2010) there tends not to be large scale erosion and export of POC.

Peatlands are nutrient-poor environments and are characterised as places where plant available P is limited (Clymo, 1984) and this explains why a strong seasonal trend was not observed in [SRP]. However [P] have been acknowledged to be highest in summer month (Kieckbusch & Schrautzer, 2007) and [TP] did show a similar seasonal trend to those of [DOC], suggesting export of DOC and TP are at least partly controlled by similar mechanisms, e.g. biological activity and discharge (Waldron et al., 2009; Murray, 2012). The seasonal increase in [DOC] and [TP] is most likely the cause for maxima observed in [chlorophyll *a*] (Figure 5.16). Hours of daylight and temperature will increase during spring and summer months and these are significant influences on growth and so [chlorophyll *a*], and the spring maxima (and conversely winter minima) that occurred at Gordonbush are common (Balbi, 2000).

[TON] exhibited the opposite seasonal trends to [DOC] and [TP], with maxima observed in the winter and minima in the summer (Figure 5.8). This pattern has been observed in many peatlands sites (Chapman et al., 2001). It is caused by lower biological demand for N in winter months subsequently causing a reduction in soil retention of N, meaning sources of N are more readily exported from soils (Black et al., 1993; Chapman et al., 2001; Turner et al., 2003; Kieckbusch & Schrautzer, 2007). The range of [TON] is larger in the winter events compared to summer events demonstrating the excess N available for export in the winter compared to summer and that discharge is again an important pathway for transporting N from peatlands soils (Aitkenhead-Peterson et al., 2003; Aitkenhead-Peterson et al., 2005; Dillon & Molot, 2005).

Generally, inputs of N to the ecosystem are low; agricultural activity in the catchments is limited to deer grazing and non-use of agricultural fertilisers, which are rich in N (Mattsson et al., 2005; Taylor & Townsend, 2010). Gordonbush is also located in a rural setting in a sparsely-populated region of the country, therefore inputs of atmospheric N, i.e. N sources from car emissions will be low (Cundill et al., 2007), resulting in generally low [TON] observed at Gordonbush compared to other locations (see section 5.5.2 and Table 5.3).

### 5.5.1.2 [DOC] and [POC] hysteresis at Gordonbush

Hysteresis loops have been described to have five basic patterns: single-line, single-line with loop, clockwise loop, anticlockwise loop and Fo8 loops (Williams, 1989). However (Evans & Davies, 1998) created six loops based on the differing influence of surface, soil and groundwater sources for any given hydrological event (Figure 5.17). Clockwise loops indicate [maximum] is reached before peak discharge (Evans & Davies, 1998) and where source material is easily erodible (Sander et al., 2011). Anticlockwise loops imply a sufficient supply of the determinant after peak discharge has occurred to keep concentrations elevated (Williams, 1989; Gao & Josefson, 2012). Fo8 loops are indicative of a combination of multiple processes which trigger clockwise and anticlockwise loops during the same hydrological event (Seeger et al., 2004; Sander et al., 2011). Complex hysteresis patterns such as Fo8 loops, are hard to link to a single factor, therefore their existence indicates the determinant is not controlled solely by discharge (Gao & Josefson, 2012).

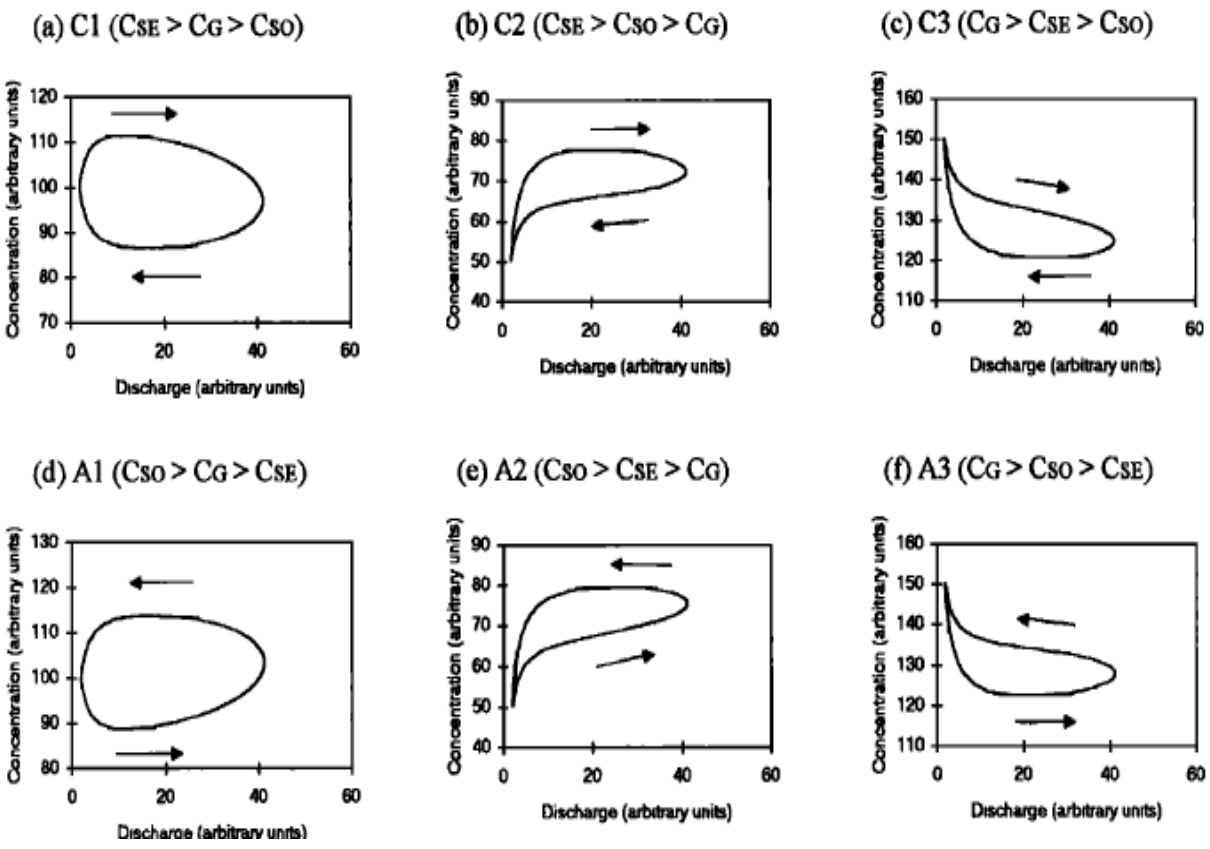


**Figure 5.17 - Classification of discharge-concentration hysteresis loops**
Clockwise (C1, C2 and C3) and anticlockwise (A1, A2, A3) hysteresis loops are produced when a particular source of water (surface, soil or groundwater flow) is dominant during any a hydrological event. This figure was taken from (Evans & Davies, 1998), $C_{SE}$ = Surface flow, $C_{SO}$ = Soil flow and $C_G$ = Groundwater flow.

The majority of hysteresis observed for summer and spring-autumn storm events were anticlockwise, A2, loops. The initial shapes of these loops, where [DOC] increases quickly at start of the event contemporaneously with discharge, suggests shared flow pathways. Between events, especially during summer, peat surfaces can dry out making them more hydrophobic (Holden et al., 2004; Michel et al., 2004) such that rainfall cannot be absorbed, contributing to peatland rivers typically flashy response at beginning of storm events (Holden & Burt, 2003b) where discharge and surface flow increase quickly. Sources of DOC on surface soil layers are quickly transported by surface flow causing a large change in [DOC] at this time (Adamson et al., 2001). If the influence of surface flow was maintained or was dominant throughout the duration of the event, [DOC] would decrease with discharge and create a C2 loop. Instead, A2 loops imply that the dominant source of DOC on the falling limb, but also overall throughout the whole event, is soil flow. As peat surfaces re-wet during the event, percolation increases and DOC is released from the soil profile as this subsurface source of water becomes more dominant. When surface flow is reduced and surface sources of DOC have been exhausted, [DOC] is maintained on falling limb by supply of soil flow which has an abundance of DOC. The mechanism of subsurface DOC transport through riparian soils has been acknowledged as major flux during storm events (McGlynn & McDonnell, 2003; Sanderman et al., 2009).

The change to clockwise, C2, loops for winter storm occurs as the DOC pool is smaller than in summer or spring-autumn (Freeman et al., 2001a; Worrall & Burt, 2004; Evans et al., 2005) as there is lower production of DOC and / or the pool has become reduced due to flushing out in earlier events (Worrall et al., 2002; Hood et al., 2006; Worrall et al., 2008). Thus, because surface sources of C are reduced, an increase in surface flow and discharge is not followed by increase in [DOC]. Additionally when these events occurred, the ground may have been frozen and surface run-off becomes the dominant source of water contributing DOC to river system. As water percolates less easily through the upper soils (Strohmeier et al., 2013), soil flow becomes a less dominant source than surface flow at these times. Furthermore, water from snow melt, which has very low C content, may have increase the surface flow and subsequently caused a dilution in [DOC] (Laudon et al., 2004).

Cross-over loops (or Fo8 loops) occur more often in GB12 compared to GB11 or GB10, due to its smaller catchment size. Clockwise hysteresis loops are usually dominant in catchments <10 $km^2$ (GB12 is 5.14 $km^2$) (Seeger et al., 2004) - although soil flow has a greater influence than surface flow, and this should result in an anti-clockwise loop, the catchment is sufficiently small that soil flow (containing additional source of C and DOC) reaches the river before peak discharge and creates a clockwise loop (Gao & Josefson, 2012).

The same clockwise rotation loops (C2) exhibited for [POC] hysteresis in all rivers across all events reflects the hierarchy of surface > soil > groundwater flow controlling [POC]. Supply of sediment sources must be readily available on rising limb of events from surface soil layers but become exhausted before maximum discharge is reached (Evans & Davies, 1998; Chanat et al., 2002). [POC] and hysteresis results from Gordonbush are in agreement with the acknowledgment [POC] are variable and episodic in their rate of export during hydrological events (Hope et al., 1997b; Pawson et al., 2008; Dinsmore et al., 2010; Dyson et al., 2011) and difficult to predict in absence of long-term monitoring data sets (Dinsmore et al., 2013).

#### 5.5.1.3 POC-TP relationships and hysteresis

Although seasonality was observed in [TP], it was less pronounced than that of [DOC] – rather the largest [TP] recorded were closely associated the largest storm events and coincided with some of the highest [POC] recorded (Figure 5.2 & Figure 5.5). This indicates both [POC] and [TP] are more strongly controlled by river discharge and rainfall intensity (capable of transporting larger suspended loads) than biological activity and temperature. When hysteresis diagrams of [POC] and [TP] are plotted (Figure 5.13) this interpretation is supported as their loops follow the same pattern, implying a common hydrological flow pathway between both determinants and therefore their sources are likely to be similar. Thus, it is not surprising there is a statistically significant correlation between [POC] and [TP] (Figure 5.13).

Furthermore, it was observed some of the highest [POC] noted during this research were simultaneously recorded in all three rivers during summer storm events (Figure 5.2). When there are periods of no rainfall before a summer storm, the soil surface can dry up and crack. When a heavy rainfall event does eventually occur, the soil surface is susceptible to erosion and leads to increased [POC]. This further indicates antecedent conditions and size of storm events are more influential than seasonality determining [POC] and [TP]. The largest [POC] occur in spring-autumn and winter and may indicate a response to peat drying in summer facilitating erosion with higher autumn-spring flows, or it may just be a response to higher discharge causing more erosion.

Since [POC] and [TP] were well correlated in all three rivers (Figure 5.13) this signifies that most the TP being transported is in insoluble form. This conclusion is reinforced when average percentages of [TP] which were made up of [SRP] are calculated, with the results as follows, GB10 = ~48%, GB11 = ~18% and GB12 = ~16%.

### 5.5.1.4 TON hysteresis and DOC-TON relationship

Hysteresis analyses of [TON] show summer storm events are dominated by A3 loops and winter events by C3 loops. This seasonal change in hydrological controls is reflected in, and supported by, previous observations and interpretation of a winter maxima and summer minima in [TON]. In winter months the relative abundance of N in soil layers increases thus causing surface run-off to become a more influential source of TON during this time, resulting in C3 clockwise loops where groundwater > surface > soil. In the summer, as N is depleted at the surface due to biological uptake, inputs from the soil profile outweigh those from the surface and A3 anticlockwise loops are observed where groundwater > soil > surface. It was noted that GB12 consistently displays C3 loops regardless of season. In catchments <10 $km^2$ surface run-off sources are commonly more influential than source of N from the soil profile as the catchments are better hydrologically connected and surface run-off is transferred into streams quicker and more efficiently (Seeger et al., 2004). Since GB12 catchment size is 5.14 $km^2$ this explains why only C3 loops are observed.

It has been acknowledged N inputs to peatland catchments are dominated by precipitation (i.e. atmospheric fallout) (Adamson et al., 1998) and atmospheric sources of N (precipitation containing $NO_3^-$) have been found to be delivered directly to streams during winter events (Sebestyen et al., 2008). Although this process might be contributing to seasonal changes in [TON] observed at Gordonbush it contradicts the hysteresis analyses that suggest [TON] is mostly influenced by groundwater sources during storm events. Quantifying the effect of atmospheric N sources on aquatic [TON] has not been possible during this research and so it is unknown if this is significant. However, the inverse [DOC]-[TON] relationship observed in Gordonbush data (Figure 5.15) has been noted in other studies (Inamdar et al., 2004; Aitkenhead-Peterson et al., 2005; Goodale et al., 2005; Evans et al., 2006b; Clark et al., 2008; Waldron et al., 2009; Taylor & Townsend, 2010; Daniels et al., 2012).

The use of fertilisers and increases in atmospheric N deposition caused by thermal industrial processes was thought to lead to increases in N species in surface waters (Galloway et al., 2008), including those in peatland catchments. However, it has been hypothesised that larger amounts of labile C lead to N immobilisation and denitrification by heterophic microbes (Taylor & Townsend, 2010). This process can occur in areas surrounding streams which can cause nitrate levels to decrease and therefore reduce $NO_3^-$ exported in rivers (Goodale et al., 2005). Subsequently soils with high C content i.e. peatlands, have been identified as areas less susceptible to $NO_3^-$ leaching (Evans et al., 2006b) and TOC/TON ratios are highest in peat-dominated catchments (Mattsson et al.,

2015). It has been proposed that during the start of hydrological storm events, $NO_3^-$ in stream water is derived from groundwater sources which are displaced by infiltrating precipitation (Inamdar et al., 2004). As the storm event progresses, DOC sources from surface run-off, and through-flow from soils when they become saturated and subsequently dominate, dilute the influence of $NO_3^-$ inputs (Inamdar et al., 2004; Aitkenhead-Peterson et al., 2005). This combined with higher labile C depressing nitrate production (Goodale et al., 2005) contributes to inverse [DOC]-[TON] relationships seen in peatlands, and observed at Gordonbush. These conclusions and interpretation are also supported by hysteresis analyses of [TON] which suggest that groundwater is the dominant source controlling [TON] in the Gordonbush rivers.

The inverse [DOC]-[TON] relationship occurs in GB11 and GB12 but not in GB10; the major difference between them is the legacy of forest felling in the Bull Burn Plantation in Allt Mhuilin (GB10) catchment. It is possible the increased breakdown of harvesting residues may have contributed an additional source N (Cummins & Farrell, 2003; Tetzlaff et al., 2007) in GB10, enough to mask the inverse [DOC]-[TON] relationship that otherwise exists. However, DOC-TON interactions are complex and merit additional investigations as type (not concentration) of C species, i.e. low-weight vs. high-weight molecular, may be the most important factor controlling N release from peat soils (Saari et al., 2009). In addition, C:N have been used in empirical models to predict annual DOC fluxes with a high degree of accuracy therefore further understanding of DOC-TON interactions could assist future estimates of C fluxes from peatlands, especially under changing climatic conditions (Aitkenhead & McDowell, 2000).

#### 5.5.1.5 DOC-SRP relationships

The curvi-linear [DOC]-[SRP] relationships are intriguing (Figure 5.15) and provide an understanding of the process of macronutrient export. Two interpretations are proposed below.

1. The highest [DOC] (above >25 mg $l^{-1}$) and low [SRP] are associated with high flow conditions in summer (August) events. Summer months are times when P uptake by vegetation is at a maximum and hence leads to lower levels of available P in the soil profile. So, at times of year when [DOC] is high [SRP] will be low due to plant uptake. Alternatively, SRP and DOC are coming from different sources during an event and SRP is exhausted earlier than DOC.

2. Peatland soils are largely water logged and the fastest rates of decomposition of organic matter occur in the surface layers. Therefore, it is likely that largest

concentrations of SRP can also be found in the top / surface soil (Steinmann, 1997). During storm events the SRP in the top layers of soil will be quickly transported into surrounding streams by surface run-off, however as peatlands are nutrient-limited environments, the pools of SRP are relatively small and become exhausted early in the event (on rising limb of storm hydrograph) before discharge reaches a maximum. As maximum [DOC] (supplemented by DOC sourced from deeper within soil profile as it becomes saturated and more hydrologically connected) and event discharge are approached, smaller quantities of SRP are available for export from top soil and the relatively poor solubility (and source) of SRP in deeper parts of the soil profile. Subsequently, as a maximum on a storm hydrograph is approached, and on the falling limb, [SRP] begin to decrease back towards zero. This export mechanism is similar to that explained by Knorr (2013) regarding DOC and by (Rigler, 1979) for SRP. I propose that [DOC] of ~20 mg $l^{-1}$ represents a critical flow rate where the majority of available SRP has been transported and thereafter quantities only decrease.

The curvi-linear shape of [DOC]-[SRP] is not seen as clearly in GB10 compared to GB11 and GB12, and this is comparable to differences between the catchments seen for [DOC]-[TON] inverse relationships. Similar reasons for this observation could be applicable where there is an additional P input in GB10 due to forest felling debris: [SRP] is higher for a given [DOC] suggesting an additional source of P (on the assumption all catchments should behave the same unless there is a mechanism otherwise). The possible impact of forest felling is discussed in more depth in a later section looking at inter-catchment differences (see section 5.5.4).

## 5.5.2 A comparison of Gordonbush drainage [macronutrient] to other sites

The range of [DOC] and [POC] recorded between all three catchments at Gordonbush are comparable to other studied northern temperate peatland sites (Table 5.5). [TP] are comparable to other cited peatland study sites in Scotland, Ireland, Finland and Canada. [SRP] measured at Gordonbush are at the lower end of the ranges found in the literature. Mean [$NO_3^-$], of which [TON] represents a possible maximum, have been documented to be < 1000 µg $l^{-1}$ far north east Scotland (i.e. Caithness and Sutherland region) (Betton et al., 1991; Chapman et al., 2001). Gordonbush is in this range as mean [TON] are less than < 1000 µg $l^{-1}$ and comparable with other peatland studies, but at the lower end of the ranges reported.

| Research field site, peatland & sample type | DOC & POC (mg $l^{-1}$) | TP & SRP (µg $l^{-1}$) | TON (µg $l^{-1}$) | Author (s) |
|---|---|---|---|---|
| **Scotland** | | | | |
| River Dee Basin, NE Scotland | 1 – 33 | 2 – 255 | 14 – 2340 | (Dawson et al., 2004; |
| Blanket bog & river | <1 – 22.9 | | | Dawson et al., 2011; |
| | | | | Dawson et al., 2012) |
| 3 sites across Scotland | | | <10 – 853 | (Dawson et al., 2008) |
| Mixed & river | | | | |
| River Dee Basin, NE Scotland | | | 0 – 1000 | (Black et al., 1993) |
| Blanket bog & river | | | | |
| Various sites in Scotland | | | <10 – 3005 | (Chapman et al., 2001) |
| Upland ombrotrophic & stream | | | | |
| NE Scotland and Mid-Wales | (POC) | | | (Dawson et al., 2002) |
| Upland ombrotrophic & stream | <1 - 67 | | | |
| Brocky Burn, NE Scotland | 5 – 40 | | | (Billett et al., 2006) |
| Upland ombrotrophic & stream | | | | |
| Braes of Doune, Central Scotland | 2 – 35 | | | (Grieve & Gilvear, 2008) |
| Blanket peat & streams | | | | |
| Loch Ard, Central Scotland | 5 – 25 | 3 – 50 | 0 – 83 | (Tetzlaff et al., 2007) |
| Upland ombrotrophic & stream | | | | |
| Auchencorth Moss, SE Scotland | 4 – 88 | | | (Dinsmore et al., 2013) |
| Lowland ombrotrophic & stream | <1 – 17.8 | | | |
| Whitelee, SW Scotland | 3 – 57 | 0 – 340 | 0 – 2440 | (Waldron et al., 2009; |
| Upland ombrotrophic & stream | <1 – 23.4 | 0 – 275 | | Murray, 2012) |
| Arecleoch, SW Scotland | 3 – 65 | | | (van Niekerk, 2012) |
| Upland ombrotrophic & stream | 1 – 138 | | | |
| **UK & Ireland** | | | | |
| Moor House, NE England | 5 – 40 | | 0 – 400 | (Adamson et al., 1998; |
| Blanket bog & stream | | | | Clark et al., 2009) |
| River Ashop, NE England | 1 – 46 | | | (Pawson et al., 2012) |
| Blanket bog & stream | <1 – 1230 | | | |
| Hexhamshire, NE England | 7 – 208 | | | (Rowson et al., 2010) |
| Blanket bog & stream | 3 – 102.6 | | | |
| Hexhamshire, NE England | 3 – 24 | | | (Worrall & Burt, 2008) |
| Upland peat & rivers | | | | |
| Upper Teesdale, NE England | | | 0 – 450 | (Cundill et al., 2007) |
| Upland peat & streams | | | | |
| Upper Teesdale, NE England | | 0 – 300 | 0 – 500 | (Turner et al., 2003) |
| Upland peat & streams | | | | |
| W Ireland | 25 – 85 | | 0 – 2000 | (Cummins & Farrell, |
| Blanket-forested & streams | | | | 2003) |
| Burrishoole, W Ireland | | 0 – 530 | | (Rodgers et al., 2010) |
| Blanket bog & stream | | | | |
| **Rest of the World** | | | | |
| Southern Finland | 0 – 75 | 0 – 50 | 10 – 540 | (Nieminen, 2004) |
| Upland forested & stream | | | | |
| Vilppula, S Finland | | 0 – 500 | | (Kaila et al., 2014) |
| Boreal forested peat & stream | | | | |
| Ontario, Canada | | 0 – 300 | 0 – 4700 | (Devito & Dillon, 1993) |
| Fen & stream | | | | |
| Alberta, Canada | | (SRP) | | (Thormann & Bayley, |
| Fen & rivers | | 9 – 100 | | 1997) |
| **Gordonbush** | 1 – 49 | <LOQ-265 | <LOQ - 141 | This study |
| Blanket bog & stream | <0.1 – 22 | <LOQ - 39 | | |

**Table 5.5 - Values of [DOC], [POC], [TP], [SRP] and [TON] ranges from other peatland sites**
A description of where research was undertaken (as well as peatland type & sample type), range of [] macronutrients measured lead author of paper and year of publication is documented in the table above. 'Mixed' peatland type means a combination of ombrotrophic, minerotrophic or both, were investigated. Not every example presented highlighted the LOQ (<0.15 µg $l^{-1}$) of their [SRP] and [TON] so '0' (zero) values do not necessarily mean no trace of determinants was measured when analysed so caution has been taken when comparing and contextualising these minimum values.

### 5.5.3 Water Quality at Gordonbush

Annual mean [TP] for GB10 and GB11 (Table 5.3), is of "Good" water quality where GB12 annual mean is of "High" status in comparison to Table 5.2. When mean [SRP] are considered, all three rivers meet standards of the highest river water quality standard presented in Table 5.2. Lower ranges of [SRP] should be expected as northern peatlands such as Gordonbush are P (nutrient)-limited environments (Aerts et al., 2001). Over the research period there is a decrease in mean [SRP] observed in GB10 during events (Figure 5.6). This reduction may suggest that any impact of windfarm activities on SRP was only noticed in GB10 during the first 6-12 months of construction (August 2010 to August 2011). This may be related to forestry felling in GB10 catchment. [SRP] in GB11 and GB12 were consistently recorded in the "High" river quality bracket and there is a suggestion that [SRP] decreases over time (Figure 5.6), similar to trends observed in GB10. However, since GB12 was not affected by windfarm construction and trends seen in that catchment and GB11 are the same, it may signify that there were no SRP related windfarm impacts in GB11 and results recorded are measures of natural variability.

The only enforced water quality standard relating to [TON] is the EU Drinking Water Directive which outline nitrate ($NO_3^-$) levels must be <50 mg $l^{-1}$ (standard set in relation to severely limit methemoglobinemia cases in infants). The range of [TON] measured at Gordonbush (up to maximum of 140.8 µg $l^{-1}$) is far less than this limit. This is not unexpected as peatlands are considered N-limited environments (Chapman et al., 2001; Cundill et al., 2007).

### 5.5.4 Inter-catchment differences and assessment of the overall impact of windfarm construction on stream water chemistry

DOC, POC, TP and SRP concentrations generally followed the trend GB10 > GB11 ≥ GB12. Stream [DOC] has been positively correlated with catchment characteristics including size (Grieve, 1994; Dawson et al., 2002; Kortelainen et al., 2006), soil type and peat coverage (Hope et al., 1994; Dillon & Molot, 1997; Hope et al., 1997a; Hope et al., 1997b; Aitkenhead et al., 1999; Gergel et al., 1999; Aitkenhead-Peterson et al., 2007; Mattsson et al., 2007). When plotted, mean [DOC] for all three Gordonbush catchments (Figure 5.3), the ranked order of the catchments match the size and specific peat coverage: GB10 28.87 $km^2$ with 84% amount of peat coverage, GB11 15.39 $km^2$ with 64% and GB12 5.14 $km^2$ with 17% (Figure 3.2). Discharge increases with catchment size, so given links between [POC] and discharge it is unsurprising the ranked order matches [DOC]. Historically cut drainage channels can aid peat erosion (Evans & Lindsay, 2010) and a survey conducted at Gordonbush in 2010 (Milne, 2010) mapped a greater number

of drainage channels in GB10 catchment compared to GB11 and none were recorded in GB12 catchment (Figure 3.14). This could also be contributing to the observed differences.

Increases in aquatic [POC] in peatland catchment have been attributed to anthropogenic activity (Mattsson et al., 2005). In eroding peatlands where deep gully erosion occurs [POC] can peak at 800-1200 mg $l^{-1}$ (Pawson et al., 2008; Pawson et al., 2012) and flux values can be higher than DOC losses (Evans et al., 2006b; Pawson et al., 2008). Since windfarm construction involves considerable amounts of soil disturbance and peat excavation it might be hypothesised that [POC] should increase in construction-affected catchments because of increased areas of unconsolidated soil material and greater potential for particulate transport during storm events. A clear increase in [POC] is not observed during or after the construction phase in GB10 and GB11 compared to GB12 and the ranking order and magnitude in [POC] between different catchments is consistent. This suggests that management practices and silt settling ponds used along drainage channels near to road networks on site have been successful in mitigating any impact of increased silt material entering the main rivers, Allt Mhuilin and Allt Smeorail (Figure 5.18).

Catchment characteristics including peat coverage (Dillon & Molot, 1997), may also influence [TP] and so the ranked order of the catchments. Forest felling may also be a significant factor; the Bull Burn plantation located in GB10 catchment was felled in May 2010. Forest harvesting is known to increase nutrient concentrations in adjacent rivers (Feller, 2005) which can cause deterioration of water of quality downstream (Nieminen, 2004; Kaila et al., 2012).

Increases in P (Dillon & Molot, 1997; Ahtiainen & Huttunen, 1999; Cummins & Farrell, 2003; Nieminen, 2003, 2004; Rodgers et al., 2010; Kaila et al., 2012) and [DOC] (Neal et al., 1998; Cummins & Farrell, 2003; Nieminen, 2004; Tetzlaff et al., 2007; Muller & Tankere-Muller, 2012; Murray, 2012) export due to deforestation in peatland catchments have been noted. Decomposition of felled debris is complex and its rate is dependent on many factors such as moisture conditions, temperature and microbial activity (Laiho & Prescott, 2004; Prescott, 2005; Kaila et al., 2012). However, the organic matter left behind after felling (brash) creates a labile pool of C (Nieminen, 2004; Tetzlaff et al., 2007) and P (Piirainen et al., 2004; Kaila et al., 2012).

**Figure 5.18 - Examples of sediment sumps at Gordonbush**
Above are two examples of the use of sediment sumps at Gordonbush, installed during the period of wind farm construction. Sumps were utilised as part of road and borrow pit drainage network. The sumps primary purpose was to collect and stop large volumes of silt ultimately entering water and river courses during periods of intensive surface run-off. The sumps were periodically emptied so their primary purpose was maintained effectively. Photographs were taken by (Knotts & Sloman, 2013).

Sample collection did not start until July 2010 (when felling had already started) so no data exists for prior to foresting felling in the Bull Burn Plantation for comparison. [SRP] were consistently highest in GB10 and the lack of forest harvesting in GB11 and GB12, combined with extremely low [SRP] recorded in those catchments (majority <5 µg $l^{-1}$) indicates that P is mostly found in particulate form in catchments at Gordonbush in the absence of forestry felling activities. We suggest that the legacy of felling in GB10 is a likely cause of observed increased soluble phosphorous, i.e. [SRP], between it and the other two catchments (GB11 and GB12) (Figure 5.7). Generally, a decreasing mean [SRP] trend can be observed from GB10 and P concentrations have returned to pre-felling conditions within four years at other sites (Rodgers et al., 2010). This suggests a rapid release of P shortly after harvesting, but with decreasing flux over time.

In Finnish peatland catchments clear-cutting increased export of C and nutrient, sometimes for periods >10 years; however the increases are only significant if clear cutting exceeds 30% of catchment area (Palviainen et al., 2014). The Bull Burn Plantation covered an area ~15 % of the total Allt Mhuilin catchment area. In addition, the generally higher rates of primary production in GB10 than GB11 and GB12 (Figure 5.16) may be a response to higher [SRP] and [TP].

The ranking order of [DOC] between catchments stayed consistent throughout the research period (Figure 5.2). Although recorded maximum and mean [DOC] increase

yearly between 2010 and 2012 in GB10, the same is not observed in GB11 and GB12. This observed mean [DOC] increase in GB10 in addition to higher [SRP] measured in this catchment would suggest that the legacy of forest felling is contributing to an increase in C export compared to GB11 (affected by windfarm construction but not forest felling) and GB12 (no windfarm construction or forest felling). This supports the conservative conclusion that the impact of windfarm construction, excluding forest felling, on [DOC] is minimal. Additionally, the use of mean [determinants] to determine impact of changes in river systems has been proven to be an effective method (Lessels & Bishop, 2014).

This interpretation is also further feasible if yearly increases in [DOC] in GB10 could be partly due to periods of frost and cold winter conditions in the previous years (Haei et al., 2013). The winter of 2010/2011 were very cold (Met Office, 2013b) which can cause [DOC] in the soil to increase in following spring and summer (Agren et al., 2010b; Haei et al., 2010; Agren et al., 2012) and though this process would be active in GB11 and GB12, it perhaps had a greater effect in GB10 given the larger area of peat within the catchment thus contributing to an increase in maximum [DOC] observed. However, concentration data alone is sufficient to be certain of any potential impact caused and this issue has to be considered further when calculating C fluxes per unit area (Chapter 6).

Increases in [$NO_3$] have been observed after periods of forest felling (Cummins & Farrell, 2003; Tetzlaff et al., 2007) however this is has not always been translated into increases in N export (Kaila et al., 2012). Although it was suggested earlier that observations of a lack of an inverse relationships between [DOC]-[TON] in GB10 could be due to forest felling activities the changes in [TON] within and between the catchments at Gordonbush (Figure 5.9) is probably best described as seasonal and an impact of forest felling is not detected.

Nitrate concentrations have been positively correlated with percentage catchment coverage of brown forest soils, and negatively correlated with peat (Chapman et al., 2001; Aitkenhead-Peterson et al., 2005). GB10 contains the highest percentage of brown forest soils (4% compared to 2% in GB11 and 0% in GB12) but also highest percentage of peat (84%, compared to 64% in GB11 and 17% in GB12) and this particular distribution may contribute to the variation in [TON] seen between the catchments.

Unfortunately, data collected prior to forest felling was limited (spot samples collected by Dr. Dargie for WQMP between December 2009 and August 2010) and did not allow a direct “before and after” assessment of [DOC], [POC], [TP] and [SRP] in GB10. However, in summary, the observations of elevated [SRP] and small increases in [DOC] in GB10, compared to GB11 and GB12, and the greater rates of primary production, suggest forest

felling has impacted on water quality. This impact is very small and water quality (as determined by the new standards set by (UK TAG, 2013)) overall varied between “Good” and “High” status throughout the research period. There is no signal of impact from construction activities of the windfarm.

## 5.6 Summary of stream-water chemistry at Gordonbush

Typical seasonal trends in DOC, TP and TON have been observed in all Gordonbush time series. All ranges of determinants measured are comparable with other systems that do not host a windfarm. Standards of water quality relating to [SRP] were either “Good” or “High” throughout the duration of the study period with little or no deterioration in water quality standards or increase in mean concentrations during the sample collection period.

Hysteresis analysis has demonstrated that [DOC] export varies between catchments, rising and falling limbs and throughout different time periods in the year. This observation crucially informs approaches to construct aquatic organic C fluxes (chapter 6). Hysteresis analysis has also help highlight the magnitude of storm events is most probably more important than seasonality in controlling [POC] and [TP]. Hysteresis analysis supported and reinforced interpretations of seasonal changes in [TON]. The inverse relationship found between [DOC]-[TON] at Gordonbush has been commonly observed in other studies, but the curvi-linear relationship between [DOC]-[SRP] could be related to an exhaustion of SRP sources in the topsoil on rising limb of storm events before sources of DOC are increased as deeper parts of the peat profile become more hydrologically connected (and SRP sources are limited) as a storm event develops.

POC, TP, SRP and TON concentrations retain a catchment ranking order and magnitude varies little throughout the research period. The windfarm affected (GB10, 11) and control catchments (GB12) are behaving similarly. Although they decreased over time, the elevated [SRP] measured in GB10 compared to GB11 and GB12, suggest the likelihood of higher C and nutrients measured in GB10 might to be related to the legacy of forest felling - the decomposition of the harvested debris left behind in the Bull Burn plantation adjacent to Allt Mhuilin river. Additionally, both [DOC]-[SRP] and [DOC]-[TON] relationships in GB10 may be masked by increased nutrient supply from forest felling debris. However, apart from forest felling, there is no evidence that windfarm construction activities are impacting macronutrient fluvial concentrations, and/or causing a deterioration in water quality (where there are standards to assess this). However, total efflux is also a function of discharge and whether an impact is more prevalent when discharge is accounted for and this is explored further in the following flux chapter.

# 6 Constructing aquatic organic carbon fluxes to assess the impact of windfarm construction

## 6.1 Abstract

Whether windfarms increase fluvial C export is a key question. To answer this, accurate export budgets must be calculated. Here, I use the time series of [C] and corresponding discharge to calculate annual catchment export budgets for three complete hydrological years, from August 2010 to September 2013. Further I use different approaches to explore the sensitivity of the flux calculation method on the C export budget estimate, for example, linear regression and the traditional 'Method 5' (Walling & Webb, 1985) were used. Based on results of hysteresis analysis presented in the previous chapter, linear regression (when data was separated by the time of year and rising or falling limbs of storm events) was selected as the method to estimate fluxes. In addition, multiple linear regression (MLR) methodology was explored to investigate if aquatic organic C fluxes could be estimated and improved compared to results using linear regression. Analysis showed air temperature and alkalinity were the best descriptors to utilise to infer measured [DOC]. However, alkalinity was not measured continuously throughout the research so MLR analysis undertaken could not provide further aquatic organic C fluxes estimates. Total annual aquatic organic C fluxes calculated using linear regression techniques ranged from 3-38 g C $m^{-2}$ $yr^{-1}$ for Allt Mhuilin (GB10), Allt Smeorail (GB11) and Old Town Burn (GB12). This range is similar to aquatic C flux estimates for other UK and northern hemisphere peatlands sites (10-100 g C $m^{-2}$ $yr^{-1}$). Although maintaining the same ranked position of GB10 > GB11 > GB12, C fluxes in GB12 showed little inter-annual variation; this was not the same with GB10 and GB11. C flux estimates dropped by ~35 % between 2011-2013 in GB10 and by ~25% during the same time period at GB11. These changes imply that C fluxes may have been more elevated in GB10 and GB11 in 2011 and 2012, compared to GB12, and this may be a consequence of windfarm construction activities in both catchments. Only a three year data set was collected, and so assessing the cause of inter-annual variability was challenging, but the decrease in exports in 2013 and a return to closer ranges across the catchments, suggest that if there was an impact of the windfarm, it was short-lived. To advance estimations of aquatic organic C fluxes from peatlands in the future, it is recommended the best predictive variables identified during MLR analysis are continuously measured. However, a model which integrates both empirical data and processed-based modelling is advocated as the best future strategy.

## 6.2 Introduction

C is lost from peatland systems through gaseous and aquatic pathways (Billett et al., 2006; Moody et al., 2013). Aquatic organic C fluxes are typically simpler to measure, than non-aquatic fluxes (gaseous and inorganic C sources), given aquatic systems unidirectional export where all losses occur at a single location, the catchment outlet (Billett et al., 2010). Concentration time series of aquatic organic C species (DOC and POC) do not show total C losses and consideration of these alone cannot be used to deduce changes in C export, which also depends on discharge on discharge.

Indeed, river fluxes constitute a concentration e.g., [C], multiplied by a discharge (Hirsch et al., 1991; Cohn, 2005). Thus where (semi-)continuous time series of concentration and discharge coexist, the flux can be calculated. River discharge time series are relatively easy to calculate from continuous stage height records', providing a ratings curve exists (see section 3.12). Continuous [DOC] and [POC] time series are not commonly available as continuous measurement of aquatic organic C determinants (or any other macronutrient) is expensive (Cohn, 2005) and *in-situ* data logging devices directly measuring both parameters are not currently available. Systems for measuring [DOC] continuously *in-situ* (instruments making indirect measurement through UV-visible spectrometry (Sandford et al., 2010; Grayson & Holden, 2012), are available e.g., TriOS (www.trios.de) and s::can (www.s-can.at) but are again expensive and thus far have not been used extensively in academic research. Therefore, to calculate an annual aquatic organic C flux, forms of interpolation are needed between manually sampled measurements (Hinton et al., 1997).

Finding links between changes in physical parameters that reflect changes in aquatic organic C export is essential to this interpolation. Discharge is a key driver of aquatic C export (Grieve, 1990; Hope et al., 1994; Hinton et al., 1997; Schiff et al., 1997; Hinton et al., 1998; Schiff et al., 1998; Clark et al., 2007; Dawson & Smith, 2007; Worrall & Burt, 2007a; Dawson et al., 2008; Clark et al., 2009). Therefore, it is logical to use methods involving discharge to predict [C]. To understand and identify which approach to estimating aquatic organic C export (using discharge) is best aligned with field export mechanisms, hysteresis analysis can also prove to be a helpful tool and was undertaken in the previous chapter (5).

'Method 5', utilising flow weighted mean concentrations and mean annual discharge (Verhoff et al., 1980; Walling & Webb, 1985) has been a popular and favoured procedure for calculating river load fluxes (e.g. aquatic organic C fluxes) for a number of years (Hope et al., 1997a; Dawson et al., 2002; Worrall et al., 2003; Billett et al., 2004; Dawson et al.,

2004; Pawson et al., 2008; Rowson et al., 2010; Pawson et al., 2012) and was recommended by Paris Commission for measurement of river fluxes (Littlewood, 1992). C fluxes, using the 'Method 5' technique, are commonly estimated using samples of concentration collected at weekly, fortnightly or monthly intervals (Grayson & Holden, 2012). However, large proportions of overall C fluxes are exported during short time periods of high flow (Evans et al., 1999; Holden & Burt, 2003b) which are not regularly captured during routine sampling programmes (Clark et al., 2007) as peatland streams respond rapidly to discharge events with short-lived (flashy) hydrograph peaks due to the surrounding soils being permanently in, or closely, to a waterlogged condition (Price, 1992; Holden, 2005b; Evans et al., 2014). It has been estimated that approx. 50 % of aquatic C fluxes totals are exported within 10 % of highest flows (Hinton et al., 1997; Clark et al., 2007). Not characterising such events can lead to significant errors in calculating total aquatic C fluxes (Clark et al., 2007) using techniques such as 'Method 5' (Grayson & Holden, 2012).

By employing a sampling strategy focussed in capturing storm events, this research project has aimed to better account for the significance of aquatic C fluxes during periods of high discharge, especially in the late summer when the 'autumn flush' occurs (Mitchell & McDonald, 1992) as abundant sources of C that have accumulated due to microbial breakdown of soil as it dries during the summer, are washed into river by heavy rainfall (Grayson & Holden, 2012). Due to having an increased sampling frequency over a wider range of hydrological conditions, alternative flux estimations have been investigated rather than simply using averaging approaches e.g., 'Method 5'. The aim is to refine the flux estimates by investigating statistical relationships between physical parameters and measured [C] data to infer [C] when no samples were collected, using both linear (can [C] be inferred successfully using stage/discharge) and MLR (e.g. can estimates be improved by using more than one variables, e.g. discharge and temperature) techniques. Log linear models are often used for this purpose because of its relatively inexpensive cost of acquiring the data utilised (Horowitz, 2003) compared to measuring and recording multiple chemical or biological parameters *in-situ*. In some examples discharge parameters can explain up 50 % of total variability in river load estimates (Cohn et al., 1992).

Ultimately these budgets are being constructed to assess if aquatic organic C fluxes, have been affected by windfarm construction, which may be masked when considering a concentration time series alone. This is undertaken by examining inter-annual variations between catchments affected by windfarm construction (GB10 and GB11) and the control site (GB12).

# 6.3 Methods

Inorganic forms of C (e.g. $CO_2$) are exported in fluvial systems (Billett et al., 2006; Waldron et al., 2007; Alin et al., 2011; Aufdenkampe et al., 2011) and can represent a significant proportion of terrestrial C losses from peatlands (Moody et al., 2013). However this research project has only accounted for aquatic organic C (DOC & POC) losses within export budgets from Gordonbush catchments as it was not logistically possible to measure DIC and nutrients so the focus was on the latter due to its importance in assessing water quality.

All methods relevant to sample collection and analysis are described in the methodology chapters 3 & 4. Here I document: additional methods used to generate data utilised to construct aquatic organic C fluxes; a description of flux calculations utilising various linear regressions; an explanation of how aquatic organic C fluxes are estimated using 'Method 5' (Walling & Webb, 1985) river load calculation technique; MLR techniques utilised to create an equation to infer [DOC] based on more than one variable.

## 6.3.1 Estimating aquatic organic carbon fluxes

### 6.3.1.1 Collection of data used to estimate fluxes

Gordonbush [DOC] and [POC] datasets collected between August 2010 and September 2013, include samples taken during event sampling, spot samples and monthly samples collected as part of WQMP between December 2009 and December 2012 (collected by Dr. Tom Dargie). Stage height records are displayed in Appendix B and discharge has been estimated through stage-discharge ratings curve (see section 3.12 and Appendix D) from data collected by ISCO 2150 flow meter.

### 6.3.1.2 Linear regression

Aquatic organic C fluxes have been calculated by investigating if there was a statistically significant linear relationship between stage or discharge and [C] using three different approaches. This has been undertaken to take into account the temporal variation in [DOC] which is apparent in the time series data (see section 6.3.1.2) and the intra-event. As concentration-discharge relationships for a range of river solutes are commonly linear on when both axes are logged (double-log) (Godsey et al., 2009) in all approaches I assessed if a stronger statistical relationship could be found by transforming the data by using natural logs (ln). Applying log transformations can make data sets "appear" less highly skewed, more normally distributed and more interpretable (MacDonald, 2009). The regression equation (either linear, $2^{nd}$ order polynomial (quadratic) or double log linear

form) that produced the highest $R^2$ and lowest p-values was then used to infer [DOC/POC] continuously from August 2010 to September 2013 as described below.

The three approaches were:

- All [DOC] and [POC] data has been used to create a single regression equation to estimate [DOC] and [POC] from discharge or stage height (at 15 minute resolution). **(Code – All Data)**
- [DOC] and [POC] data have been considered seasonally, creating three separate regression equations with stage height or discharge. The three time periods were defined as follows: Summer (samples collected in June, July, August and September); Winter (December, January, February); Spring-Autumn (March, April, May, October, November). **(Code – Seasonal)**
- The data categorised into three time periods was further split into two groups based on where the samples were collected on the rising or falling limb of a hydrological event. This created six linear relationships that inferred [DOC] and [POC] for each river based on discharge or stage height on both limbs of storm hydrographs. **(Code – Seasonal + R&F limbs)**

Approaches like this for dividing data sets to find the best relationships between discharge and concentration have been used elsewhere, e.g., Horowitz (2003). For comparison with these more detailed approaches, two other estimates of aquatic organic C fluxes were made, which assumed [DOC] and [POC] remained constant in the time period between two adjacent sampling data points. The first comparison used all storm event and spot sampling data (Event & Spot samples); the second used only spot sample data and no storm event data (Spot samples), an approach typical of many sampling programmes.

### 6.3.1.3 Estimating aquatic organic carbon fluxes using 'Method 5'

Continuous [C] are often estimated using a flow-weighted mean [C] (e.g., (Dinsmore et al., 2013)). 'Method 5' (Verhoff et al., 1980; Walling & Webb, 1985) utilises this technique, producing an averaged value then multiplies it by annual mean discharge (commonly referred to as 'Q') to estimate downstream export of any determinant a user requires,

$$Total\ Annual\ Load = Q_r \times \frac{\sum_{i=1}^{n}[C_i \times Q_i]}{\sum_{i=1}^{n} Q_i} \quad (6.1)$$

for the 'Method 5' Eqn (6.1) $C_i$ = instantaneous concentration associated with individual samples, $Q_i$ = instantaneous discharge at time of sampling, $Q_r$ = annual mean discharge and n = number of samples.

Standard errors of fluxes calculated from 'Method 5' equations can also be estimated using total annual discharge and variance of flow weighted mean concentration (Hope et al., 1997b). The method was used to compare the aquatic organic C flux results from Gordonbush to other studies that have used the same technique and the flux estimations of other techniques employed in this research project.

A flow weighted average mean [DOC] and [POC] was calculated using all samples collected (storm events, spot and WQMP samples) in an individual (hydrological) year to calculate aquatic C flux estimates, **(Code - Method 5 (all data))**. In addition, an aquatic C flux was calculated using a flow-weighted average mean [DOC] and [POC] that only utilised the spot and monthly WQMP samples **(Code - Method 5 (Spot))**. This was to test the sensitivity of including storm events in the Method 5 approach.

| Summary of all flux calculation methods | |
|---|---|
| **Code Name** | **Technique and data used** |
| Linear and Non-Linear techniques | |
| **All data** | All [DOC] & [POC] data |
| **Seasonal** | Split into 3 time periods |
| **Sea. + R&F limbs** | Split into 3 time periods & rising and falling limbs |
| **Event & spot samples** | linear [C] assumed between data points using all data collected |
| **Spot samples** | linear [C] assumed between data points using only spot samples |
| Utilising Method 5 methodology techniques | |
| **Method 5 (all data)** | Method 5 methodology using all data |
| **Method 5 (Spot)** | Method 5 methodology using only spot samples |

**Table 6.1 - Summary of flux calculations used in Chapter 6**
Code names and a brief description of the technique and data used for each flux calculation method is presented above. The table is split documenting linear and non-linear techniques and Method 5 methodology.

#### 6.3.1.4 Multiple linear regression

All multiple linear and stepwise regressions were undertaken in the statistical software package Minitab v16. Given that DOC commonly constitutes the large majority of aquatic organic C fluxes (Dinsmore et al., 2013), it was investigated whether [DOC] (rather than [POC]) could be inferred continuously using well-defined and easily measureable physical parameters.

Stepwise regression methods were used to identify the most significant variables that best described changes in [DOC]. Stepwise methods stop when the addition of a new variable is not significant to the constructed equation (Draper & Smith, 1998). These variables were selected from a list of physical and chemical parameters, based on an understanding of known factors that influence and control C export from peatlands

systems. These included stage height, discharge, pH, alkalinity, water temperature, air temperature (considered as weekly, fortnightly and four weekly averages), days since last rainfall (considered in two forms, when rainfall was >1 mm and when >5 mm) and day of the year (a proxy for seasonality). Information on air temperature and days since rainfall data were provided courtesy of the West Clyne weather station located just outside Brora, (http://monadh.com/wcl.php) (Cranfield, 2013) which is part of the Scottish Weather Network (http://www.scottishweather.net/).

Some other descriptors were considered: the net change in discharge between consecutive samples and also whether the [DOC] was measured on the rising or falling limbs of storm hydrographs. It was important that any variables selected whilst stepwise regression was undertaken were not auto-correlated, e.g. rainfall and discharge would be correlated as discharge tends to respond to rainfall increases. For such interactions only one variable was selected.

# 6.4 Results

## 6.4.1 Discharge/stage – [C] linear regression

Hysteresis analysis indicates that describing [DOC] and [POC] from stage or discharge is best approached by considering rising and falling limbs separately (section 5.4.3). To consider this approach all the data collected from GB11 sampling point are compared with the data separated into rising and falling limbs. This comparison for GB10 and GB12 can be found in Appendix E. GB11 was selected to be presented as its catchment was affected by windfarm development and its flow regime was never restricted, i.e. the old hydro-electric dam at times influenced flow regime at GB10 before it was removed in April 2013. Throughout the linear regression analysis, relationships between stage/discharge-[C] were commonly non-linear and indicative of power functions, e.g. (Agren et al., 2010a). Since $R^2$ values and p-values cannot be calculated for non-linear regressions, therefore double-log transformations were performed for the majority of discharge/stage-[C] relationships. This supported linear regression to assess if the relationships found could statistically support an estimation of an aquatic organic C flux.

## 6.4.2 Discharge/stage vs. DOC – GB11

The $R^2$ for the double natural log (ln) form of discharge plotted against all [DOC] is only 0.20, indicative of a weak measure of goodness of fit but with a p value (<0.001) which is highly significant (Figure 6.1). The same data divided into three time periods produces linear functions (winter is a polynomial) with stronger $R^2$ values whilst retaining highly significant p values: summer (0.56), spring-autumn (0.57) and winter (0.21) (Figure 6.2).

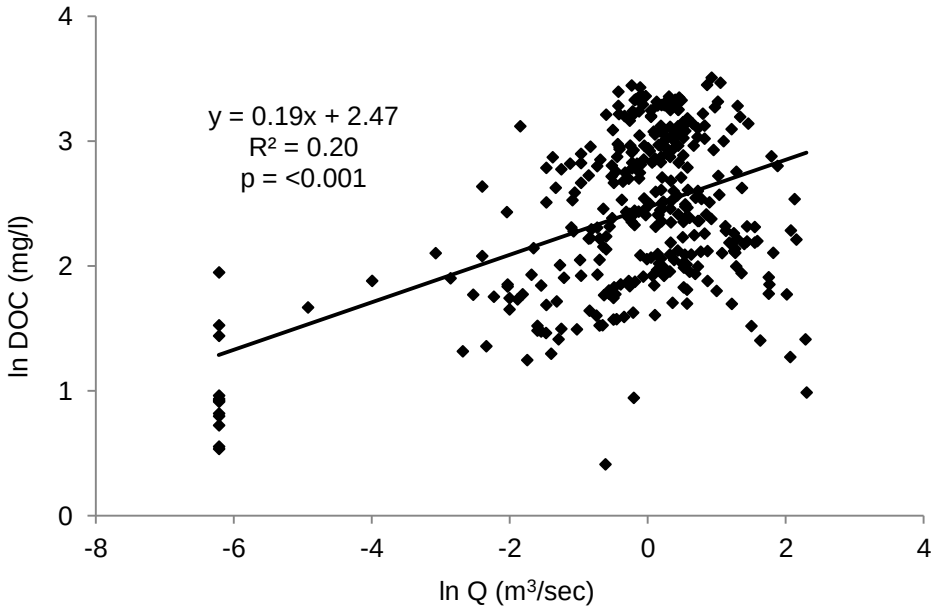


**Figure 6.1 - Discharge plotted against all [DOC] data**
The best fit equation of the presented linear relationship, $R^2$ and p-value are displayed.

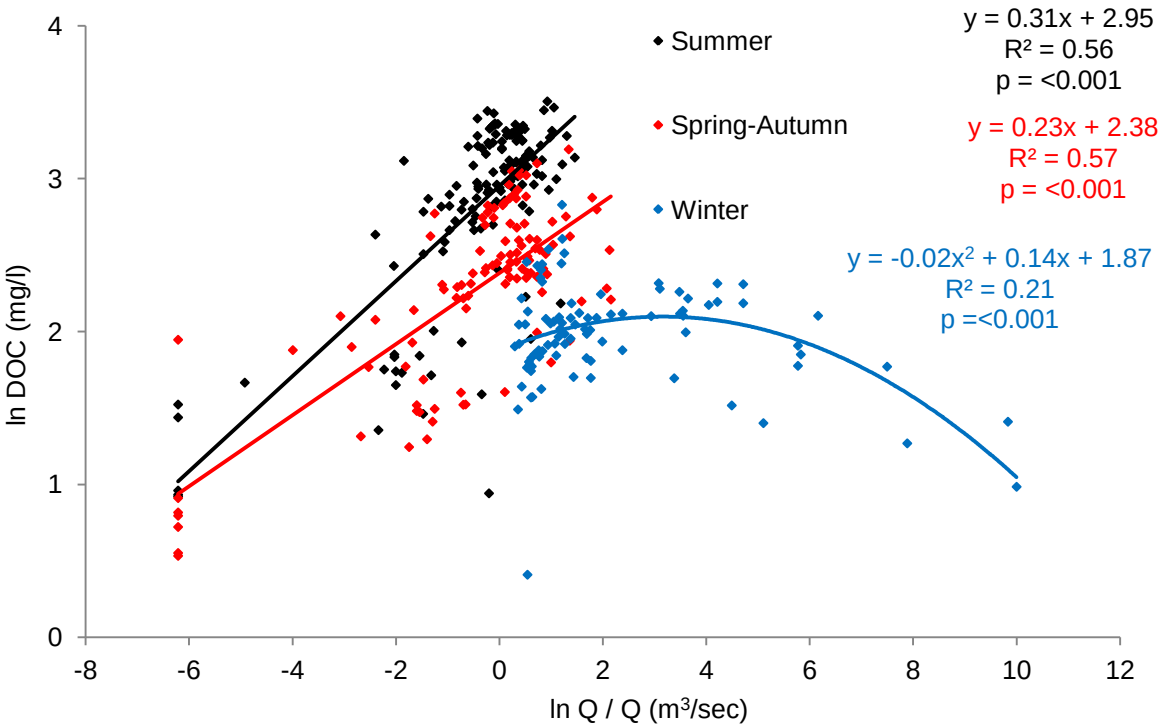


**Figure 6.2 - Discharge plotted against [DOC] data split by time period**
[DOC] data in the above figure has been divided into three time period categories which broadly map seasons, summer, spring-autumn and winter depending on when a sample was collected. The respective linear functions, $R^2$ and p-values are presented in the same colours as the data points.

When the summer, spring-autumn and winter data, are further separated into rising and falling limbs (Figure 6.3), two equations are generated for each time period. $R^2$ values increased in only one equation for each time period (summer rising, spring-autumn falling, winter rising) than the linear relationships for these three categories. Generally, rising limb $R^2$ values were higher than those on the falling limb for all rivers, however there were two exceptions, GB11 (Figure 6.3B) and GB10 (Figure E.3) spring-autumn falling limbs. For summer and spring-autumn plots (Figure 6.3A&B), there is still considerable scatter in the data and, rising and falling limb data and equations trend-lines overlap. The falling limb linear regressions plot above the rising limb, indicating generally higher [DOC] for similar discharges than the rising limb (Figure 6.3 and Appendix E). Rising and falling limb equations are also highly significant for GB11, as well as GB10 and GB12.

For winter rising and falling limb relationships, polynomial equations best described the [DOC] collected (Figure 6.3C&D), with a general trend of [DOC] decreasing as discharge increases which is the opposite of summer and spring-autumn relationships. The winter rising limb has a more pronounced negative relationship than the flatter falling limb, indicating that [DOC] on falling limbs show a smaller rate of change than those on rising limb. Although the winter rising limb equation is highly significant it should be noted the falling limb is only weakly significant, $p < 0.05$. Only having a p-value of <0.05 applies for

'winter' and 'winter rising limb' for GB10. Furthermore, 'winter falling limb' relationships for GB10 and GB12 are not statistically significant, i.e., p = >0.05 (Table E.1 & E.3).

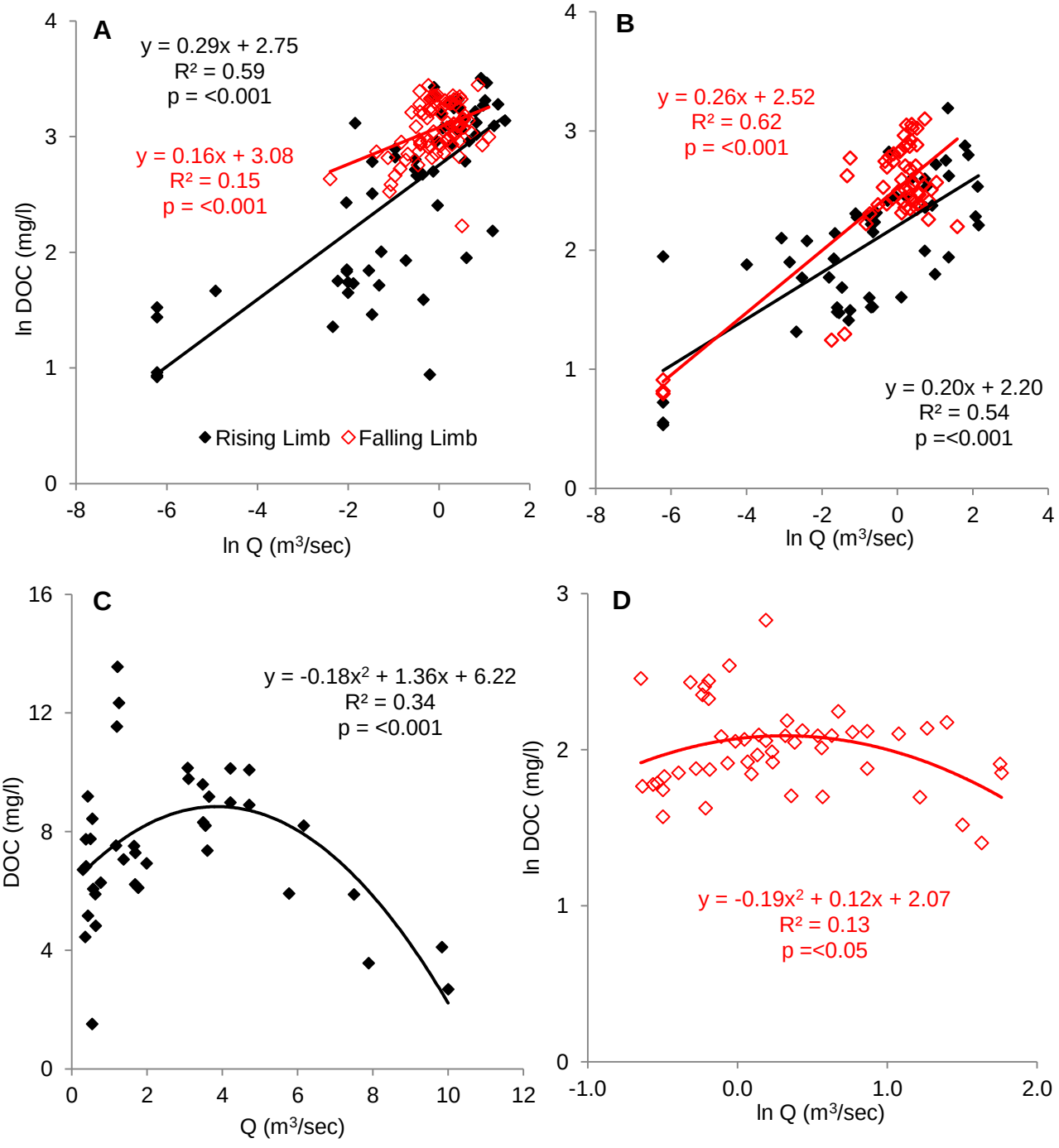


**Figure 6.3 – Discharge plotted against [DOC] data split by time period and split into rising and falling limbs**

A = Summer rising and falling linear relationships. B = Spring-autumn rising and falling linear relationships. For graphs A & B y-axis of [DOC] and x-axis of discharge (Q - $m^3$/sec) have had a natural log (ln) conversion. C = Winter rising limb data. D = Winter falling limb data. Graph C is simply discharge plotted against [DOC] whereas in graph D both y-axis and x-axis have a ln applied to them. The black data represents [DOC] on rising limb of storm events, the red show data on falling limb, a legend is shown on graph A. The linear or polynomial equations best describing the data are presented along with $R^2$ and p values on every graph.

## 6.4.3 Discharge/stage vs. POC – GB11

The relationship between all [POC] and stage height is quite well-described by a polynomial, $R^2 = 0.59$ (Figure 6.4A). However, although [POC] in Gordonbush rivers does not exhibit a strong seasonal pattern (see Figure 5.3) and all events show similar behaviour (the same hysteresis pattern) three different and highly statistically significant relationships exist for the three seasonal categories (Figure 6.4B&C). $R^2$ values improve in winter (0.85) and spring-autumn (0.60) relationships when split 'seasonally', but this is reduced for the summer data (0.36).

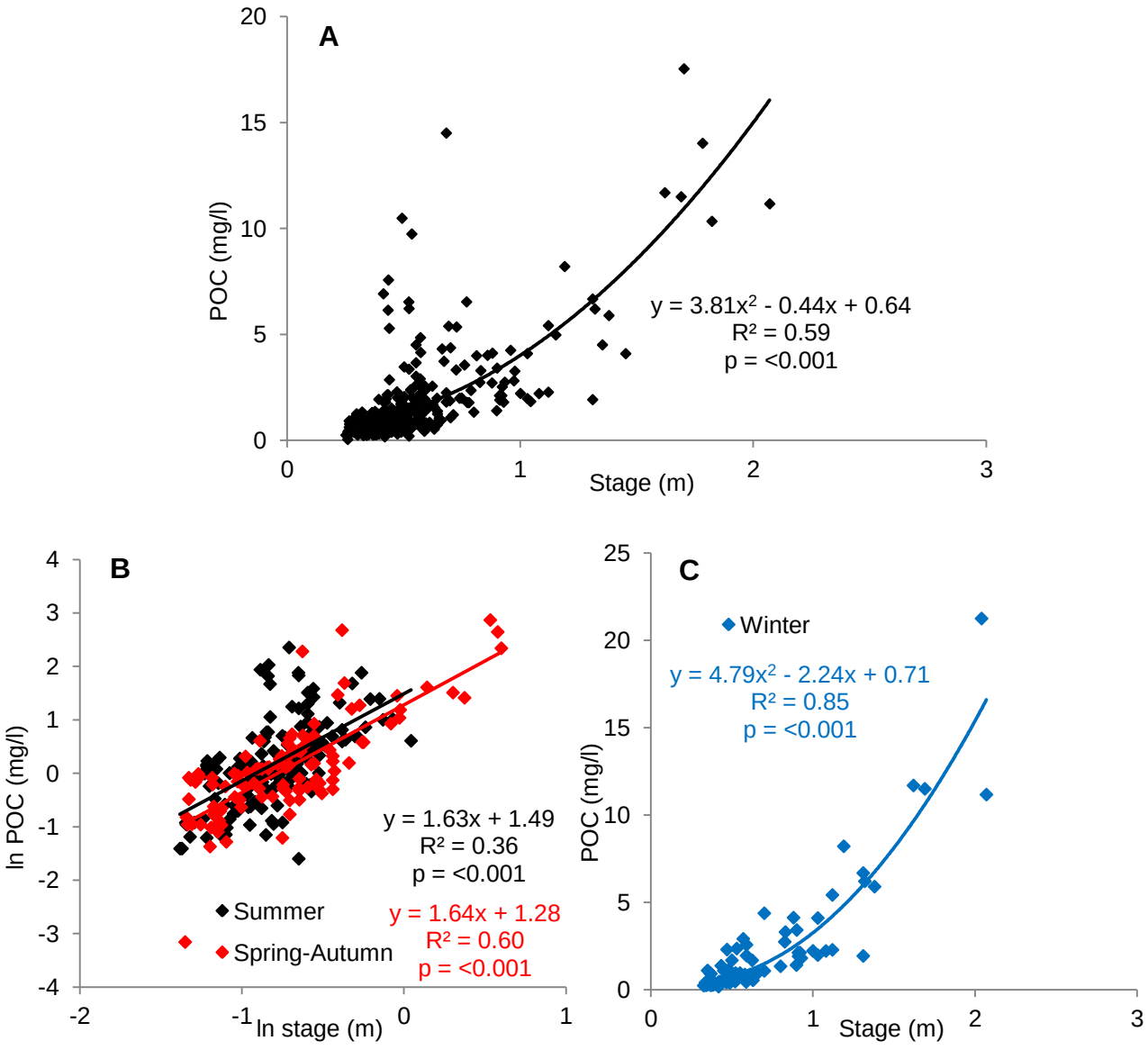


**Figure 6.4 - Stage/discharge plotted against all [POC] and [POC] split by time period**
A = Stage height plotted against all [POC] data. B = [POC] split by time period, showing summer and spring-autumn data. Both axes have been ln transformed. C = stage height plotted against winter [POC] data. The equation of the polynomial/linear equation, $R^2$ value and p value are presented on each graph. The colour coding for data split by time period, summer = black, spring-autumn = red and winter = blue, is the same colour scheme used when [DOC] was presented.

When [POC] data are split into rising and falling limb relationships with discharge, $R^2$ values increase on the rising limbs (summer and spring-autumn) and decrease on falling limb (summer, spring-autumn and winter) but the two lines overlap (Figure 6.5) indicating that POC export will be broadly consistent on both rising and falling storm hydrographs limbs for the same discharge or stage height value.

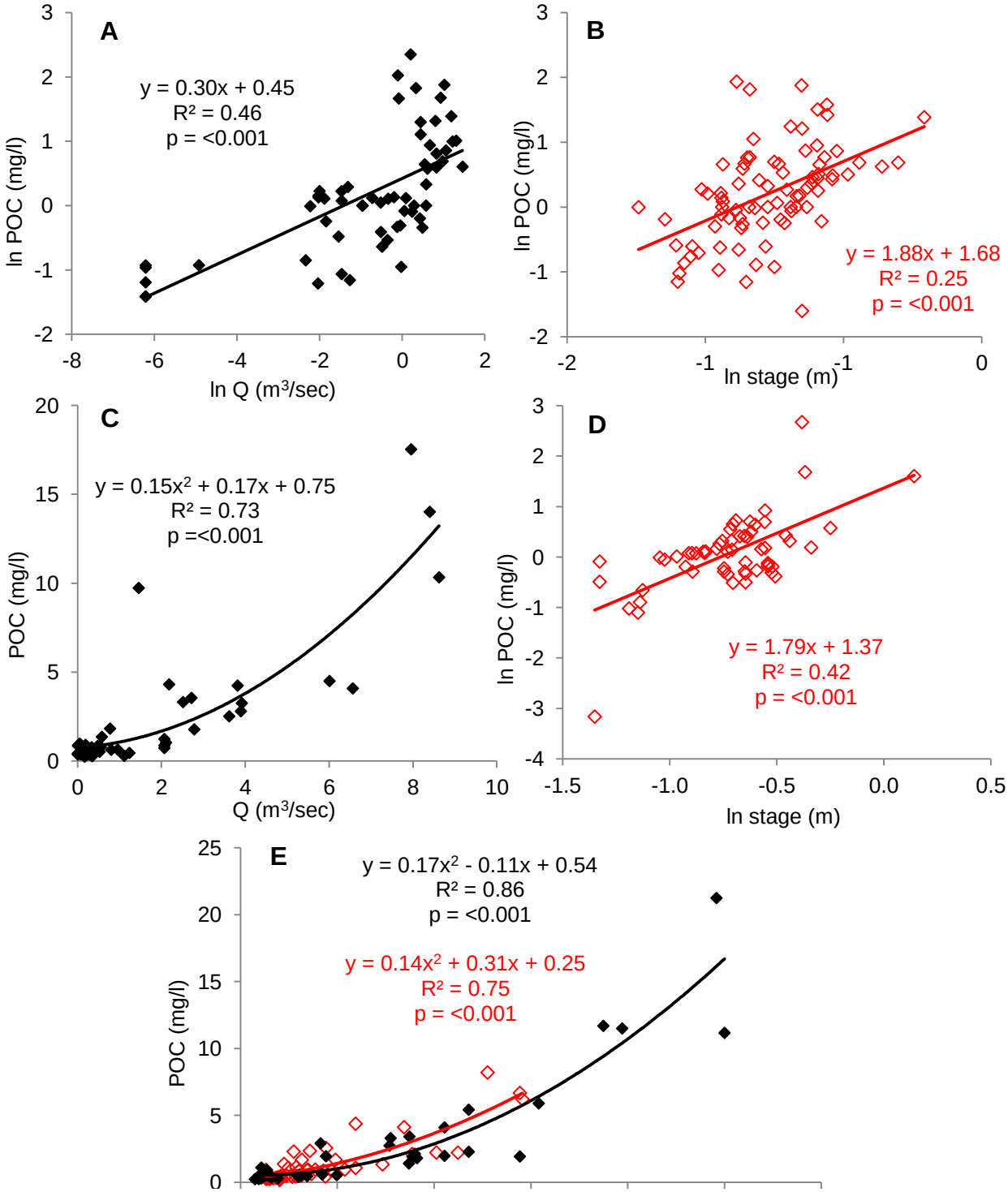


**Figure 6.5 – Discharge/stage plotted against [POC] split by time period as well as rising and falling limbs**

A = Summer rising limb data (double ln axis with discharge). B = Summer falling limb data (double ln axis with stage). C = Spring-autumn rising limb data (Q vs. [POC]). D = Spring-autumn falling limb data (double ln axis with stage). E = Winter rising and falling limb (Q vs. [POC]). The black data represents [DOC] on rising limb of storm events, the red show data on falling limb, a legend is shown on graph A. The linear or polynomial equations best describing the data is presented along with $R^2$ and p values on every graph.

Generally, [POC] rising limb equations had higher $R^2$ values when compared to falling limb equations, the exception being summer rising and falling limb equations for GB12 (Table E.3).

## 6.4.4 Aquatic organic carbon flux estimations

Table 6.2 aquatic organic C fluxes that have been estimated using techniques described in Methods section 6.3 of this chapter and the regression equations presented in section 6.4.2 (DOC) and 0 (POC) for GB11, (Appendix E for GB10 and for GB12). The % contribution of DOC to the overall C export is differentiated in the table below.

| River and flux method | All Flux results are quoted in g C $m^{-2}$ $yr^{-1}$ Hydrological Year | | | | | | | |
|---|---|---|---|---|---|---|---|---|
| | **2010** | | **2011** | | **2012** | | **2013** | |
| | **Flux** | **%DOC** | **Flux** | **%DOC** | **Flux** | **%DOC** | **Flux** | **%DOC** |
| **GB10 - Allt Mhuilin (28.9 $km^2$)** | | | | | | | | |
| **All Data** | 3.1 | 94 | 26.1 | 93 | 23.3 | 93 | 22.1 | 93 |
| **Seasonal** | 4.4 | 94 | 24.8 | 92 | 19.7 | 93 | 16.6 | 91 |
| **Seasonal with R&F Limbs** | 4.6 | 94 | 24.6 | 92 | 19.9 | 93 | 16.3 | 92 |
| **Method 5 (All Data)** | 4.5 | 94 | 37.3 | 93 | 28.4 | 89 | 19.8 | 87 |
| **Method 5 (spot)** | 4.4 | 96 | 24.4 | 94 | 19.1 | 96 | 24.4 | 91 |
| **Spot Sample** | 5.1 | 94 | 22.4 | 95 | 17.0 | 95 | 20.1 | 95 |
| **Event & Spot Samples** | 5.1 | 94 | 25.3 | 96 | 20.5 | 94 | 17.0 | 92 |
| **Specific Q ($m^3$ $km^{-2}$) (10^6)** | 0.15 | | 1.17 | | 1.06 | | 0.98 | |
| **GB11 Allt Smeorail (15.4 $km^2$)** | | | | | | | | |
| **All Data** | 1.8 | 90 | 15.3 | 88 | 13.9 | 89 | 14.8 | 85 |
| **Seasonal** | 2.7 | 94 | 15.0 | 90 | 13.4 | 91 | 11.2 | 84 |
| **Seasonal with R&F Limbs** | 2.9 | 94 | 15.1 | 92 | 13.9 | 93 | 11.3 | 87 |
| **Method 5 (All Data)** | 3.3 | 93 | 25.5 | 93 | 18.8 | 89 | 15.0 | 61 |
| **Method 5 (spot)** | 3.4 | 95 | 12.9 | 95 | 11.4 | 87 | 15.0 | 94 |
| **Spot Sample** | 3.2 | 92 | 11.9 | 93 | 12.2 | 94 | 10.2 | 93 |
| **Event & Spot Samples** | 3.2 | 94 | 14.0 | 94 | 12.9 | 92 | 11.2 | 83 |
| **Specific Q ($m^3$ $km^{-2}$) (10^6)** | 0.15 | | 1.14 | | 1.06 | | 1.02 | |
| **GB12 Old Twn Burn (5.1 $km^2$)** | | | | | | | | |
| **All Data** | 2.2 | 89 | 13.1 | 89 | 13.9 | 89 | 14.4 | 88 |
| **Seasonal** | 3.2 | 93 | 12.7 | 92 | 12.8 | 91 | 11.1 | 88 |
| **Seasonal with R&F Limbs** | 3.2 | 94 | 12.9 | 93 | 12.7 | 92 | 11.2 | 90 |
| **Method 5 (All Data)** | 4.1 | 92 | 22.6 | 94 | 22.6 | 90 | 16.4 | 74 |
| **Method 5 (spot)** | - | - | 2.7 | 85 | 3.1 | 89 | 3.8 | 97 |
| **Spot Sample** | 3.5 | 87 | 16.1 | 96 | 8.3 | 90 | 9.8 | 91 |
| **Event & Spot Samples** | 4.1 | 93 | 14.2 | 95 | 14.8 | 93 | 10.8 | 87 |
| **Specific Q ($m^3$ $km^{-2}$) (10^6)** | 0.22 | | 1.31 | | 1.29 | | 1.26 | |

**Table 6.2 - Aquatic organic C flux estimate results**
Hydrological year 2010 only contains a flux estimate for months Aug. and Sept. 2010, hence flux estimates are considerably lower than other years when fluxes for the full hydrological year have been calculated. % DOC reflects percentage of DOC export makes up total annual C flux. Specific Q ($m^3$ $km^{-2}$) is annual discharge in $m^3$ in each hydrological year divided by catchment size ($km^2$) for each river (presented next to name of river). The value of Specific Q presented has further been divided by a factor of 10^6 (1 million) for ease of display.

For complete hydrological years aquatic C flux estimates ranged from 2.7 to 37.3 g C $m^{-2}$ $yr^{-1}$ between all methods of calculations and all rivers. The highest C flux estimate in all three rivers was calculated in 2011 (Table 6.2) using the 'Method 5 (all data)' technique each time and this method produced the highest of all flux estimates in all three rivers across all studied years (exception, GB10 – 2013). 'Method 5 (all data)' also produced the largest range of flux estimates between 2011-2013 for GB10 and GB11 (Table 6.2). The lowest C flux estimate of all methods used was calculated in 2013 for GB10 and GB11 but the technique ('Seasonal with R&F limbs' and 'Spot sample' respectively) that gave this result was different for each river. For GB12, the lowest C flux estimate was in 2011 but again a different technique to the comparable result in GB10 and GB11 was different ('Method 5 (spot)'). Between on all techniques and all years, estimates for GB10 vary the most, followed by GB12 and finally GB11.

Considering only complete hydrological years, annual discharge of all three rivers followed 2011 > 2012 > 2013. Generally, this trend was also reflected in C flux estimates using most techniques for GB10 and GB11 (Table 6.2). Noticeable exceptions to this pattern are flux estimates which were based on spot sampling data. This result is not surprising as discharge was used as a variable to infer aquatic [C] using linear and non-linear regression relationships. Results from GB12 do not show the same relationship where C flux estimates correspond to increases in annual discharge. This suggests that the choice of flux estimation techniques, rather than annual discharge, exerts a stronger influence on C flux estimates.

GB10, where [DOC] were generally higher, always had higher export estimates than GB11 and GB12. Exports estimations for GB11 and GB12 are very similar for 'All data', 'Seasonal' and 'Event and Spot samples' approaches. Both 'Seasonal with R&F limbs' and 'Method 5 (spot samples)', calculate greater exports in GB11 than GB12 for all hydrological years. GB11 flux estimate is higher in 2011 for 'Method 5 (all data)' compared to GB12 but lower in 2012 and 2013 using the same technique. The opposite is apparent for 'Spot samples' estimations when comparing GB11 and GB12.

The contribution of DOC to the total aquatic organic C flux estimates ranged from 61 – 97 % (with only two values <80 %). The 'Method 5 (spot)' technique yielded the highest % DOC contributions of all the methods in all rivers, GB10 96 % (2012), GB11 95 % (2011) and GB12 97 % (2013) (Table 6.2). The average % DOC contribution across all of the three rivers, techniques and years was 91 % clearly indicating DOC is the main component of the aquatic organic C fluxes estimated.

Time series graphs displaying all flux estimates for each river are presented (Figure 6.6).

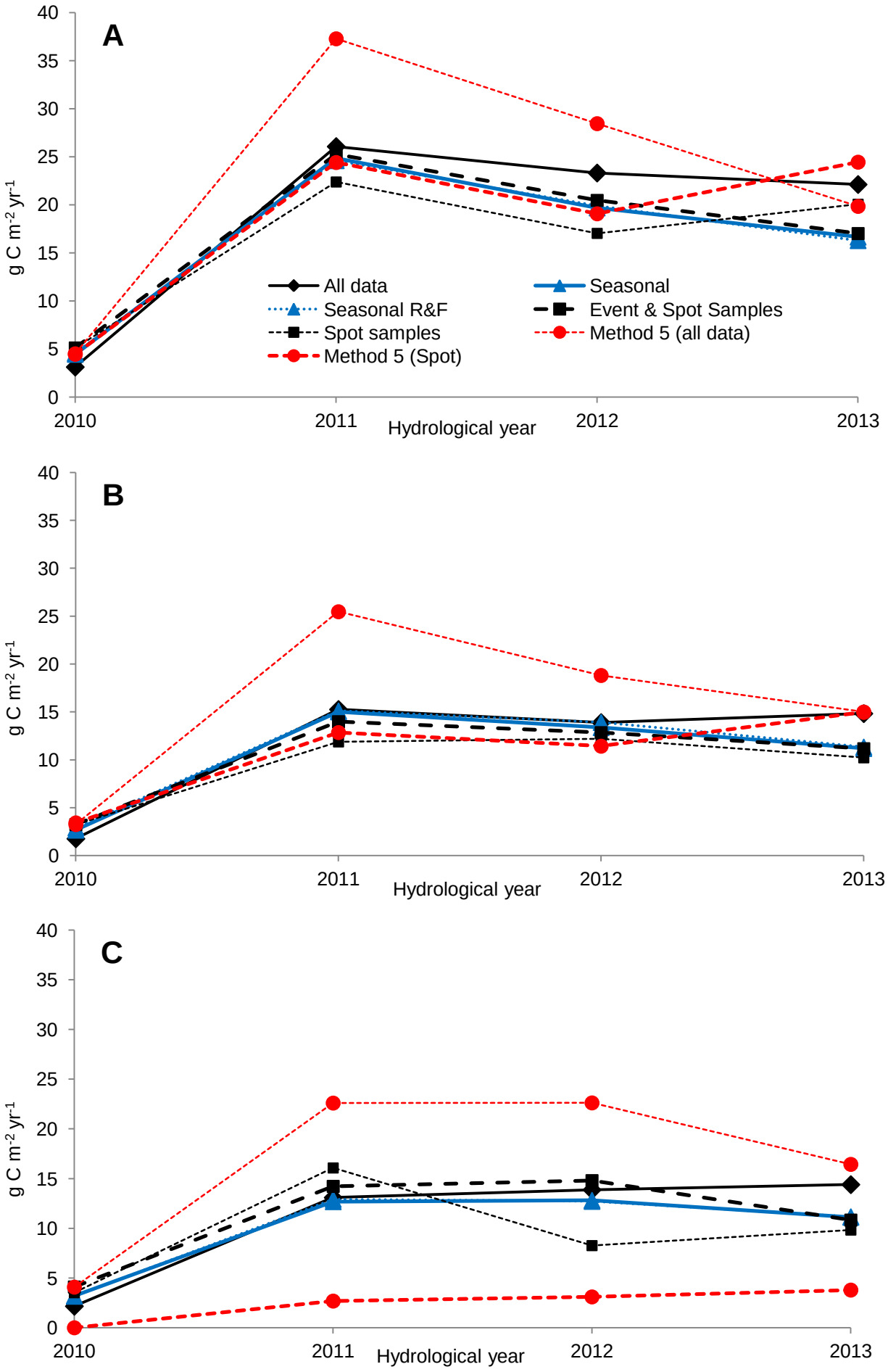


**Figure 6.6 - Time series of all flux estimation methods**
A = GB10 (Allt Mhuilin), B = GB11 (Allt Smeorail), C = GB12 (Old Town Burn). The legend in Figure 6.6A also applies to 6.6B and 6.6C. It should be noted values for 2010 are considerably lower than 2011, 2012 and 2013 as the aquatic C flux for 2010 was not based on a complete hydrological year (only August and September 2010).

## 6.4.5 Identification of 'best' variables using stepwise regression

DOC is the dominant component and source of aquatic organic C in all Gordonbush rivers; this is acknowledged in other studies (e.g., Dawson et al. (2004)), therefore it was prioritised to investigate if [DOC], than [POC] could be modelled using MLR. Two approaches were explored, one where MLR equations utilised the 'best' set of variables, and one where only variables readily measurable *in-situ* are utilised (Table 6.3). Thus, two equations were generated for each river (Table 6.4).

| Stepwise regression results | VARIABLES | | | | | |
|---|---|---|---|---|---|---|
| | **Avg. Air Temp** | | **Alkalinity** | **pH** | **Days since Rain** | |
| River | **4 week** | **1 week** | | | **>1mm** | **>5mm** |
| **GB10** with Alk | 52.0 | | 25.2 | | 0.3 | |
| **GB10** with pH | 52.0 | | | 12.5 | 2.0 | |
| **GB11** with Alk | 37.8 | | 26.2 | | 0.3 | |
| **GB11** with pH | 37.8 | | | 12.1 | 2.3 | |
| **GB12** with Alk | | 25.4 | 41.0 | | | 0.7 |
| **GB12** with pH | | 28.1 | | 8.1 | | |

**Table 6.3 - Stepwise regression results indicating the 'best' set of variables to infer [DOC]**
The table displays the % contribution of each variable to [DOC] variation for all equations in Table 6.4. Each variable was statistically significant to at least p value <0.05.

| River and Method | Equation ([DOC] =) | $R^2$ | Mallow c-p | S |
|---|---|---|---|---|
| **GB10** with Alkalinity | 7.39 - (0.415 * Alk) + (2.13 * 4 week AT) - (0.243 * Days rain >1mm) | 0.78 | 4.0 | 4.5 |
| **GB10** with pH | 22.6 - (3.02 * pH) + (1.9 * 4 week AT) - (0.557 * Days rain >1mm) | 0.66 | 4.0 | 5.5 |
| **GB11** with Alkalinity | 4.66 - (0.420 * Alk) + (1.56 * 4 week AT) - (0.222 * Days rain >1mm) | 0.64 | 5.0 | 4.5 |
| **GB11** with pH | 17.1 - (2.57 * pH) + (1.4 * 4 week AT) - (0.473 * Days rain >1mm) | 0.52 | 3.6 | 5.2 |
| **GB12** with Alkalinity | 7.34 - (0.314 * Alk) + (1.18 * 1 week AT) - (0.0875 * Days rain >5mm) | 0.67 | 6.0 | 4.0 |
| **GB12** with pH | 19.3 - (2.27 * pH) + (0.887 * 1 week AT) | 0.36 | 3.0 | 5.8 |

**Table 6.4 - Multiple linear regression equations for all three Gordonbush rivers**
Two equations are presented for each river, one an alkalinity variable term and another with pH substituted instead. In the equations 'Alk' = Alkalinity and '4 week AT' = 4 week average air temperature, 'Days Rain >1 mm' = Days since rainfall was >1 mm. The adjusted $R^2$ (Adj. $R^2$), Mallows c-p and S values are given. The Mallows c-p is a measure of model precision and the S value indicates of the average distance between measured values and those predicted by the modelled regression line. A smaller Mallows c-p value, close to the number of predictors in the model plus the constant, indicates the model is relatively precise in estimating the true regression coefficients and better at inferring future responses (Minitab support). The p values for all the MLR equations were highly significant, i.e. p <0.001.

Modelled equations generated by the forward selection of the 'best' variables always had higher $R^2$ values and this is most likely attributed to the inclusion of alkalinity (which was not measured *in situ*). Adjusted $R^2$ are larger for GB10 equations than GB11 and GB12. Average air temperature proved to be the best descriptor of [DOC] in two of the three

rivers (GB10 and GB11). A four week average air temperature was a more effective indicator of seasonality for GB10 and GB11 whereas for GB12 a one week average worked better when predicting measured [DOC].

In equations using the 'best' variables, a four weekly average air temperature accounted for over half of variability in [DOC], GB10 (52 % of 77.5 % total) and GB11 (37.8 % of 64.3 % total), whereas a one week average air temperature only described approx. a quarter of the 66.9 % total in GB12. Alkalinity, was the second most influential descriptor, explaining ~25 % of the variance in GB10 and GB11, but was the principle indicator in GB12, accounting for 41 % of the 66.9 % total. "Days since rainfall" also appeared as significant variable for all sites. For GB10 and GB11 "days since rain > 1mm" was retained whereas "days since rain > 5 mm" described better for GB12.

In the absence of alkalinity, pH emerged as a significant descriptor. However adjusted $R^2$ values decreased by over 10 % in GB10 and GB11 and over 30 % in GB12. 'Days since rainfall > 1mm' became a stronger descriptor in absence of 'Alkalinity' in GB10 and GB11, but was not significant in the secondary equation generated for GB12.

## 6.4.6 Comparison of measured vs. modelled [DOC]

When measured [DOC] are plotted against modelled [DOC] it is unsurprising $R^2$ values for the resulting equations are relatively high, GB10 = 0.78, GB11 = 0.65 and GB12 =0.68, and all the relationships are highly significant, $p < 0.001$. From the equations presented for all three rivers in Figure 6.7 (next page) it is clear that GB10 has the largest gradient (0.80) compared to GB11 (0.68) and GB12 (0.69) which are similar. The gradients of equations for all 3 rivers are <1 indicating that the MLR results under-predict measured [DOC] values. The intercept for all equations are between ~4-5 suggesting an offset of 4-5 mg $l^{-1}$ between inferred results and measured [DOC] values. This is reinforced when S values are noted for each river, GB10 = 4.02, GB11 = 3.79 and GB12 = 3.39, respectively. Prediction intervals, at 95 % level, imply that [DOC] can be modelled to within ±10 mg $l^{-1}$ level of a field sample measurement.

Unfortunately, the 'best' variables were not continuously measured through the research at Gordonbush. This meant that it was not possible to construct a continuous [DOC] time series or subsequently an aquatic organic C flux by proxy using the results of MLR analysis.

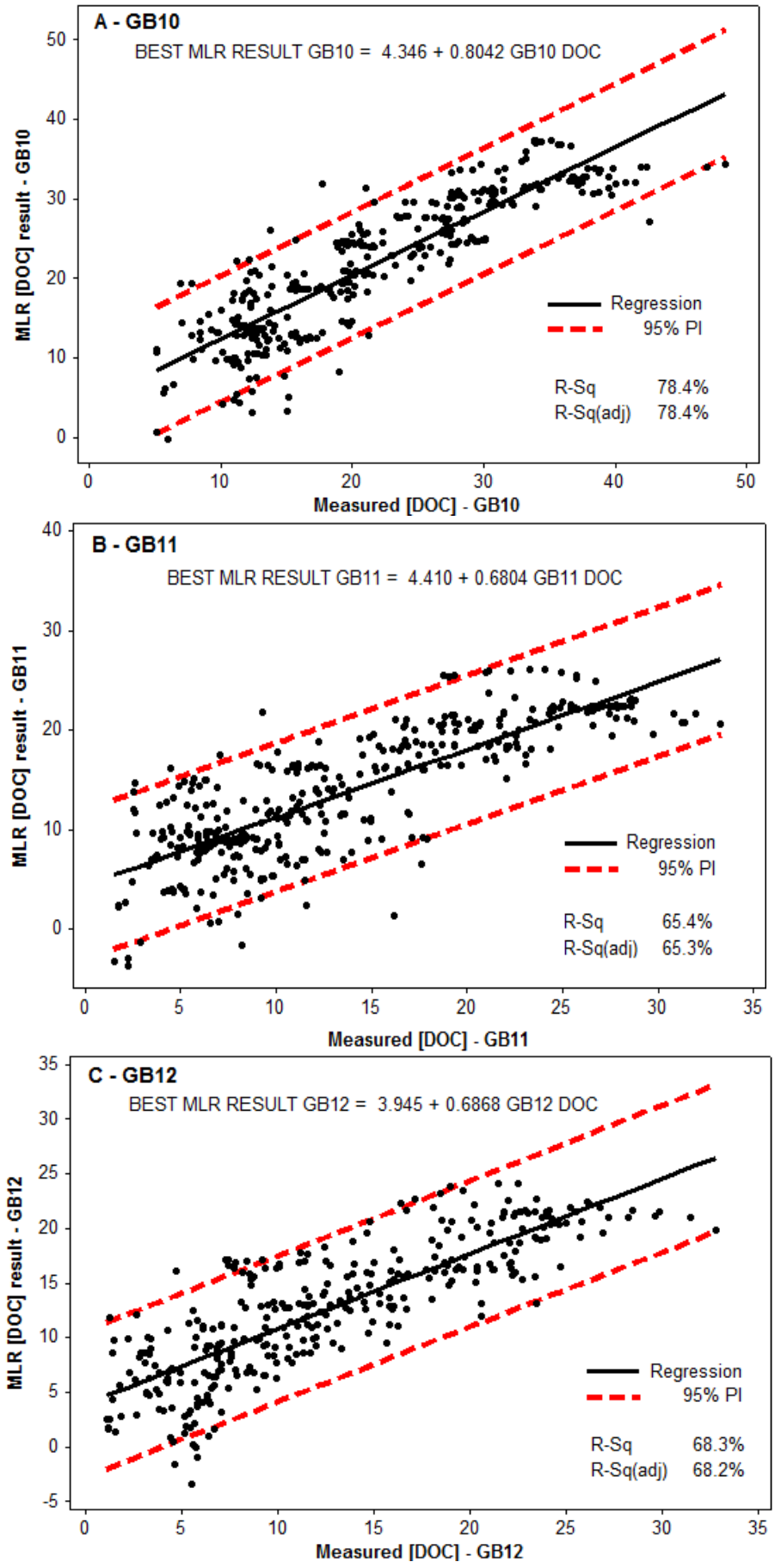


**Figure 6.7 – Measured [DOC] vs. [DOC] predicted by multiple linear regression**
A = GB10, B = GB11 and C = GB12. Regression equations are presented for measured [DOC] on the x-axis, plotted against [DOC] results generated by multiple linear regression equations (e.g. MLR [DOC] result) on y-axis. The linear equation (top of graph in block capitals), $R^2$ value, adjusted $R^2$ (R-Sq(adj.)) (which are quoted in percentage terms rather than -1 to 1), trend-line (black solid line) and prediction intervals (red dashed lines) are displayed on each graph. All linear regressions presented are highly significant, p value <0.001.

# 6.5 Discussion

## 6.5.1 Evaluation of aquatic organic carbon flux estimation techniques and choice of 'best' model

The strengths and limitations of each flux estimation technique will be discussed based on acknowledged controls on the export of aquatic C from peatland systems as in addition to statistical robustness.

### 6.5.1.1 Linear and multiple linear regression

The large amount of scatter surrounding the linear regression equations and generally relatively low $R^2$ values when discharge is plotted against all [DOC] and [POC] (Figure 6.1 and Figure 6.4A) suggests linear regression might be too simplistic an approach for estimating aquatic organic C fluxes. This finding is not surprising for although discharge is widely acknowledged an important factor in controlling aquatic [C], it is not the only one. Time series data (Chapter 5) showed a clear seasonal trend in fluvial [DOC]. To incorporate, at very least, discharge and seasonality into a single regression requires MLR analysis.

Air temperature was identified as an important descriptor of [DOC] in the MLR, a result found in other studies (Kohler et al., 2009), presumably as it acts as a proxy for seasonality in production of DOC (Worrall et al., 2004a). Similar temperatures occur in spring and autumn, so it was expected that hydrologic descriptors would also be important, particularly as discharge is a dominant control on [DOC] (Clark et al., 2007, 2008; Dawson et al., 2011), but this was not the case. Both pH and alkalinity were better descriptors of changes in [DOC] than hydrological variables. Increased aquatic DOC loading can result in a decrease of river pH (Austnes et al., 2010; Sandford et al., 2010; Knorr, 2013), associated with fulvic and humic acid contents of the DOC component (Tipping & Hurley, 1988; Evans et al., 2005). Alkalinity is effectively a proxy for inorganic [C] in poorly buffered waters (Neal et al., 1998; Jarvie et al., 2001), so as [DOC] increases and pH decreases, alkalinity also decreases and results in an inverse relationship being produced between the two factors (Waldron et al., 2007; Speed et al., 2010). In this instance, it describes [DOC] well as it also varies with hydrology. This inverse relationship was evident in all studied Gordonbush rivers and data collected from GB10 sampling point is shown as an example below (Figure 6.8).

DOC release from peatlands has been positively correlated with rainfall (Worrall & Burt, 2007a) but also with the previous weeks' and month's temperature, signalling past temperatures directly affect DOC availability (Harrison et al., 2008; Yurova et al., 2008;

Agren et al., 2010b). Time between hydrological events has been known to influence DOC export, with [DOC] increasing once re-wetted after period of drought (Worrall et al., 2006b; Worrall & Burt, 2008; Clark et al., 2012; Oswald & Branfireun, 2014) and so it is not surprising that "days since last rainfall" was a significant descriptor. There are catchment specific differences: >1mm (GB10 and GB11); >5mm (GB12).

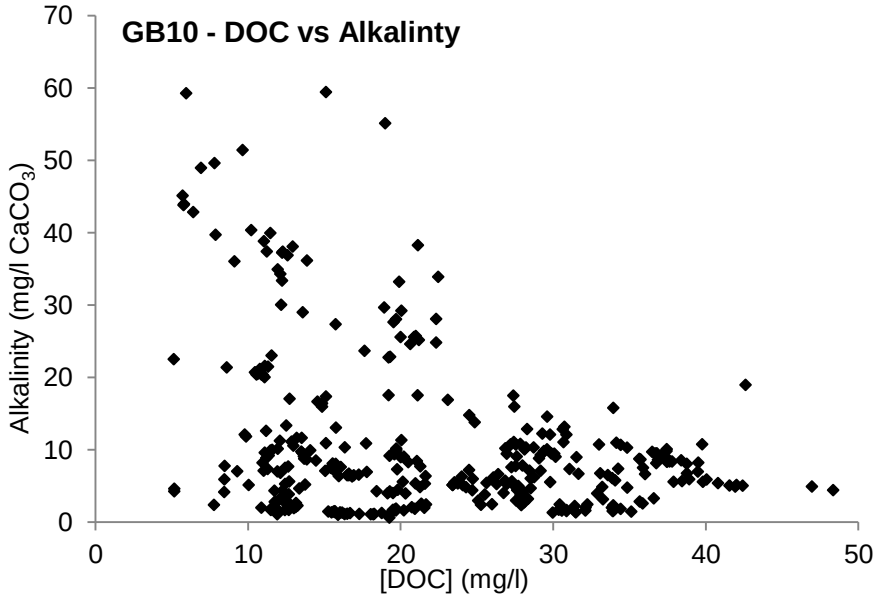


**Figure 6.8 - Inverse relationships between [DOC] and Alkalinity, an example from GB10**
The graph shows all analysed [DOC] data plotted against all measures of alkalinity recorded during this research at GB10 sampling point.

It is known other physical catchment characteristics can influence DOC export (e.g. catchment size, (Grieve, 1994); peat coverage, (Aitkenhead et al., 1999), (Hope et al., 1997a); soil type and overall peat depth, (Hope et al., 1994; Hope et al., 1997b). The aim of this MLR was to model [DOC] in each individual catchment and such equations have been produced for each. For this purpose it was not worthwhile to consider catchment characteristics listed above as these are static variables and would not have affected the results. It is recognised that if a single equation was to be constructed to predict/compare [DOC] between all three rivers at Gordonbush, then these descriptors may have become more significant.

Unfortunately, the limitation to using MLR results to construct aquatic organic C (DOC) fluxes (despite this being the preferred over linear regression) was key variables identified were not measured continuously throughout the research at Gordonbush. Thus approaches had to be found to improve linear regressions using discharge as a predictor to infer aquatic organic [C].

Similar to time series data, hysteresis analysis (Chapter 5) indicated hydrological controls vary with time. This was indicated by the prominence of A2 loops in the summer and spring-autumn storm events (in all rivers), where high [DOC] are maintained after peak discharge whereas in winter months C2 loops were prevalent, indicating [DOC] decreases after peak discharge and lower [DOC] for similar discharge values on the falling compared to the rising limb (see hysteresis analysis results in section 5.4.3). Furthermore, the occurrence of Fo8 during hysteresis analysis of discharge-[DOC] data from all Gordonbush rivers clearly signifies a complexity of C export than cannot be described solely by stage or discharge using a singular linear equation.

Splitting the [C] data into three different time periods ('Seasonal' method) accounts for known seasonal variation in fluvial [DOC] and highlights a seasonal aspect to [POC] which was not noticeable from time series and hysteresis analysis. The seasonal approach still assumes that [C] on the rising and falling limbs are the same, which by the fact hysteresis loops could be constructed, demonstrated this is not true. Splitting data into time periods and hydrologically ('Seasonal with R&F limbs') seems like the best process-informed approach in modelling the nature of C export and has essentially tried to account for more variables affecting C export than just stage/discharge. However, for all rivers, adopting this approach still results in a reduction of $R^2$ values in at least one of the rising or falling limb relationships compared to the linear equations produced when data was only split by the time periods chosen (summer, spring-autumn and winter). This highlights the limitations of using linear regression to infer [C] and export which is influenced by multiple factors, highlighted by MLR analysis.

For linear equations, the lowest $R^2$ values of all time split aquatic organic [C] data occur in winter for [DOC]. Less data was collected during winter storm events (~85 samples in each river) compared to summer (~150 samples) and spring-autumn (~110 samples) events and could partly explain why $R^2$ values are lower for winter linear regressions despite the fitted line overall describing the data quite well in most cases. Positive linear relationships were observed in summer and spring-autumn time periods as [DOC] generally increased with stage/discharge however this was not the case for winter events. [DOC] and stage/discharge produced negative regressions for 'winter' (Figure 6.2) and 'winter rising' (Figure 6.3C) and [DOC] remained fairly constant despite changes in discharge on falling limb (Figure 6.3D). This lack of slope may also be a contributing factor why the winter falling limb regression was not significant.

The 'winter' relationships observed also suggest a dilution of [DOC] during winter storm events most likely caused by the influence of snow melt (which is low in [DOC] (Agren et al., 2012)) contributing an additional source of water. Unfortunately, there was not enough

data to split winter events into snow melt only but targeting more of these events in future studies would be a worthwhile consideration and could improve $R^2$ values and statistical significance of these types of linear regressions. The occurrence of non-significant linear regressions (p values >0.05) for GB10 and GB12 winter falling limb relationships is certainly a major drawback to using the 'Seasonal with R&F limbs' approach to estimate aquatic organic C fluxes. It is acknowledged far more (long-term) research is needed to fully understand the role of winter climatic conditions on C export dynamics (Haei & Laudon, 2015) and this research shows too that it is challenging to estimate aquatic organic C fluxes using linear regression techniques that are statistically robust even if and when the best-informed approaches are used.

#### 6.5.1.2 'Method 5' methodology

The accuracy of flux estimates using 'Method 5' are influenced by sampling frequency related both to the quantity and seasonal spread of DOC and POC data collected (Littlewood et al., 1998). The time intervals between individual [DOC] and [POC] measurements varies between different studies, however long-term studies (greater than one year) tend to sample somewhere between a daily and monthly basis. A bias of samples collected at any particular time of year will greatly influence the calculated flux e.g. dominance of summer samples over winter would skew estimates to a higher predicted C flux as the [C] is greater during the summer.

Since emphasis was on event rather than regular spot sampling at Gordonbush, the annual flux estimates, particular the flow-weighted mean concentration (FWMC) will be influenced by having more data of higher concentrations. Although FWMC associated with 'Method 5 – All data' is representative of [C] across a wider range of hydrological conditions, more summer than winter storm events were sampled each year. This leads to the FWMC for 'Method 5 (all data)' being more influenced by summer [DOC] which is higher than winter [DOC]. Thus, it is unsurprising that 'Method 5 (All data)' predicted the highest fluxes, as the data used to calculate it was mostly summer storm event data. Base flow conditions collected on a more intermittent scale over course of the year may produce a more comparable FWMC budget with the other approaches. Ideally, when using finer resolution event sampling data compared to only spot samples ('Method 5 – Spot'), to calculate a more representative budget using FWMC, an equal amount of storm events at different times of year, over a representative hydrological conditions, should be included.

Estimates from 'Method 5 – Spot' are more comparable to the estimates produced by the best linear regression technique 'Seasonal and R&F Limbs' than 'Method 5 – (All data)'

(Table 6.2 and Figure 6.6). Fluxes calculated based on lower sampling frequencies are subject to larger errors than studies with higher frequencies (Strohmeier et al., 2013). However, fluxes calculated from samples collected on 30 minute intervals were similar to fluxes from samples collected on a daily, weekly and monthly basis (Koehler et al., 2009) emphasising that, depending on the method of flux calculation, including more data does not necessarily produce a considerably better predictability of river flux.

#### 6.5.1.3 Assuming constant [C] between sampling

Estimating fluxes by assuming that concentration does not change between sampling points, was another method used to produce an estimate of aquatic C flux. The method is based on an understanding that this calculation can over-estimate [C] in one time period, but equally can under-estimate in another time period. The estimates this method ('Event & Spot samples' and 'Spot samples') have produced for Gordonbush catchments are comparable to with the estimates generated by the favoured linear regression technique ('Seasonal & R&F limbs') in GB10 and GB11 and next best ('Seasonal') in GB12 (Table 6.2 and Figure 6.6). This is likely because spot samples were generally collected at regular intervals throughout the research period, so the times when high [C] samples (particularly in the summer and late autumn months) were collected and C export was likely over-estimated (especially during periods of low flow), is counter-balanced by times when [C] were low and C export under-estimated (most probably during event flow) during winter and early spring months.

#### 6.5.1.4 Exploring limitations of flux estimations and choice of 'best' model

It is important to discuss known sources of variability associated with all the C fluxes estimates presented. There were numerous sources of variability associated with each flux estimate, meaning statistical uncertainty could not be computed easily. These sources of variability included: albeit relatively small, variability associated with analysis of [DOC] and [POC] and the measurement of stage height data; estimates of discharge using the ISCO 2105 flow meter; confidence intervals associated stage-discharge ratings curve for each river; variability with cross-correlation analysis for periods of time when stage height needed to be reconstructed; variability related to the individual regression equations used to infer [DOC] and [POC]. This difficulty in constraining uncertainty is a limitation for all flux techniques estimations and overcoming this would be a priority in any future research related to this topic.

All flux estimation methods show broadly the same C flux trends across the three rivers. This is to be expected, as except for 'Spot' and 'Event & Spot samples' estimates, all other methods infer [C] based on discharge. The 'Spot' and 'Event & Spot samples'

techniques should be excluded from being considered an optimum flux estimation choice. Although the results calculated for this research were comparable with more advanced techniques, the techniques which assume constant [C] between sampling ('Spot' and 'Event & Spot samples') are deemed to lack sensitivity and are overly reliant on samples being collected at regular intervals to ensure high [C] are counter balanced with low [C] samples. Thus, these estimates are not generally considered to give the best representation of true C fluxes.

When using 'Method 5', data used should be evenly distributed based on the time of year the sample was collected and hydrological flow conditions, and as this research was focussed on storm event sampling flux estimates from this method will not be representative.

Therefore, it must be decided which of the linear regression flux methods offers the most representative aquatic organic C flux estimate. Log-linear (double or single log) regression equations used for estimating river fluxes (like those used in 'Seasonal' and Seasonal with R&F limb' methods) tend to under-predict 'real' [DOC] and [POC] for a given discharge, therefore producing a low bias when final fluxes are computed (Ferguson, 1986; Cohn et al., 1989; Cohn et al., 1992). The scatter of data around a regression line on a logarithmic (to base e or 10) scale tends to under-predict high values in data sets and over-predict low values for variability associated with that particular equation (Walling & Webb, 1988; Helsel & Hirsch, 2002; Horowitz, 2003) such that in some cases, river fluxes have been underestimated by up to 50 % (Ferguson, 1986; Cohn et al., 1989).

However, over longer timeframes, the variability associated with such load estimates using log-linear models become smaller as the over and under predictions are more likely to balance each other out, for e.g. variability for suspended sediment river load totals were estimated to be <1 % for monitoring data sets 5 years or longer (Horowitz, 2003). Using the three year data set (2010-2013) of [DOC] and [POC], collected at Gordonbush during various hydrological conditions and time periods, most likely captured 'true' natural variability. Analysing three years worth of data also reduces bias associated e.g. to a storm event being sampled any single year which could have contained extremely high, or low, [C]. Furthermore, it is acknowledged the key to good discharge-concentration relationships used in flux estimates appears to be how well the specific regression line(s) average out the scatter in any given data set rather than how well the resulting equations fits all the data points (Horowitz, 2003). Therefore, the strength of the linear regression used should not solely be based on its ability to predict individual [DOC] at any given time, i.e. its $R^2$ value, but instead be assessed on how representative is it of [DOC] more broadly in that season or on that rising/falling limb. That all aquatic organic C fluxes using

linear regressions ('All data', 'Seasonal' and 'Seasonal with R&F limbs') give similar results promotes the idea that a regression dissecting the middle of the data set rather passing through all points works well, i.e. 'All data'.

Due to the understanding gained from hysteresis analysis on how C is exported, and despite the limitations highlighted, I consider that the linear regressions where data is split by time period, and into rising and falling limbs, best describe DOC flux. It has previously been recommended that different relationships could be used for the rising and falling limbs of event hydrographs when using log-linear relationships in river flux calculations (Cohn et al., 1992). Although descriptive relationships are often improved by supplementation of more data, which should lead to more accurate budget estimates, the data scatter in the regression relationships is such that the individual linear regression equations used in 'Seasonal' and 'Seasonal and R&F limbs' method are quite similar (see tables of equations for each river in Appendix E). Thus both estimates are comparable and the maximum difference in C flux estimates between the two techniques in any one year for each specific river itself gives an indication of uncertainty around the flux estimates calculated.

Advanced statistical methods and framework set out in (Cohn, 2005) (the paper gives an example involving orthophosphate aquatic fluxes) should be considered in the future to better estimate confidence intervals on not only individual discharge-concentration relationships but also variability associated with stage-discharge ratings curves for the three rivers studied. The (quasi) maximum likelihood estimation ((Q)MLE) or adjusted maximum likelihood estimation (AMLE) have been recommended as a better estimates of variability associated with regression model coefficients (Cohn, 2005). Applying such variability estimates have been shown to provide satisfactory estimates for macronutrient river fluxes (Cohn et al., 1992).

### 6.5.2 Contextualising carbon fluxes at Gordonbush with other sites

The full hydrological year organic C flux estimates (using the 'Seasonal with Rising and Falling Limbs' method, considered to be most representative) for catchments GB10 and GB11 (affected by windfarm construction, Table 6.6), are similar to other fluxes estimates for UK peatland sites, including two others affected by windfarm developments (Table 6.5). Full hydrological year estimates for the control catchment, GB12 are just below or on the lower limit of aquatic fluxes in Table 6.6. It has previously been acknowledged that catchment size and peat coverage have been positively correlated with aquatic C fluxes (Grieve, 1994; Hope et al., 1994, 1997a; Aitkenhead et al., 1999). Therefore, regardless of

windfarm construction, the catchment ranking of C fluxes, GB10 > GB11 > GB12 is not surprising given the same ranking is also observed with catchment size and peat coverage within each catchment: 28.87 $km^2$ and 84 % peat coverage for GB10, 15.39 $km^2$ and 33 % peat coverage for GB11 and 5.14 $km^2$ and 17 % peat coverage for GB12.

| Study area | Sampling frequency | (g C $m^{-2}$ $yr^{-1}$) | Authors |
|---|---|---|---|
| British survey, 85 regions | Monthly | 10-103 | (Hope et al., 1997b) |
| NE Scotland & Mid-Wales | Weekly – Bi weekly | 12-19 | (Dawson et al., 2002) |
| Moor House | Weekly | 12-47 | (Worrall et al., 2003) |
| Glen Dye | Weekly-bi weekly | 18-31 | (Dawson et al., 2004) |
| Dee Valley | Two-weekly | 2-11 | (Aitkenhead-Peterson et al., 2007) |
| Auchencorth Moss | Weekly | 21-33 | (Billett et al., 2004) |
| Peak District | Hourly to bi-weekly | ~92 | (Pawson et al., 2008) |
| Peak District | 15 minutes to 11 days | 29-106 | (Pawson et al., 2012) |
| Hexamshire Common | 8 hourly to weekly | ~ 34-40, ~75-95 | (Rowson et al., 2010) |
| Auchencorth Moss | Approx. weekly | ~17-25 | (Dinsmore et al., 2013) |
| Cottage Hill Sike | Two-weekly | 50-65 | (Holden et al., 2012a) |
| **Studies below measured aquatic C flux from peatlands affected by windfarm construction** | | | |
| Gordonbush, NE Scotland | Storm event based* | 11-25 | This study |
| Whitelee, SW Scotland | Two-weekly* | 10-42 | (Murray, 2012) |
| Arecleoch, SW Scotland | Every 1-2 days | 34-55 | (van Niekerk, 2012) |
| Braes of Doune, C Scotland | Storm event based | 19-25 | (Grieve & Gilvear, 2008) |

**Table 6.5 - Aquatic organic carbon fluxes from other peatland sites**
Fluxes from a range of peatland sites in Scotland, England and Wales, where g C $m^{-2}$ $yr^{-1}$ comprises the sum of DOC and POC fluxes. Unless stated with a '*' all authors used the 'Method 5'. * - This study used aforementioned techniques to calculate presented C flux ranges, Murray (2012) used a simple [C] x Q to calculate C export every two weeks and assumed this was constant in between sampling points.

Climate will also influence the size of the aquatic C flux. Gordonbush estate is located in the far north-east of Scotland where it is colder (mean annual temperature 1981-2010 was approx 5-6°C (Met Office, 2014)) and drier (average annual rainfall 1981-2010 was approx. 1250-1500 mm, (Met Office, 2014)) than many other areas of peatland considered in Table 6.5. Temperature and hydrological conditions have been acknowledged as main drivers of C export (Dawson & Smith, 2007; Dawson et al., 2008) therefore given the cooler and drier environment, biological activity (C production) may be reduced and lower rainfall may flush less DOC out of peat soil profiles or erode peat to generate POC. Furthermore, the highest estimates in Table 6.5 (Pawson et al., 2008; Rowson et al., 2010; Pawson et al., 2012) were calculated in areas where peat erosion is quite severe and because of that it is common POC components of fluxes can be considerably higher than DOC as a result (Evans & Warburton, 2007; Evans et al., 2014). It has been estimated typical POC fluxes for undisturbed peatlands are commonly <10 g C $m^{-2}$ $yr^{-1}$ (Hope et al., 1997b) whilst for severely eroding systems POC fluxes can exceed 100 g C $m^{-2}$ $yr^{-1}$ (Worrall et al., 2011). Since POC contributions were low (typically <10 %) for

Gordonbush aquatic organic C flux estimates, this gives an initial indication there has been a limited impact of windfarm construction considering the soil disturbance activities in GB10 and GB11 could have potentially promoted more erosion in these catchments.

### 6.5.3 Assessment of windfarm impact on carbon fluxes

Whether there is an impact of windfarm construction on C fluxes can be assessed by comparison with a control site and/or comparison of flux estimates with other similar sites to assess if the export is considerably higher. Laudon et al. (2011) argues the sensitivity of C export (particularly DOC) ultimately depends on changes with individual landscapes. All catchments at Gordonbush are broadly similar so hydrology will provide a first order control and as all catchments have similar specific Q estimates, a comparison between catchments fluxes can be undertaken. Therefore to assess whether Gordonbush windfarm construction activities affect aquatic C fluxes, the relative ranking of the windfarm catchments can be compared to one another and to the control. C flux results from 'Seasonal' and 'Seasonal with R&F limbs' have been considered when assessing a potential windfarm impact on C fluxes (see Figure 6.9 and Table 6.6 for summary of C flux results). Although a change in ranked position would be considered to indicate inter-catchment changes in C export, the magnitude of change in estimates between hydrological years will also be considered when concluding if a windfarm impact has been observed in calculated C fluxes.

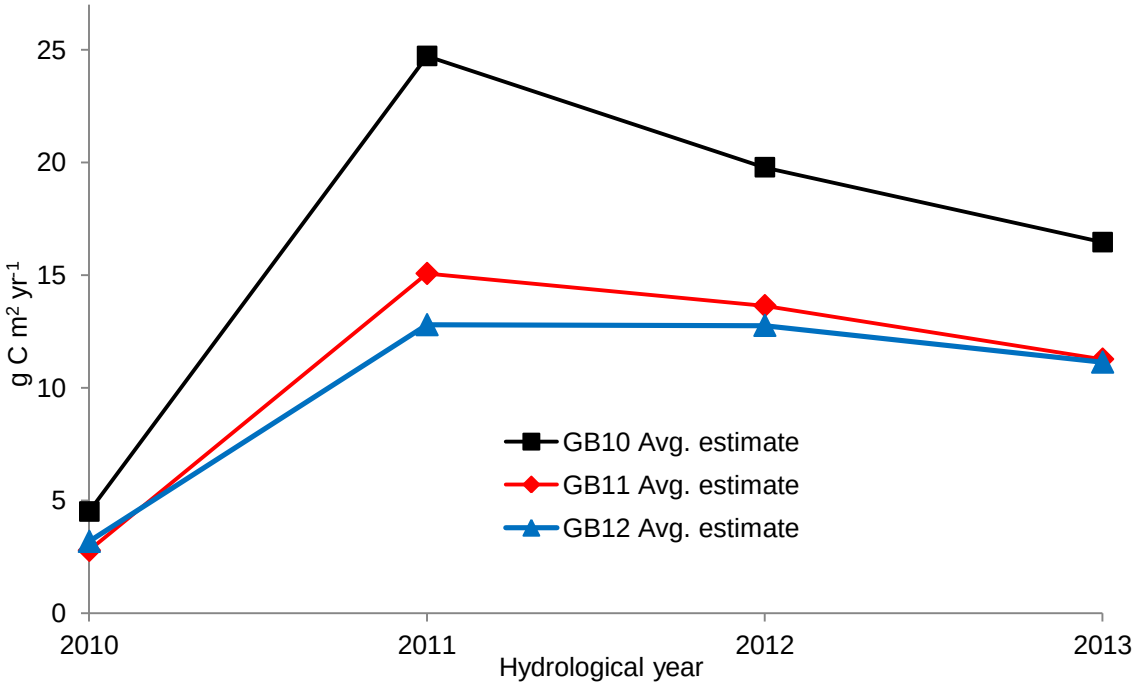


**Figure 6.9 – Time series of best C flux estimate for Gordonbush rivers**
The graph above is essentially an illustration of Table 6.6. The solid black (GB10), red (GB11) and blue (GB12) lines represent the average of both best C flux estimates.

| C flux units (g C $m^{-2}$ $yr^{-1}$) | Hydrological Year | | | |
|---|---|---|---|---|
| | **2010** | **2011** | **2012** | **2013** |
| River and flux calculation method | **Annual C flux estimates** | | | |
| **GB10 - Allt Mhuilin** | | | | |
| **Seasonal** | 4.4 | 24.8 | 19.7 | 16.6 |
| **Seasonal with R&F Limbs** | 4.6 | 24.6 | 19.9 | 16.3 |
| **Avg. between two methods above** | 4.5 | 24.7 | 19.8 | 16.5 |
| **Specific Q (10^6)** | 0.15 | 1.17 | 1.06 | 0.98 |
| **GB11 - Allt Smeorail** | | | | |
| **Seasonal** | 2.7 | 15.0 | 13.4 | 11.2 |
| **Seasonal with R&F Limbs** | 2.9 | 15.1 | 13.9 | 11.3 |
| **Avg. between two methods above** | 2.8 | 15.1 | 13.6 | 11.3 |
| **Specific Q (10^6)** | 0.15 | 1.14 | 1.06 | 1.02 |
| **GB12 - Old Town Burn** | | | | |
| **Seasonal** | 3.2 | 12.7 | 12.8 | 11.1 |
| **Seasonal with R&F Limbs** | 3.2 | 12.9 | 12.7 | 11.2 |
| **Avg. between two methods above** | 3.2 | 12.8 | 12.8 | 11.1 |
| **Specific Q (10^6)** | 0.22 | 1.31 | 1.29 | 1.26 |

**Table 6.6 - Gordonbush C flux estimates**
The table above shows C flux results for the two best considered flux estimation methods, 'Seasonal' and 'Seasonal with R&F limbs' for all three rivers, GB10, GB11, GB12, and all studied hydrological years. Please note that 2010 estimate only considers 2 months worth of data. Also included are average results of the two best methods and the specific discharge calculated for each year and river with the value presented at 10^6 for ease of presentation.

The average C flux estimates between 'Seasonal' and 'Seasonal with R&F Limbs' flux methods (Figure 6.9), show that the ranked order of GB10 > GB11 > GB12 is maintained in every hydrological year, similarly observed with [DOC] and [POC] data. However, the magnitude of change of C fluxes between the catchments is not the same each year (data from 2010 is excluded for this comparison as C fluxes were not representative of a full hydrological year). C fluxes in GB10 and GB11 show a greater magnitude of inter-annual variation than GB12. For GB10 C flux decreases 20 % from 2011 to 2012 and a further 17 % between 2012 and 2013. Overall in GB10 C fluxes decrease 35 % between 2011 and 2013. For GB11 C flux estimates decrease 9 % between 2011 and 2012 and a further 17 % between 2012 and 2013 equates to a decrease of 25 % from 2011 to 2013 (Table 6.6). In comparison GB12 estimates are the same in 2011 and 2012 and drop 14 % in 2013. In Figure 6.9, the highlighted differences are represented by change in gradients between the time series lines linking C fluxes estimates in consecutive years.

These changes imply that C fluxes may have been elevated in GB10 and GB11 compared to GB12 in 2011 and 2012, and this may be a consequence of windfarm construction activities in both catchments. Annual discharge was also higher in these years and so these higher exports may represent more soil-flushing considering they both contain more peat than GB12. Furthermore increases in [DOC] and [TP] time series were observed at

GB10 (Chapter 5) during the same time period. Together, these observations suggest that the increased C exports are a signal of disturbance due to the windfarm construction activities (including forest felling). In 2013 differences between all catchments are at their smallest as C flux estimates in GB10 and GB11 continue to decrease. This could represent recovery from the majority of landscape disturbance associated with construction of windfarm infrastructure which occurred mainly between August 2010 and April 2012. This could suggest that if there was an impact, it was short-lived.

Given the close proximity of the three studied catchments, we would expect their respective specific annual discharges to be similar (Hendriks, 2010). Despite all the potential variability associated with discharge calculation, specific annual discharges are similar each studied year for GB10 and GB11 (Table 6.6), with values for GB12 being elevated in comparison. If discharge has been over-estimated in GB12, this would result in an overestimate of the estimates of C fluxes presented, thus GB12 C fluxes would be lower than stated, in turn further increasing the differences previously highlighted and strengthening the interpretation that a windfarm impact has been observed.

Having considered the highlighted areas of measurement variability and the limitations of the 'best' flux method used, confidence in the validity of C flux estimates made at Gordonbush is retained and conclusions of a possible windfarm impact in windfarm affected catchments, GB10 and GB11 is maintained.

### 6.5.4 Application and advancement of aquatic carbon modelling

From the results of this research, future studies should not aim to produce aquatic C fluxes without the use of automated equipment or implementation of an intensive sampling strategy. Any equations modelling [DOC] from continuously logging environmental monitoring equipment will probably be site-specific. Despite this, focussing on continual measurement of air temperature, days between rainfall events and a proxy for alkalinity, e.g. pH, should be encouraged at all sites to produce more detailed time series. In turn, this might allow the opportunity for C fluxes to be calculated more precisely in the absence of a specialised *in-situ* river DOC sensor. To improve the model created and reduce prediction intervals of the equation, future MLR analysis inferring [DOC] could potentially include other variables, such as conductivity, which have been observed to be strongly correlated with [DOC] data (Daniel et al., 2002; Waterloo et al., 2006). Conductivity and pH are usually well correlated (potentially auto-correlated when used in MLR) as both are related to the concentration of charged ions in solution (conductivity is the sum of the contribution of all charged ions in solution and pH is a measure of $[H^+]$ ions). Therefore, conductivity could be measured and used as an alternative to pH as conductivity sensor

technology is inexpensive and requires little maintenance. Alternatively, using only physical characteristics of the landscape such as altitude, runoff and peatland cover, [DOC] has been modelled with high statistical significance using regression models, the results of which were applicable at multiple sites across the same region (Agren et al., 2010a).

Empirical (regression) models can effectively utilise large data sets and efficiently show general trends (Futter & de Wit, 2008). However, the results from MLR analysis showed [DOC] could only be predicted to ± 10 mg $l^{-1}$ (Figure 6.7) which when accounted for when estimating an aquatic organic C flux could result in large (i.e. +50 %) errors limits. Empirical modelling is also constrained by the data sets that are available (Zhang et al., 2013) whereas alternatively, process-based modelling attempts to assign mathematical equations to the mechanisms controlling environmental parameters and are better suited at simulating future projections (e.g. changes in climate changes) than empirical models (Futter & de Wit, 2008). Alternative methods to empirical modelling which are more statistically advanced include: Bayesian modelling (Arhonditsis et al., 2008), varying coefficient models (Ferguson et al., 2007, 2009), or general additive modelling (Ryder et al., 2014), however, all these methods require a greater statistical knowledge and understanding. In-stream [DOC] is not exclusively controlled by one factor (Jutras et al., 2011), therefore simply inferring linear patterns between different variables to offer predictions of fluxes is not the best strategy. Table 6.7 (next page) briefly describes some of the process-based and integrated models which have been developed to infer aquatic [DOC].

In the future, to better infer [DOC] and advance modelling of aquatic organic C fluxes at Gordonbush and other peatland sites, alternatives approaches (to the ones explored in this research) should be investigated. I would advocate a model which integrates both empirical data and processed-based modelling; linking measured data and conceptual thinking of processes involved in the transfer of C from terrestrial to aquatic environment, e.g. (Agren et al., 2014). I would suggest trying to integrate collected [DOC] data with a hydrological model called, “Grid to Grid”, developed by Centre to for Ecology and Hydrology. “Grid to Grid” translates rainfall intensity into river flows to try to predict river flooding in the UK (Bell et al., 2007).

Furthermore, I would suggest that DOC fluxes are best described by trying to link rainfall intensity to the time taken for soils to reach a particular moisture point(s) where C starts being transferred into rivers. Mathematical equations and factors that affect rates of C transfer from soil profiles to rivers would need to be integrated into the “Grid to Grid” model but knowledge gained from current models (Table 6.7) could help assist the

estimation of these rates. I propose that such an approach would offer a significant improvement to the linear regression or MLR approaches explored in this research.

| Type of model and brief description | |
|---|---|
| **Process based** | **Author(s)** |
| Uses soil moisture & temperature as main descriptors of [DOC]. Initial model modified to made applicable in forested areas | (Grieve, 1991; Boyer et al., 2000) |
| Links DOC fluxes to soil types and DOC adsorption in different parts of soil profile | (Neff & Asner, 2001) |
| DyDOC model uses litter production, precipitation air & soil temperature to predict DOC | (Michalzik et al., 2003) |
| Uses soil moisture & water table fluctuations as main descriptors of [DOC] | (Worrall & Burt, 2005) |
| Links [DOC] to weather conditions, biological activity physical attributes of catchment and hydrological pathways | (Futter et al., 2007; Futter & de Wit, 2008) |
| **Integration of empirical and process based** | |
| DOC-3 model based on daily weather variations (ForHym process based model (Balland et al., 2006)) and digital elevation model to infer how wet peat is (utilising data from (Meng et al., 2005)) | (Jutras et al., 2011) |
| Similar to DOC-3 but includes and integrates an additional process based model simulating decomposing forest litter and thus extra source of DOC (Zhang et al., 2007; Zhang et al., 2010) | (Zhang et al., 2013) |
| Uses landscape-mixing model based predicting water-chemistry, i.e. DOC from landscape properties, e.g. sub-surface geology, slope angles and drainage patterns | (Agren et al., 2014) |

**Table 6.7 - Examples of models developed to infer aquatic [DOC]**
The table above is divided into two sections, Process based and Integrated models. A brief description of each model is given accompanied by the relative author(s).

## 6.6 Summary of constructing aquatic organic carbon fluxes

Hysteresis analysis is a powerful tool in deciding how to construct C export budgets as the understanding of processes informs decisions of which model is most appropriate. Partitioning the data by time period (i.e. accounting for seasonality) and into rising and falling limb seems to effectively represent the processes of C export and reflect the 'best' choice flux calculation method using linear regression. Whilst other approaches were broadly comparable, 'Method 5 all data' is not appropriate for this study as the data sets contain a large quantity of storm event data.

In general, the best flux estimates are comparable with other UK peatland sites where aquatic organic C fluxes have been calculated. Differences that occur compared to other sites could be climatic and there is evidence that some differences between the studied rivers may be attributed to differences in peat coverage within each catchment. Having a semi-continuous [DOC] time series would also be valuable in assessing if there was a

continued impact from wind-farm construction in the future at Gordonbush or indeed any other similarly affected site. Therefore, although MLR analysis did not result in aquatic organic C fluxes estimates being calculated the results could be applied (and a proxy developed) in the future at Gordonbush or at other sites.

One practical application of this knowledge gained could be to investigate the effect changes in aquatic organic [C] have on economically important on fish populations. The largest inter-annual changes in C export were recorded in the largest river, the Allt Mhuilin and feeds directly into River Brora, an important salmon fishing river. Although such an impact study was not undertaken as part of this research but such an investigation in the future would definitely benefit from a continuous [DOC] time series as well as better monitor transport of terrestrial C to the oceans. Additionally, as previously stated integrating both empirical and process-based modelling represents the 'best' strategy for improving aquatic organic C flux estimates.

Though maintaining the same ranked position of GB10 > GB11 > GB12 throughout the research period, calculated C fluxes from windfarm affected catchments (GB10 and GB11) compared to the control (GB12), indicate an increase in C flux in 2011 and 2012. As such there is evidence of a windfarm construction related impact on aquatic organic C flux at Gordonbush. This conclusion raises the question how effectively can these losses, albeit short-lived, be off-set? This is why investigations into the variability of C sequestration rates within peatlands, and receiving water bodies, (next chapter) and the effectiveness of remedial work (in terms of reducing C export) are needed (chapter 8 looks at the effectiveness of drain-blocking). This extra knowledge will allow us to better understand the fate of C export from source to sink as well as how this may have changed in the past to contextualise modern change, and help predict how they may change in the future and consequently how to manage these areas appropriately.

# 7 Carbon sequestration in peats and lakes at Gordonbush estate

## 7.1 Abstract

Investigating long-term C sequestration rates is essential if modern aquatic C fluxes are to be properly contextualised and an integrated assessment of catchment wide C cycling is to be achieved, necessary to better understand if Gordonbush is a C sink or C source. This information is also useful when assessing impacts of windfarm construction. In this chapter the C sequestration rates for lake and peat cores are calculated and the modern day sediment export into Loch Brora from the Gordonbush windfarm development is measured. Peat started to form ~9000 cal. yr. BP ago with long term average rates of accumulation of 0.33 – 0.34 mm $yr^{-1}$. Calculated C sequestration rates ranged from 10 – 57 g C $m^{-2}$ $yr^{-1}$, where long term average rates of C accumulation were 20.8 and 24.4 g C $m^{-2}$ $yr^{-1}$ from the two peat cores collected. It was difficult to establish a robust chronology for the sediment core recovered from Loch Brora. Estimates for calculated long-term sedimentation rates of 0.16 cm $yr^{-1}$ and a C sequestration rate of 61.8 g C $m^{-2}$ $yr^{-1}$ (range was 22-85 g C $m^{-2}$ $yr^{-1}$) will need to be refined. As a result, examining the historical links between catchment C sequestration rates and sediment export dynamics from C 'source' (Gordonbush peats) to the C 'sink' (Loch Brora sediments) was not possible.

The modern-day maximum sedimentary fluxes into Loch Brora, calculated from *in-situ* sediment trap samples, coincide with periods of high river discharges, suggesting a first order control on sediment delivery to the lake. Sedimentary C fluxes from windfarm hosting catchment, GB11, were higher than for the control site GB12. Given the difference in characteristics between the two catchments (size, peat coverage, abundance of erodible material), these differences could be natural. However, whether windfarm construction has had a short-term impact on sediment efflux cannot be discerned because of the limited time series data collected and the difficulties associated with quantifying the effect of specific construction activities. More time is needed to assess if this differences between GB11 and GB12 sedimentary fluxes are transient, catchment-specific or coincident with the windfarm construction, which also may have a longer-term impact. This is an important future research need. Additionally, estimates of Loch Brora C sequestration rates (although not definitive) imply only approx. 8 % of particulate material exported is sequestered long-term into lake sediments. This suggests Loch Brora is not currently, and will not be in the future, a strong C 'sink' for any potential increases in sediment export due to disturbance of peat by windfarm construction activities or natural erosional processes.

## 7.2 Introduction

Peatlands are important terrestrial C stores (Yu et al., 2010) containing an estimated 455 to 547 Gt of C globally (Gorham, 1991; Turunen et al., 2002), and their presence and condition greatly influences the global C cycle (Yu, 2011). Since the end of the last ice age peatlands have sequestered enough $CO_2$ to lower global temperature by 1.5-2°C (Holden, 2005b). Lake sediments are also important sites where C is stored and sequestered, mineralized, or transported to downstream ecosystems (Hanson et al., 2011). The importance and incorporation of lake-C dynamics in global C cycle models is only just being realised (Kortelainen et al., 2004; Cole et al., 2007; Anderson et al., 2009; Battin et al., 2009; Tranvik et al., 2009; Ferland et al., 2012; Raymond et al., 2013). Land-cover and land use change strongly influences C export from terrestrial ecosystems (Grieve & Gilvear, 2008), as well as primary productivity (Smith et al., 1999) and organic C burial rates in lakes (Kortelainen et al., 2004; Anderson et al., 2009). However, the impact of land use change on C sequestration within peats (Ostle et al., 2009) and lakes (Heathcote & Downing, 2012) is currently poorly constrained.

The Gordonbush windfarm catchments drain into Loch Brora. Using sediment chronologies enables consideration of longer-term variability in C accumulation and export from peatlands and lacustrine C sequestration. From this, controls influencing changes in C export from peatland 'sources' to lake sediment 'sinks' over the last few millennia can be investigated. In turn, monitoring of modern sedimentary fluxes from rivers draining peatland catchments into Loch Brora will help assess i) how much sediment is delivered and if there is an impact of windfarm construction and ii) lake C burial efficiency by comparison with historical C sequestration rates. Using sedimentary archives to assess how sensitive peatlands are likely to be to modern anthropogenic disturbance is a relatively untested method. However, the nature of the landscape within the Gordonbush Estate, and the construction of the windfarm development, provided an opportunity to test this novel approach.

The main aims of this chapter are to:

1. Quantify the range of peat and lake C sequestration rates over time.
2. Quantify rates of mass sediment and C (POC) delivery to lake from peatland catchments.
3. Compare peat and lake C sequestration results from Gordonbush with other sites and identify the key controls on the sensitivity of such rates and if observed changes are common elsewhere.

## 7.3 Methods

### 7.3.1 Peat and lake coring

Peat cores were recovered from Gordonbush peatland using a 0.5 m Russian corer, and lake sediment cores were recovered from Loch Brora using a gravity corer for the mud-water interface, and a square-rod Livingstone piston corer for longer sediment sequence. Two peat cores were collected; one from an undisturbed site (GB1) and one from a location subject to historical peat cutting activity (GB2 (cut)) (see section 3.10 and map Figure 3.12). This approach was taken not only to investigate potential variability in peat accumulation from two different sites (one undisturbed and another disturbed by historical peat cutting activities) but to contextualise and assess the balance between C sequestration and aquatic C losses. This type of activity allows better understanding of the peatland C cycle at Gordonbush and whether the ecosystem is currently a net sink or source of C. This information can also aid a better-informed assessment of the 'green credentials' and potential C related impact of building windfarms on peatlands. A core from Loch Brora (LB10) was collected from a site 5.3 metres deep, near to where the Allt Smeorail River enters the lake (see sections 3.9 and map Figure 3.11).

### 7.3.2 Post-coring sedimentary analysis

Total organic matter was determined using weight loss on ignition at 550°C at 1-cm resolution for all peat and lake cores (section 4.2.1). A combination of radiometric $^{210}$Pb/$^{137}$Cs (using bulk freeze dried peat and lake sediment samples) and AMS $^{14}$C (humic acids extracted from bulk peat and lake sediment samples dating) were used to establish geochronologies and calculate sedimentation rates for core collected (section 4.2.3).

In addition, sediment traps were used to estimate modern sediment fluxes into Loch Brora from two inlet rivers, one whose catchment is affected by windfarm construction (Allt Smeorail), and one which is a control site (Old Town Burn). More information on sediment trap methodology can be found in section 3.8.

### 7.3.3 Age-depth modelling using *Bacon*

Age models were constructed using the *Bacon* software package for R (*Bacon* manual,(Blaauw & Christen, 2014)). Age-depth models are constructed utilising Bayesian statistics and the Markov Chain Monte Carlo (MCMC) methodology, given a set of radiocarbon ages (Blaauw & Christen, 2011; Christen & Perez, 2011; Goring et al., 2012). All calibrated ages are quoted in years before 1950 A.D., 'cal. yr. BP' as is convention (Reimer et al., 2004).

*Bacon* requires the following information to be provided by the user before any accumulation rates are calculated: an accumulation rate prior probability (i.e., a measure of uncertainty related to accumulation rates, in this case a gamma distribution which is based on previous work on various sediment cores (Goring et al., 2012)); section thickness, which dictates the resolution of calculated accumulation rates and ages of sediment within any core. This term is also a measure of the flexibility of the age-depth model; a model with larger section thickness can appear rigid with abrupt changes in accumulation rates; using a section thickness that is smaller means the model will appear smoother but may be over-fitted and not representative of the sediment core if it is calculated, e.g., using a disproportionally small number of radiocarbon ages. *Bacon* software contains an option suggesting a suitable resolution given dating data entered and a 4 cm resolution was advised for Gordonbush data provided. This resolution was considered appropriate given the (six for each peat core and four for Loch Brora lake core) $^{14}$C dates obtained. Ideally, and if financial budgets had allowed, a higher number of peat and lake core samples would have been $^{14}$C dated and would have allowed a finer resolution to be used.

Finally, *Bacon* users must provide a memory term defining how much the accumulation rate of a particular depth in a core depends on the depth above it as well as additionally providing information of any depths of known accumulation hiatuses (*Bacon* manual, (Blaauw & Christen, 2014)). All this information allows a tailored and highly core specific age-depth model to be produced with a continuous and smoothed range of accumulation rates. The way *Bacon* utilises Bayesian statistics to create sedimentary chronologies is more statistically robust than previous programmes e.g., connecting data points using linear regressions (Blaauw & Christen, 2005; Blaauw, 2010) which is now acknowledged as an unsuitable technique for examining environmental change over Holocene timescales (Yeloff et al., 2006). As a result, *Bacon* software has been endorsed as the best methodology for quantifying age-depth models for peats and provides the best estimates of changing uncertainties throughout any sediment record (Langdon et al., 2012).

# 7.4 Results

## 7.4.1 Peat Cores

### 7.4.1.1 Sedimentological properties of peat cores

To calculate C sequestration histories for Gordonbush peat and Loch Brora (see section 7.4.2), stratigraphic variations in sediment properties including dry bulk density and total organic C are essential (Tolonen & Turunen, 1996; Chapman et al., 2009): percentage water (% Water), loss on ignition at 550°C (% $LOI_{550}$), and % $LOI_{550}$ converted to grams of C per dry $cm^3$ of sediment (g C $cm^3$) are presented (Figure 7.1A-C).

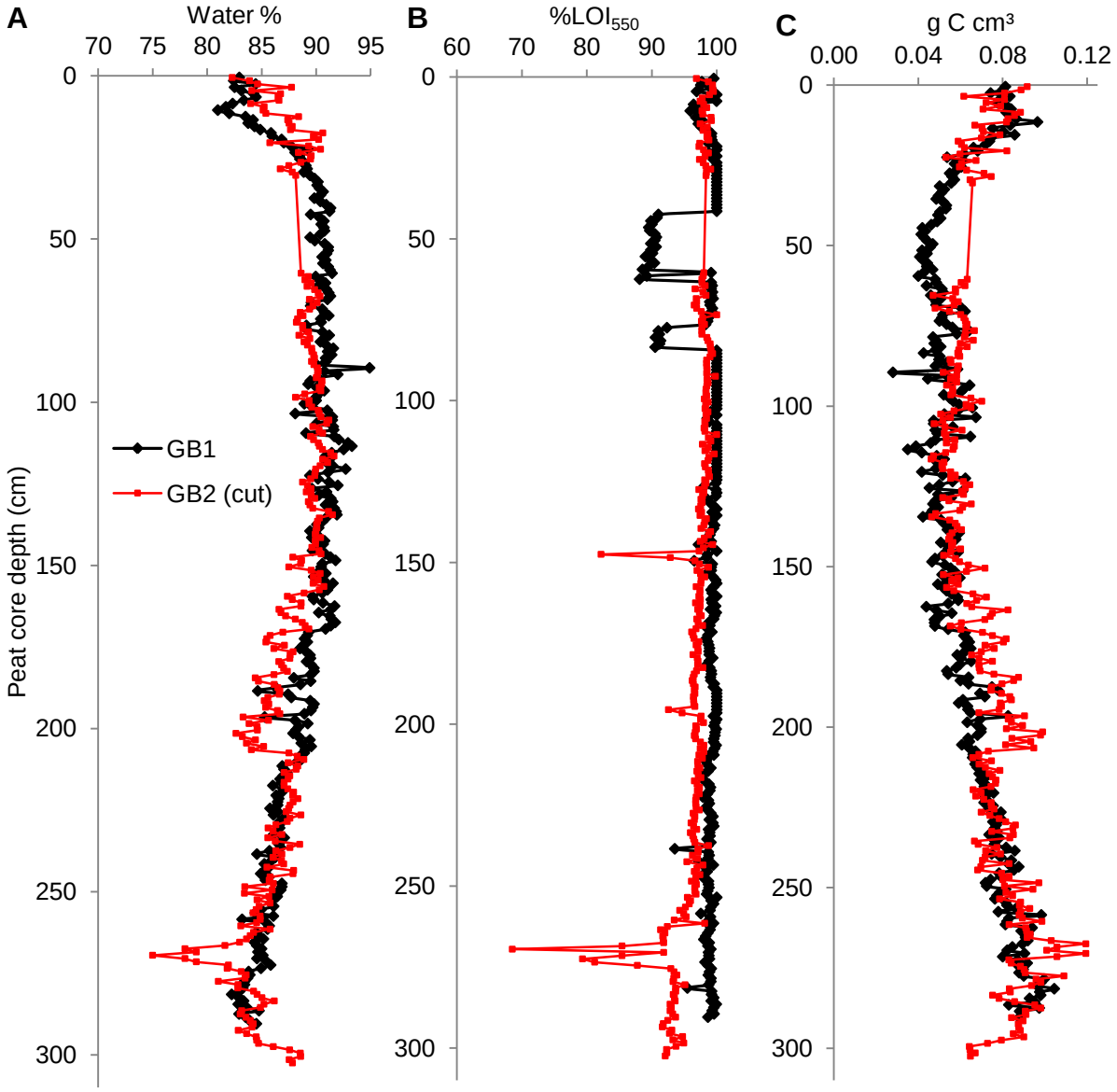


**Figure 7.1 - Physical properties (Water %, $\%LOI_{550}$, g C $cm^3$)**
All data presented for peat cores GB1 and GB2 (cut) has a 1 cm resolution. GB1 data is represented by black diamonds, GB2 (cut) data is represented by red squares. A = Water percentage of sediments, B = $\%LOI_{550}$ of each sample, C = dry density carbon content (g C $cm^3$). In all 3 diagrams above GB2 core has a straight red line going from 30 to 60 cm. This represents the removal of material by peat cutting activities at GB2 and has been incorporated so both GB1 and GB2 can be compared on like for like basis. A description of how the value of the cut was estimated is available in subsequent section 7.4.1.3.

Percent water ranges between 75 – 95 % and generally increases from the base of the core to ~150 cm (Figure 7.1A). Water percentage stays constant at ~90 % from 150 to 50 cm and then decrease towards surface sediments. GB1 and GB2 (cut) show natural variability between locations, despite close proximity. Calculated % $LOI_{550}$ ranges mostly between 95 – 100 % in both cores (Figure 7.1B), with data from GB1 and GB2 cores consistently within error of each other. As peat is almost exclusively decaying organic matter and proportions of C between peats differ very little (Chapman et al., 2009) such high %LOI results are not surprising. There are two periods in GB1 where %LOI decreases to approx. 90 %: between 42-62 cm and 77-84 cm. In GB2 (cut), exceptions to %LOI between 95-100 % are at 148 cm (82 %) and 270 cm (69 %) and generally 250-300 cm where it is lower (Figure 7.1B). Dry bulk density C content (g C $cm^3$) ranges between 0.03-0.12 g C $cm^3$ in both cores, showing the inverse general trends observed in water percentage (Figure 7.1C): an increase from basal depths to 150 cm, a period of generally constant values approx. 0.05-0.06 g C $cm^3$ then an increase from approx. 50 cm to surface sediments. Bulk density reflects local moisture conditions on the peatland surface and greatly influences variation in C sequestration rates in peats (Chapman et al., 2009), e.g., peat layers with high bulk densities commonly indicate drier conditions (Yu et al., 2003). However, to accurately construct C sequestration histories, bulk density (g C $cm^3$) data, needs to be combined with a core chronology. Calculated bulk density indicate, throughout both peat profiles studies C sequestration rates cannot be assumed to be constant. For this reason and also to understand rates of C sequestration, age profiles have to be constructed.

### 7.4.1.2 $^{210}$Pb and $^{14}$C dating results

GB1 shows a peak of unsupported $^{210}$Pb at 1.5 cm, then a decrease and trend to zero after 4.5 cm (Figure 7.2A). There is a peak in the top 2 cm of GB1 $^{137}$Cs profile that could signify a combination of historic peaks in atmospheric, and subsequent deposition of $^{137}$Cs during 1963 and 1986, related to a time period prior to ban of atomic weapons testing in 1963 and 1986 Chernobyl nuclear disaster (Appleby, 2001) (Figure 7.2B). By comparison in GB2 (cut) core site we do not observe either the typical $^{210}$Pb or $^{137}$Cs profiles (Figure 7.2A&B), which means a $^{210}$Pb age model for GB2 (cut) peat core is less reliable than that calculated for GB1. For GB1, the constant rate of supply (CRS) model (Appleby & Oldfield, 1978) for estimating ages of sediment from $^{210}$Pb data was used to produce an age model for the top 5 cm of the GB1 core (Figure 7.2C). The oldest calculated age from the $^{210}$Pb CRS model is 1821 AD at 4.5 cm. From this an apparent average accumulation rate over the last ~190 years is estimated to be 0.24 mm $yr^{-1}$ (Figure 7.2C).

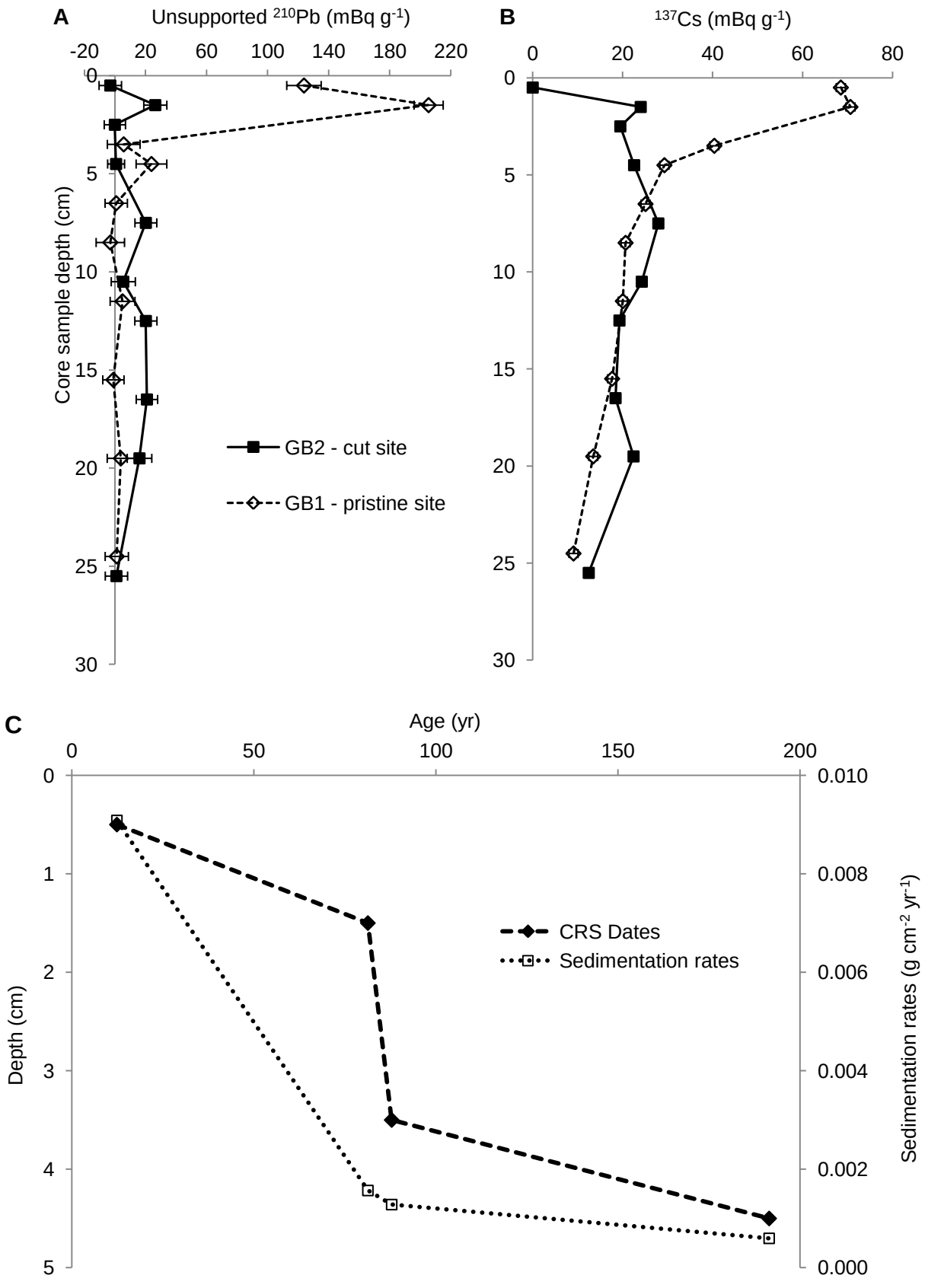


**Figure 7.2 - $^{210}$Pb and $^{137}$Cs peat profiles and 210Pb age-depth model**
Fallout radionuclide concentrations are presented versus depth. A = GB1 & GB2 (cut) peat core Unsupported $^{210}$Pb profile, B = GB1 & GB2 (cut) peat core $^{137}$Cs profile. Errors bars (1δ) are displayed on all sample results for $^{210}$Pb and $^{137}$Cs measurements. The ages of sediments, for both peat cores have been calculated using $^{210}$Pb data (graphs A & B) in conjunction with the CRS (constant rate of supply) model. Sedimentation rates are presented on secondary y-axis (right-hand side), age is plotted on x-axis. C = CRS derived $^{210}$Pb age-depth model for GB1 peat core.

| Peat core ID code | Material | Sample depth (cm) | $\delta^{13}C$ (‰) | AMS $^{14}C$ | Error (±) | Calculated age (cal. yr. BP) | | |
|---|---|---|---|---|---|---|---|---|
| | | | | | | Median | Min. | Max. |
| **GB1 (non-cut)** | | | | | | | | |
| SUERC-46754 | Peat | 25.5 | -27.2 | 1048 | 29 | 936 | 787 | 1039 |
| SUERC-42928 | Peat | 57.5 | -27.7 | 1739 | 25 | 1653 | 1547 | 1787 |
| SUERC-49279 | Peat | 75.5 | -27.5 | 2328 | 29 | 2298 | 2121 | 2416 |
| SUERC-42927 | Peat | 149.5 | -28.6 | 3598 | 29 | 3903 | 3756 | 4048 |
| SUERC-49283 | Peat | 175.5 | -27.8 | 4001 | 30 | 4470 | 4365 | 4606 |
| SUERC-46756 | Peat | 199.5 | -27.7 | 4438 | 27 | 5112 | 4891 | 5277 |
| SUERC-42929 | Peat | 285.5 | -27.2 | 7931 | 30 | 8676 | 8369 | 8913 |
| **GB2 (cut site)** | | | | | | | | |
| SUERC-46757 | Peat | 27.5 | -27.2 | 1464 | 26 | 1316 | 1203 | 1402 |
| SUERC-42930 | Peat | 57.5 | -27.4 | 2640 | 29 | 2767 | 2580 | 2863 |
| SUERC-46758 | Peat | 99.5 | -27.2 | 3354 | 29 | 3614 | 3468 | 3761 |
| SUERC-42931 | Peat | 134.5 | -29.4 | 4144 | 24 | 4629 | 4425 | 4809 |
| SUERC-46759 | Peat | 200.5 | -29.3 | 4973 | 29 | 5781 | 5598 | 5959 |
| SUERC-42932 | Peat | 261.5 | -29.2 | 7640 | 30 | 8351 | 7889 | 8550 |

**Table 7.1 - Peat core $^{14}C$ dating results**
Seven samples from GB1 and six from GB2 (cut) cores, were 14C dated. Median, minimum and maximum calculated ages (cal. yr. BP) were derived from age-depth modelling performed by *Bacon* software utilising IntCal13 calibration curve, Bayesian theory statistics and Markov Chain Monte Carlo (MCMC) techniques. It should be noted that GB2 sample depths entered into *Bacon* were adjusted to accommodate the estimated 30 cm of peat removed from the site during cutting (see next section 7.4.1.3). For example, the median radiocarbon age at 99.5 cm for GB2 was 3614 but we think that represents an accumulation depth of 129.5 cm. Therefore, sample depth 57.5 cm became 87.5 cm, 99.5 cm became 129.5 cm etc.

Results of AMS $^{14}C$ dating of peats cores GB1 and GB2 (cut) are presented above (Table 7.1). The youngest and oldest median calculated ages (cal. yr. BP) present in GB1 are 936 cal. yr. BP and 8676 cal. yr. BP respectively. The range of any particular age estimation for GB1 is consistently between 240-300 years from 25.5 cm to 175.5 cm sample depths whereas the two deepest sample depths aged have ranges of ~400 and ~550 respectively. For GB2, the range of calculated ages is between ~300 and ~400 years down to 200.5 cm, but for sample depth 261.5 cm the range is of ages is 625 years.

When both cores are sampled at the same depth there are differences in median calculated ages (GB1 at 25.5 cm = 936 cal. yr. BP, GB2 at 27.5 cm = 1341 cal. yr. BP; GB1 at 57.5 cm = 1653 cal. yr. BP, GB2 at 57.5 cm = 2722 cal. yr. BP; and GB1 at 199.5 cm = 5112 cal. yr. BP, GB2 at 200.5 cm = 5784 cal. yr. BP). GB1 core was 291 cm long and GB2 (cut) core 274 cm. However, GB2 (cut) was taken at a historical peat cutting site so peat has been lost from the profile and therefore it is not surprising that calculated ages are not synchronous with the same depths at each site. However, when the oldest $^{14}C$ dates are extrapolated, the median age for bottom of each core was estimated (using *Bacon* software) to be very similar for each core, 8887 cal. yr. BP for GB1 and 8883 cal. yr. BP for GB2.

### 7.4.1.3 Estimating depth of peat removal from cut site

In order to make direct comparisons between age-depth models, accumulation and C sequestration histories of GB1 and GB2 (cut) peat cores, the depth of peat removed from the peat cutting site, GB2 (cut) needs to be accommodated. The local gamekeeper considered that generally approx. 0.3 m of top soil was removed before cutting was undertaken to access more humified peat (Rowantree, 2013). Then, as much as 0.3-0.9 m could be removed before the top soil was placed back in the cut area (Rowantree, 2013). It was observed that there was 0.3 m difference between the GB2 coring site and the surrounding peat, indicating the depth of the cut was of approx. 0.3 m. Additionally, peat depth work undertaken by SSER shows peat depths to be 3 m in the area surrounding GB2 (SSER, 2012); the length of GB2 core recovered was 2.7 m and if 0.3 m is added to this to account for the peat removed, it suggests the true depth of peat was 3 m and this agrees with SSER data. The removal of peat at GB2 (cut) is most likely the reason why a reliable $^{210}$Pb age-model could not be produced due to surface disturbance and also why $^{14}$C ages differ from GB1 results for similar sample depths (Table 7.1). A schematic of the peat-cutting process is provided (Figure 7.3). To account for the peat cutting hiatus in GB2, 30 cm was added to each sample depth below 30 cm (i.e. 31 cm becomes 61 cm, etc).

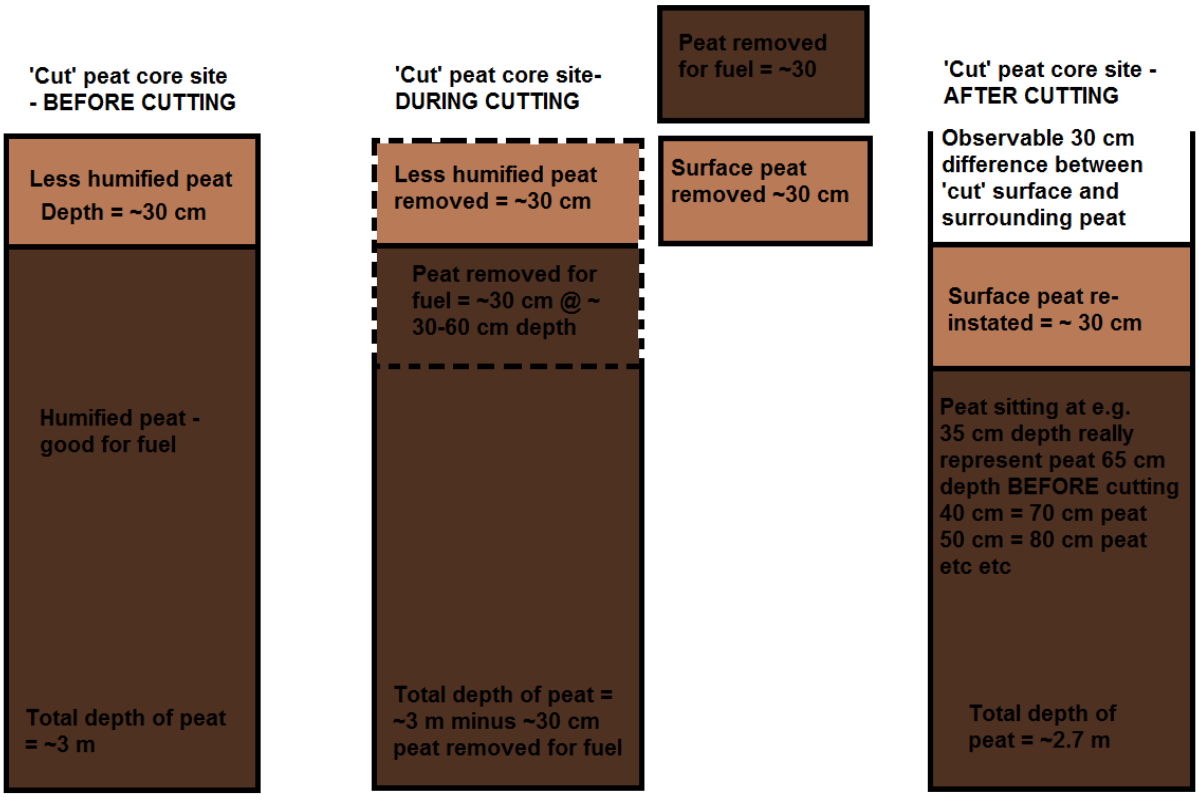


**Figure 7.3 - Schematic cross-section of peat profile before, during and after cutting**
The above diagram illustrates peat cutting at GB2 (cut) site.

### 7.4.1.4 Estimates of peat C sequestration over time

C sequestration histories for the peat cores were generated using *Bacon* (output from age-depth modelling analysis undertaken in *Bacon* is presented in Appendix G) based on core C content and accumulation. C sequestration rates are conventionally expressed as g C $m^{-2}$ $yr^{-1}$ (Tolonen et al., 1992; Anderson, 2002), see section 4.2.4 for how these are calculated. Long term average accumulation and C sequestration rates relate to the accumulated mass of sediment and C, respectively, above peat-mineral contact as a function of the basal age of the peat (Tolonen & Turunen, 1996; Turunen et al., 2002; Turunen, 2008). Only mean accumulation and C sequestration rates generated are presented (Figure 7.4A-B). A summary table displaying maximum, minimum and averages values of all mean accumulation results is presented below (Table 7.2).

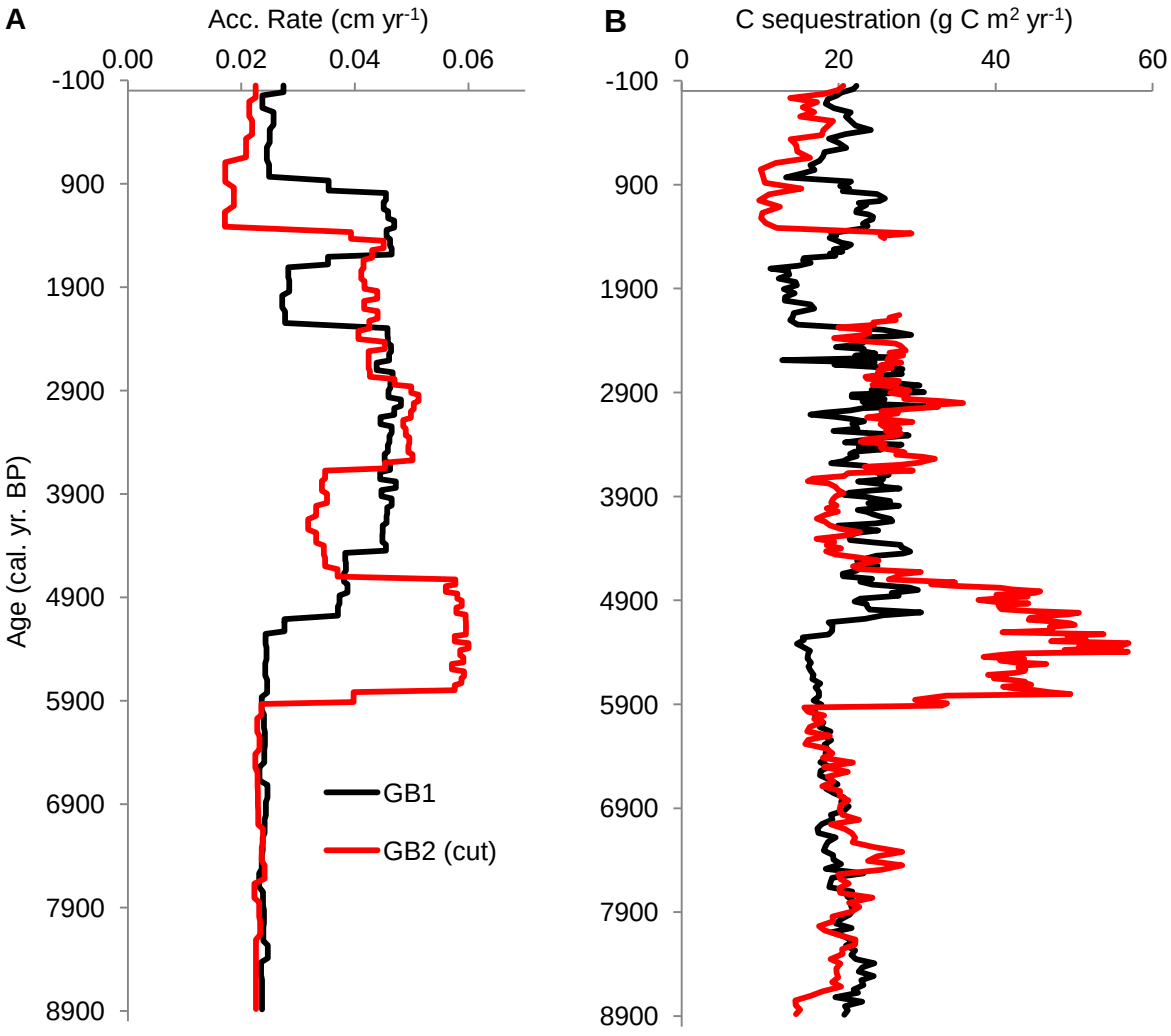


**Figure 7.4 - Peat accumulation and C sequestration histories**
A & B = Mean peat accumulation (A) and C sequestration (B) rate histories, GB1 peat core is presented in black and GB2 (cut) in red. Accumulation ($cm^{-1}$ $yr^{-1}$) and C sequestration (g C $m^{-2}$ $yr^{-1}$) rates are both plotted against median age estimates (y-axis) generated by *Bacon* for each core's age-depth model. The y-axis contains negative values as 0 cal BP = 1950 A.D. therefore any year after 1950 is represented by negative number, e.g. 2010 A.D. = -60. Where GB2 (cut) data is not continuous (graph B), this represents the estimated period of sequestration hiatus created by peat removal at the site for which we have no carbon content (g C $cm^3$) existed to make a C sequestration estimate during this time.

| Core site | Accumulation rates (cm $yr^{-1}$) | | | C sequestration (g C $m^{-2}$ $yr^{-1}$) | | | Long term averages | |
|---|---|---|---|---|---|---|---|---|
| | Min | Max. | Avg. | Min | Max. | Avg. | (cm $yr^{-1}$) | (g C $m^{-2}$ $yr^{-1}$) |
| Peat - GB1 | 0.023 | 0.048 | 0.035 | 11.3 | 31.1 | 21.3 | 0.033 | 20.8 |
| Peat - GB2 (cut) | 0.017 | 0.060 | 0.039 | 9.9 | 57.0 | 27.3 | 0.034 | 24.4 |

**Table 7.2 - Summary of peat core accumulation and C sequestration rates**
A summary of minimum, maximum and average values of all mean values calculated by *Bacon* regarding accumulation and C sequestration rates of Gordonbush peat cores. Long terms averages of accumulation and C sequestration are also presented in the far right columns of the table.

The calculated accumulation rate ranges for both peat cores are similar: GB1 (0.023-0.048 $cm^{-1}$ $yr^{-1}$) and GB2 (cut) (0.017-0.060 $cm^{-1}$ $yr^{-1}$) (Table 7.2). The biggest difference between the two peat cores occurs during 5900-4900 cal. yr. BP, 4600-3600 cal. yr. BP, 2300-1700 cal. yr. BP and 1500-700 cal. yr. BP (Figure 7.4A). This could be an artefact caused by the density of radiocarbon dates used for each core. For example, there is an 86-cm gap between the lowermost two AMS $^{14}C$ dates in GB1 (286 and 200 cm), whereas GB2 (cut) samples only have a 60 cm (291 and 231 cm) (refer back to Table 7.1). For a more direct comparison, it would have been better if the density of radiocarbon dated samples had been the same for each core. Since the long term average accumulation rates vary only slightly, (GB1 - 0.033 and GB2 – 0.034 $cm^{-1}$ $yr^{-1}$) it suggests that accumulation histories between both sites are similar.

Minimum C sequestration ranges are similar, GB1 - 11.29 g C $m^{-2}$ $yr^{-1}$ and GB2 – 9.89 g C $m^{-2}$ $yr^{-1}$, however the maximum calculated are quite different, GB1 - 31.08 g C $m^{-2}$ $yr^{-1}$ and GB2 – 56.94 g C $m^{-2}$ $yr^{-1}$ (Table 7.2). Since g C $cm^3$ values are similar for both peat cores (Figure 7.1C), the biggest difference in C sequestration histories between the two cores will coincide when the largest difference in accumulation rates occurs, mainly 5900-4900 cal. yr. BP. Excluding this period, both cores have C sequestration rates between ~10 and ~37 g C $m^{-2}$ $yr^{-1}$ throughout (Figure 7.4B). Long term average C sequestration rates (commonly referred to as 'LORCA' (Tolonen & Turunen, 1996)) for both peat cores are comparable, GB1 = 20.8 g C $m^{-2}$ $yr^{-1}$ and GB2 = 24.4 g C $m^{-2}$ $yr^{-1}$ (Table 7.2).

Trends in C sequestration rates (Figure 7.4B) match those observed in accumulation rate profiles for both cores (Figure 7.4A). From basal depth, trends in C sequestration are broadly similar in both GB1 and GB2, ranging for ~15-25 g C $m^{-2}$ $yr^{-1}$ between 9000-5900 cal. yr. BP. The largest disparity in C sequestration rates between GB1 and GB2 occurs from 5900-4700 cal. yr. BP; GB2 increases to a profile maximum of ~57 g C $m^{-2}$ $yr^{-1}$ at 5300 cal. yr. BP and rates stay between ~30-57 g C $m^{-2}$ $yr^{-1}$ during this period. Although C sequestration increase in GB1 from ~17 to ~30 g C $m^{-2}$ $yr^{-1}$ during the same period, the timing of change is different the magnitude smaller than that observed in GB2. Generally, C sequestration rates in both cores fluctuate between ~15-30 g C $m^{-2}$ $yr^{-1}$ from 4900 to

2200 cal. yr. BP, with similar rates between both cores observed at ~4500, 3300 and 3000-2600 cal. yr. BP. The second largest disparity between C sequestration rates occurs between 1300-900 cal. yr. BP, where GB1 rates are ~20-30 g C $m^{-2}$ $yr^{-1}$ compared to GB2 rates which range between ~10-15 g C $m^{-2}$ $yr^{-1}$. From 900 cal. yr. BP to surface sediments, both cores show a generalised increasing trend in C sequestration rates where estimates in both cores converge to ~20 g C $m^{-2}$ $yr^{-1}$ at the surface. The position of where the (red) line tracing C sequestration rates in GB2 breaks and restarts (Figure 7.4B), is our estimation of the accumulation hiatus caused by the removal of peat due to cutting activities which took place in 1950s and 1960s (Rowantree, 2013).

The relatively small number of $^{14}C$ age determinations means the minimum and maximum age estimations generated by *Bacon* are not well-constrained around the mean accumulation values. Consequently, it is not practical to present calculated minimum and maximum values, as they are not wholly representative of true accumulation or C sequestration rates within any of the cores.

## 7.4.2 Loch Brora core

The same layout of results presented for peat cores, will be used for the Loch Brora lake core results. Sedimentological properties are followed by $^{210}$Pb and $^{14}$C dating results and then accumulation and C sequestration histories for Loch Brora are presented.

### 7.4.2.1 Sedimentological properties of lake core

Percentage water (% Water), loss on ignition at 550°C (% $LOI_{550}$), and % $LOI_{550}$ converted to grams of C per dry cm$^3$ of sediment (g C cm$^3$) are presented for Loch Brora sediment core (Figure 7.5A-B).

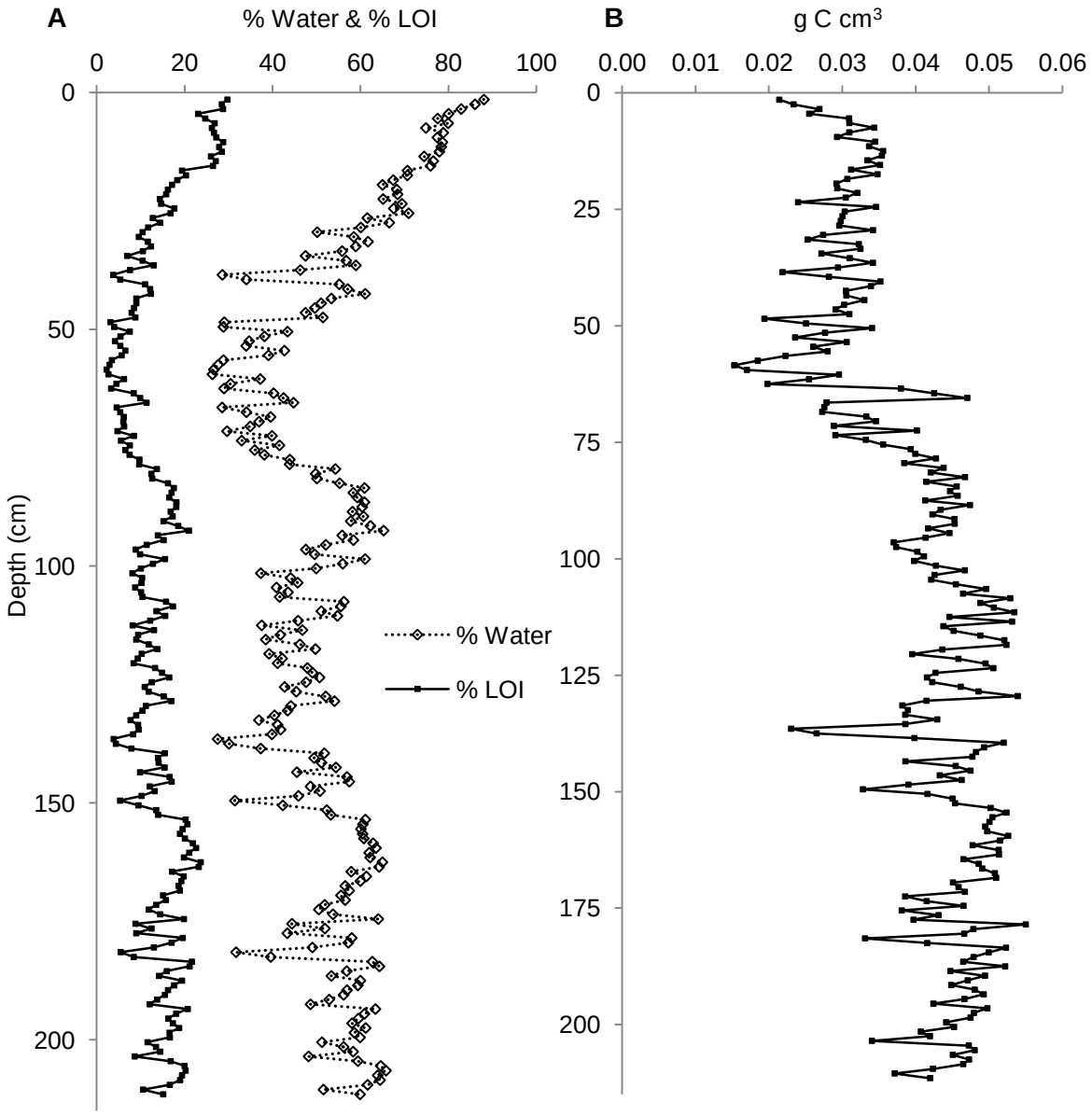


**Figure 7.5 - Physical properties (Water %, %LOI and g C cm$^3$) for Loch Brora sediment core**
All data presented for Loch Brora lake sediment core (LB10) has a 1 cm resolution. A legend is presented where Water % and %LOI are displayed on the same graph. A = Water percentage of sediments and %LOI of each sample, B = dry density carbon content (g C cm$^3$).

Water percentage and $\%LOI_{550}$ correspond throughout length of Loch Brora sediment (Figure 7.5A). Water percentage ranges from 22-88 % and $\%LOI_{550}$ from 2-28 %. Even though there are fluctuations between individual data points, values are consistently between 40-65 % (water) and 7-23 % ($LOI_{550}$) from basal depths to 85 cm. A decreasing trend in $\%LOI_{550}$ is apparent from 85 cm to 77 cm and then $\%LOI_{550}$ increases from here to the surface sediments. Dry weight density C content ranges between 0.015-0.055 g C $cm^3$ (Figure 7.5B). Generally, g C $cm^3$ ranges between 0.04-0.055 between basal depths and 110 cm. Bulk density of C in Loch Brora core seems to change at ~60 cm, and here C content ranges between 0.02-0.04 to 10 cm before finally decreasing towards surface sediments.

### 7.4.2.2 $^{210}$Pb and $^{14}$C dating results

The unsupported $^{210}$Pb concentrations for the top 32 cm of the Loch Brora core (LB10) decline from 1007 Bq $kg^{-1}$ at 2 cm to 31 Bq $kg^{-1}$ at 32 cm and decrease to zero with increasing depth (Figure 7.6A), which is typical of $^{210}$Pb profiles for sequentially deposited lake sediments (Appleby, 2001). Concentrations of $^{137}$Cs vary mostly between 1000 and 1300 Bq $kg^{-1}$ throughout the core however peaks are observed at 15.5 cm (2865 Bq $kg^{-1}$) and 12.5 cm (2225 Bq $kg^{-1}$) (Figure 7.6B). The peak at 15.5 cm is likely to be associated with the atmospheric testing of nuclear weapons with maximum fallout in 1963, while the other at 12.5 cm, it most likely derived from the 1986 Chernobyl nuclear disaster when high levels of $^{137}$Cs were released into the atmosphere (Appleby, 2008).

Based on a CRS model of $^{210}$Pb, the Loch Brora core has a date of 1863 AD at 31.5 cm, (Figure 7.6C) giving an accumulation rate of 0.22 cm $yr^{-1}$ at the top of the core. The CRS model also estimates 1986 A.D. to be between 12.5 and 13.5 cm, which is in agreement with the interpretation of a peak in $^{137}$Cs at 12.5 cm linked to the fallout of the 1986 Chernobyl nuclear disaster. Another peak in $^{137}$Cs profile is observed at 15.5 cm and this might have assumed this to be an indication of 1963 A.D. peak. However, our CRS model approximates 1963 A.D to occur at 20.5 cm. Despite this, the CRS model is still the best tool available to estimate ages for sediments less than 150 years (Appleby & Oldfield, 1978; Oldfield et al., 1979; Appleby, 2008). In comparison, when the Constant Initial Concentration (CIC) model was tested (alternative to CRS model) it grossly over-aged the sediments. Based on the CRS model, sedimentation rates calculated vary between 0.01-0.2 g $cm^{-2}$ $yr^{-1}$ over the last 150 years. Sedimentation rates increased markedly close to surface sediments (0.16 g $cm^{-2}$ $yr^{-1}$ at >0.5 years) (Figure 7.2C), but these sediment layers have the lowest density as they are less compacted compared to deeper sediment layers. This has the effect of predicting higher rates of sedimentation; however these are not representative of longer-term trends.

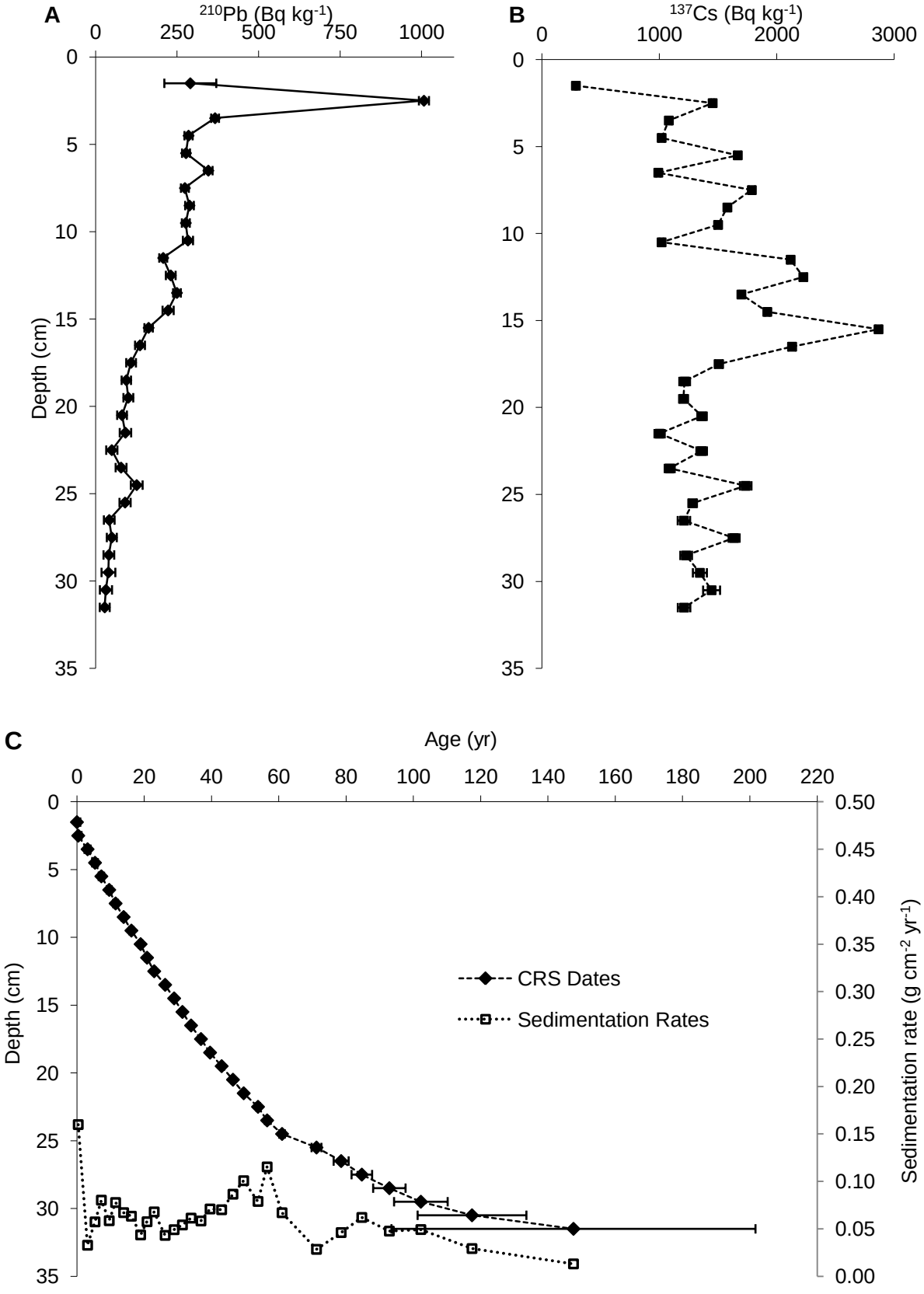


**Figure 7.6 - 210Pb and 137Cs lake profile and 210Pb age-depth model**
Fallout radionuclide concentrations are presented versus depth. A = Loch Brora (LB10) Unsupported $^{210}$Pb profile, B = Loch Brora (LB10) $^{137}$Cs profile. Errors bars (1δ) are displayed on all sample results for $^{210}$Pb and $^{137}$Cs measurements. The ages of the Loch Brora core sediments have been calculated using $^{210}$Pb data (graphs A&B) in conjunction with the CRS (constant rate of supply) model. Sedimentation rates are presented on secondary y-axis (right-hand side), age is plotted on x-axis. C = CRS derived $^{210}$Pb age-depth model for GB1 peat core, B = CRS derived $^{210}$Pb age-depth model for Loch Brora lake sediment core

Presented below is a table of results of $^{14}C$ dating of Loch Brora core samples (Table 7.3).

| Lab core ID code | Material | Sample depth (cm) | $\delta^{13}C$ (‰) | AMS $^{14}C$ | Error (±) | Calculated age (cal. yr. BP) | | |
|---|---|---|---|---|---|---|---|---|
| | | | | | | Median | Min. | Max. |
| **Loch Brora core LB10** | | | | | | | | |
| SUERC-51015 | Lake | 106.5 | -28.4 | 2017 | 29 | *585* | *435* | *755* |
| SUERC-51016 | Lake | 130.5 | -28.6 | 1922 | 29 | *748* | *591* | *929* |
| SUERC-51017 | Lake | 159.5 | -28.6 | 1885 | 29 | *947* | *794* | *1132* |
| SUERC-51018 | Lake | 208.5 | -28.6 | 1335 | 29 | *1278* | *1184* | *1498* |

**Table 7.3 - Loch Brora $^{14}C$ dating results**
Results from Loch Brora lake sediment core (LB10) are presented above. Median, minimum and maximum calculated ages (cal. yr. BP) were derived from age-depth modelling performed by Bacon software utilising IntCal13 calibration curve, Bayesian theory statistics and Markov Chain Monte Carlo (MCMC) techniques. The "Calculated age (cal. yr. BP)" were all calculated utilising only the reported $^{14}C$ age for the deepest sample depth dated, 208.5 cm. This ensured calculated ages followed a stratigraphic order which was not the case when samples were analysed. **However**, **by only using this $^{14}C$ age the age-depth for this core is compromised and the results have been italicised to reflect this unreliability.**

The AMS $^{14}C$ ages from Loch Brora (Table 7.3) do not fall in stratigraphic order and get younger with depth. After receiving these initial results, efforts were made to date macrofossils but unfortunately insufficient quantity of suitable material was found. This issue caused difficulty in generating reasonable age-depth models. For this reason it is impossible to establish a robust record of C sequestration. The Loch Brora sediment was collected in a series of overlapping cores, which is standard practice in palaeolimnological studies (Figure 7.7), meaning there is no evidence to support an inversion of the core(s) which might have explained the results of the samples analysed for radiocarbon. Therefore, one approach is to assume the bottom depth is correct and use this to constrain the whole profile. Old $^{14}C$ age estimates are not uncommon in lake sediments, and can be caused by a variety of reasons, but in this case the most likely is the in wash of pre-aged sediment. It is conceivably that erosion of peat from the Gordonbush catchment brings old C in the form of both particulate and dissolved organic/inorganic C. Therefore, the analysis of C sequestration rates and long term C accumulation rates for Loch Brora are tentative.

The deepest $^{14}C$ date, which by inference represents the basal age of core at 208.5 cm, 1335 ± 29 (see Table 7.3), was used to configure sediment accumulation rates. This may be incorrect, and as it is the youngest age it is acknowledged it will calculate the largest sequestration rates so a comparison of C losses must be viewed cautiously. However, this approach was the only way to create an age-depth model in *Bacon*. When the median calculated age at 208.5 cm is extrapolated back using *Bacon* a basal age for the core of 1301 cal. yr. BP is produced. Based on this basal age, the long-term average

accumulation rate is estimated to be 0.16 cm $yr^{-1}$ for Loch Brora sediments. The average accumulation rate estimated from our $^{210}Pb$ dating results is 0.22 cm $yr^{-1}$, the $^{14}C$ accumulation rates are similar, with the slight difference between the near surface and long term rates of accumulation could be an artefact of sediment compaction.

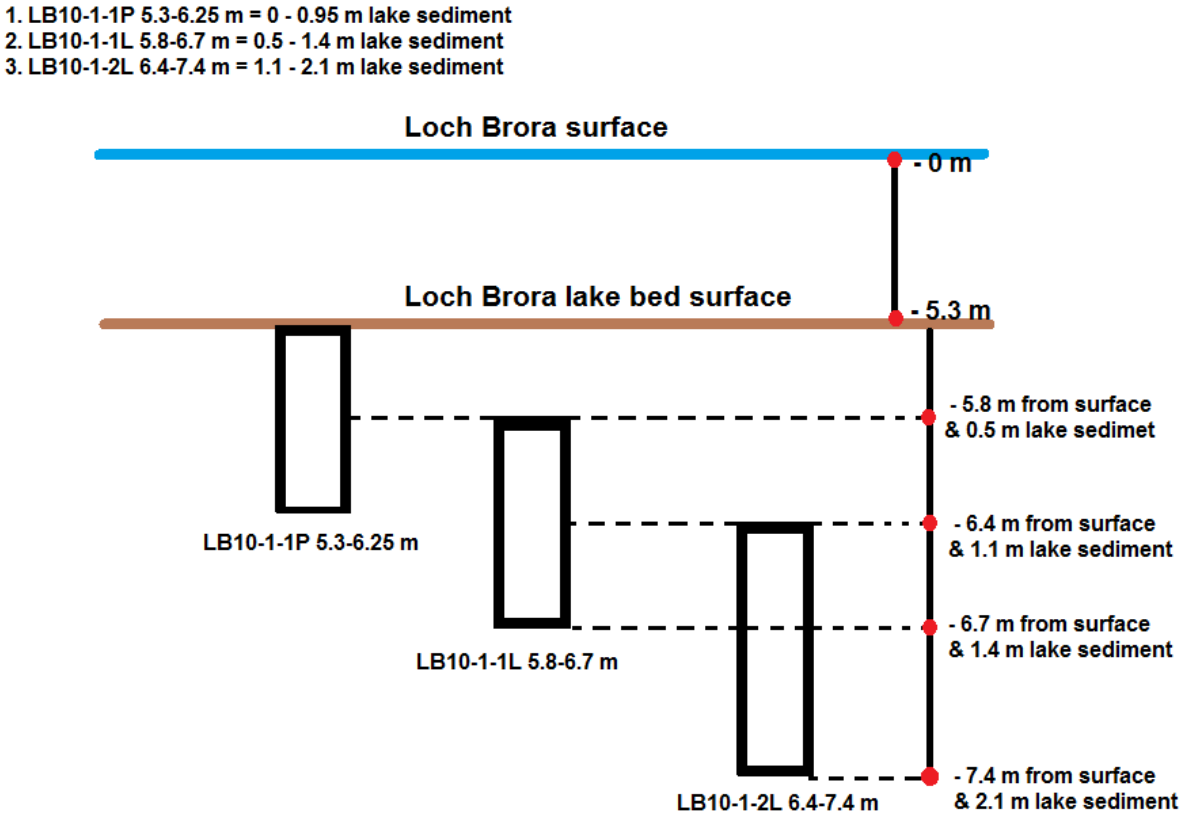


**Figure 7.7 - Schematic of Loch Brora sediment coring methodology**
It should be noted the diagram above is not drawn to scale and is only an illustration. The cores were coded using standard Paleolimnology practice for example **LB10-1-1P 5.3-6.25 m**, coring location and year is given first (**LB10** = Loch Brora 2010), coring site within the lake in case multiple cores are collected (**1** = 1st coring site), coring method and number (**1P** = 1st Piston core / **1L** = 1st Livingstone core) and finally depth of core from lake surface (**5.3-6.25 m** = 5.3 m was depth of water and 0.95 m core was retrieved so 5.3 + 0.95 = 6.25 m). Radiocarbon samples 106.5 cm and 130.5 cm were extracted from LB10-1-1L 5.8-6.7m and samples 159.5 cm and 208.5 cm from LB10-1-2L 6.4-7.4m. If either or even both cores were inverted, given the radiocarbon results, a sequential depth to age profile would not be produced.

### 7.4.2.3 Estimates of lake C sequestration over time

Lake sediment accumulation and C sequestration rates histories, based on age-depth models produced by *Bacon* (refer to Appendix G for *Bacon* output), are presented (Figure 7.8). A the summary table displaying maximum, minimum and averages values of all mean accumuulation results is also presented (Table 7.4).

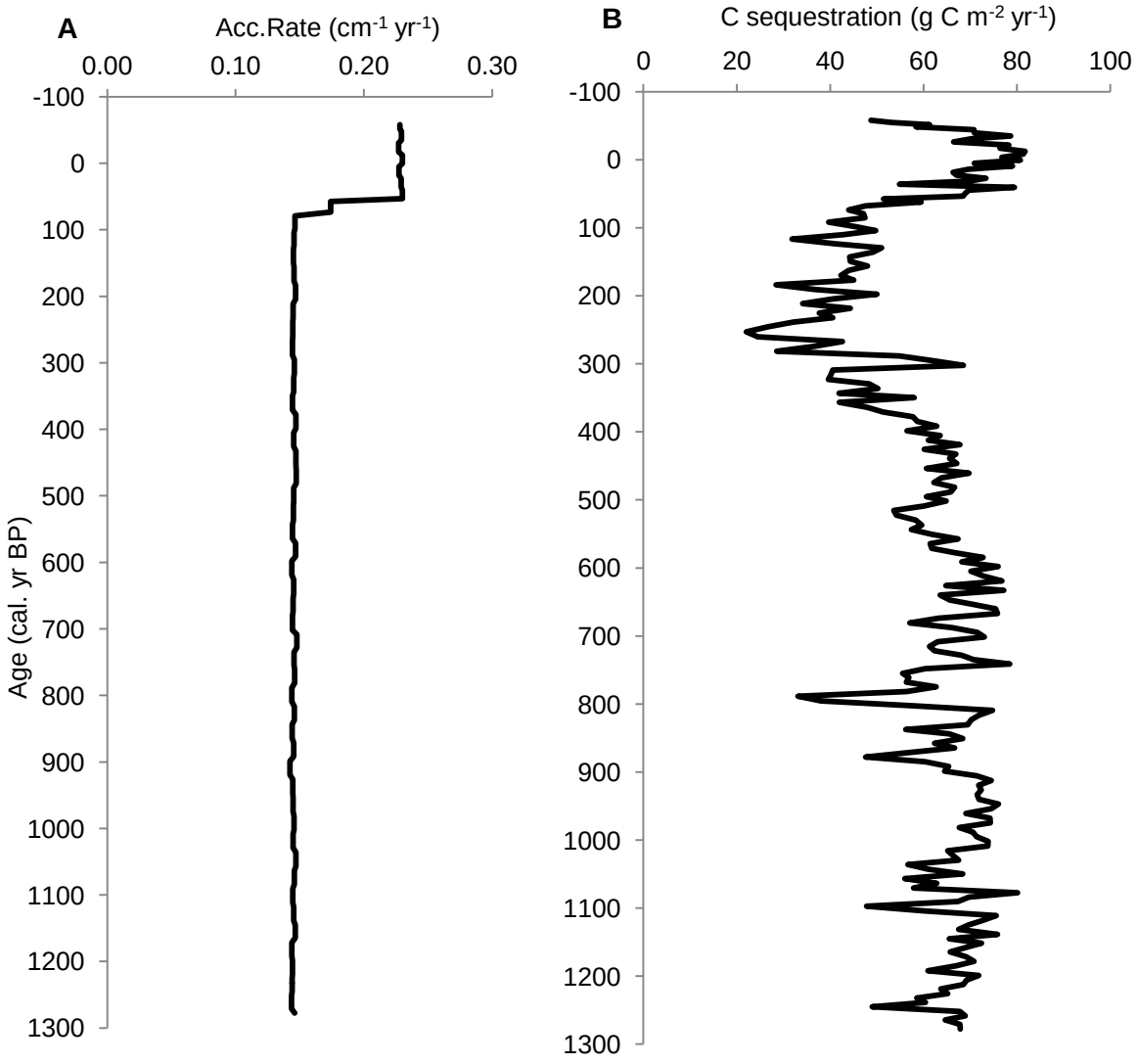


**Figure 7.8 - Lake accumulation and C sequestration histories**
A & B = Lake accumulation (A) and C sequestration (B) rate histories. Accumulation (cm $yr^{-1}$) and C sequestration (g C $m^{-2}$ $yr^{-1}$) rates are plotted against median age estimates (y-axis) generated by *Bacon* for lake core age-depth model. The y-axis contains negative values as 0 cal BP = 1950 A.D. therefore any year after 1950 is represented by negative number, e.g. 2010 A.D. = -60.

| Core site | Accumulation rates (cm $yr^{-1}$) | | | C sequestration (g C $m^{-2}$ $yr^{-1}$) | | | Long term averages | |
|---|---|---|---|---|---|---|---|---|
| | Min | Max. | Avg. | Min | Max. | Avg. | (cm $yr^{-1}$) | (g C $m^{-2}$ $yr^{-1}$) |
| Lake - LB10 | 0.142 | 0.230 | 0.157 | 22.1 | 81.8 | 61.0 | 0.156 | 61.8 |

**Table 7.4 - Summary of Loch Brora accumulation and C sequestration histories**
A summary of minimum, maximum and average values of all mean values calculated by *Bacon* regarding accumulation and C sequestration rates of Gordonbush LB10 core. Long terms averages of accumulation and C sequestration are also presented in the far right columns of the table.

The age model for Loch Brora generates a constant accumulation rate of 0.15 cm $yr^{-1}$ between 85 cal. yr. BP and basal age of ~1280 cal. yr. BP (Figure 7.8A). This is a consequence of utilising only one radiocarbon age dated from Loch Brora sediments: the age model assumes a linear sedimentation rate between the used basal age and $^{210}Pb$ dating results. Between ~80 and 40 cal. yr. BP, accumulation rates increase from ~0.15 to ~0.23 cm $yr^{-1}$, and then stay constant from that point to surface sediments.

Rates of C sequestration range between 22-82 g C $m^{-2}$ $yr^{-1}$, with an average of 61.0 g C $m^{-2}$ $yr^{-1}$ throughout the core and a long term average of 61.8 g C $m^{-2}$ $yr^{-1}$ (Table 7.4). C sequestration rates are relatively constant throughout the majority of the lake core and the variability observed can be traced to changes in C content of individual sediment layers (Figure 7.5B). The majority of C sequestration rate estimations fluctuate between ~57-78 g C $m^{-2}$ $yr^{-1}$ between 1300-600 cal. yr. BP, and then there is a general decrease from ~75 g C $m^{-2}$ $yr^{-1}$ at 600 cal. yr. BP to ~25 g C $m^{-2}$ $yr^{-1}$ at 250 cal. yr. BP (Figure 7.8B). Rates of C sequestration then generally increase from ~25 to 80 g C $m^{-2}$ $yr^{-1}$ up to 0 cal. yr. BP before decreasing towards ~48 g C $m^{-2}$ $yr^{-1}$ in surface sediments.

## 7.4.3 Modern sedimentary C fluxes in Loch Brora

### 7.4.3.1 Mass sedimentary and C flux time series

Total mass and C sediment flux (normalised to catchment size) time series for GB11 and GB12 show similar patterns over time (Figure 7.9A) but with more variability in the total mass of sediment in GB11 than GB12. The largest sediment and C fluxes occurred between 29/11/12 and 8/1/13 at GB11 (19.57 g $m^{-2}$ $d^{-1}$, 0.51 g C $m^{-2}$ $d^{-1}$) and GB12 (2.30 g $m^{-2}$ $d^{-1}$, 0.41 g $m^{-2}$ $d^{-1}$). However, there are times when small increases in mass sediment flux at GB11, e.g. did not result in corresponding increases in C flux.

Median grain size shows similar trends to mass and C flux with larger ranges recorded in GB11 than GB12 (Figure 7.9B-C). Peaks in median grain size at GB11 matched with peaks in mass sediment flux. In comparison, median grain size at GB12 is more constant throughout time series and the small peaks observed do not coincide with mass and C sediment flux maximums. The maximum mass, C sediment fluxes, and median grain size recorded at GB11 occur after some of the biggest storm events recorded on the Allt Smeorail hydrograph (Figure 7.9D).

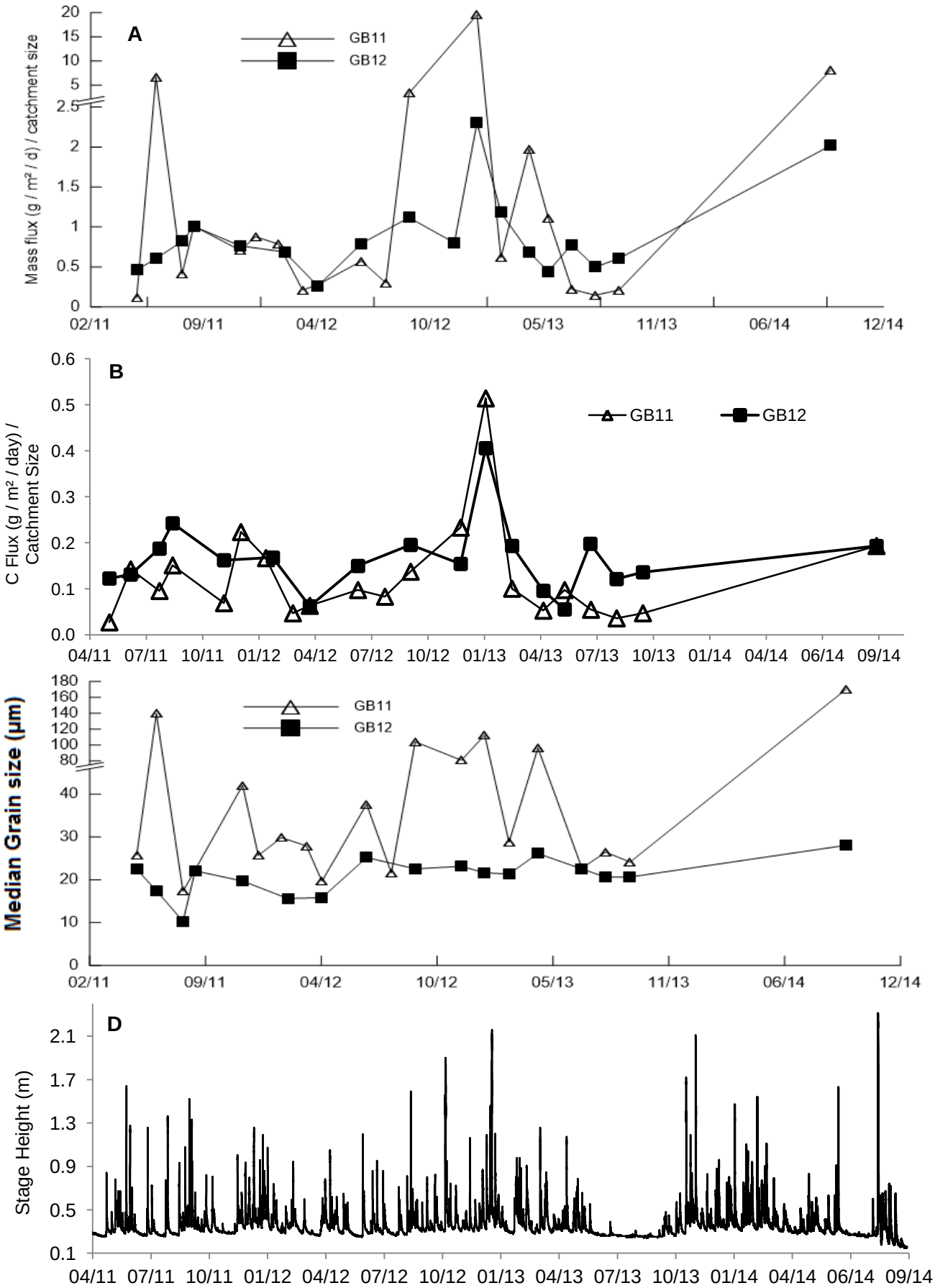


**Figure 7.9 - Mass, carbon and grain size sediment flux time series and GB11 hydrograph**
All graphs have a time line of April 2011 to October 2013, displayed on GB11 hydrograph. A = Mass flux ((g $m^{-2}$ $day^{-1}$) / catchment size), B = Carbon flux ((g C $m^{-2}$ $day^{-1}$) / catchment size), C = median grain size, D = Allt Smeorail (GB11) hydrograph from March 27th 2011 through to 24th September 2014. There is a missing value of median grain size on 14/5/13 for GB12, from the sample collected there was insufficient material to undertake grain size analysis. Please note the relevant breaks in scale on the y-axis on graphs A and C.

Annual mass and C sediment fluxes (Table 7.5) have been calculated from averaged daily rates presented in Figure 7.9A & B. The values in Table 7.5 represent sediment and C delivered to each sediment trap location and have not been scaled for the catchment size of the related rivers delivering the sediment. Also presented is a bar graph depicting the specific annual dischage from GB11 for hydrological years 2011-2014 (Figure 7.10).

| **Sampling site** | Year (Sept. – Sept.) | Annual mass flux (g $m^{-2}$ $yr^{-1}$) | Annual C flux (g C $m^{-2}$ $yr^{-1}$) |
|---|---|---|---|
| **GB11 (Allt Smeorail)** | *2010-2011 | 10054 | 502 |
| Catchment size 15.39 $km^2$ | 2011-2012 | 4662 | 553 |
| | 2012-2013 | 18227 | 835 |
| *(Based on 6 months data from | 2013-2014 | 45314 | 1086 |
| Mar. 2011 to Sept. 2011) | **Average** | **21374** | **794** |
| **GB12 (Old Town Burn)** | *2010-2011 | 1256 | 298 |
| Catchment size 5.14 $km^2$ | 2011-2012 | 1118 | 234 |
| | 2012-2013 | 1686 | 315 |
| | 2013-2014 | 3784 | 363 |
| | **Average** | **2179** | **317** |
| **Loch Brora (LB10)** | **Long term average C sequestration rate = 61.8 g C $m^{-2}$ $yr^{-1}$** | | |

**Table 7.5 - Annual mass sediment and C fluxes calculated from Loch Brora sediment traps**
Annual sedimentary fluxes were calculated from September to September to closely match hydrological year. Sediment traps were installed on 27th March 2011 so annual fluxes for 2010-2011 were extrapolated based on samples collected between March 2011 and September 2011. All values have units of g C $m^{-2}$ $yr^{-1}$ unless stated. Also included is the long term average C sequestration rate from Loch Brora sediment core, noting this is an insecure estimate.

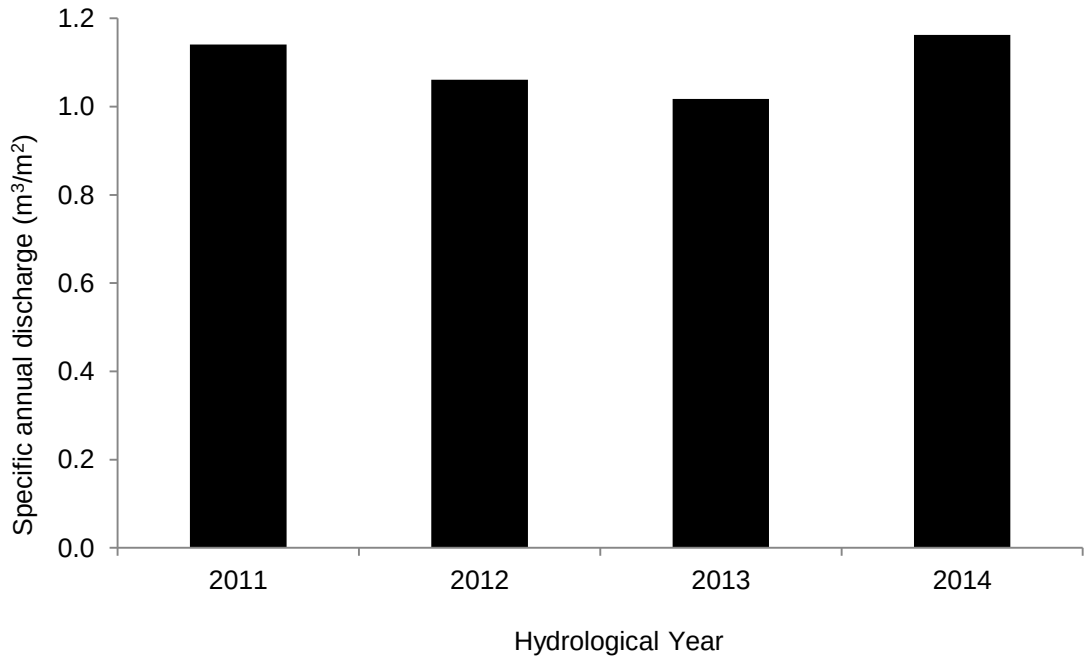


**Figure 7.10 – Specific annual discharge from GB11 (Allt Smeorail river) 2011-2014**
Specific annual discharge has been caluclated by dividing annual discharge ($m^3$) by size ($m^2$) of Allt Smeorail catchment.

The largest calculated annual and C fluxes at both sampling points coincide with the year with the largest specific annual discharge (2014). Calculated annual mass and C fluxes are consistently higher at GB11 than GB12. The range in mass and C fluxes is also larger in GB11 (4662-45314 g $m^{-2}$ $yr^{-1}$ and 502-1086 g C $m^{-2}$ $yr^{-1}$ resepctively) than GB12 (1118-3784 g $m^{-2}$ $yr^{-1}$ and 234-363 g C $m^{-2}$ $yr^{-1}$ resepctively). Average annual mass fluxes are almost 10 times higher in GB11 (21374 g $m^{-2}$ $yr^{-1}$) compared to GB12 (2179 g $m^{-2}$ $yr^{-1}$) where average C fluxes are only twice as large. Even when average annual mass fluxes are scaled for catchments size, GB11 sedimentary flux (1389 g $m^{-2}$ $yr^{-1}$ / $km^2$) is still over three times larger than GB12 (424 g C $m^{-2}$ $yr^{-1}$ / $km^2$). When the average annual C flux from GB11 are compared to long term C sequestration rates of the Loch Brora core, it suggests that only approx. 8 % of C entering the lake is sequestred on a long term basis.

### 7.4.3.2 Relationship between sediment flux and grain size

For GB11 data sediment flux rate is significantly and postiviely correlated with median grain size (PCC = 0.7, p = <0.01, n = 21) (Figure 7.11A), but the same relationship is not significant in GB12 (PCC = 0.38, p = >0.05, n = 18) (Figure 7.11B). At both sites larger median grain size is negatively correlated with % C in the sample (GB11 (Figure 7.11C), PCC = -0.89, p = <0.01, n = 21, GB12 (Figure 7.11D), PCC = -0.58, p = <0.05, n = 18). Similar to the relation between median grain size and mass sediment flux, this relationship is statistically stronger in GB11 than GB12.

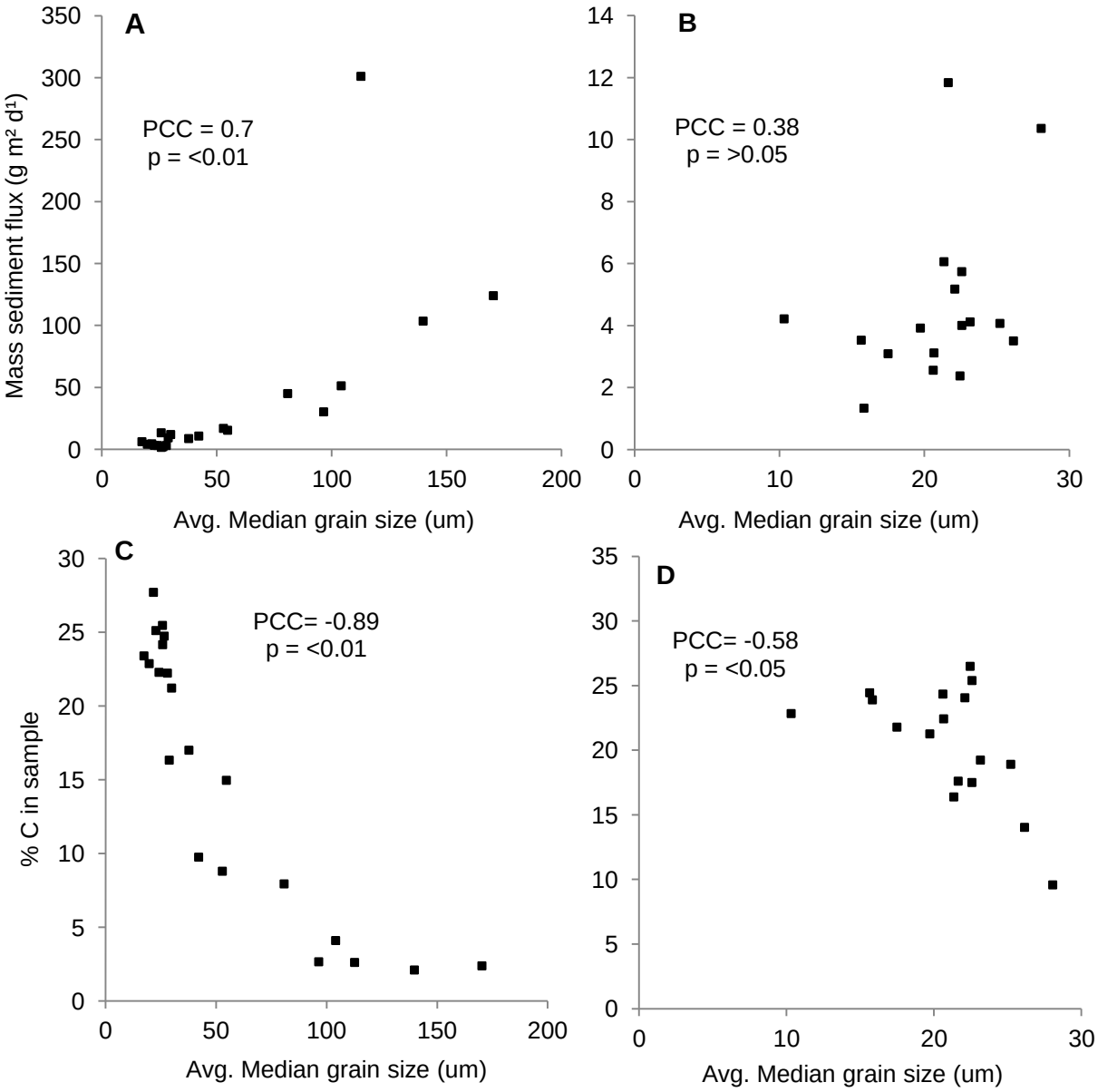


**Figure 7.11 - Mass flux and % C plotted against median grain size**
A = Avg. median grain size vs. mass flux (GB11), B = Avg. median grain size vs. mass flux (GB12), C = Avg. median grain size vs. % C in sample (GB11), D = Avg. median grain size vs. % C in sample (GB12). Average median grain size is always plotted on x-axis; mass flux and % C in sample are plotted on y-axis. The average median grain size is given as three replicates were analysed for each sample analysed. Equations and $R^2$ values of best fit relationships are presented on each graph.

# 7.5 Discussion

## 7.5.1 Assessing age-depth models & controls on C sequestration

### 7.5.1.1 Peat core age-model

Without identifying tephra layers, errors associated with radiocarbon dating can make it difficult to compare records from the same geographical location (Langdon & Barber, 2004; Mauquoy et al., 2004; Charman et al., 2006; Blundell et al., 2008). In the case of Gordonbush peat cores, the different density of dates measured for each core created the biggest problem when attempting to compare both peat records and accurately judge the offset created at GB2 (cut) by peat cutting activities. Peat sites within close proximity have shown contrasting C sequestration signals over last 2000 years (Langdon & Barber, 2005), but we would expect general trends to be the same. When a 30 cm correction was applied to the GB2 (cut), the general trends in g C $cm^3$ are well-matched between the two cores (Figure 7.1C) which suggests this 30 cm estimates the amount of peat lost (equivalent to ~900-1000 years of accumulation). Also, the long-term accumulation rates would be expected to be similar given the close proximity of the two sites, and this is the case (GB1 - 0.033 cm $yr^{-1}$ and GB2 (cut) - 0.034 cm $yr^{-1}$), which further supports our estimate of peat loss.

Long term average peat accumulation rates based on $^{14}C$ dating results (GB1 - 0.033 cm $yr^{-1}$ and GB2 (cut) - 0.034 cm $yr^{-1}$) are higher than those based on $^{210}Pb$ (GB1 - 0.024 cm $yr^{-1}$). Given the difference in time-scales associated with both techniques ($^{14}C$ = 9000 years; $^{210}Pb$ = 150 years) the variations observed are not surprising. However, both results are of similar orders of magnitude and peat accumulation rates calculated by *Bacon* throughout the whole core are similar based on $^{210}Pb$ dating results, most notably ~9000 to ~6000 cal. yr. BP (Figure 7.4A). This supports the results from GB1 $^{210}Pb$ age-depth. There are difficulties associated with constraining a 150-year-old $^{210}Pb$ peat-core age-model due to its slow development and growth, meaning discrepancies in calculated surface C sequestration rates between both peat core sites (Figure 7.4A). The fact that a robust $^{210}Pb$ age-depth model could not be produced for GB2 (cut) due to peat cutting activities will have also contributed to the discrepancies in estimation of surface accumulation rates.

Further, C sequestration rates may not be accurate in layers close to the surface of the peat, as it is still decomposing and not completely humidified (Turunen et al., 2004; Billett et al., 2010). Ideally a smaller sampling resolution of peat could give a more detailed $^{210}Pb$ and recent accumulation history; however different coring equipment allowing a greater size of sample to be extracted would have been required.

Peat accumulation rates in GB1 and GB2 cores, 0.017-0.06 cm $yr^{-1}$, (Table 7.2), are similar to mean accumulation rates of peats in the Western Ross region of Scotland (approx. 100 miles west south west of Gordonbush), of 0.042 – 0.057 cm $yr^{-1}$ (Anderson, 2002) and other North American peatlands (0.028 – 0.065 cm $yr^{-1}$), which have grown since approx. 7000 cal. yr. BP (Gorham et al., 2012). Accumulation rates in peat over the last millennia in North America have also remained constant (Gorham et al., 2003), a pattern similar to the estimated accumulation rates for both Gordonbush peat cores (Figure 7.4A).

#### 7.5.1.2 What are the controls on peat C sequestration?

The majority of peatlands located at high latitudes (>40° N) in the Northern hemisphere developed after the last deglaciation (Vitt et al., 2005; Beilman et al., 2010; Billett et al., 2010; Yu, 2012). Thus the maximum basal ages of any Northern Hemisphere peatland is <16500 cal. yr. BP (MacDonald et al., 2006). Basal ages of ~9000 cal. yr. BP in Gordonbush is consistent with the time-frame of peatland development between 11000 and 7000 cal. yr. BP (Anderson, 2002; MacDonald et al., 2006), which is also correlated with low atmospheric [$CO_2$] (Yu et al., 2011; Pendea & Chmura, 2012). The age of Gordonbush peats are therefore comparable with basal ages of peat cores taken in Scotland (Western Ross, (Anderson, 2002)) and Finland (Juutinen et al., 2013).

Based on the current age-models it is clear peat C sequestration rates at Gordonbush are naturally variable over time. GB1 and GB2 (cut) have similar long term rates of peat accumulation, but show natural variability in C sequestration rates. This is most likely due to site-specific variation that influences sequestration rates i.e. the micro-topography (hummock or hollow), the position of the water table and the vegetation present. Areas with higher water tables support more *Sphagnum* growth and increased C sequestration rates compared to drier areas. (Belyea & Clymo, 2001; Turunen et al., 2004; Strack & Waddington, 2007; Strack et al., 2008). The trend is for C sequestration rates to be more variable over the last ~5000 years (10-31 g C $m^{-2}$ $yr^{-1}$ across both cores) compared to rates up to this point (14-25 g C $m^{-2}$ $yr^{-1}$) (Figure 7.4B) and this has been observed at other peat sites in Finland (Tolonen & Turunen, 1996). Broadly, sensitivity in C sequestration rates is thought to be predominately influenced by hydro-climatic and geomorphic conditions (Quillet et al., 2013), and such peat archives are regularly used to examine changes in climate throughout the Holocene period (Cook et al., 1998; Chambers & Charman, 2004; Charman, 2007; Blundell et al., 2008).

The accumulation of peat results from an imbalance between plant production and decomposition, and if the later surpasses the former, release of $CO_2$ increases and the

peat becomes a net C source; equally if the opposite happens peats are net sinks of C (Quinty & Rochefort, 2003; Barber & Langdon, 2007; Charman, 2007; Charman et al., 2009). Warm and wet conditions favour peatland growth and C sequestration (Yu, 2011). Conversely, cold and dry periods limit peat growth and reduce C sequestration rates (Frolking et al., 2001).

Maxima C sequestration rates at Gordonbush are observed at ~7300, ~4800, ~3000, ~1300-1150 and 920-860 cal. yr. BP, respectively (Figure 7.4B) concomitant with maxima C sequestration in other studies. These higher C sequestration rates have been associated with reconstructed maxima in air temperature and annual precipitation rates at a global scale (Mayewski et al., 2004) but also specifically in Canada (Vitt et al., 2000; Frolking & Roulet, 2007), the UK and Ireland (Charman et al., 2006; Blundell et al., 2008) as well as studies of peat cores in Northern Scotland (Anderson, 1998; Anderson et al., 1998). The Holocene Thermal Maximum (HTM), between 9000-5000 cal. yr. BP in Northeast Canada (Kaufman et al., 2004), has been linked to maximum C sequestration (Mauquoy et al., 2008; Jones & Yu, 2010; Yu et al., 2010), which are recorded in GB2 (40-57 g C $m^{-2}$ $yr^{-1}$) between 5800-5000 cal. yr. BP (Figure 7.4B). A notable rise in C sequestration in the GB2 (cut) core from 3700-3500 cal. yr. BP (Figure 7.4B) is concurrent with similar rises in C sequestration rates attributed to an abrupt change to a much warm wetter climate in Scotland enhancing peat growth and reducing decomposition rates (Anderson, 1998; Anderson et al., 1998). A broad-scale cooling between 6800-6000 cal. yr. BP caused a decrease in C sequestration (Langdon et al., 2003; Yu, 2011) and this climatic effect is potentially reflected in both Gordonbush peat cores as C sequestration rates decrease from ~20 g C $m^{-2}$ $yr^{-1}$ to ~16 g C $m^{-2}$ $yr^{-1}$ in GB1 and GB2 (cut) during this time period. A decreasing C sequestration trend is apparent in both cores at this time (Figure 7.4B) despite accumulation rates being constant (Figure 7.4A).

#### 7.5.1.3 Are Gordonbush peat C sequestration rates similar to other sites?

Both the range and the long term average C sequestration rate calculated from Gordonbush peat cores are comparable to the global/regional range of values calculated for other northern hemisphere temperate regions during the Holocene (5 – 72 g C $m^{-2}$ $yr^{-1}$) (Table 7.6) (Gorham, 1991; Tolonen & Turunen, 1996; Vitt et al., 2000; Turunen et al., 2002; Turunen et al., 2004; Nilsson et al., 2008).

| C sequestration rates (g C $m^2$ $yr^{-1}$) | Research field site | Author(s) / Reference |
|---|---|---|
| | **Worldwide studies** | |
| 29 | Global average | (Gorham, 1991) |
| 5 – 40 (Average 18.6) | Northern Peatlands | (Yu et al., 2009; Yu, 2011) |
| | **Canada** | |
| 19.4 | Western Canada | (Vitt et al., 2000) |
| 19 ± 8 | 15 bogs across Canada | (Turunen et al., 2004) |
| ~20 | Mer Bleue, Canada | (Nigel T. Roulet et al., 2007) |
| 19 – 24 | Alberta, Canada | (Flanagan & Syed, 2011) |
| | **Northern Europe/ Boreal** | |
| 17.2 | Western Siberia, Russia | (Turunen et al., 2001) |
| 5 – 36 | Western Siberia, Russia | (Beilman et al., 2009) |
| 19 – 69 | Western Siberia, Russia | (Borren et al., 2004) |
| ~26 | Finnish average | (Tolonen & Turunen, 1996) |
| ~18.5 | Finnish Holocene avg. | (Turunen et al., 2002) |
| 14 – 72 | Store Mosse, S Sweden | (Belyea & Malmer, 2004) |
| 23 | Northern Sweden | (Nilsson et al., 2008) |
| | **Scotland** | |
| 10 – 36 | 3 bogs in W Ross, Scotland | (Anderson, 2002) |
| 10 – 60 (average = 20-25) | Gordonbush, NE Scotland | This study |

**Table 7.6 - C sequestration rates from various peat core studies**
Authors and a brief description of field site location along with C sequestration rates are documented above from a range of different studies.

### 7.5.1.4 Loch Brora core age-model

Due to the non-stratigraphic nature of $^{14}C$ results associated with the Loch Brora sediment core, this record cannot be regarded as a definitive estimate of C sequestration. This means that a comparison between peat and lake cores to assess potential 'sink-to-source' controls of C sequestration rates is not possible. It would have been preferable to analyse plant macrofossils for AMS $^{14}C$ dating (Nilsson et al., 2001), but this type of material was very sparse in the sediment cores.

Thus, from one basal age, the calculated long-term accumulation rates for AMS $^{14}C$ (0.16 cm $yr^{-1}$) and $^{210}Pb$ (0.22 cm $yr^{-1}$) age-models are similar, which supports the tentative age-depth model for Loch Brora. Average accumulation rates for last 150 years at Gordonbush are similar to results reported in Loch Coire Fionnarich (located in NW Scotland but also surrounded by peatland) (Kattel, 2009). Excluding this example, there is very little data available on sedimentation rates or basal ages (also relevant later on when comparing C sequestration rates) of other lakes within the vicinity of Loch Brora in NE Scotland for comparison. Sedimentation rates in Loch Brora are at the lower range of rates measured in an upland temperate catchment in Northern England (0.16-1.12 cm $yr^{-1}$) (Hatfield et al., 2008).

#### 7.5.1.5 What are the controls on lake C sequestration?

Notwithstanding the issues associated with the reliability of the Loch Brora chronology, the results do suggest that C sequestration is not constant over time (Figure 7.8B) and there is a degree of natural variability regardless of assumed uniform sedimentation rates. Similar to peat, lake C sequestration is controlled by hydrological and climatic conditions (Adrian et al., 2009). Therefore, changes in C sequestration rates observed throughout Loch Brora core are likely to be driven by changes in climate and will be dictated by local conditions. The locations of the Loch Brora core site was selected close to the mouth of the Allt Smeorail river so the sediment retrieved would be influenced by, and reflect, the nature of sedimentation sourced from the peatlands of Gordonbush estate. However, Loch Brora drains over 90 % of the River Brora catchment, (approx. 400 $km^2$) therefore its sediments are also influenced by landscape C inputs and outputs from a far larger area (Kortelainen et al., 2013; Anderson et al., 2014). Various land-uses (and anthropogenic impacts) will all influence C sequestration rates within Loch Brora but unfortunately are out of the scope of this research.

Physical controls including oxic conditions on the lake bed and lake morphometry also influence C sequestration. Whether the bottom waters of Loch Brora are aerobic (leading to mineralisation of C and reduced sequestration) or anaerobic (conversely promotes C sequestration) environment will affect C burial efficiency (Jansson et al., 2000; Hanson et al., 2004; Sobek et al., 2009; Einola et al., 2011; Sobek et al., 2011; Gudasz et al., 2012; Fenner & Freeman, 2013). Small deep lakes are more efficient at sequestrating C than large flat ones (Hanson et al., 2011; Ferland et al., 2012; Kortelainen et al., 2013; Ferland et al., 2014). Loch Brora, being relatively shallow with a mean depth of 6.9 m and a surface area of 2.3 $km^2$, falls into the large flat category and a relatively low C burial efficiency rate should be expected.

#### 7.5.1.6 Are Loch Brora C sequestration rates comparable to other sites?

The calculated long-term average C sequestration rate for Loch Brora (61.8 g C $m^{-2}$ $yr^{-1}$) falls broadly within range of other studies (Table 7.7), but this is considerably higher than average global lake C sequestration rates of 10-15 g C $m^{-2}$ $yr^{-1}$ (Mulholland & Elwood, 1982; Tranvik et al., 2009). Some of the studies presented are from boreal-forested regions where allochthonous sediment delivery processes are likely to be driving C accumulation (Gudasz et al., 2012). Additionally, higher C sequestration rates have been associated with anthropogenic activities including intensive agricultural (Van Oost et al., 2007; Quinton et al., 2010) and forest-felling (Houghton, 2005) rather than being driven from the nature of their surrounding landscapes.

| C sequestration rates (g C $m^{-2}$ $yr^{-1}$) | Research field site | Author (s) / References |
|---|---|---|
| | **Worldwide sites** | |
| 5 – 14 | Global review | (Tranvik et al., 2009) |
| up to 70 | N Hemisphere (temperate) | (Dean & Gorham, 1998) |
| 19 – 24 | Global boreal lakes | Molot & Dillon (1996) |
| 10 – 15 | Global review | (Mulholland & Elwood, 1982) |
| 5 – 55 | Northern temperate lakes | (Hanson et al., 2014) |
| | **North America** | |
| 1 – 10 (11 lakes) | Quebec, Canada | (Ferland et al., 2014) |
| 9 – 31 | Wisconsin & Michigan, USA (boreal lakes) | (Buffam et al., 2011) |
| 39 – 162 (7 lakes) | Midwestern USA (glacial lakes) | (Heathcote & Downing, 2012) |
| 3 – 184 (116 lakes) modern day avg. = 39 | Minnesota, USA (boreal forests to prairies) | (Anderson et al., 2013) |
| | **Northern Europe** | |
| <5 | Boreal lakes, Finland | (Kortelainen et al., 2004) |
| 22 – 82 (mean = 61.8) | Gordonbush, NE Scotland | This study |

**Table 7.7 - C sequestration rates in various lake core studies**
Authors and brief description of field site location along with C sequestration rates are documented above from a range of different studies.

Lake C sequestration rates are more variable and approx. three times larger than rates calculated for Gordonbush peats (Loch Brora = 61.8 g C $m^{-2}$ $yr^{-1}$ and GB1 = 20.7 g C $m^{-2}$ $yr^{-1}$) and similarly the long-term sediment accumulation rates are five times larger in the lake than the peat (Loch Brora = 0.16 $cm^{-2}$ $yr^{-1}$ and GB1 = 0.033 $cm^{-2}$ $yr^{-1}$). This is not surprising given the difference in catchment scale (Loch Brora ~400 $km^2$, Gordonbush peatlands <30 $km^2$), and the likely increased magnitude of sediment and C inputs to the lake. Again, the uncertainty associated with the Loch Brora chronology limits a more detailed interpretation.

### 7.5.2 What is controlling POM and POC delivery from peat to lake systems?

The greatest sediment flux to Loch Brora is synchronous with storm events (Figure 7.9D) suggesting a strong hydrological control on sediment delivery to the lake. Furthermore, during large storm events there are elevated [POC] (Chapter 5, see POC time series section 5.4.1.2). There is no seasonal pattern in [POC] in the sediment traps, which suggests no strong biological control on sediment delivery to the lake. This is not surprising, as higher river discharges are capable of transporting larger sediment loads and bigger-sized particles (Webb et al., 1997) and grain size increases with mass flux support this inference (Figure 7.11A). Annual sedimentary fluxes are largest at both monitoring sites in 2013-2014 (Table 7.5). Three of the five largest storm events recorded throughout the full research period occurred between September 2013 and September

2014. Conversely, the lowest annual mass flux estimations were made in 2011-2012, when there was only one recorded storm event in GB11 where maximum stage height was >1.5 m. This reinforces that discharge is a primary control on sediment flux at Gordonbush. If so, it is possible that one or two of the largest storm events are responsible for the majority of annual sediment transport from the rivers to the loch. Similar conclusions have been made about sediment delivery in other study (Marttila & Klove, 2010).

Clearly, there is intra-lake variability of sediment fluxes, indicated by differences in results between the two sediment trap sampling points. This might relate to the different sizes of GB11 and GB12 catchments. GB11 is larger and therefore has more abundant potential sources of material available for transport than GB12. However, given the relative inter-annual variation in annual mass fluxes (Table 7.5), the calculated totals suggest GB11 (Allt Smeorail) catchment has more areas susceptible to erosion and transport of particulate material during the largest storm events, compared to GB12. The fact such a clear relationship between mass flux and grain size as well mass flux and % C are not seen in GB12 (Figure 7.11B&D) compared to GB11 (Figure 7.11A&C) supports this explanation. Despite these differences, the influence of the River Brora and the quantity of sediment it contributes to calculated sedimentary flux totals is currently unknown, but cannot be ignored. The shape of Loch Brora and the relatively-sheltered position of the sediment trap sampling point at GB12 mean that it was less influenced by water and sediment through-flow associated with River Brora compared to GB11.

The estimation that approximately only 8 % of C entering the lake at GB11 is being sequestered on a long-term basis is comparable with a study of five Finnish lakes where average burial rates were ~14 % (Einola et al., 2011). In boreal lakes in Quebec burial rates were highly variable, between 4 – 62 %, where C sedimentary fluxes were measured between 10-50 g C $m^{-2}$ $yr^{-1}$ but long term average C sequestration rates were 1 – 10 g C $m^{-2}$ $yr^{-1}$ (Ferland et al., 2014). No additional data was collected to comment on the fate of the remaining ~92 % of sedimentary C deposited, but assuming it did not accumulate in the sediments it has to have been either mineralized and degassed to atmosphere or simply transported to the ocean (8 miles further downstream) unaltered (Hanson et al., 2011; Ferland et al., 2014). Both of these processes are sensitive to changes in environmental conditions including oxygen exposure time of sediments (Sobek et al., 2009; Sobek et al., 2011) and hydrologic residence times (Hanson et al., 2014).

Unfortunately, there are few similar studies using sediment traps to compare and further contextualise Gordonbush results in terms of intra-lake variability or whether the annual sediment and C fluxes I have measured are typical or not.

### 7.5.3 Can an impact of windfarm construction be detected from sedimentary information collected?

Peat C sequestration rates are variable over time, most likely due to long-term climatic changes. Some of these are associated with changes in surface wetness and precipitation (Charman et al., 2006), therefore windfarm activities that require peat to be drained and water tables lowered will likely have an impact on C sequestration in those areas. Since peat accumulates so slowly, rather than using $^{210}$Pb, peat accumulation rates could be better gauged by the use of crank wires outlined by Clymo (1970) and utilised in other studies, e.g. Waddington et al. (2003).

Aquatic organic C fluxes (8-25 g C $m^{-2}$ $yr^{-1}$) and peat C sequestration (long-term average 20-25 g C $m^{-2}$ $yr^{-1}$) rates from Gordonbush catchments have been estimated. However, to contextualise these results within the complete C cycle of Gordonbush's ecosystem, and to assess whether Gordonbush is a sink or source of C, estimates of net ecosystem exchange (NEE) are needed. NEE represents organic C available for storage within the system or loss from it by export or non-biological oxidation (Lovett et al., 2006) but it has not been measured at Gordonbush during this research. The combined aquatic and peat sequestration C fluxes represent the minimum NEE value needed for Gordonbush to remain a C 'sink', approx. -30-50 g C $m^{-2}$ $yr^{-1}$. Data presented (Table 7.8) shows that values in this range have been measured at other northern temperate peatland sites. If NEE assessment were undertaken at Gordonbush, a better assessment of windfarm impact could be made in relation to peat and lake C sequestration rates.

| NEE (g C $m^{-2}$ $yr^{-1}$) | Research field site & peatland type | Author(s) / Reference |
|---|---|---|
| | **North America** | |
| -40.2 ± 40.5 | Ontario, Canada (Ombrotrophic) | (Roulet et al., 2007) |
| -10 to -76 | Ontario, Canada (Ombrotrophic) | (Lafleur et al., 2003) |
| -144 | Alberta, Canada (Minerotrophic) | (Syed et al., 2006) |
| -189 ± 47 | Alberta, Canada (Minerotrophic) | (Flanagan & Syed, 2011) |
| -69 ± 33 | Wisconsin & Michigan, USA (Mixed) | (Buffam et al., 2011) |
| | **Europe** | |
| 0 to -60 | Europe wide (Mixed) | (Janssens et al., 2005) |
| 5.1 ± 28 | S Sweden (Ombrotrophic) | (Lund et al., 2012) |
| -48 to -61 | Sweden (Minerotrophic) | (Sagerfors et al., 2008) |
| | **UK & Ireland** | |
| -40 to -70 | UK wide (Mixed) | (Cannell et al., 1993) |
| -28 to -120 | 4 sites across UK (Mixed) | (Billett et al., 2010) |
| -74.2 ± 21.9 | Central Scotland (Ombrotrophic) | (Dinsmore et al., 2013) |
| -13 to -84 | Ireland (Ombrotrophic) | (Koehler et al., 2011) |

**Table 7.8 – Calculated NEE rates from other northern temperate peatland sites**
'Mixed' implies a combination ombrotrophic and minerotrophic peatland sites were studied

Sediment trap data shows greater sedimentary and C export in higher flows so it is not unreasonable to expect both to increase in wetter hydrological years. Other anthropogenic activities (mostly agriculture) have resulted in catchment disturbance and increases in macronutrient and sediment export (Smith et al., 1999; Houghton, 2005; Mattsson et al., 2005; Van Oost et al., 2007; Quinton et al., 2010; Anderson et al., 2014; Pacheco et al., 2014). As such, the Gordonbush windfarm development could be responsible for the large differences between GB11 and GB12 in annual mass sedimentary fluxes per unit catchment. Previously, increases in sedimentary export have been directly attributed to windfarm construction in Scotland, e.g. Braes of Doune (Grieve & Gilvear, 2008). However, at Gordonbush the time scale of observation is too short to be certain that this is a windfarm-induced difference and not site-specific differences that would be maintained in time as a function of sediment trap position within the loch (although sited in an area considered likely dominated by river in flow). Also catchment differences are important. GB11 and GB12 are not matched catchments and differ in size, peat coverage and thus likely erosion susceptibility. Thus direct comparisons between the two must be recognised to have some limitations.

When Loch Brora core and sediment trap data are compared, there is an indication Loch Brora is not a strong sink for C losses from the peatland. Once C is lost from the peatland it will most likely to be mineralised to $CO_2$ or transported further downstream to the ocean (Hanson et al., 2011). Therefore, if the windfarm construction did cause of some of the differences between sediment trap data from GB11 and GB12, evidence suggests that Loch Brora would not necessarily act as a strong C 'sink' of windfarm induced C losses. In a similar physical landscape design, and a lake with higher organic C burial could be an advantage in planning windfarm design.

## 7.6 Summary of C sequestration and sedimentary export

Peat records at Gordonbush have comparable basal ages (~9000 cal. yr. BP), calculated C sequestration rate ranges (10-58 g C $m^{-2}$ $yr^{-1}$) as well as long term average C sequestration rates (20.8 and 24.4 g C $m^{-2}$ $yr^{-1}$) to other sites in Northern Hemisphere. Due to the non-sequential nature of radiocarbon results a robust age-model could not be constructed for the Loch Brora sediment core therefore the calculated range C sequestration rates of 22-82 g C $m^{-2}$ $yr^{-1}$, and long term average of 61.8 g C $m^{-2}$ $yr^{-1}$, are acknowledged as not being definitive estimates and must be treated cautiously. Unfortunately similar studies are rare in NE Scotland so local contextualisation of these estimates is not possible. C sequestration histories of peat and lake cores are naturally variable over time and the main controls on this are most likely climatic. Periods of maxima C sequestration observed in other peat cores associated with known climatic

events were also found in Gordonbush peat cores, e.g. high C sequestration rates observed between 5800-5000 cal. yr. BP could be related to HTM (Yu et al., 2010); increased C sequestration rates between 3700-3500 cal. yr. BP are concurrent with results from other Scottish peat cores and have been related to a wetter and warmer climate during this period (Anderson et al., 1998); increases C sequestration between ~1500-1000 cal. yr. BP are induced by a wetter climate (Charman et al., 2006).

Maxima in mass sedimentary fluxes indicate discharge is a controlling factor of sediment delivery to Loch Brora and GB11 exports more C per unit are than GB12. Windfarm construction activities (including excavation of two on-site borrow pits) were prevalent in GB11 (Allt Smeorail) but more time is needed to assess if this difference is transient, coincident with the windfarm construction, or catchment-specific. This is an important future research need. Although C sequestration results from Loch Brora must be viewed cautiously, comparing the calculated values with rates of modern sediment delivery, it was estimated organic C burial efficiency was approx. 8 %, which is comparable to other studies (Einola et al., 2011; Ferland et al., 2014). The physical characteristics of Loch Brora suggest it should have low C sequestration efficiency rates and low potential for being a strong long-term terrestrial 'sink' of sedimentary C fluxes and any subsequent increases from Gordonbush peatland catchments in the future.

Anthropogenic disturbance may increase sediment and macro-nutrient export from uplands areas, but this signal was not strong, or even discernible at Gordonbush. There is now a longer term record for comparison if more construction activities are planned in order to extend the current size of the windfarm. Furthermore, studies that quantify the effect of anthropogenic disturbance within peats and lakes need to be widened from the currently limited examples that exist (Billett et al., 2010), e.g. focussing on whether constructing windfarms on peatlands in catchments with a lakes can be detected in lake sediment records.

# 8 Peatland restoration at Gordonbush

## 8.1 Abstract

In this chapter I consider how drain-blocking may affect water table and aquatic C concentrations. WTD recorded by PTs show a similar response to downstream river stage height, i.e. when it rains WTD rises and stage height increases, and during extended dry periods the opposite occurs. This suggests WTD at PT locations is controlled mainly by meteorological conditions (rainfall delivery and evapotranspiration) and drainage. Manual measurements in dip-wells indicate that drainage channels have the greatest influence on WTD between 0 – 2 metres from the drain, beyond which WTD remains more constant. No statistically significant difference was detected between mean WTD of dip-well data before and after blocking in relation to distance from individual drains or a comparison between drain and control data. Therefore, there is limited evidence to suggest that drain-blocking has had a positive effect on raising WTD over the first year. WTD PT time series data indicates, during the particularly dry summer of 2013, water table drawdown was greater and recovery longer in the drained area compared to the non-drained area, suggesting that the net effect of multiple parallel drains can cause water table drawdown at a significant distance (~25 m) from the drainage channel.

[DOC] in drains shows a seasonal pattern similar to those in peatland rivers, with late summer maxima and winter minima. The time series indicates that maximum [DOC] increased in the year proceeding blocking which has been noted in other studies, but this maximum was probably influenced by a long drought period in the year after blocking (2013) which was not apparent the year before. Although maximum [DOC] increased after blocking, there was no statistically significant difference between [DOC] collected up and downstream of drainage channel inputs for samples collected before and after blocking. This suggests drain-blocking has had little impact on the larger site [DOC] signature one year after drain-blocking. However, as discharge from drainage channels was not measured, a potential reduction in DOC export cannot be assessed.

## 8.2 Introduction

The latest updated Kyoto Protocol gives peatland restoration new legitimacy as a climate change mitigation activity (Bonn et al., 2014b), allowing such restoration to be a contributing activity in reducing a country's GHG emissions (Ramchunder et al., 2009). Also in the UK, other EU-wide policies (e.g. EU Habitat Directive and WFD) support improvements to peatland habitats (Holden et al., 2007b; Holden, 2008; Wilson et al., 2010; Bonn et al., 2014b). Restoration programmes are widespread across the UK,

(Armstrong et al., 2010) as a result of conservation bodies (e.g., IUCN) and local government organisations (e.g., SNH) advocating these natural habitats as providers of important ecosystems services (Bain et al., 2011; Evans et al., 2014). Some of these include climate regulation via C sequestration and storage, water regulation (helps prevent flooding), and peatlands represent palaeo-environmental archives and habitats for internationally important wildlife (Bonn et al., 2014a).

A common form of peatland restoration is drain-blocking (Holden, 2008; Armstrong et al., 2009; Evans et al., 2014). This started in the UK in 1980s to reverse trends of erosion and C losses by raising water tables and encouraging the establishment of peat-forming species e.g. *Sphagnum* (Peacock et al., 2013b). Actively blocking drains raises water tables (Worrall et al., 2007a; Armstrong et al., 2010; Wilson et al., 2011a) and can help reduce C losses from peatland through reduced DOC export. Additionally, drain-blocking helps prevent soil erosion and lessen POC export (Evans & Warburton, 2007; Holden et al., 2007a; Parry et al., 2014) as soils are able to better withstand periods of drought (Wilson et al., 2011b). Organic soils also possess a low capacity for nutrient (P & N) retention and are vulnerable to leaching losses (Otabbong et al., 2009). Permanently water-logged peatland, where aerobic decomposition is minimal, represents the best conditions for macronutrient (C, P & N) retention and minimising export (Kieckbusch & Schrautzer, 2007; Otabbong et al., 2009; Dunne et al., 2010). Ensuring that effective management practices are implemented, e.g. drain-blocking, contributes to restoring degraded peatlands from C sources back to C stores (Evans et al., 2014).

Furthermore, drain-blocking is seen as one solution to the problems caused by increasing [DOC] (Strack et al., 2011) which are faced by water companies sourcing drinking supplies from peatlands. Processes which aim to reduce the colour of DOC-rich water by chlorination can create potentially carcinogenic by-products (Turner et al., 2013; Martin-Ortega et al., 2014). This problem, although less pertinent in the Highlands of Scotland (due to public water resources being sourced from lochs and reservoirs), is a key peatland management issue in the rest of the UK as over 50 % of all utilised water supplies are sourced from peatland areas (Tang et al., 2013).

The majority of drains at Gordonbush were cut in 1950s and 1960s (Milne, 2010; Rowantree, 2013). Observations of other drainage systems in Caithness and Sutherland suggest that lack of restoration or mis-management can lead to extensive degradation and erosion of peatland sites (Wilkie & Mayhew, 2003). Therefore, a commitment was made at Gordonbush to implement a programme of drain-blocking to raise water table levels with the aim of promoting *Sphagnum* growth, increasing water-retaining potential and reducing C export from the peat. Reduced C export would support increased C

sequestration and so “offset C” lost during construction, thus reducing the windfarm payback time. Additionally these wetter areas were desirable to create a suitable habitat for birds (Douglas & Pearce-Higgins, 2014), such as the golden plover and dunlin, which may have been displaced by windfarm construction activities (SSER, 2009; Douglas et al., 2011).

There is also continual debate and controversy on the scale of impact regarding the drawdown of water tables and potentially a reduction in C sequestration rates in peat soils related to, and caused by, windfarm construction activities (particularly those involving excavation of large volumes of peat to install road networks and foundations for turbines bases). Unfortunately, it was not possible to design a monitoring programme to investigate these issues directly due to Gordonbush being a fully operational construction site during the research period. Thus it was decided to work in conjunction with the HMP at the drain-blocking site to investigate the impact of man-made drainage channels on the drawdown of water tables. Whilst the studied drainage channels are smaller than some subsurface structures in the windfarm, they still provide an analogue. In particular I was interested in comparing detailed water table records, placed at a reasonable distance from drainage channels, to see how far or if any impact could be detected.

The over-arching aim is this chapter is to assess if drain-blocking raised the water table and changed [DOC] in the drainage channels. The observation period was 3 years (June 2011 to September 2014), with studied drainage channels blocked in September 2012, one year after monitoring had began. More specifically this research aimed to:

1. Quantify the effect of artificial channel drainage on water table drawdown before and after drain-blocking, particularly considering lateral extent;

2. Investigate if there is any change in [DOC] in drains before and after blocking by direct comparison but also to investigate changes in [DOC] in rivers downstream of the drains to further assess if [DOC] had changed;

3. Compare Gordonbush with other sites where drains have been blocked to assess if the observed changes here are typical.

# 8.3 Methods

## 8.3.1 Water table depth and DOC data collection and handling

Chapter 3 details the methods for monitoring water table measurement (section 3.11), continuously and manually, and for DOC sampling and analysis. Multiple dip-wells and piezometers are required for reliable measurements of WTD across a site scale (Allott et al., 2009) so PTs and dip-wells were installed in June 2011 0.5, 1, 2, 5, 10 and 20 metres from each side of each studied drain (drain transect) and at 10 metre intervals in a non-drained area (control transect). One PT was installed in a drained and non-drained area in order to produce a detailed time series of water table dynamics (logging WTD every 1 hour) and ensure the manually measurements were broadly representative. These PTs were positioned to be as far as possible from the drains (distance ~ 25 m either side) in the middle of the drained area transect, and in the middle of the control transect. Installing more PTs was not possible due to financial constraints and so the distance of 25 m was chosen to avoid the localised draw-down of the water table near the drainage channel (Holden et al., 2006; Holden, 2008; Erwin, 2009; Holden et al., 2011). Data from PTs allowed assessment and informed understanding of the extent of the hydrological impact of drainage channels, such as those excavated during windfarm construction (Dawson & Smith, 2007; Grieve & Gilvear, 2008; Ostle et al., 2009; Ramchunder et al., 2009). Such understanding is critical for informing the calculation of the 'carbon payback time' (Nayak et al., 2008; Nayak et al., 2009). For ease, the maps of drains monitored and the associated control site are detailed here (Figure 8.1A&B).

The time series presented are from June 2011 to September 2014, but [DOC] was measured only during the core field season from August 2011 to September 2013. Unfortunately due to water ingress, the PT located in the Drain Transect stopped working in November 2013. Further, the control PT output between 29/11/12 and 20/2/13 suggested erratic and unrealistic changes in water table height. This problem was investigated by the manufactures of the PT (Waterra, In-Situ Inc. ®) and we decided to smooth the data set: a running average of the previous 24 hours of data was calculated, and this output is presented in Figure 8.10 for the affected period. Despite this the time series appears different for this time period to the drain WTD profile, when other periods are similar. Thus I assume greater uncertainty in data for this time period. Additionally, this data has not been included when descriptive statistics have been calculated (Table 8.5), frequency distributions have been plotted (Figure 8.11) or during correlation analysis of WTD at control PT site and stage height in Allt Smeorail (Figure 8.12 and Table 8.6). Appendix H details how data recorded by PTs was converted into a continuous WTD time series.

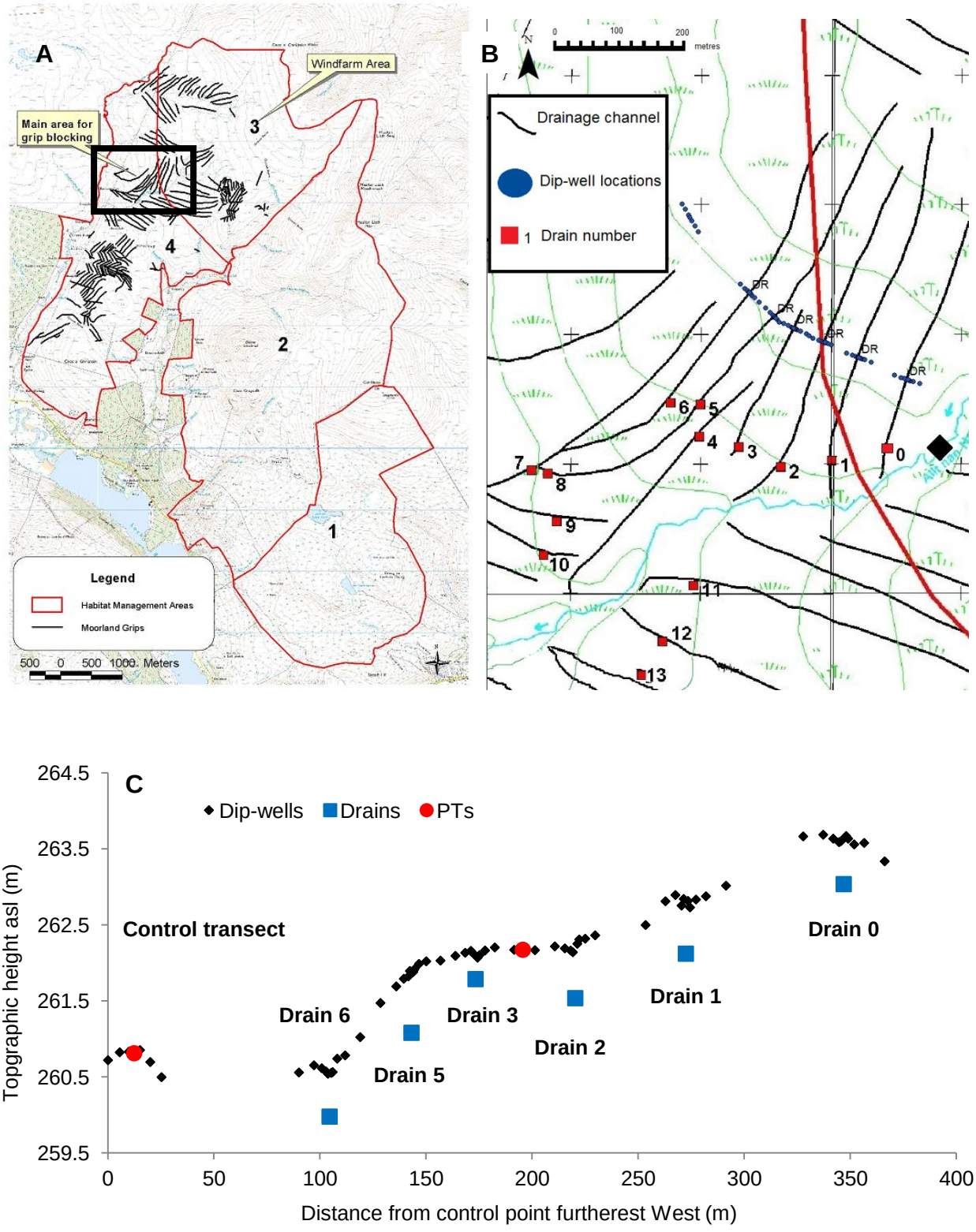


**Figure 8.1 - Maps of drain-blocking site and GPS points of installed dip-wells and PTs**
A = shows Gordonbush estate and marks locations of drains in black. B = a more detailed map of the area highlighted in black is presented. Blue dots (right Map) represent dip-well positions (adapted from Milne, 2010). The dots to the NW of the diagram represent the control site. Drains 0, 1, 2, 3, 5, and 6 all drain into Allt nan Nathraichen river (blue thin on map B); a tributary of Allt Mhuilin which was sampled upstream of where any of the drains drain into the river (marked by black diamond). C = a cross sectional view of drain-blocking transect. The position of installed dip-wells (black diamonds), PTs (red circles) and drains (blue squares) are plotted in a West-East transect, with distance from the most western installed dip-well in the control transect (x-axis) against topographic height (m) above sea level (asl) (y-axis). Sites were chosen to maintain topographic control between the drain and control transect whilst needing to measure water table perpendicular to the drain. The range in topographic height is only 3 m and slope above and below the profiles was comparable.

### 8.3.2 Blockage of the drainage channels

Various materials have been used to block drains: wooden boards, plywood, plastic sheeting, plastic piling, peat turves (blocks) and heather bales (Ramchunder et al., 2009). Slope, direction of water flow and dimensions of the drains will all influence what restoration method is most suitable to use (Crushell et al., 2009; Landry & Rochefort, 2012). Peat turves are ideally suited where the cross-sectional area of the channel is less than 0.7 $m^2$ and angles of drainage slopes are less than 3°; steeper than this and water simply flows around damming obstacles and back into the drains (Armstrong et al., 2009; Armstrong et al., 2010). This method was considered suitable for blocking Gordonbush drains and has been recommended as the best and most cost effective drain-blocking method (Armstrong et al., 2009). As is convention, peat turf material was sourced upstream of dam locations and suitably packed to create a robust seal. Also, escape routes were cut adjacent to dams so that water flows over the surrounding peat surface and not around the dam and back into the drains (Armstrong et al., 2009). Drains at Gordonbush were blocked in early September 2012.

### 8.3.3 Pooling of water around PT locations

During the research it became evident that water began pooling around PTs sites at both drain and control locations. Photographs taken on a routine monitoring visit on 29$^{th}$ November 2012 shows evidence of water pooling and that the problem was more severe at drain PT site than control (Figure 8.2).This may be caused by a compression of peat surface (Whittington & Price, 2006) in the area due to increased human activity involved with monitoring the sites and/or local deer being attracted to them (rubbing themselves or gnawing at them). This is being introduced here as it is believed to have influenced WTD data collected from PTs at both drained and non-drained (control) sites. Consequently, when WTD was being estimated from located logged at PT locations, the data implied the water table was above the surface by several cms for extended periods of time. Therefore, there is some uncertainty about the absolute values presented, but the trends in WTD are still representative.

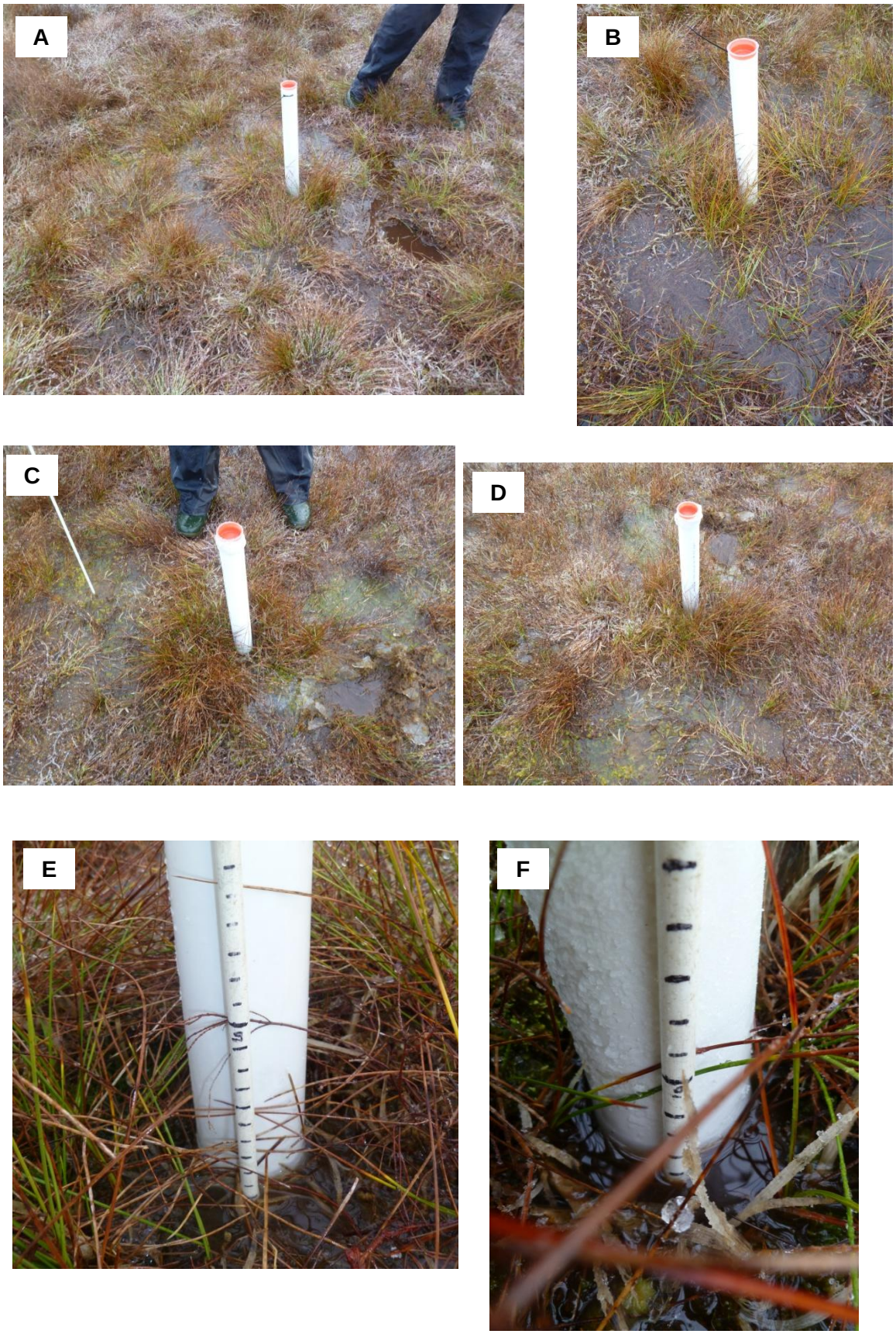


**Figure 8.2 - Photographs of water pooling around PT sites on 29th November 2012**
All photographs were taken by Ben Smith. A & B shows water pooling around drain PT site, C & D around the control PT. E (drain PT) & F (control PT) shows WTD ~10 cm and ~ 6 cm from peat surface respectively, indicating the water pooling appears more severe at drain PT compared to control PT in terms of measured WTD.

### 8.3.4 Statistical analysis

A linear modelling programme in R ('lm' command) was used to infer if any statistical differences were apparent between manual WTD measurements (as a function of stage height), collected from dip-wells positioned various distances from the drains, before and after blocking. Additionally, differences between data collected from drain transect and the control sites were studied to infer any statistically significant differences before and after blocking. The concept being considered was if drain-blocking had no effect there should not be a statistically significance difference between data collected before and after drain-blocking techniques had been installed. A similar analysis has previously been used in a before-after-control-impact (BACI) type study by Malloy & Price (2014).

Linear regression and correlation were utilised to test if the relationship between WTD, at sites where control and drain PTs were located, and stage height response (used as a proxy in the absence of rainfall data being collected) in the Allt Smeorail (sampling point GB6) differed before and after blocking. Similar to WTD dip-well data, if blocking had no effect it would be expected relationships between control PT and drain PT sites would remain unchanged and/or show the same differences of WTD response with stage throughout the study period. Paired t-tests were used to help assess the magnitude of change in [DOC] from drains before and after blocking. Additionally, frequency distributions (used in a similar study in Shantz & Price (2006)) and box-plot diagrams have been utilised to illustrate aspects of descriptive statistics associated with data collected from the drain-blocking study undertaken at Gordonbush.

## 8.4 Results

### 8.4.1 Visual responses of effect of drain-blocking

Photographs are presented of drainage channels at Gordonbush drain-blocking study site before and after blocking in September 2012 had taken place (Figure 8.3) as well as examples of water pooling behind peat turves (Figure 8.4).

Quantitative vegetation monitoring was not undertaken during the drain-blocking monitoring period. However, the observed increase of *Sphagnum* infilling of drains after drain-blocking (Figure 8.4) signifies slower flow and so water must be more effectively being stored (trapped) in drainage channels to allow such colonisation – most *Sphagnum* species prefer water-logged conditions (Quinty & Rochefort, 2003). In addition, increased surface vegetation growth in turn will slow water flow via drainage channels due to increased roughness and help reduce overall water export.

**BEFORE Drain-blocking** **AFTER Drain-blocking**

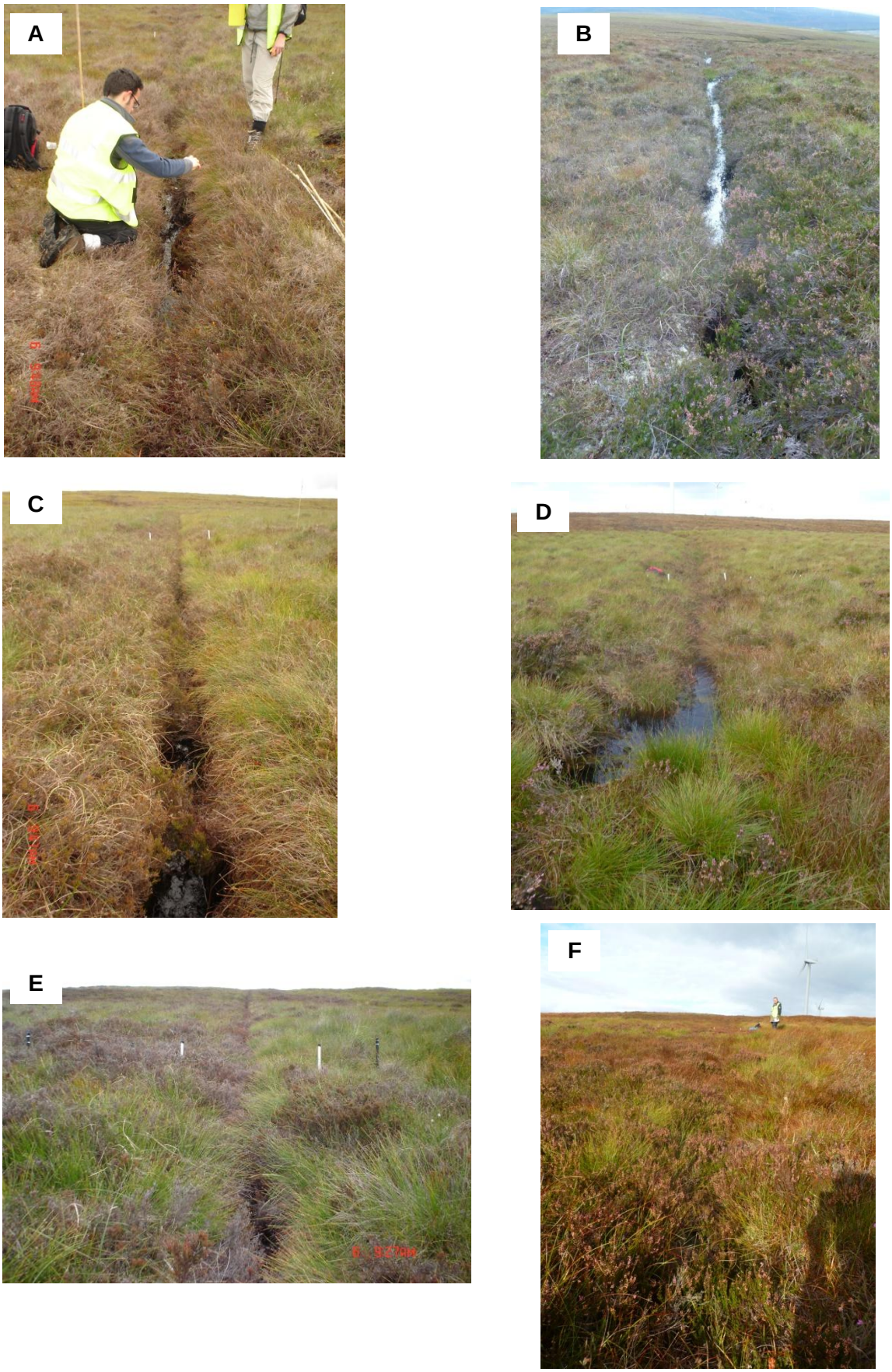


**Figure 8.3 - Pictures of ditches at Gordonbush before and after drain-blocking**
A, C, E (LHS) show drains 3, 5 and 6 respectively on 6/8/11, one year before drain blocking had been initiated. Photographs B, D, F (RHS) show the same drains on 24/9/14, two years after blocking had been completed in September 2012. More water is present after blocking. Also, due to infilling of the ditch by newly-established vegetation the outline of the drain is less clear than earlier (compare F to E).

**Examples of *Sphagnum* growth and water pooling behind peat turves after blocking**

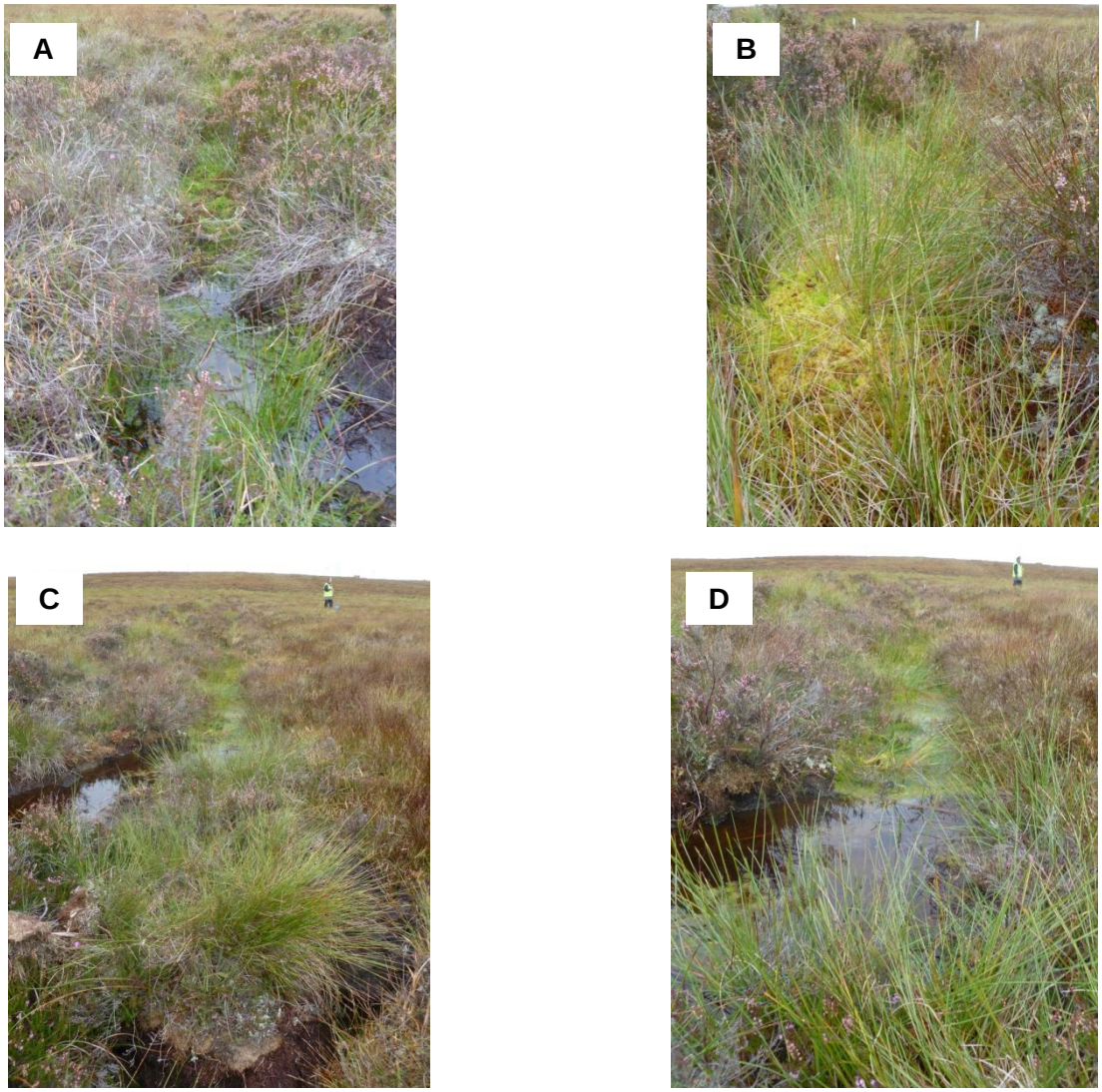


**Examples of drain-blocking using peat turves**

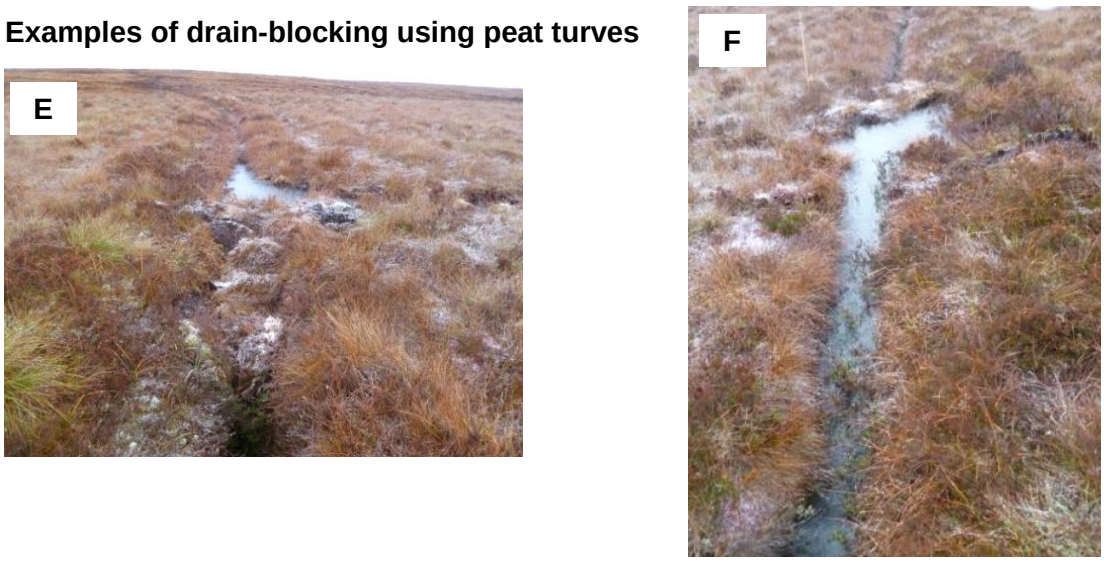


**Figure 8.4 - Examples of *Sphagnum* growth, water pooling and peat turve drain-blocking**
A & B = show *Sphagnum* becoming re-established in drains. C & D = show increased water pooling behind peat turves and subsequently more *Sphagnum* due more water-logged conditions. Photographs A-D were taken in Sept. 2014. Photographs E & F were taken in November 2012.

## 8.4.2 Water table depth in drain and control transect dip-wells

Water table depths were manually measured on 23 separate occasions from installed dip-wells, 13 times before drain-blocking (using peat turves) was undertaken in early September 2012 (June 2011 to August 2012), and monitored 10 times afterwards (September 2012 to September 2013 and one additional date in September 2014).

### 8.4.2.1 Temporal variation in water table depths

The range of manually recorded WTDs in all dip-wells was -52.5 cm to +13.5 cm (drain 0 had biggest range of individual transects, -48.5 cm to +13.5 cm, a range of 62 cm across the monitored area). A summary table of descriptive statistics for all (both before and after blocking, Aug. 2011 – Sept. 2014) WTD data collected from dip-wells (Table 8.1) and related box-plots (Figure 8.5) are presented for each drain and the control transect.

| Site | n | Min. | Max. | Mean | SE Mean | SD | Median (Q2) | Q1 | Q3 |
|---|---|---|---|---|---|---|---|---|---|
| Control | 161 | -40.0 | 9.0 | -2.1 | 0.6 | 7.8 | 0.0 | 3.5 | 2.3 |
| Drain 6 | 270 | -52.5 | 7.0 | -7.7 | 0.6 | 10.3 | -5.0 | -11.6 | -0.5 |
| Drain 5 | 270 | -42.5 | 4.5 | -7.5 | 0.5 | 8.8 | -5.0 | -10.6 | -1.0 |
| Drain 3 | 247 | -38.0 | 10.0 | -2.6 | 0.4 | 6.4 | -1.5 | -5.0 | 1.5 |
| Drain 2 | 270 | -37.5 | 7.0 | -4.5 | 0.5 | 8.4 | -1.5 | -8.6 | 1.0 |
| Drain 1 | 270 | -46.0 | 9.5 | -3.1 | 0.6 | 9.3 | -1.0 | -6.1 | 2.6 |
| Drain 0 | 270 | -48.5 | 13.5 | -4.2 | 0.6 | 9.3 | -2.0 | -8.0 | 1.0 |

**Table 8.1 - Summary of descriptive statistics for manual WTD measured from dip-wells**
Data from all 6 drain transects and the control transect is presented, n = number of individual WTD measurements, Min. = minimum, Max. = maximum, SE Mean = standard error of the mean, Q1 = 1st / lower / 25th percentile quartile, Q3 = 3rd / upper. 75th quartile. The units for all data are cm.

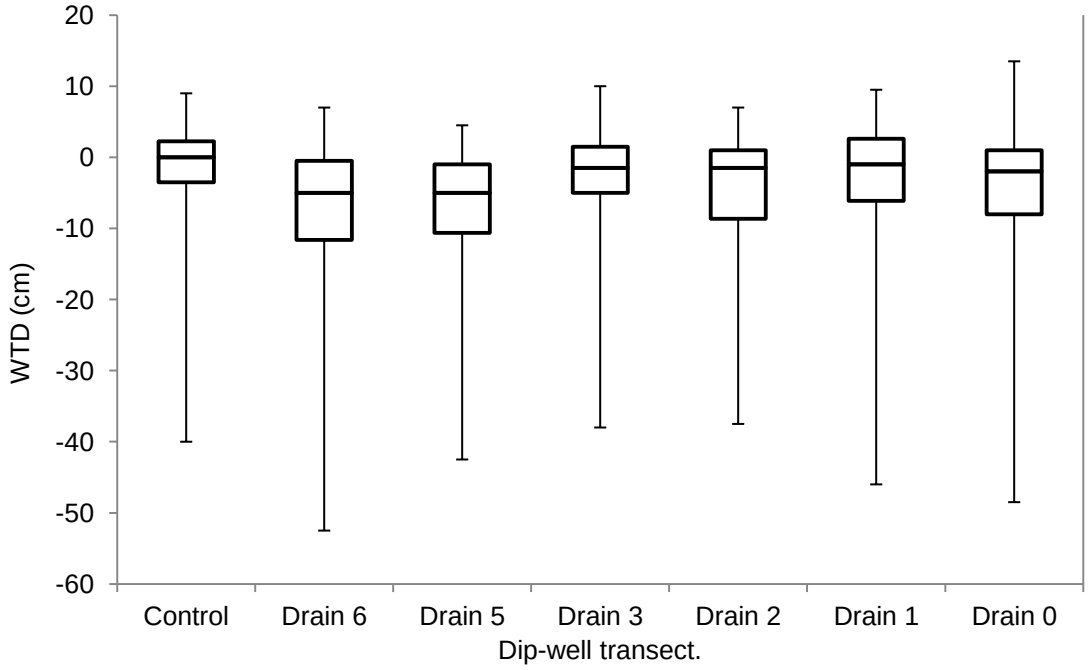


**Figure 8.5 - Box-plots of minimum and maximum WTD data collected from dip-wells**
Box-plots show median (line within the box), Q1 (the lower box outline), Q3 (the upper box outline) as well as minimum and maximum values (the error bars/whiskers).

Mean values from all drain transects and control transect are negative, ranging from -2 to -8 cm, the highest observed in the control transect and lowest in Drain 6 and 5 transect. Median for all drains transects are negative, the only positive median was recorded at the control transect and the same trend is observed for Q1 values. Drains 0 to 6 can be considered replicates of each other and although variation can be observed between them, it is small and generally box-plots of data collected from each site show similar trends.

The dates when the minimum and maximum WTD was observed in dip-wells located at each drain and control transect are presented in Table 8.2.

| Drain No. / Control | Min. WTD (cm) | Date & Position | Max. WTD (cm) | Date & Position |
|---|---|---|---|---|
| Control | -40.0 | 5/8/2013 @ 50 m | 7.0 | 9/1/13 @ 20 m |
| 6 | -52.5 | 5/8/2013 @ 5 m E | 7.0 | 9/1/13 @ 10 m E |
| 5 | -42.5 | 5/8/2013 @ 1 m E | 4.5 | 9/1/13 @ 20 m E |
| 3 | -38.0 | 5/8/2013 @ 10 m E | 10.0 | 29/11/12 @ 10 m W |
| 2 | -37.5 | 5/8/2013 @ 1 m E | 7.0 | 9/1/13 @ 20 m E |
| 1 | -46.0 | 5/8/2013 @ 1 m E | 9.5 | 9/1/13 @ 2 m W |
| 0 | -48.5 | 5/8/2013 @ 0.5 m E | 13.5 | 9/1/13 @ 20 m E |

**Table 8.2 - Maxima and Minima WTDs manually recorded in dip-wells across all transects**
The data is presented as control and then drain 6-0 to represent the sequence of dip-well transects west to east across drain-blocking site, matching how the sites are represented in cross-section (Figure 8.1).

In four of the six drain dip-well transects (Drain no. 5, 2, 1 and 0) the minima WTDs are located closest to the drainage channel at either 0.5 or 1 m. Maximum WTDs were recorded at 5 m from the drainage channel along Drain 6 transect and at 10 m along Drain 3. The minima WTD recorded in dip-wells occurred on 5/8/13 across all transects and coincided with a period between May-September 2013 when river levels were constantly low (Figure 8.10). Maxima WTD in dip-wells occurred in five of the six drain transects at either 10 or 20 metres, the furthest two dip-well locations from the drainage channel. The one exception was Drain 1 where maxima WTD of +9.5 cm was recorded 2 m from the main drain channel. All maxima WTDs occurred during winter months. Except for Drain 3 transect, maxima WTD in dip-wells occurred on 9/1/13 after a period of multiple storm events occurring in the previous month.

### 8.4.2.2 Spatial variation in water table depth across transects

The spatial variation in WTDs across drain and control transects was examined by plotting a frequency distribution (Figure 8.6) as well the means of all WTDs recorded before (pre) and after (post) blocking, between June 2011 and September 2013, at each dip-well location (Figure 8.7).

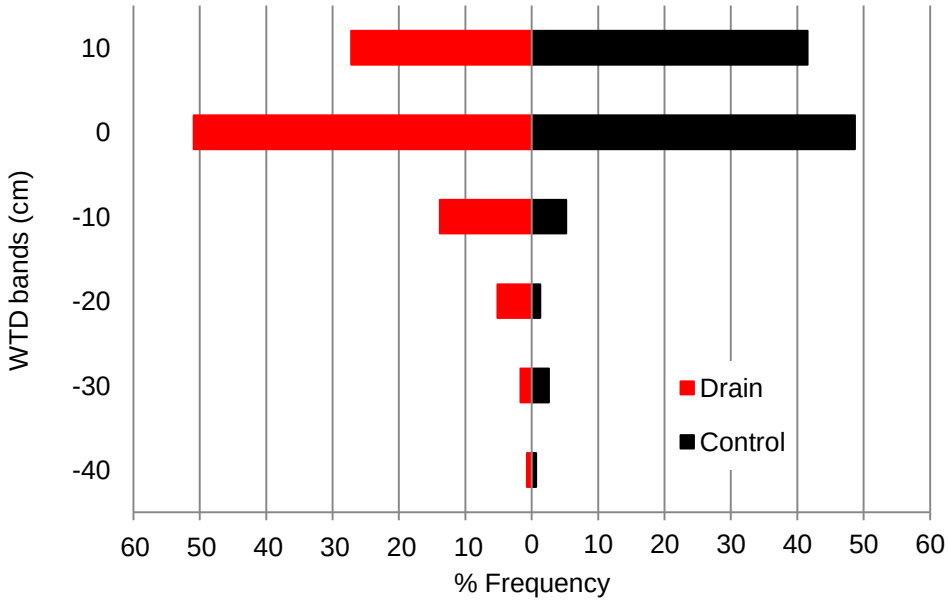


**Figure 8.6 - Frequency distribution of WTD dip-well data**
The above diagram illustrates the frequency (%) of particular WTD measurements in bands of 10 cm from -40 to +10 cm (y-axis), however the -40 band = WTD measured between <50 and -40 cm, -30 band = WTD measured between <40 and -30 cm, etc. Only WTD measurements which had a frequency of >0.5 % are presented. The drain data is pooled (n = 1526) and the control was the single transect (n = 154).

The majority of WTD measurements in dip-wells were recorded between -10 and +10 cm in both control and drain transects. Over 90 % of WTD observations in the control transects were recorded in this range whereas it was 80 % in the drain transects. Only 5 % all of WTD observations in the control transects were recorded between -10 and -20 cm, whereas in drain transects the figure was almost three times as much, at just under 15 %. Recorded WTD below -40 cm had the smallest frequency in dip-wells at both control and drain transects of 1 %.

Mean results for each numbered drain and control transect are presented in Figure 8.7A-G along with a graph plotting the mean of all means in Figure 8.7H. Data in the plots below have been topographically corrected for WTD. Similar graphs which have been normalised for topography (similar to mean of all means plot) are presented in Appendix I.

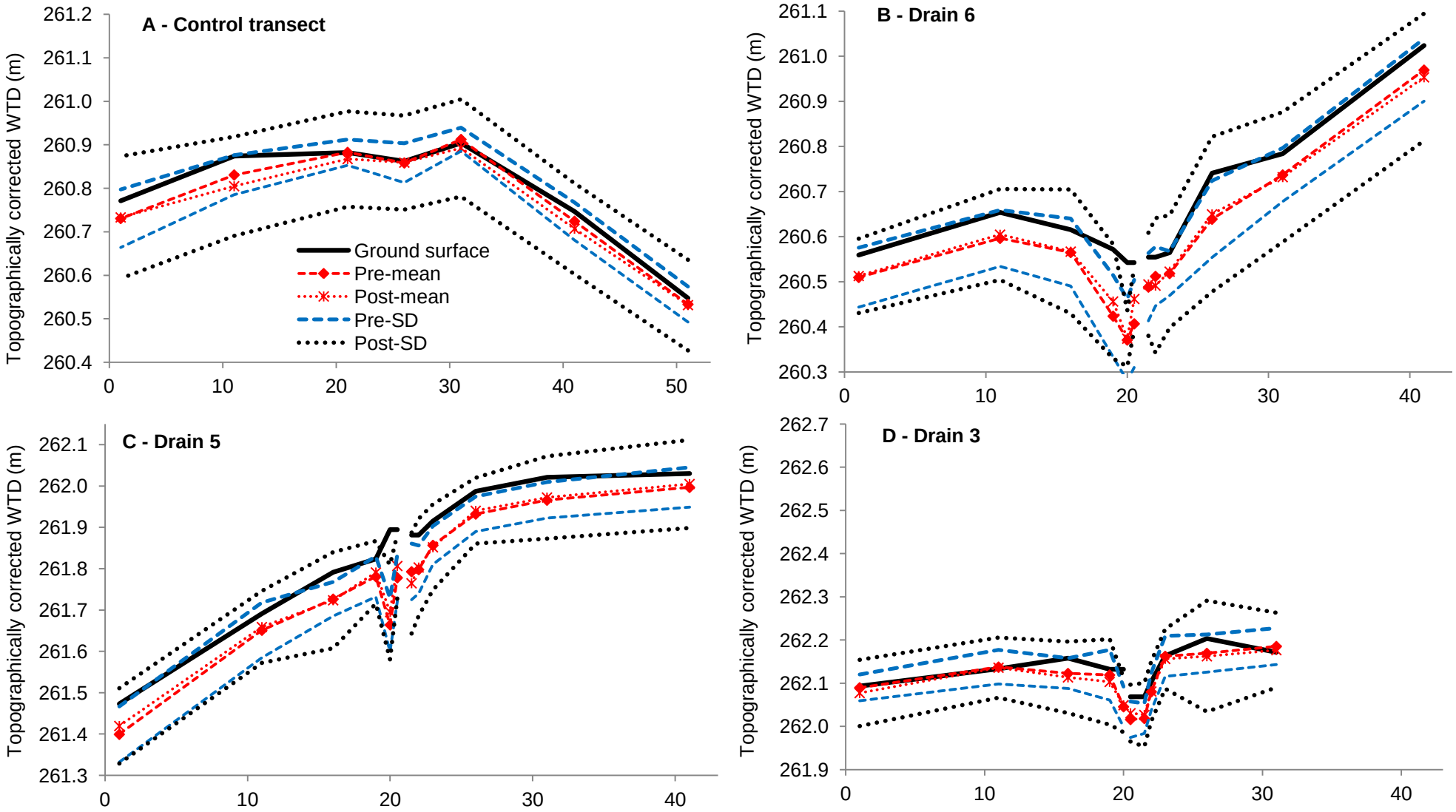


**Figure 8.7 - Water table depth for control dip-well transect, drain 1-6 and means of all drains, a W-E transect**
Mean WTD, of 23 manual measurements between Jun. 2011 and Sept. 2014, are presented in red, with red diamonds and red asterisks measurements before (n = 14) and after drain-blocking (n = 9) respectively. The thick solid black line represents the ground surface with WTDs presented relative to this. The blue (pre-blocking) and black (post-blocking) dashed lines represent standard deviations (SD) of the mean WTD. For comparison between drains, the y-axis is over the same range of 0.8 m. The dip-wells are drawn to scale: 0.5, 1, 2, 10, and 20 metres from each side of the drain, and the gap is the drain. The names of each drain and corresponding letter A – H are displayed in top left hand corner of individual plots. Plots E – H are on next page. The layout of the graphs is the same order they are presented in Figure 8.1C showing the topographic heights of all drains and dip-wells. The legend is only present on graph A. In graph H, the y = 0 line represents the peat surface from which WTD was calculated from.

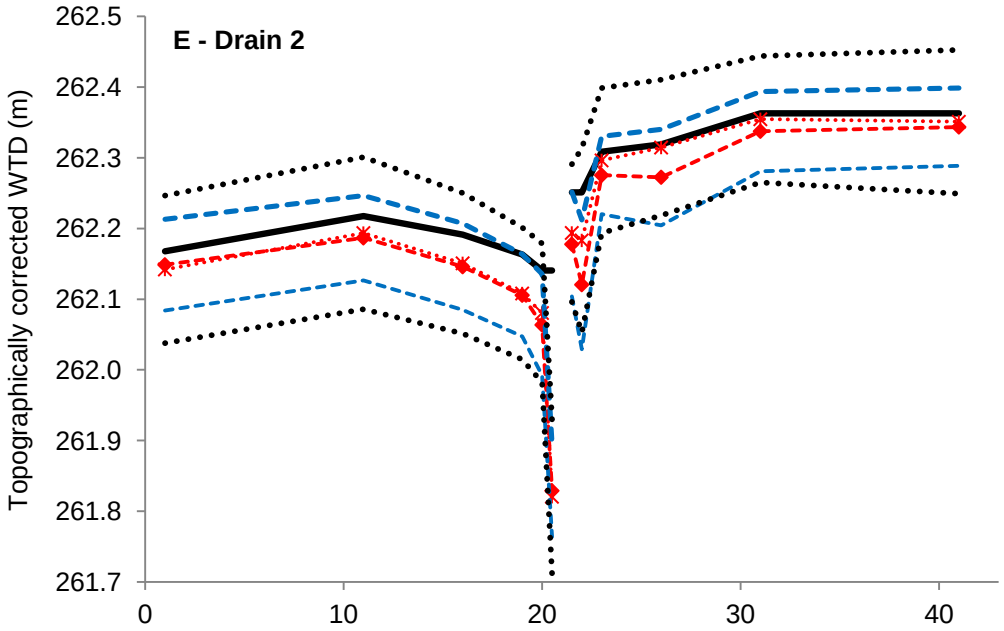
E - Drain 2
Topographically corrected WTD (m)
262.5
262.4
262.3
262.2
262.1
262.0
261.9
261.8
261.7
0
10
20
30
40

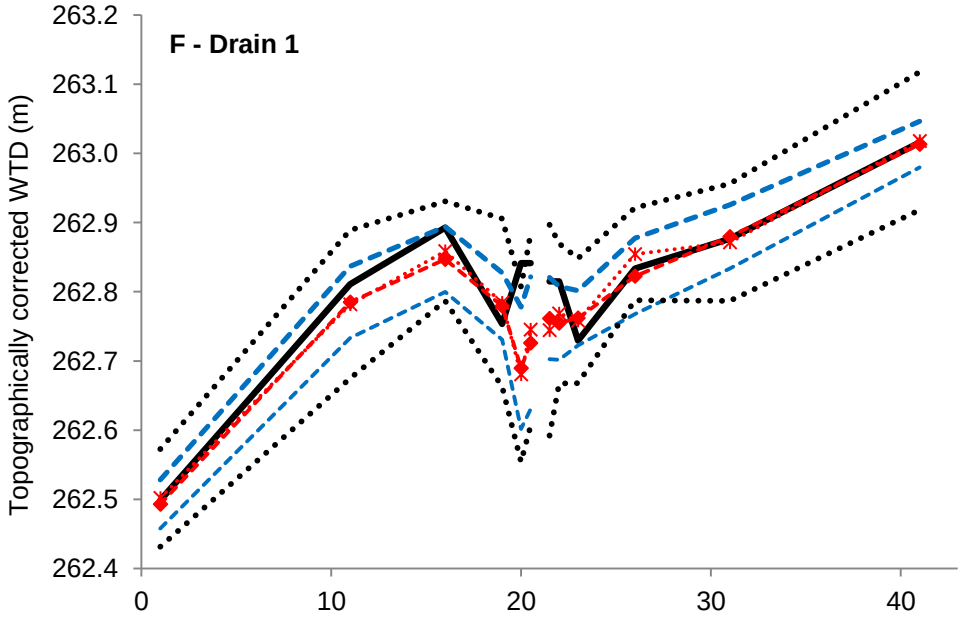
F - Drain 1
Topographically corrected WTD (m)
263.2
263.1
263.0
262.9
262.8
262.7
262.6
262.5
262.4
0
10
20
30
40

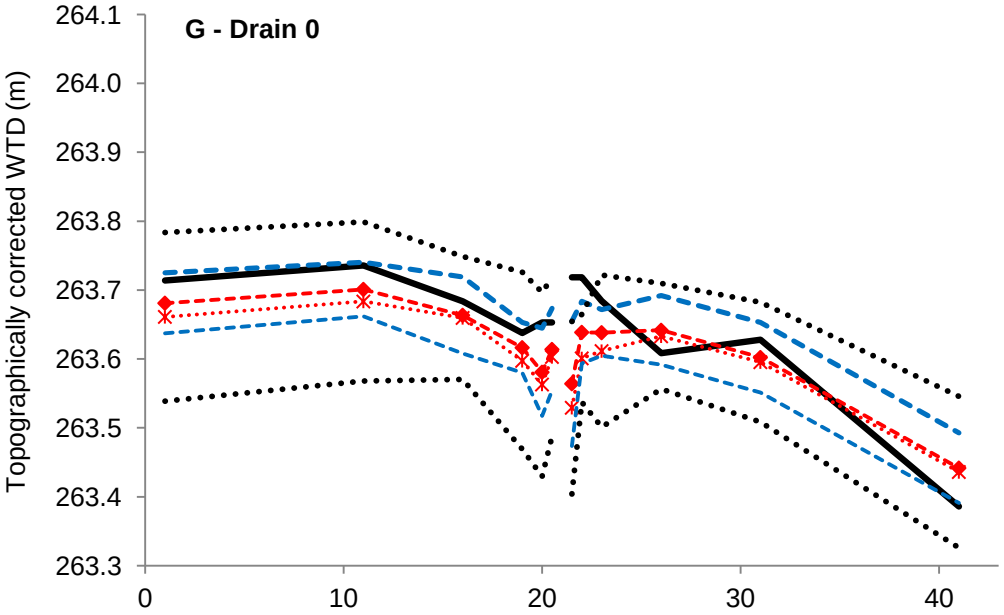
G - Drain 0
Topographically corrected WTD (m)
264.1
264.0
263.9
263.8
263.7
263.6
263.5
263.4
263.3
0
10
20
30
40

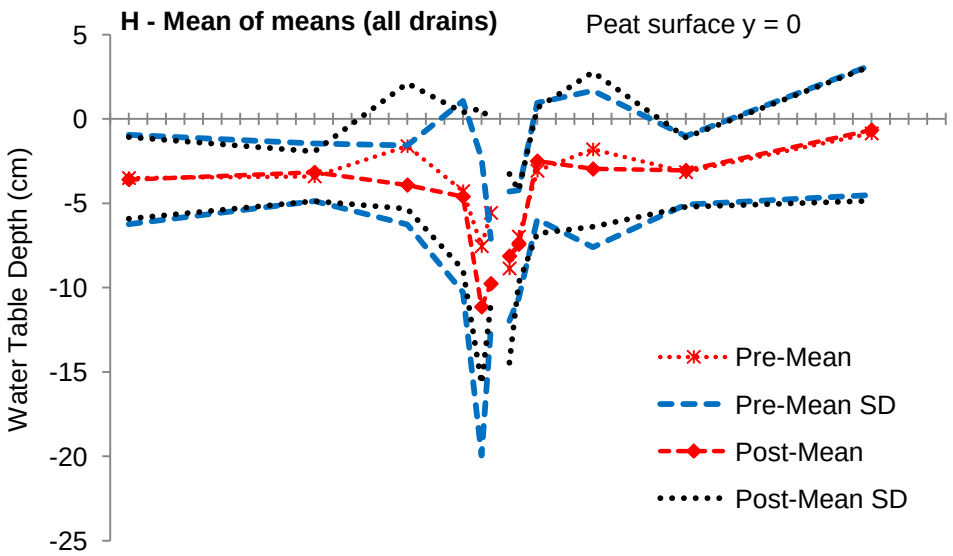
H - Mean of means (all drains)
Peat surface y = 0
Water Table Depth (cm)
5
0
-5
-10
-15
-20
-25
Pre-Mean
Pre-Mean SD
Post-Mean
Post-Mean SD

When tested using a linear model in R, from the WTD dip-well data collected, distance from the drain was highly significant ($p < 0.000$) in describing WTD. The manual measurements of WTD either side of the drains indicate that maximum mean WTDs were observed in dip-wells located 2 m to 0.5 m from the drainage channels. These are also the areas where mean WTDs show the greatest variation (SD is the largest) and deviate the most from the topography of the surface (Figure 8.7). The largest mean and individual manually measured WTD occur at 10 and 20 m distance (Figure 8.7 and Table 8.2) and mean WTDs before and after blocking also show the least variation for 20 m dip-well locations. This all indicates water table drawdown occurs most within 2 metres of the drain and influence of the drain on water table drawdown lessens with increased distance from the drainage channel.

Figure 8.7A-G shows that topographically corrected mean WTDs during periods before and after blocking are consistently located below the ground surface in both control and drain transects. Except for drain 0, all drain transects generally slope up in west to east direction yet there is no obvious indication of influence of slope as mean WTDs broadly follow the topography of the land (including control transect). This is most evident in data from dip-wells located between 2 and 20 m from drainage channels. Figure 8.7H (Mean of means of all drains) does show WTDs in dip-wells the same distance from the drainage channel to be lower on the western edges compared to the eastern one.

In all drains (and mean of all drains), except drain 1, the maximum WTDs both before and after drain-blocking were observed at 20 m locations (Figure 8.7B-G). As a result of a peat levee (created in drain production), located 1 m away from the drain on the eastern side of drains 1 and 3 and western edge of drains 1 and 0, WTD mean depth is higher – this is expected as micro-topography greatly influences WTD (Macrae et al., 2013) and can change significantly over small scales and gradients (Strack & Waddington, 2007; Strack et al., 2008).

### 8.4.2.3 Variation in water table depth before and after drain-blocking

Frequency distributions graphs are presented for WTD measured in dip-wells before and after blocking (Figure 8.8).

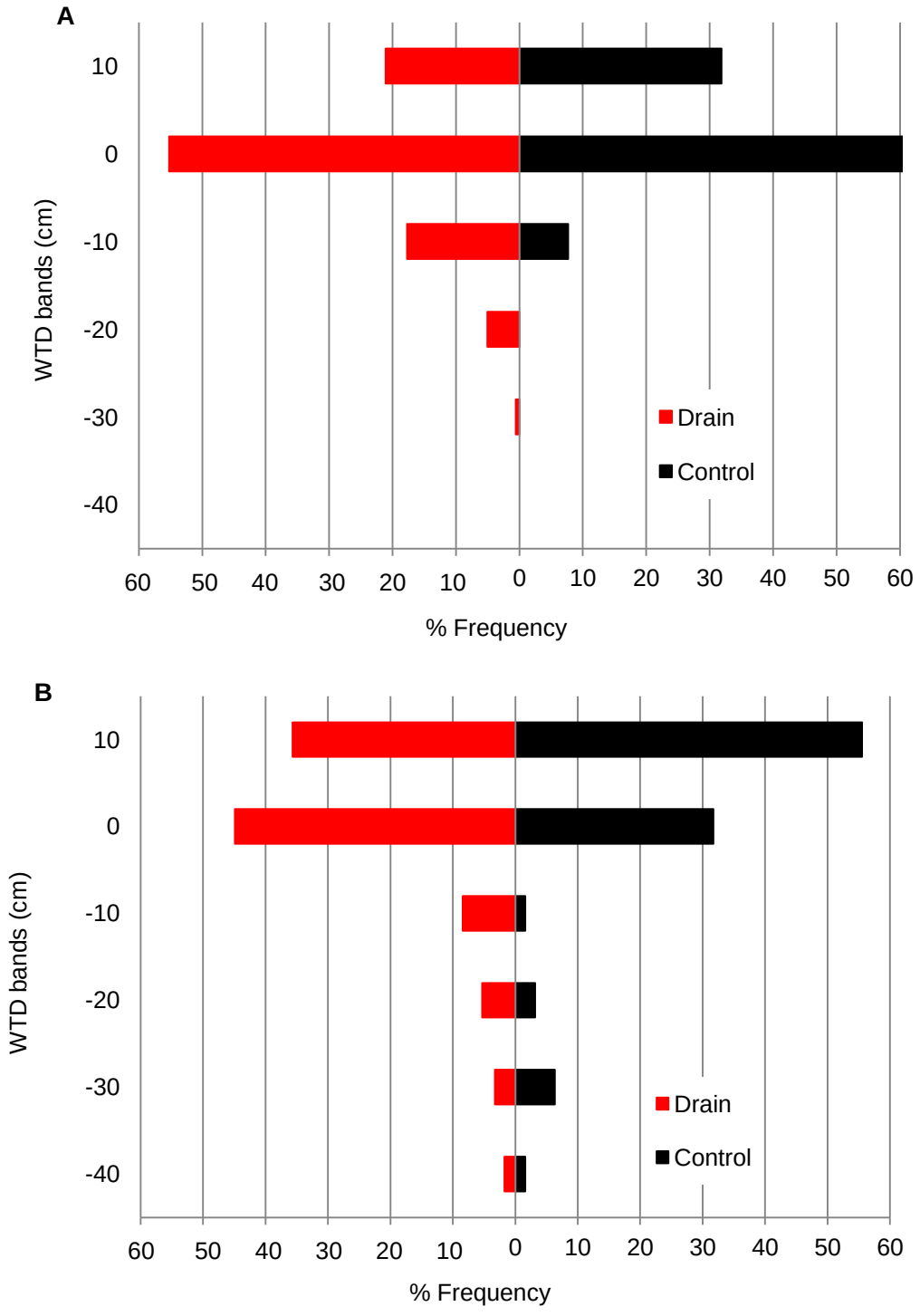


**Figure 8.8 - Frequency distribution plots for WTD dip-well data before and after blocking**
A = data collected in the pre-blocking period, August 2011 to September 2012 (Control n = 91, Drain n = 887). B = data collected in the post-blocking period, September 2012 to September 2013 (Control n = 63, Drain n = 639). Only frequencies >0.5 % are displayed.

Water table depths ranging between -10 and +10 cm dominate distributions in both drain and control transect. WTDs within this range increase from 76 % before blocking to 81 % after blocking, but decrease from 92 % in the control before blocking, to 88 % afterwards. The trend change in frequency distributions between <10 to 0 cm (0 band on graphs) and >0 to 10 cm (10 band on graphs) is also the same between drain and control transects before and after blocking, but the magnitude differs substantially. For the drain transects the frequency of the 0 band decreases from 55 % to 45 % and the 10 band increases from 21 % to 36 %. For the control transect, the 0 band decreases from 60 % to 32 % but 10 band increases from 32 % to 56 %. During the period of pre-blocking no WTD <20 cm was measured in dip-wells across control transect, but in the period after blocking such values accounted for ~10 % of all WTDs recorded. In the Drain transects, the occurrence of WTDs <20 cm after blocking increased to 10 %, compared to 6 % before.

Linear models, using R and R studio, were used to test if there was a statistically significant change in mean WTDs measured in dip-wells for data collected before and after drain-blocking. Analysis was undertaken on whether a statistically significant change ($p<0.05$) of mean WTD had been observed with distance of each dip-well from the drain transects (as a function of stage height, independent of the control transect), and WTD between drain and control transects, firstly across each drain, then across the distance dip-wells were positioned. This was undertaken for all transects. The ANOVA results of the analysis just described are presented in Table 8.3 along with some descriptive statistics of WTD dip-well data (across all drains) before and after blocking (Table 8.4). Tukey-style box-plots (produced in R), associated with the three main relationships tests (distance from drains, drain vs. control (all drains) and drain vs. control (all distances)) are presented in Figure 8.9.

Linear modelling results show for all analysis undertaken, even for individual distances and individual drains, no statistically significant difference was found between WTD data collected from dip-wells, before or after drain-blocking had been implemented (Table 8.3). Further, the box-plots (Figure 8.9) indicate very little variation before and after blocking. Visually, the response in mean WTDs before and after drain-blocking is not consistent across all drain transects but in general data shows little variation (Figure 8.7A-G) indicating the lack of statistically significant change. The greatest difference between mean pre- and post-blocking WTDs is observed in drain 2 (Figure 8.7E) on the eastern edge, where all post-blocking mean WTDs are consistently higher than those calculated during pre-blocking period. When comparing drain vs. control across each drain, the p values for Drain 2 and Drain 0 are on the threshold of being statistically significant. P values are not without errors and the probability of incorrectly rejecting the null hypothesis for level of significance at a 0.05 level can be at least 23 % and typically close to 50 %

(Sellke et al., 2001), therefore any difference between before and after at Drain 2 and 0 must be considered marginal. Generally, mean WTD before and after blocking at each site are comparable and SD between all drains and between drains and control are similar for all data before and all data after blocking, further indicating a lack of change in WTD dip-well data (Table 8.4).

| Relationship tested | DF | f-value | p-value |
|---|---|---|---|
| **Distance from Drains** | | | |
| Dip-wells at all distances | 807 | 0.33 | 0.56 |
| 0.5 m | 117 | 0.56 | 0.46 |
| 1 m | 135 | 0.14 | 0.71 |
| 2 m | 135 | 0.07 | 0.79 |
| 5 m | 135 | 0.64 | 0.43 |
| 10 m | 135 | 0.01 | 0.91 |
| 20 m | 135 | 0.00 | 0.95 |
| **Drain vs. Control (Drains)** | | | |
| All drains | 136 | 2.61 | 0.11 |
| Drain 6 | 21 | 0.79 | 0.38 |
| Drain 5 | 21 | 2.09 | 0.16 |
| Drain 3 | 21 | 0.05 | 0.83 |
| Drain 2 | 21 | 4.34 | 0.05 |
| Drain 1 | 21 | 2.12 | 0.16 |
| Drain 0 | 21 | 4.44 | 0.05 |
| **Drain vs. Control (Distances)** | | | |
| All distances | 133 | 1.65 | 0.20 |
| 0.5 m | 18 | 2.35 | 0.14 |
| 1 m | 21 | 0.96 | 0.34 |
| 2 m | 21 | 2.35 | 0.14 |
| 5 m | 21 | 3.43 | 0.08 |
| 10 m | 21 | 1.15 | 0.30 |
| 20 m | 21 | 0.13 | 0.71 |

**Table 8.3 - Linear modelling results of WTD dip-well data comparing before & after blocking**
DF = degrees of freedom, the f and p-values associated with each analysis are presented in the table above. Statistical significance is defined by p value < 0.05. Therefore, all relationships tested are deemed not statistically significant.

| | Before blocking | | | | | After blocking | | | | |
|---|---|---|---|---|---|---|---|---|---|---|
| **Site** | **n** | **Mean** | **SE Mean** | **SD** | **Median** | **n** | **Mean** | **SE Mean** | **SD** | **Median** |
| Drain 0 | 150 | -3.6 | 0.6 | 7.1 | -2.8 | 120 | -5.0 | 1.1 | 11.5 | -2.0 |
| Drain 1 | 150 | -3.4 | 0.6 | 7.7 | -2.0 | 120 | -2.8 | 1.0 | 11.0 | 0.3 |
| Drain 2 | 150 | -5.4 | 0.6 | 7.2 | -2.8 | 120 | -3.5 | 0.9 | 9.6 | -5.0 |
| Drain 3 | 137 | -2.5 | 0.4 | 5.0 | -2.0 | 110 | -2.7 | 0.7 | 7.9 | -0.9 |
| Drain 5 | 150 | -7.8 | 0.6 | 7.5 | -6.0 | 120 | -7.1 | 0.9 | 10.2 | -3.5 |
| Drain 6 | 150 | -8.0 | 0.7 | 8.4 | -6.0 | 120 | -7.4 | 1.1 | 12.3 | -3.0 |
| Control | 91 | -1.9 | 0.5 | 4.7 | -1.0 | 70 | -2.4 | 1.3 | 10.6 | 0.3 |

**Table 8.4 - Descriptive statistics of WTD dip-well data before and after blocking**
The number of samples used to calculate statistics, n, are presented for time periods before and after blocking.

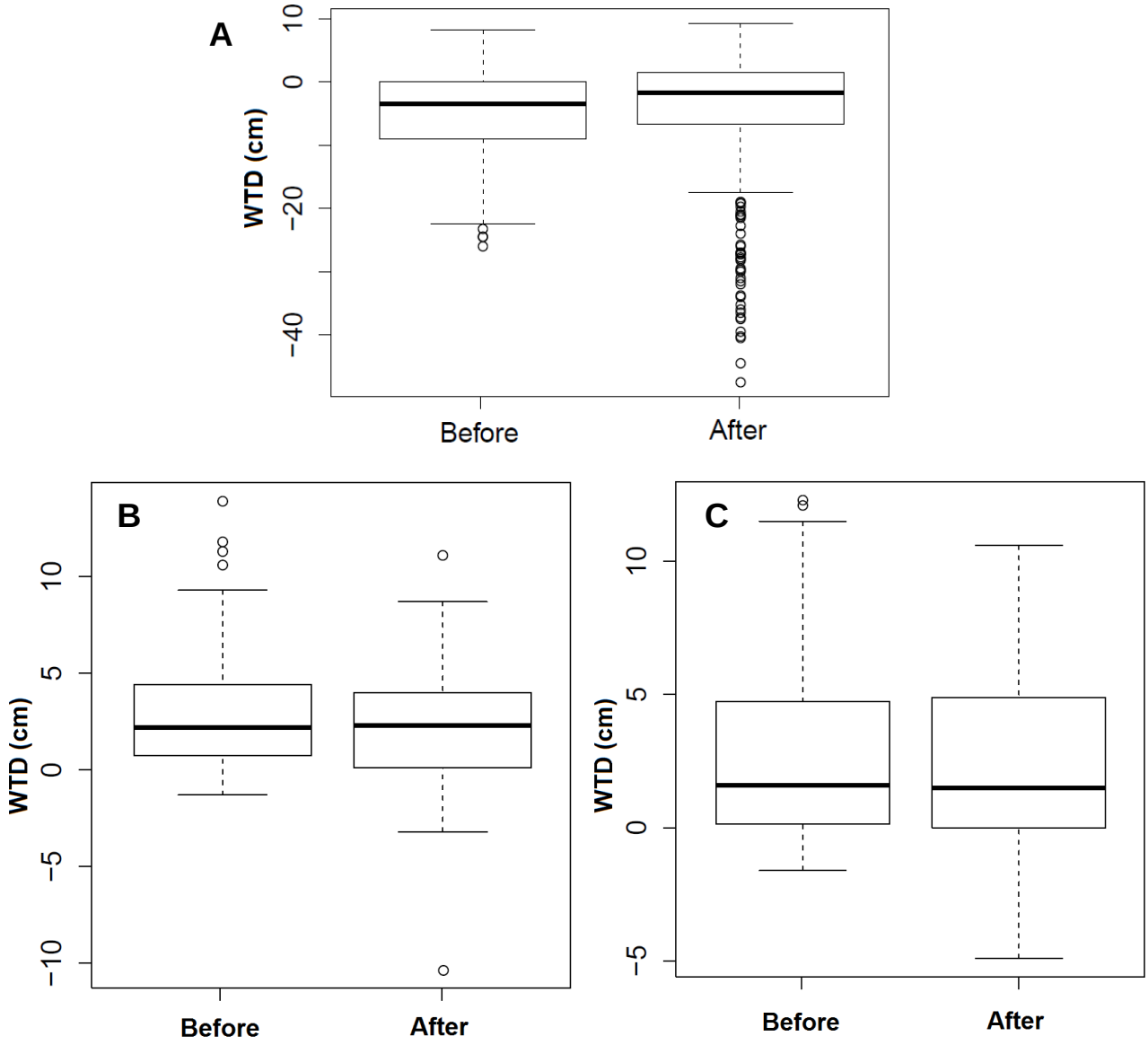


**Figure 8.9 - Tukey-style box-plots of linear modelling results**
Tukey-style box-plots show the lowest WTD still within 1.5 inter-quartile range of the lower quartile, and the highest WTD still within 1.5 inter-quartile range of the upper quartile. In relation to headings in Table 8.3 A = Distance from Drains (Dip-wells at all distances). B = Drain vs. Control (All drains). C = Drain vs. Control (All distances).

## 8.4.3 Variation in PT water table depths and inter-site comparison

### 8.4.3.1 Temporal and spatial variation in water table depths

Figure 8.10 shows the times series of WTD at each PT location, within drain and control dip-well transects respectively. The methodology for creating both times series is presented in Appendix H. Inferring WTD from data recorded by both PTs can only be predicted to an uncertainty of ± 10 cm (Appendix H). The time series data shows the WTD to be above the peat surface for extended periods of time up to +20 cm. This is unusual; however, when the prediction intervals (± 10 cm) are considered the data could be regarded as 'normal' WTD values. In addition, the hydrograph of the Allt Smeorail river, from the PT located at GB6 sampling point, is also shown with the PT WTD data.

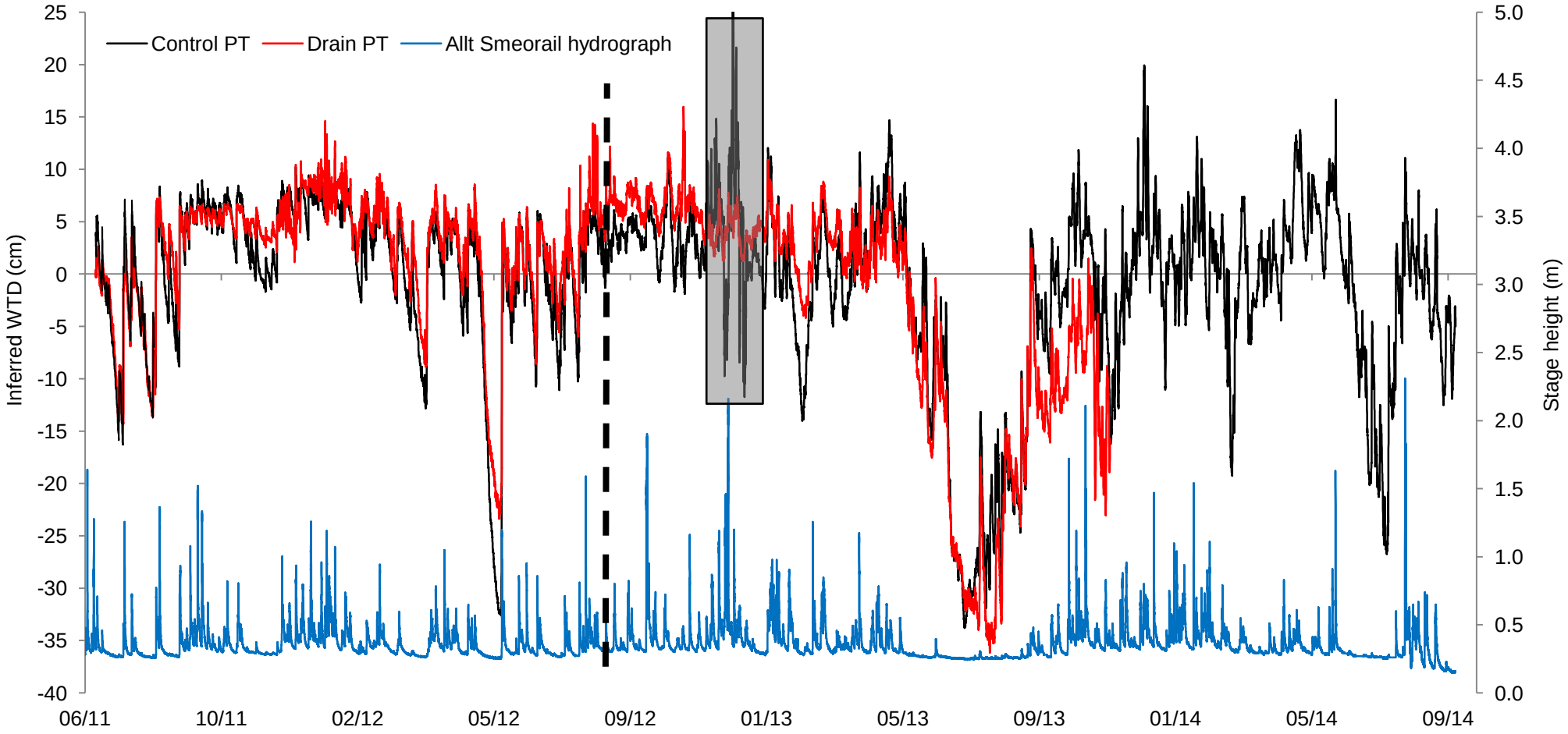


**Figure 8.10 – Water table depth from PTs at drain-blocking site and hydrograph for Allt Smeorail for comparison from 15/6.11 to 24/9/14**
Water table depth (y=axis) for the drain PT (Red) and control PT (Black), where. Y = 0 is the peat surface from which water table depth was measured. The yy-axis is stage height (metres) and the blue line is the hydrograph for Allt Smeorail. Note the Drain PT record ends on 24/11/13 due to suspected water ingress damaging the PT. The black line marks when drain-blocking was undertaken in the first week of September 2012. The shaded area covers the period between 29/11/12 and 9/1/13 and relates to a period when data from control PT had a greater uncertainty. Please note this data has been excluded for statistics analysis of control PT WTD time series data, this includes descriptive statistics in Table 8.5, frequency distributions in Figure 8.11 and linear regression plots between control PT data and stage height from Allt Smeorail in Figure 8.12.

Table 8.5 presents the summary statistics from all data logged by the two PTs.

| | Summary WTD statistics, for a given record | | | | | |
|---|---|---|---|---|---|---|
| **PT position as a function of ~annual observation** | **Min. (cm)** | **Max. (cm)** | **Range (cm)** | **Mean (cm)** | **Median (cm)** | **No. days WTD (<0)** |
| **Control PT** | | | | | | |
| Jun. 2011 - Sept. 2012 (459 days) | -32.6 6/6/12 | +10.2 8/12/11 | 42.8 | +0.8 | +2.8 | 165 (36%) |
| **Before-blocking** | | | | | | |
| Sept. 2012 - Sept. 2013 (324 days*) | -33.8 19/7/13 | +14.7 14/5/13 | 48.5 | -4.5 | +0.1 | 146 (45%) |
| **After- blocking** | | | | | | |
| Sept. 2013 - Sept. 2014 (373 days) | -26.8 26/7/14 | +19.9 24/12/13 | 46.7 | -0.8 | +0.3 | 147 (39%) |
| **After-blocking** | | | | | | |
| **Drain PT** | | | | | | |
| Jun. 2011 - Sept. 2012 (459 days) | -23.4 4/6/12 | +14.6 3/1/12 | 38.0 | +2.3 | +4.1 | 107 (23%) |
| **Before-blocking** | | | | | | |
| Sept. 2012 - Sept. 2013 (365 days) | -36.2 10/8/13 | +16.0 13/11/12 | 52.1 | -3.0 | +3.0 | 125 (34%) |
| **After-blocking** | | | | | | |
| Sept. 2013 - Nov. 2013 (69 days) | -23.1 on 20/11/13 | +1.5 17/9/13 | 24.6 | -9.8 | -10.0 | 68 (n/a) |
| **After-blocking** | | | | | | |

**Table 8.5 – Descriptive statistics for WTD from the control and drain PTs**
Drain-blocking was completed in early September 2012 and periods before and after blocking are related to this date. The records presented match hydrological years as closely possible given the start and end dates of monitoring as well as the date drain-blocking was completed. The asterisk associated with control PT Sept. 2012 – Sept. 2013 indicates data from 29/11/12 and 9/1/13 has been excluded as has a greater uncertainty associated with it. The first number in the 'No. days WTD (<0)' column represents the absolute number of days the WTD was recorded as being negative for that period of time. However, all monitoring years vary in length, therefore to compare 'No. days WTD (<0)' between different years, the absolute 'No. days WTD (<0)' has been expressed as a percentage. It is the percentage value that gives the best representative value for data between the three monitoring time periods indicated in the table to be compared. This calculation was not undertaken for drain PT 'Sept. 2013- Nov. 2013', as the fact WTD was <0 for all days in this record except one. The drain PT malfunctioned during Nov. 2013 and so this record was considerably shorter.

Unfortunately long-term rainfall data were not collected on site for comparison with water table dynamics, but a nearby hydrograph can act as a proxy. The drains flow into the Allt Mhuilin river, however due to mechanical failure the Allt Mhuilin stage height record ended in June 2013. Thus the adjacent Allt Smeorail hydrograph is shown relative to the PT-WTD profiles as a proxy for the influence of rainfall, soil moisture and evapotranspiration, and drainage of water table dynamics (Figure 8.10).

When both control and drain PTs were operational, they generally show the same temporal and spatial trends. The time series graph of WTD from PTs (Figure 8.10) indicates WTD at both sites is highly dynamic and not static: the lowest water table occurs in the summer months and the highest in the winter months. The lowest water tables (31/3/12, 6/6/12, 27/2/13, 6/8/13, 26/7/14) are apparent during period of low stage heights i.e. there is a drop in water table due to evapotranspiration and lack of recharge of run-off

is observed in the stage height record. The opposite is also true. When it rains, there is a responsive increase in water table and stream run-off increases e.g. 6/6/12, 19/8/12, 7/3/13, 2/11/14 and 11/8/14. Water table is consistently <0 from May to September 2013 and this coincided with an extended period of river base flow (Figure 8.10).

Similar time series of positive and negative mean values are found in control and drained sites in both 2011-2012 and 2012-2013. Positive median values are observed at both control and drain sites for the period before blocking (2011-2012) and the first year after blocking (2012-2013). In addition, the number of days WTD was <0 increases from 2011-2012 to 2012-2013 (from 36 % to 45 % in control transect and 23 % to 34 % in drain transect, respectively, Table 8.5). Throughout the study period, the overall minimum (control = -33.8 cm, drain = -36.2 cm) and maximum (control = 19.9 cm, drain = 16.0 cm) WTD values (and therefore overall total ranges) recorded at both sites are similar but there are differences in the timing of when these values were recorded between Control and Drain PT locations.

The WTDs at the drain PT site were consistently higher than control PT by approx. 3-6 cm, until around 10/4/13 (Figure 8.10). It was expected that WTD would be lower than in the drained area. The trends and differences between the control and drain PT time series are relatively small, supporting an interpretation that drainage has little or no effect 20 m out from the drainage channel - indicated by limited variation in mean WTD in dip-well data located between 2 m and 20 m (Figure 8.7). However, contrary to this assumption during, and after, the drought period between May-September 2013, lower WTD is observed in drain PT compared to control PT (the opposite trend was apparent previously). This may suggest (given the location of the drain PT, 25 m away from both drain 2 and 3 respectively) that there is an impact on WTD beyond 20 m from any drainage channel in areas where multiple parallel channels are present. This will be considered further in the discussion.

#### 8.4.3.2 Variation in water table depth before and after drain-blocking

From the WTD data collected from both control and drain PT sites, it was important to assess what effect, if any, drain-blocking had on WTD, as well as whether WTD response in a site located within an area of drainage (drain PT site) was different to that of a non-drained area (control PT site). The null hypothesis was drainage would have no effect and WTD response at both sites should be the same, before and after blocking, as they are subject to the same meteorological conditions, which are known to predominately influence WTD (the size of acrotelm and catotelm in a peat soil profile) (Clymo, 1984; Evans et al., 1999).

To understand more easily differences in WTDs between the control and drain PT sites, before and after drain-blocking, frequency distributions have been plotted for both these periods. Unfortunately, the drain PT was not operational for the full second year after-blocking so a comparison of WTD PT time series from both sites can only be undertaken from August 2011 to November 2013 (Figure 8.11).

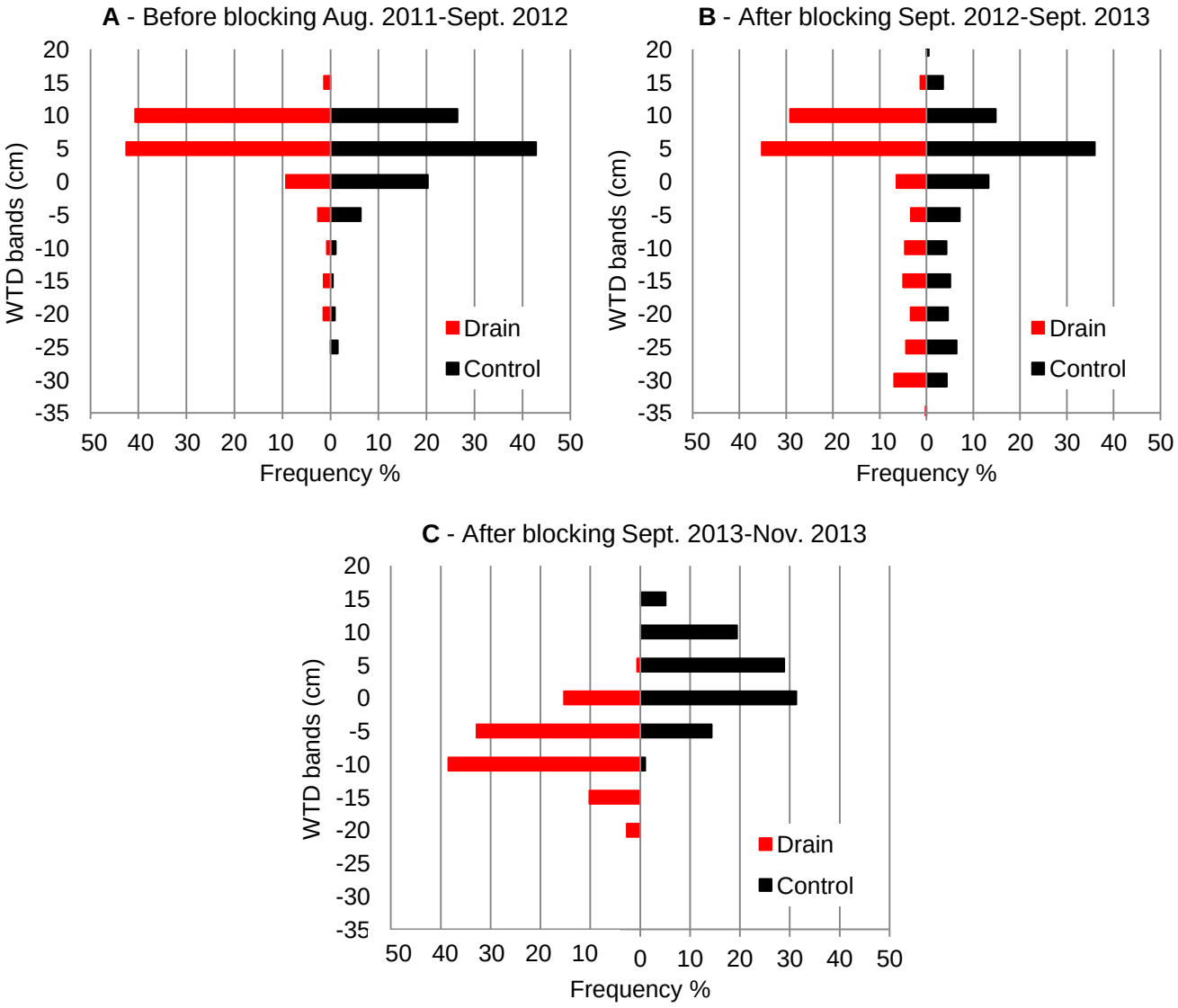


**Figure 8.11 - Frequency distributions for WTD PT time series data**
On the y-axis WTDs are split into 5 cm bands, i.e. -35 = all WTDs measured between > -40 cm and 35 cm, -30 = WTDs between > -35 cm and -30 cm and so on. Due to the much larger volume of WTD data collected from PTs compared to manual WTD measurements (presented earlier Figure 8.6 and Figure 8.8) the resolution of data presented has been increased to every 5 cm. Only frequencies >0.5% are presented.

At both control and drain PT sites there is an increase in the frequency of WTDs recorded >-25 cm (Figure 8.11A vs. B): approximately 10 % of all observations at both sites are recorded below -25 cm; previously this occurred <2 % of the time. In the same period at both sites there is a ~20% reduction in WTDs >0 cm, (control 69 % of WTD >0 cm in graph A to 51 % in graph B; for drain PT data the decrease was 84 % to 64 %).

Frequency distributions for WTDs in graphs A and B are quite similar for both sites however this is not the case for graph C (Figure 8.11). Despite the graph representing WTDs measured at the same time, the majority (71 %) of WTD observations at the drain PT were between -5 and -15 cm, whereas 60 % of WTDs at the control site were recorded between 0 and 10 cm. No WTD were recorded >5 cm at drain PT between Sept. 2013 and Nov. 2013, compared to 24 % at control PT. Conversely, 13 % of WTD observations at drain PT were < -15 cm compared to none at control PT.

To further assess whether WTD response changed after drain-blocking between the control or drain PT sites, stage height was plotted against WTD at both sites (Figure 8.12).

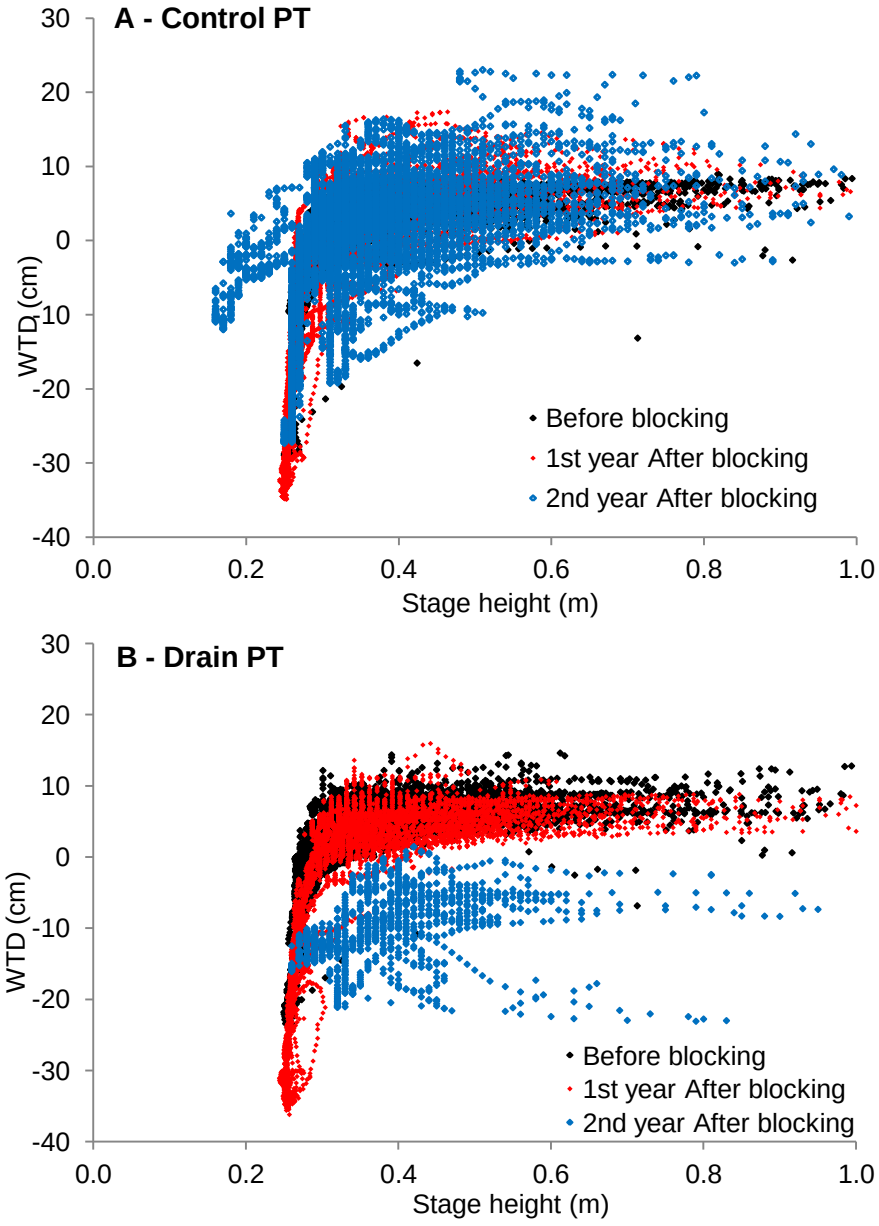


**Figure 8.12 - Stage height (GB6) plotted against control and drain PT WTD**
To better emphasise and distinguish inter-annual trends, stage height is only presented up to a maximum of 1.0 m. Individual years when monitoring took place are plotted in different colours, Before blocking (Aug. 2011 – Sept. 2012) = black, 1st year After blocking (Sept. 2012 – Sept. 2013) = black, 2nd year After blocking (Sept. 2013 – Sept. 2014) = blue. For Drain PT 2nd year. After blocking refers to Sept. 2013 – Nov. 2013 time period.

From the control PT site, generally the same relationship is seen between stage and WTD in all three monitoring years, before and after blocking (Figure 8.12). The same is not observed with the drain PT site. WTD response before and the 1st year after blocking plot is very similar (the data almost fully overly each other). However, in the second year after blocking (albeit a reduced data set) the relationship between stage and WTD is different, with much lower WTD for a similar stage height range. For comparison, data recorded during the time period when PTs at control and drain sites were both operational in the second year after blocking, September 2013 to November 2013, is shown for the control profile only along with data recorded before, and the first year after blocking (Figure 8.13). Here we see the reduced data set from September 2013 to November 2014 presented still overlaps data recorded the year before blocking as well as the first year after drain-blocking, which is different from what is observed when the drain PT data was examined.

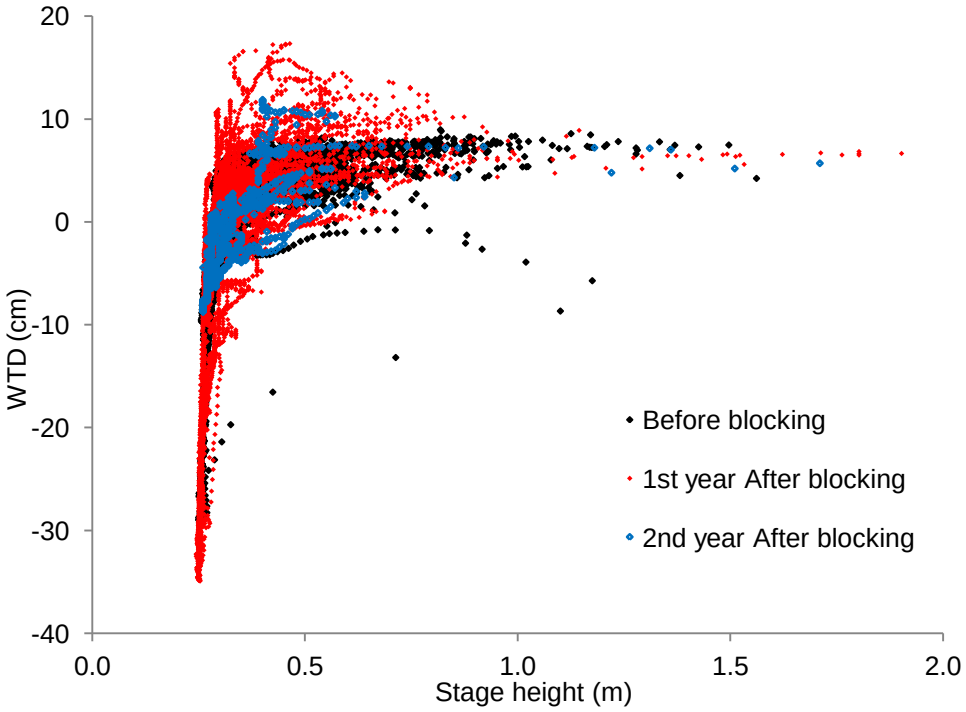


**Figure 8.13 – Stage height (GB6) plotted against control PT WTD**
The above is the same as graph A – Control PT in Figure 8.12 except data shown for '2nd year After blocking' (in blue), only covers the time period when the Drain PT was also operational, September 2013 to November 2013.

Correlation analysis was carried out on WTD and stage height data sets for each PT site and the results (Table 8.6) reflect what is observed (Figure 8.12).

| Monitoring Period | Control PCC | p-value | Drain PCC | p-value |
|---|---|---|---|---|
| Before blocking | 0.51 | 0.000 | 0.47 | 0.000 |
| 1st year After blocking | 0.51 | 0.000 | 0.45 | 0.000 |
| 2nd year After blocking (Sept. 2013 – Nov. 2013) | 0.56 | 0.000 | 0.26 | 0.000 |
| 2nd year After blocking (Sept. 2013 – Sept. 2014) | 0.43 | 0.000 | n/a | n/a |

**Table 8.6 - Correlation analysis of PT WTD vs. GB6 stage height**
PCC = Pearson's correlation coefficient. Monitoring time periods are consistent with all figures.

The null hypothesis is that drain-blocking should have no effect on WTD at both sites. Therefore, correlation between stage and WTD should not change at a particular site regardless of year. For control and drain PT sites, PCC are constant (or show little variation) for both before blocking and first year after blocking periods. For the time period both control and drain PTs were operational in second year after blocking (September 2013 to November 2013), the PCC for control PT site shows a small increase from 0.51 to 0.56 however PCC at the drain PT site shows a large relatively large decrease in comparison from 0.45 to 0.26 (Table 8.6). When the PCC result for all data from the second year after blocking (September 2013 to September 2014) for the control site is examined, there is a small decrease from 0.51 to 0.43 compared to the previous two years. However, as the data plotted in Figure 8.13 illustrates, the relationship between stage height and WTD at the control PT site remains very similar to previous year's data. The unusually dry meteorological conditions during the summer of 2013 have to be acknowledged as part cause of the trends in the data observed but this analysis indicates WTD response is not the same before and after blocking at both sites.

## 8.4.4 Time series of [DOC] within drainage channels

A time series of [DOC] of samples collected from the six drains, Allt nan Nathraichen (AN) and Allt Mhuilin rivers, is presented (Figure 8.14). [DOC] from both rivers have been included as a way of assessing how a drained peatland area contributes to catchment export of DOC.

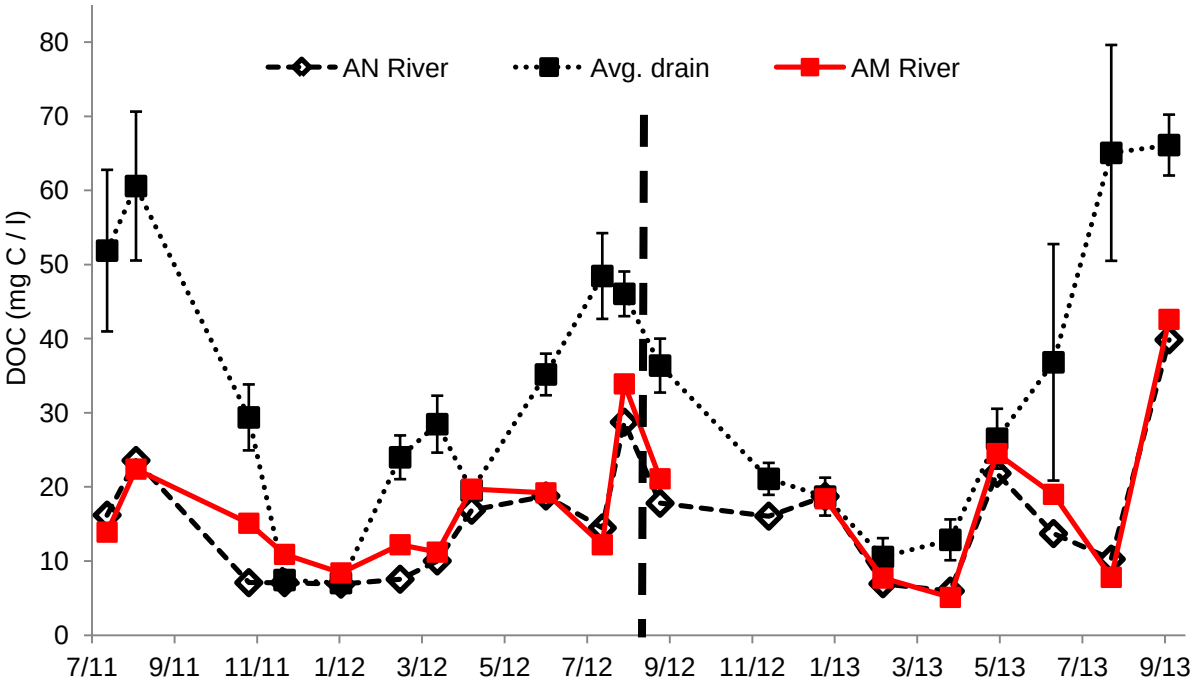


**Figure 8.14 - [DOC] time series from drain-blocking area and nearby rivers, 6/8/11 to 16/9/13**
The black squares and associated error bars represent mean [DOC] and ± SD of all six drains when sampled. The [DOC] of samples Allt nan Nathraichen (AN) river, collected upstream of where the studied drains enter the river, are represented by black hollow diamonds. [DOC] of samples collected from Allt Mhuilin at sampling point GB10, represents a point downstream where water from the drains enter the catchment wide river network, are represented by red squares. The dashed vertical black line marks the when all drains were blocked using peat turves in early Sept. 2012.

Table 8.7 displays descriptive statistics of [DOC] measured before and after blocking.

| Units = mg C $l^{-1}$ | Before blocking (Aug. 2011 - Sept 2012) | | | | | After blocking (Sep. 2012 - Sept 2013) | | | | |
|---|---|---|---|---|---|---|---|---|---|---|
| **Site** | **n** | **Mean** | **SD** | **Min.** | **Max.** | **n** | **Mean** | **SD** | **Min.** | **Max.** |
| AM (GB10) | 11 | 16.3 | 7.2 | 5.1 | 33.9 | 8 | 18.3 | 12.2 | 5.1 | 42.6 |
| AN | 11 | 14.3 | 7.4 | 6.0 | 28.7 | 9 | 16.8 | 10.2 | 6.0 | 39.8 |
| Drain 0 | 11 | 31.9 | 16.2 | 7.0 | 56.5 | 9 | 30.7 | 24.9 | 10.4 | 76.8 |
| Drain 1 | 11 | 29.7 | 15.0 | 6.1 | 53.8 | 9 | 27.1 | 17.5 | 8.7 | 60.2 |
| Drain 2 | 11 | 33.1 | 20.8 | 7.0 | 65.5 | 9 | 30.7 | 18.5 | 9.2 | 65.9 |
| Drain 3 | 11 | 30.7 | 15.1 | 6.5 | 46.9 | 9 | 34.8 | 22.8 | 8.7 | 73.6 |
| Drain 5 | 11 | 36.7 | 22.2 | 7.6 | 72.6 | 9 | 38.0 | 26.2 | 10.9 | 80.1 |
| Drain 6 | 10 | 31.2 | 19.0 | 7.3 | 69.0 | 9 | 34.7 | 19.1 | 15.4 | 65.9 |
| Avg. Drain | 65 | 32.5 | 17.8 | 7.0 | 60.6 | 54 | 32.7 | 20.8 | 10.5 | 66.1 |

**Table 8.7 – Summary [DOC] statistics from Allt nan Nathraichen (AN) and Allt Mhuilin (AM) rivers and drains 0-6**

DOC concentrations in all drains ranged from 6 mg C $l^{-1}$ (January 2012) to 80 mg C $l^{-1}$ (August 2013) (Figure 8.14). As with the rivers, drain [DOC] show the seasonal pattern of late summer maxima and winter minima, with inter-drain variation greatest in summer months (June to August). Mean drain [DOC] in 2013, June (36.8 mg C $l^{-1}$), August (65.1 mg C $l^{-1}$) and September (66.1 mg C $l^{-1}$) 2013 after drain-blocking, were higher than the comparable time in 2012 before blocking, 35.2 mg C $l^{-1}$, 46.1 mg C $l^{-1}$ and 36.4 mg C $l^{-1}$ respectively (Figure 8.14). Mean ± SD of [DOC] was largest in drain 5, before and after blocking (Table 8.7). River [DOC] from AN and AM sampling points ranged between 5-6 mg C $l^{-1}$ (April 2013) and 40-43 mg C $l^{-1}$ (September 2013), respectively, and always had lower [DOC] than the contemporaneous drain samples. When [DOC] from AN and AM rivers are compared before and after drain-blocking a different trend is observed to drain [DOC]. [DOC] from AM and AN rivers are very similar before and after blocking, apart from period between November 2011 and April 2012 before blocking where [DOC] in AM were higher than AN (Figure 8.14).

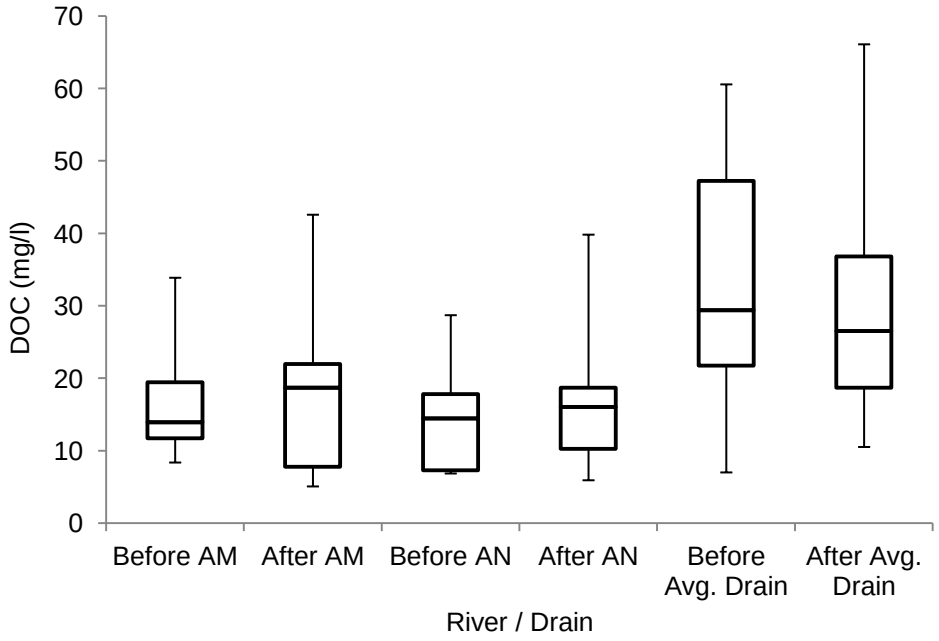


**Figure 8.15 - River and Drain [DOC] box-plots before and after blocking**
Displayed are minimum-maximum style box-plots based on data presented in Table 8.7.

Apart from drain 6, in both rivers and all drains higher maximum [DOC] were recorded after blocking compared to before, reflected in larger SDs of mean [DOC] at all sites after blocking (Table 8.7, Figure 8.15). The mean (Table 8.7) and median (the horizontal line in each box, Figure 8.15) [DOC] increase in both rivers after blocking, but the mean of the drain average [DOC] stays the same after blocking (32.5 mg C $l^{-1}$ before vs. 32.7 mg C $l^{-1}$ after, Table 8.7) and the median decreases slightly (Figure 8.15).

Paired t-tests analysis was undertaken on differences between river [DOC] (both rivers) compared to the average drain [DOC], before and after blocking, and between the two river [DOC] (Table 8.8). The null hypothesis is that if drain blocking has no effect, the difference in the mean [DOC] between river samples and drain samples should not change before and after blocking. Similarly there should be no difference between rivers [DOC].

Paired t-tests

| | Before blocking | | | | | After blocking | | | | |
|---|---|---|---|---|---|---|---|---|---|---|
| **Relationship** | **n** | **Mean** | **SE Mean** | **SD** | **p** | **n** | **Mean** | **SE Mean** | **SD** | **p** |
| AN vs. Avg. Drain | 11 | -18.3 | 4.1 | 13.5 | 0.000 | 9 | -15.9 | 5.8 | 17.4 | 0.000 |
| AM vs. Avg. Drain | 11 | -16.3 | 4.6 | 15.4 | 0.000 | 8 | -15.8 | 6.6 | 18.7 | 0.000 |
| AM vs. AN | 11 | 2.0 | 1.0 | 3.3 | 0.07 | 8 | 1.4 | 0.9 | 2.5 | 0.17 |

**Table 8.8 - River and Drain [DOC] data paired t-tests results**
AN = Allt nan Nathraichen and AM = Allt Mhuilin, n = number of samples compared from each river in each test.

The mean differences between AN/AM vs. Avg. Drain decreases after blocking, whilst SE mean and SD increases and both data sets are statistically different from one another ($p < 0.000$) (Table 8.8). The same is true for AM vs. AN samples except, the difference between [DOC] samples collected from AM and AN were not statistically different from each other, either before ($p = 0.07$) or after blocking ($p = 0.17$). It should be noted SE mean and SD are likely to increase in any analysis where sample size gets smaller and this is the case in all analysis undertaken in Table 8.8.

Therefore since differences in mean [DOC] decreased between rivers and drains samples, drain blocking could have been responsible for this and could have reduced [DOC] in the drains. However, the differences between the rivers did not change and this may be expected between the two sites if the drains contributed to the AM [DOC] significantly.

## 8.5 Discussion

The continuously logged WTD reveals that the water table is dynamic. Most peatlands have WTD within 40 cm of ground surface 80 % of the year (Holden, 2005b) and this seems to occur also at Gordonbush. Although on-site rainfall data was not available, the fastest rates of change was coincide with storm events which followed drought (evidenced by constant stage low height before event flow), with WTDs increasing by up to ~8 cm over a one hour period (two examples included 9/7/2011 and 7/9/2013). Downstream discharge data shows that the largest decreases in WTDs are contemporaneous with low flow period and highest WTDs occur during high flow periods. This reveals that the WTDs at Gordonbush are highly sensitive to meteorological factors, namely precipitation ('push' factor) and evapotranspiration ('pull' factor). Water table depth is known to rise rapidly following rainfall events and recharge of water in peatlands happens quickly after prolonged dry weather (Evans et al., 1999). Dry periods during the summer months can result in extended periods of water table drawdown (Lafleur et al., 2005; Allott et al., 2009) and the study site at Gordonbush behaves similarly (Figure 8.10).

The depth of the water table within a peatland soil is affected by many factors making peatland hydrology a complex subject area (Holden, 2005b, 2008). In this discussion WTD at Gordonbush will continue to be described in terms of simplified 'push' and 'pull' meteorological factors and the impact and influence of artificial drainage will be explored further. Firstly though, the effect of topography on WTDs at Gordonbush needs considered.

### 8.5.1 Quantifying the effect of topography on water table drawdown

From west to east (control transect to dip-well position at 20 E in drain 0 transect), over a distance of ~370 m, GPS data indicate an elevation increase of 3 m (Figure 8.1C). This equates to an average slope angle of ~ + 0.5° (up-slope in west-east direction). Topography and topographic features are known to influence and control peatland hydrology (Holden & Burt, 2003a, b; Holden, 2005a; McNamara et al., 2008). Mapping topographically corrected mean WTD along the drain-blocking study site transect (Figure 8.7) suggests that WTD broadly follows topography. Distance from any drain had no statistically significant affect on WTDs data collected from dip-wells, before or after blocking (Table 8.3 and Figure 8.9), indicating topography is likely to be a systematic control across the site at Gordonbush.

Water table drawdown is likely to be greater on the down-slope of drainage channels (Holden et al., 2006; Lindsay & Freeman, 2008) and the effect is exaggerated on steeper slopes (Allott et al., 2009). Although the slope is very gentle across the study site transect at Gordonbush, lower WTDs may occur more frequently on western than eastern sides of the drainage channels. However, this is observed only at drain 2 and thus mean WTDs are plotted (Figure 8.7E&H). Spatial variation in soil moisture has been attributed to micro-topographic features (Belyea & Baird, 2006). However, it has also been suggested that although topography is a key control on WTD at a landscape scale, it does not always explain well local variations in WTD across a small scale (Allott et al., 2009). From Gordonbush data it is evident the presence of drainage channels have more influence over water table drawdown than slope. There is a drain ~ 60 m away whose top end is mapped approx. 5 m lower than the control transect, (Figure 8.1B). However, as it appears that shallow slope has little influence on WTD then it is unlikely that this channel negatively influences the WTD in the control transect.

### 8.5.2 Quantifying the effect of drainage channels on water table drawdown

The WTD dip-well data shows drainage (distance from the drain) affects WTD. The plots of mean WTD indicate this effect is most pronounced within 2 metres of study drains (Figure 8.7). The influence of channels can be up to 5 metres, with no surface water common within 2 metres, e.g., (Allott et al., 2009; Wilson et al., 2010) and Gordonbush shows a similar response.

However, WTD data collected from PTs at control and drain sites suggests drainage channels affect WTD at a greater distance than 2 metres. The observed change in WTD response to stage and decrease in correlation coefficient after exceptionally dry summer of 2013 (Met Office, 2013a) at drain PT, was in contrast to the constant WTD-stage relationship observed at the control PT site (Figure 8.12 and Table 8.6). Drainage density can affect WTD as soil water through-flow in drainage areas can be more efficient and transfer of water to drains is faster, taking it away from surrounding (non-drained) areas (Allott et al., 2009). The time series shows this response, with water table drawdown greater in areas surrounding drainage channels (lowest WTDs recorded at drain PT in May-September 2013). Data The PTs shows WTD recovery (i.e. time taken for soil profiles to become saturated again) is longer in areas of peat with historic drainage channels. This signifies peat in drained areas is more susceptible to drying out than undisturbed areas and indicates under extreme dry periods drainage channels can affect WTD up to a 25 m distance (distance of drain PT from closest drainage channel).

WTD is modelled to be impacted as far as 400 m or more from drainage channels (Holden, 2005b, a, 2008) and if occurring, it is possible similar WTD drawdown will occur when wind-farm infrastructure, e.g. drainage networks for roads, are implemented on peatlands (e.g. (Lindsay & Freeman, 2008; Lindsay, 2010)). WTD drawdown has been postulated to be expected at least 20 m out from common-sized drains (Lindsay & Freeman, 2008) and the PT time series from Gordonbush shows such a response.

At Gordonbush it is clear the impact of meteorological conditions (predominately the drought May-September 2013) and the presence of drainage channels have a far greater control than topography on WTD as this time period caused the largest drop in water table at the control and drained site. However, to understand better the additional impact of effect of drain-blocking, future research should also consider installing PTs for further comparison in drained areas which are not blocked and in more than one control site. Furthermore, additional PTs located < 25 m from drainage channels may better help quantify any “positive” lateral effects that drain-blocking may have on raising water tables closer to the drainage channels themselves. The increased response from different land use treatments from multiple time series would allow more confident interpretation

## 8.5.3 What is the effect of drain-blocking?

### 8.5.3.1 Water table depth

Peat surfaces may become more saturated after blocking (Wilson et al., 2010) so the effectiveness of drain-blocking was assessed by comparing average WTD in the period after, to before drain-blocking. There is no statistically significant difference in WTDs measured before or after blocking, either as a function of distance from the drains, or comparing drains vs. the control in relation to WTD across each drain, or at every distance from the drains a dip-well was positioned. Assessing the longer-term effectiveness of drain-blocking using the WTD dip-well data is limited as manual WTD monitoring did not take place between September 2013 and September 2014 (2$^{nd}$ year post-blocking).

When manual WTD data from drain transects is collated (Figure 8.7H), the largest rises in mean WTD before and after drain-blocking occur at a 2 m distance from the drainage channel. Therefore, any effect of drain-blocking raising WTD within the peat soil profile may be limited within the immediate vicinity (2 m) of the channel in the early period after drain-blocking. WTD rises have been measured at other sites after blocking e.g. average of +2 cm over a 2 year period (Wilson et al., 2010) and +9 cm within 10 months after blocking (Worrall et al., 2007a). These were also measured using by manually measuring WTD in dip-wells located either side of drainage channels. Comparing water-table depth data from one site to another is not always valid due to variation in peat physical

properties and climates between sites (Baird, 2012). Additionally, changes in WTD can take more than one year to respond positively to blocking activities (Wilson et al., 2010). Despite drain 2 and drain 0 showing a marginal statistically significant difference between mean WTD and the control site (Table 8.3), there is insufficient evidence to suggest that WTDs have risen due to drain-blocking activities. Manual dip-well measurement monitoring finished in September 2013 which may have been insufficiently long to detect a raised water table response.

Meteorological conditions strongly control water table depth in peatland (Whittington & Price, 2006; Moore et al., 2013). The spring of 2011 was exceptionally warm and dry (Met Office, 2011) which may explain the lower water tables at the start of monitoring. The calendar year of 2012 (which included 9 months of pre-blocking data) was one of the wettest in recorded history in the UK and the summer months were some of the wettest recorded during the last century (Met Office, 2012). The increased surface run-off sources, reduction in evapotranspiration losses would have kept WTDs high during this period – indeed the majority of WTDs in dip-wells were recorded between -10 and +10 cm (Figure 8.6) and PT logged positive WTDs for over 200 days during 2012 (Figure 8.10). In the summer of 2013 an extended period of dry weather from May through to September (Met Office, 2013a) caused a prolonged WTD drawdown during this period, and as a consequence WTD did not recover > 0 cm until ~3 months afterwards.

The combination of these meteorological conditions, the loss (drain PT failure) and limitations in data (dip-well measured stopped September 2013), makes comprehensively assessing the effectiveness of drain-blocking challenging. Although there is evidence drawdown in the drained area was greater and WTD recovery was longer than a non-drained area during a drought period (June to September 2013), a WTD time series from an unblocked drained area would help confirm this.

Local meteorological conditions are very important in the timeline of change after blocking drains and short term monitoring may not allow a response to blocking to be observed if there is a stronger ‘climatic ‘ driver acting during the monitoring period. Therefore, longer-term monitoring is needed to fully assess the effectiveness of drain-blocking to raise WTDs and, if any, the spatial extent of any lateral increase. The dip-wells and control PT are still in position and thus the opportunity exists to return and make further measurements. Generally there is strong scientific evidence that peat restoration shows good ecological responses within 5 years (Martin-Ortega et al., 2014) so it is recommended that monitoring continues (Bonn et al., 2014b) at Gordonbush over this sort of time-scale and if possible beyond. The understanding generated here gives a framework to build on.

Beyond assessing whether drain-blocking can effectively raise WTDs, future monitoring should also investigate the consequent impacts of changing hydrology with a view to vegetation succession. Such research would be an important contribution to site-specific understanding of C storage: WTD directly influences vegetation present (Charman, 2002; Evans & Warburton, 2007) and in turn affects the larger C balance. For example, colonisation of *Eriophorum sp*. in blocked drained areas has led to increases of $CH_4$ emissions (Cooper et al., 2014; Green et al., 2014) and at some sites emissions from re-wetted peatland areas have remained elevated compared to undisturbed peatlands for 30 years after restoration (Vanselow-Algan et al., 2015). Establishing *Sphagnum sp*., either initially (Green et al., 2014) or in a succession to grasses (e.g. *Eriophorum sp*.) (Cooper et al., 2014), is acknowledged as the best way to reduce $CH_4$ emissions from drain-blocked sites in the long-term. Additionally, the effect of drain-blocking on vegetation changes and subsequent [DOC] (and DOC fluxes) was not undertaken during this research but this activity has been suggested as an area of interest worthy of investigation in any future research (see Chapter 9, section 9.3.5). Therefore WTD monitoring and vegetation management is important if drain-blocking/re-wetting of peatland is to be successful and ultimately improve a peatlands C sink potential (Cooper et al., 2014), including drain-blocked areas at Gordonbush.

Observations made at Gordonbush could prove to be important as the wind-farm payback calculator (Nayak, 2008) tries to predict influence and impact of drainage channels on WTD draw-down and relate this to expected C losses during construction. It should be noted that the effect of drainage on WTD at Gordonbush has been investigated across a series of parallel drains, which is a different scenario to singular drainage channels which may be involved in elements of windfarm construction, e.g. trenches for cabling, building road networks and associated drainage channels. However, this research shows that even small (~0.5 m wide and ~0.5-0.7 m deep) drains, can affect WTD at a distance from drainage channels. If drainage channels associated with wind-farm construction are wider and (perhaps more importantly) deeper than the drains studied in this research, this could alter, potentially increasing, 'carbon payback time' of the Gordonbush wind-farm. If wind-farm developments incorporate restoration programmes as part of their HMPs, and drain-blocking within these areas raise WTDs, then it is likely to contribute to off-setting C losses caused by construction through the higher water tables benefits of an increasing likelihood of reduced DOC export, decreased aerobic decomposition of peat soil profile and increased C sequestration potential (Wallage et al., 2006; Strack & Waddington, 2007; Holl et al., 2009; Wilson et al., 2011b; Armstrong et al., 2012).

### 8.5.3.2 [DOC] in drainage channels

The ranges of [DOC] measured in drains at Gordonbush (6-77 mg C $l^{-1}$), before and after blocking, are comparable to other studies (5-120 mg C $l^{-1}$) (Table 8.9), the exception being some extremely high [DOC], >200 mg C $l^{-1}$, where the catchments were acknowledged as being extensively and densely drained (Gibson et al., 2009).

| | Recorded [DOC] (mg $l^{-1}$) | | | |
|---|---|---|---|---|
| **Field site** | **Overall range** | **Pre / (un) blocked** | **Post-blocking** | **Author** |
| Gordonbush | 6-80 (mean ~32) | 6 – 73<br>Mean = 33 | 8 – 77<br>Mean = 36 | This study |
| N Pennines, England | 5-70 | 5 – 30<br>Mean = 17 | 5 – 70<br>Mean = 33 | (Worrall et al., 2007a) |
| NE Scotland & N England | 5-95 | Mean = 31 | Mean = 23 | (Armstrong et al., 2010) |
| Oughtershaw, N England | 5-120 | 5-120<br>Med. = 40 | 5-60<br>Med. = 15 | (Wallage et al., 2006) |
| Upper Teesdale, England | 10-80 | 10-70 | 15-75 | (Turner et al., 2013) |
| Teesdale, England | 10-220 | 20-120<br>Med. = ~40 | 10-220<br>Med. = ~40 | (Gibson et al., 2009) |
| Lake Vyrnwy, Mid-Wales | Means = 25-35 | Means = 25-30 | Means = 30-50 | (Wilson et al., 2011a) |
| UK national survey | 4.7 – 114, Mean ~34 | n/a | n/a | (Armstrong et al., 2012) |

**Table 8.9 - [DOC] from other UK drain-blocking sites**
When possible information is given on ranges of [DOC] measured when drains were pre-blocked (or unblocked) and post-blocked during both periods in the highlighted studies. Mean and median (represented by 'Med.') [DOC] have been quoted when available.

It appears that at Gordonbush, the minimum, maximum and mean [DOC] increased at all drain sampling sites the year after blocking (also Table 8.7). This has been observed in four of the seven studies presented (Worrall et al., 2007a; Gibson et al., 2009; Wilson et al., 2011a; Turner et al., 2013).

Statistically significant increases in [DOC], or non-significant decreases (Gibson et al., 2009; Turner et al., 2013), have been found after blocking (2 years) at other restoration sites (Kalbitz & Geyer, 2002; Worrall et al., 2007b; Waddington et al., 2008; Wilson et al., 2011a). A meta-analysis of data from UK lowland peat in England and Wales, found average [DOC] was 27.3 mg C $l^{-1}$ greater in drained areas compared to un-drained sites but overall re-wetting initiatives, such as drain-blocking, do not currently demonstrate a conclusive or corresponding decrease in [DOC] (Haddaway et al., 2014). Water colour and [DOC] from areas where drains have been blocked may decrease by up to 70 % compared to similar samples from unblocked drains (Wallage et al., 2006; Armstrong et al., 2010), presented in Table 8.9. Further, DOC production is said to decrease over time (months) in permanently wet soils (Blodau & Moore, 2003); however, it is acknowledged that drain-blocking techniques will not have the desired effects in every location (Holden et

al., 2006; Armstrong et al., 2010). Unfortunately monitoring of [DOC] in drainage channels stopped in September 2013 so there is no data to interpret impact on [DOC] in the second year after blocking.

DOC quality, measured using spectrophotometry, was not investigated during this research and it may have been interesting to consider this to see if the composition of DOC reflects a change in source. For example DOC export has come from deeper layers of humified peat and has higher aromaticity (Frank et al., 2014) (deemed lower quality), and vice versa (Strack et al., 2015) (deemed higher quality). Quality of DOC determines its bioavailability (Kalbitz et al., 2003) and areas of *Sphagnum* growth (see Figure 8.4) are associated with low aromatic, high-quality DOC (Strack et al., 2015). Re-wetting peatlands through drain-blocking can reduce aromaticity of DOC, i.e. DOC exported from areas where WTD is low and deep peat layers are exposed and can be oxidised, and improve water quality downstream of the restored site (Frank et al., 2014). Therefore, measuring the quality of DOC can help indicate both vegetation characteristics of the surrounding area as well as water quality and is an additional parameter to assess the effectiveness of drain-blocking, or more generally peatland restoration. If possible it should be measured in any future monitoring of DOC from blocked drains at Gordonbush.

#### 8.5.3.3 Relationship between [DOC] in drainage channels and rivers

The Allt nan Nathraichen (AN) river sampling point was located upstream of where monitored drainage channels enter the river (Figure 8.1B). [DOC] in the drainage channels was always greater in relation to [DOC] samples collected from AN sampling point (Figure 8.14). The catchment area above the sampling point of the AN river has fewer drainage channels than the drain-blocking study site (Figure 8.1A). This suggests that [DOC] in AN river was lower as fewer direct routes for soil DOM to be exported were present without subsequent in-stream processing.

The simplest interpretation of the increased [DOC] in the drains observed after blocking (Figure 8.14 and Table 8.7) however may be a response to the drought between May and September 2013 (Met Office, 2013a). Largest [DOC] coincide with an extended period of stable base flow suggesting reduced soil run-off. Prolonged periods of water table draw down (and evapotranspiration) can result in increased DOC production (Mitchell & McDonald, 1992; Clark et al., 2009; Gibson et al., 2009) (as outlined in section 2.3.2.3). In addition to the biochemical production controls, evaporation from the surface of standing water bodies (as may have occurred within the blocked drains, Figure 8.14) can increase [DOC] (Armstrong et al., 2010).

Since samples were collected under differing conditions and samples sizes were not the same, [DOC] from drain samples, collected before and after blocking, could not be directly compared to each other to infer any effect of drain-blocking on [DOC]. Therefore, differences between [DOC] samples from the drains had to be compared to samples from both rivers, AM and AN. If drain-blocking was to have a positive effect on reducing [DOC] we might expect to see a decrease in the difference between samples collected from the drains compared to samples from AM and AN. Additionally, if there was any reduction in [DOC] caused by drain-blocking, we would expect the difference between [DOC] in downstream AM river (GB10) compared to the AN river to be smaller after blocking than before (as the drain input upstream of AM reduces).

A difference in mean [DOC] is observed, before and after blocking, for AM vs. Average Drain decreasing 0.5 mg C $l^{-1}$ (-16.3 before to -15.8 after) and for AN vs. Average Drain decreasing by 2.4 mg C $l^{-1}$ (-18.3 before to -15.9 after) respectively. Although individually the differences between AM/AN vs. Average Drain [DOC] values are statistically significant both before and after blocking, when before and after blocking mean [DOC] values for AM/AN vs. Average Drain are directly compared the differences were within the limits of the mean plus SE (Table 8.8). Additionally, as there is no statistically significant difference between AM and AN [DOC] samples before or after blocking it appears blocking has little impact on the larger site [DOC] signature.

The lack of difference between AM and AN is probably because, although the sampling point on Allt Mhuilin will be fed by DOC-rich water from the drain, as nearer the catchment outlet it, unlike AN, will be influenced by multiple inflows including various small streams (which is not the case for AN) and potentially could be masking any positive effect of drain-blocking on [DOC]. These additional inflows could dilute the influence of [DOC] input upstream subsequently increasing the difference between [DOC] recorded within the drains and [DOC] at the AM sampling point. Conversely, additional areas of drained (and unblocked) peat downstream of AN (see Figure 8.1) could be supplying even greater amounts of DOC rich water which will be fully mixed in the Allt Mhuilin river before [DOC] is recorded at sampling point AM. From the data gathered, it is difficult to tell the influence of either dilution or extra DOC supply processes that are prevalent in the Allt Mhuilin river. Future increased spatial sampling between AM and AN river sampling points would further understanding of DOC sources (from drainage channels as well as wider catchment) and transport pathways in the catchment and help better assess the impact of drain-blocking on reducing [DOC].

To determine whether drain-blocking had a positive effect on reducing DOC export at Gordonbush, discharge from drainage channels would have had to be measured to

estimate fluxes (such data was not collected during this research due to resource limitations). This is something which should be considered in the future. Reductions in DOC export have been observed in periods after drain-blocking has been implemented (Quinty & Rochefort, 2003; Gibson et al., 2009; Strack & Zuback, 2013). Drain-blocked areas should allow the surrounding peatland to retain more water, reducing peak flows (Quinty & Rochefort, 2003). Thus, the area becomes more buffered to extreme events (e.g. flooding risks) and consequently increased releases of DOC and POC during storm events (Wilson et al., 2011b). The retention of water stops production of "fresh" DOC in aerobic layers due to shallower water tables (Holden & Burt, 2003a, b) as more anaerobic conditions develop. Some drain-blocking studies initially measured reductions in DOC export within 1-2 years of drain-blocking, but this was attributed to decreases in water yield rather than concentration (Gibson et al., 2009; Turner et al., 2013). [DOC] increased in the Gordonbush drains post-blocking, supporting a similar interpretation here.

The greatest water colour, [DOC] and DOC export reductions were only observed at some sites following a 10 year period after restoration programmes had been initiated (Strack & Zuback, 2013) further emphasising, the need for long-term monitoring programmes to fully assess impact of blocking (Holl et al., 2009; Armstrong et al., 2010; Wilson et al., 2010). However, antecedent conditions greatly influence [DOC] (Grand-Clement et al., 2014), therefore these must be properly accounted for assessing the impact of blocking on [DOC] for any particular data set. Estimated recovery from horticultural peat extraction sites following restoration, such that sites that were C sources become sinks, is 6-10 years (Waddington et al., 2010).

In summary, although drains were blocked, in the first year after blocking local meteorological has had a greatest affect on [DOC]. Monitoring of [DOC] at Gordonbush would need to continue for several years to fully assess if drain-blocking has a positive effect on reducing [DOC] - approximately 5 years was the timescale suggested to observe a WTD impact of drain-blocking (Martin-Ortega et al., 2014). The addition of monitoring discharge from the drains and vegetation surveys would enhance future assessment.

## 8.6 Conclusions

Drain-blocking activities can help increase water table levels thus reducing DOC production and fluvial organic C export (Wilson et al., 2011b) – the benefit to downstream water quality is such that this is considered a good peatland management tool (Wilson et al., 2011a). Furthermore, wetter conditions (higher water tables) promote increased rates of C sequestration (Clymo, 1984; Kalbitz et al., 2000). As such drain-blocking was undertaken at Gordonbush.

WTD has been shown to be very dynamic and change quickly (hourly) in response to meteorological conditions, especially rainfall after dry periods. This dynamic response is hidden when only manual measures of WTD are considered and justifies the needs for investment and installation of instruments capable of measuring changes at a sub-hour frequency. Such equipment becomes important when trying to consider and quantify the effect of water table drawdown related to aspects of wind-farm construction on peatlands as well as how long monitoring should continue after construction has finished, quantifying the legacy of any impact.

No statistically significant differences in WTDs before and after drain-blocking were detected. Water table drawdown is greatest up to 2 metres from drainage channels and this continues to be so in the first year after the drains have been blocked. Observations from WTD in PT time series indicate that drainage channels have an impact up to 25 m and that drained areas of peat are more susceptible to increased water table drawdown during periods of drought. Drain-blocking does not seem to have an immediate effect strong enough to buffer climatic conditions in the first year after blocking. For extreme events this is unlikely anyway – the ‘control’ water table also responded and this site is less susceptible to enhanced drainage. Thus the exceptional dry summer in 2013 may have offset potentially positive responses.

[DOC] in drainage channels was greater in summer months after drain-blocking had been implemented. However this could also reflect meteorological forcing (June-September 2013 drought) and associated evaporation increasing [DOC] rather than re-wetting up of oxidised peat. Despite a reduction in mean [DOC] between drain and river samples, a positive effect of drain-blocking reducing [DOC] cannot be concluded from one years’ post-blocking data. Future work estimating discharge from drains and increased spatial sampling of [DOC] is recommended to further deduce the longer-term impact of blocking.

Thus to accommodate short-term variability in response induced by other factors, monitoring programmes may have to be longer e.g., one to five year periods after blocking

(Holl et al., 2009; Armstrong et al., 2010; Wilson et al., 2010). Additional monitoring is advised not only to further assess the impact of drain-blocking might have on data collected during this study (inclusion of PTs near to drainage channels to better assess changes in WTD) but to expand knowledge of interactions between ecology and hydrology. Having a better understanding of the wider implications of carbon cycling at the drain-blocking site will help assess if peatland restoration is improving the C sink potential of these areas. This should include vegetation surveys to monitor if blocking if helping re-establishment of more *Sphagnum* species (Armstrong et al., 2010; Armstrong et al., 2012; Peacock et al., 2013b) and the source of the DOC as assessed from quality (Strack et al., 2015). If considering a full-site C balance, whether drain-blocking impacts $CH_4$ emissions (Cooper et al., 2014) could be explored – drainage systems are easier to study that the terrestrial system in this context as gas concentrations are more homogenous along length.

The HMP has other objectives, and it may be of interest to assess if the drain-blocking has attracted local wading nesting species who like a wetter habitat. e.g. golden plover and dunlin (Douglas & Pearce-Higgins, 2014). This is a goal of SSER's Gordonbush HMP. Additionally, the general public, stakeholders and landowners perhaps need a better appreciation of the magnitude of time needed for improvements, e.g. WTD increases to occur at drained sites, and that restoration rates will differ from site to site. In turn this requires the science community to better communicate results of such studies and the other benefits of peatland restoration to the general public and their well-being e.g. reduced [DOC] leads to less chlorination and potential carcinogenic by-products in drinking water supplies (Martin-Ortega et al., 2014) or in a Highland context, maintaining optimal conditions in commercially and ecologically important rivers for salmonids.

# 9 Conclusions

## 9.1 Abstract

The evidence from chapters 5 and 6 demonstrates that windfarm construction may have increased C and P export in affected catchments; however, the results suggest that this impact may only be short lived (<2 years). Peat C sequestration rates at Gordonbush are comparable to similar locations, and along with aquatic organic C fluxes, provide an understanding of minimum sequestration rates required for this wind-developed site to maintain a C 'sink' status. In Chapter 8, even 2 years after drain blocking had been initiated, the water table still responded strongly to meteorological conditions (predominately rain and temperature). While it may be an effective long-term (>5 years) restoration tool, the process of drain blocking does not yield significant rises in WTD in the short term (<2 years). Furthermore, during very dry periods, and even 25 m from drainage channels, data suggests water table drawdown was more severe in areas of high-density drainage than a control (un-drained) site. Future research should focus on reducing uncertainty in areas of the C cycle already measured, e.g. refining estimates of C export through improved DOC modelling, modern sediment export estimates, and identifying sources of C. Additional best management practices to current guidelines are:

1. Continuation of regular monitoring of aquatic C and P species to fully assess the impacts of windfarm construction in future years.
2. Monitoring sediment accumulation in construction site silt traps.

Overall, this research has contributed to the wider knowledge base by producing additional estimates of aquatic organic C fluxes, peat and lake C sequestration rates in the North East Scotland region, as well as novel data documenting sediment export from peatlands. In addition, the extent of water table draw down in densely drained areas could be utilised to improve estimates of 'carbon payback' times for windfarms.

## 9.2 Summary of key findings

Understanding biochemical processes in disturbed peatlands is essential to assessing the impact of windfarms, as society strives for increased energy capacity. This understanding can then be used to inform the decision-making process on how to manage, and restore, our peatlands responsibly (Zak et al., 2010). This type of research is also becoming a core part of many Habitat Management Plans (HMP) for windfarm sites and is in keeping with Principle 4 of 'Windfarms and Peatland Good Practise' to 'support applied research into key areas of peatland science relevant to understanding the impacts of development on the various peatland qualities including biodiversity, C and hydrology' (Scottish Renewables et al., 2012).

My PhD thesis had two principal aims:

1. To assess if windfarm construction causes changes in river [C] and [macronutrients] and if so, how long the response prevails for.

2. To examine particulate C and sediment accumulation and export from the landscape over timescales longer than windfarm construction, to provide a historical context for assessing the significance of potential losses during the construction period.

My research shows that aquatic [C], [P] and [N] species were within observed ranges of similar biogeochemical studies at other northern peatland locations, including both sites impacted by windfarm construction and 'natural' undisturbed peatlands. The water quality in all three rivers, assessed using site-specific criteria for [P] outlined in the EU WFD, was 'High' or 'Good' status throughout the data collection period, spanning both construction and post-construction stages between July 2010 and September 2013. Annual aquatic organic C fluxes of 9-25 g C $m^{-2}$ $yr^{-1}$ are similar to other comparable sites. DOC accounted for ~90 % of total aquatic organic C fluxes, and hysteresis plots proved to be an effective tool to separate different [C]-discharge relationships; not only through different periods of the year, but also on rising and falling limbs of storm hydrographs.

Without any pre-construction data it is a challenge to assess the scale, prevalence and potential impact of windfarm construction on [macronutrient], water quality and aquatic C fluxes in real time. However, [P] was higher in GB10 than GB11 and GB12. Since GB10 was the only catchment affected by forest felling (Bull Burn Plantation) it is likely that organic debris left behind after felling (and subsequent breakdown of this material) are the source of this [P]. The concentrations decreased at GB10 throughout the research period indicating the impact was largest in the first year after felling.

C export from GB12 showed little inter-annual variation, whereas flux estimates decreased each year between 2011-2013 in both GB10 and GB11. Compared to the control catchment of GB12, these changes imply that C fluxes have become elevated in GB10 and GB11 in 2011 and 2012. Discharge was also higher in these years and so these higher exports may represent more soil-flushing. However, this change in GB10 together with the increase in [P] suggests that the increased exports are a signal of disturbance from the windfarm. The relative short time-scale of the data set (three years) means that fully assessing inter-annual variability in C fluxes between catchments is challenging. Calculated C fluxes in 2013 were comparable in all three catchments

suggesting that if there was an impact it was possibly short-lived, again indicative of a similar response in [P].

Average long-term peat C sequestration rates were calculated between 20-25 g C $m^{-2}$ $yr^{-1}$ at the two sites in Gordonbush, which falls within the ranges reported from other northern temperate peatlands. Due to the uncertainties in the core chronology from Loch Brora a direct comparison of C sequestration to peat cores was not made, and therefore assessing if a sink-source relationship existed between these two terrestrial C-stores was difficult.

Establishing a robust chronology for the Loch Brora core was not possible meaning determining the long-term C sequestration for the lake was difficult. The distribution of radiocarbon ages for the sediment core was not stratigraphically aligned, with a number of older dates occurring towards the top of the core. The most parsimonious explanation for this is that pre-aged carbon has been incorporated into the lake sediments from old DOC or POC that has eroded from the peat catchment. The 'young' radiocarbon age at the base of the core would be more difficult to explain, and therefore we assume it has been lain down *in situ*. However, all estimates based on this resulting age model must remain conservative. If this basal age is used, it calculates a long-term average C sequestration in Loch Brora of 61.8 g C $m^{-2}$ $yr^{-1}$, which provides an upper limit of any potential annual C storage. A long term average lake C sequestration rate of 61.8 g C $m^{-2}$ $yr^{-1}$ only suggests ~8 % of POC delivered to Loch Brora contributes to this sequestration. This upper limit is comparable to other organic C burial efficiencies in Finnish lakes located in peatlands (Einola et al., 2011; Sobek et al., 2011; Fenner & Freeman, 2013). While this figure implies that Loch Brora sediment will not act as a strong C 'sink' for any potential increased POC losses, greater chronological control may revise this figure down.

Contextualising modern and historic sedimentary C export is hampered by a lack of similar studies, but most sediment appears to be delivered to Loch Bora during only a small number of the biggest storm events. Even when normalised for catchment size, the average mass of sediment collected at GB11 sediment trap was three times greater than GB12. Whether this is a result of the physical differences in catchment characteristics between the two or a windfarm-related impact is difficult to assess. In any case, the calculated peat and lake C sequestration, and modern sediment export suggests that the flow of organic C is a key terrestrial and aquatic process at Gordonbush and it provides a baseline for further assessment of disturbance (Figure 9.1).

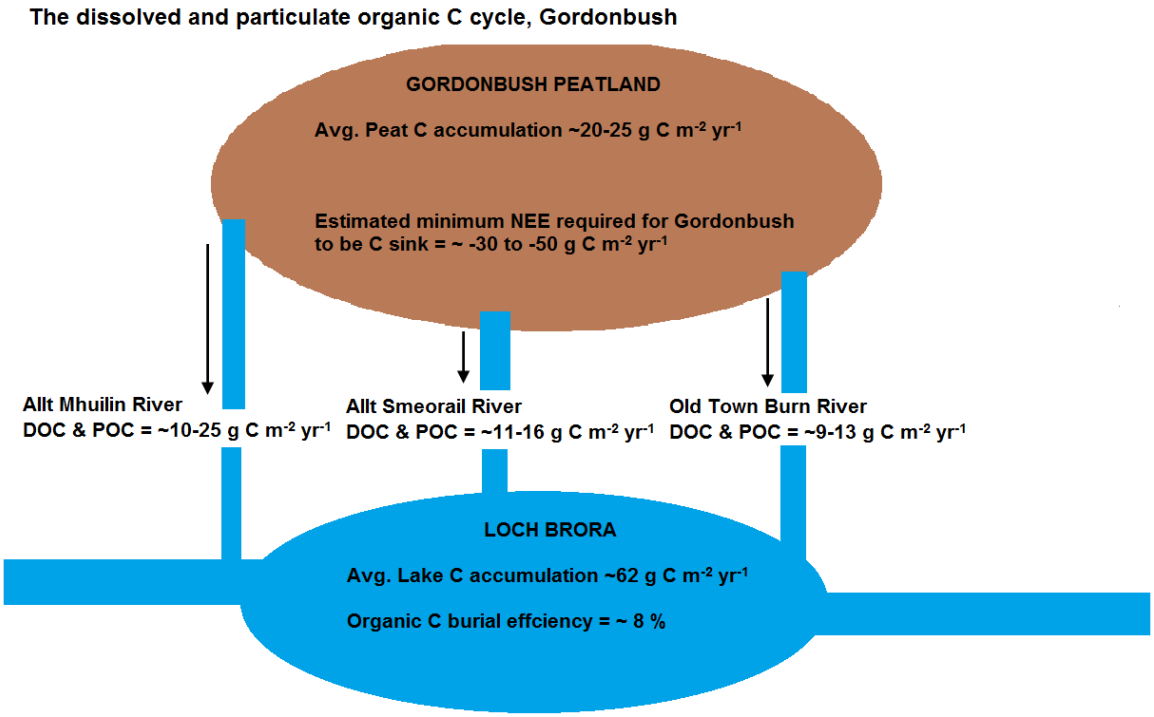


**Figure 9.1 - The dissolved and particulate organic C cycle, Gordonbush**

Aquatic organic C fluxes and peat C sequestration rates are of similar scales (Figure 9.1). Therefore, it can be estimated NEE rates would need to be between -30 and -50 g C $m^{-2}$ $yr^{-1}$ for Gordonbush peats to be a C 'sink'. Although measurements of peatland NEE were out-with this research, the advanced understanding of C cycling, generated over several years (Figure 9.1) provides a basis for exploration of the full C cycle to ascertain whether of Gordonbush is a sink or source of C.

## 9.3 Potential research directions

This research has contributed to a better understanding of the impacts of windfarm construction within a peatland environment on C and nutrient cycling. Future research should balance targeting subject areas crucial to reducing uncertainty associated with current understanding. Additionally, during this research certain topic areas have emerged which would generally benefit from extra study, irrespective of whether the C-rich landscape hosts a windfarm.

### 9.3.1 Development of *in-situ* sensor technology and remote modelling of DOC

Given the labour intensive and expensive nature of collecting event sampling data, I would propose that effort should be spent developing a cost-effective, portable device capable of

measuring [DOC] *in-situ*. Devices and sensors currently exist that measure [DOC] via spectrophotometery (Sandford et al., 2010) (manufacturers e.g., TriOS and s::can) and they provide much higher data resolution than manual sampling. However, these systems rely on complex algorithms, which are needed to convert wavelength measurements into [DOC], and are not particularly portable. If a cost-effective and portable system could be developed that measured [DOC] *in-situ* the higher resolution data would generate greater detail of aquatic DOC export in many different climate locations (peatland distributed globally and among different climatic zones). This type of technology would help increase understanding of the terrestrial C cycle as well as better monitor and detect changes within ecosystems, e.g. potentially induced by climate change.

Estimations of DOC fluxes (the main component of aquatic organic C fluxes) are not commonplace and a cheaper alternative, compared to spectrophotometry sensors, could be to focus on measurement of variables highlighted to be significant using MLR analysis to characterise aquatic [C] (and subsequently calculated C fluxes): air temperature, alkalinity and days since rainfall. However, in the future, it would be advised that more time could be spent developing more advanced models of [DOC] and export. DOC-discharge dynamics are complex and affected by weather, location, specific flow paths and residence times pertaining to surface water and groundwater (Futter & de Wit, 2008; Mei et al., 2012). To improve estimating aquatic organic C fluxes from peatlands, or any other terrestrial environment, an approach that integrates empirical data and process-based modelling (e.g. modelling the rate of transfer of DOC from soil profile to rivers under varying hydrological conditions) should be adopted.

### 9.3.2 Investigation of C sequestration in NE Scotland

Different climate change scenarios predict conflicting outcomes for peat and C sequestration: increased photosynthetic active radiation (PAR) could lead to enhanced *Sphagnum* (Loisel et al., 2012) growth and subsequently increases in C accumulation rates in peatlands (Loisel & Yu, 2013; Quillet et al., 2013). Conversely, more droughts will cause peats to dry out and decomposition to exceed sequestration rates (Charman et al., 2009; Charman et al., 2013). In lakes, any predicted rise in temperatures will likely increase organic C mineralisation and reduced sequestration (Gudasz et al., 2010) whereas anthropogenic activities and landscape disturbance will continue to cause lakes to become more eutrophic (Smith, 2003) potentially enhancing C sequestration rates (Anderson et al., 2014; Pacheco et al., 2014).

Understanding how significant C sequestration and export changes, within and from, peat and lakes will be in the future relative to the past would still have a stronger foundation by

a better understanding of long-term C sequestration in lakes and peatlands. Given the lack of literature found to locally contextualise Gordonbush results, I would suggest more research of this nature is needed in NE Scotland. The Flow Country is Europe's largest expanse of blanket bog and thus an important area of soil C storage (estimated to store 400 million tonnes of C (SNH, 2014)). Therefore, examining how C cycling within this region has changed in the past may aid better understanding of current changes and help design and implement management practices which will offset some of the negative effects of climate change (IPCC, 2014a). Relating to this research, obtaining a robust radiocarbon chronology from Loch Brora and a number of other lochs in the region would be a priority. This in turn would allow a more thorough investigation of the magnitude of influence peat systems exert on lake C capture within different catchments. How both ecosystems have responded to past climate change will help infer C cycling changes that might occur in the future so extra investigation is needed (Sobek et al., 2009; Buffam et al., 2011; Yu, 2012; Anderson et al., 2014; Pacheco et al., 2014).

Environmental conditions can greatly affect C sequestration in peats and lakes. This in turn affects the ecology so tracking changes in species assemblages can help infer past environmental conditions. In peats the level of the water table can greatly influence C sequestration rates. Investigating diatom assemblages in peat cores has been successfully used as method of paeleo-climatic reconstruction, in particular bog-surface wetness (Hargan et al., 2015). In lakes, C sequestration is said to generally be lower in heterotrophic (Einola et al., 2011; Sobek et al., 2011; Fenner & Freeman, 2013) compared to autotrophic lakes (Jansson et al., 2000; Hanson et al., 2004; Gudasz et al., 2012). Analysis of biogenic silica within Loch Brora sediment may help to understand switches between heterotrophic and autotrophic environments (Fritz & Anderson, 2013) helping to identify natural variability in ecological status and how this influences lake C sequestration. Additionally, similar to peats, diatom analysis could be applied to Loch Brora core sediment to investigate changes in climate over the 1000s of year's timescale and, to sediment trap samples to assess seasonal changes in species population. Tracking modern day diatoms species, indicative of particular environmental conditions including nutrient status and acidity levels, could help evaluate any potential ecological impact of windfarm construction (i.e. any potential extended draw down of water tables) as well as further contextualise diatom analysis results from historic peat and lake sediments. Assessing past ecological changes may help influence management policies to ensure that lakes are net sinks rather net sources of C to mitigate future climate change affects.

### 9.3.3 Identifying sources of C and refining modern sediment export estimates

To refine estimates of sedimentary export and better assess the impact of windfarm construction, it would be valuable to continue monitoring sediment traps located in Loch Brora. This monitoring might be aided by deployment of additional sediment traps in this area to try gaining more information on the natural variability of sediment export at the mouths of both Allt Smeorail (GB11) and Old Town Burn (GB12) rivers and how representative the sediment yields measured here are of sediment delivery.

It may be worthwhile to obtain radiocarbon dates for samples collected from sediment traps. This would help distinguish the source of sedimentary C from the catchment. It might be hypothesised that catchments that are unaffected by construction or disturbance would export predominately 'young' C, whereas wind-farm affected catchments, construction activities may expose deeper and older layers of peat that could be susceptible to erosion and old POC export.

Floculation of DOC can increase POC inputs and contribute to C sequestration (Dillon & Molot, 1997; von Wachenfeldt et al., 2008) but the extent and controls on the mechanism are poorly understood (von Wachenfeldt & Tranvik, 2008; Anderson et al., 2014). Considering DOC accounts for ~90 % of aquatic organic C export, future research quantifying DOC-POC floculation rates would be worthwhile and further add to knowledge of C sequestration controls in Loch Brora but and the wider terrestrial-aquatic C cycle.

### 9.3.4 Investigation of gaseous C losses from peats and lakes

This research has focussed on aquatic and sedimentary C fluxes and it would be interesting to investigate gaseous C losses on the Gordonbush estate in three areas:

1. The scale of $CO_2$ evasion from rivers during the full range of hydrological conditions, similar to aquatic sampling of [DOC] and [POC] undertaken on this project, e.g., (Dinsmore & Billett, 2008).
2. The installation of an Eddy Covariance tower on the peatland plateau within the catchment area of Allt Mhuilin (GB10) or Allt Smeorail (GB11) catchments, would allow $CO_2$ and $CH_4$ emissions from peatland surface to be monitored and NEE rates could be calculated (Koehler et al., 2011).
3. Given it was estimated that ~90 % of particulate C deposited in the lake was not sequestered on a long-term basis, a study designed to investigating the fate of this particulate C would be worthwhile (Aufdenkampe et al., 2011; Raymond et al., 2013).

By measuring $CO_2$ evasion from rivers, a more detailed understanding of aquatic (organic and inorganic) C fluxes from Gordonbush catchments would be generated. Calculating peatland NEE would allow the significance of calculated of peat sequestration rates and aquatic C budgets to be fully assessed, and an evaluation of Gordonbush's current C storing status (i.e., sink or source).

Through measuring $CO_2$ evasion from Loch Brora, rates of mineralisation could be estimated and the proportion of C sequestered in lake sediment or transported further downstream could be better gauged. This type of information would offer a better insight into the fate of C transferred between peatland and lake ecosystems at Gordonbush and add to the relatively small field of whole catchment C balance studies (Worrall et al., 2003; Dawson & Smith, 2007; Worrall et al., 2009; Billett et al., 2010; Rowson et al., 2010; Buffam et al., 2011; Worrall et al., 2011; Dinsmore et al., 2013).

The research areas suggested in this section and the previous three sections (9.3.1, 9.3.2 and 9.3.3) would all enhance understanding of the terrestrial C cycle but also allow a broader perspective (and knowledge) to be gained between processes transferring C from fluvial and terrestrial pools (C sources) to the oceanic environment (C sinks).

### 9.3.5 Continued monitoring at (drain-blocking) peatland restoration site

There remains a need to further understand how best to restore degraded peatland sites. One suggestion is to undertake more meta-data analyses using data collected from multiple peatland sites (Evans et al., 2014). The IUCN has a target of restoring 1 million hectares of peatlands in the UK back to 'good condition' by 2020 (Bain et al., 2011) and studies have been commissioned to help identify conservation priorities e.g., (Artz et al., 2014). However, it is important that realistic restoration targets are determined and palaeoecological studies (e.g. the study of diatoms by (Hargan et al., 2015) previously mentioned) can help provide an historical context of blanket peatland condition, i.e. bog surface wetness, and support future peatland management (Blundell & Holden, 2015). To fully assess the effectiveness of drain-blocking at the Gordonbush peatland restoration site I would advise the following:

1. Water table depth monitoring should continue for at least another 3 years as statistically significant positive effects, e.g. rises in water table, have not been observed until 5 years of monitoring has been undertaken (Martin-Ortega et al., 2014). The installation of additional PTs may be advantageous; locating one in an area of drainage channels which has not been blocked could be used to compare with data collected from the drain PT used in this research, which indicated WTD

was still affected 25 m away in a densely drained area. Further, a PT located within 2-5 m of a drainage channel could help detect and quantify how long it takes for drain-blocking to raise WTD closest to the drains.

2. Vegetation type distribution can be an indication of WTD (Lafleur et al., 2005; McNamara et al., 2008) and influences [DOC] export from peatland catchments (Armstrong et al., 2012). Establishing peat-forming *Sphagnum* species is seen as a crucial step to return areas of suspected C sources e.g. drainage channels, back to C sinks (Glatzel et al., 2004; Waddington et al., 2010). Considering this, it may be beneficial to survey vegetation at the drain-blocking site and investigate if any potential positive affects in raising WTDs and reduced [DOC] and export are observed in the present plant communities. Also vegetation monitoring can relate, by proxy, to GHG emissions and quantifying the impact of these, especially $CH_4$, can help assess the timescale taken for drain-blocking sites to re-establish C sink status (Vanselow-Algan et al., 2015).

3. Monitoring of [DOC] should be continued but combined with the estimation of discharge from drainage channels so DOC exports can be calculated and the effectiveness of drain-blocking as a technique to reduce DOC export, and actively encouraging the retention of C within peatland, can be critically assessed. Analysing DOC quality may also help assess the effectiveness of drain-blocking to reduce C export and increase WTD (Strack et al., 2015). Similar to the effects of drainage on DOC, lower water tables and subsequently increased aeration and decomposition can increased P and N export from peatlands (Devito & Dillon, 1993; Zak & Gelbrecht, 2007; Geurts et al., 2010) and decrease their effectiveness as natural nutrient sinks (Zak et al., 2008). This response, coupled with a changing future climate projecting increased rainfall intensity (IPCC, 2014a), and hydrological flow being an important control on P release from peats (Dunne et al., 2010), means enhanced aquatic nutrient availability could cause ecological related problems downstream (Kjaergaard et al., 2012; Surridge et al., 2012). Given the economic and ecological importance of high water quality in Scottish Highland rivers to maintain healthy salmonid populations then integrated monitoring with related organisations this type of problem could affect, more investigation of P and N export from drain blocking areas might be worthwhile.

To achieve goals of peatland restoration, the benefits of restoration need to be measured and better communicated to the general public and landowners. The scientific community need to demonstrate and translate more effectively how the condition of peatlands might affect society's well-being, e.g., reduced [DOC] leads to less chlorination and potential

carcinogenic by-products in drinking water supplies (Martin-Ortega et al., 2014); peat restoration can significantly reduce GHG emissions helping meet climate targets and goals of other policies (EU Habitats directive and WFD (Bonn et al., 2014b). Additionally, scientists need inform and get the general public to appreciate, the magnitude of any improvements and the time taken for such improvement to be noticed (e.g. WTD rise from drain-blocking), will differ from site to site (Martin-Ortega et al., 2014).

## 9.4 Recommended future management practices for building infrastructure projects on peatlands

It has been suggested that building windfarms on peatlands may not result in net C savings, and so by siting windfarms on peatlands in good condition should be avoided (Maslen Environmental, 2009; Smith et al., 2014). However, if such renewable energy projects are to be constructed on terrestrial carbon stores, guidance exists to minimise C loss: 'Good practice windfarm construction' (Scottish Renewables et al., 2013), peat excavation and re-use (Scottish Renewables & SEPA, 2012) and 'Good practice principles' (Scottish Renewables et al., 2012). It is important to consider how this research and proposed future research could augment the best management practices that should be followed when constructing on peatland. Relevant present guidelines are first presented below:

1. Peat excavation should always be minimised with regards to depth and extent when and where possible.
    a. Track length should be minimised, building on the shallowest peat.
    b. Run necessary cabling alongside existing roads
    c. Only open up borrow pits on the shallowest peats to minimise size and number. Borrow pits should only be opened when it is not viable to import aggregate from off-site.
    d. Full planning must be in place regarding all excavation and how this is going to be used, i.e. backfill borrow pits
2. Peat should be handled carefully retaining the structure and integrity of excavated materials and should always be re-instated as soon as possible. Excavated pieces of peat should be large as they dry out slower, also spraying peat to keep moist, both measures increases successful re-instatement. Moving peat around sites should be avoided.
3. Windfarm infrastructure, e.g. roads, should be constructed in a way where catchment drainage characteristics are maintained and this involves evaluating track design during the construction process, meaning potential changes from previously planned designs.

4. The use of silt traps to prevent excess sediment from roads or borrow pits freely entering water-courses. This measure is also recommended by (Nayak et al., 2008; Nayak et al., 2009).
5. Submerged foundations, capable of withstanding uplift due to water pressure, should be employed at turbines bases to maintain natural hydrology rather than draining peat.
6. Developers should take pro-active action on peatland restoration initiatives, e.g. drain-blocking.

Increases in sedimentary export have been directly attributed to wind-farm construction in Scotland before due to poor contingency drainage infrastructure (Grieve & Gilvear, 2008). For silt traps (recommendation No. 5), to maintain their effectiveness, they need to be regularly cleaned out especially after periods of heavy rainfall. This practice was employed at Gordonbush but an additional approach to routine emptying could be to monitor sediment accumulation depth which may highlight areas of particularly high and changes in erosion rates, such that mitigation practices could be implemented more efficiently.

In addition to recommendation No. 6, to reduce loss of stored C, is it important to maintain a high water table, and drain blocking has been shown to be a cost-effective restoration management tool to do this. Engagement with all stakeholders is an important part of this process where the benefits of such actions should be clearly presented, funding for restoration initiatives made available and reliable information on best practices to follow (Connolly & Holden, 2013).

As increases in [SRP] and [TP] were observed in Allt Mhuilin, adjacent to forest felling activities, a further recommendation could included the installation of buffer zones around felled forestry areas. Grassed buffer zones are more effective at retaining P after forest harvesting than non-grassed zones (Asam et al., 2012). However, this may not be appropriate to the habitat and so peatland vegetation in a buffer strip could also help, as it can act as a long-term P sink and slow the flow of water increasing soil contact time and likelihood of absorbance (Asam et al., 2012). Although brash mats are used to improve soil bearing capacity of harvesting machinery (Asam et al., 2012), best practice could include clearing felled forestry material as this may reduce impact of nutrient concentrations in adjacent streams. Leaving mulched material would be a bad idea as mulching methods can increase P release (Rodgers et al., 2010).

Furthermore, in addition to increases in [P], potential increases in aquatic [C] have been observed at Gordonbush in the first and second years following the start of construction

activities in windfarm affected catchments. Therefore, regular monitoring of [C] and [SRP], especially in the initial stages of construction when soil disturbance (or forest felling) is at a maximum, would allow early detections of increased C and nutrient export such that mitigation practices could be implemented e.g., grass seeding immediately after felling (O'Driscoll et al., 2011). Designing a monitoring programme where measurements are taken prior to, as well as at multiple controls and impacted sites during construction is necessary to really assess impact. Doing so helps separating the effects of inter-annual variability from a construction impact and improves the robustness of any analysis. Therefore, regular and well designed monitoring, before, throughout and after construction would allow the establishment of long term data sets which would be a fantastic resource to fully understand impact of windfarm construction activities at Gordonbush in the coming years and other peatland windfarm developments.

## 9.5 Research contributions to the wider-knowledge base

Environmental impact assessments on the legacy of windfarm construction on peatlands remain rare. This research has helped to add to the existing knowledge base and provide some new information which can be potentially utilised in future studies. The main contributions are summarised below:

1. Estimates of aquatic organic C fluxes in the North East of Scotland are lacking and so this research helps create a data set as detailed as found elsewhere in other parts of Northern Europe. These results add to the evidence that in these systems seasonality and discharge remain important drivers of changes in [DOC], and DOC is the dominant component of aquatic organic C fluxes from northern temperate peatlands.
2. This is only the second study (the other being (Murray, 2012)) to show increased [SRP] and [TP] in a river adjacent to a forest felled area as a result of windfarm construction activities.
3. Estimates of peat and lake (even though Loch Brora results must be treated cautiously) C sequestration rates have been calculated in an area where previous studies are not numerous. This could also be of value to palaeo-environmental researchers interested in Holocene climate change (as evidenced by C sequestration rates). Studies examining rates of sediment export from peatlands, by using sediment trap data, do not appear to have been undertaken elsewhere, so this research is highly novel.
4. A novel curvi-linear relationship was identified between [DOC]-[SRP] which is worthy of further investigation to fully assess what mechanisms are controlling SRP export from peatland ecosystems.

5. I demonstrated that in absence of *in-situ* [DOC] sensor, monitoring alkalinity, pH, air temperature and rainfall could offer the best way of inferring [DOC] from the measurement of physical parameters.
6. While evidence suggests the impact on WTD is most severe ~2 m from drainage channels, data from PTs imply the effect of increased drainage density can influence WTD to a distance of ~25 m away. Lateral extension of drainage impacts has previously been suggested (e.g. to 20 m, Lindsay 2010), but this is one of few studies to investigate this area in more detail. Evidence collated at Gordonbush also suggests that meteorological conditions exert the most control on WTDs compared to drainage channels or, less so, topography.
7. This research has highlighted key gaps in peatland science knowledge, how certain data could be better constrained and areas where future research should focus. Therefore, this research and the data collected has provided a good basis for additional work to be undertaken which in the future could better inform inputs required by the 'carbon payback calculator' to assess the environmental impact of windfarm construction.

In summary, this research has led to a greater understanding of landscape adaption and resilience, with particular reference to effects of windfarm construction on the C cycle within peatland environments. The discussion on future research directions has highlighted exciting and novel opportunities that could be explored, and would enhance the results from this work. The scope of future research possibilities demonstrates the wide range and complexity of terrestrial C and nutrient cycling. However, in current funding regimes, fully integrated programmes are unlikely. Thus more cost-effective and automated (including remote modelling) alternatives need to be explored (Bonn et al., 2014b). Understanding the value of ecosystems services of peatlands remains crucial for selecting and designing effective policies that will best utilise, sustain and restore them (Reed et al., 2014). Knowledge exchange activities have not been explored here, but this may be a sensible approach to assessing where best, in the future, to focus effort so as scientific interest and stakeholders needs are fully integrated.

# Appendices

# Appendix A – Reconstructing stage heights

The collection of stage height data from the three studied rivers at Gordonbush did not start until November 2010 in GB10 and GB11 and December 2011 in GB12. However, aquatic organic C fluxes were calculated from when storm event sampling began which was in August 2010. Therefore, an approach was required to reconstruct stage height during the missing time periods (presented in Table A.1) so that discharge, needed to compile aquatic organic C fluxes, could be estimated. Stage height data also needed to be inferred from June to September 2013 in GB10 as a fault occurred at the PT located there in June 2013 and it was not operational after this date.

| River | Recorded Stage | Missing Stage |
|---|---|---|
| **GB10** | 17/11/10 to 24/6/13 | 1/8/10 to 17/11/10 and 24/6/13 to 16/9/13 |
| **GB11** | 18/11/10 to 16/9/13 | 1/8/10 to 18/11/10 |
| **GB12** | 13/12/11 to 16/9/13 | 1/8/10 to 13/12/11 |

**Table A.1 - Recorded and missing stage height data**
Dates of recorded and missing stage height in all three Gordonbush rivers.

To reconstruct missing stage height data, relationships between long-term SEPA monitoring stage height records at Bruachrobie ((NC) 892039) on the River Brora and installed PTs in Gordonbush river catchments were investigated. For each relationship considered time lags between data sets were identified and corrected for using cross-correlation techniques. This was possible as both River Brora and Gordonbush stage height data sets had a resolution of 15 minutes. Figure A.1 demonstrates the time lag between River Brora and Gordonbush rivers (stage from GB10 is used an example).

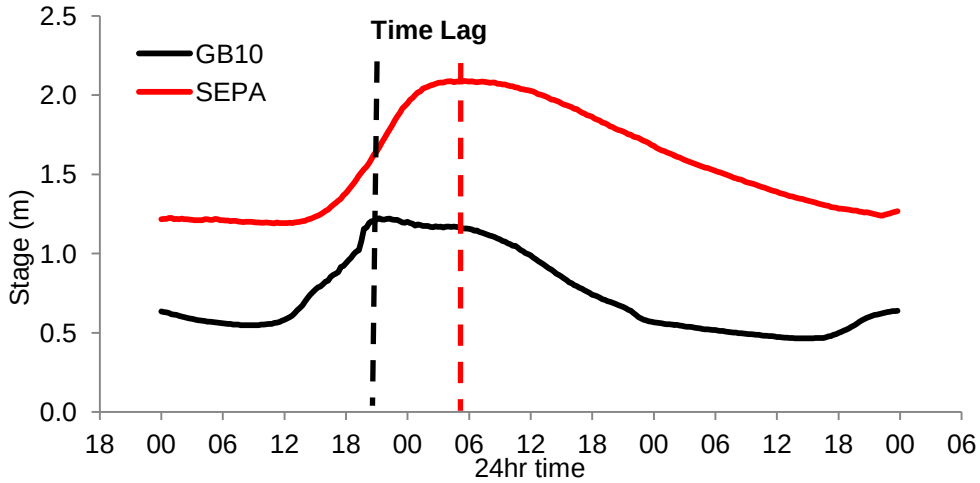


**Figure A.1 - Gordonbush and River Brora stage height time lag**
Stage height profiles show a storm event which occurred in January 2011. Black and red dashed lines highlight when peak stage height was reached in both rivers, for GB10 it was 4/1/12 21:15 (1.22 m) and SEPA (River Brora) 5/1/12 05:30 (2.09 m).

Stronger relationships between stage height data sets were produced when both data sets were log transformed to improve homoscedasticity (McDonald, 2009). After cross-correlation analysis, the lag time that was most statistically significantly between the two data sets was selected and data sets shifted accordingly. For example, the most significant lag time between GB10 and River Brora data sets was 9 hours, therefore when regressed; stage height of River Brora at 12am (midnight) was done so to infer stage height of GB10 at 3pm the previous day.

After the appropriate time lag had been applied, it was investigated whether regressing data sets using natural log transformations (again to reduce skewness) or the original data produced a better predictive relationship after time lag was applied. Where River Brora data was being used to infer stage height in GB10 untransformed stage height worked best, but for GB6 (located further upstream on Allt Smeorail than main sampling point GB11) and GB12, regressing stage height using data sets with natural log transformations produced a more significant linear fitted line. Table A.2 displays what cross-correlations were undertaken for each river, the data gap of stage height that the analysis help to fill, the value and statistical significance of the lag time and the resultant linear equation used to infer missing stage height from each river as well as the $R^2$ value of that relationship.

| River | Data Gap | Cross-Correlation data set | Lag number and time (hrs) | Lag significance (-1 to +1) | $R^2$ of Linear Regression |
|---|---|---|---|---|---|
| **Allt Mhuilin (GB10)** | 1/8/10 to 17/11/10 | River Brora (RB) (SEPA) | -36 = 9 hours | 0.90 | 0.83 |
| Regression | **GB10 SH** = 0.03 + (0.40*(RB SH)) – (0.11*(RB $SH^2$)) + (0.09*(RB $SH^3$)) | | | | |
| **Allt Mhuilin (GB10)** | 24/6/13 to 16/9/13 | GB12 (Uni. of Glasgow) | -3 = 0.75 hours | 0.88 | 0.79 |
| Regression | **GB10 SH** = 0.04 + (1.44*(GB12 Stage)) + (0.26*(GB12 $Stage^2$)) | | | | |
| **Allt Smeorail (GB6)** | 1/8/10 to 18/11/10 | River Brora (RB) (SEPA) | -47 = 11.75 hrs | 0.84 | 0.72 |
| Regression | **Ln GB6 SH** = -0.88 + (0.88*(ln RB SH)) +(0.32*(ln RB $SH^2$)) + (0.23*(ln RB $SH^3$)) | | | | |
| **Old Town Burn (GB12)** | 1/8//10 to 18/11/10 | River Brora (RB) (SEPA) | -40 = 10 hours | 0.86 | 0.74 |
| Regression | **Ln GB12 SH** = -1.41 + (1.02 * (ln RB SH)) + (0.09 * (ln RB $SH^2$)) | | | | |
| **Old Town Burn (GB12)** | 18/11/10 to 13/12/11 | Allt Smeorail (MNV Ltd) | +4 = 1 hour | 0.92 | 0.88 |
| Regression | **GB12 SH** = -0.11 + (1.14 * (GB6 SH)) - (0.76 * (GB6 $SH^2$)) + (0.21 * (GB6 $SH^3$)) | | | | |

**Table A.2 - River Brora Gordonbush river stage height time lags and regression equations**
The resolution of stage height datasets was 15 minutes so lag number were divided by 4 to give time lag in hours. Lag significance is measured on -1 to +1 scale, 0 meaning zero correlation, -1 and +1 equating to perfect negative or positive correlations respectively and the values presented represent the significance of the stated lag time. "$R^2$ of Linear Regression" is measure of fit between the two stage height data sets after the lag time has been applied and the equation associated was used to reconstruct stage height. This regression equation is presented for each cross-correlation undertaken. Stage height has been abbreviated to 'SH' in all regression equations in the table above.

As GB6 was located further upstream compared to GB10 and GB12 (where stage height was recorded near respective catchment outlets), this likely contributed to data from GB6 and River Brora being skewed the most. This is reflected by the most significant lag time between River Brora and GB6 points, of 11.75 hours, being the greatest of the three rivers (Table A.2). For GB12, when GB6 data existed, a better relationship was found with GB6 than River Brora data ($R^2$ = 0.88 for GB6 vs. GB12 compared to River Brora vs. GB12 = 0.74, Table A.2). Reasons for this are most probably related to the fact GB6 and GB12 have a greater geographical proximity and relatively similar catchments sizes, compared to GB12 and River Brora. Therefore, a GB6-GB12 relationship was used to predict GB12 stage height between November 2010 and December 2011 and River Brora data was used to predict GB12 stage height from November 2010 back to August 2010. A similar protocol was followed to process and reconstruct data as described earlier.

The types of linear equations that were selected were based on which gave the best fitted line. All relationships in Table A.2 are based on using the river specific "Cross-correlation data set" as the predictor variable (x) to estimate response variable (y) which is GB10, GB6 or GB12. Data from cross-correlation analysis regarding the use of River Brora data used to infer GB10 stage height from 1/8/10 to 17/11/10 is given as an example. A diagram of cross-correlation lag significance and the resultant linear regression is presented.

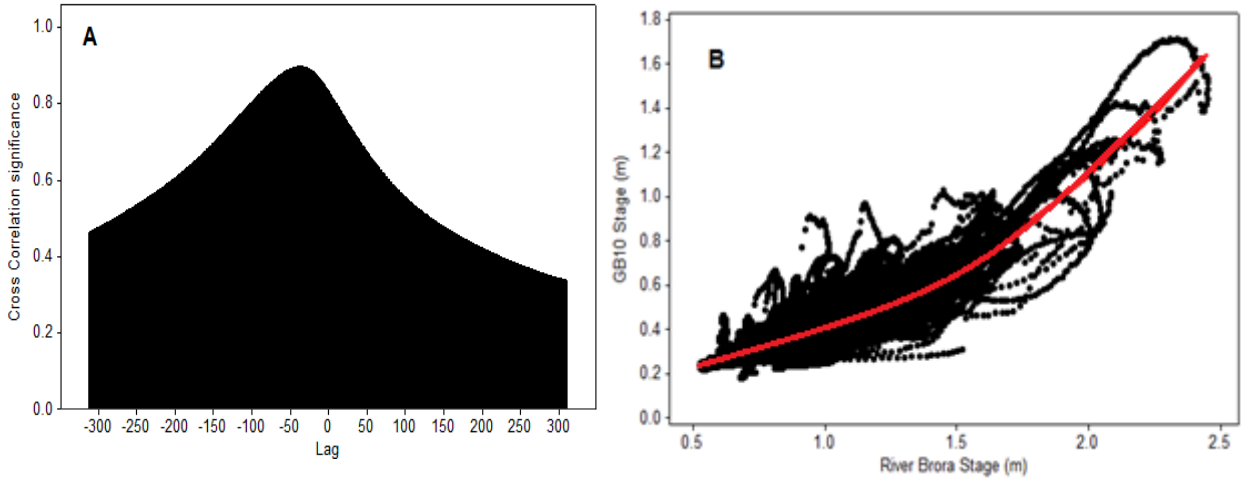


**Figure A.2 - Cross correlation lag significance and inferred stage height linear regression**
A = output of cross-correlation analysis of River Brora and GB10 stage height data. Lag significance peaks at -36. B = Resultant regression plot produced used to infer GB10 stage height from River Brora data. The red line shows the linear regression best fit line, the equation of which is presented in Table A.1 and had an $R^2$ value of 0.83.

# Appendix B – Complete stage height profiles

Below are the fully reconstructed stage height profile for all three studied rivers, Allt Mhuilin (GB10), Allt Smeorail (GB11) and Old Town Burn (GB12). GB10 and GB12 stage records run from 1st August 2010 to 16th September 2013. Data for GB11 stage was recorded for an extra year and is displayed from 1st August 2010 to 24th September 2014.

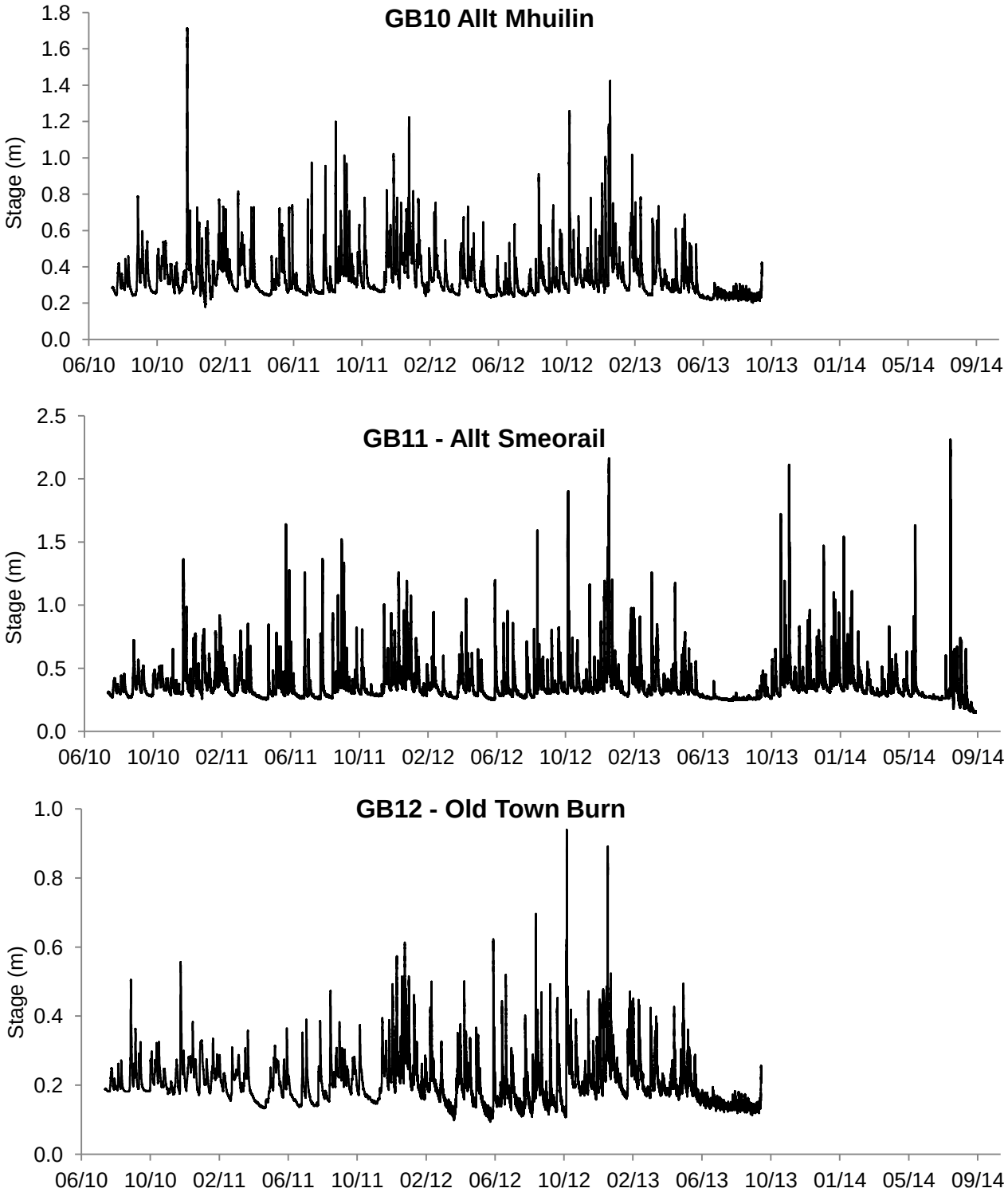


**Figure B.1 - Stage height profiles of all three studied Gordonbush rivers, Aug. 2010 to Sept. 2014**

# Appendix C – Editing discharge data

Some data collected by the ISCO 2150 flow meter (see section 3.6) was rejected. For example, during the largest storm events, the sensor moved from its original position on the river bed (where relationships between stage and cross-sectional area of river was pre-programmed into ISCO logger) and so was not collecting data relevant to where the ratings curve was collected. Alternatively, the quality of data collected by the sensor was of inadequate and not suitable for statistical use. This section will explain the criteria and data quality checks that were used identify these problems and present ISCO 2150 signal quality charts for discharge data used in construction of stage-discharge relationships for each river, Allt Mhuilin, Allt Smeorail and Old Town Burn.

## Sensor displacement

Precautions were taken during original deployment to ensure displacement did not occur however the problem transpired in the two largest rivers, the Allt Mhuilin and Allt Smeorail. During the storm event, 11th - 15th October 2012, the ISCO logger was deployed at sampling point GB11 (initially deployed 10/9/2012). The flow meter sensor became detached as the event approached its maximum discharge and was lost. Data was only used in creation of stage-discharge relationship before any suspected movement of the sensor took place. This was the only incident of sensor displacement in Allt Smeorail.

The ISCO logger was deployed in Allt Mhuilin at sampling point GB10 between 29/11/2012 to 10/4/2013. Upon returning to download data from instrument on 8/1/2013 and 10/4/2013, the sensor was not found in its original position, therefore it had moved. To identify what data could be used, the ISCO data was compared to the co-located GB10 MNV Ltd PT as the relationship should be linear e.g. Figure C.1. As a result, data from 15/12/12 to 8/1/13 and 9/3/13 to 10/4/13 to was rejected.

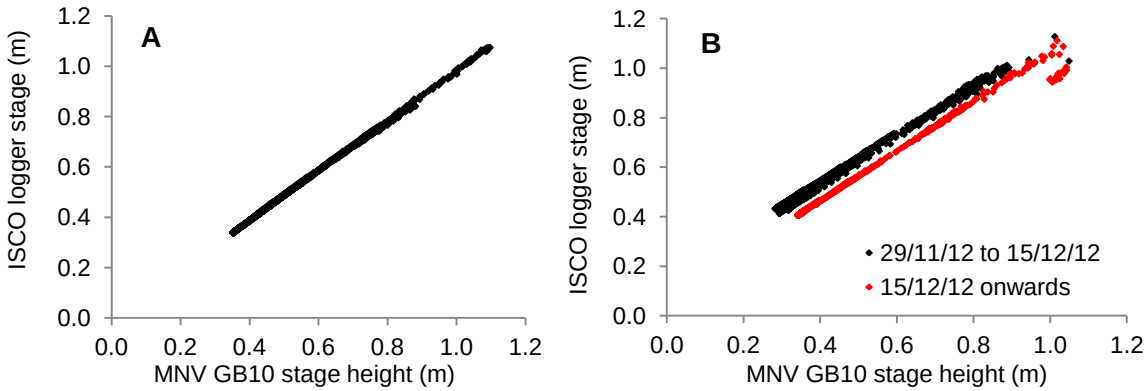


**Figure C.1 - Differences in stage heights of ISCO logger and MNV Ltd equipment at GB10**
A = an illustration of a 'good' relationship between ISCO and MNV Ltd pressure transducer between 8/1/13 and 19/2/13 indicating no sensor displacement during this time period. B = graph displays difference in stage height relationship after 15/12/12.

## ISCO 2150 flow meter data quality

Data was also rejected when it was apparent that the measurement of discharge it was recording was of poor quality, indicated by data collected by ISCO logger. Two signal diagnostics were recorded for every velocity reading taken, i) signal strength and ii) spectrum strength. A strong signal occurs when multiple particles are present within the flow stream for ultrasonic waves to hit and return a signal. In natural rivers, signal strength should typically be 40-65 % according to the manufacture. Spectrum strength is a proxy for strength of flow hydraulics in the stream and gives information on how much of the signal transmitted is received again by the sensor. A value of 100 % implies all of signals transmitted were received and 0 % effectively means no water is flowing. ISCO manufactures quote spectrum strength to typically be 40-60 % in natural streams, although a minimum of 20 % spectrum strength is needed and recommended for data collected to be considered valid. Presented (Figure C.2) is a signal quality chart for ISCO 2150 which acts a guide for users to check the validity of the discharge data they have collected.

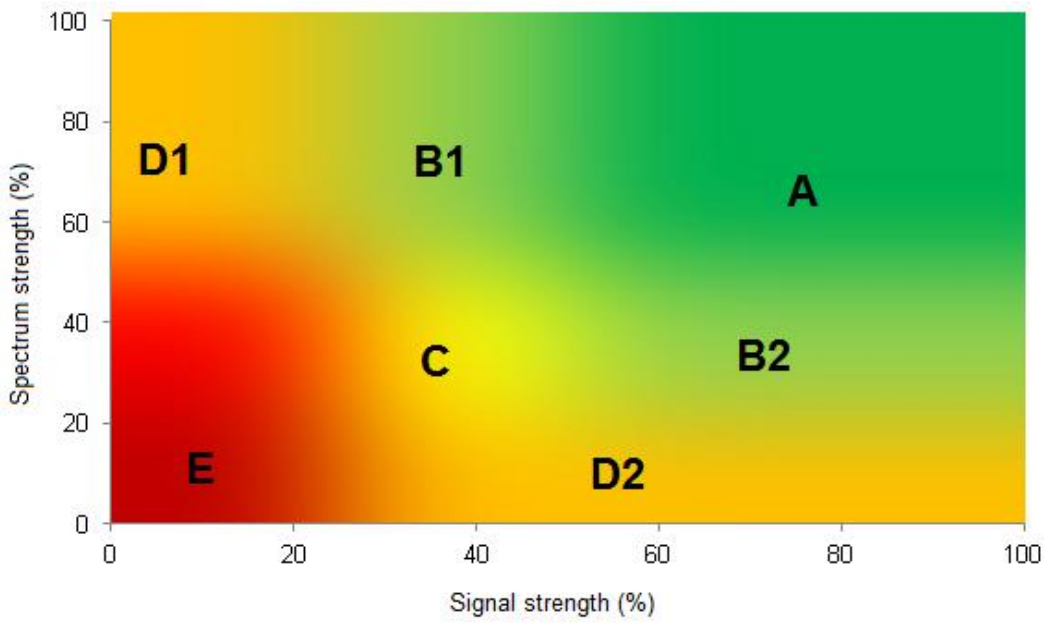


**Figure C.2 - ISCO 2150 signal quality chart**
A = excellent solids content and excellent velocity hydraulics. B1 = medium signal strength strong spectrum, low solids content but excellent hydraulics. B2 = good signal strength, low spectrum, questionable hydraulics (possible cause of this is debris on the sensor). C = fair signal and spectrum strength, data quality may be suspect. D1. Strong spectrum, good hydraulics but weak signal potentially caused by clean water. D2 = strong signal, weak spectrum, good particle concentration but suspect hydraulics. E = weak signal and spectrum strength, poor application and data is very suspect.

Ideally, all data would plot in the A, B1 and B2, areas signifying the greatest quality of data. The data handling procedure was to first discard data generated during periods of sensor displacement, and then discard data that did not meet minimum 20 % spectrum strength threshold. Low signal and spectrum strength problems normally resulted during period of known low flow where velocity of water column past the sensors was very slow and also contained very few suspended particles. Also, during low flow, algal growth and fine sediment build-up on the sensor was sometimes present and this most probably affected spectrum strength. It was only convenient to check ISCO logger approx. once every 6 weeks so low battery life also was suspected of contributing to poor signal and spectrum strength data days prior to download dates. Below is an example of signal quality charts for data used to create stage-discharge relationships (Figure C.3).

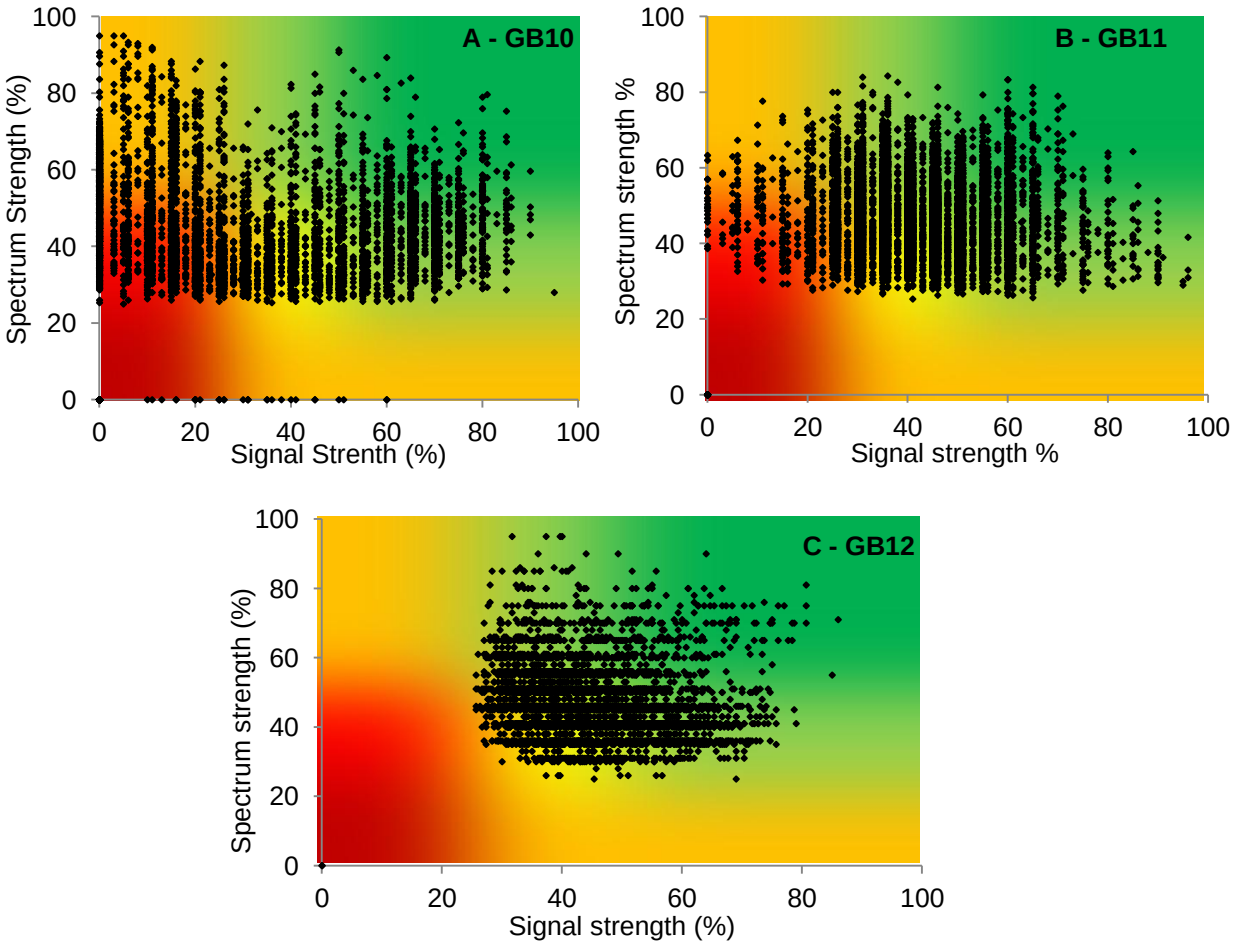


**Figure C.3 - Signal Quality of Gordonbush discharge data**
Graphs show discharge data used to construct stage-discharge relationships (black dots) with the ISCO 2150 signal quality chart overlain. A = GB10, Allt Mhuilin, B = GB11, Allt Smeorail, C = GB12 Old Town Burn.

Data signal quality for Old Town Burn (GB12) is the best of all three rivers with all data sitting in A, B1, B2 or C classes. Although some data from Allt Mhuilin and Allt Smeorail sit in C, D1 and E zones, none of the data sits in D2 zone which corresponds to weak hydraulics. Thus it was concluded high-quality data was used in the construction of stage-discharge relationships at Gordonbush.

# Appendix D – Stage-discharge relationships and flow duration curves

The following sections contain data collected relating to the creation of stage-discharge relationships for the Allt Mhuilin (GB10) and Old Town Burn (GB12) rivers. This section follows the same format as Chapter 3 section 3.12 which presented data relating to Allt Smeorail (GB11) river. Therefore, data will be presented indicating time periods discharge was estimated using ISCO 2150 velocity logger equipment; flow duration curves for the research period (again measured stage height at each river has been used as a proxy for discharge in these graphs); ISCO logger position during deployment and resulting (stage-discharge) plot of all collected ISCO logger data; and a collated definitive stage-discharge relationship for each river which was used, when necessary, to calculate a discharge throughout the research at each river. As long-term stage height was collected at the same sampling point as discharge was calculated at both GB10 and GB12 there was no need to present data justifying the use of stage height data at different point as was the case for GB11.

## Allt Mhuilin (GB10)

The following time series graph shows stage recorded at GB10 throughout this research, highlighting periods when ISCO logger equipment was deployed to estimate discharge.

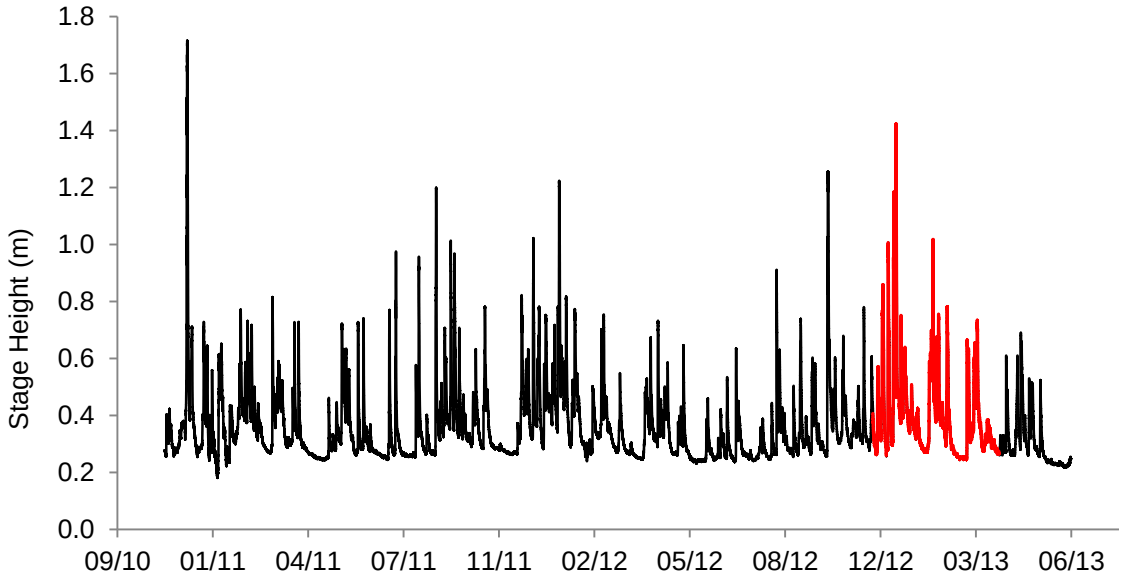


**Figure D.1 - GB10 hydrograph highlighting periods of ISCO logger deployment**
The black line represents the hydrograph time series from 17th November 2010 to 24th June 2013 collected from MNV installed logger positioned near catchment outlet of Allt Mhuilin river (sampling point GB10). The red line represents time period when ISCO 2150 flow logger was placed in Allt Mhuilin river at sampling point GB10 from 29/11/2012 to 10/4/2013.

The ISCO 2150 flow logger was positioned in Allt Mhuilin at sampling point GB10, the same location where MNV Ltd had pressure transducer equipment measuring stage height. This position was chosen because of the uniformity of the river channel, the river banks were steep and almost vertical and the river bed was relatively flat meaning calculating cross-sectional areas of river profiles much easier due to this approx. rectangular shape.

A flow duration curve for GB10 is presented below.

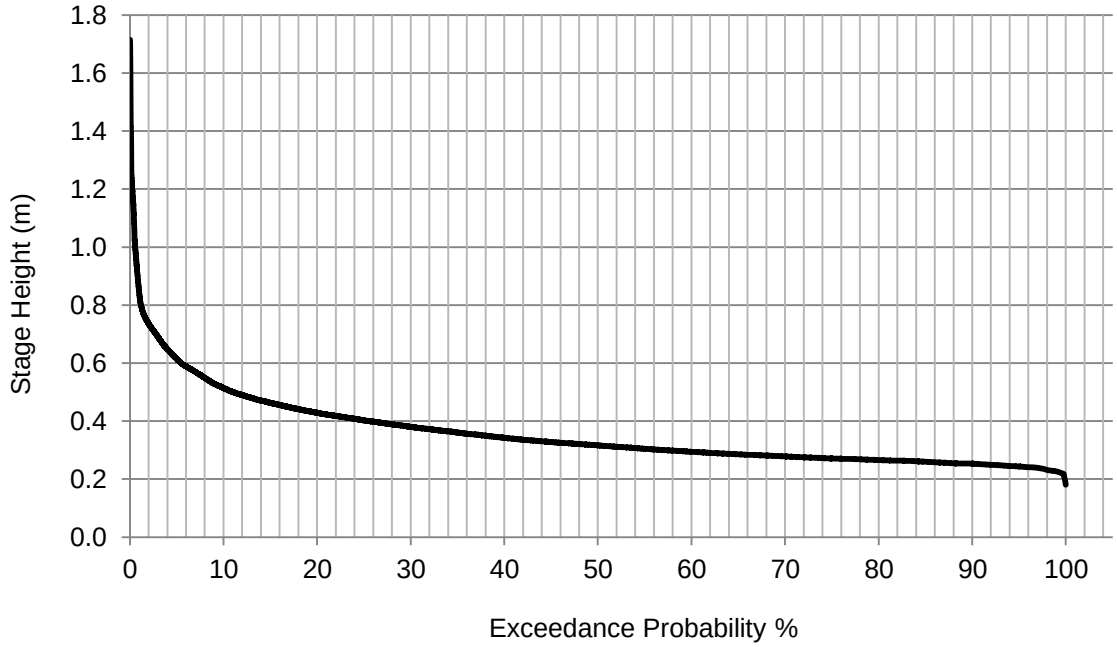


**Figure D.2 - GB10 flow duration curve**
A flow duration curve ranks stage heights recorded over time and produces a percentage value for the amount of time, during a designated period, a particular stage height has occurred or been exceeded.

Maximum stage height ever recorded at GB10 between November 2010 and June 2013 was 1.629 m on 11/12/2010, the minimum was 0.094 m on 11/1/2011. The maximum stage recorded while ISCO logger was positioned at GB10 was 1.46 m (23/12/2012) however, for data quality purposes (see section Appendix C), the maximum stage height used in stage-discharge equation was 0.999 m on 31/1/2013 and had an exceedance probability of 0.46 %. The minimum stage recorded during ISCO logger deployment was 0.214 m on 2/12/2012 and had an exceedance probability of 68 %. The hydrograph (Figure D.1) and flow duration curve (Figure D.2) demonstrates the ISCO logger deployment period captured typical low and high flows, giving confidence the stage-discharge relationship describes well this system.

The ISCO logger has a limited horizontal reach (approx. 3 metres). In GB10 the channel is wider than this (~9 metres) and so as river velocity may vary across the channel I moved

the logger within the channel, approx. every 6 weeks, to compare estimates of discharge and be sure that the stage-discharge relationship is accurate. A cross-sectional profile is presented (Figure D.3) for all three positions the ISCO logger was deployed in at GB10.

Figure D.4 shows data collected related to the positions where the ISCO logger was deployed.

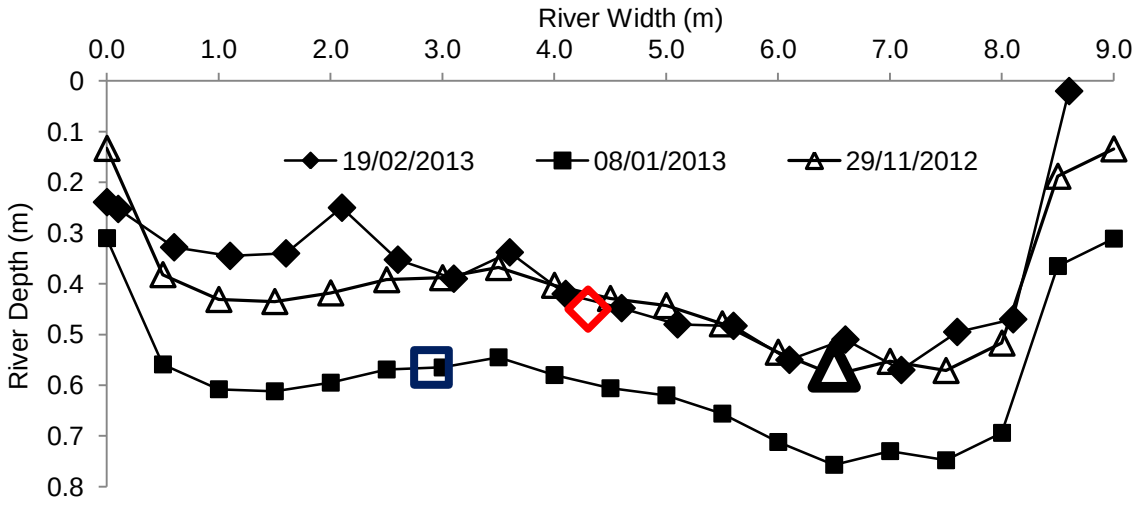


**Figure D.3 - ISCO logger positions at GB10**
Cross-sectional river profiles are shown for survey dates of Allt Mhuilin river. The profiles are represented looking in an upstream direction to river flow. The coloured shapes are markers for the location of where the ISCO logger was placed after a specific survey had taken place. The shapes (diamond, triangle and square) of the markers match up with the shapes linked by the black lines used to represent cross-sectional profiles recorded on different dates the river was surveyed.

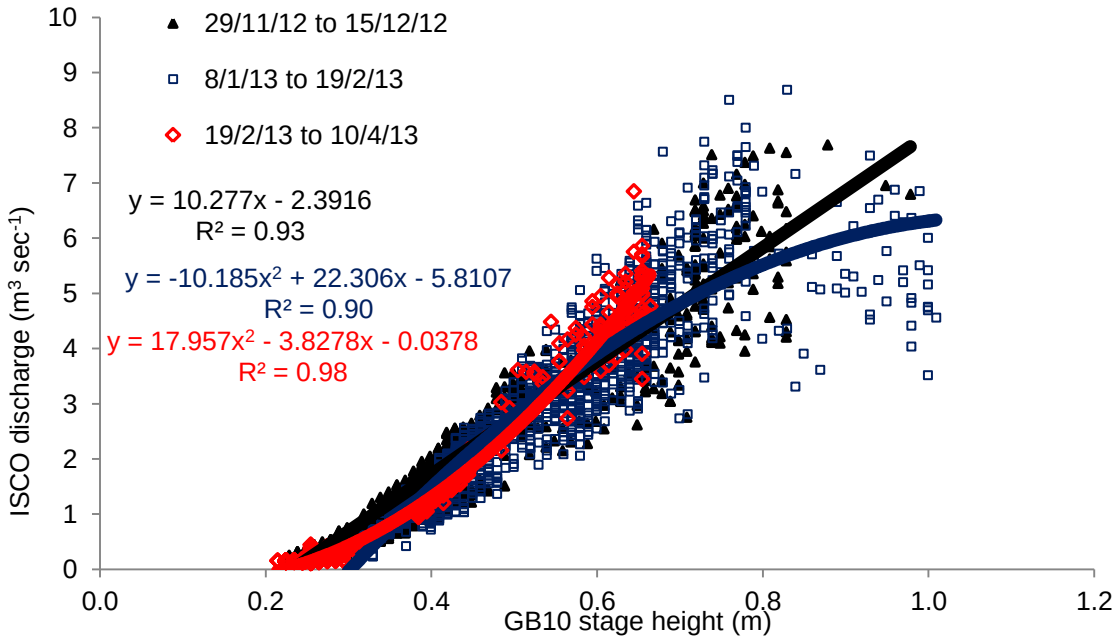


**Figure D.4 - Stage plotted against collated ISCO discharge data from GB10**
Edited, quality controlled, discharge data collected from ISCO logger when placed in at GB10 over different dates plotted against stage height from GB10 pressure transducer. The colours used for each date are the same as used in Figure D.3. The equations for each line are shown in each dates representative colour. The fitted lines to all the equations are shown in deep shades of black blue and red respectively.

Using only one of the data sets shown in Figure D.4 may give a biased discharge result (over or under estimation). Combining all three data sets accommodates natural uncertainty in estimating discharge in a wide channel to give a better stage height-discharge relationship (Figure D.5).

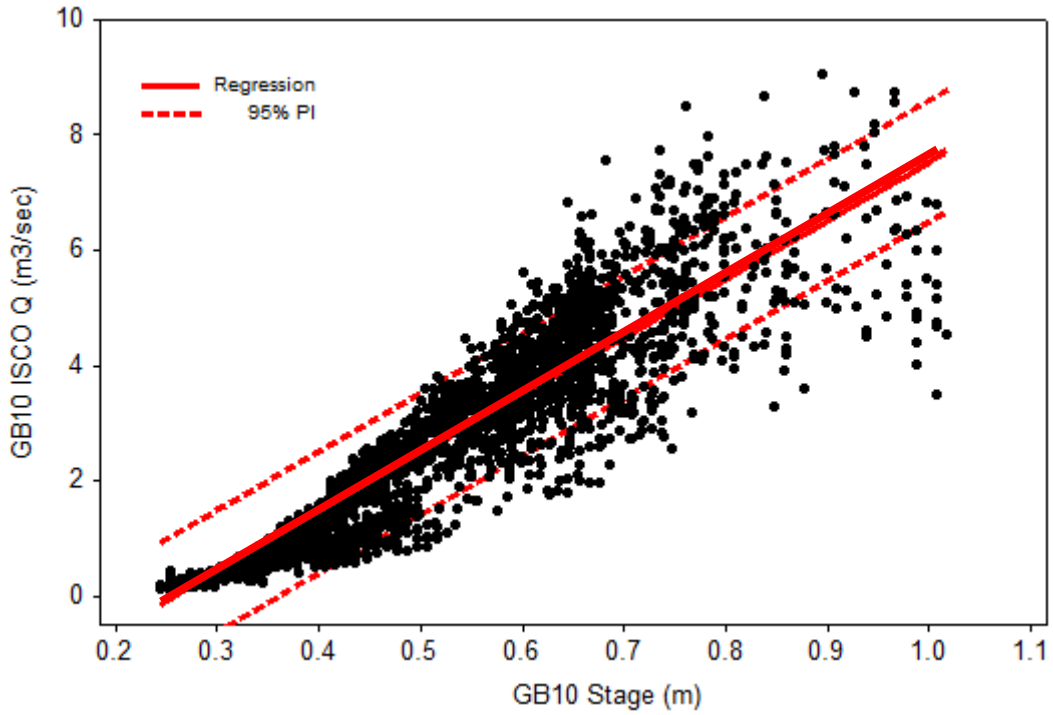


**Figure D.5 - Stage-discharge ratings curve for GB10**
All collated discharge data is plotted against corresponding stage height data from GB10. The red line shows the best fit linear relationship through the data. The dashed red lines are the prediction intervals for the fitted line.

The final stage-discharge relationship for GB10 produced a best fit linear relationship (Discharge = 10.16 * GB10 stage) – 2.614) with a $R^2$ = 0.9 and a p = <0.01.

## Old Town Burn (GB12)

In the Old Town Burn river (GB12), the ISCO logger was placed a small distance (approx. 100 m) down-stream of where stage height was recorded using an In-Situ Rugged 100 Troll. The particular location was once again chosen for its flat river bed and steep-sided river bank characteristics. The sampling point at GB12 was approx. three metres wide therefore deployment of only one ISCO sensor was needed to characterise the river velocities.

The following time series graph shows hydrograph for when stage height was recorded PT equipment at GB12 and highlights when ISCO logger equipment was deployed in the river.

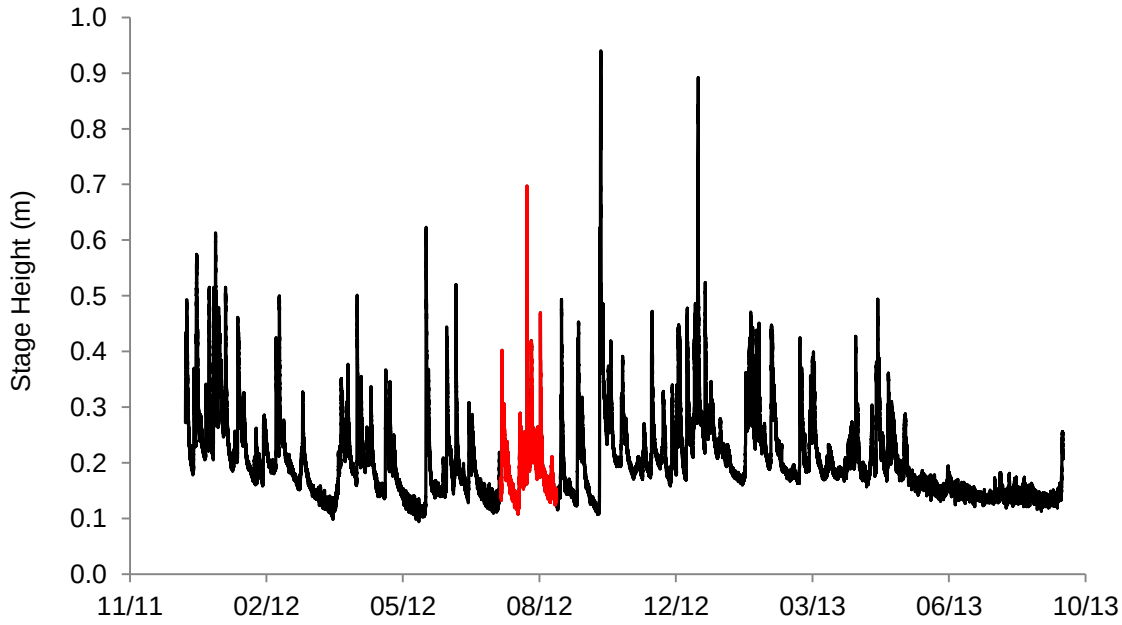


**Figure D.6 - GB12 hydrograph highlighting periods of ISCO logger deployment**
GB12 stage height, recorded by Rugged Troll 100 between December 2011 and September 2013, is shown in black and the time period when ISCO logger was deployment in Old Town Burn near GB12 are highlighted in red, 31/7/12 to 10/9/12.

Figure D.7 presents a flow duration curve for all stage height measured using PT equipment at GB12 during this research.

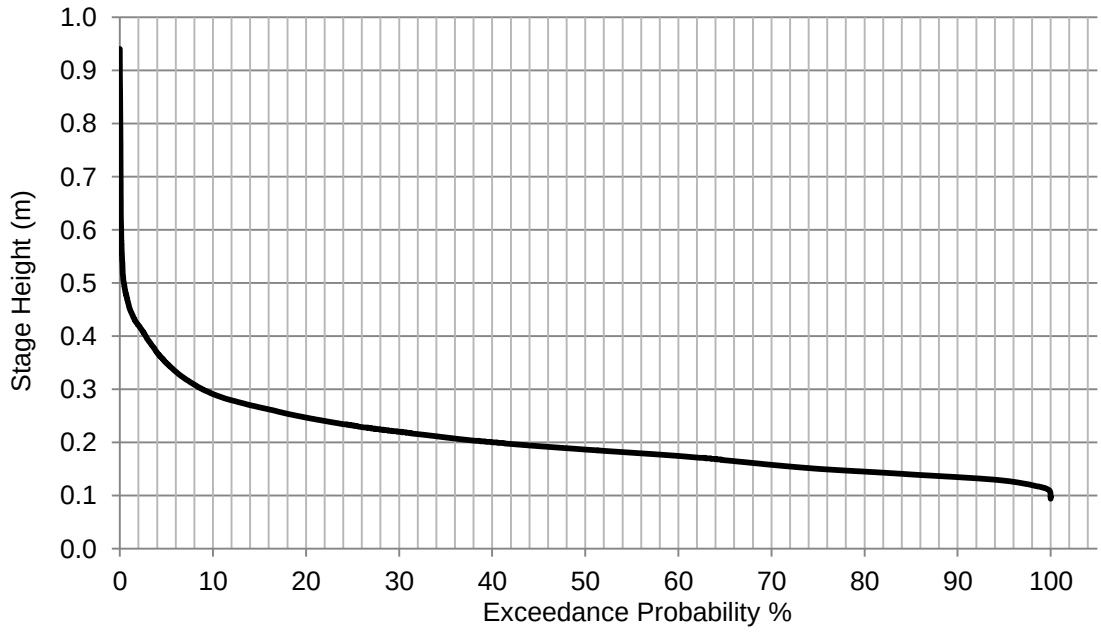


**Figure D.7 - GB12 flow duration curve**
Stage height values recorded between December 2011 and September 2013 from Rugged Troll 100 pressure transducer plotted as a function of percentage of time that value was equalled or exceeded.

During ISCO logger deployment, the maximum and minimum stage heights recorded at GB12 were 0.71 m (19/8/12) and 0.125 m (13/8/12). This does not capture the largest

flow, 0.94 m (12/10/12) and 0.09 m (1/6/2012) but the flow duration curve for GB12 (Figure D.7), allows estimate that 0.71 m represents the top 0.1 % of measured and ranked stage height values, 0.125 m is equivalent to 96.3 %, and so our stage-discharge relationship represents the hydrological range of GB12 well.

A cross sectional diagram of GB12 river at the sampling where ISCO logger equipment was deployed between 31/7/12 and 10/9/12 is presented.

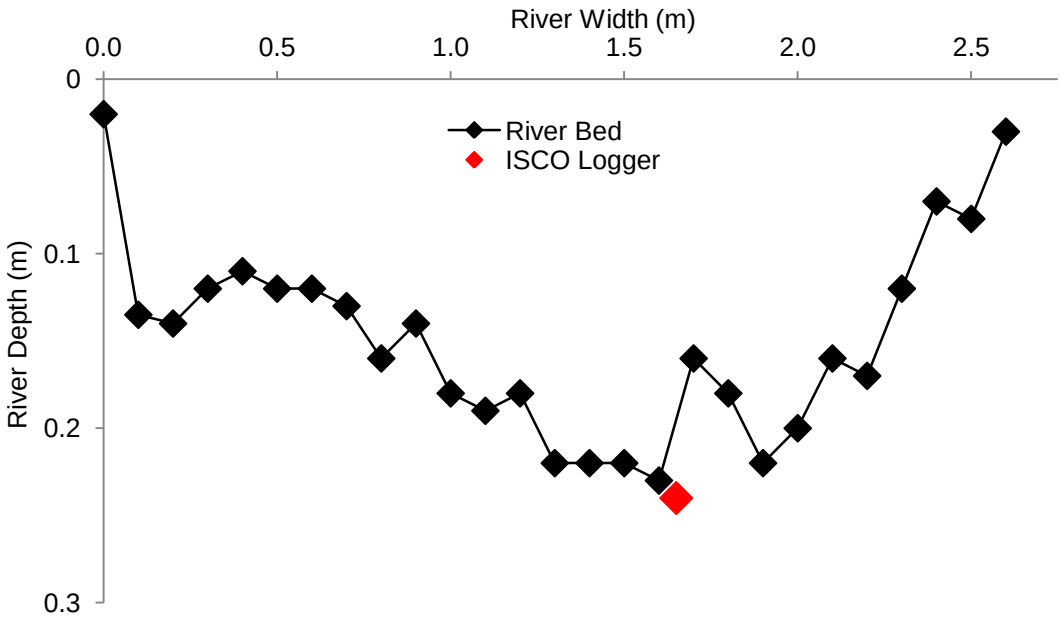


**Figure D.8 - Cross section of GB12 and ISCO logger position**
The black diamonds represent individual measurements of stage height for river cross-section at ISCO logger position near GB12. The red diamond indicates the position where the ISCO logger was placed on the river bed.

As indicated on Figure D.8, the ISCO logger was placed in the deepest part of the river channel. This decision was made as the fastest flows tend to occur above the deepest parts of any river channel allowing us to collect data which would best estimate maximum permissible discharge and avoid potentially under-estimation.

Below is the data set of discharge values calculated during ISCO logger deployment period and corresponding stage height measurements from GB12 (Figure D.9).

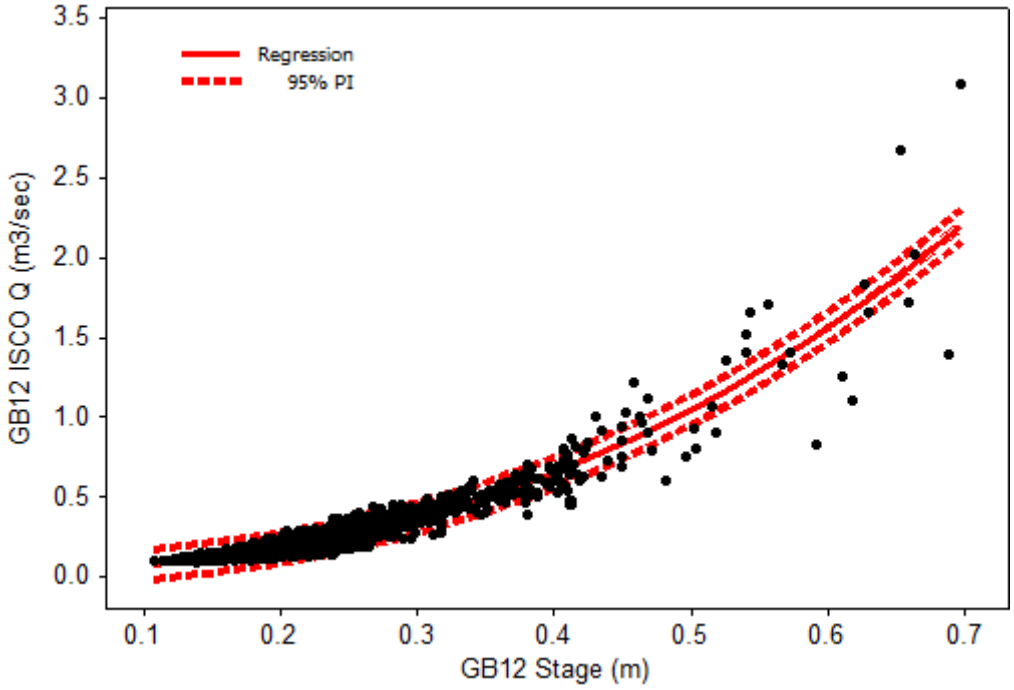


**Figure D.9 - Stage-discharge ratings curve for GB12**
All collated discharge data is plotted against corresponding stage height data from GB12. The red line shows the best fit linear relationship through the data. The dashed red lines are the prediction intervals for the fitted line.

The relationship fitted to the data is a cubic (Discharge = $(2.493 * \text{GB12 stage})^3 + (2.505 * \text{GB12 stage})^2 + (0.1453 * \text{GB12 stage}) + 0.03382$) and strong with $R^2 = 0.9$ and $p = <0.01$. There is less scatter above 0.4 m stage height than below it as less data was collected when stage height was this high. Variability in discharge data has increased in all three river datasets at the largest discharge estimates. Variability associated with measurement of discharge will increase as discharge increases and the data from all three river datasets indicates there is more variability in river velocities measured by ISCO logger equipment as stage increases potentially caused by greater turbulence in river channels during these periods.

The type of non-linear, i.e. cubic, relationship best describing stage-discharge ratings curve for GB12 is what is typically expected for ratings curves for rivers (as stage increases, the velocity of water and cross-sectional area of river also increases, meaning not only more is there a great volume of water but it is moving faster). However, linear relationships for GB10 and GB11 fitted the data collected better. When non-linear best-fit relationships were applied from data collected at GB10 and GB11, the resulting relationships predicted discharge decreased as stage height increased at a certain point. This is not an intuitive or fundamentally correct relationship for any stage-discharge ratings curve therefore that is why non-linear relationships were not used for GB10 and GB11.

# Appendix E – Linear regressions of aquatic organic C data

This appendix chapter contains linear regressions of discharge and stage height data plotted against aquatic organic C data for Allt Mhuilin (GB10) and Old Town Burn (GB12) river sampling points. The resulting linear equations were used to construct aquatic organic C fluxes (both DOC and POC) for GB10 and GB12 using the same methods outline in Chapter 6 where examples from the Allt Smeorail (GB11) sampling point were presented. Stage/discharge will be plotted against all [DOC] collected, this data will then be presented divided based on one of three time periods it was collected during 'Summer', 'Spring-Autumn' or 'Winter'. Finally, data from each time period will be presented individually highlighting data collected on the rising and falling limbs of storm hydrographs separately. The falling limb data is always displayed in a red colour. The same format used for presenting [DOC] will be applied when presenting stage/discharge [POC] data. A collated table of all linear equations and associated $R^2$ values is presented for all three rivers at the end of this appendix section.

## Allt Mhuilin (GB10)

Stage/discharge vs. [DOC]/[POC] are presented for GB10 below. A title in the top left-hand corner of each graph will detail the nature of the data presented. A best fit relationship will be highlighted and the resulting equation, $R^2$ and associated p value for this relationship will be presented on the graph. Where appropriate the colour of text of equations, $R^2$ and p values match that of the data and specific trend-line.

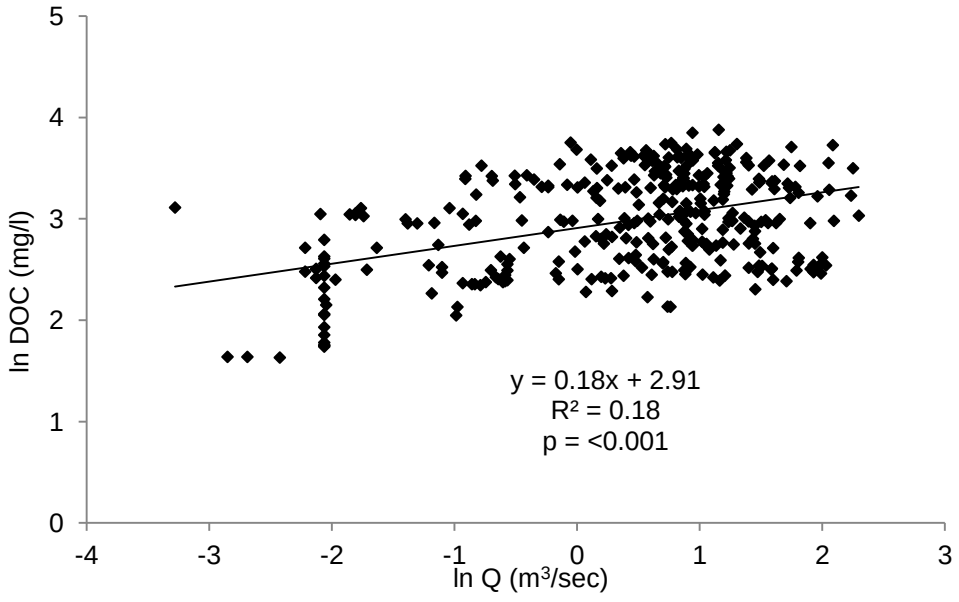


**Figure E.1 - Discharge plotted against [DOC] for all collected data in GB10**

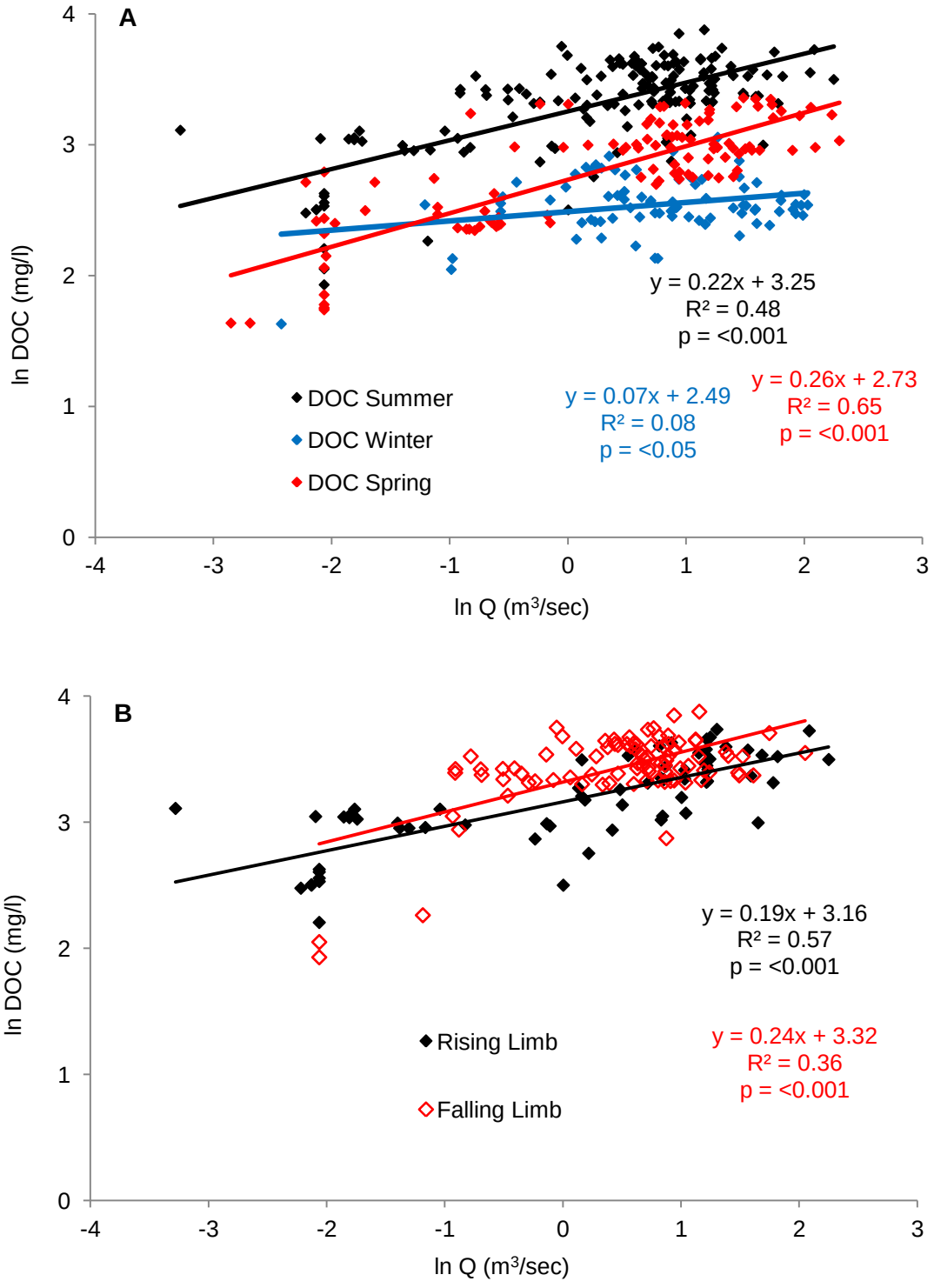


**Figure E.2 – 'Seasonal' and 'Summer' rising and falling limb relationships**
A = GB10 [DOC] split by time period. B = 'Summer' rising and falling limb relationships

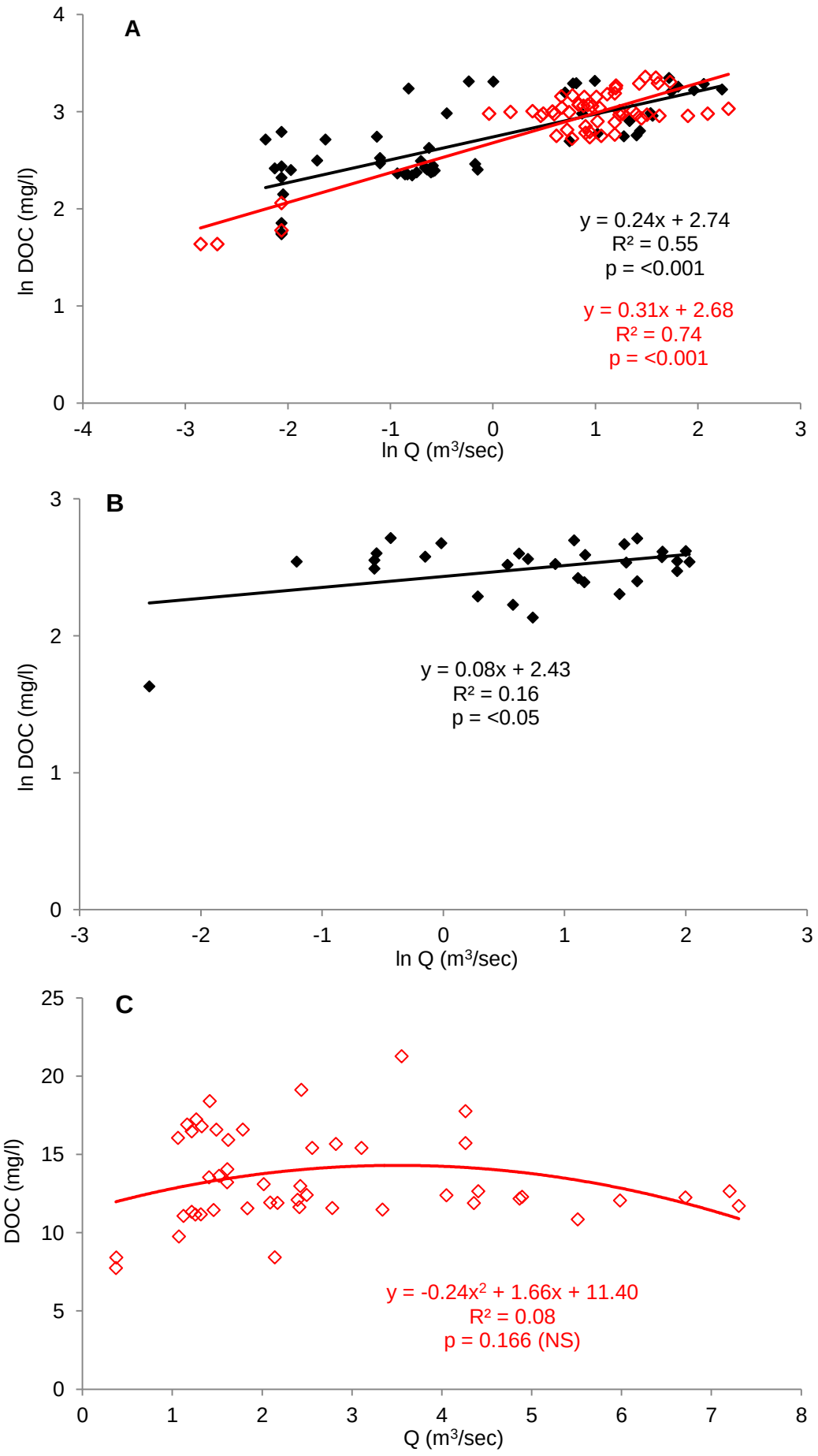


**Figure E.3 - Rising and falling limb relationships for GB10 in Spring-Autumn and Winter**
A = Spring-Autumn rising and falling limbs. B = Winter rising limb. C = Winter falling limb

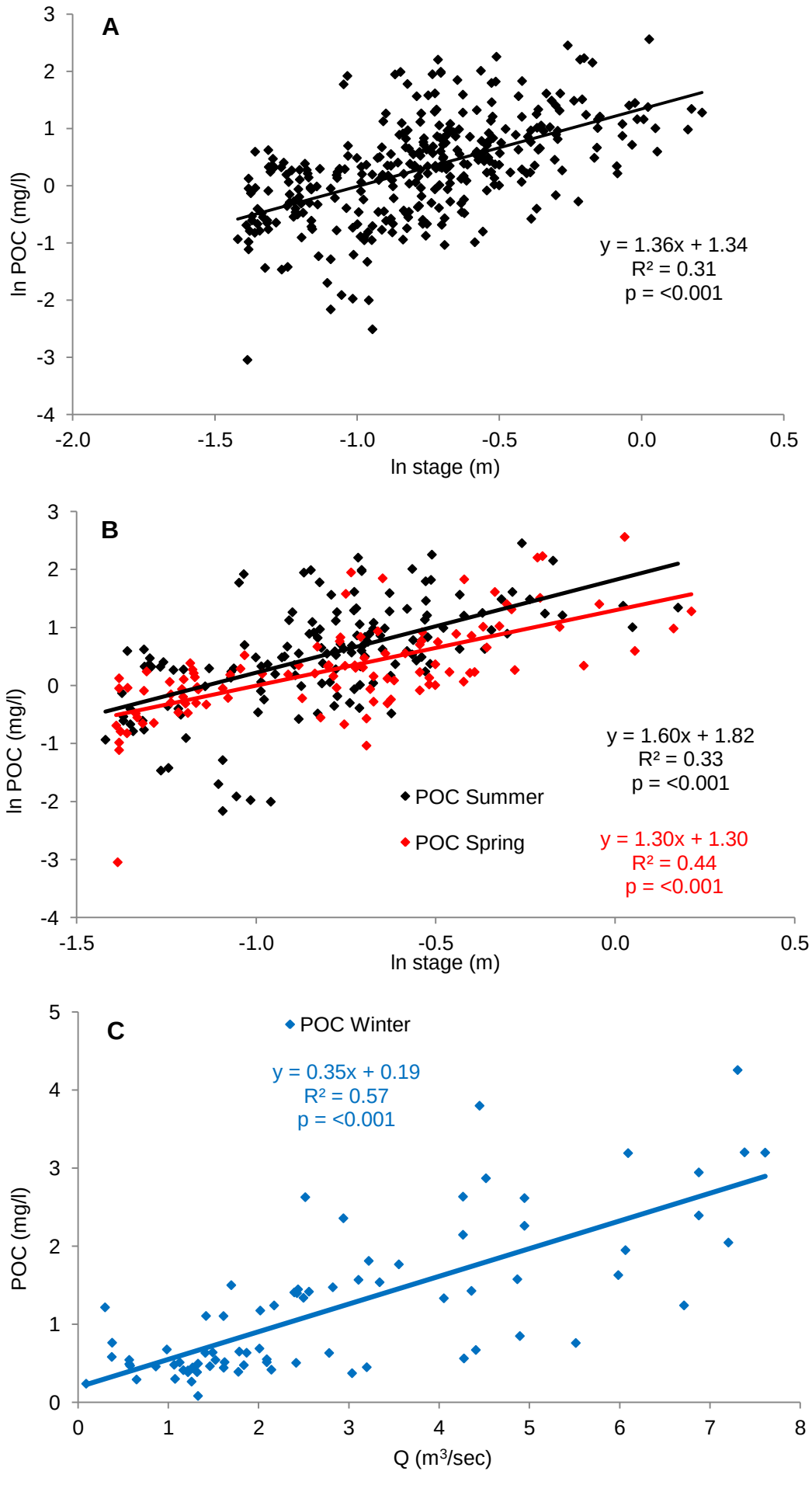


**Figure E.4 – Stage/discharge plotted against [POC] for GB10**
A = All [POC] data plotted against stage. B = Data split into summer and spring-autumn time periods. C = Data split into winter time period

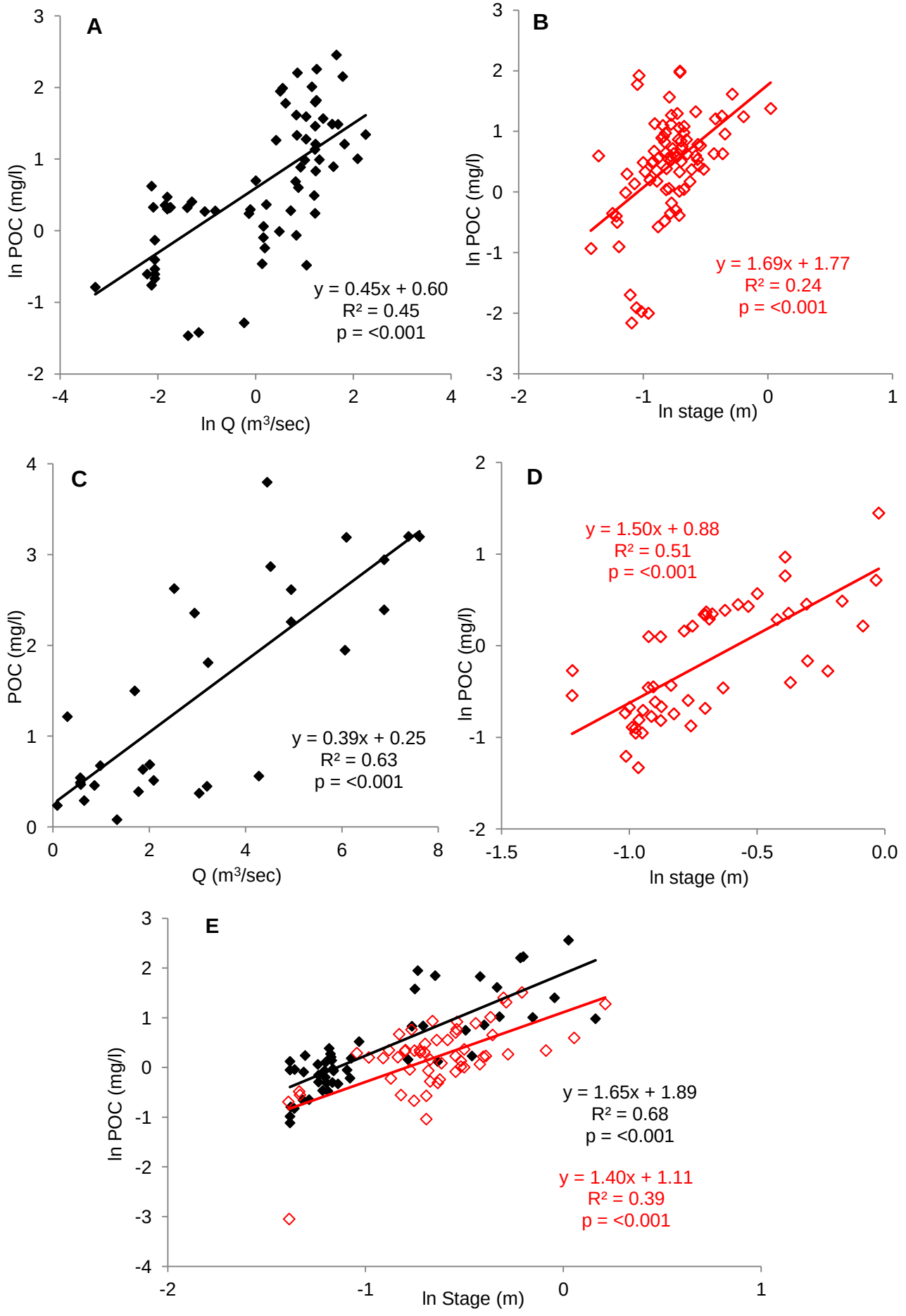


**Figure E.5 - Time split rising and falling limb relationships for GB10 [POC] data**
A = Summer rising limb. B = Summer falling limb. C = Winter rising limb. D = Winter falling limb. E = Spring-autumn rising and falling limbs

# Old Town Burn (GB12)

Stage/discharge vs. [DOC]/[POC] are presented for GB12 below. The same information presented at start of previous section (Allt Mhuilin - GB10) applies in this section.

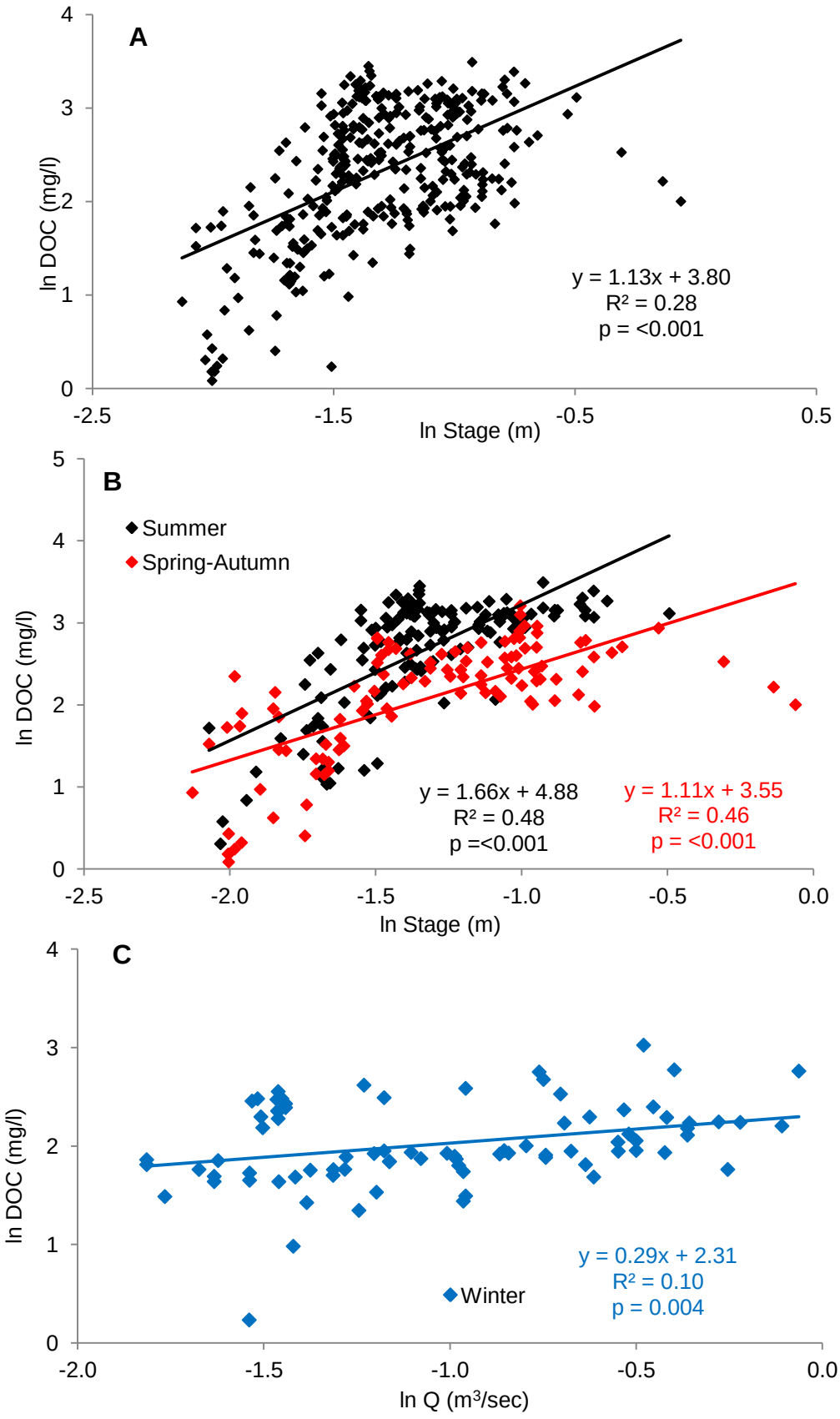


**Figure E.6 - Stage/discharge plotted against all and time split [DOC] data for GB12**
A = All [DOC] data for GB12 plotted against stage. B = [DOC] split into Summer and Spring-autumn time periods. C = [DOC] split into winter time period

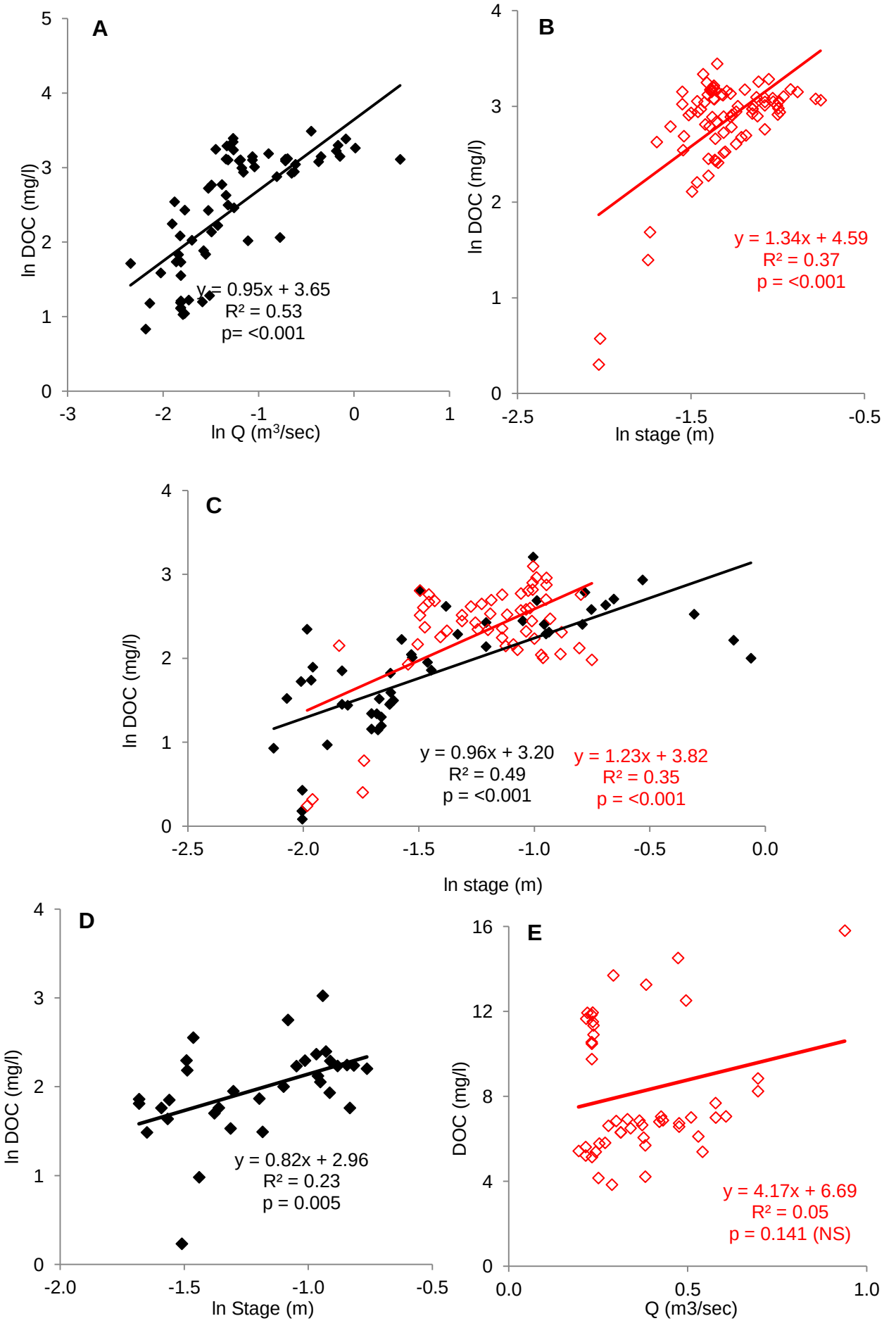


**Figure E.7 - Time split with rising and falling limbs for GB12 [DOC] data**
A = Summer rising limb. B = Summer falling limb. C = Spring-autumn rising and falling limbs. D = Winter rising limb. E = Winter falling limb.

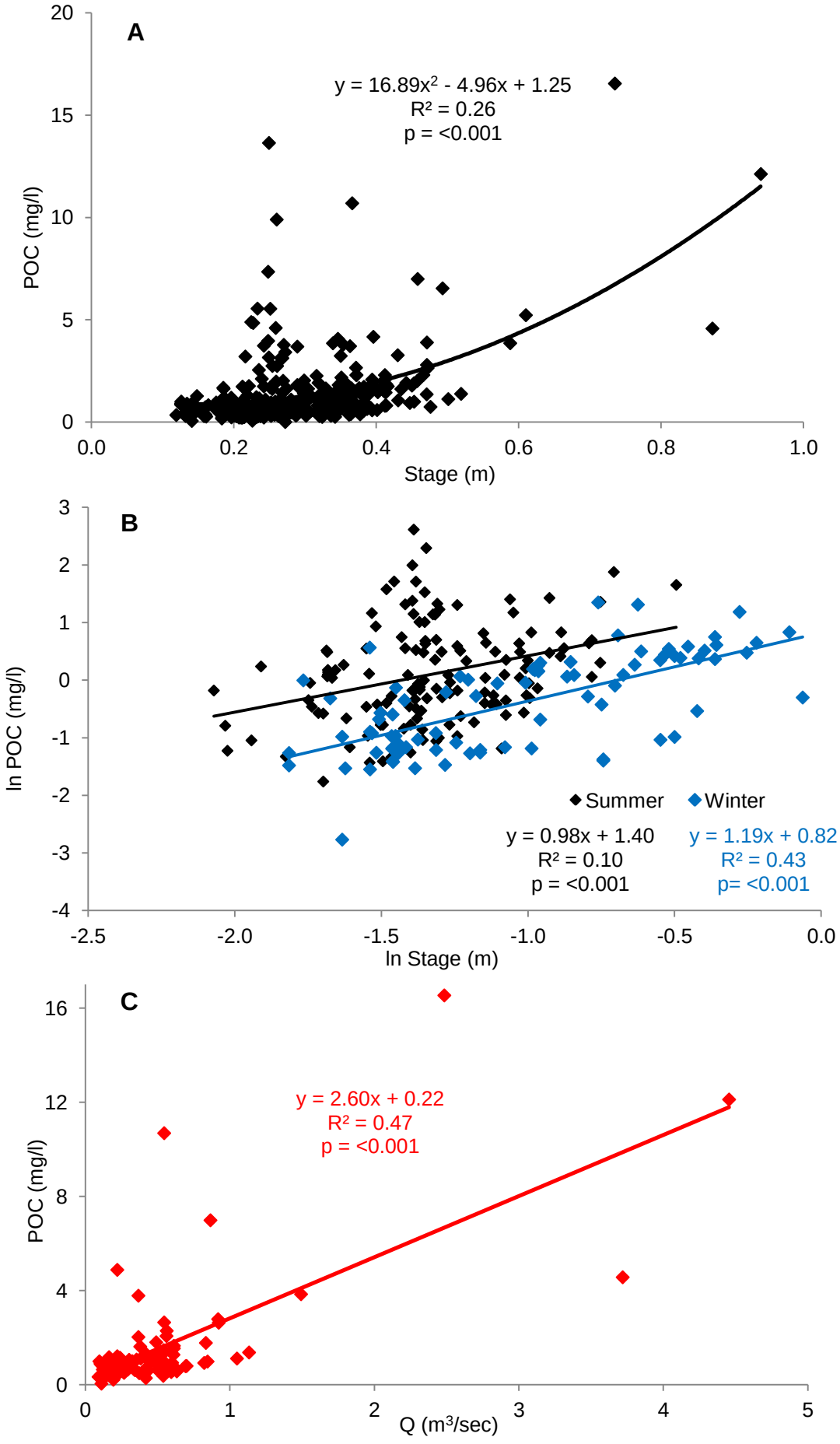


**Figure E.8 - Stage/discharge plotted against [POC] data from GB12**
A = All [POC] data. B = [POC] data split by time period, Summer and Winter. C = [POC] data split by time period, Spring-Autumn.

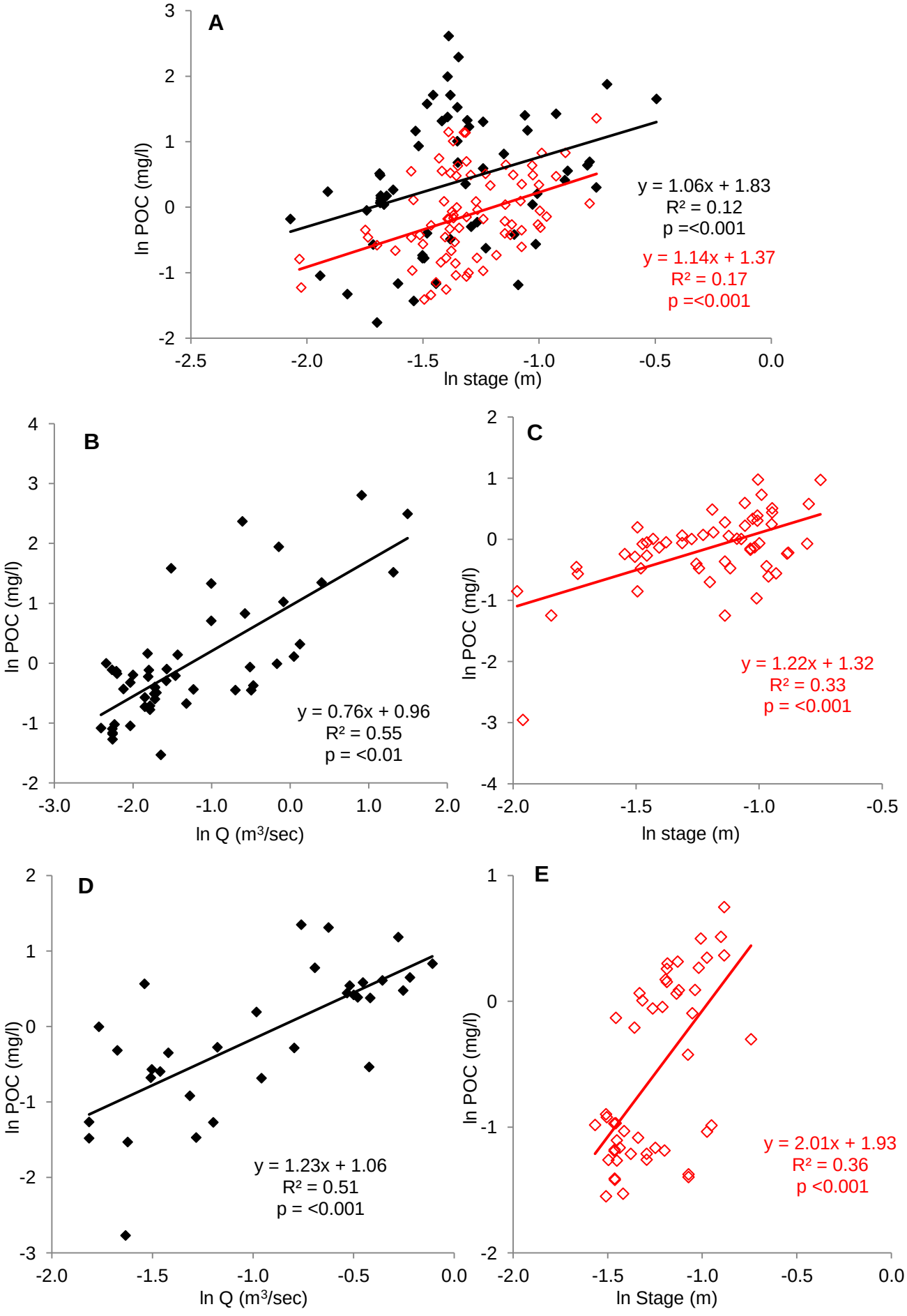


**Figure E.9 - [POC] data from GB12 split by time period and rising and falling limbs**
A = Summer rising and falling limb. B = Spring-Autumn rising limb. C = Spring-Autumn falling limb. D = Winter rising limb. E = Winter falling limb.

# Tables of regression equations used to create Gordonbush aquatic organic C fluxes

Below are three tables, one for each river, GB10, GB11 and GB12, containing details of regression equations used to create aquatic organic C fluxes at Gordonbush. Details are given on the relationship used, e.g., ln Q vs. ln DOC, the type of regression line utilised, e.g., 'Linear', the equation of the regression line and then the $R^2$ value, p-value ('p') and the S value ('S') of that resulting the relationship. Some abbreviations have been used in the table to save space, these include; **Q** = discharge, **s** = Stage height, **ln DOC** = natural log of [DOC], **Linear.** = linear regression line and **Polynomial.** = 2nd order polynomial / quadratic equation.

The following table contains data relating to regression equations related to calculation of aquatic organic C fluxes from Allt Mhuilin river – GB10.

| **Allt Mhuilin – GB10** | | |
|---|---|---|
| | **DOC** | **POC** |
| **All Data** | ln Q vs. ln DOC = Linear<br>y = 2.91 + (0.18 * ln Q)<br>$R^2$ = 0.18 p = 0.000 S = 0.44 | ln s vs. ln POC = Linear<br>y = 1.34 + (1.36 * ln s)<br>$R^2$ = 0.31 p = 0.000 S = 0.73 |
| **Summer** | ln Q vs. ln DOC = Linear<br>y = 3.25 + (0.22 * ln Q)<br>$R^2$ = 0.48 p = 0.000 S = 0.26 | ln s vs. ln POC = Linear<br>y = 1.82 + (1.6 * ln s)<br>$R^2$ = 0.33 p = 0.000 S = 0.74 |
| **Winter** | ln Q vs. ln DOC = Linear<br>y = 2.49 + (0.07 * ln Q)<br>$R^2$ = 0.08 p = 0.014 S = 0.21 | Q vs. POC = Linear<br>y = 0.19 + (0.35 * Q)<br>$R^2$ = 0.57 p = 0.000 S = 0.63 |
| **Spring-Autumn** | ln Q vs. ln DOC = Linear<br>y = 2.73 + (0.26 * ln Q)<br>$R^2$ = 0.65 p = 0.000 S = 0.25 | ln s vs. ln POC = Linear<br>y = 1.3 + (1.3 * ln s)<br>$R^2$ = 0.44 p = 0.000 S = 0.60 |
| **Summer Rising** | ln Q vs. ln DOC = Linear<br>y = 3.16 + (0.19 * ln Q)<br>$R^2$ = 0.57 p = 0.000 S = 0.24 | ln Q vs. ln POC = Linear<br>y = 0.60 + (0.45 * ln Q)<br>$R^2$ = 0.45 p = 0.000 S = 0.70 |
| **Summer Falling** | ln Q vs. ln DOC = Linear<br>y = 3.32 + (0.24 * ln Q)<br>$R^2$ = 0.36 p = 0.000 S = 0.24 | ln s vs. ln POC = Linear<br>y = 1.77 + (1.69 * ln s)<br>$R^2$ = 0.24 p = 0.000 S = 0.76 |
| **Winter Rising** | ln Q vs. ln DOC = Linear<br>y = 2.43 + (0.08 * ln Q)<br>$R^2$ = 0.16 p = 0.028 S = 0.44 | Q vs. POC = Linear<br>y = 0.25 + (0.39 * Q)<br>$R^2$ = 0.63 p = 0.000 S = 0.73 |
| **Winter Falling** | Q vs. DOC = Polynomial<br>y = 11.39 + (1.66 * Q) – (0.24 * $Q^2$)<br>$R^2$ = 0.08 p = 0.166 S = 2.83 | ln s vs. ln POC = Linear<br>y = 0.88 + (1.50 * ln s)<br>$R^2$ = 0.51 p = 0.000 S = 0.45 |
| **Spring-Autumn Rising** | ln Q vs. ln DOC = Linear<br>y = 2.74 + (0.24 * ln Q)<br>$R^2$ = 0.55 p = 0.000 S = 0.30 | ln s vs. ln POC = Linear<br>y = 1.89 + (1.65 * ln s)<br>$R^2$ = 0.68 p = 0.000 S = 0.51 |
| **Spring-Autumn Falling** | ln Q vs. ln DOC = Linear<br>y = 2.68 + (0.31 * ln Q)<br>$R^2$ = 0.74 p = 0.000 S = 0.19 | ln s vs. ln POC = Linear<br>y = 1.11 + (1.40 * ln s)<br>$R^2$ = 0.39 p = 0.000 S = 0.55 |

**Table E.1 - Regression equations used to construct aquatic C flux estimates for GB10**

The next table contains data relating to regression equations related to calculation of aquatic organic C fluxes from Allt Smeorail river – GB11.

| **Allt Smeorail – GB11** | | |
|---|---|---|
| | **DOC** | **POC** |
| **All Data** | ln Q vs. ln DOC = Linear<br>y = 2.47 + (0.19 * ln Q)<br>$R^2$ = 0.20 p = 0.000 S = 0.58 | s vs. POC = Polynomial<br>y = 0.64 - (0.44 * s) + (3.81 * $s^2$)<br>$R^2$ = 0.59 p = 0.000 S = 1.62 |
| **Summer** | ln Q vs. ln DOC = Linear<br>y = 2.95 + (0.311 * ln Q)<br>$R^2$ = 0.56 p = 0.000 S = 0. | ln s vs. ln POC = Linear<br>y = 1.54 + (1.68 * ln s)<br>$R^2$ = 0.36 p = 0.000 S = 0.67 |
| **Winter** | Q vs. ln DOC = Polynomial<br>y = 1.87 + (0.14 * Q) – (0.02 * $Q^2$)<br>$R^2$ = 0.21 p = 0.000 S = 0.31 | s vs. POC = Polynomial<br>y = 0.71 + (2.24 * s) + (4.79 * $s^2$)<br>$R^2$ = 0.85 p = 0.000 S = 1.26 |
| **Spring-Autumn** | ln Q vs. ln DOC = Linear<br>y = 2.38 + (0.23 * ln Q)<br>$R^2$ = 0.56 p = 0.000 S = 0.38 | ln s vs. ln POC = Linear<br>y = 1.28 + (1.64 * ln s)<br>$R^2$ = 0.60 p = 0.000 S = 0.58 |
| **Summer Rising** | ln Q vs. ln DOC = Linear<br>y = 2.75 + (0.29 * ln Q)<br>$R^2$ = 0.59 p = 0.000 S = 0.50 | ln Q vs. ln POC = Linear<br>y = 0.45 + (0.30 * ln Q)<br>$R^2$ = 0.46 p = 0.000 S = 0.69 |
| **Summer Falling** | ln Q vs. ln DOC = Linear<br>y = 3.08 + (0.16 * ln Q)<br>$R^2$ = 0.15 p = 0.000 S = 0.21 | ln s vs. ln POC = Linear<br>y = 1.68 + (1.88 * ln s)<br>$R^2$ = 0.25 p = 0.000 S = 0.66 |
| **Winter Rising** | Q vs. DOC = Polynomial<br>y = 6.22 + (1.36 * Q) – (0.18 * $Q^2$)<br>$R^2$ = 0.34 p = 0.001 S = 2.09 | Q vs. POC = Polynomial<br>y = 0.54 - (0.11 * Q) + (0.17 * $Q^2$)<br>$R^2$ = 0.86 p = 0.000 S = 1.62 |
| **Winter Falling** | ln Q vs. ln DOC = Polynomial<br>y = 2.07 + (0.12 * Q) – (0.19 * $Q^2$)<br>$R^2$ = 0.13 p = 0.043 S = 0.27 | Q vs. POC = Polynomial<br>y = 0.25 - (0.31 * Q) + (0.14 * $Q^2$)<br>$R^2$ = 0.75 p = 0.000 S = 0.88 |
| **Spring-Autumn Rising** | ln Q vs. ln DOC = Linear<br>y = 2.20 + (0.20 * ln Q)<br>$R^2$ = 0.54 p = 0.000 S = 0.39 | Q vs. POC = Polynomial<br>y = 0.75 + (0.17 * Q) + (0.15 * $Q^2$)<br>$R^2$ = 0.73 p = 0.000 S = 1.85 |
| **Spring-Autumn Falling** | ln Q vs. ln DOC = Linear<br>y = 2.52 + (0.26 * ln Q)<br>$R^2$ = 0.62 p = 0.000 S = 0.32 | ln s vs. ln POC = Linear<br>y = 1.37 +(1.79 * ln s)<br>$R^2$ = 0.42 p = 0.000 S = 0.58 |

**Table E.2 - Regression equations used to construct aquatic C flux estimates for GB11**

The next table contains data relating to regression equations related to calculation of aquatic organic C fluxes from Old Town Burn river – GB12.

| **Old Town Burn – GB12** | | |
|---|---|---|
| | **DOC** | **POC** |
| **All Data** | ln s vs. ln DOC = Linear<br>y = 3.8 + (1.13 * ln s)<br>$R^2$ = 0.28 p = 0.000 S = 0.60 | s vs. POC = Polynomial<br>y = 1.25 - (4.96 * s) + (16.89 * $s^2$)<br>$R^2$ = 0.26 p = 0.000 S = 1.57 |
| **Summer** | ln s vs. ln DOC = Linear<br>y = 4.88 + (1.60 * ln s)<br>$R^2$ = 0.48 p = 0.000 S = 0.49 | ln s vs. ln POC = Linear<br>y = 1.40 + (0.98 * ln s)<br>$R^2$ = 0.10 p = 0.000 S = 0.82 |
| **Winter** | ln Q vs. ln DOC = Linear<br>y = 2.31 + (0.29 * ln Q)<br>$R^2$ = 0.10 p = 0.004 S = 0.41 | ln s vs. ln POC = Linear<br>y = 0.82 + (1.19 * ln s)<br>$R^2$ = 0.44 p = 0.000 S = 0.63 |
| **Spring-Autumn** | ln s vs. ln DOC = Linear<br>y = 3.55 + (1.11 * ln s)<br>$R^2$ = 0.46 p = 0.000 S = 0.53 | Q vs. POC = Linear<br>y = 0.22 + (2.60 * Q)<br>$R^2$ = 0.47 p = 0.000 S = 1.66 |
| **Summer Rising** | ln Q vs. ln DOC = Linear<br>y = 3.65 + (0.95 * ln Q)<br>$R^2$ = 0.53 p = 0.000 S = 0.55 | ln s vs. ln POC = Linear<br>y = 1.83 + (1.06 * ln s)<br>$R^2$ = 0.12 p = 0.005 S = 0.94 |
| **Summer Falling** | ln s vs. ln DOC = Linear<br>y = 4.59 + (1.34 * ln s)<br>$R^2$ = 0.37 p = 0.000 S = 0.41 | ln s vs. ln POC = Linear<br>y = 1.37 + (1.14 * ln s)<br>$R^2$ = 0.17 p = 0.001 S = 0.72 |
| **Winter Rising** | ln s vs. ln DOC = Linear<br>y = 2.96 + (0.82 * ln s)<br>$R^2$ = 0.23 p = 0.005 S = 0.45 | ln Q vs. ln POC = Linear<br>y = 1.06 + (1.23 *ln Q)<br>$R^2$ = 0.51 p = 0.000 S = 0.68 |
| **Winter Falling** | Q vs. DOC = Linear<br>y = 6.69 + (4.17 * Q)<br>$R^2$ = 0.05 p = 0.141 S = 3.15 | ln s vs. ln POC = Linear<br>y = 1.93 + (2.01 * ln s)<br>$R^2$ = 0.36 p = 0.000 S = 0.56 |
| **Spring-Autumn Rising** | ln s vs. ln DOC = Linear<br>y = 3.20 + (0.96 * ln s)<br>$R^2$ = 0.48 p = 0.000 S = 0.56 | ln Q vs. ln POC = Linear<br>y = 0.96 + (0.76 * ln Q)<br>$R^2$ = 0.55 p = 0.000 S = 0.68 |
| **Spring-Autumn Falling** | ln s vs. ln DOC = Linear<br>y = 3.82 + (1.23 * ln s)<br>$R^2$ = 0.35 p = 0.000 S = 0.50 | ln s vs. ln POC = Linear<br>y = 1.32 + (1.22 * ln s)<br>$R^2$ = 0.33 p = 0.000 S = 0.51 |

**Table E.3 - Regression equations used to construct aquatic C flux estimates for GB12**

# Appendix F – Data associated with $^{210}$Pb radiometric dating of peat and lake cores

## $^{210}$Pb from GB1 and GB2 peat cores

Below are tables and graphs outlining data associated with $^{210}$Pb radiometric dating undertaken on Gordonbush peat samples from cores GB1 and GB2 (cut).

| Depth (cm) | Cumulative Dry Mass (g cm$^{-2}$) | Total $^{210}$Pb Bq Kg$^{-1}$ | Error (1σ) | Supported $^{210}$Pb Bq Kg$^{-1}$ | Error (1σ) | Unsupported $^{210}$Pb Bq Kg$^{-1}$ | Error (1σ) |
|---|---|---|---|---|---|---|---|
| **GB1** | | | | | | | |
| 0.50 | 0.112 | 134.86 | 15.58 | 11.09 | 6.97 | 123.77 | 11.28 |
| 1.50 | 0.240 | 214.84 | 14.30 | 9.41 | 4.76 | 205.42 | 9.53 |
| 3.50 | 0.352 | 17.38 | 15.34 | 11.69 | 6.08 | 5.69 | 10.71 |
| 4.50 | 0.467 | 34.34 | 14.79 | 10.48 | 5.32 | 23.86 | 10.06 |
| 6.50 | 0.608 | 10.63 | 9.69 | 9.83 | 4.94 | 0.80 | 7.31 |
| 8.50 | 0.734 | 8.91 | 13.24 | 11.99 | 5.36 | -3.08 | 9.30 |
| 11.50 | 0.866 | 15.09 | 11.04 | 10.15 | 5.20 | 4.93 | 8.12 |
| 15.50 | 0.991 | 9.18 | 9.64 | 10.25 | 4.26 | -1.07 | 6.95 |
| 19.50 | 1.126 | 12.61 | 11.98 | 8.79 | 5.90 | 3.82 | 8.94 |
| 24.50 | 1.270 | 15.45 | 10.21 | 14.30 | 5.02 | 1.15 | 7.61 |
| **GB2 (cut)** | | | | | | | |
| 0.50 | 0.136 | 1.05 | 10.48 | 4.14 | 4.22 | -3.10 | 7.35 |
| 1.50 | 0.270 | 32.24 | 10.66 | 5.83 | 4.43 | 26.40 | 7.54 |
| 2.50 | 0.403 | 5.24 | 10.82 | 5.35 | 3.10 | -0.11 | 6.96 |
| 4.50 | 0.535 | 8.76 | 6.13 | 8.05 | 4.94 | 0.71 | 5.54 |
| 7.50 | 0.679 | 38.01 | 10.24 | 17.80 | 4.06 | 20.21 | 7.15 |
| 10.50 | 0.809 | 15.92 | 11.39 | 10.50 | 4.40 | 5.41 | 7.89 |
| 12.50 | 0.945 | 31.08 | 10.32 | 10.87 | 4.18 | 20.21 | 7.25 |
| 16.50 | 1.089 | 30.36 | 10.08 | 9.46 | 3.95 | 20.90 | 7.02 |
| 19.50 | 1.216 | 30.36 | 11.57 | 14.32 | 4.52 | 16.04 | 8.05 |
| 25.50 | 1.350 | 10.61 | 10.54 | 9.69 | 4.08 | 0.92 | 7.31 |

**Table F.1 - $^{210}$Pb concentrations in GB1 and GB2 (cut) peat cores from Gordonbush**

| Depth (cm) | Dry Mass (g cm$^{-2}$) | Chronology Date (AD) | Age (yr) | Error (±) | Sedimentation Rate g cm$^{-2}$ yr$^{-1}$ | cm yr$^{-1}$ | Error (±) |
|---|---|---|---|---|---|---|---|
| 0.5 | 0.112 | 2000 | 12.34 | 1.5 | 0.0091 | 0.041 | 0.001 |
| 1.5 | 0.240 | 1931 | 81.30 | 46.0 | 0.0016 | 0.018 | 0.001 |
| 3.5 | 0.352 | 1925 | 87.84 | 172.3 | 0.0013 | 0.040 | 0.003 |
| 4.5 | 0.467 | 1821 | 191.55 | 1759.8 | 0.0006 | 0.023 | 0.005 |

**Table F.2 - $^{210}$Pb chronology of GB1 peat core**

| GB1 Depth (cm) | $^{137}$Cs Bq Kg$^{-1}$ | Error (1σ) | GB2 (cut) Depth (cm) | $^{137}$Cs Bq Kg$^{-1}$ | Error (1σ) |
|---|---|---|---|---|---|
| 0.50 | 68.51 | 2.57 | 0.50 | 0.01 | 1.80 |
| 1.50 | 70.66 | 2.28 | 1.50 | 24.02 | 1.86 |
| 3.50 | 40.39 | 2.43 | 2.50 | 19.49 | 1.90 |
| 4.50 | 29.29 | 2.35 | 4.50 | 22.56 | 1.83 |
| 6.50 | 25.09 | 1.94 | 7.50 | 27.94 | 1.78 |
| 8.50 | 20.66 | 2.09 | 10.50 | 24.26 | 1.91 |
| 11.50 | 20.05 | 1.98 | 12.50 | 19.30 | 1.83 |
| 15.50 | 17.67 | 2.08 | 16.50 | 18.43 | 1.73 |
| 19.50 | 13.46 | 1.96 | 19.50 | 22.43 | 1.93 |
| 24.50 | 9.08 | 1.82 | 25.50 | 12.47 | 1.84 |

**Table F.3 - Artificial fallout radionuclide concentrations in GB1 and GB2 peat cores**

# $^{210}$Pb from Loch Brora sediment core

Below are tables and graphs outlining data associated with $^{210}$Pb radiometric dating undertaken on lake core sediment samples from Loch Brora (LB10).

| Depth (cm) | Cumulative Dry Mass (g cm$^{-2}$) | Unsupported $^{210}$Pb Bq Kg$^{-1}$ | Error (1σ) | $^{210}$Pb inventory Bq m$^{-2}$ | Error (1σ) | $^{137}$Cs Inventory Bq m$^{-2}$ | Error (1σ) |
|---|---|---|---|---|---|---|---|
| 1.5 | 0.05 | 290 | 79.7 | 195 | 53 | 288.1 | 7.1 |
| 2.5 | 0.12 | 1007 | 15.4 | 1351 | 21 | 1452.8 | 12.5 |
| 3.5 | 0.24 | 366 | 12.0 | 992 | 32 | 1079.6 | 24.1 |
| 4.5 | 0.38 | 285 | 12.6 | 794 | 35 | 1018.3 | 25.1 |
| 5.5 | 0.54 | 277 | 12.2 | 922 | 40 | 1667.0 | 28.8 |
| 6.5 | 0.65 | 346 | 12.9 | 702 | 26 | 990.0 | 17.8 |
| 7.5 | 0.83 | 274 | 12.2 | 826 | 37 | 1786.7 | 25.9 |
| 8.5 | 0.97 | 288 | 13.3 | 742 | 34 | 1578.4 | 22.8 |
| 9.5 | 1.13 | 276 | 12.1 | 814 | 36 | 1499.4 | 25.7 |
| 10.5 | 1.21 | 283 | 15.6 | 529 | 29 | 1018.0 | 16.8 |
| 11.5 | 1.34 | 207 | 12.1 | 553 | 32 | 2117.2 | 22.8 |
| 12.5 | 1.50 | 230 | 14.9 | 777 | 50 | 2225.4 | 29.4 |
| 13.5 | 1.63 | 249 | 11.9 | 582 | 28 | 1697.9 | 20.2 |
| 14.5 | 1.76 | 222 | 17.0 | 497 | 38 | 1918.6 | 19.4 |
| 15.5 | 1.89 | 162 | 12.9 | 478 | 38 | 2865.9 | 25.3 |
| 16.5 | 2.07 | 136 | 15.2 | 502 | 56 | 2129.0 | 31.7 |
| 17.5 | 2.23 | 108 | 14.9 | 424 | 58 | 1505.5 | 34.1 |
| 18.5 | 2.46 | 94 | 14.4 | 489 | 75 | 1214.4 | 45.5 |
| 19.5 | 2.72 | 100 | 15.0 | 430 | 65 | 1205.3 | 37.8 |
| 20.5 | 3.04 | 81 | 14.9 | 368 | 68 | 1362.7 | 40.0 |
| 21.5 | 3.36 | 91 | 17.5 | 438 | 84 | 1001.1 | 43.4 |
| 22.5 | 3.71 | 49 | 17.1 | 251 | 87 | 1359.3 | 44.9 |
| 23.5 | 3.99 | 78 | 16.6 | 367 | 79 | 1087.2 | 42.5 |
| 24.5 | 4.30 | 126 | 18.1 | 676 | 97 | 1734.3 | 49.2 |
| 25.5 | 4.57 | 90 | 17.1 | 368 | 70 | 1282.6 | 36.4 |
| 26.5 | 4.98 | 41 | 16.4 | 250 | 99 | 1208.1 | 52.9 |
| 27.5 | 5.33 | 49 | 15.3 | 267 | 83 | 1635.9 | 46.8 |
| 28.5 | 5.76 | 40 | 16.4 | 233 | 95 | 1227.1 | 49.7 |
| 29.5 | 6.25 | 39 | 21.2 | 259 | 141 | 1344.1 | 59.7 |
| 30.5 | 6.65 | 31 | 18.6 | 261 | 155 | 1443.9 | 72.1 |
| 31.5 | 7.04 | 28 | 15.2 | 168 | 93 | 1209.5 | 53.1 |

**Table F.4- $^{210}$Pb and $^{137}$Cs concentrations from Loch Brora sediment core**

Loch Brora sediment core $^{210}$Pb dating chronology from 1.5-31.5 cm is presented below.

| Depth (cm) | Dry Mass (g cm$^{-2}$) | Chronology Date (AD) | Age (yr) | Error ( + / -) | Sedimentation Rate g cm$^{-2}$ yr$^{-1}$ | Sedimentation Rate cm yr$^{-1}$ |
|---|---|---|---|---|---|---|
| 1.5 | 0.026 | 2010 | 0 | 1.0 | | |
| 2.5 | 0.088 | 2010 | 0 | 1.0 | 0.160 | 6.55 |
| 3.5 | 0.179 | 2008 | 3 | 0.9 | 0.033 | 1.11 |
| 4.5 | 0.305 | 2006 | 5 | 0.8 | 0.057 | 0.84 |
| 5.5 | 0.456 | 2004 | 7 | 0.8 | 0.080 | 0.76 |
| 6.5 | 0.593 | 2001 | 10 | 0.7 | 0.059 | 0.68 |
| 7.5 | 0.741 | 2000 | 11 | 0.7 | 0.078 | 0.65 |
| 8.5 | 0.901 | 1997 | 14 | 0.7 | 0.067 | 0.61 |
| 9.5 | 1.047 | 1995 | 16 | 0.6 | 0.063 | 0.59 |
| 10.5 | 1.166 | 1992 | 19 | 0.6 | 0.044 | 0.55 |
| 11.5 | 1.276 | 1990 | 21 | 0.5 | 0.058 | 0.55 |
| 12.5 | 1.421 | 1988 | 23 | 0.5 | 0.068 | 0.54 |
| 13.5 | 1.561 | 1985 | 26 | 0.5 | 0.043 | 0.52 |
| 14.5 | 1.692 | 1982 | 29 | 0.4 | 0.049 | 0.50 |
| 15.5 | 1.825 | 1980 | 31 | 0.4 | 0.054 | 0.49 |
| 16.5 | 1.983 | 1977 | 34 | 0.4 | 0.061 | 0.49 |
| 17.5 | 2.154 | 1974 | 37 | 0.4 | 0.058 | 0.47 |
| 18.5 | 2.347 | 1971 | 40 | 0.4 | 0.071 | 0.47 |
| 19.5 | 2.588 | 1968 | 43 | 0.4 | 0.070 | 0.45 |
| 20.5 | 2.879 | 1965 | 46 | 0.4 | 0.087 | 0.44 |
| 21.5 | 3.200 | 1961 | 50 | 0.5 | 0.101 | 0.43 |
| 22.5 | 3.535 | 1957 | 54 | 0.6 | 0.079 | 0.42 |
| 23.5 | 3.848 | 1954 | 57 | 0.7 | 0.115 | 0.42 |
| 24.5 | 4.145 | 1950 | 61 | 0.8 | 0.067 | 0.40 |
| 25.5 | 4.436 | 1940 | 71 | 1.5 | 0.028 | 0.36 |
| 26.5 | 4.773 | 1932 | 79 | 2.2 | 0.046 | 0.34 |
| 27.5 | 5.154 | 1926 | 85 | 3.1 | 0.062 | 0.32 |
| 28.5 | 5.544 | 1918 | 93 | 4.8 | 0.048 | 0.31 |
| 29.5 | 6.005 | 1909 | 102 | 8.0 | 0.049 | 0.29 |
| 30.5 | 6.449 | 1894 | 117 | 16.2 | 0.029 | 0.26 |
| 31.5 | 6.844 | 1863 | 148 | 54.1 | 0.013 | 0.21 |

**Table F.5 - $^{210}$Pb chronology of Loch Brora**

# Appendix G – Age-depth modelling output from *Bacon* V2.2

Utilising *Bacon* V2.2 programme within in R software, an age-depth model was produced for each of the following sediment cores; GB1 (undisturbed peat core), GB2 (cut peat core) and Loch Brora (LB10). A 4 cm resolution was used for both peat and lake cores. Based on this resolution and the input of analysed radiocarbon and $^{210}$Pb samples, *Bacon* calculated calibrated radiocarbon ages and sediment accumulation rates throughout all studied cores (see section 4.3.2 for more details relating to the *Bacon* programme). This data was fundamental to the calculation of peat and Loch Brora core C sequestration histories presented in Chapter 7. A visual representation of peat and Loch Brora age-depth models produced is displayed below (Figure G.1), the figure caption is on the next page.

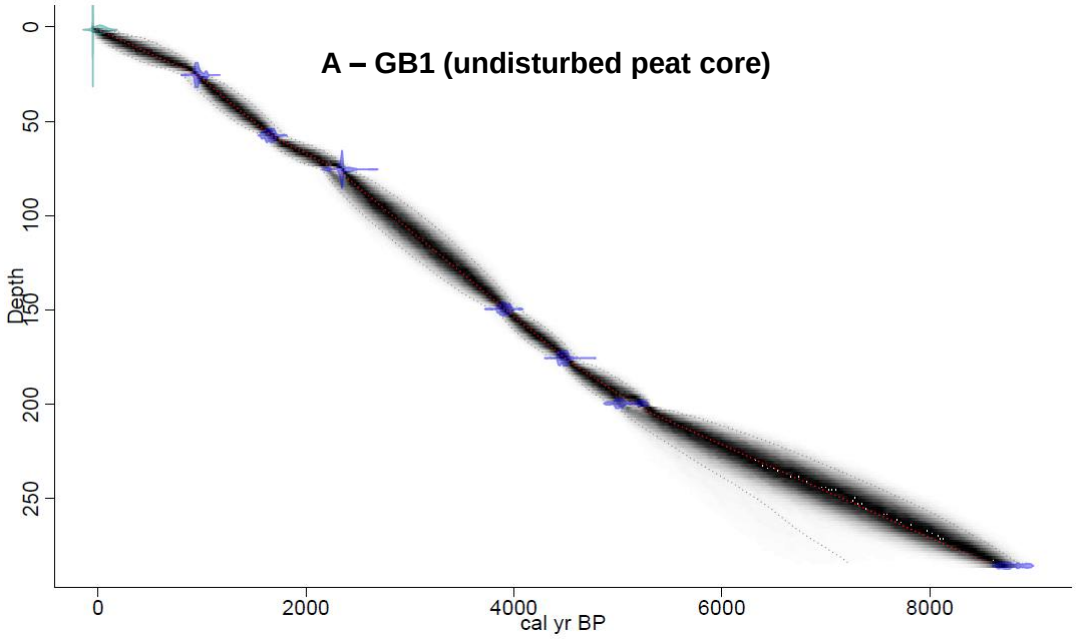


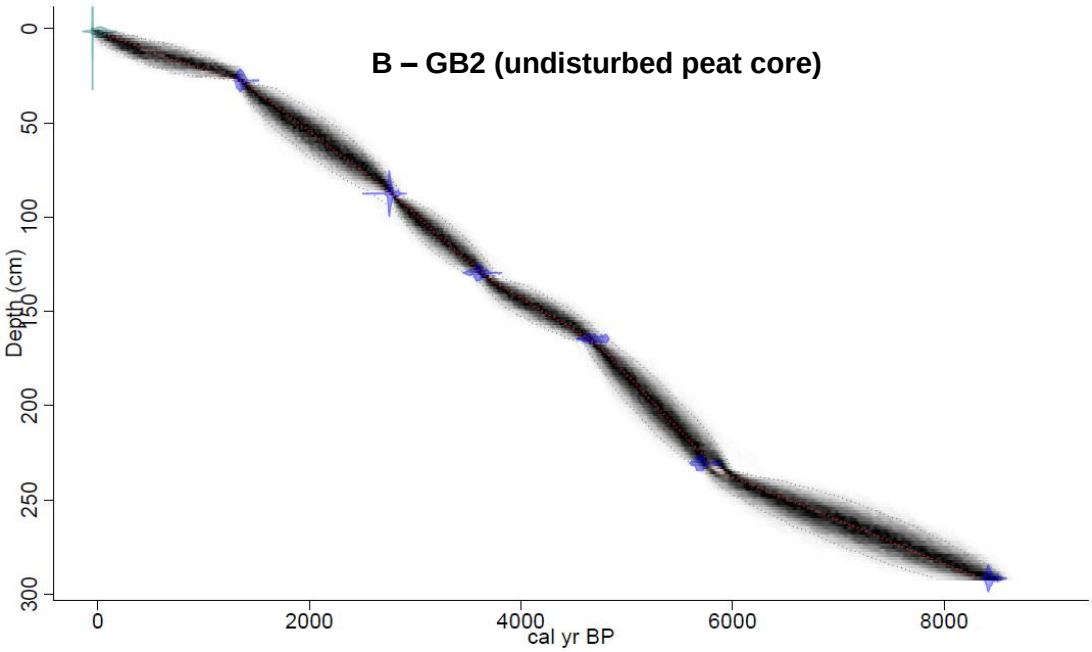

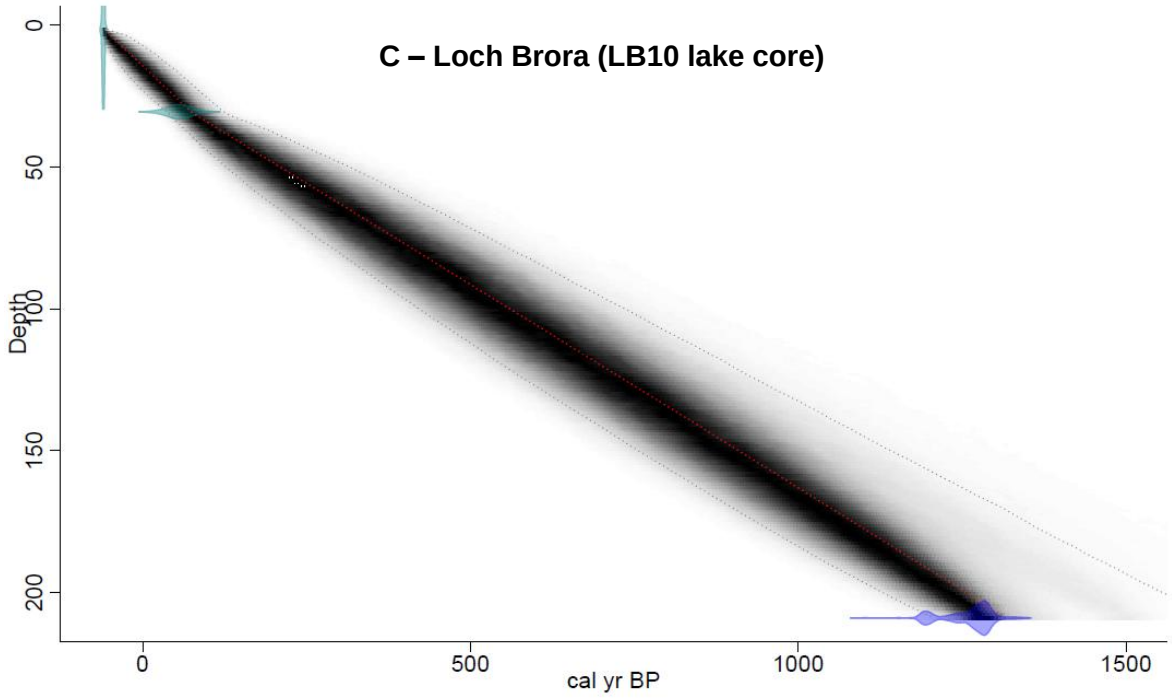


**Figure G.1 - Age-depth modelling output from *Bacon***
A = GB1 peat core age-depth model, B = GB2 (cut) peat core, C = Loch Brora (LB10) lake core. On all graphs the x-axis unit is calibrated years before (cal. yr. BP) and y-axis unit is depth in centimetres (cm). All graphs presented are outputs generated by using *Bacon* software in R. The shaded areas around the red line represent all statistically possible age estimations for any given depth based on multiple MCMC iterations. These areas become larger when the gap between any two adjacent radiocarbon samples is bigger. The darker the shaded areas represent the most likely age estimates. The red line itself represents the 'best' age model based on all MCMC iterations. The blue dots and associated error bars represent provided radiocarbon ages. The green lines near 0 cm depth represent age estimates provided from $^{210}$Pb dating.

From the age models produced, both accumulation of peat in these cores have very similar trends (Figure G.1A&B). This model inference supports our peat-cutting estimate of 30 cm. The wide green bands at the top of the core illustrate the uncertainty associated with $^{210}$Pb dating from surface sediments. Even though a successful $^{210}$Pb chronology could not be constructed for GB2 due to disturbance at the site, estimated ages and associated errors within top 2 cm (depth of estimated hiatus) of GB1 $^{210}$Pb chronology were used in the GB2 age-depth model. There is only one AMS $^{14}$C age anchoring the base of the Loch Brora core, and therefore the limits of the error surrounding the age model estimates are constant from ~32 cm; the limit of $^{210}$Pb analysis (Figure G.1C).

# Appendix H – Methodology for inferring WTD from PT data sets

The data recorded by the PTs located in the drain-blocking transect, the drain and control PTs (data presented in Chapter 8), was not a direct measure of the water table depth (WTD), rather they measured pressure and thus the height of water above the PT (Figure H.1, 'C'). Therefore, a method was needed to infer WTD from data recorded by both PTs.

A schematic representation of how WTD was measured is presented (Figure H.1). Subtracting the values of 'B' from 'A' gave a manual value of WTD. The series of manual WTD measurements, recorded at control and drain PTs, and corresponding PT data values have been used to create linear relationships so a continuous WTD profile could be inferred. It should be noted there was a need to correct some of the PT data and methodology for this is outlined later in this chapter.

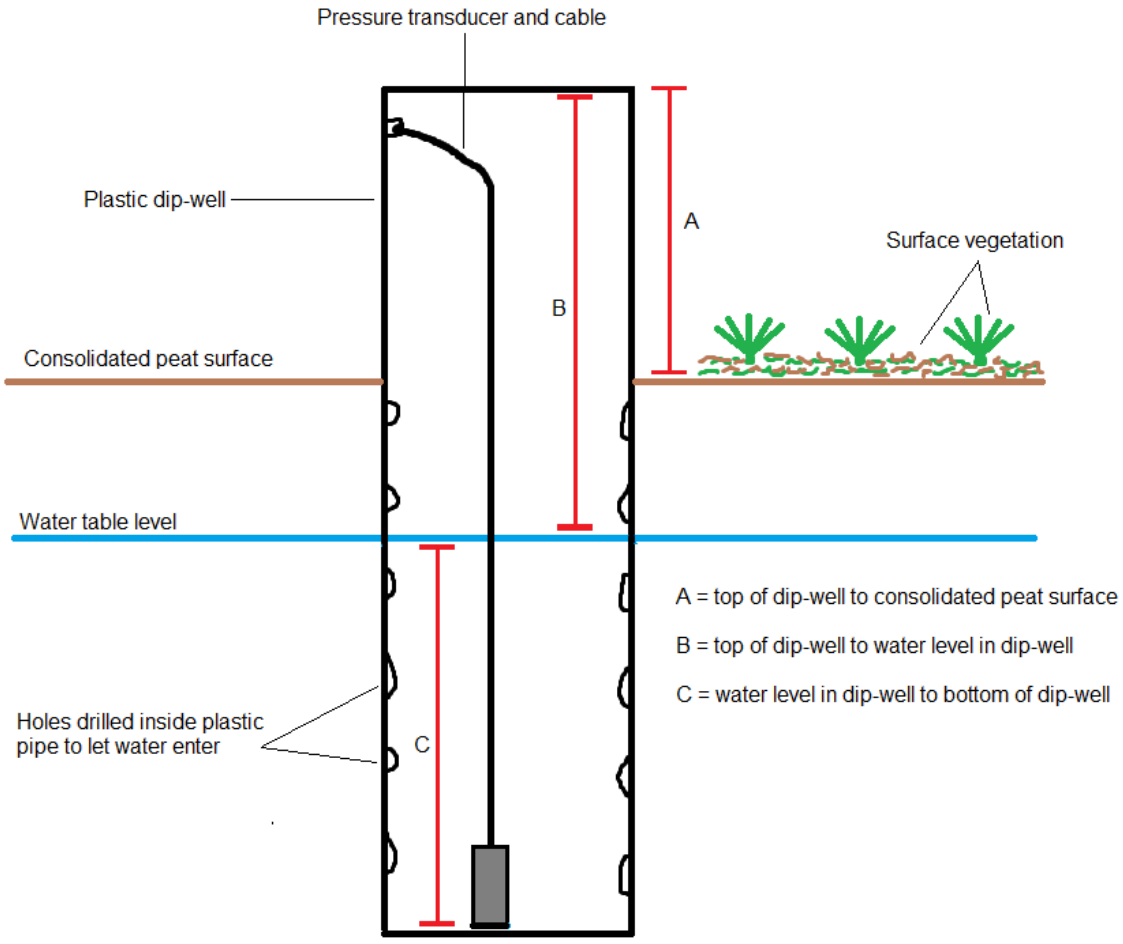


**Figure H.1 – Schematic representation of how WTD was recorded**
The diagram above demonstrates what measurements were taken manually and automatically by pressure transducers in order to calculate water table depth in dip-wells. Each time data were downloaded from both drain and control PTs, the height of the dip-well casing above the consolidated peat surface ('A') and the distance between the top of the dip-well casing to the water table depth ('B') were measured. 'B' was measured using a graduated hollow cane (at 1 cm resolution), blowing into the pipe whilst lowering it into the dip-well. When bubbles were heard, the depth the cane had been lowered to be recorded (also explained in Chapter 3, section 3.11.3).

In addition, it was investigated if using an 'anchor point' for inferring WTD gave differing results. The method was in effect a one point calibration and assumed perfect linearity between manual WTD and PT value after the first measurement, i.e. the PT value is used as an offset, e.g., if manual WTD = -5 cm and PT value = 90 cm, the 'anchor point' method would infer manual WTD = -6 cm would equate to PT value = 89 cm etc. such for the above example the following linear equation, y = 1x – 95 (i.e. WTD = PT value – 95) would describe relationship between WTD and PT values.

## Inferring WTD using linear regression

In principal the manual measurements of WTD and the PT values should form a good 1:1 relationship. The relationships constructed from both Control and Drain PT sites are presented below (Figure H.2 & Figure H.3).

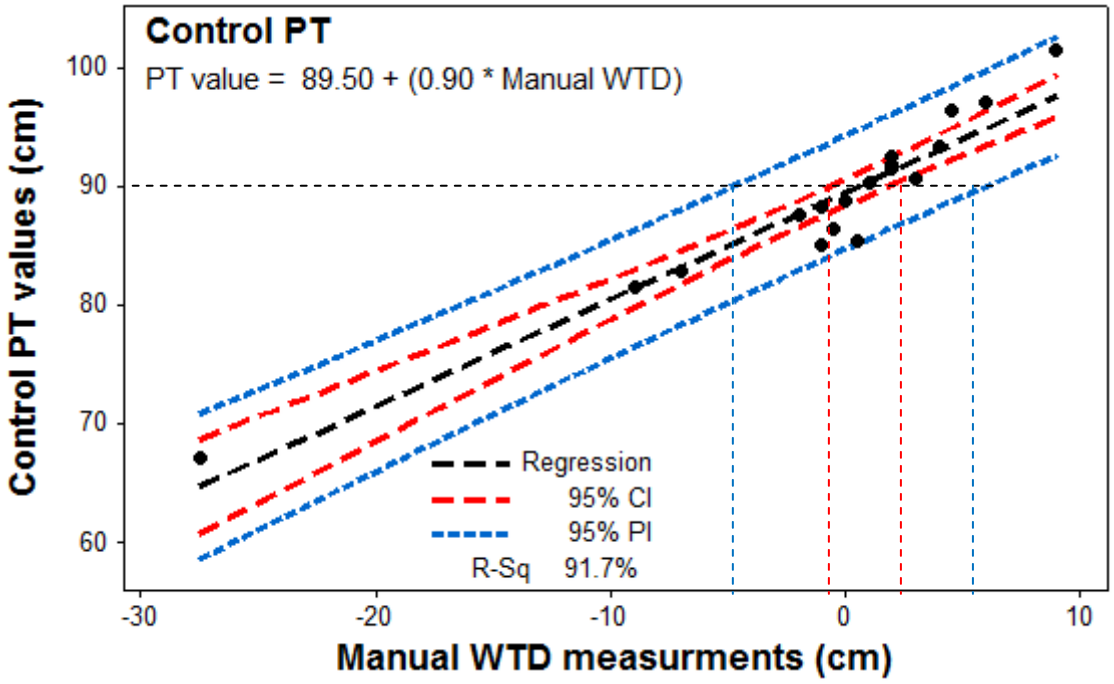


**Figure H.2 - Linear relationship of manual WTD plotted against Control PT data**
The equation for the linear regression line (black) if displayed, along with the $R^2$ value, 95% confidence intervals (red) and 95% prediction intervals (blue). An example is given how the size of the confidence interval and prediction intervals of the regression relate to uncertainty of manual WTD associated with the Control PT value of 90 cm. The confidence intervals encompass 2.5 cm, between -0.5 to ~2 cm and prediction intervals 10 cm, between -5 cm and + 5 cm.

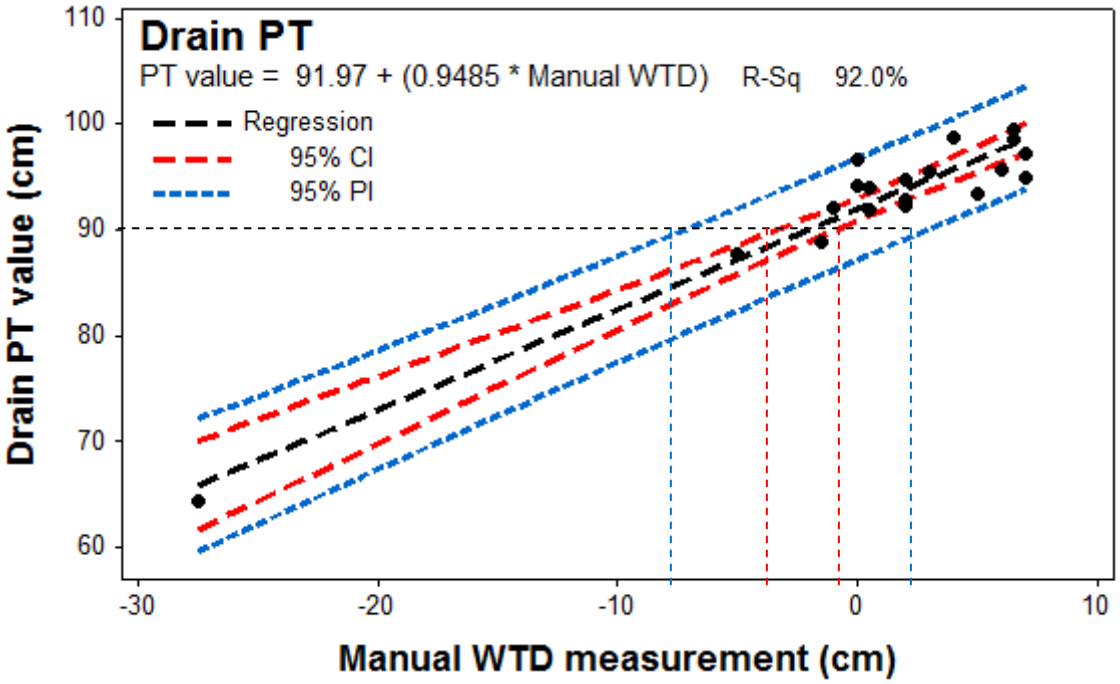


**Figure H.3 - Linear relationship between manual WTD plotted against Drain PT data**
The equation for the linear regression line (black) if displayed, along with the $R^2$ value, 95% confidence intervals (red) and 95% prediction intervals (blue). An example is given how the size of the confidence interval and prediction intervals of the regression relate to uncertainty of manual WTD associated with the Drain PT value of 90 cm. The confidence intervals encompass ~3 cm, between ~-3.6 to ~-0.6 cm and prediction intervals ~10 cm, between -7.5 cm and + 2.5 cm.

The linear regression relationships used to infer WTD for both Control and Drain PT sites have high $R^2$ = 0.92 (both) and a p = <0.01 (both), indicating the relationships are highly significant. Using 'inverse regression' methodology (Draper & Smith, 1998; Miller & (Edited by Thompson, 2006) the confidence intervals of the linear regressions for both sites indicate the line of best fit is within ± 2-3 cm of the manually measured WTD, the prediction intervals for both relationships indicate WTD can only be inferred on average of ± 10 cm based on the data points collected (Figure H.2 & Figure H.3). These prediction intervals therefore represent large differences and correspond to some of the sources of variability that were associated with manually collected WTD measurements, some examples are: the accuracy of the graduations on the hollow pipe used, the weather conditions (i.e. wind speed) affecting when the bubbles are heard, when you hear bubbling depends on how windy, how deep the water table is as sound will be lost as it travels by absorbance.

Figure H.4 displays time series of WTD using multiple point calibration and 'anchor point' techniques from both Control and Drain PT sites. Table H.1 and Table H.2 also show some key statistics from both approaches inferring WTD time series. Both PTs were initially installed on 15/6/11 but were re-installed on 6/8/11 to fit a bigger plastic dip-well casing. Thus, due to a lack of manual WTD data points collected between 15/6/11 and 6/8/11, constructing a linear relationship for this time period was not feasible. Therefore

the 'anchor point' was exclusively used to infer WTD at this time and so, in the tables that follow no data is presented for WTD inferred by the linear relationships (Figure H.4) between 15/6/11 and 5/8/11.

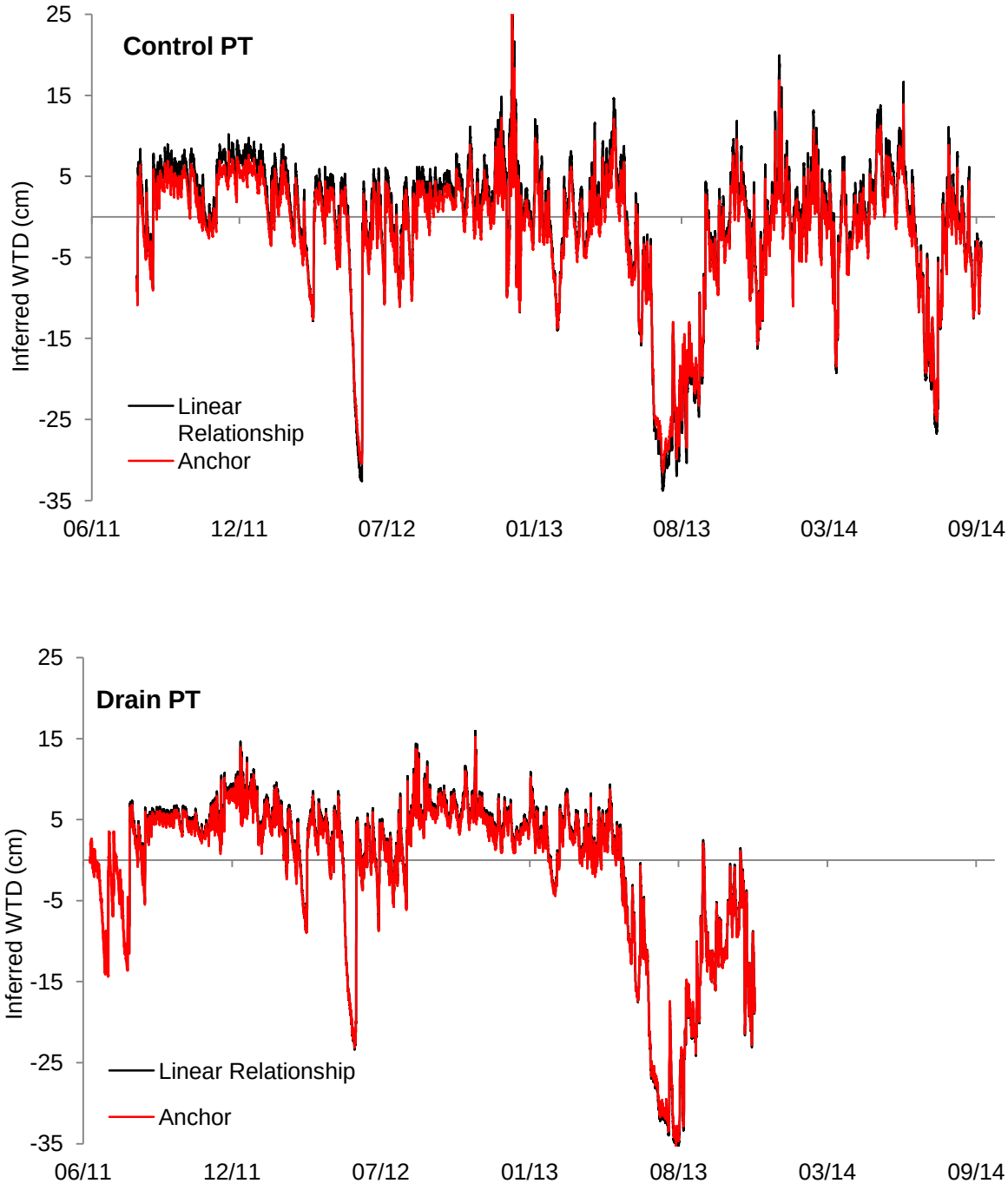


**Figure H.4 - Continuously inferred WTD times series from Control and Drain PTs**
WTD profiles based on linear relationships presented in Figure H.2 (Control PT) and Figure H.3 (Drain PT) are presented (black) along with WTD inferred using the 'anchor point' technique (red). The 'anchor point' equations used for the Control PT between 15/6/11 and 5/8/11 were y = 1x – 63.587 and from 6/8/11 to the end of the data record (24/9/14) y = 1x - 90.612 respectively. The 'anchor point' equations used for the Drain PT between 15/6/11 and 5/8/11 were y = 1x – 68.11 and from 6/8/11 to the end of the data record (24/11/13) y = 1x - 92.665 respectively The Drain PT is shorter as the PT ceased working on 24/11/13, thought to be due to water ingress. The Control PT continued to record data up to 24/9/14 when it was last downloaded.

| **CONTROL PT** | | | Linear Regression | Anchor |
|---|---|---|---|---|
| **Date of Download** | **PT reading (cm)** | **Manual WTD (cm)** | **Inferred WTD (cm)** | **Inferred WTD (cm)** |
| *15/06/2011 17:30* | | *-1* | *n/a* | *1.9* |
| *23/06/2011 10:15* | | *-2* | *n/a* | *-1.4* |
| *05/08/2011 17:00* | *56.587* | *-7* | *n/a* | *-7.0* |
| **After re-installation the 2nd continuous record started on 6/8/11** | | | | |
| 27/08/2011 13:10 | 81.612 | -9 | -8.8 | -9.0 |
| *17/11/2011 10:14* | *90.081* | *-6* | *0.6* | *-0.5* |
| 13/12/2011 13:45 | 97.016 | 6 | 8.4 | 6.4 |
| 23/01/2012 12:39 | 96.382 | 4.5 | 7.6 | 5.8 |
| 03/02/2012 12:45 | 88.301 | -1 | -1.3 | -2.3 |
| 06/03/2012 09:24 | 87.567 | -2 | -2.1 | -3.0 |
| 02/04/2012 14:38 | 90.376 | 1 | 1.0 | -0.2 |
| 27/04/2012 09:30 | 93.376 | 4 | 4.3 | 2.8 |
| 20/06/2012 09:09 | 91.448 | 2 | 2.2 | 0.8 |
| 31/07/2012 09:37 | 86.483 | -0.5 | -3.3 | -4.1 |
| 16/08/2012 09:25 | 91.844 | 2 | 2.6 | 1.2 |
| 11/09/2012 09:42 | 90.748 | 3 | 1.4 | 0.1 |
| *29/11/2012 12:03* | *91.318* | *7.5* | *2.0* | *0.7* |
| *09/01/2013 09:47* | *88.931* | *5.5* | *-0.6* | *-1.7* |
| *20/02/2013 11:22* | *84.294* | *1.5* | *-5.8* | *-6.3* |
| 10/04/2012 10:49 | 88.757 | 0 | -0.8 | -1.9 |
| 14/05/2013 10:26 | 101.487 | 9 | 13.3 | 10.9 |
| 24/06/2013 14:23 | 85.484 | 0.5 | -4.5 | -5.1 |
| 05/08/2013 12:32 | 67.088 | -27.5 | -24.9 | -23.5 |
| 16/09/2013 14:50 | 92.481 | 2 | 3.3 | 1.9 |
| 24/09/2014 15:40 | 85.006 | -1 | -5.0 | -5.6 |
| **Basic statistics from inferred time series June 2011 to Sept. 2014** | | | | |
| **Method** | Linear | Anchor | | |
| Mean | -1.5 | -2.5 | | |
| Minimum | 19.9 | 16.8 | | |
| Maximum | -33.8 | -31.5 | | |
| Total Range | 53.7 | 48.3 | | |
| Median | 1.2 | 0.0 | | |

**Table H.1 - Control PT site data**
Dates of downloads corresponding Control PT values and manual WTD measurements are presented in comparison to WTD values inferred using the linear regression and anchor point techniques. Some basic statistics relating to data presented in the time series (Figure H.4) are presented at the bottom of the table for each technique. The data highlighted in italics was excluded when creating the linear relationship between manual WTD and PT value, reasons for which are given later on in this chapter, section 0 PT data correction.

| **DRAIN PT** | | | Linear Regression **Inferred** | Anchor **Inferred** |
|---|---|---|---|---|
| **Date of Download** | **PT reading (cm)** | **Manual WTD (cm)** | **WTD (cm)** | **WTD (cm)** |
| 15/06/2011 18:00 | | -31 | *n/a* | -0.31 |
| 23/06/2011 10:45 | | -31 | *n/a* | -0.96 |
| 05/08/2011 16:00 | 61.61 | -6.5 | *n/a* | -6.5 |
| **After re-installation the 2nd continuous record started on 6/8/11** | | | | |
| 27/08/2011 14:27 | 87.665 | -5 | -4.5 | -5.0 |
| 17/11/2011 11:16 | 95.544 | 3 | 3.8 | 2.9 |
| 13/12/2011 13:28 | 100.733 | no data | 9.2 | 8.1 |
| 23/01/2012 12:25 | 98.603 | 6.5 | 7.0 | 5.9 |
| 03/02/2012 12:30 | 96.724 | 0 | 5.0 | 4.1 |
| 06/03/2012 09:00 | 92.136 | -1 | 0.2 | -0.5 |
| 02/04/2012 14:24 | 94.059 | 0.5 | 2.2 | 1.4 |
| 27/04/2012 09:30 | 95.74 | 6 | 4.0 | 3.1 |
| 20/06/2012 10:13 | 92.912 | 2 | 1.0 | 0.2 |
| 31/07/2012 09:37 | 91.919 | 0.5 | 0.0 | -0.7 |
| 16/08/2012 09:05 | 94.745 | 2 | 2.9 | 2.1 |
| 11/09/2012 09:29 | 98.66 | 4 | 7.1 | 6.0 |
| 29/11/2012 11:45 | 97.254 | 7 | 5.6 | 4.6 |
| 09/01/2013 09:35 | 94.891 | 7 | 3.1 | 2.2 |
| 20/02/2013 11:04 | 92.271 | 2 | 0.3 | -0.4 |
| 10/04/2012 10:21 | 94.142 | 0 | 2.3 | 1.5 |
| 14/05/2013 10:11 | 99.56 | 6.5 | 8.0 | 6.9 |
| 24/06/2013 13:32 | 88.859 | -1.5 | -3.3 | -3.8 |
| 05/08/2013 13:12 | 64.393 | -27.5 | -29.1 | -28.3 |
| 16/09/2013 14:40 | 93.399 | 5 | 1.5 | 0.7 |
| **reliable data ends on approx. 24/11/13 @ 10:00 (due to suspected water ingress)** | | | | |
| **Basic statistics from inferred time series June 2011 to Nov. 2013** | | | | |
| **Methods** | Linear | Anchor | | |
| Mean | -3.5 | -4.0 | | |
| Minimum | 16.0 | 14.4 | | |
| Maximum | -36.1 | -35.0 | | |
| Range | 52.1 | 49.5 | | |
| Median | 3.2 | 2.3 | | |

**Table H.2 - Drain PT site data**
Dates of downloads corresponding Control PT values and manual WTD measurements are presented in comparison to WTD values inferred using the linear regression and anchor point techniques. Some basic statistics relating to data presented in the time series (Figure H.4) are presented at the bottom of the table for each technique.

The time series of WTD profiles using linear and 'anchor point' relationships show general trends throughout the monitoring period are the same (Figure H.4). Furthermore, when the basic statistics are compared for linear and 'anchor' techniques for both Control (Table H.1) and Drain (Table H.2) PTs, there are only slight differences between values. Paired t-test results between linear and 'anchor point' inferred values for all download dates indicate there is a significant difference ($p < 0.05$) between the both Control and Drain PT

sets of data but means differ by only ~1 cm (Control PT = 1.06 cm and Drain PT = 0.77 cm).

It is noticeable WTD is inferred to be above > 0 cm for extended time periods. Although this is not unrealistic considering WTD is measured from the peat surface and not the vegetation surface and the previously highlighted issue of pooling of water around PT sites, the magnitude of some WTDs inferred, especially > 5 cm could be considered to be unusual. This could indicate the linear relationships are perhaps not correctly inferring WTD, however, the magnitude of the prediction intervals should be considered (Figure H.2 & Figure H.3). Therefore, the large of amount of WTD data inferred > 0 cm is only a reflection of the range, number and measurement variability of manual WTD data points collected, rather than an inherent problem inferring WTD using the linear regression or any inaccuracies of the PT data recorded.

Although the time series and basic statistics for the 'anchor point' method produces similar results compared to linear relationships used to infer WTD, the linear equations base the relationship between PT data and manual measurements on several rather than one data point. Thus, I opted to use the linear regression approach as although the uncertainty is large (± 10 cm), I can constrain and predict it which is something I cannot do with the 'anchor point' approach.

## PT data correction

Both PTs had to be corrected for two main reasons: the first was changes in values caused by movement of the PTs themselves during download periods and the second were spikes caused by electrical noise. Instances of both were identified and data sets were corrected and adjusted accordingly. Examples of both types of disturbance caused by downloading data from PTs and suspected electrical noise are presented (Figure H.6 & Figure H.5).

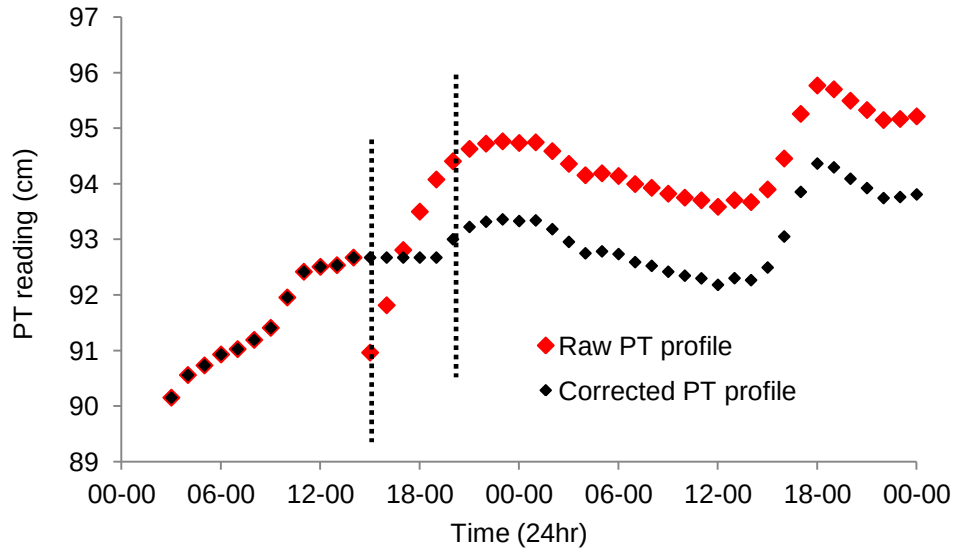


**Figure H.6 – An example of human induced disturbance in PT data and relative correction.** The example above is from the control PT record and a download which occurred on 2/4/12 at 14:38. The red markers are representative of the raw PT data and the black markers represent the corrected data. The left dashed black line represents the first data point after the time of downloading when a disturbance has clearly taken place. The right dashed black line represents the extent of the data correction and where it is assumed the PT is once again stable and the data it is recording starts representing 'natural' changes after the disturbance period. In this example the raw PT data is moved down to counteract the disturbance caused by movement induced when data was downloaded.

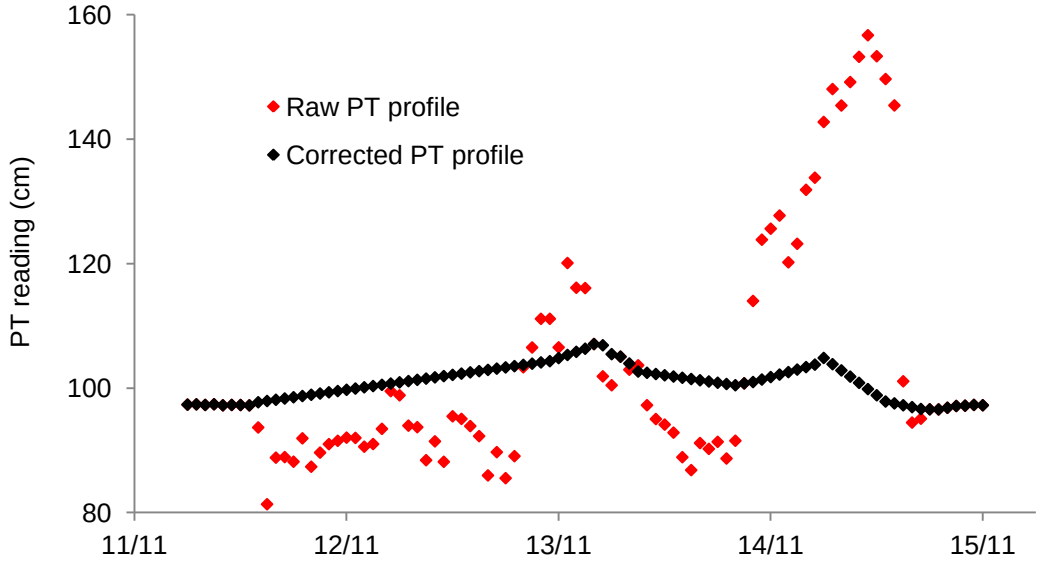


**Figure H.5 – An example of electrical noise disturbance in PT data**
This example is taken from data from drain PT during 12/11/12 and 15/11/12. The changes recorded by the PT (raw data) range from 80 to 160 cm. This 80 cm range in WTD change over 3 days was deemed unrealistic and due to electrical noise. Having examined river hydrograph data there was a small storm event on 13/11/12 and this is why the corrected data shows an increase in WTD to this point. Correcting or reconstructing periods of data like this so the most representative WTD changes are reflected in the PT profile was not a straightforward, and challenging, task. However, meteorological conditions were used to inform the correction process to make the best possible estimate of WTD at PT sites when these 'spikes' occurred.

Examples of human induced disturbance (Figure H.6) were common as it was extremely difficult to remove the connecting component of the PT from the plastic casing without

disturbing the PT position even slightly. However, these disturbances occurred exclusively during download periods so were easily isolated and fixed.

The irregularities in the PT data sets caused by electrical noise (Figure H.5) were most prevalent in the Control PT data between download dates 29/12/2012 and 20/2/13. During this time period, sporadic measurements showed changes on 80 cm in a few hours, which is clearly unrealistic for water table movement in a peat soil. This issue was mitigated by using a 24 hour running average during the affect period but it is accepted there is a greater uncertainty associated with data collected during the period. This fact was acknowledged when the WTD time series was presented in Chapter 8. Also, due to this problem, manual WTD measurements and corresponding PT value data points recorded during this time period were excluded when establishing a linear relationship to infer WTD on a continuous basis. In addition, barring the November 2012 to February 2013 time period for Control PT data, other instances of 'spikes' were much more isolated in both data sets, such instances commonly only occurred once every two months.

Furthermore, one additional data point collected on the 17/11/11 from Control PT was excluded from the construction of the linear relationship between manual WTD and PT values. On this date, both PTs were removed from their plastic cases to be 'winter-proofed'. This stemmed for concern that during the winter months freezing temperatures may permanently damage the PT sensors so it was decided to protect them. Therefore, a condom filled with vodka (40 % alcohol freezes at ~(-27°C)) was securely fastened to each PT, with the sensory part of the PT submersed in vodka. A similar disturbance did not seem to be caused when collecting the equivalent manual WTD measurement at the drain PT so this data point was included. Finally, the data record for the drain PT ended on 24/11/13 due to suspected water ingress permanently damaging the sensor. The control PT remained in working order up to the last download date of 24/9/14.

# Appendix I – WTD in dip-wells along drain transect

Below I present graphs showing manually collected WTD data from dip-wells located within all six drain transects at the Gordonbush drain blocking site (Figure I.1, the caption is on the following page). The following plots have been normalised for topographic height compared to plots presented in section 8.4.2.2 where data was topographically corrected.

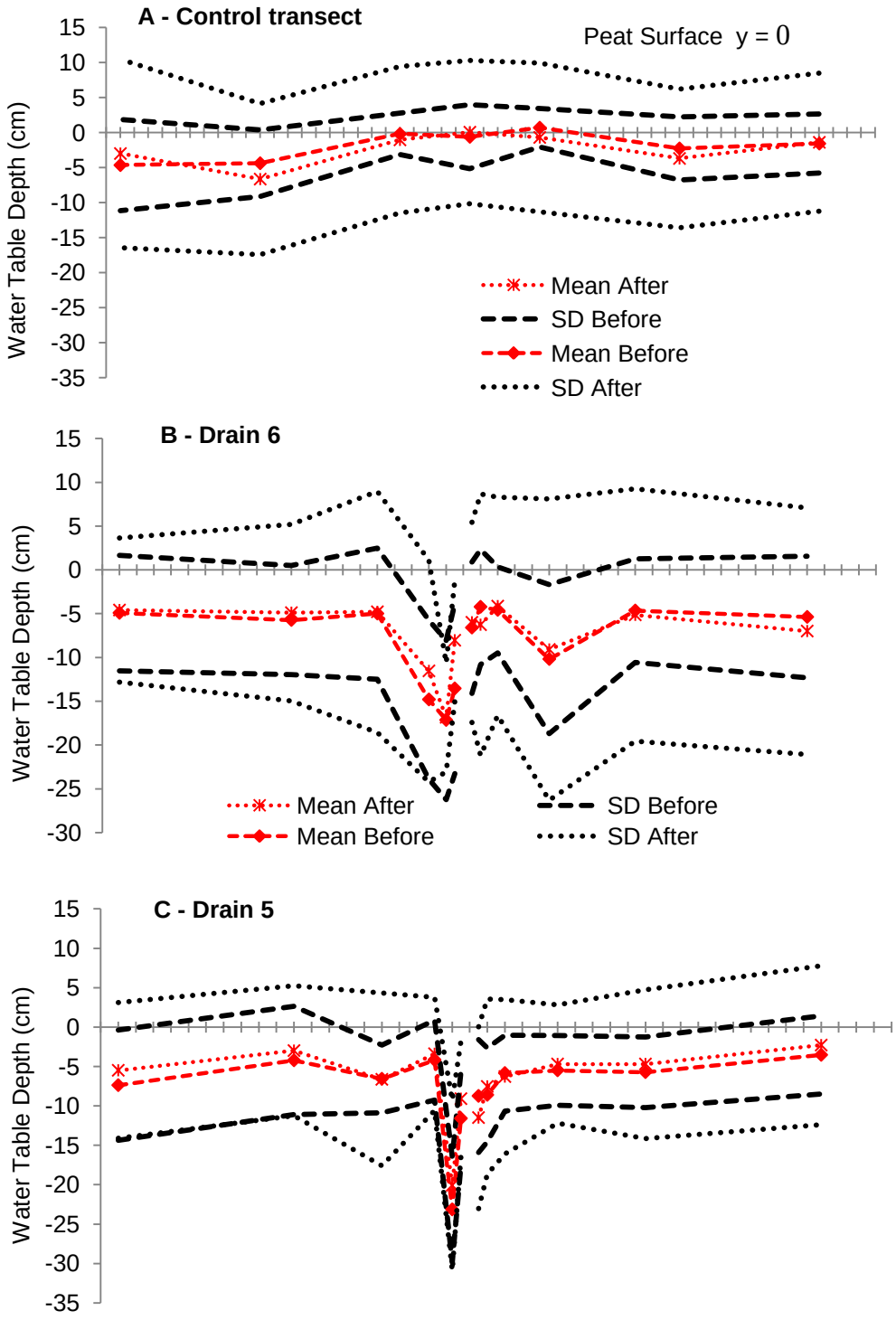

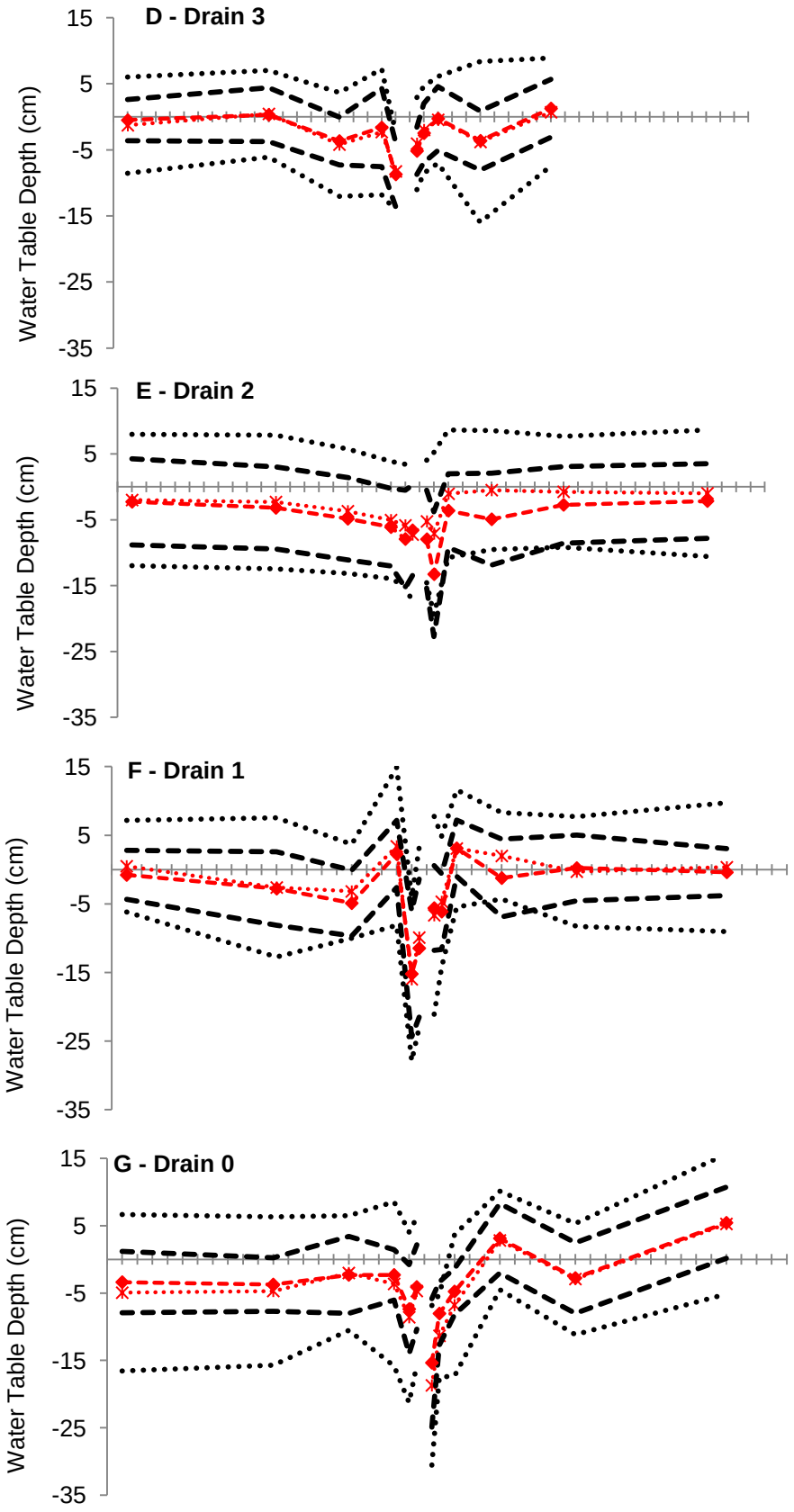


**Figure I.1 – Topographically normalised plots of mean WTD measured at dip-wells (W-E) transects** Mean WTD, of 23 manual measurements between Jun. 2011 and Sept. 2014, are presented in red, with red diamonds and red asterisks measurements before (n = 14) and after drain-blocking (n = 9) respectively. The black lines represent standard deviations (SD) of the mean WTD, the thick dashed lines represents data before and thin dashed lines after" drain-blocking. The y = 0 line represents the peat surface from which WTD was calculated from. The dip-wells are drawn to scale: 0.5, 1, 2, 10, and 20 metres from each side of the drain, and the gap is the drain. The names of each drain and corresponding letter A – G are displayed in top left hand corner of individual plots. The legend is only present on graph A.

# References

Adamson, J.K., Scott, W.A. and Rowland, A.P. (1998) 'The dynamics of dissolved nitrogen in a blanket peat dominated catchment', *Environmental Pollution,* 99(1), 69-77.

Adamson, J.K., Scott, W.A., Rowland, A.P. and Beard, G.R. (2001) 'Ionic concentrations in a blanket peat bog in northern England and correlations with deposition and climate variables', *European Journal of Soil Science,* 52(1), 69-79.

Adrian, R., O'Reilly, C.M., Zagarese, H., Baines, S.B., Hessen, D.O., Keller, W., Livingstone, D.M., Sommaruga, R., Straile, D., Van Donk, E., Weyhenmeyer, G.A. and Winder, M. (2009) 'Lakes as sentinels of climate change', *Limnology and Oceanography,* 54(6), 2283-2297.

Aerts, R., Wallén, B., Malmer, N. and De Caluwe, H. (2001) 'Nutritional constraints on Sphagnum-growth and potential decay in northern peatlands', *Journal of Ecology,* 89(2), 292-299.

Agren, A., Buffam, I., Bishop, K. and Laudon, H. (2010a) 'Modeling stream dissolved organic carbon concentrations during spring flood in the boreal forest: A simple empirical approach for regional predictions', *Journal of Geophysical Research-Biogeosciences,* 115.

Agren, A., Haei, M., Kohler, S.J., Bishop, K. and Laudon, H. (2010b) 'Regulation of stream water dissolved organic carbon (DOC) concentrations during snowmelt; the role of discharge, winter climate and memory effects', *Biogeosciences,* 7(9), 2901-2913.

Agren, A.M., Buffam, I., Cooper, D.M., Tiwari, T., Evans, C.D. and Laudon, H. (2014) 'Can the heterogeneity in stream dissolved organic carbon be explained by contributing landscape elements?', *Biogeosciences,* 11(4), 1199-1213.

Agren, A.M., Haei, M., Blomkvist, P., Nilsson, M.B. and Laudon, H. (2012) 'Soil frost enhances stream dissolved organic carbon concentrations during episodic spring snow melt from boreal mires', *Global Change Biology,* 18(6), 1895-1903.

Ahtiainen, M. and Huttunen, P. (1999) 'Long-term effects of forestry managements on water quality and loading in brooks', *Boreal Environment Research,* 4, 101-114.

Aitkenhead-Peterson, J.A., Alexander, J.E. and Clair, T.A. (2005) 'Dissolved organic carbon and dissolved organic nitrogen export from forested watersheds in Nova Scotia: Identifying controlling factors', *Global Biogeochemical Cycles,* 19(4), GB4016.

Aitkenhead-Peterson, J.A., McDowell, W.H. and Neff, J.C. (2003) '2 - Sources, Production, and Regulation of Allochthonous Dissolved Organic Matter Inputs to Surface Waters' in Findlay, S.E.G. and Sinsabaugh, R.L., eds., *Aquatic Ecosystems*, Burlington: Academic Press, 25-70.

Aitkenhead-Peterson, J.A., Smart, R.P., Aitkenhead, M.J., Cresser, M.S. and McDowell, W.H. (2007) 'Spatial and temporal variation of dissolved organic carbon export from gauged and ungauged watersheds of Dee Valley, Scotland: Effect of land cover and C:N', *Water Resources Research,* 43(5), W05442.

Aitkenhead, J.A., Hope, D. and Billett, M.F. (1999) 'The relationship between dissolved organic carbon in stream water and soil organic carbon pools at different spatial scales', *Hydrological Processes,* 13(8), 1289-1302.

Aitkenhead, J.A. and McDowell, W.H. (2000) 'Soil C:N ratio as a predictor of annual riverine DOC flux at local and global scales', *Global Biogeochemical Cycles,* 14(1), 127-138.

Algesten, G., Sobek, S., Bergstrom, A.K., Agren, A., Tranvik, L.J. and Jansson, M. (2004) 'Role of lakes for organic carbon cycling in the boreal zone', *Global Change Biology,* 10(1), 141-147.

Alin, S.R., Rasera, M., Salimon, C.I., Richey, J.E., Holtgrieve, G.W., Krusche, A.V. and Snidvongs, A. (2011) 'Physical controls on carbon dioxide transfer velocity and flux in low-gradient river systems and implications for regional carbon budgets', *Journal of Geophysical Research-Biogeosciences,* 116.

Allison, L.E. (1965) 'Organic carbon' in Black, C.A., ed. *Methods of Soil Analysis Part 2*, USA: Madison: American Society of Agronomy, 1367-1378.

Allott, T.E.H., Evans, M.G., Lindsay, J.B., Agnew, C.T., Freer, J.E., Jones, A. and Parnell, M. (2009) *Water tables in Peak District blanket peatlands* UK: Partnership, M.f.t.F.: Moors for the Future Partnership, available: https://www.escholar.manchester.ac.uk/api/datastream?publicationPid=uk-ac-man-scw:18867&datastreamId=FULL-TEXT.PDF [Accessed 21/1/15].

Aminot, A. and Rey, F. (2000) 'Standard procedure for the determination of chlorophyll a by spectroscopic methods', *International Council for the Exploration of the Sea*, 1-12.

Anderson, A.R., Ray, D. and Pyatt, D.G. (2000) 'Physical and hydrological impacts of blanket bog afforestation at Bad a′ Cheo, Caithness: the first 5 years', *Forestry,* 73(5), 467-478.

Anderson, D.E. (1998) 'A reconstruction of Holocene climatic changes from peat bogs in north-west Scotland', *Boreas,* 27(3), 208-224.

Anderson, D.E. (2002) 'Carbon accumulation and C/N ratios of peat bogs in North-West Scotland', *Scottish Geographical Journal,* 118(4), 323-341.

Anderson, D.E., Binney, H.A. and Smith, M.A. (1998) 'Evidence for abrupt climatic change in northern Scotland between 3900 and 3500 calendar years BP', *The Holocene,* 8(1), 97-103.

Anderson, N.J., Bennion, H. and Lotter, A.F. (2014) 'Lake eutrophication and its implications for organic carbon sequestration in Europe', *Global Change Biology*, n/a-n/a.

Anderson, N.J., D'Andrea, W. and Fritz, S.C. (2009) 'Holocene carbon burial by lakes in SW Greenland', *Global Change Biology,* 15(11), 2590-2598.

Anderson, N.J., Dietz, R.D. and Engstrom, D.R. (2013) 'Land-use change, not climate, controls organic carbon burial in lakes', *Proceedings of the Royal Society B: Biological Sciences,* 280(1769), 20131278.

Appleby, P.G. (2001) 'Chronstratigraphic Tecniques in Recent Sediments' in Last, W.M. and Smol, J.P., eds., *Tracking Environmental Change USing Lake Sediments, Volume 1: Basin Analysis, Coring and Chronological Techniques*, Dordrecht, Netherlands: Kluwer Academic Publishers, 171-203.

Appleby, P.G. (2008) 'Three decades of dating recent sediments by fallout radionuclides: a review', *The Holocene,* 18(1), 83-93.

Appleby, P.G., Nolan, P.J., Gifford, D.W., Godfrey, M.J., Oldfield, F., Anderson, N.J. and Battarbee, R.W. (1986) '210Pb dating by low background gamma counting', *Hydrobiologia,* 143(1), 21-27.

Appleby, P.G. and Oldfield, F. (1978) 'The calculation of lead-210 dates assuming a constant rate of supply of unsupported 210 Pb to the sediment', *CATENA,* 5(1), 1-8.

Appleby, P.G. and Oldfieldz, F. (1983) 'The assessment of 210Pb data from sites with varying sediment accumulation rates', *Hydrobiologia,* 103(1), 29-35.

Aquatic Research Instruments, A.R.I. (2013) 'ARI Russian Peat Borer', *Aqautic Research News* [online], available: http://www.aquaticresearch.com/russian_peat_borer.htm [Accessed 12/11/2014]

Arhonditsis, G.B., Papantou, D., Zhang, W., Perhar, G., Massos, E. and Shi, M. (2008) 'Bayesian calibration of mechanistic aquatic biogeochemical models and benefits for environmental management', *Journal of Marine Systems,* 73(1–2), 8-30.

Armstrong, A., Holden, J., Kay, P., Foulger, M., Gledhill, S., McDonald, A.T. and Walker, A. (2009) 'Drain-blocking techniques on blanket peat: A framework for best practice', *Journal of Environmental Management,* 90(11), 3512-3519.

Armstrong, A., Holden, J., Kay, P., Francis, B., Foulger, M., Gledhill, S., McDonald, A.T. and Walker, A. (2010) 'The impact of peatland drain-blocking on dissolved organic carbon loss and discolouration of water; results from a national survey', *Journal of Hydrology,* 381(1–2), 112-120.

Armstrong, A., Holden, J., Luxton, K. and Quinton, J.N. (2012) 'Multi-scale relationship between peatland vegetation type and dissolved organic carbon concentration', *Ecological Engineering,* 47(0), 182-188.

Artz, R.R.E., Donnelly, D., Andersen, R., Mitchell, R., Chapaman, S.J., Smith, J., Smith, P., Cummins, R., Balana, B. and Cuthbert, A. (2014) *Managing and restoring blanket bog to benefit biodiversity and carbon balance - a scoping study*, SNH: Scottish Natural Heritage,available: http://www.snh.org.uk/pdfs/publications/commissioned_reports/562.pdf [Accessed 10/9/15].

Asam, Z.U.Z., Kaila, A., Nieminen, M., Sarkkola, S., O'Driscoll, C., O'Connor, M., Sana, A., Rodgers, M. and Xiao, L.W. (2012) 'Assessment of phosphorus retention efficiency of blanket peat buffer areas using a laboratory flume approach', *Ecological Engineering,* 49(0), 160-169.

Aufdenkampe, A.K., Mayorga, E., Raymond, P.A., Melack, J.M., Doney, S.C., Alin, S.R., Aalto, R.E. and Yoo, K. (2011) 'Riverine coupling of biogeochemical cycles between land, oceans, and atmosphere', *Frontiers in Ecology and the Environment,* 9(1), 53-60.

Austnes, K., Evans, C.D., Eliot-Laize, C., Naden, P.S. and Old, G.H. (2010) 'Effects of storm events on mobilisation and in-stream processing of dissolved organic matter (DOM) in a Welsh peatland catchment', *Biogeochemistry,* 99(1-3), 157-173.

Bailly-Comte, V., Martin, J.B. and Screaton, E.J. (2011) 'Time variant cross correlation to assess residence time of water and implication for hydraulics of a sink-rise karst system', *Water Resources Research,* 47(5), W05547.

Bain, C.G., Bonn, A., Stoneman, R., Chapman, S., Coupar, A., Evans, M., Gearey, B., Howat, M., Joosten, H., Keenleyside, C., Labadz, J., Lindsay, R., Littlewood, N., Lunt, P., Miller, C.J., et al. (2011) *IUCN UK Commission  Inquiry on Peatlands*, IUCN UK Peatland Programme, E.: available: [Accessed 10/3/12].

Baird, A.J. (2012) 'Critical review of widths of drainage influence associated with artificial drains in blanket bog, with particular reference to the 2011 update of the Scottish Government Carbon Calculator Tool', *Countryside Council for Wales (CCW),* Contract Science Report(No. 1015).

Balbi, D.M. (2000) 'Suspended chlorophyll in the River Nene, a small nutrient-rich river in eastern England: long-term and spatial trends', *Science of The Total Environment,* 251, 401-421.

Ball, D.F. (1964) 'LOSS-ON-IGNITION AS AN ESTIMATE OF ORGANIC MATTER AND ORGANIC CARBON IN NON-CALCAREOUS SOILS', *Journal of Soil Science,* 15(1), 84-92.

Balland, V., Bhatti, J., Errington, R., Castonguay, M. and Arp, P.A. (2006) 'Modeling snowpack and soil temperature and moisture conditions in a jack pine, black spruce and aspen forest stand in central Saskatchewan (BOREAS SSA)', *Canadian Journal of Soil Science,* 86(2), 203-217.

Barber, K.E. and Langdon, P.G. (2007) 'What drives the peat-based palaeoclimate record? A critical test using multi-proxy climate records from northern Britain', *Quaternary Science Reviews,* 26(25–28), 3318-3327.

Barker, S., Diz, P., Vautravers, M.J., Pike, J., Knorr, G., Hall, I.R. and Broecker, W.S. (2009) 'Interhemispheric Atlantic seesaw response during the last deglaciation', *Nature,* 457(7233), 1097-U50.

Battin, T.J., Luyssaert, S., Kaplan, L.A., Aufdenkampe, A.K., Richter, A. and Tranvik, L.J. (2009) 'The boundless carbon cycle', *Nature Geosci,* 2(9), 598-600.

Bazeley, R. (2013) *Analytical issues involved in river water sampling, storage and analysis: Whitelee and Gordonbush catchments, and beyond*, Undergraduate dissertation, Environmental Chemistry department, School of Chemistry, University of Glasgow: University of Glasgow, unpublished.

Beaudoin, A. (2003) 'A comparison of two methods for estimating the organic content of sediments', *Journal of Paleolimnology,* 29(3), 387-390.

Beilman, D.W., MacDonald, G.M., Smith, L.C. and Reimer, P.J. (2009) 'Carbon accumulation in peatlands of West Siberia over the last 2000 years', *Global Biogeochemical Cycles,* 23(1), GB1012.

Beilman, D.W., MacDonald, G.M. and Yu, Z. (2010) 'The northern peatland carbon pool and the Holocene carbon cycle', *PAGES (Past Global Changes) News,* 18(1).

Bell, V.A., Kay, A.L., Jones, R.G. and Moore, R.J. (2007) 'Development of a high resolution grid-based river flow model for use with regional climate model output', *Hydrology and Earth System Sciences,* 11(1), 532-549.

Belyea, L.R. (1996) 'Separating the effects of litter quality and microenvironment on decomposition rates in a patterned peatland', *Oikos,* 77(3), 529-539.

Belyea, L.R. and Baird, A.J. (2006) 'Beyond "The limits to peat bog growth": Cross-scale feedback in peatland development', *Ecological Monographs,* 76(3), 299-322.

Belyea, L.R. and Clymo, R.S. (1999) 'Do hollows control the rate of peat bog growth?', *Patterned mires: origin and development, flora and fauna,*

Belyea, L.R. and Clymo, R.S. (2001) 'Feedback control of the rate of peat formation', *Proceedings of the Royal Society of London. Series B: Biological Sciences,* 268(1473), 1315-1321.

Belyea, L.R. and Malmer, N. (2004) 'Carbon sequestration in peatland: patterns and mechanisms of response to climate change', *Global Change Biology,* 10(7), 1043-1052.

Best, E.K. (1976) 'AN AUTOMATED METHOD FOR DETERMINING NITRATE NITROGEN IN SOIL EXTRACTS', *Queensland Journal of Agricultural and Animal Sciences,* 33(2), 161-166.

Betton, C., Webb, B.W. and Walling, D.E. (1991) *RECENT TRENDS IN NO3-N CONCENTRATION AND LOADS IN BRITISH RIVERS, Sediment and Stream Water Quality in a Changing Environment : Trends and Explanation*.

Billett, M.F., Charman, D.J., Clark, J.M., Evans, C.D., Evans, M.G., Ostle, N.J., Worrall, F., Burden, A., Dinsmore, K.J., Jones, T., McNamara, N.P., Parry, L.E., Rowson, J.G. and Rose, R. (2010) 'Carbon balance of UK peatlands: current state of knowledge and future research challenges', *Climate Research,* 45, 13-29.

Billett, M.F., Deacon, C.M., Palmer, S.M., Dawson, J.J.C. and Hope, D. (2006) 'Connecting organic carbon in stream water and soils in a peatland catchment', *Journal of Geophysical Research: Biogeosciences,* 111(G2), G02010.

Billett, M.F. and Moore, T.R. (2008) 'Supersaturation and evasion of CO2 and CH4 in surface waters at Mer Bleue peatland, Canada', *Hydrological Processes,* 22(12), 2044-2054.

Billett, M.F., Palmer, S.M., Hope, D., Deacon, C., Storeton-West, R., Hargreaves, K.J., Flechard, C. and Fowler, D. (2004) 'Linking land-atmosphere-stream carbon fluxes in a lowland peatland system', *Global Biogeochemical Cycles,* 18(1), GB1024.

Björck, S. and Wohlfarth, B. (2001) '14C Chronostratigraphic Techniques in Paleolimnology' in Last, W. and Smol, J., eds., *Tracking Environmental Change Using Lake Sediments*, Springer Netherlands, 205-245.

Blaauw, M. (2010) 'Methods and code for ‘classical’ age-modelling of radiocarbon sequences', *Quaternary Geochronology,* 5(5), 512-518.

Blaauw, M. and Christen, J.A. (2005) 'Radiocarbon peat chronologies and environmental change', *Journal of the Royal Statistical Society: Series C (Applied Statistics),* 54(4), 805-816.

Blaauw, M. and Christen, J.A. (2011) 'Flexible Paleoclimate Age-Depth Models Using an Autoregressive Gamma Process', *Bayesian Analysis,* 6(3), 457-474.

Blaauw, M. and Christen, J.A. (2014) 'Bacon manual - v2.2',

Black, K.E., Lowe, J.A.H., Billett, M.F. and Cresser, M.S. (1993) 'OBSERVATIONS ON THE CHANGES IN NITRATE CONCENTRATIONS ALONG STREAMS IN 7 UPLAND MOORLAND CATCHMENTS IN NORTHEAST SCOTLAND', *Water Research,* 27(7), 1195-1199.

Blodau, C. and Moore, T.R. (2003) 'Experimental response of peatland carbon dynamics to a water table fluctuation', *Aquatic Sciences,* 65(1), 47-62.

Blundell, A., Charman, D.J. and Barber, K.E. (2008) 'Multiproxy late Holocene peat records from Ireland: towards a regional palaeoclimate curve', *Journal of Quaternary Science,* 23(1), 59-71.

Blundell, A. and Holden, J. (2015) 'Using palaeoecology to support blanket peatland management', *Ecological Indicators,* 49, 110-120.

Bonn, A., Allott, T.E.H., Evans, M., Joosten, H. and Stoneman, R. (2014a) *Peatland Restoration for Ecoystem Services,* Cambridge: University Press Cambridge.

Bonn, A., Reed, M.S., Evans, C.D., Joosten, H., Bain, C.G., Farmer, J.G., Emmer, I., Couwenberg, J., Moxey, A., Artz, R., Tanneberger, F., von Unger, M., Smyth, M. and Birnie, D. (2014b) 'Investing in nature: Developing ecosystem service markets for peatland restoration', *Ecosystem Services,* (0).

Borren, W., Bleuten, W. and Lapshina, E.D. (2004) 'Holocene peat and carbon accumulation rates in the southern taiga of western Siberia', *Quaternary research,* 61(1), 42-51.

Boyer, E.W., Hornberger, G.M., Bencala, K.E. and McKnight, D.M. (2000) 'Effects of asynchronous snowmelt on flushing of dissolved organic carbon: a mixing model approach', *Hydrological Processes,* 14(18), 3291-3308.

Bradley, R.I., Milne, R., Bell, J., Lilly, A., Jordan, C. and Higgins, A. (2005) 'A soil carbon and land use database for the United Kingdom', *Soil Use and Management,* 21(4), 363-369.

Bragg, O.M. (2002) 'Hydrology of peat-forming wetlands in Scotland', *Science of The Total Environment,* 294(1-3), 111-129.

Bragg, O.M. and Tallis, J.H. (2001) 'The sensitivity of peat-covered upland landscapes', *CATENA,* 42(2–4), 345-360.

British Geological Survey, U.K. (2014) *Gordonbush Geology*, sheet BGS 1:50000, Edinburgh: EDINA Geology Digimap Service, (Geology Roam).

British Parliament, U.K. (2013) *Common Debates*, available: http://www.publications.parliament.uk/pa/cm201314/cmhansrd/cm130911/text/130911w0002.htm#130911w0002.htm_spnew14 [Accessed 9/9/14].

Brodie, R.S., Hostetler, S. and Slatter, E. (2008) 'Comparison of daily percentiles of streamflow and rainfall to investigate stream–aquifer connectivity', *Journal of Hydrology,* 349(1–2), 56-67.

Brooks, P.D., McKnight, D.M. and Bencala, K.E. (1999) 'The relationship between soil heterotrophic activity, soil dissolved organic carbon (DOC) leachate, and catchment-scale DOC export in headwater catchments', *Water Resources Research,* 35(6), 1895-1902.

Bruneau, P.M.C. and Johnson, S.M. (2014) *Scotland's peatland - definitions & information resources*, Edinburgh: (SNH), S.N.H.: Scottish Natural Heritage (SNH), available: http://www.snh.org.uk/pdfs/publications/commissioned_reports/701.pdf [Accessed 2/3/15].

Buffam, I., Turner, M.G., Desai, A.R., Hanson, P.C., Rusak, J.A., Lottig, N.R., Stanley, E.H. and Carpenter, S.R. (2011) 'Integrating aquatic and terrestrial components to construct a complete carbon budget for a north temperate lake district', *Global Change Biology,* 17(2), 1193-1211.

Cannell, M.G.R., Dewar, R.C. and Pyatt, D.G. (1993) 'Conifer plantations on drained peatlands in Britain: a net gain or loss of carbon?', *Forestry,* 66(4), 353-369.

Chambers, F.M., Beilman, D.W. and Yu, Z. (2010) 'Methods for determining peat humification and for quantifying peat bulk density, organic matter and carbon content for palaeostudies of climate and peatland carbon dynamics', *Mires and Peat,* 7.

Chambers, F.M. and Charman, D.J. (2004) 'Holocene environmental change: contributions from the peatland archive', *The Holocene,* 14(1), 1-6.

Chanat, J.G., Rice, K.C. and Hornberger, G.M. (2002) 'Consistency of patterns in concentration-discharge plots', *Water Resources Research,* 38(8).

Chapman, P.J., Edwards, A.C. and Cresser, M.S. (2001) 'The nitrogen composition of streams in upland Scotland: some regional and seasonal differences', *Science of The Total Environment,* 265(1-3), 65-83.

Chapman, S.J., Bell, J., Donnelly, D. and Lilly, A. (2009) 'Carbon stocks in Scottish peatlands', *Soil Use and Management,* 25(2), 105-112.

Charman, D. (2002) *Peatland and Environmental Change,* London & New York: Wiley & Sons.

Charman, D.J. (1992) 'BLANKET MIRE FORMATION AT THE CROSS LOCHS, SUTHERLAND, NORTHERN SCOTLAND', *Boreas,* 21(1), 53-72.

Charman, D.J. (2007) 'Summer water deficit variability controls on peatland water-table changes: implications for Holocene palaeoclimate reconstructions', *The Holocene,* 17(2), 217-227.

Charman, D.J., Barber, K.E., Blaauw, M., Langdon, P.G., Mauquoy, D., Daley, T.J., Hughes, P.D.M. and Karofeld, E. (2009) 'Climate drivers for peatland palaeoclimate records', *Quaternary Science Reviews,* 28(19–20), 1811-1819.

Charman, D.J., Beilman, D.W., Blaauw, M., Booth, R.K., Brewer, S., Chambers, F.M., Christen, J.A., Gallego-Sala, A., Harrison, S.P., Hughes, P.D.M., Jackson, S.T., Korhola, A., Mauquoy, D., Mitchell, F.J.G., Prentice, I.C., et al. (2013) 'Climate-related changes in peatland carbon accumulation during the last millennium', *Biogeosciences,* 10(2), 929-944.

Charman, D.J., Blundell, A., Chiverrell, R.C., Hendon, D. and Langdon, P.G. (2006) 'Compilation of non-annually resolved Holocene proxy climate records: stacked Holocene peatland palaeo-water table reconstructions from northern Britain', *Quaternary Science Reviews,* 25(3–4), 336-350.

Chow, A.T., Tanji, K.K. and Gao, S.D. (2003) 'Production of dissolved organic carbon (DOC) and trihalomethane (THM) precursor from peat soils', *Water Research,* 37(18), 4475-4485.

Christ, M. (2014) 'Operating Manual Freeze Dryer ALPHA 1-4 LD-2', Version 0203(

Christen, J.A. and Perez, S.E. (2011) *A New Robust Statistical Model for Radiocarbon Data, 2011*.

Clark, J.M., Ashley, D., Wagner, M., Chapman, P.J., Lane, S.N., Evans, C.D. and Heathwaite, A.L. (2009) 'Increased temperature sensitivity of net DOC production from ombrotrophic peat due to water table draw-down', *Global Change Biology,* 15(4), 794-807.

Clark, J.M., Bottrell, S.H., Evans, C.D., Monteith, D.T., Bartlett, R., Rose, R., Newton, R.J. and Chapman, P.J. (2010) 'The importance of the relationship between scale and process in understanding long-term DOC dynamics', *Science of The Total Environment,* 408(13), 2768-2775.

Clark, J.M., Chapman, P.J., Adamson, J.K. and Lane, S.N. (2005) 'Influence of drought-induced acidification on the mobility of dissolved organic carbon in peat soils', *Global Change Biology,* 11(5), 791-809.

Clark, J.M., Heinemeyer, A., Martin, P. and Bottrell, S.H. (2012) 'Processes controlling DOC in pore water during simulated drought cycles in six different UK peats', *Biogeochemistry,* 109(1-3), 253-270.

Clark, J.M., Lane, S.N., Chapman, P.J. and Adamson, J.K. (2007) 'Export of dissolved organic carbon from an upland peatland during storm events: Implications for flux estimates', *Journal of Hydrology,* 347(3–4), 438-447.

Clark, J.M., Lane, S.N., Chapman, P.J. and Adamson, J.K. (2008) 'Link between DOC in near surface peat and stream water in an upland catchment', *Science of The Total Environment,* 404(2–3), 308-315.

Clymo, R. (1970) 'The growth of Sphagnum: methods of measurement', *The Journal of Ecology*, 13-49.

Clymo, R.S. (1984) 'THE LIMITS TO PEAT BOG GROWTH', *Philosophical Transactions of the Royal Society of London Series B-Biological Sciences,* 303(1117), 605-654.

Clymo, R.S. (1987) 'THE ECOLOGY OF PEATLANDS', *Science Progress,* 71(284), 593-614.

Clymo, R.S. (1992) 'Models of peat growth', *Suo (Helsinki),* 43(4-5), 127-136.

Clymo, R.S., Turunen, J. and Tolonen, K. (1998) 'Carbon Accumulation in Peatland', *Oikos,* 81(2), 368-388.

Clyne Heritage Society, C.H.S. (2013) 'The history of Clyne parish', [online], available: http://www.clyneheritage.com/pages/parish.html [accessed 6/6/14]

Cohn, T.A. (2005) 'Estimating contaminant loads in rivers: An application of adjusted maximum likelihood to type 1 censored data', *Water Resources Research,* 41(7).

Cohn, T.A., Caulder, D.L., Gilroy, E.J., Zynjuk, L.D. and Summers, R.M. (1992) 'THE VALIDITY OF A SIMPLE STATISTICAL-MODEL FOR ESTIMATING FLUVIAL CONSTITUENT LOADS - AN EMPIRICAL-STUDY INVOLVING NUTRIENT LOADS ENTERING CHESAPEAKE BAY', *Water Resources Research,* 28(9), 2353-2363.

Cohn, T.A., Delong, L.L., Gilroy, E.J., Hirsch, R.M. and Wells, D.K. (1989) 'Estimating constituent loads', *Water Resources Research,* 25(5), 937-942.

Cole, J.J., Prairie, Y.T., Caraco, N.F., McDowell, W.H., Tranvik, L.J., Striegl, R.G., Duarte, C.M., Kortelainen, P., Downing, J.A., Middelburg, J.J. and Melack, J. (2007) 'Plumbing the Global Carbon Cycle: Integrating Inland Waters into the Terrestrial Carbon Budget', *Ecosystems,* 10(1), 172-185.

Connolly, J. and Holden, N.M. (2013) 'CLASSIFICATION OF PEATLAND DISTURBANCE', *Land Degradation & Development,* 24(6), 548-555.

Cook, G.T., Dugmore, A.J. and Shore, J.S. (1998) 'The influence of pretreatment on humic acid yield and C-14 age of Carex peat', *Radiocarbon,* 40(1), 21-27.

Cooper, M.D.A., Evans, C.D., Zielinski, P., Levy, P.E., Gray, A., Peacock, M., Norris, D., Fenner, N. and Freeman, C. (2014) 'Infilled Ditches are Hotspots of Landscape Methane Flux Following Peatland Re-wetting', *Ecosystems,* 17(7), 1227-1241.

Cooper, R., Thoss, V. and Watson, H. (2007) 'Factors influencing the release of dissolved organic carbon and dissolved forms of nitrogen from a small upland headwater during autumn runoff events', *Hydrological Processes,* 21(5), 622-633.

Costa, J.E., Spicer, K.R., Cheng, R.T., Haeni, P.F., Melcher, N.B., Thurman, E.M., Plant, W.J. and Keller, W.C. (2000) 'Measuring stream discharge by non-contact methods: A proof-of-concept experiment', *Geophysical Research Letters,* 27(4), 553-556.

Cowell, R. (2010) 'Wind power, landscape and strategic, spatial planning-The construction of 'acceptable locations' in Wales', *Land Use Policy,* 27(2), 222-232.

Cranfield, R.F. (2013) 'Weather observation data (2009-2013) from West Clyne Farm, Brora, Sutherland',

Crushell, P.H., Smolders, A.J.P., Schouten, M.G.C., Roelofs, J.G.M. and van Wirdum, G. (2009) 'The origin and development of a minerotrophic soak on an Irish raised bog: an interpretation of depth profiles of hydrochemistry and peat chemistry', *Holocene,* 19(6), 921-935.

Cummins, T. and Farrell, E.P. (2003) 'Biogeochemical impacts of clearfelling and reforestation on blanket-peatland streams - II. major ions and dissolved organic carbon', *Forest Ecology and Management,* 180(1-3), 557-570.

Cundill, A.P., Chapman, P.J. and Adamson, J.K. (2007) 'Spatial variation in concentrations of dissolved nitrogen species in an upland blanket peat catchment', *Science of The Total Environment,* 373(1), 166-177.

Daniel, M.H.B., Montebelo, A.A., Bernardes, M.C., Ometto, J., DeCamargo, P.B., Krusche, A.V., Ballester, M.V., Victoria, R.L. and Martinelli, L.A. (2002) 'Effects of urban sewage on dissolved oxygen, dissolved inorganic and organic carbon, and electrical conductivity of small streams along a gradient of urbanization in the Piracicaba River basin', *Water Air and Soil Pollution,* 136(1-4), 189-206.

Daniels, S.M., Evans, M.G., Agnew, C.T. and Allott, T.E.H. (2012) 'Ammonium release from a blanket peatland into headwater stream systems', *Environmental Pollution,* 163, 261-272.

Dargie, T. (2012a) *Gordonbush Water Quality Monitoring Programme Site Map*, sheet

Dargie, T. (2012b) *Gordonbush Wind Farm Water Quality Monitoring Final Report*, Services, N.E.: available: [Accessed 7/2/13].

Davidson, E.A. and Janssens, I.A. (2006) 'Temperature sensitivity of soil carbon decomposition and feedbacks to climate change', *Nature,* 440(7081), 165-173.

Dawson, J.J.C., Adhikari, Y.R., Soulsby, C. and Stutter, M.I. (2012) 'The biogeochemical reactivity of suspended particulate matter at nested sites in the Dee basin, NE Scotland', *Science of The Total Environment,* 434, 159-170.

Dawson, J.J.C., Billett, M.F., Hope, D., Palmer, S.M. and Deacon, C.M. (2004) 'Sources and sinks of aquatic carbon in a peatland stream continuum', *Biogeochemistry,* 70(1), 71-92.

Dawson, J.J.C., Billett, M.F., Neal, C. and Hill, S. (2002) 'A comparison of particulate, dissolved and gaseous carbon in two contrasting upland streams in the UK', *Journal of Hydrology,* 257(1–4), 226-246.

Dawson, J.J.C. and Smith, P. (2007) 'Carbon losses from soil and its consequences for land-use management', *Science of The Total Environment,* 382(2–3), 165-190.

Dawson, J.J.C., Soulsby, C., Tetzlaff, D., Hrachowitz, M., Dunn, S.M. and Malcolm, I.A. (2008) 'Influence of hydrology and seasonality on DOC exports from three contrasting upland catchments', *Biogeochemistry,* 90(1), 93-113.

Dawson, J.J.C., Tetzlaff, D., Speed, M., Hrachowitz, M. and Soulsby, C. (2011) 'Seasonal controls on DOC dynamics in nested upland catchments in NE Scotland', *Hydrological Processes,* 25(10), 1647-1658.

Dean, W.E. (1974) 'DETERMINATION OF CARBONATE AND ORGANIC-MATTER IN CALCAREOUS SEDIMENTS AND SEDIMENTARY-ROCKS BY LOSS ON IGNITION - COMPARISON WITH OTHER METHODS', *Journal of Sedimentary Petrology,* 44(1), 242-248.

Dean, W.E. and Gorham, E. (1998) 'Magnitude and significance of carbon burial in lakes, reservoirs, and peatlands', *Geology,* 26(6), 535-538.

DECC, D.o.E.a.C.C. (2011) *Valuation of Energy Use and Greenhouse Gas Emissions for Appraisal and Evaluation. Guidance Table 1-24: Supporting the Tool kit and the*

*Guidance.Table 1: ElectricityEmissions Factors to 2100.*, Government, U.: available: ⟨http://www.decc.gov.uk/en/content/cms/about/ec_social_res/iag_guidance/iag_guidance.aspx⟩. [Accessed 1/6/14].

DEFRA, D.f.E., Food and Rural Affairs. (2010) 'Nitrate', *http://dwi.defra.gov.uk/consumers/advice-leaflets/nitrate.pdf,*

Devito, K.J. and Dillon, P.J. (1993) 'THE INFLUENCE OF HYDROLOGIC CONDITIONS AND PEAT OXIA ON THE PHOSPHORUS AND NITROGEN DYNAMICS OF A CONIFER SWAMP', *Water Resources Research,* 29(8), 2675-2685.

Dillon, P.J. and Molot, L.A. (1997) 'Effect of landscape form on export of dissolved organic carbon, iron, and phosphorus from forested stream catchments', *Water Resources Research,* 33(11), 2591-2600.

Dillon, P.J. and Molot, L.A. (2005) 'Long-term trends in catchment export and lake retention of dissolved organic carbon, dissolved organic nitrogen, total iron, and total phosphorus: The Dorset, Ontario, study, 1978–1998', *Journal of Geophysical Research: Biogeosciences,* 110(G1), G01002.

Dinsmore, K.J. and Billett, M.F. (2008) 'Continuous measurement and modeling of CO2 losses from a peatland stream during stormflow events', *Water Resources Research,* 44(12), W12417.

Dinsmore, K.J., Billett, M.F. and Dyson, K.E. (2013) 'Temperature and precipitation drive temporal variability in aquatic carbon and GHG concentrations and fluxes in a peatland catchment', *Global Change Biology,* 19(7), 2133-2148.

Dinsmore, K.J., Billett, M.F., Dyson, K.E., Harvey, F., Thomson, A.M., Piirainen, S. and Kortelainen, P. (2011) 'Stream water hydrochemistry as an indicator of carbon flow paths in Finnish peatland catchments during a spring snowmelt event', *Science of The Total Environment,* 409(22), 4858-4867.

Dinsmore, K.J., Billett, M.F., Skiba, U.M., Rees, R.M., Drewer, J. and Helfter, C. (2010) 'Role of the aquatic pathway in the carbon and greenhouse gas budgets of a peatland catchment', *Global Change Biology,* 16(10), 2750-2762.

Douglas, D.J.T., Bellamy, P.E. and Pearce-Higgins, J.W. (2011) 'Changes in the abundance and distribution of upland breeding birds at an operational wind farm', *Bird Study,* 58(1), 37-43.

Douglas, D.J.T., Follestad, A., Langston, R.H.W. and Pearce-Higgins, J.W. (2012) 'Modelled sensitivity of avian collision rate at wind turbines varies with number of hours of flight activity input data', *Ibis,* 154(4), 858-861.

Douglas, D.J.T. and Pearce-Higgins, J.W. (2014) 'Relative importance of prey abundance and habitat structure as drivers of shorebird breeding success and abundance', *Animal Conservation,* 17(6), 535-543.

Draper, N.R. and Smith, H. (1998) *Applied Regression Analysis, 3rd Edition,* 3 ed*.,* University of Michigan: Wiley.

Drew, S., Waldron, S., Gilvear, D., Grieve, I., Armstrong, A., Bragg, O.M., Brewis, F., Cooper, M., Dargie, T., Duncan, C., Harris, L., Wilson, L., McIver, C., Padfield, R. and Shah, N. (2013) 'The price of knowledge in the knowledge economy: Should development of peatland in the UK support a research levy?', *Land Use Policy,* 32(0), 50-60.

Dunne, E.J., Clark, M.W., Mitchell, J., Jawitz, J.W. and Reddy, K.R. (2010) 'Soil phosphorus flux from emergent marsh wetlands and surrounding grazed pasture uplands', *Ecological Engineering,* 36(10), 1392-1400.

Dyson, K.E., Billett, M.F., Dinsmore, K.J., Harvey, F., Thomson, A.M., Piirainen, S. and Kortelainen, P. (2011) 'Release of aquatic carbon from two peatland catchments in E. Finland during the spring snowmelt period', *Biogeochemistry,* 103(1-3), 125-142.

Eaton, A.D., Clesceri, L.S., Rice, E.W. and Greenberg, A.E. (2005) *Standard methods for examination of water and wastewater,* 21st ed*.,* American Public Health Association.

Einola, E., Rantakari, M., Kankaala, P., Kortelainen, P., Ojala, A., Pajunen, H., Mäkelä, S. and Arvola, L. (2011) 'Carbon pools and fluxes in a chain of five boreal lakes: A dry and wet year comparison', *Journal of Geophysical Research: Biogeosciences,* 116(G3), n/a-n/a.

EPA, U.S.E.P.A. (2015a) 'Phosphorus', *Water: Monitoring & Assessment* [online], available: http://water.epa.gov/type/rsl/monitoring/vms56.cfm [Accessed 18/2/15]

EPA, U.S.E.P.A. (2015b) 'Total Alkalinity', *Water: Monitoring & Assessment* [online], available: http://water.epa.gov/type/rsl/monitoring/vms510.cfm [Accessed 18/2/15]

Erwin, K.L. (2009) 'Wetlands and global climate change: the role of wetland restoration in a changing world', *Wetlands Ecology and management,* 17(1), 71-84.

European Union, E.U. (2012) *EU on the Implementation of the Water Framework Directive (2000/60/EC) River Basin Management Plans*, Brussels: European Union, available: http://ec.europa.eu/environment/water/water-framework/pdf/CWD-2012-379_EN-Vol3_UK.pdf [Accessed 15/4/14].

Eurostat, E.C. (2012) 'Agri-environmental indicator - nitrate pollution of water', [online], available:http://epp.eurostat.ec.europa.eu/statistics_explained/index.php/Agri-environmental_indicator_-_nitrate_pollution_of_water [Accessed 15/4/14]

Evans, C. and Davies, T.D. (1998) 'Causes of concentration/discharge hysteresis and its potential as a tool for analysis of episode hydrochemistry', *Water Resources Research,* 34(1), 129-137.

Evans, C.D., Bonn, A., Holden, J., Reed, M.S., Evans, M.G., Worrall, F., Couwenberg, J. and Parnell, M. (2014) 'Relationships between anthropogenic pressures and ecosystem functions in UK blanket bogs: Linking process understanding to ecosystem service valuation', *Ecosystem Services,* (0).

Evans, C.D., Chapman, P.J., Clark, J.M., Monteith, D.T. and Cresser, M.S. (2006a) 'Alternative explanations for rising dissolved organic carbon export from organic soils', *Global Change Biology,* 12(11), 2044-2053.

Evans, C.D., Jones, T.G., Burden, A., Ostle, N., Zieliński, P., Cooper, M.D.A., Peacock, M., Clark, J.M., Oulehle, F., Cooper, D.J. and Freeman, C. (2012) 'Acidity controls on dissolved organic carbon mobility in organic soils', *Global Change Biology,* 18(11), 3317-3331.

Evans, C.D., Monteith, D.T. and Cooper, D.M. (2005) 'Long-term increases in surface water dissolved organic carbon: Observations, possible causes and environmental impacts', *Environmental Pollution,* 137(1), 55-71.

Evans, C.D., Reynolds, B., Jenkins, A., Helliwell, R.C., Curtis, C.J., Goodale, C.L., Ferrier, R.C., Emmett, B.A., Pilkington, M.G., Caporn, S.J.M., Carroll, J.A., Norris, D., Davies, J.

and Coull, M.C. (2006b) 'Evidence that soil carbon pool determines susceptibility of semi-natural ecosystems to elevated nitrogen leaching', *Ecosystems,* 9(3), 453-462.

Evans, M. and Lindsay, J. (2010) 'Impact of gully erosion on carbon sequestration in blanket peatlands', *Climate Research,* 45(1), 31-41.

Evans, M. and Warburton, J. (2007) 'The geomorphology of upland peat: pattern, process, form',

Evans, M. and Warburton, J. (2008) 'Frontmatter' in *Geomorphology of Upland Peat*, Blackwell Publishing Ltd, i-xviii.

Evans, M.G., Burt, T.P., Holden, J. and Adamson, J.K. (1999) 'Runoff generation and water table fluctuations in blanket peat: evidence from UK data spanning the dry summer of 1995', *Journal of Hydrology,* 221(3), 141-160.

Falck Renewables, F.R. (2013) 'Kilbraur', [online], available: http://www.falckrenewables.eu/attivita/elenco/kilbraur/overview.aspx?sc_lang=en [Accessed 6/9/12]

Feller, M.C. (2005) 'FOREST HARVESTING AND STREAMWATER INORGANIC CHEMISTRY IN WESTERN NORTH AMERICA: A REVIEW1', *JAWRA Journal of the American Water Resources Association,* 41(4), 785-811.

Fenner, N. and Freeman, C. (2011) 'Drought-induced carbon loss in peatlands', *Nature Geoscience,* 4(12), 895-900.

Fenner, N. and Freeman, C. (2013) 'Carbon preservation in humic lakes; a hierarchical regulatory pathway', *Global Change Biology,* 19(3), 775-784.

Ferguson, C.A., Bowman, A.W., Scott, E.M. and Carvalho, L. (2007) 'Model comparison for a complex ecological system', *Journal of the Royal Statistical Society: Series A (Statistics in Society),* 170(3), 691-711.

Ferguson, C.A., Bowman, A.W., Scott, E.M. and Carvalho, L. (2009) 'Multivariate varying-coefficient models for an ecological system', *Environmetrics,* 20(4), 460-476.

Ferguson, R.I. (1986) 'River Loads Underestimated by Rating Curves', *Water Resources Research,* 22(1), 74-76.

Ferland, M.E., del Giorgio, P.A., Teodoru, C.R. and Prairie, Y.T. (2012) 'Long-term C accumulation and total C stocks in boreal lakes in northern Quebec', *Global Biogeochemical Cycles,* 26.

Ferland, M.E., Prairie, Y.T., Teodoru, C.R. and del Giorgio, P.A. (2014) 'Linking organic carbon sedimentation, burial efficiency, and long-term accumulation in boreal lakes', *Journal of Geophysical Research: Biogeosciences*, 2013JG002345.

Fiorillo, F. and Doglioni, A. (2010) 'The relation between karst spring discharge and rainfall by cross-correlation analysis (Campania, southern Italy)', *Hydrogeology Journal,* 18(8), 1881-1895.

Flanagan, L.B. and Syed, K.H. (2011) 'Stimulation of both photosynthesis and respiration in response to warmer and drier conditions in a boreal peatland ecosystem', *Global Change Biology,* 17(7), 2271-2287.

Flowers, H. (2014) 'Technicon Autoanalyser II Method Handbook',

Forestry Commission Scotland, F. (2011) *Forests and Water*, Edinburgh: Forestry Commission, available: http://www.forestry.gov.uk/PDF/FCGL007.pdf/$FILE/FCGL007.pdf [Accessed 14/5/14].

Forestry Commission Scotland, F. (2015) 'Woodland expansion: the Scottish Government's plan for reducing greenhouse gas emissions has a target of increasing planting to 10,000 hectares of new woodland each year', *Woodland Expansion* [online], available:http://scotland.forestry.gov.uk/supporting/management/annual-review/woodland-expansion [Accessed 15/9/15]

Fraga, M.I., Romero-Pedreira, D., Souto, M., Castro, D. and Sahuquillo, E. (2009) 'Assessing the impact of wind farms on the plant diversity of blanket bogs in the Xistral Mountains (NW Spain)', *Mires and Peat,* 4.

Frank, S., Tiemeyer, B., Gelbrecht, J. and Freibauer, A. (2014) 'High soil solution carbon and nitrogen concentrations in a drained Atlantic bog are reduced to natural levels by 10 years of rewetting', *Biogeosciences,* 11(8), 2309-2324.

Freeman, C., Evans, C.D., Monteith, D.T., Reynolds, B. and Fenner, N. (2001a) 'Export of organic carbon from peat soils', *Nature,* 412(6849).

Freeman, C., Fenner, N., Ostle, N.J., Kang, H., Dowrick, D.J., Reynolds, B., Lock, M.A., Sleep, D., Hughes, S. and Hudson, J. (2004) 'Export of dissolved organic carbon from peatlands under elevated carbon dioxide levels', *Nature,* 430(6996), 195-198.

Freeman, C., Fenner, N. and Shirsat, A.H. (2012) 'Peatland geoengineering: an alternative approach to terrestrial carbon sequestration', *Philosophical Transactions of the Royal Society A: Mathematical, Physical and Engineering Sciences,* 370(1974), 4404-4421.

Freeman, C., Ostle, N. and Kang, H. (2001b) 'An enzymic 'latch' on a global carbon store - A shortage of oxygen locks up carbon in peatlands by restraining a single enzyme', *Nature,* 409(6817), 149-149.

Fritz, S.C. and Anderson, N.J. (2013) 'The relative influences of climate and catchment processes on Holocene lake development in glaciated regions', *Journal of Paleolimnology,* 49(3), 349-362.

Frolking, S., Roulet, N. and Fuglestvedt, J. (2006) 'How northern peatlands influence the Earth's radiative budget: Sustained methane emission versus sustained carbon sequestration', *Journal of Geophysical Research-Biogeosciences,* 111(G1).

Frolking, S. and Roulet, N.T. (2007) 'Holocene radiative forcing impact of northern peatland carbon accumulation and methane emissions', *Global Change Biology,* 13(5), 1079-1088.

Frolking, S., Roulet, N.T., Moore, T.R., Richard, P.J.H., Lavoie, M. and Muller, S.D. (2001) 'Modeling Northern Peatland Decomposition and Peat Accumulation', *Ecosystems,* 4(5), 479-498.

Futter, M.N., Butterfield, D., Cosby, B.J., Dillon, P.J., Wade, A.J. and Whitehead, P.G. (2007) 'Modeling the mechanisms that control in-stream dissolved organic carbon dynamics in upland and forested catchments', *Water Resources Research,* 43(2).

Futter, M.N. and de Wit, H.A. (2008) 'Testing seasonal and long-term controls of streamwater DOC using empirical and process-based models', *Science of The Total Environment,* 407(1), 698-707.

Galloway, J.N., Townsend, A.R., Erisman, J.W., Bekunda, M., Cai, Z., Freney, J.R., Martinelli, L.A., Seitzinger, S.P. and Sutton, M.A. (2008) 'Transformation of the nitrogen cycle: recent trends, questions, and potential solutions', *Science,* 320(5878), 889-892.

Gao, P. and Josefson, M. (2012) 'Event-based suspended sediment dynamics in a central New York watershed', *Geomorphology,* 139, 425-437.

Geist, H. (2006) *Our Earth's Changing Land: An Ecyclopedia of Land-Use and Land-Cover Change,* Greenwood Press.

Gergel, S.E., Turner, M.G. and Kratz, T.K. (1999) 'DISSOLVED ORGANIC CARBON AS AN INDICATOR OF THE SCALE OF WATERSHED INFLUENCE ON LAKES AND RIVERS', *Ecological Applications,* 9(4), 1377-1390.

Geurts, J.J.M., Smolders, A.J.P., Banach, A.M., de Graaf, J., Roelofs, J.G.M. and Lamers, L.P.M. (2010) 'The interaction between decomposition, net N and P mineralization and their mobilization to the surface water in fens', *Water Research,* 44(11), 3487-3495.

Gibson, H.S., Worrall, F., Burt, T.P. and Adamson, J.K. (2009) 'DOC budgets of drained peat catchments: implications for DOC production in peat soils', *Hydrological Processes,* 23(13), 1901-1911.

Givelet, N., Le Roux, G., Cheburkin, A., Chen, B., Frank, J., Goodsite, M.E., Kempter, H., Krachler, M., Noernberg, T., Rausch, N., Rheinberger, S., Roos-Barraclough, F., Sapkota, A., Scholz, C. and Shotyk, W. (2004) 'Suggested protocol for collecting, handling and preparing peat cores and peat samples for physical, chemical, mineralogical and isotopic analyses', *Journal of Environmental Monitoring,* 6(5), 481-492.

Glatzel, S., Basiliko, N. and Moore, T. (2004) 'Carbon dioxide and methane production potentials of peats from natural, harvested, and restored sites, eastern Quebec, Canada', *Wetlands,* 24(2), 261-267.

Glatzel, S., Kalbitz, K., Dalva, M. and Moore, T. (2003) 'Dissolved organic matter properties and their relationship to carbon dioxide efflux from restored peat bogs', *Geoderma,* 113(3-4), 397-411.

Glew, J.R. (1988) 'A portable extruding device for close interval sectioning of unconsolidated core samples', *Journal of Paleolimnology,* 1(3), 235-239.

Glew, J.R., Smol, J.P. and Last, W.M. (2001) 'Sediment core collection and extrusion' in *Tracking environmental change using lake sediments*, Springer, 73-105.

Godsey, S.E., Kirchner, J.W. and Clow, D.W. (2009) 'Concentration–discharge relationships reflect chemostatic characteristics of US catchments', *Hydrological Processes,* 23(13), 1844-1864.

Godwin, H. (1962) 'Half-life of Radiocarbon', *Nature,* 195(4845), 984-984.

Goodale, C.L., Aber, J.D., Vitousek, P.M. and McDowell, W.H. (2005) 'Long-term Decreases in Stream Nitrate: Successional Causes Unlikely; Possible Links to DOC?', *Ecosystems,* 8(3), 334-337.

Gorham, E. (1957) 'The Development of Peat Lands', *The Quarterly Review of Biology,* 32(2), 145-166.

Gorham, E. (1991) 'NORTHERN PEATLANDS - ROLE IN THE CARBON-CYCLE AND PROBABLE RESPONSES TO CLIMATIC WARMING', *Ecological Applications,* 1(2), 182-195.

Gorham, E., Janssens, J.A. and Glaser, P.H. (2003) 'Rates of peat accumulation during the postglacial period in 32 sites from Alaska to Newfoundland, with special emphasis on northern Minnesota', *Canadian Journal of Botany-Revue Canadienne De Botanique,* 81(5), 429-438.

Gorham, E., Lehman, C., Dyke, A.S., Clymo, D. and Janssens, J.A. (2012) 'Long-term carbon sequestration in North American peatlands', *Quaternary Science Reviews,* 58(0), 77-82.

Goring, S., Williams, J.W., Blois, J.L., Jackson, S.T., Paciorek, C.J., Booth, R.K., Marlon, J.R., Blaauw, M. and Christen, J.A. (2012) 'Deposition times in the northeastern United States during the Holocene: establishing valid priors for Bayesian age models', *Quaternary Science Reviews,* 48, 54-60.

Grand-Clement, E., Luscombe, D.J., Anderson, K., Gatis, N., Benaud, P. and Brazier, R.E. (2014) 'Antecedent conditions control carbon loss and downstream water quality from shallow, damaged peatlands', *Science of The Total Environment,* 493, 961-973.

Grayson, R. and Holden, J. (2012) 'Continuous measurement of spectrophotometric absorbance in peatland streamwater in northern England: implications for understanding fluvial carbon fluxes', *Hydrological Processes,* 26(1), 27-39.

Green, S.M., Baird, A.J., Boardman, C.P. and Gauci, V. (2014) 'A mesocosm study of the effect of restoration on methane (CH4) emissions from blanket peat', *Wetlands Ecology and management,* 22(5), 523-537.

Grieve, I. and Gilvear, D. (2008) 'Effects of wind farm construction on concentrations and fluxes of dissolved organic carbon and suspended sediment from peat catchments at Braes of Doune, central Scotland.', *Mires and Peat,* (4).

Grieve, I.C. (1990) 'Seasonal, hydrological, and land management factors controlling dissolved organic carbon concentrations in the loch fleet catchments, Southwest Scotland', *Hydrological Processes,* 4(3), 231-239.

Grieve, I.C. (1991) 'A model of dissolved organic carbon concentrations in soil and stream waters', *Hydrological Processes,* 5(3), 301-307.

Grieve, I.C. (1994) 'Dissolved organic carbon dynamics in two streams draining forested catchments at loch ard, Scotland', *Hydrological Processes,* 8(5), 457-464.

Gudasz, C., Bastviken, D., Premke, K., Steger, K. and Tranvik, L.J. (2012) 'Constrained microbial processing of allochthonous organic carbon in boreal lake sediments', *Limnology and Oceanography,* 57(1), 163-175.

Gudasz, C., Bastviken, D., Steger, K., Premke, K., Sobek, S. and Tranvik, L.J. (2010) 'Temperature-controlled organic carbon mineralization in lake sediments', *Nature,* 466(7310).

Haddaway, N., Burden, A., Evans, C., Healey, J., Jones, D., Dalrymple, S. and Pullin, A. (2014) 'Evaluating effects of land management on greenhouse gas fluxes and carbon balances in boreo-temperate lowland peatland systems', *Environmental Evidence,* 3(1), 5.

Haei, M. and Laudon, H. (2015) 'Carbon dynamics and changing winter conditions: a review of current understanding and future research directions', *Carbon,* 12, 15763-15808.

Haei, M., Oquist, M.G., Buffam, I., Agren, A., Blomkvist, P., Bishop, K., Lofvenius, M.O. and Laudon, H. (2010) 'Cold winter soils enhance dissolved organic carbon concentrations in soil and stream water', *Geophysical Research Letters,* 37.

Haei, M., Oquist, M.G., Kreyling, J., Ilstedt, U. and Laudon, H. (2013) 'Winter climate controls soil carbon dynamics during summer in boreal forests', *Environmental Research Letters,* 8(2).

Hanson, P.C., Buffam, I., Rusak, J.A., Stanley, E.H. and Watras, C. (2014) 'Quantifying lake allochthonous organic carbon budgets using a simple equilibrium model', *Limnology and Oceanography,* 59(1).

Hanson, P.C., Hamilton, D.P., Stanley, E.H., Preston, N., Langman, O.C. and Kara, E.L. (2011) 'Fate of Allochthonous Dissolved Organic Carbon in Lakes: A Quantitative Approach', *Plos One,* 6(7).

Hanson, P.C., Pollard, A.I., Bade, D.L., Predick, K., Carpenter, S.R. and Foley, J.A. (2004) 'A model of carbon evasion and sedimentation in temperate lakes', *Global Change Biology,* 10(8), 1285-1298.

Hargan, K.E., Ruhland, K.M., Paterson, A.M., Holmquist, J., MacDonald, G.M., Bunbury, J., Finkelstein, S.A. and Smol, J.P. (2015) 'Long-term successional changes in peatlands of the Hudson Bay Lowlands, Canada inferred from the ecological dynamics of multiple proxies', *Holocene,* 25(1), 92-107.

Harrison, A.F., Taylor, K., Scott, A., Poskitt, J., Benham, D., Grace, J., Chaplow, J. and Rowland, P. (2008) 'Potential effects of climate change on DOC release from three different soil types on the Northern Pennines UK: examination using field manipulation experiments', *Global Change Biology,* 14(3), 687-702.

Hatfield, R.G., Maher, B.A., Pates, J.M. and Barker, P.A. (2008) 'Sediment dynamics in an upland temperate catchment: changing sediment sources, rates and deposition', *Journal of Paleolimnology,* 40(4), 1143-1158.

Heathcote, A.J. and Downing, J.A. (2012) 'Impacts of Eutrophication on Carbon Burial in Freshwater Lakes in an Intensively Agricultural Landscape', *Ecosystems,* 15(1), 60-70.

Heaton, T.J., Blackwell, P.G. and Buck, C.E. (2009) 'A BAYESIAN APPROACH TO THE ESTIMATION OF RADIOCARBON CALIBRATION CURVES: THE INTCAL09 METHODOLOGY', *Radiocarbon,* 51(4), 1151-1164.

Heiri, O., Lotter, A.F. and Lemcke, G. (2001) 'Loss on ignition as a method for estimating organic and carbonate content in sediments: reproducibility and comparability of results', *Journal of Paleolimnology,* 25(1), 101-110.

Helsel, D.R. and Hirsch, R.M. (2002) *Statistical Methods in Water Resources, Techniques of Water-Resources Investigations of the USGS - Book 4 Hydrologic Analysis and Interpretation*.

Hendriks, M.R. (2010) *Introduction to Physical Hydrology,* UK: Oxford University Press.

Henriksen, A. (1965) 'AN AUTOMATIC METHOD FOR DETERMINING LOW-LEVEL CONCENTRATIONS OF PHOSPHATES IN FRESH AND SALINE WATERS', *Analyst,* 90(1066), 29-&.

Heras, P. and Infante, M. (2009) 'Wind farms and mires in the Basque Country and north-west Navarra, Spain', *Mires and Peat,* 4.

Hinton, M.J., Schiff, S.L. and English, M.C. (1997) 'The significance of storms for the concentration and export of dissolved organic carbon from two Precambrian Shield catchments', *Biogeochemistry,* 36(1), 67-88.

Hinton, M.J., Schiff, S.L. and English, M.C. (1998) 'Sources and flowpaths of dissolved organic carbon during storms in two forested watersheds of the Precambrian Shield', *Biogeochemistry,* 41(2), 175-197.

Hirsch, R.M., Alexander, R.B. and Smith, R.A. (1991) 'Selection of methods for the detection and estimation of trends in water quality', *Water Resources Research,* 27(5), 803-813.

Holden, J. (2005a) 'Controls of soil pipe frequency in upland blanket peat', *Journal of Geophysical Research-Earth Surface,* 110(F1).

Holden, J. (2005b) 'Peatland hydrology and carbon release: why small-scale process matters', *Philosophical Transactions of the Royal Society A: Mathematical, Physical and Engineering Sciences,* 363(1837), 2891-2913.

Holden, J. (2008) *Upland hydrology, Drivers of Environmental Change in Uplands*.

Holden, J. and Burt, T.P. (2003a) 'Hydrological studies on blanket peat: the significance of the acrotelm-catotelm model', *Journal of Ecology,* 91(1), 86-102.

Holden, J. and Burt, T.P. (2003b) 'Runoff production in blanket peat covered catchments', *Water Resources Research,* 39(7).

Holden, J., Chapman, P.J. and Labadz, J.C. (2004) 'Artificial drainage of peatlands: hydrological and hydrochemical process and wetland restoration', *Progress in Physical Geography,* 28(1), 95-123.

Holden, J., Chapman, P.J., Palmer, S.M., Kay, P. and Grayson, R. (2012a) 'The impacts of prescribed moorland burning on water colour and dissolved organic carbon: A critical synthesis', *Journal of Environmental Management,* 101(0), 92-103.

Holden, J., Evans, M.G., Burt, T.P. and Horton, M. (2006) 'Impact of Land Drainage on Peatland Hydrology', *J. Environ. Qual.,* 35(5), 1764-1778.

Holden, J., Gascoign, M. and Bosanko, N.R. (2007a) 'Erosion and natural revegetation associated with surface land drains in upland peatlands', *Earth Surface Processes and Landforms,* 32(10), 1547-1557.

Holden, J., Shotbolt, L., Bonn, A., Burt, T.P., Chapman, P.J., Dougill, A.J., Fraser, E.D.G., Hubacek, K., Irvine, B., Kirkby, M.J., Reed, M.S., Prell, C., Stagl, S., Stringer, L.C., Turner, A., et al. (2007b) 'Environmental change in moorland landscapes', *Earth-Science Reviews,* 82(1–2), 75-100.

Holden, J., Smart, R.P., Dinsmore, K.J., Baird, A.J., Billett, M.F. and Chapman, P.J. (2012b) 'Natural pipes in blanket peatlands: major point sources for the release of carbon to the aquatic system', *Global Change Biology,* 18(12), 3568-3580.

Holden, J., Wallage, Z.E., Lane, S.N. and McDonald, A.T. (2011) 'Water table dynamics in undisturbed, drained and restored blanket peat', *Journal of Hydrology,* 402(1–2), 103-114.

Holl, B.S., Fiedler, S., Jungkunst, H.F., Kalbitz, K., Freibauer, A., Drosler, M. and Stahr, K. (2009) 'Characteristics of dissolved organic matter following 20 years of peatland restoration', *Science of The Total Environment,* 408(1), 78-83.

Hood, E., Gooseff, M.N. and Johnson, S.L. (2006) 'Changes in the character of stream water dissolved organic carbon during flushing in three small watersheds, Oregon', *Journal of Geophysical Research-Biogeosciences,* 111(G1).

Hope, D., Billett, M.F. and Cresser, M.S. (1994) 'A review of the export of carbon in river water: Fluxes and processes', *Environmental Pollution,* 84(3), 301-324.

Hope, D., Billett, M.F. and Cresser, M.S. (1997a) 'Exports of organic carbon in two river systems in NE Scotland', *Journal of Hydrology,* 193(1–4), 61-82.

Hope, D., Billett, M.F., Milne, R. and Brown, T.A.W. (1997b) 'EXPORTS OF ORGANIC CARBON IN BRITISH RIVERS', *Hydrological Processes,* 11(3), 325-344.

Horowitz, A.J. (2003) 'An evaluation of sediment rating curves for estimating suspended sediment concentrations for subsequent flux calculations', *Hydrological Processes,* 17(17), 3387-3409.

Houghton, R.A. (2005) 'Aboveground Forest Biomass and the Global Carbon Balance', *Global Change Biology,* 11(6), 945-958.

Hruska, J., Kram, P., McDowell, W.H. and Oulehle, F. (2009) 'Increased Dissolved Organic Carbon (DOC) in Central European Streams is Driven by Reductions in Ionic Strength Rather than Climate Change or Decreasing Acidity', *Environmental Science & Technology,* 43(12), 4320-4326.

Hughes, M.P. and Dowse, G. (2012) *The state of Scotland's lowland raised bogs in 2012: interim findings from a survey of 58 Scottish lowland raised bogs and analysis of change since 1994/95*, Edinburgh: Scottish Wildlife Trust, available: http://scottishwildlifetrust.org.uk/docs/002__057__publications__policies__The_state_of_Scotlands_lowland_raised_bogs_full_report___June_2012__1340123493.pdf [Accessed 6/6/14].

Inamdar, S.P., Christopher, S.F. and Mitchell, M.J. (2004) 'Export mechanisms for dissolved organic carbon and nitrate during summer storm events in a glaciated forested catchment in New York, USA', *Hydrological Processes,* 18(14), 2651-2661.

Ingram, H.A.P. (1978) 'SOIL LAYERS IN MIRES - FUNCTION AND TERMINOLOGY', *Journal of Soil Science,* 29(2), 224-227.

IPCC (2007) 'Climate Change 2007: Synthesis Report', *Contribution of Working Groups I, II, and III to the Forth Assessment Report of the Intergovernmental Panel on Climate Change,* IPCC(Geneva), Switzerland, 2007.

IPCC (2014a) *Climate Change 2014: Impacts, Adaptation, and Vulnerability. Part A: Global and Sectoral Aspects. Contribution of Working Group II to the Fifth Assessment Report of the Intergovernmental Panel on Climate Change [Field, C.B., V.R. Barros, D.J. Dokken, K.J. Mach, M.D. Mastrandrea, T.E. Bilir, M. Chatterjee, K.L. Ebi, Y.O. Estrada, R.C. Genova, B. Girma, E.S. Kissel, A.N. Levy, S. MacCracken, P.R. Mastrandrea, and L.L. White (eds.)],* Cambridge, United Kingdom and New York, NY, USA: Cambridge University Press.

IPCC (2014b) *Climate Change 2014: Impacts, Adaptation, and Vulnerability. Part B: Regional Aspects. Contribution of Working Group II to the Fifth Assessment Report of the Intergovernmental Panel on Climate Change [Barros, V.R., C.B. Field, D.J. Dokken, M.D. Mastrandrea, K.J. Mach, T.E. Bilir, M. Chatterjee, K.L. Ebi, Y.O. Estrada, R.C. Genova, B. Girma, E.S. Kissel, A.N. Levy, S. MacCracken, P.R. Mastrandrea, and L.L. White (eds.)],* Cambridge, United Kingdom and New York, NY, USA: Cambridge University Press.

Ireland, A.W., Booth, R.K., Hotchkiss, S.C. and Schmitz, J.E. (2013) 'A comparative study of within-basin and regional peatland development: implications for peatland carbon dynamics', *Quaternary Science Reviews,* 61, 85-95.

Janssens, I.A., Freibauer, A., Schlamadinger, B., Ceulemans, R., Ciais, P., Dolman, A.J., Heimann, M., Nabuurs, G.J., Smith, P., Valentini, R. and Schulze, E.D. (2005) 'The carbon budget of terrestrial ecosystems at country-scale - a European case study', *Biogeosciences,* 2(1), 15-26.

Jansson, M., Bergstrom, A.K., Blomqvist, P. and Drakare, S. (2000) 'Allochthonous organic carbon and phytoplankton/bacterioplankton production relationships in lakes', *Ecology,* 81(11), 3250-3255.

Jarvie, H.P., Neal, C., Smart, R., Owen, R., Fraser, D., Forbes, I. and Wade, A. (2001) 'Use of continuous water quality records for hydrograph separation and to assess short-term variability and extremes in acidity and dissolved carbon dioxide for the River Dee, Scotland', *Science of The Total Environment,* 265(1-3), 85-98.

Jeffrey, S.W. and Humphrey, G.F. (1975) 'NEW SPECTROPHOTOMETRIC EQUATIONS FOR DETERMINING CHLOROPHYLLS A, B, C1 AND C2 IN HIGHER-PLANTS, ALGAE AND NATURAL PHYTOPLANKTON', *Biochemie Und Physiologie Der Pflanzen,* 167(2), 191-194.

Joensuu, S., Ahti, E. and Vuollekoski, M. (2002) 'Effects of Ditch Network Maintenance on the Chemistry of Run-off Water from Peatland Forests', *Scandinavian Journal of Forest Research,* 17(3), 238-247.

Jones, M.C. and Yu, Z.C. (2010) 'Rapid deglacial and early Holocene expansion of peatlands in Alaska', *Proceedings of the National Academy of Sciences of the United States of America,* 107(16), 7347-7352.

Joosten, H., A., S., Couwenberg, J., Laine, J. and Smith, P. (2013) 'The role of peatlands in climate regulation' in Bonn, A., Allott, T.E.H., Evans, M., Joosten, H. and Stoneman, R., eds., *Peatland Restoration and Ecosystem Services*, Cambridge: Cambridge University Press.

Jutras, M.F., Nasr, M., Castonguay, M., Pit, C., Pomeroy, J.H., Smith, T.P., Zhang, C.F., Ritchie, C.D., Meng, F.R., Clair, T.A. and Arp, P.A. (2011) 'Dissolved organic carbon concentrations and fluxes in forest catchments and streams: DOC-3 model', *Ecological Modelling,* 222(14), 2291-2313.

Juutinen, S., Valiranta, M., Kuutti, V., Laine, A.M., Virtanen, T., Seppa, H., Weckstrom, J. and Tuittila, E.S. (2013) 'Short-term and long-term carbon dynamics in a northern peatland-stream-lake continuum: A catchment approach', *Journal of Geophysical Research-Biogeosciences,* 118(1), 171-183.

Kaila, A., Asam, Z.U.Z., Sarkkola, S., Xiao, L.W., Lauren, A., Vasander, H. and Nieminen, M. (2012) 'Decomposition of harvest residue needles on peatlands drained for forestry - Implications for nutrient and heavy metal dynamics', *Forest Ecology and Management,* 277, 141-149.

Kaila, A., Sarkkola, S., Lauren, A., Ukonmaanaho, L., Koivusalo, H., Xiao, L.W., O'Driscoll, C., Asam, Z.U.Z., Tervahauta, A. and Nieminen, M. (2014) 'Phosphorus export from drained Scots pine mires after clear-felling and bioenergy harvesting', *Forest Ecology and Management,* 325, 99-107.

Kalbitz, K. and Geyer, S. (2002) 'Different effects of peat degradation on dissolved organic carbon and nitrogen', *Organic Geochemistry,* 33(3), 319-326.

Kalbitz, K., Schmerwitz, J., Schwesig, D. and Matzner, E. (2003) 'Biodegradation of soil-derived dissolved organic matter as related to its properties', *Geoderma,* 113(3–4), 273-291.

Kalbitz, K., Solinger, S., Park, J.H., Michalzik, B. and Matzner, E. (2000) 'Controls on the dynamics of dissolved organic matter in soils: A review', *Soil Science,* 165(4), 277-304.

Kaplan, L.A. (1994) 'A FIELD AND LABORATORY PROCEDURE TO COLLECT, PROCESS, AND PRESERVE FRESH-WATER SAMPLES FOR DISSOLVED ORGANIC-CARBON ANALYSIS', *Limnology and Oceanography,* 39(6), 1470-1476.

Kattel, G.R. (2009) 'Application of sediment traps in global change research in mountain lakes', *Journal of Mountain Science,* 6(3), 228-239.

Kaufman, D.S., Ager, T.A., Anderson, N.J., Anderson, P.M., Andrews, J.T., Bartlein, P.J., Brubaker, L.B., Coats, L.L., Cwynar, L.C., Duvall, M.L., Dyke, A.S., Edwards, M.E., Eisner, W.R., Gajewski, K., Geirsdottir, A., et al. (2004) 'Holocene thermal maximum in the western Arctic (0-180 degrees W)', *Quaternary Science Reviews,* 23(5-6), 529-560.

Keddy, P.A. (2010) *Wetland ecology: principles and conservation,* 2nd ed.*,* Cambridge, UK: Cambridge University Press.

Kettridge, N., Turetsky, M.R., Sherwood, J.H., Thompson, D.K., Miller, C.A., Benscoter, B.W., Flannigan, M.D., Wotton, B.M. and Waddington, J.M. (2015) 'Moderate drop in water table increases peatland vulnerability to post-fire regime shift', *Scientific reports,* 5.

Kieckbusch, J.J. and Schrautzer, J. (2007) 'Nitrogen and phosphorus dynamics of a re-wetted shallow-flooded peatland', *Science of The Total Environment,* 380(1-3), 3-12.

Kjaergaard, C., Heiberg, L., Jensen, H.S. and Hansen, H.C.B. (2012) 'Phosphorus mobilization in rewetted peat and sand at variable flow rate and redox regimes', *Geoderma,* 173, 311-321.

Klein, M. (1984) 'ANTI CLOCKWISE HYSTERESIS IN SUSPENDED SEDIMENT CONCENTRATION DURING INDIVIDUAL STORMS - HOLBECK CATCHMENT - YORKSHIRE, ENGLAND', *CATENA,* 11(2-3), 251-257.

Kleinen, T., Brovkin, V. and Schuldt, R.J. (2012) 'A dynamic model of wetland extent and peat accumulation: results for the Holocene', *Biogeosciences,* 9(1), 235-248.

Knorr, K.H. (2013) 'DOC-dynamics in a small headwater catchment as driven by redox fluctuations and hydrological flow paths - are DOC exports mediated by iron reduction/oxidation cycles?', *Biogeosciences,* 10(2), 891-904.

Knotts, R. and Sloman, R. (2013) *Gordonbush Wind Farm Development: Photographs 2010-2013* Knotts, R., ed.

Koehler, A.K., Murphy, K., Kiely, G. and Sottocornola, M. (2009) 'Seasonal variation of DOC concentration and annual loss of DOC from an Atlantic blanket bog in South Western Ireland', *Biogeochemistry,* 95(2-3), 231-242.

Koehler, A.K., Sottocornola, M. and Kiely, G. (2011) 'How strong is the current carbon sequestration of an Atlantic blanket bog?', *Global Change Biology,* 17(1), 309-319.

Koh, L.P., Butler, R.A. and Bradshaw, C.J.A. (2009) 'Conversion of Indonesia's peatlands', *Frontiers in Ecology and the Environment,* 7(5), 238-238.

Kohler, S.J., Buffam, I., Seibert, J., Bishop, K.H. and Laudon, H. (2009) 'Dynamics of stream water TOC concentrations in a boreal headwater catchment: Controlling factors and implications for climate scenarios', *Journal of Hydrology,* 373(1-2), 44-56.

Kortelainen, P., Mattsson, T., Finér, L., Ahtiainen, M., Saukkonen, S. and Sallantaus, T. (2006) 'Controls on the export of C, N, P and Fe from undisturbed boreal catchments, Finland', *Aquatic Sciences,* 68(4), 453-468.

Kortelainen, P., Pajunen, H., Rantakari, M. and Saarnisto, M. (2004) 'A large carbon pool and small sink in boreal Holocene lake sediments', *Global Change Biology,* 10(10), 1648-1653.

Kortelainen, P., Rantakari, M., Pajunen, H., Huttunen, J.T., Mattsson, T., Juutinen, S., Larmola, T., Alm, J., Silvola, J. and Martikainen, P.J. (2013) 'Carbon evasion/accumulation ratio in boreal lakes is linked to nitrogen', *Global Biogeochemical Cycles,* 27(2), 363-374.

Kreutzweiser, D.P., Hazlett, P.W. and Gunn, J.M. (2008) 'Logging impacts on the biogeochemistry of boreal forest soils and nutrient export to aquatic systems: A review', *Environmental Reviews,* 16, 157-179.

Kritzberg, E.S., Cole, J.J., Pace, M.M. and Graneli, W. (2006) 'Bacterial growth on allochthonous carbon in humic and nutrient-enriched lakes: Results from whole-lake C-13 addition experiments', *Ecosystems,* 9(3), 489-499.

Kuusisto, E. (1996) *Chapter 12 - Hydrological Measurements*, United Nations Environment Programme & World Health Organization, available: http://www.who.int/water_sanitation_health/resourcesquality/wqmchap12.pdf [Accessed 3/3/15].

Lafleur, P.M., Hember, R.A., Admiral, S.W. and Roulet, N.T. (2005) 'Annual and seasonal variability in evapotranspiration and water table at a shrub-covered bog in southern Ontario, Canada', *Hydrological Processes,* 19(18), 3533-3550.

Lafleur, P.M., Roulet, N.T., Bubier, J.L., Frolking, S. and Moore, T.R. (2003) 'Interannual variability in the peatland-atmosphere carbon dioxide exchange at an ombrotrophic bog', *Global Biogeochemical Cycles,* 17(2), 1036.

Laiho, R. and Prescott, C.E. (2004) 'Decay and nutrient dynamics of coarse woody debris in northern coniferous forests: a synthesis', *Canadian Journal of Forest Research,* 34(4), 763-777.

Lambert, S.D. and Graham, N.J.D. (1995) 'REMOVAL OF NONSPECIFIC DISSOLVED ORGANIC-MATTER FROM UPLAND POTABLE WATER-SUPPLIES .1. ADSORPTION', *Water Research,* 29(10), 2421-2426.

Landry, J. and Rochefort, L. (2012) *The drainage of peatlands: impacts and rewetting techniques*, Quebec, Canada: University of Laval, available: [accessed Accessed].

Langdon, P.G. and Barber, K.E. (2004) 'Snapshots in time: precise correlations of peat-based proxy climate records in Scotland using mid-Holocene tephras', *The Holocene,* 14(1), 21-33.

Langdon, P.G. and Barber, K.E. (2005) 'The climate of Scotland over the last 5000 years inferred from multiproxy peatland records: inter-site correlations and regional variability', *Journal of Quaternary Science,* 20(6), 549-566.

Langdon, P.G., Barber, K.E. and Hughes, P.D.M. (2003) 'A 7500-year peat-based palaeoclimatic reconstruction and evidence for an 1100-year cyclicity in bog surface wetness from Temple Hill Moss, Pentland Hills, southeast Scotland', *Quaternary Science Reviews,* 22(2–4), 259-274.

Langdon, P.G., Brown, A.G., Caseldine, C.J., Blockley, S.P.E. and Stuijts, I. (2012) 'Regional climate change from peat stratigraphy for the mid- to late Holocene in central Ireland', *Quaternary International,* 268(0), 145-155.

Laudon, H., Berggren, M., Agren, A., Buffam, I., Bishop, K., Grabs, T., Jansson, M. and Kohler, S. (2011) 'Patterns and Dynamics of Dissolved Organic Carbon (DOC) in Boreal Streams: The Role of Processes, Connectivity, and Scaling', *Ecosystems,* 14(6), 880-893.

Laudon, H., Kohler, S. and Buffam, I. (2004) 'Seasonal TOC export from seven boreal catchments in northern Sweden', *Aquatic Sciences,* 66(2), 223-230.

Ledesma, J.L.J., Kohler, S.J. and Futter, M.N. (2012) 'Long-term dynamics of dissolved organic carbon: Implications for drinking water supply', *Science of The Total Environment,* 432, 1-11.

Lessels, J.S. and Bishop, T.F.A. (2014) 'Using the precision of the mean to estimate suitable sample sizes for monitoring total phosphorus in Australian catchments', *Hydrological Processes*, n/a-n/a.

Lichvarova, M. (2001) 'Nitrogen compounds in water' in Virtanen, T., ed. *Water Chemistry*, Banska Bystrica, Slovakia: Pedagogicka spolocnost Jana Amosa Komenskeho, 19-24.

Limpens, J., Berendse, F., Blodau, C., Canadell, J.G., Freeman, C., Holden, J., Roulet, N., Rydin, H. and Schaepman-Strub, G. (2008) 'Peatlands and the carbon cycle: from local processes to global implications - a synthesis', *Biogeosciences,* 5(5), 1475-1491.

Lindsay, R.A. (2010) *Peatbogs and Carbon : A Critical Synthesis*, Scotland, R.: Environmental Research Group, University of East London, available: [Accessed 16/5/13].

Lindsay, R.A., Charman, D.J., Everingham, F., O'Reilly, R.M., Palmer, M.A., Rowell, T.A. and Stroud, D.A. (1988) *The flow country: The peatlands of Caithness and Sutherland, The flow country: The peatlands of Caithness and Sutherland.*

Lindsay, R.A. and Freeman, J. (2008) *Lewis Wind Power (LWP) Environmental Impact Statements (EIS) 2004 and 2006 – A Critical Review*, Peatland Research Unit School of Health and Bioscience University of East London, available: [Accessed 1/6/14].

Littlewood, I.G. (1992) 'Estimating contaminant loads in rivers: a review', *Report - Institute of Hydrology,* (117), 81 pp.

Littlewood, I.G., Watts, C.D. and Custance, J.M. (1998) 'Systematic application of United Kingdom river flow and quality databases for estimating annual river mass loads (1975–1994)', *Science of The Total Environment,* 210, 21-40.

Livingstone, D.A. (1955) 'A LIGHTWEIGHT PISTON SAMPLER FOR LAKE DEPOSITS', *Ecology,* 36(1), 137-139.

Loisel, J., Gallego-Sala, A.V. and Yu, Z. (2012) 'Global-scale pattern of peatland Sphagnum growth driven by photosynthetically active radiation and growing season length', *Biogeosciences,* 9(7), 2737-2746.

Loisel, J. and Yu, Z.C. (2013) 'Recent acceleration of carbon accumulation in a boreal peatland, south central Alaska', *Journal of Geophysical Research-Biogeosciences,* 118(1), 41-53.

Lorenzen, C. (1967) 'Determination of chlorophyll and pheopigments:spectrophotometric equations', *Limnol. Oceanogr.,* 12(2), 343-346.

Lovett, G.M., Cole, J.J. and Pace, M.L. (2006) 'Is Net Ecosystem Production Equal to Ecosystem Carbon Accumulation?', *Ecosystems,* 9(1), 152-155.

Lumsdon, D.G., Stutter, M.I., Cooper, R.J. and Manson, J.R. (2005) 'Model assessment of biogeochemical controls on dissolved organic carbon partitioning in an acid organic soil', *Environmental Science & Technology,* 39(20), 8057-8063.

Lund, M., Christensen, T.R., Lindroth, A. and Schubert, P. (2012) 'Effects of drought conditions on the carbon dioxide dynamics in a temperate peatland', *Environmental Research Letters,* 7(4).

MacDonald, G.M., Beilman, D.W., Kremenetski, K.V., Sheng, Y.W., Smith, L.C. and Velichko, A.A. (2006) 'Rapid early development of circumarctic peatlands and atmospheric CH4 and CO2 variations', *Science,* 314(5797), 285-288.

MacKenzie, A.B., Hardie, S.M.L., Farmer, J.G., Eades, L.J. and Pulford, I.D. (2011) 'Analytical and sampling constraints in Pb-210 dating', *Science of The Total Environment,* 409(7), 1298-1304.

Macrae, M.L., Devito, K.J., Strack, M. and Waddington, J.M. (2013) 'Effect of water table drawdown on peatland nutrient dynamics: implications for climate change', *Biogeochemistry,* 112(1-3), 661-676.

Malloy, S. and Price, J.S. (2014) 'Fen restoration on a bog harvested down to sedge peat: A hydrological assessment', *Ecological Engineering,* 64, 151-160.

Martin-Ortega, J., Allott, T.E.H., Glenk, K. and Schaafsma, M. (2014) 'Valuing water quality improvements from peatland restoration: Evidence and challenges', *Ecosystem Services,* 9(0), 34-43.

Marttila, H. and Klove, B. (2010) 'Dynamics of erosion and suspended sediment transport from drained peatland forestry', *Journal of Hydrology,* 388(3-4), 414-425.

Maslen Environmental, M.E. (2009) *Assessing Impacts of Wind Farm Development on Blanket Peatland in England: Part 1 Final Report*, Natural England Commissioned Report NECR032, Natural England Website: available: http://publications.naturalengland.org.uk/publication/43010 [Accessed 8/10/15].

Mattsson, T., Kortelainen, P., Lepistö, A. and Räike, A. (2007) 'Organic and minerogenic acidity in Finnish rivers in relation to land use and deposition', *Science of The Total Environment,* 383(1–3), 183-192.

Mattsson, T., Kortelainen, P. and Räike, A. (2005) 'Export of DOM from Boreal Catchments: Impacts of Land Use Cover and Climate', *Biogeochemistry,* 76(2), 373-394.

Mattsson, T., Kortelainen, P., Raike, A., Lepisto, A. and Thomas, D.N. (2015) 'Spatial and temporal variability of organic C and N concentrations and export from 30 boreal rivers induced by land use and climate', *The Science of the total environment,* 508.

Mauquoy, D., Van Geel, B., Blaauw, M., Speranza, A. and van der Plicht, J. (2004) 'Changes in solar activity and Holocene climatic shifts derived from 14C wiggle-match dated peat deposits', *The Holocene,* 14(1), 45-52.

Mauquoy, D., Yeloff, D., Van Geel, B., Charman, D.J. and Blundell, A. (2008) 'Two decadally resolved records from north-west European peat bogs show rapid climate changes associated with solar variability during the mid–late Holocene', *Journal of Quaternary Science,* 23(8), 745-763.

Mayewski, P.A., Rohling, E.E., Stager, J.C., Karlén, W., Maasch, K.A., Meeker, L.D., Meyerson, E.A., Gasse, F., van Kreveld, S. and Holmgren, K. (2004) 'Holocene climate variability', *Quaternary research,* 62(3), 243-255.

McDonald, J.H. (2009) *Handbook of biological statistics,* Sparky House Publishing Baltimore, MD.

McGlynn, B.L. and McDonnell, J.J. (2003) 'Role of discrete landscape units in controlling catchment dissolved organic carbon dynamics', *Water Resources Research,* 39(4).

McNamara, N.P., Plant, T., Oakley, S., Ward, S., Wood, C. and Ostle, N. (2008) 'Gully hotspot contribution to landscape methane (CH4) and carbon dioxide (CO2) fluxes in a northern peatland', *Science of The Total Environment,* 404(2-3), 354-360.

Mei, Y., Hornberger, G.M., Kaplan, L.A., Newbold, J.D. and Aufdenkampe, A.K. (2012) 'Estimation of dissolved organic carbon contribution from hillslope soils to a headwater stream', *Water Resources Research,* 48.

Meng, F.R., Arp, P., Sangster, A., Brun, G.L., Rencz, A.N., Hall, G.E., Holmes, J., Lean, D.R. and Clair, T.A. (2005) 'Modeling dissolved organic carbon, total and methyl mercury in Kejimkujik freshwaters', *Mercury Cycling in a Wetland-Dominated Ecosystem: Multidisciplinary Study*, 267-284.

Met Office, M.O. (2011) 'Exceptionally warm and dry Spring 2011', *Past weather events* [online], available: http://www.metoffice.gov.uk/climate/uk/interesting/2011_spring [accessed 3/9/15]

Met Office, M.O. (2012) '2012- a wet year', *Weather case studies* [online], available: http://www.metoffice.gov.uk/learning/learn-about-the-weather/weather-phenomena/case-studies/2012-a-wet-year http://www.metoffice.gov.uk/news/releases/archive/2012/second-wettest-summer [Accessed 15/2/15]

Met Office, M.O. (2013a) 'Summer 2013', *Climate summaries* [online], available: http://www.metoffice.gov.uk/climate/uk/summaries/2013/summer

http://www.metoffice.gov.uk/climate/uk/interesting/2013-heatwave [Accessed 15/2/15]

Met Office, M.O. (2013b) 'Winter 2010/2011', *Climate Summarises - 2011 weather summaries* [online], available: http://www.metoffice.gov.uk/climate/uk/summaries/2011/winter [August 2013].

Met Office, M.O. (2014) 'Kinbrace climate 1981-2010', *UK climate averages* [online], available:http://www.metoffice.gov.uk/public/weather/climate/gfm5qbgxz[Accessed 1/1/11]

MEWAM (1992) 'Methods for the examination of waters and associated materials - Phosphorus and silicon in waters, effluents and sludges.' in HMSO, ed.

Michalzik, B., Tipping, E., Mulder, J., Lancho, J.F.G., Matzner, E., Bryant, C.L., Clarke, N., Lofts, S. and Esteban, M.A.V. (2003) 'Modelling the production and transport of dissolved organic carbon in forest soils', *Biogeochemistry,* 66(3), 241-264.

Michel, J.C., Morel, P. and Riviere, L.M. (2004) 'The importance of hydric history on the physical properties and wettability of peat' in Alsanius, B., Jensen, P. and Asp, H., eds., *Proceedings of the International Symposium on Growing Media & Hydroponics*, 275-281.

Miller, J.N. and (Edited by Thompson, M. (2006) 'Uncertainties in concentrations estimated from calibration experiments ', *Analytical Methods Committe Technical Brief (The Royal Society of Chemistry),* (22).

Milne, F. (2010) *Report to SSE: Gordonbush Wind Farm Habitat Management Plan; report of survey to identify ditches for blocking*, Northern Ecological Services: Northern Ecological Services, available: http://www.northecol.co.uk/index.html [Accessed 1/2/12].

Milne, R. and Brown, T.A. (1997) 'Carbon in the vegetation and soils of Great Britain', *Journal of Environmental Management,* 49(4), 413-433.

Mitchell, G. and McDonald, A.T. (1992) 'Discolouration of water by peat following induced drought and rainfall simulation', *Water Research,* 26(3), 321-326.

Monteith, D.T., Stoddard, J.L., Evans, C.D., de Wit, H.A., Forsius, M., Hogasen, T., Wilander, A., Skjelkvale, B.L., Jeffries, D.S., Vuorenmaa, J., Keller, B., Kopacek, J. and Vesely, J. (2007) 'Dissolved organic carbon trends resulting from changes in atmospheric deposition chemistry', *Nature,* 450(7169), 537-U9.

Moody, C.S., Worrall, F., Evans, C.D. and Jones, T.G. (2013) 'The rate of loss of dissolved organic carbon (DOC) through a catchment', *Journal of Hydrology,* 492(0), 139-150.

Moore, P.A., Pypker, T.G. and Waddington, J.M. (2013) 'Effect of long-term water table manipulation on peatland evapotranspiration', *Agricultural and Forest Meteorology,* 178–179, 106-119.

Mornsjo, T. (1971) 'PEATLAND TYPES AND THEIR REGIONAL DISTRIBUTION IN SOUTH SWEDEN', *Geologiska Foreningens i Stockholm Forhandlingar,* 93(PART 3), 587-600.

Mulholland, P.J. and Elwood, J.W. (1982) 'The role of lake and reservoir sediments as sinks in the perturbed global carbon cycle', *Tellus,* 34(5), 490-499.

Muller, F.L.L. and Tankere-Muller, S.P.C. (2012) 'Seasonal variations in surface water chemistry at disturbed and pristine peatland sites in the Flow Country of northern Scotland', *Science of The Total Environment,* 435, 351-362.

Mullin, J.B. and Riley, J.P. (1955) 'THE SPECTROPHOTOMETRIC DETERMINATION OF NITRATE IN NATURAL WATERS, WITH PARTICULAR REFERENCE TO SEA-WATER', *Analytica Chimica Acta,* 12(5), 464-480.

Murphy, J. and Riley, J.P. (1962) 'A MODIFIED SINGLE SOLUTION METHOD FOR DETERMINATION OF PHOSPHATE IN NATURAL WATERS', *Analytica Chimica Acta,* 26(1), 31-&.

Murray, H.S. (2012) *Assessing the impact of windfarm-related disturbance on streamwater carbon, phosphorus and nitrogen dynamics: A case study of the Whitelee catchments*, unpublished thesis (Thesis), University of Glasgow.

Nayak, D.R., Miller, D., Nolan, A., Smith, P. and Smith, J. (2008) *Calculating carbon savings from wind farm on Scottish peat lands Final Report corrected 29/6/10*, Edinburgh: Scottish Government, available: http://www.scotland.gov.uk/Resource/Doc/917/0117390.pdf [Accessed 1/4/11].

Nayak, D.R., Miller, D., Nolan, A., Smith, P. and Smith, J.U. (2009) 'Calculating carbon budgets of wind farms on Scottish peatlands', *Mires and Peat,* 4, Article 09.

Neal, C. and Hill, S. (1994) 'Dissolved inorganic and organic carbon in moorland and forest streams: Plynlimon, Mid-Wales', *Journal of Hydrology,* 153(1), 231-243.

Neal, C., House, W.A. and Down, K. (1998) 'An assessment of excess carbon dioxide partial pressures in natural waters based on pH and alkalinity measurements', *Science of The Total Environment,* 210(1-6), 173-185.

Neal, C., Reynolds, B., Neal, M., Hughes, S., Wickham, H., Hill, L., Rowland, P. and Pugh, B. (2003) 'Soluble reactive phosphorus levels in rainfall, cloud water, throughfall, stemflow, soil waters, stream waters and groundwaters for the Upper River Severn area, Plynlimon, mid Wales', *Science of The Total Environment,* 314, 99-120.

Neal, C., Reynolds, B., Neal, M., Wickham, H., Hill, L. and Williams, B. (2004) 'The impact of conifer harvesting on stream water quality: the Afon Hafren, mid-Wales', *Hydrology and Earth System Sciences Discussions,* 8(3), 503-520.

Neal, C., Robson, A.J., Neal, M. and Reynolds, B. (2005) 'Dissolved organic carbon for upland acidic and acid sensitive catchments in mid-Wales', *Journal of Hydrology,* 304(1), 203-220.

Neff, J.C. and Asner, G.P. (2001) 'Dissolved organic carbon in terrestrial ecosystems: Synthesis and a model', *Ecosystems,* 4(1), 29-48.

Nieminen, M. (2003) 'Effects of clear-cutting and site preparation on water quality from a drained Scots pine mire in southern Finland', *Boreal Environment Research,* 8(1), 53-59.

Nieminen, M. (2004) 'Export of dissolved organic carbon, nitrogen and phosphorus following clear-cutting of three Norway spruce forests growing on drained peatlands in southern Finland', *Silva Fennica,* 38(2), 123-132.

Nilsson, M., Klarqvist, M., Bohlin, E. and Possnert, G. (2001) 'Variation in C-14 age of macrofossils and different fractions of minute peat samples dated by AMS', *Holocene,* 11(5), 579-586.

Nilsson, M., Sagerfors, J., Buffam, I., Laudon, H., Eriksson, T., Grelle, A., Klemedtsson, L., Weslien, P. and Lindroth, A. (2008) 'Contemporary carbon accumulation in a boreal oligotrophic minerogenic mire - a significant sink after accounting for all C-fluxes', *Global Change Biology,* 14(10), 2317-2332.

O'Driscoll, C., Rodgers, M., O'Connor, M., Asam, Z.-u.-Z., de Eyto, E., Poole, R. and Xiao, L. (2011) 'A Potential Solution to Mitigate Phosphorus Release Following Clearfelling in Peatland Forest Catchments', *Water, Air, & Soil Pollution,* 221(1-4), 1-11.

OFGEM, O.o.G.a.E.M. (2014) *Renewables Obligation (RO)*, OFGEM, available: https://www.ofgem.gov.uk/environmental-programmes/renewables-obligation-ro [Accessed 1/2/15].

Oldfield, F. and Appleby, P.G. (1984) 'A combined radiometric and mineral magnetic approach to recent geochronology in lakes affected by catchment disturbance and sediment redistribution', *Chemical Geology,* 44(1–3), 67-83.

Oldfield, F., Appleby, P.G., Cambray, R.S., Eakins, J.D., Barber, K.E., Battarbee, R.W., Pearson, G.R. and Williams, J.M. (1979) '210 Pb, 137 Cs and 239 Pu Profiles in Ombrotrophic Peat', *Oikos,* 33(1), 40-45.

Oldfield, F., Richardson, N. and Appleby, P.G. (1995) 'Radiometric dating (210Pb, 137Cs, 241Am) of recent ombrotrophic peat accumulation and evidence for changes in mass balance', *The Holocene,* 5(2), 141-148.

Oosthoek, K.J.W. (2005) 'The origins and evolution of community forests in Scotland, 1919-2002', [online], available: http://www.eh-resources.org/community_forest.html [accessed 9/9/14]

Ostle, N.J., Levy, P.E., Evans, C.D. and Smith, P. (2009) 'UK land use and soil carbon sequestration', *Land Use Policy,* 26, S274-S283.

Oswald, C.J. and Branfireun, B.A. (2014) 'Antecedent moisture conditions control mercury and dissolved organic carbon concentration dynamics in a boreal headwater catchment', *Water Resources Research,* 50(8), 6610-6627.

Otabbong, E., Fristedt, A. and Otabbong, I.R. (2009) 'Phosphorus status, disposition and seasonal dynamics in the Swedish Kristianstad Riparian Histosol Wetlands', *Acta Agriculturae Scandinavica Section B-Soil and Plant Science,* 59(2), 179-188.

Pacheco, F.S., Roland, F. and Downing, J.A. (2014) 'Eutrophication reverses whole-lake carbon budgets', *Inland Waters,* 4(1), 41-48.

Page, S., Hoscilo, A., Wosten, H., Jauhiainen, J., Silvius, M., Rieley, J., Ritzema, H., Tansey, K., Graham, L., Vasander, H. and Limin, S. (2009) 'Restoration Ecology of Lowland Tropical Peatlands in Southeast Asia: Current Knowledge and Future Research Directions', *Ecosystems,* 12(6), 888-905.

Page, S.E., Rieley, J.O. and Banks, C.J. (2011) 'Global and regional importance of the tropical peatland carbon pool', *Global Change Biology,* 17(2), 798-818.

Palviainen, M., Finer, L., Lauren, A., Launiainen, S., Piirainen, S., Mattsson, T. and Starr, M. (2014) 'Nitrogen, Phosphorus, Carbon, and Suspended Solids Loads from Forest Clear-Cutting and Site Preparation: Long-Term Paired Catchment Studies from Eastern Finland', *Ambio,* 43(2), 218-233.

Parry, L.E., Holden, J. and Chapman, P.J. (2014) 'Restoration of blanket peatlands', *Journal of Environmental Management,* 133, 193-205.

Pastor, J., Solin, J., Bridgham, S.D., Updegraff, K., Harth, C., Weishampel, P. and Dewey, B. (2003) 'Global warming and the export of dissolved organic carbon from boreal peatlands', *Oikos,* 100(2), 380-386.

Patterson, L. and Cooper, D.J. (2007) 'The use of hydrologic and ecological indicators for the restoration of drainage ditches and water diversions in a mountain fen, cascade range, California', *Wetlands,* 27(2), 290-304.

Pawson, R.R., Evans, M.G. and Allott, T.E.H.A. (2012) 'Fluvial carbon flux from headwater peatland streams: significance of particulate carbon flux', *Earth Surface Processes and Landforms,* 37(11), 1203-1212.

Pawson, R.R., Lord, D.R., Evans, M.G. and Allott, T.E.H. (2008) 'Fluvial organic carbon flux from an eroding peatland catchment, southern Pennines, UK', *Hydrology and Earth System Sciences,* 12(2), 625-634.

Peacock, M., Burden, A., Cooper, M., Dunn, C., Evans, C.D., Fenner, N., Freeman, C., Gough, R., Hughes, D., Hughes, S., Jones, T., Lebron, I., West, M. and Zielinski, P. (2013a) 'Quantifying dissolved organic carbon concentrations in upland catchments using phenolic proxy measurements', *Journal of Hydrology,* 477, 251-260.

Peacock, M., Evans, C.D., Fenner, N. and Freeman, C. (2013b) 'Natural revegetation of bog pools after peatland restoration involving ditch blocking-The influence of pool depth and implications for carbon cycling', *Ecological Engineering,* 57, 297-301.

Pendea, I.F. and Chmura, G.L. (2012) 'A high-resolution record of carbon accumulation rates during boreal peatland initiation', *Biogeosciences,* 9(7), 2711-2717.

Peterson, B.J., Deegan, L., Helfrich, J., Hobbie, J.E., Hullar, M., Moller, B., Ford, T.E., Hershey, A., Hiltner, A., Kipphut, G., Lock, M.A., Fiebig, D.M., McKinley, V., Miller, M.C., Vestal, J.R., et al. (1993) 'BIOLOGICAL RESPONSES OF A TUNDRA RIVER TO FERTILIZATION', *Ecology,* 74(3), 653-672.

Piirainen, S., Finér, L., Mannerkoski, H. and Starr, M. (2004) 'Effects of forest clear-cutting on the sulphur, phosphorus and base cations fluxes through podzolic soil horizons', *Biogeochemistry,* 69(3), 405-424.

Piotrowska, N., Blaauw, M., Mauquoy, D. and Chambers, F.M. (2011) 'Constructing deposition chronologies for peat deposits using radiocarbon dating', *Mires and Peat,* (7).

Prescott, C.E. (2005) 'Do rates of litter decomposition tell us anything we really need to know?', *Forest Ecology and Management,* 220(1–3), 66-74.

Preston, M.D., Eimers, M.C. and Watmough, S.A. (2011) 'Effect of moisture and temperature variation on DOC release from a peatland: Conflicting results from laboratory, field and historical data analysis', *Science of The Total Environment,* 409(7), 1235-1242.

Pribyl, D.W. (2010) 'A critical review of the conventional SOC to SOM conversion factor', *Geoderma,* 156(3-4), 75-83.

Price, J.S. (1992) 'BLANKET BOG IN NEWFOUNDLAND .2. HYDROLOGICAL PROCESSES', *Journal of Hydrology,* 135(1-4), 103-119.

Quillet, A., Garneau, M. and Frolking, S. (2013) 'Sobol' sensitivity analysis of the Holocene Peat Model: What drives carbon accumulation in peatlands?', *Journal of Geophysical Research-Biogeosciences,* 118(1), 203-214.

Quinton, J.N., Govers, G., Van Oost, K. and Bardgett, R.D. (2010) 'The impact of agricultural soil erosion on biogeochemical cycling', *Nature Geosci,* 3(5), 311-314.

Quinty, F. and Rochefort, L. (2003) *Peatland Restoration Guide,* Second Edition ed., Quebec, Canada: Candian Sphagnum Peat Moss Association and New Brunswick Depaertment of Natural Reseources and Energy.

Rafelski, L.E., Piper, S.C. and Keeling, R.F. (2009) 'Climate effects on atmospheric carbon dioxide over the last century', *Tellus Series B-Chemical and Physical Meteorology,* 61(5), 718-731.

Ramchunder, S.J., Brown, L.E. and Holden, J. (2009) 'Environmental effects of drainage, drain-blocking and prescribed vegetation burning in UK upland peatlands', *Progress in Physical Geography,* 33(1), 49-79.

Raymond, P.A., Hartmann, J., Lauerwald, R., Sobek, S., McDonald, C., Hoover, M., Butman, D., Striegl, R.G., Mayorga, E., Humborg, C., Kortelainen, P., Durr, H., Meybeck, M., Ciais, P. and Guth, P. (2013) 'Global carbon dioxide emissions from inland waters', *Nature,* 503(7476), 355-359.

Reed, M.S., Bonn, A., Evans, C., Glenk, K. and Hansjürgens, B. (2014) 'Assessing and valuing peatland ecosystem services for sustainable management', *Ecosystem Services,* (0).

Reimer, P.J., Baillie, M.G.L., Bard, E., Bayliss, A., Beck, J.W., Bertrand, C.H.J., Blackwell, P.G., Buck, C.E., Burr, G.S., Cutler, K.B., Damon, P.E., Edwards, R.L., Fairbanks, R.G., Friedrich, M., Guilderson, T.P., et al. (2007) *IntCal04 terrestrial radiocarbon age calibration, 0-26 cal kyr BP, 2007*.

Reimer, P.J., Baillie, M.G.L., Bard, E., Bayliss, A., Beck, J.W., Bertrand, C.J.H., Blackwell, P.G., Buck, C.E., Burr, G.S., Cutler, K.B., Damon, P.E., Edwards, R.L., Fairbanks, R.G., Friedrich, M., Guilderson, T.P., et al. (2004) 'IntCal04 terrestrial radiocarbon age calibration, 0-26 cal kyr BP', *Radiocarbon,* 46(3), 1029-1058.

Reimer, P.J., Baillie, M.G.L., Bard, E., Bayliss, A., Beck, J.W., Blackwell, P.G., Ramsey, C.B., Buck, C.E., Burr, G.S., Edwards, R.L., Friedrich, M., Grootes, P.M., Guilderson, T.P., Hajdas, I., Heaton, T.J., et al. (2009) 'INTCAL09 AND MARINE09 RADIOCARBON AGE CALIBRATION CURVES, 0-50,000 YEARS CAL BP', *Radiocarbon,* 51(4), 1111-1150.

Reimer, P.J., Baillie, M.G.L., Bard, E., Bayliss, A., Beck, J.W., Blackwell, P.G., Ramsey, C.B., Buck, C.E., Burr, G.S., Edwards, R.L., Friedrich, M., Grootes, P.M., Guilderson,

T.P., Hajdas, I., Heaton, T.J., et al. (2011) *IntCal09 and Marine09 Radiocarbon Age Calibration Curves, 0-50,000 Years cal BP, 2011*.

Reimer, P.J., Bard, E., Bayliss, A., Beck, J.W., Blackwell, P.G., Bronk Ramsey, C., Buck, C.E., Cheng, H., Edwards, R.L., Friedrich, M., Grootes, P.M., Guilderson, T.P., Haflidason, H., Hajdas, I., Hatté, C., et al. (2013) *IntCal13 and Marine13 Radiocarbon Age Calibration Curves 0–50,000 Years cal BP, 2013*.

Reimer, P.J., Brown, T.A. and Reimer, R.W. (2008) *Discussion: Reporting and Calibration of Post-Bomb 14C Data, 2008*.

Renou-Wilson, F. and Farrell, C.A. (2009) 'Peatland vulnerability to energy-related developments from climate change policy in Ireland: the case of wind farms', *Mires and Peat,* 4, Article 08.

Rigler, F.H. (1979) 'The export of phosphorus from Dartmoor catchments: a model to explain variations of phosphorus concentrations in streamwater', *Journal of the Marine Biological Association of the United Kingdom,* 59(03), 659-687.

Robards, K., McKelvie, I.D., Benson, R.L., Worsfold, P.J., Blundell, N.J. and Casey, H. (1994) 'DETERMINATION OF CARBON, PHOSPHORUS, NITROGEN AND SILICON SPECIES IN WATERS', *Analytica Chimica Acta,* 287(3), 147-190.

Rodgers, M., O'Connor, M., Healy, M.G., O'Driscoll, C., Asam, Z.U.Z., Nieminen, M., Poole, R., Muller, M. and Xiao, L.W. (2010) 'Phosphorus release from forest harvesting on an upland blanket peat catchment', *Forest Ecology and Management,* 260(12), 2241-2248.

Roulet, N.T., Lafleur, P.M., Richard, P.J.H., Moore, T.R., Humphreys, E.R. and Bubier, J.L. (2007) 'Contemporary carbon balance and late Holocene carbon accumulation in a northern peatland', *Global Change Biology,* 13(2), 397-411.

(2013) *Gordonbush Estate and surrounding area: current and historical information* available: [accessed 16/2/1].

Rowland, A.P. and Haygarth, P.M. (1997) 'Determination of total dissolved phosphorus in soil solutions', *Journal of Environmental Quality,* 26(2), 410-415.

Rowson, J.G., Gibson, H.S., Worrall, F., Ostle, N., Burt, T.P. and Adamson, J.K. (2010) 'The complete carbon budget of a drained peat catchment', *Soil Use and Management,* 26(3), 261-273.

Ruesch, A. and Gibbs, H.K. (2008) *New IPCC Tier-1 Global Biomass Carbon Map For the Year 2000*, sheet Oak Ridge, Tennessee: Oak Ridge National Laboratory,

Ryder, E., de Eyto, E., Dillane, M., Poole, R. and Jennings, E. (2014) 'Identifying the role of environmental drivers in organic carbon export from a forested peat catchment', *The Science of the total environment,* 490.

Saari, P., Saarnio, S., Kukkonen, J.V.K., Akkanen, J., Heinonen, J., Saari, V. and Alm, J. (2009) 'DOC and N2O dynamics in upland and peatland forest soils after clear-cutting and soil preparation', *Biogeochemistry,* 94(3), 217-231.

Sagerfors, J., Lindroth, A., Grelle, A., Klemedtsson, L., Weslien, P. and Nilsson, M. (2008) 'Annual CO2 exchange between a nutrient-poor, minerotrophic, boreal mire and the atmosphere', *Journal of Geophysical Research: Biogeosciences,* 113(G1), G01001.

Sander, G.C., Zheng, T., Heng, P., Zhong, Y. and Barry, D.A. (2011) 'Sustainable soil and water resources: modelling soil erosion and its impact on the environment', *19th International Congress on Modelling and Simulation (Modsim2011)*, 45-56.

Sanderman, J., Lohse, K.A., Baldock, J.A. and Amundson, R. (2009) 'Linking soils and streams: Sources and chemistry of dissolved organic matter in a small coastal watershed', *Water Resources Research,* 45(3).

Sandford, R.C., Bol, R. and Worsfold, P.J. (2010) 'In situ determination of dissolved organic carbon in freshwaters using a reagentless UV sensor', *Journal of Environmental Monitoring,* 12(9), 1678-1683.

Schiff, S., Aravena, R., Mewhinney, E., Elgood, R., Warner, B., Dillon, P. and Trumbore, S. (1998) 'Precambrian shield wetlands: Hydrologic control of the sources and export of dissolved organic matter', *Climatic Change,* 40(2), 167-188.

Schiff, S.L., Aravena, R., Trumbore, S.E., Hinton, M.J., Elgood, R. and Dillon, P.J. (1997) 'Export of DOC from forested catchments on the Precambrian Shield of Central Ontario: Clues from C-13 and C-14', *Biogeochemistry,* 36(1), 43-65.

Schilstra, A.J. (2001) 'How sustainable is the use of peat for commercial energy production?', *Ecological Economics,* 39(2), 285-293.

Scotland's Soils, S.S. (2014a) 'Scotland's soil - key facts', *Scotland's soils* [online], available: http://www.soils-scotland.gov.uk/about/key-fact#5 [accessed 12/2/15]

Scotland's Soils, S.S. (2014b) 'Soil Organic Matter', *State of Scotland's soils* [online], available: http://www.soils-scotland.gov.uk/context/organic [accessed 12/2/15]

Scottish Government, S.G. (2011) *2020 Routemap for Renewable Energy in Scotland*, www.gov.scot: Scottish Goverment Publications, available: http://www.scotland.gov.uk/Topics/Business-Industry/Energy/UpdateRenewableRoutemap [Accessed 12/2/15].

Scottish Government, S.G. (2012) *More clean energy 'essential for Scotland'*, www.gov.scot: Scottish Goverment Publications, available: http://www.scotland.gov.uk/News/Releases/2012/10/Renewables30102012 [Accessed 12/2/15].

Scottish Government, S.G. (2014) *Onshore wind farms FAQs*, www.gov.scot: Scottish Goverment Publications, available: http://www.scotland.gov.uk/Topics/Business-Industry/Energy/Energy-sources/19185/17852-1/WindFAQ [Accessed 12/2/15].

Scottish Government, S.G. and DECC, D.o.E.a.C.C. (2014a) *Renewable Electrcity Statistics for Scotland*, www.gov.scot: Scottish Goverment Publications, available: http://www.scotland.gov.uk/Resource/0044/00447302.pdf [Accessed 12/2/15].

Scottish Government, S.G. and DECC, D.o.E.a.C.C. (2014b) *Renewable Planning Statistics - Summary Tables*, www.gov.scot: Scottish Goverment Publications, available: http://www.scotland.gov.uk/Topics/Statistics/Browse/Business/Energy/planningdata [Accessed 12/2/15].

Scottish Renewables, S.R. (2013) 'Scotland's renewables industry displaces record amount of CO2', *News* [online], available: http://www.scottishrenewables.com/news/scotlands-renewables-industry-displaces-CO2/ [accessed 16/2/15]

Scottish Renewables, S.R. (2014) 'What is Onshore wind?', *Onshore* [online], available: http://www.scottishrenewables.com/technologies/onshore-wind/ [accessed 16/2/15]

Scottish Renewables, S.R., RSPB, R.P.f.P.o.B., Scottish Wildlife Trust, S., World Wide Fund for Nature, W. and Friends of the Earth Scotland, F. (2012) 'Wind farms and peatland - Good practice principles',

Scottish Renewables, S.R. and SEPA, S.E.P.A. (2012) *Developments on peatland: Guidance on the assessment of peat volumes, reuse of excavated peat and the minimisation of waste*, Scotland: Joint publication by Scottish Renewables & SEPA, available: http://www.scottishrenewables.com/publications/guidance-assessment-peat-volumes-reuse-excavated/ [Accessed 1/9/14].

Scottish Renewables, S.R., SNH, S.N.H., SEPA, S.E.P.A., Forestry Commission Scotland, F. and Historic Scotland, H. (2013) *Good practice during wind farm construction*, Scotland: available: http://www.snh.gov.uk/planning-and-development/renewable-energy/onshore-wind/good-practice-during-windfarm-const/ [Accessed 1/9/14].

Sebestyen, S.D., Boyer, E.W., Shanley, J.B., Kendall, C., Doctor, D.H., Aiken, G.R. and Ohte, N. (2008) 'Sources, transformations, and hydrological processes that control stream nitrate and dissolved organic matter concentrations during snowmelt in an upland forest', *Water Resources Research,* 44(12), W12410.

Seeger, M., Errea, M.P., Begueria, S., Arnaez, J., Marti, C. and Garcia-Ruiz, J.M. (2004) 'Catchment soil moisture and rainfall characteristics as determinant factors for discharge/suspended sediment hysteretic loops in a small headwater catchment in the Spanish pyrenees', *Journal of Hydrology,* 288(3-4), 299-311.

Sellke, T., Bayarri, M.J. and Berger, J.O. (2001) 'Calibration of ρ values for testing precise null hypotheses', *The American Statistician,* 55(1), 62-71.

Shantz, M. and Price, J. (2006) 'Hydrological changes following restoration of the Bois-des-Bel Peatland, Quebec, 1999–2002', *Journal of Hydrology,* 331(3), 543-553.

Smith, J., Nayak, D.R. and Smith, P. (2012) 'Avoid constructing wind farms on peat', *Nature,* 489(7414), 33-33.

Smith, J., Nayak, D.R. and Smith, P. (2014) 'Wind farms on undegraded peatlands are unlikely to reduce future carbon emissions', *Energy Policy,* 66(0), 585-591.

Smith, L.C., MacDonald, G.M., Velichko, A.A., Beilman, D.W., Borisova, O.K., Frey, K.E., Kremenetski, K.V. and Sheng, Y. (2004) 'Siberian peatlands a net carbon sink and global methane source since the early Holocene', *Science,* 303(5656), 353-356.

Smith, M.D., Knapp, A.K. and Collins, S.L. (2009) 'A framework for assessing ecosystem dynamics in response to chronic resource alterations induced by global change', *Ecology,* 90(12), 3279-3289.

Smith, R.L. (1990) *Ecology and field biology, Ecology and field biology.*

Smith, V.H. (2003) 'Eutrophication of freshwater and coastal marine ecosystems - A global problem', *Environmental Science and Pollution Research,* 10(2), 126-139.

Smith, V.H., Tilman, G.D. and Nekola, J.C. (1999) 'Eutrophication: impacts of excess nutrient inputs on freshwater, marine, and terrestrial ecosystems', *Environmental Pollution,* 100(1–3), 179-196.

SNH, S.N.H. (2005) *The Peatlands of Caithness & Sutherland Management Strategy 2005-2015*, Scottish Natural Heritage, available: http://www.snh.org.uk/pdfs/scottish/nhighland/PeatlandsStrategy.pdf [Accessed 7/5/13].

SNH, S.N.H. (2012) *Identification of carbon-rich soil mapping units*, SNH Internal Coms Strategy, available: http://www.snh.gov.uk/docs/A602512.pdf [Accessed 6/6/14].

SNH, S.N.H. (2013a) *Onshore Wind Farms in Scotland (August 2013)*, sheet http://www.snh.gov.uk/docs/A1055080.pdf: Ordnance Survey,

SNH, S.N.H. (2013b) 'Site Details for Caithness and Sutherland Peatlands', *Sitelink - A Map of Scotland SSSIs* [online], available: http://gateway.snh.gov.uk/sitelink/siteinfo.jsp?pa_code=8218 [accessed 6/6/14]

SNH, S.N.H. (2014) 'The Peatland Partnerships March 2014 Newsletter',

Sobek, S., Durisch-Kaiser, E., Zurbrugg, R., Wongfun, N., Wessels, M., Pasche, N. and Wehrli, B. (2009) 'Organic carbon burial efficiency in lake sediments controlled by oxygen exposure time and sediment source', *Limnology and Oceanography,* 54(6), 2243-2254.

Sobek, S., Zurbrugg, R. and Ostrovsky, I. (2011) 'The burial efficiency of organic carbon in the sediments of Lake Kinneret', *Aquatic Sciences,* 73(3), 355-364.

Soupir, M.L., Mostaghimi, S. and Mitchem, C. (2009) 'A COMPARATIVE STUDY OF STREAM-GAGING TECHNIQUES FOR LOW-FLOW MEASUREMENTS IN TWO VIRGINIA TRIBUTARIES', *Journal of the American Water Resources Association,* 45(1), 110-122.

Speed, M., Tetzlaff, D., Soulsby, C., Hrachowitz, M. and Waldron, S. (2010) 'Isotopic and geochemical tracers reveal similarities in transit times in contrasting mesoscale catchments', *Hydrological Processes,* 24(9), 1211-1224.

SSER, S.a.S.E.R. (2009) *Gordonbush Estate Habitat Managment Plan*, Renewables, S.a.S.E.: available: [Accessed 1/6/10].

SSER, S.a.S.E.R. (2012) 'Gordonbush peat record - geotechnical record',

SSER, S.a.S.E.R. (2014) 'Gordonbush', *What We Do: Our Projects and Assets* [online], available: http://sse.com/whatwedo/ourprojectsandassets/renewables/gordonbush/ [accessed 18/1/15]

Strack, M., Toth, K., Bourbonniere, R. and Waddington, J.M. (2011) 'Dissolved organic carbon production and runoff quality following peatland extraction and restoration', *Ecological Engineering,* 37(12), 1998-2008.

Strack, M. and Waddington, J.M. (2007) 'Response of peatland carbon dioxide and methane fluxes to a water table drawdown experiment', *Global Biogeochemical Cycles,* 21(1), GB1007.

Strack, M., Waddington, J.M., Bourbonniere, R.A., Buckton, E.L., Shaw, K., Whittington, P. and Price, J.S. (2008) 'Effect of water table drawdown on peatland dissolved organic carbon export and dynamics', *Hydrological Processes,* 22(17), 3373-3385.

Strack, M. and Zuback, Y.C.A. (2013) 'Annual carbon balance of a peatland 10 yr following restoration', *Biogeosciences,* 10(5), 2885-2896.

Strack, M., Zuback, Y.C.A., McCarter, C. and Price, J.S. (2015) 'Changes in dissolved organic carbon quality in soils and discharge 10 years after peatland restoration', *Journal of Hydrology,* 527, 345-354.

Strohmeier, S., Knorr, K.H., Reichert, M., Frei, S., Fleckenstein, J.H., Peiffer, S. and Matzner, E. (2013) 'Concentrations and fluxes of dissolved organic carbon in runoff from a forested catchment: insights from high frequency measurements', *Biogeosciences,* 10(2), 905-916.

Stuiver, M. and Reimer, P.J. (1993) 'EXTENDED C-14 DATA-BASE AND REVISED CALIB 3.0 C-14 AGE CALIBRATION PROGRAM', *Radiocarbon,* 35(1), 215-230.

Surridge, B.W.J., Heathwaite, A.L. and Baird, A.J. (2012) 'Phosphorus mobilisation and transport within a long-restored floodplain wetland', *Ecological Engineering,* 44, 348-359.

Syed, K.H., Flanagan, L.B., Carlson, P.J., Glenn, A.J. and Van Gaalen, K.E. (2006) 'Environmental control of net ecosystem CO2 exchange in a treed, moderately rich fen in northern Alberta', *Agricultural and Forest Meteorology,* 140(1-4), 97-114.

Tallis, J.H. (1998) 'Growth and degradation of British and Irish blanket mires', *Environmental Reviews,* 6(2), 81-122.

Tang, R., Clark, J.M., Bond, T., Graham, N., Hughes, D. and Freeman, C. (2013) 'Assessment of potential climate change impacts on peatland dissolved organic carbon release and drinking water treatment from laboratory experiments', *Environmental Pollution,* 173, 270-277.

Taylor, P.G. and Townsend, A.R. (2010) 'Stoichiometric control of organic carbon-nitrate relationships from soils to the sea', *Nature,* 464(7292), 1178-1181.

Teledyne ISCO, I. (2013) '2150 Area Velocity Module', *2100 Series Flow Modules* [online], available: http://www.isco.com/products/products3.asp?PL=2021010 [accessed 12/2/14]

Teledyne ISCO, I. (2013) '3700 Full-Size Portable Sampler', *Automatic Water Samples* [online], available: http://www.isco.com/products/products3.asp?PL=201101030 [accessed 12/2/14]

Tetzlaff, D., Malcolm, I.A. and Soulsby, C. (2007) 'Influence of forestry, environmental change and climatic variability on the hydrology, hydrochemistry and residence times of upland catchments', *Journal of Hydrology,* 346(3-4), 93-111.

Thormann, M.N. and Bayley, S.E. (1997) 'Decomposition along a moderate-rich fen-marsh peatland gradient in boreal Alberta, Canada', *Wetlands,* 17(1), 123-137.

Thurman, E.M. (1985) *Organic Geochemistry of Natural Waters, Developments in Biogeochemistry,* Lancaster: Kluwer Academic Publishers Group.

Tipping, E. and Hurley, M.A. (1988) 'A MODEL OF SOLID-SOLUTION INTERACTIONS IN ACID ORGANIC SOILS, BASED ON THE COMPLEXATION PROPERTIES OF HUMIC SUBSTANCES', *Journal of Soil Science,* 39(4), 505-519.

Tipping, E., Smith, E.J., Bryant, C.L. and Adamson, J.K. (2007) 'The organic carbon dynamics of a moorland catchment in N. W. England', *Biogeochemistry,* 84(2), 171-189.

Tipping, E. and Woof, C. (1991) 'THE DISTRIBUTION OF HUMIC SUBSTANCES BETWEEN THE SOLID AND AQUEOUS PHASES OF ACID ORGANIC SOILS - A DESCRIPTION BASED ON HUMIC HETEROGENEITY AND CHARGE-DEPENDENT SORPTION EQUILIBRIA', *Journal of Soil Science,* 42(3), 437-448.

Tolonen, K. and Turunen, J. (1996) 'Accumulation rates of carbon in mires in Finland and implications for climate change', *The Holocene,* 6(2), 171-178.

Tolonen, K., Vasander, H., Damman, A. and Clymo, R.S. (1992) 'Preliminary estimate of long-term carbon accumulation and loss in 25 boreal peatlands'.

Tosh, D.G., Montgomery, W.I. and Reid, N. (2014) *A review of the impacts of wind energy developments on biodiversity*, Research and Development Series No. 14/02, (NIEA), N.I.E.A.: Queen's University Belfast and the Northern Ireland Environment Agency (NIEA), available: [accessed Accessed].

Tranvik, L.J., Downing, J.A., Cotner, J.B., Loiselle, S.A., Striegl, R.G., Ballatore, T.J., Dillon, P., Finlay, K., Fortino, K., Knoll, L.B., Kortelainen, P.L., Kutser, T., Larsen, S., Laurion, I., Leech, D.M., et al. (2009) 'Lakes and reservoirs as regulators of carbon cycling and climate', *Limnology and Oceanography,* 54(6), 2298-2314.

Tranvik, L.J. and Jansson, M. (2002) 'Climate change - Terrestrial export of organic carbon', *Nature,* 415(6874), 861-862.

Turner, B.L., Baxter, R. and Whitton, B.A. (2003) 'Nitrogen and phosphorus in soil solutions and drainage streams in Upper Teesdale, northern England: implications of organic compounds for biological nutrient limitation', *Science of The Total Environment,* 314, 153-170.

Turner, E.K., Worrall, F. and Burt, T.P. (2013) 'The effect of drain blocking on the dissolved organic carbon (DOC) budget of an upland peat catchment in the UK', *Journal of Hydrology,* 479(0), 169-179.

Turunen, J. (2008) 'Development of Finnish peatland area and carbon storage 1950-2000', *Boreal Environment Research,* 13(4), 319-334.

Turunen, J., Pitkanen, A., Tahvanainen, T. and Tolonen, K. (2001) 'Carbon accumulation in West Siberian mires, Russia.', *Global Biogeochemical Cycles,* (15), 285-96.

Turunen, J., Roulet, N.T., Moore, T.R. and Richard, P.J.H. (2004) 'Nitrogen deposition and increased carbon accumulation in ombrotrophic peatlands in eastern Canada', *Global Biogeochemical Cycles,* 18(3).

Turunen, J., Tomppo, E., Tolonen, K. and Reinikainen, A. (2002) 'Estimating carbon accumulation rates of undrained mires in Finland - application to boreal and subarctic regions', *Holocene,* 12(1), 69-80.

UK TAG, W.F.D.U.T.A.G. (2008) *UK Environmental Standards and Conditions (Phase 1) Final Report April 2008*, Water Framework Directive UK Technical Advisory Group, available: http://www.wfduk.org/sites/default/files/Media/Environmental%20standards/Environmental%20standards%20phase%201_Finalv2_010408.pdf [Accessed 15/6/12].

UK TAG, W.F.D.U.T.A.G. (2013) *Updated recommendations on phosphorus standards for rivers (River Basin Management 2015-2021)*, TAG, U.: Water Framework Directive UK Technical Advisory Group, available: [Accessed 1/2/14].

van Niekerk, M. (2012) *Understanding aquatic carbon loss from upland catchments in south west Scotland during land use change from commercial forest to wind farm*, unpublished thesis (Thesis), University of Stirling.

Van Oost, K., Quine, T.A., Govers, G., De Gryze, S., Six, J., Harden, J.W., Ritchie, J.C., McCarty, G.W., Heckrath, G., Kosmas, C., Giraldez, J.V., da Silva, J.R.M. and Merckx, R. (2007) 'The Impact of Agricultural Soil Erosion on the Global Carbon Cycle', *Science,* 318(5850), 626-629.

Vanselow-Algan, M., Schmidt, S.R., Greven, M., Fiencke, C., Kutzbach, L. and Pfeiffer, E.M. (2015) 'High methane emissions dominated annual greenhouse gas balances 30 years after bog rewetting', *Biogeosciences,* 12(14), 4361-4371.

Verhoeven, J.T.A. (2014) 'Wetlands in Europe: Perspectives for restoration of a lost paradise', *Ecological Engineering,* 66, 6-9.

Verhoff, F.H., Yaksich, S.M. and Melfi, D.A. (1980) 'RIVER NUTRIENT AND CHEMICAL TRANSPORT ESTIMATION', *American Society of Civil Engineers, Journal of the Environmental Engineering Division,* 106(3), 591-608.

Vitt, D.H., Halsey, L.A., Bauer, I.E. and Campbell, C. (2000) 'Spatial and temporal trends in carbon storage of peatlands of continental western Canada through the Holocene', *Canadian Journal of Earth Sciences,* 37(5), 683-693.

Vitt, D.H., Halsey, L.A. and Nicholson, B.J. (2005) *The Mackenzie River basin*
*The World's Largest Wetlands,* Cambridge University Press.

Vleeschouwer, F.d., Chambers, F.M. and Swindles, G.T. (2010) 'Coring and sub-sampling of peatla+ds for palaeoenvironmental research', *Mires and Peat,* 7.

von Wachenfeldt, E., Sobek, S., Bastviken, D. and Tranvik, L.J. (2008) 'Linking allochthonous dissolved organic matter and boreal lake sediment carbon sequestration: The role of light-mediated flocculation', *Limnology and Oceanography,* 53(6), 2416-2426.

von Wachenfeldt, E. and Tranvik, L.J. (2008) 'Sedimentation in boreal lakes - The role of flocculation of allochthonous dissolved organic matter in the water column', *Ecosystems,* 11(5), 803-814.

Waddington, J., Rochefort, L. and Campeau, S. (2003) 'Sphagnum production and decomposition in a restored cutover peatland', *Wetlands Ecology and management,* 11(1-2), 85-95.

Waddington, J.M. and McNeill, P. (2002) 'Peat oxidation in an abandoned cutover peatland', *Canadian Journal of Soil Science,* 82(3), 279-286.

Waddington, J.M., Plach, J., Cagampan, J.P., Lucchese, M. and Strack, M. (2009) 'Reducing the Carbon Footprint of Canadian Peat Extraction and Restoration', *Ambio,* 38(4), 194-200.

Waddington, J.M., Strack, M. and Greenwood, M.J. (2010) 'Toward restoring the net carbon sink function of degraded peatlands: Short-term response in CO2 exchange to ecosystem-scale restoration', *Journal of Geophysical Research-Biogeosciences,* 115.

Waddington, J.M., Toth, K. and Bourbonniere, R. (2008) 'Dissolved organic carbon export from a cutover and restored peatland', *Hydrological Processes,* 22(13), 2215-2224.

Waddington, J.M., Warner, K.D. and Kennedy, G.W. (2002) 'Cutover peatlands: A persistent source of atmospheric CO2', *Global Biogeochemical Cycles,* 16(1).

Waldron, S., Flowers, H., Arlaud, C., Bryant, C. and McFarlane, S. (2009) 'The significance of organic carbon and nutrient export from peatland-dominated landscapes subject to disturbance, a stoichiometric perspective', *Biogeosciences,* 6(3), 363-374.

Waldron, S., Scott, E.M. and Soulsby, C. (2007) 'Stable Isotope Analysis Reveals Lower-Order River Dissolved Inorganic Carbon Pools Are Highly Dynamic', *Environmental Science & Technology,* 41(17), 6156-6162.

Wallage, Z.E., Holden, J. and McDonald, A.T. (2006) 'Drain blocking: An effective treatment for reducing dissolved organic carbon loss and water discolouration in a drained peatland', *Science of The Total Environment,* 367(2–3), 811-821.

Walling, D.E. and Webb, B.W. (1985) 'ESTIMATING THE DISCHARGE OF CONTAMINANTS TO COASTAL WATERS BY RIVERS - SOME CAUTIONARY COMMENTS', *Marine Pollution Bulletin,* 16(12), 488-492.

Walling, D.E. and Webb, B.W. (1986) 'Solutes in river systems', *Solute processes*, 251-327.

Walling, D.E. and Webb, B.W. (1988) 'The reliability of rating curve estimates of suspended sediment yield: some further comments', *IN: Sediment Budgets. IAHS Publication,* (174).

Waterloo, M.J., Oliveira, S.M., Drucker, D.P., Nobre, A.D., Cuartas, L.A., Hodnett, M.G., Langedijk, I., Jans, W.W.P., Tomasella, J., de Araujo, A.C., Pimentel, T.P. and Estrada, J.C.M. (2006) 'Export of organic carbon in run-off from an Amazonian rainforest blackwater catchment', *Hydrological Processes,* 20(12), 2581-2597.

Webb, B.W., Phillips, J.M., Walling, D.E., Littlewood, I.G., Watts, C.D. and Leeks, G.J.L. (1997) 'Load estimation methodologies for British rivers and their relevance to the LOIS RACS(R) programme', *Science of The Total Environment,* 194–195(0), 379-389.

Wetzel, R.G. (2002) 'Dissolved organic carbon: detrital energetics, metabolic regulators, and drivers of ecosystem stability of aqyuatic ecosystems' in Findlay, S.E.G. and Sinsabaugh, R.L., eds., *Aquatic Ecosystems: Interactivity of dissovled organic matter*, USA: Elsevier Science, 508.

Wetzel, R.G. and Likens, G.E. (2002) 'Composition of biomass and pigments' in Wetzel, R.G. and Likens, G.E., eds., *Limnological Analyses*, Springer, Academic Press, 147-174.

Weyhenmeyer, G.A., Willen, E. and Sonesten, L. (2004) 'Effects of an extreme precipitation event on water chemistry and phytoplankton in the Swedish Lake Malaren', *Boreal Environment Research,* 9(5), 409-420.

White, P.A., Kalff, J., Rasmussen, J.B. and Gasol, J.M. (1991) 'THE EFFECT OF TEMPERATURE AND ALGAL BIOMASS ON BACTERIAL PRODUCTION AND SPECIFIC GROWTH-RATE IN FRESH-WATER AND MARINE HABITATS', *Microbial Ecology,* 21(2), 99-118.

Whittington, P.N. and Price, J.S. (2006) 'The effects of water table draw-down (as a surrogate for climate change) on the hydrology of a fen peatland, Canada', *Hydrological Processes,* 20(17), 3589-3600.

Wilkie, N.M. and Mayhew, P.W. (2003) 'The management and restoration of damaged blanket bog in the north of Scotland', *Transactions and Proceedings of the Botanical Society of Edinburgh and Botanical Society of Edinburgh Transactions,* 55(1), 125-133.

Williams, G.P. (1989) 'SEDIMENT CONCENTRATION VERSUS WATER DISCHARGE DURING SINGLE HYDROLOGIC EVENTS IN RIVERS', *Journal of Hydrology,* 111(1-4), 89-106.

Wilson, L., Wilson, J., Holden, J., Johnstone, I., Armstrong, A. and Morris, M. (2011a) 'Ditch blocking, water chemistry and organic carbon flux: Evidence that blanket bog restoration reduces erosion and fluvial carbon loss', *Science of The Total Environment,* 409(11), 2010-2018.

Wilson, L., Wilson, J., Holden, J., Johnstone, I., Armstrong, A. and Morris, M. (2011b) 'The impact of drain blocking on an upland blanket bog during storm and drought events, and the importance of sampling-scale', *Journal of Hydrology,* 404(3–4), 198-208.

Wilson, L., Wilson, J.D., Holden, J., Johnstone, I., Armstrong, A. and Morris, M. (2010) 'Recovery of water tables in Welsh blanket bog after drain blocking: Discharge rates, time scales and the influence of local conditions', *Journal of Hydrology,* 391(3–4), 377-386.

Worrall, F., Armstrong, A. and Holden, J. (2007a) 'Short-term impact of peat drain-blocking on water colour, dissolved organic carbon concentration, and water table depth', *Journal of Hydrology,* 337(3–4), 315-325.

Worrall, F. and Burt, T.P. (2004) 'Time series analysis of long-term river dissolved organic carbon records', *Hydrological Processes,* 18(5), 893-911.

Worrall, F. and Burt, T.P. (2005) 'Predicting the future DOC flux from upland peat catchments', *Journal of Hydrology,* 300(1–4), 126-139.

Worrall, F. and Burt, T.P. (2007a) 'Flux of dissolved organic carbon from U.K. rivers', *Global Biogeochemical Cycles,* 21(1), GB1013.

Worrall, F. and Burt, T.P. (2007b) 'Trends in DOC concentration in Great Britain', *Journal of Hydrology,* 346(3–4), 81-92.

Worrall, F. and Burt, T.P. (2008) 'The effect of severe drought on the dissolved organic carbon (DOC) concentration and flux from British rivers', *Journal of Hydrology,* 361(3–4), 262-274.

Worrall, F., Burt, T.P. and Adamson, J. (2004a) 'Can climate change explain increases in DOC flux from upland peat catchments?', *Science of The Total Environment,* 326(1–3), 95-112.

Worrall, F., Burt, T.P. and Adamson, J. (2006a) 'The rate of and controls upon DOC loss in a peat catchment', *Journal of Hydrology,* 321(1–4), 311-325.

Worrall, F., Burt, T.P. and Adamson, J.K. (2006b) 'Trends in Drought Frequency – the Fate of DOC Export From British Peatlands', *Climatic Change,* 76(3-4), 339-359.

Worrall, F., Burt, T.P., Jaeban, R.Y., Warburton, J. and Shedden, R. (2002) 'Release of dissolved organic carbon from upland peat', *Hydrological Processes,* 16(17), 3487-3504.

Worrall, F., Burt, T.P., Rowson, J.G., Warburton, J. and Adamson, J.K. (2009) 'The multi-annual carbon budget of a peat-covered catchment', *Science of The Total Environment,* 407(13), 4084-4094.

Worrall, F., Chapman, P.J., Holden, J., Evans, C., Artz, R., Smith, P. and Grayson, R. (2011) *A review of current evidence on carbon fluxes and greenhouse gas emissions from UK peatlands*, Peterborough: available: http://jncc.defra.gov.uk/pdf/jncc442_webFinal.pdf [Accessed 25/1/13].

Worrall, F., Davies, H., Bhogal, A., Lilly, A., Evans, M., Turner, K., Burt, T.P., Barraclough, D., Smith, P. and Merrington, G. (2012) 'The flux of DOC from the UK – Predicting the role of soils, land use and net watershed losses', *Journal of Hydrology,* 448–449(0), 149-160.

Worrall, F., Gibson, H.S. and Burt, T.P. (2007b) 'Modelling the impact of drainage and drain-blocking on dissolved organic carbon release from peatlands', *Journal of Hydrology,* 338(1–2), 15-27.

Worrall, F., Gibson, H.S. and Burt, T.P. (2008) 'Production vs. solubility in controlling runoff of DOC from peat soils – The use of an event analysis', *Journal of Hydrology,* 358(1–2), 84-95.

Worrall, F., Harriman, R., Evans, C.D., Watts, C.D., Adamson, J., Neal, C., Tipping, E., Burt, T.P., Grieve, I., Monteith, D.T., Naden, P.S., Nisbet, T., Reynolds, B. and Stevens, P. (2004b) 'Trends in Dissolved Organic Carbon in UK Rivers and Lakes', *Biogeochemistry,* 70(3), 369-402.

Worrall, F., Reed, M., Warburton, J. and Burt, T.P. (2003) 'Carbon budget for a British upland peat catchment', *Science of The Total Environment,* 312(1–3), 133-146.

Wright, H.E. (1967) 'A SQUARE-ROD PISTON SAMPLER FOR LAKE SEDIMENTS', *Journal of Sedimentary Petrology,* 37(3), 975-&.

Yallop, A.R., Clutterbuck, B. and Thacker, J. (2010) 'Increases in humic dissolved organic carbon export from upland peat catchments: the role of temperature, declining sulphur deposition and changes in land management', *Climate Research,* 45, 43-56.

Yeloff, D., Bennett, K.D., Blaauw, M., Mauquoy, D., Sillasoo, Ü., van der Plicht, J. and van Geel, B. (2006) 'High precision 14C dating of Holocene peat deposits: A comparison of Bayesian calibration and wiggle-matching approaches', *Quaternary Geochronology,* 1(3), 222-235.

Yu, Z. (2011) 'Holocene carbon flux histories of the world's peatlands: Global carbon-cycle implications', *The Holocene,* 21(5), 761-774.

Yu, Z. (2012) 'Northern peatland carbon stocks and dynamics: a review', *Biogeosciences Discuss.,* 9(4), 5073-5107.

Yu, Z., Beilman, D.W., Frolking, S., MacDonald, G.M., Roulet, N.T., Camill, P. and Charman, D.J. (2011) 'Peatlands and Their Role in the Global Carbon Cycle', *Eos, Transactions American Geophysical Union,* 92(12), 97-98.

Yu, Z., Beilman, D.W. and Jones, M.C. (2009) 'Sensitivity of northern peatlands to Holocene climate change, in: Carbon Cycling in Northern Peatlands' in Baird, A.J., Belyea, L.R., Comas, X., Reeve, A. and Slater, L., eds., *AGU Geophysical Monograph series*, USA: American Geophysical Unnion, 55-69.

Yu, Z., Campbell, I.D., Campbell, C., Vitt, D.H., Bond, G.C. and Apps, M.J. (2003) 'Carbon sequestration in western Canadian peat highly sensitive to Holocene wet-dry climate cycles at millennial timescales', *The Holocene,* 13(6), 801-808.

Yu, Z., Loisel, J., Brosseau, D.P., Beilman, D.W. and Hunt, S.J. (2010) 'Global peatland dynamics since the Last Glacial Maximum', *Geophysical Research Letters,* 37(13), L13402.

Yu, Z.C., Turetsky, M.R., Campbell, I.D. and Vitt, D.H. (2001) 'Modelling long-term peatland dynamics. II. Processes and rates as inferred from litter and peat-core data', *Ecological Modelling,* 145(2-3), 159-173.

Yurova, A., Sirin, A., Buffam, I., Bishop, K. and Laudon, H. (2008) 'Modeling the dissolved organic carbon output from a boreal mire using the convection-dispersion equation: Importance of representing sorption', *Water Resources Research,* 44(7), W07411.

Zak, D. and Gelbrecht, J. (2007) 'The mobilisation of phosphorus, organic carbon and ammonium in the initial stage of fen rewetting (a case study from NE Germany)', *Biogeochemistry,* 85(2), 141-151.

Zak, D., Gelbrecht, J., Wagner, C. and Steinberg, C.E.W. (2008) 'Evaluation of phosphorus mobilization potential in rewetted fens by an improved sequential chemical extraction procedure', *European Journal of Soil Science,* 59(6), 1191-1201.

Zak, D., Wagner, C., Payer, B., Augustin, J. and Gelbrecht, J. (2010) 'Phosphorus mobilization in rewetted fens: the effect of altered peat properties and implications for their restoration', *Ecological Applications,* 20(5), 1336-1349.

Zhang, C.F., Jamieson, R.C., Meng, F.R., Gordon, R.J. and Bourque, C.P.A. (2013) 'Simulation of monthly dissolved organic carbon concentrations in small forested watersheds', *Ecological Modelling,* 250, 205-213.

Zhang, C.F., Meng, F.R., Trofymow, J.A. and Arp, P.A. (2007) 'Modeling mass and nitrogen remaining in litterbags for Canadian forest and climate conditions', *Canadian Journal of Soil Science,* 87(4), 413-432.

Zhang, C.F., Trofymow, J.A., Jamieson, R.C., Meng, F.R., Gordon, R.J. and Bourque, C.P.A. (2010) 'Litter decomposition and nitrogen mineralization from an annual to a monthly model', *Ecological Modelling,* 221(16), 1944-1953.